

Plutonium Chemistry

Publication Date: May 19, 1983 | doi: 10.1021/bk-1983-0216.fw001

Plutonium Chemistry

William T. Carnall, EDITOR
Argonne National Laboratory

Gregory R. Choppin, EDITOR
The Florida State University

Based on a symposium
jointly sponsored by the
ACS Divisions of
Nuclear Chemistry and Technology
and Analytical Chemistry
at the 184th Meeting of the
American Chemical Society,
Kansas City, Missouri,
September 12–17, 1982

A C S S Y M P O S I U M S E R I E S **216**

AMERICAN CHEMICAL SOCIETY

WASHINGTON, D.C. 1983



Library of Congress Cataloging in Publication Data

Plutonium chemistry.

(ACS symposium series, ISSN 0097-6156; 216)

"Based on a symposium jointly sponsored by the ACS Divisions of Nuclear Chemistry and Technology and Analytical Chemistry, at the 184th Meeting of the American Chemical Society, Kansas City, Missouri, September 12-17, 1982."

Includes bibliographies and index.

1. Plutonium—Congresses.

I. Carnall, William T., 1927- . II. Choppin, Gregory R. III. American Chemical Society. Division of Nuclear Chemistry and Technology. IV. American Chemical Society. Division of Analytical Chemistry. V. Series.

QD181.P9P56 1983 546'.434 83-6057
ISBN 0-8412-0772-0

Copyright © 1983

American Chemical Society

All Rights Reserved. The appearance of the code at the bottom of the first page of each article in this volume indicates the copyright owner's consent that reprographic copies of the article may be made for personal or internal use or for the personal or internal use of specific clients. This consent is given on the condition, however, that the copier pay the stated per copy fee through the Copyright Clearance Center, Inc. for copying beyond that permitted by Sections 107 or 108 of the U.S. Copyright Law. This consent does not extend to copying or transmission by any means—graphic or electronic—for any other purpose, such as for general distribution, for advertising or promotional purposes, for creating new collective work, for resale, or for information storage and retrieval systems. The copying fee for each chapter is indicated in the code at the bottom of the first page of the chapter.

The citation of trade names and/or names of manufacturers in this publication is not to be construed as an endorsement or as approval by ACS of the commercial products or services referenced herein; nor should the mere reference herein to any drawing, specification, chemical process, or other data be regarded as a license or as a conveyance of any right or permission, to the holder, reader, or any other person or corporation, to manufacture, reproduce, use, or sell any patented invention or copyrighted work that may in any way be related thereto.

American Chemical

PRINTED IN THE UNITED STATES OF AMERICA

Society Library

1155 16th St., N.W.

Washington, D.C. 20036

ACS Symposium Series; American Chemical Society: Washington, DC, 1983.

ACS Symposium Series

M. Joan Comstock, *Series Editor*

Advisory Board

David L. Allara

Robert Baker

Donald D. Dollberg

Brian M. Harney

W. Jeffrey Howe

Herbert D. Kaesz

Marvin Margoshes

Donald E. Moreland

Robert Ory

Geoffrey D. Parfitt

Theodore Provder

Charles N. Satterfield

Dennis Schuetzle

Davis L. Temple, Jr.

Charles S. Tuesday

C. Grant Willson

FOREWORD

The ACS SYMPOSIUM SERIES was founded in 1974 to provide a medium for publishing symposia quickly in book form. The format of the Series parallels that of the continuing ADVANCES IN CHEMISTRY SERIES except that in order to save time the papers are not typeset but are reproduced as they are submitted by the authors in camera-ready form. Papers are reviewed under the supervision of the Editors with the assistance of the Series Advisory Board and are selected to maintain the integrity of the symposia; however, verbatim reproductions of previously published papers are not accepted. Both reviews and reports of research are acceptable since symposia may embrace both types of presentation.

PREFACE

THE CHEMISTRY OF A SINGLE ELEMENT is rarely the focal point of a symposium, but the occasion of the 40th anniversary of the first synthesis and weighing of pure compounds of plutonium suggested to us that such a symposium would be both timely and productive. The interest, enthusiasm, and stimulating interaction that the symposium generated showed that this supposition was indeed correct.

The chemistry of plutonium is unique in the periodic table. This theme is exemplified throughout much of the research work that is described in this volume. Many of the properties of plutonium cannot be estimated accurately based on experiments with lighter elements, such as uranium and neptunium. Because massive amounts of plutonium have been and are being produced throughout the world, the need to define precisely its chemical and physical properties and to predict its chemical behavior under widely varying conditions will persist. In addition to these needs, there is an intrinsic fundamental interest in an element with so many unusual properties and with so many different oxidation states, each with its own chemistry.

The symposium was designed to provide an overview of the current status of plutonium chemistry by practitioners in the various areas covered. The authors, drawn from U.S. and foreign universities and national laboratories, were encouraged to include review material to place their subjects in perspective, as well as to suggest what they believe to be productive directions for future investigation. We find it particularly useful that the contributions represent a mixture of fundamental as well as more applied environmental and process chemical research. Although we do not claim that this volume represents all areas of plutonium chemistry that are currently under active investigation, this collection does represent a reasonably broad and balanced view of the field. The contents of the volume should be useful as a reference both for those familiar with actinide chemistry and for those with limited interests who seek an introduction to the literature and current status in an area of plutonium chemistry.

We would like to thank all of the participants and contributors for their interest and cooperation, and the officers of the Division of Nuclear Chemistry and Technology, particularly the chairman, Richard Hahn, for

their encouragement and assistance from the inception of the idea to hold the symposium through its realization. We were particularly honored with the participation of one who was there when it all began and who was also celebrating other anniversaries this year, Glenn T. Seaborg.

WILLIAM T. CARNALL
Argonne National Laboratory
Argonne, Illinois 60439

GREGORY R. CHOPPIN
The Florida State University
Tallahassee, Florida 32306

December 1982

Forty Years of Plutonium Chemistry: The Beginnings

GLENN T. SEABORG

University of California, Lawrence Berkeley Laboratory and Department of Chemistry, Berkeley, CA 94720

The first isolation of a chemical compound of plutonium (a flouride) took place on August 20, 1942 and the first weighing of a pure compound (2.77 micrograms of the dioxide) on September 10, 1942. Thus this Symposium marks quite precisely the 40th anniversary of these events, the beginnings of the investigation of the macroscopic (non-tracer) chemical properties of this important synthetic element. The immediately following ultramicrochemical studies led to a definition of the IV and VI oxidation states, some properties of the metallic state, the synthesis and characterization of numerous solid compounds and the crucial testing of the first method devised for its separation and isolation in pure form after its production in the nuclear chain reaction. Later work with larger amounts, available as the result of its production in a nuclear reactor, made it possible to characterize the III and V oxidation states and many more compounds.

The last forty years have seen an extensive, world-wide investigation of the chemical properties of the synthetic element, plutonium. As a result, as much is known about the chemical properties of this element as is known about the chemical properties of most of the naturally occurring elements. The papers in this volume, presented at the Symposium on the Chemistry of Plutonium held during the Kansas City meeting of the American Chemical Society, in September, 1982, represent an up-dating of this large amount of information.

In the time and space available to me, I shall largely confine my comments to the origin of the chemical studies on this remarkable element. In so doing I shall include quotations from my Journal in order to help capture some of the flavor of this pioneering work.

0097-6156/83/0216-0001\$06.50/0
© 1983 American Chemical Society

The first isolation of a chemical compound of plutonium (a fluoride) took place on August 20, 1942 and the first weighing of a pure compound (2.77 micrograms of the dioxide) on September 20, 1942 at the wartime Metallurgical Laboratory of the University of Chicago. These events represent the beginning of the investigation of the macroscopic (non-tracer) chemical properties of plutonium and this Symposium corresponds quite precisely to the 40th anniversary of these inaugural experiments.

Tracer Chemical Investigations at Berkeley

Tracer investigations during 1941 and early 1942 at Berkeley led to a great deal of information about the chemical properties of plutonium. It was learned that it has at least two oxidation states, the higher of which is not carried by lanthanum fluoride or cerium fluoride, while the lower state is quantitatively coprecipitated with these compounds. It was established that the higher oxidation state can be obtained by treatment of the lower state with oxidizing agents such as persulfate and argentic ions, dichromate, permanganate, or periodate, and that the upper state can be reduced to a lower (rare earth fluoride-carriable) state by treatment with sulfur dioxide or bromide ion. The approximate potential of the couple plutonium (reduced)-plutonium (oxidized) was believed to be between -1.0 and -1.4 volts. It was established that plutonium in aqueous solution is not reduced to the metal by zinc, and that it does not form a volatile tetroxide. It was shown that a stable lower state of plutonium--probably plutonium (IV)--is carried by $\text{Th}(\text{IO}_3)_4$. Ether extraction was used to separate large amounts of uranyl nitrate from plutonium. Methods also were devised for the separation of plutonium from elements 90, 91, and 93.

On the basis of these facts, it was speculated that plutonium in its highest oxidation state is similar to uranium (VI) and in a lower state is similar to thorium (IV) and uranium (IV). It was reasoned that if plutonium existed normally as a stable plutonium (IV) ion, it would probably form insoluble compounds or stable complex ions analogous to those of similar ions, and that it would be desirable (as soon as sufficient plutonium became available) to determine the solubilities of such compounds as the fluoride, oxalate, phosphate, iodate, and peroxide. Such data were needed to confirm deductions based on the tracer experiments.

When the Plutonium Project was established early in 1942, for the purpose of producing plutonium via the nuclear chain reaction in uranium in sufficient quantities for its use as a nuclear explosive, we were given the challenge of developing a chemical method for separating and isolating it from the uranium and fission products. We had already conceived the principle of the oxidation-reduction cycle, which became the basis for such a separations process. This principle applied to any process involving the use of a substance which carried plutonium in one of its oxidation states but not in another. By use of this

principle, for example, a carrier could be used to carry plutonium in one oxidation state and thus to separate it from uranium and the fission products. Then the carrier and the plutonium could be dissolved, the oxidation state of the plutonium changed, and the carrier precipitated again, leaving the plutonium in solution. The oxidation state of the plutonium could again be changed and the cycles repeated. With this type of procedure, only a contaminating element having a chemistry nearly identical with plutonium would fail to separate if a number of oxidation-reduction cycles were employed. This principle, of course, applies to other types of processes, such as volatility, solvent extraction, or adsorption methods.

Move to Metallurgical Laboratory

The work on the Plutonium Project in early 1942 was centralized in the Metallurgical Laboratory of the University of Chicago. The following extract from my journal describes my arrival in Chicago with my colleague Isadore Perlman:

Sunday, April 19, 1942. This morning at 9:30 a.m. Isadore Perlman and I arrived in Chicago aboard the City of San Francisco. Although our trip from Berkeley took almost two full days, we feel that the time has not been wasted. Many lively discussions ensued in the privacy of our bedroom and, with appropriate care, in the club car regarding ways to separate element 94 chemically from uranium (that will be neutron-irradiated in chain-reacting piles) and from the fission by-products that will be produced concurrently in the neutron-irradiation process. This overall problem of element 94 isolation will occupy most of our attention for some time to come. The work of my group in the Department of Chemistry at the University of California, Berkeley, during the period August 1940 to the present, has produced much of the background information which is the basis of the Metallurgical Project. (This is the code name for the project whose mission is to produce fissionable element 94 in sufficient quantity for use in a nuclear weapon, and the project is centered at the University of Chicago.)

Our research at Berkeley has resulted in the discovery of element 94, demonstration of the slow neutron fissionability of its isotope 94^{239} , discovery and demonstration of the slow neutron fissionability of U^{233} , spontaneous fission measurements on these isotopes, discovery of 93^{237} , isolation of and nuclear measurements on U^{234} , study of the chemical properties and methods of chemical separation of element 94, demonstration of the presence of small concentrations of 94 in nature and much related information.

I have known Perlman since our undergraduate days at

UCLA. When I went to Berkeley to begin my graduate work, he also transferred to Berkeley to complete his work for a B.S. degree in chemistry. He later obtained his Ph.D. in physiology at Berkeley and after some postdoctoral work there joined my group in January and soon became a key man in this effort.

When we stepped into the street from the Chicago and Northwestern Railroad Station at Canal and Madison Streets the temperature was a cold 40° F, a rather sharp contrast to that in Berkeley when we left. Staring us in the face was the headline in the Chicago Sun, "Tokyo Fears New Bombings; Reports Fires in Four Cities" with sub-heads "Five-Hour Raid on Japanese Laid to Yanks" and "Capital, Yokohama, Kobe and Nagoya Blasted." The account went on to say, "Earlier Japanese broadcasts said attacks, which began at noon yesterday, were carried out by high-flying United States planes which swept in from several directions and started fires among the flimsy wood and paper homes of the heavily populated areas," and continued with, "Neither Washington nor General Douglas McArthur's headquarters of the United Nations forces in Australia would say that Japan has been attacked by air."

We took a cab from the station to the Shoreland Hotel (55th Street at Lake Michigan) near the University of Chicago campus. We registered here and about noon returned to the downtown area via the Illinois Central commuter line. Following lunch we attended the Chicago Theater for a Sunday matinee and saw a stage show featuring Kay Kayser's band and a movie, "Design for Scandal," with Walter Pidgeon. We had dinner, returned here to our hotel, after which I wrote to Helen, my bride-to-be.

This day marks my 30th birthday and a transition point in my life, for tomorrow I will take on the added responsibility of the 94 chemistry group at the Metallurgical Laboratory on the University of Chicago campus, the central component of the Metallurgical Project.

We went to work immediately. Other chemists were added to my group and before the end of the month we were assigned space in and moved to the area on the fourth floor of George Herbert Jones Laboratory on the University of Chicago campus (Figure 1).

Although the outline of a chemical separation process could be obtained by tracer-scale investigations, the process could not be defined with certainty until study of it was possible at the actual separation plants. Therefore, the question in the summer of 1942, was as follows: How could any separations process be tested at the concentration of plutonium that would exist several years later in the production plants when, at this time, there was not even a microgram of plutonium available? This problem was solved through an unprecedented series of experiments encompassing two major objectives. First, it was decided to attempt the production

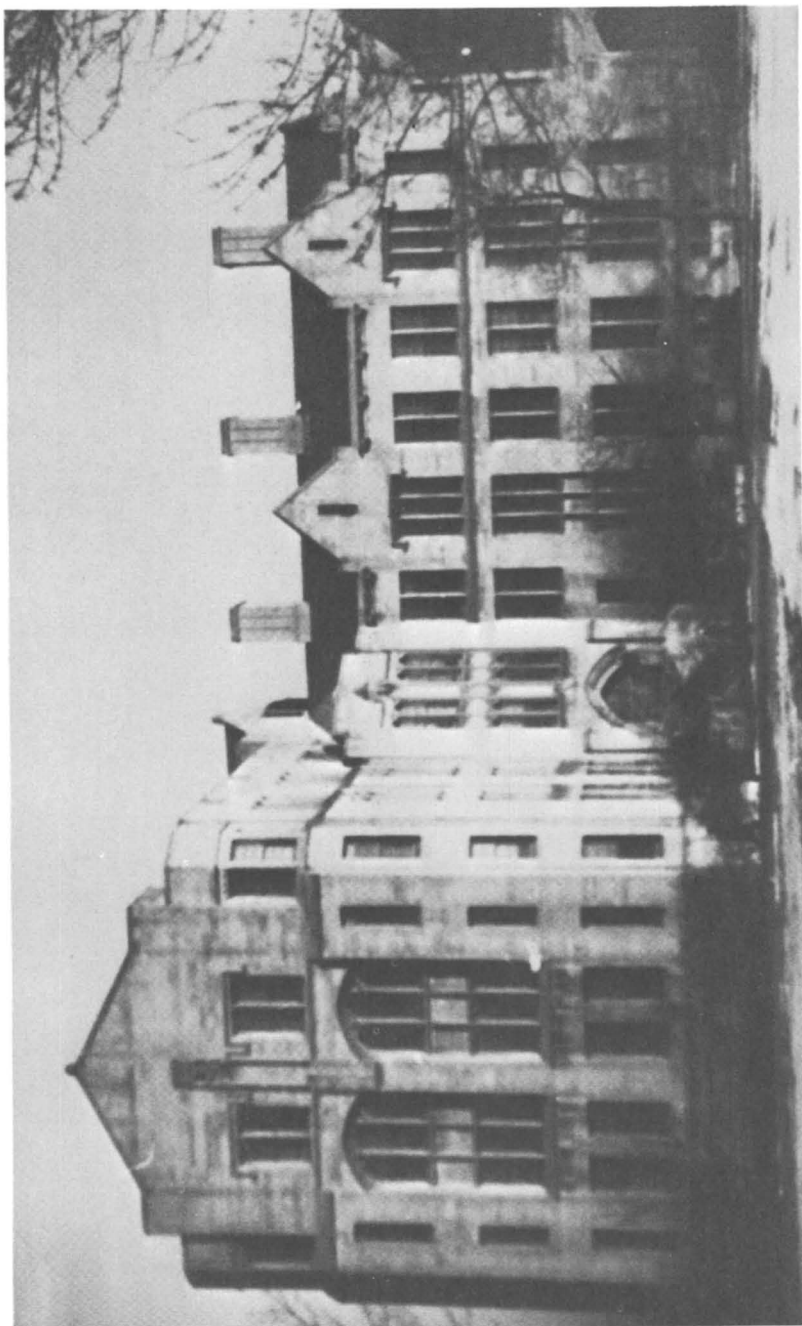


Figure 1. George Herbert Jones Laboratory. Our laboratory space on top (fourth floor) of wing at left. Rooftop work area at right end of right wing.

of an actual weighable amount of plutonium by bombarding large amounts of uranium with the neutrons from cyclotrons. It must be remembered that never before had weighable amounts of transmutation products been produced with any particle acceleration machine. Even extending this possibility to the limit, it was not anticipated that more than a few micrograms of plutonium could be produced. The second aspect of the solution of this problem involved the novel idea of attempting to work with only microgram amounts of plutonium but, at the same time, at ordinary concentrations. It was decided to undertake a program of investigation involving volumes of solutions and weighings on a scale of operations much below that of ordinary microchemistry.

We solved the first problem by bombarding large amounts of uranyl nitrate with neutrons at the cyclotrons at the University of California and Washington University; plutonium concentrates were derived from these sources through the efforts of teams of chemists who used ether extractions to separate the bulk of the uranium and an oxidation-reduction cycle with rare earth fluoride carrier to concentrate the product. I managed to convince chemists trained in the techniques of ultramicrochemistry to join us to solve the second problem--Burris B. Cunningham and Louis B. Werner of the University of California and Michael Cefola from New York University.

Isolation of Plutonium

The first isolation of plutonium was effected in room 405, Jones Laboratory, by starting with a concentrate containing the order of a microgram of plutonium in about 10 milligrams of rare earths prepared for us by Arthur C. Wahl and co-workers at Berkeley. My journal records this event as follows:

Thursday, August 20, 1942. Perhaps today was the most exciting and thrilling day I have experienced since coming to the Met Lab. Our microchemists isolated pure element 94 for the first time! This morning Cunningham and Werner set about fuming (with evolution of SO_3) yesterday's 94 solution containing about one microgram of 94^{239} , added hydrofluoric acid whereupon the reduced 94 precipitated as the fluoride, or perhaps a double fluoride, free of carrier material, from a total solution volume of 15 cubic millimeters.

This precipitate of 94, which was viewed under the microscope and which was also visible to the naked eye, did not differ visibly from the rare-earth fluorides. (Shortly after the 94 was precipitated, a considerable amount of K_2SiF_6 was observed to separate, as a result of the fact that precipitation had been performed in glass vessels. This will be avoidable in future work because we have now developed suitable fluoride-resistant micro vessels.)

From the alpha-activity remaining in the supernatant liquid after the final precipitation as a fluoride, it can be calculated, using 30,000 years as the half-life of 94^{239} , that this salt of 94 has a solubility of the order of magnitude of 10 mg of the element per liter of 6 N HF solution. This value is necessarily somewhat tentative.

By afternoon a holiday spirit prevailed in our group. Covey brought in photo floodlamps and his 35 mm camera and photographed everything in sight (Figures 2 and 3). By this time the precipitated 94 fluoride had taken on a pinkish hue. Perlman, Cefola and I, and many others including Kohman, Jaffey and their helpers, who were working in the attic laboratory on the extraction of 94^{239} from neutron-bombarded UNH, came into Room 405 to peer through the microscope at the tiny speck.

All this while, Kohman, Jaffey and their assistants were recrystallizing the UNH from the first ether extraction, which they have been doing for the last two days. In this step, the four separate solutions were taken to the roof and transferred into 14-inch evaporating dishes, set over hot plates, and heated to almost boiling. Each concentrate was kept simmering; and, as it thickened from evaporation, it was vigorously stirred. When it was evident that there remained a ratio of $6\text{H}_2\text{O}$ to one uranium nitrate by the porcelain chip test, the heating was stopped. Stirring continued, however, until the mass cooled down and hexahydrate crystals appeared. Each dish was weighed before and after emptying. The total net weight of the reconstituted UNH crystals containing the 93 and 94 is 31 lb., 10.5 oz.

The last paragraph in this extract refers to work on the separation of uranium by ether extraction as a step toward obtaining a plutonium concentrate from a large sample of neutron-irradiated uranyl nitrate.

First Weighing of Plutonium

The first weighing of a pure plutonium compound is described in the following extract from my journal:

Thursday, September 10, 1942. During the last couple of days Cunningham and Werner have been working to establish the degree of purity of the precipitate of 94 oxide that they weighed on Monday. When the 94 oxide was dissolved off the platinum weighing boat with H_2SO_4 , they oxidized with $\text{S}_2\text{O}_8^{-2} + \text{Ag}^{+2}$, followed by the addition of HF; unfortunately a precipitate appeared which must be caused by unremoved La^{+3} . This indicated that something has been holding back some La^{+3} during the LaF_3 precipitations; this

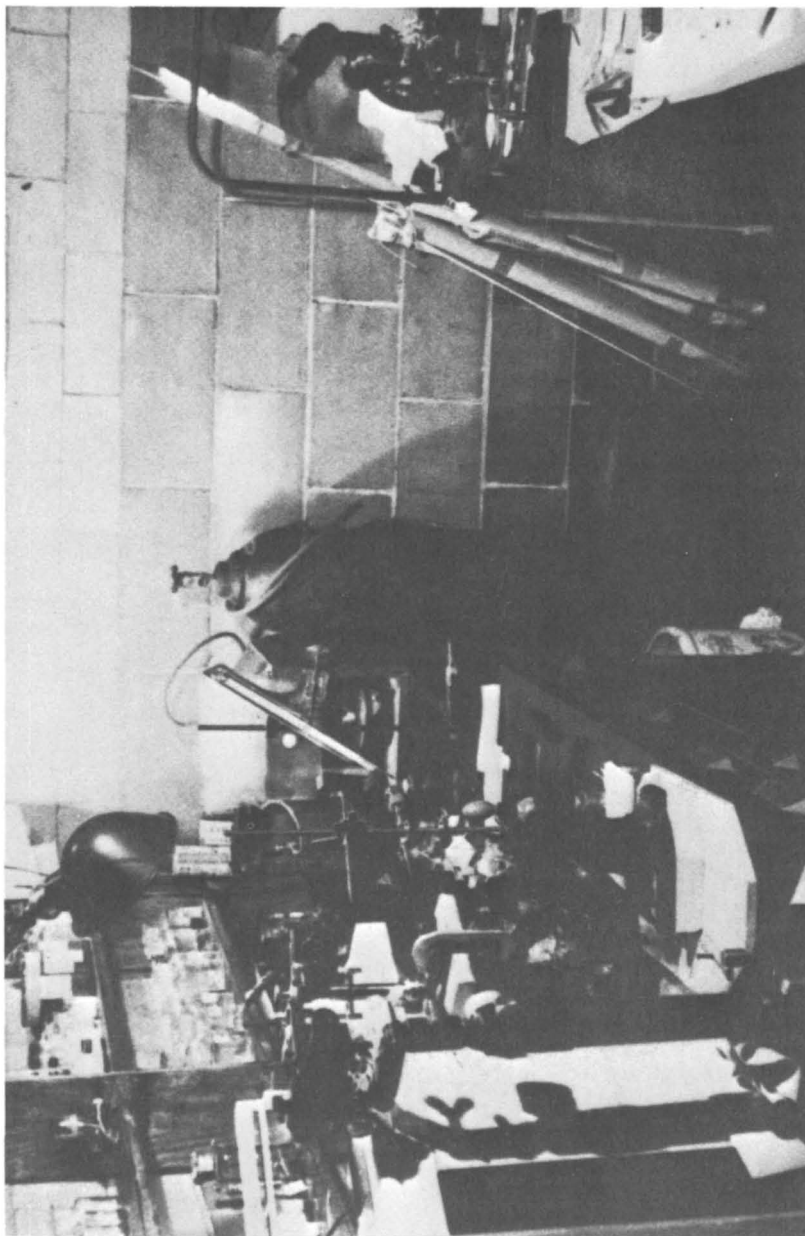


Figure 2. Room 405, Jones Laboratory, August 20, 1942.

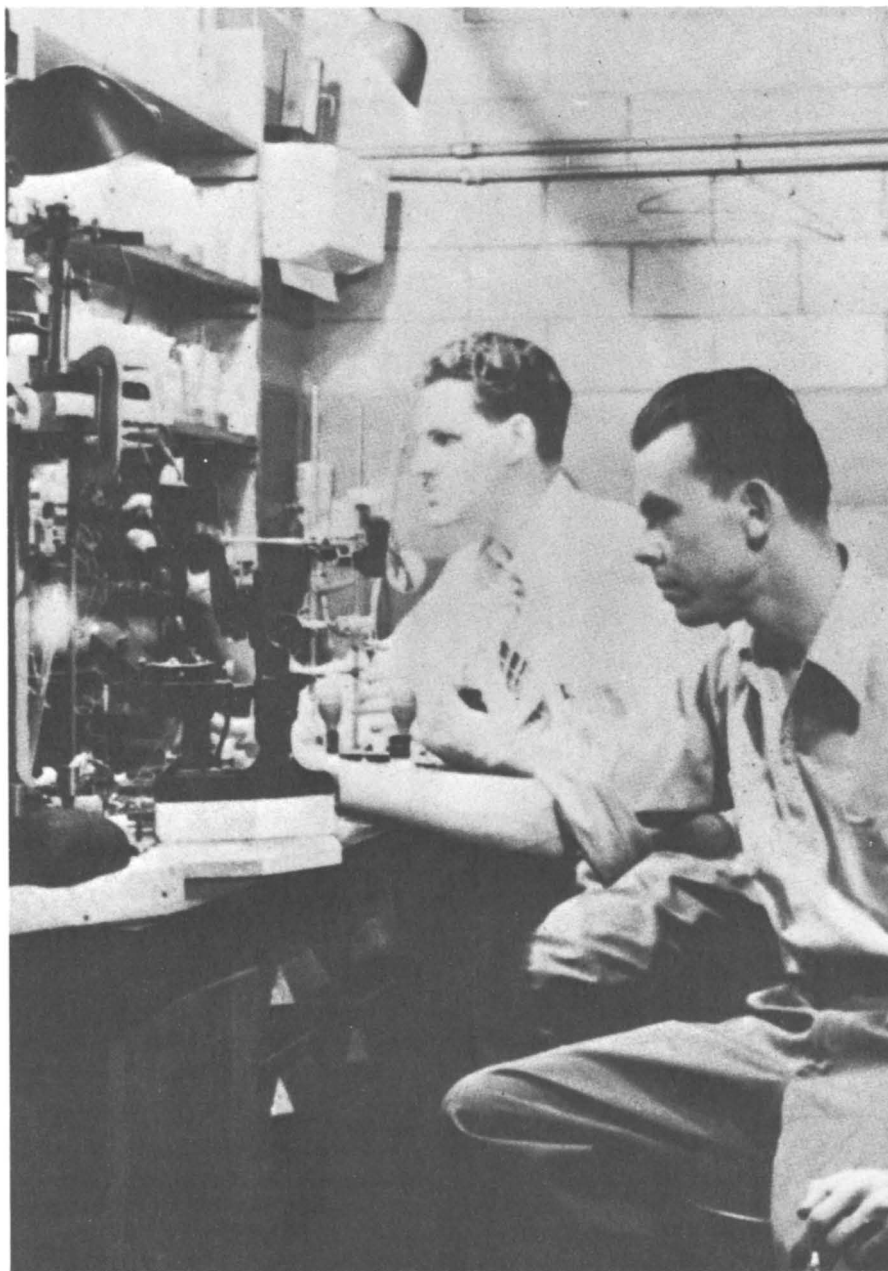


Figure 3. L. B. Werner and B. B. Cunningham, Room 405, Jones Laboratory, August 20, 1942.

led Cunningham and Werner to make an investigation of this phenomenon through the use of tracer experiments with radioactive lanthanum fission product. From these experiments they were able to conclude that the concentration of HNO_3 must be about 1 M (the concentration had been higher in their experiments) in order to insure the complete precipitation of the lanthanum fluoride from the $\text{S}_2\text{O}_8^{-2} + \text{Ag}^{+2}$ solution. They also concluded this oxidizing agent is perhaps the best to use in the oxidation-reduction cycles. Although they have been unsuccessful so far in isolating pure 94, they feel that they have now established the procedures for doing so.

Thus prepared, today Cunningham and Werner are tackling experiments with Kohman's cleaner one-fourth portion (batch no. 2) of 94^{239} isolated from the large St. Louis bombardment of UNH with cyclotron neutrons. According to Kohman's analysis, this solution contains about 8×10^6 alpha particle disintegrations per minute, corresponding to about 70 micrograms of 94^{239} , in a volume of about 18cc, together with a few inorganic (such as AgNO_3 and K_2SO_4) and other contaminants. They began by removing the 94 as the insoluble fluoride by co-precipitation with a milligram of La^{+3} . This precipitate was dissolved in a volume of 1 ml with the help of H_2SO_4 , oxidized with $\text{S}_2\text{O}_8^{-2} + \text{Ag}^{+2}$ in the presence of 1 M HNO_3 , and the La^{+3} precipitated as the fluoride by the addition of HF. After removal of the precipitate, two drops of 30% hydrogen peroxide were added to reduce the 94 (no visible precipitate appeared), 100 micrograms of La^{+3} were added as carrier, and the lanthanum fluoride precipitate incorporating the reduced 94 was removed by centrifugation. This precipitate was dissolved in 250 cubic millimeters of H_2O with the help of H_2SO_4 , and the solution again oxidized in the same manner. The La^{+3} was precipitated as the fluoride, and after its removal the 94 was reduced by fuming with H_2SO_4 in a platinum microcrucible and precipitated as the hydroxide in carrier-free form by the addition of five drops of concentrated NH_4OH . The hydroxide was packed by centrifugation in a microcone, dissolved in concentrated HNO_3 solution to which KIO_3 was added to precipitate in carrier-free form plutonous iodate. This appeared as a white bulky crystalline material. After washing with HNO_3 and KIO_3 solution, the iodate was transformed into a pale yellowish green flocculent 94 hydroxide by the addition of concentrated NH_4OH . Measurements on the alpha activity in the supernatant solutions indicated a solubility of about 0.020 grams 94 per liter for the plutonous iodate [whose formula is presumably $\text{Pu}(\text{IO}_3)_4$] and about 0.004 grams 94 per liter for the plutonous hydroxide [whose formula is presumably $\text{Pu}(\text{OH})_4 \cdot \text{XH}_2\text{O}$], using the name "plutonium" for element 94 as suggested by Wahl and me in

our Report A-135 ("The Chemical Properties of Elements 93 and 94") issued last March. The pure hydroxide was dissolved in concentrated HNO_3 and upon evaporation to dryness, the lemon-yellow crystalline plutonous nitrate [presumably of formula $\text{Pu}(\text{NO}_3)_4 \cdot \text{XH}_2\text{O}$] appeared. This was dissolved in a small volume of water resulting in a solution of pale yellow-green color. A portion of this solution was delivered onto a platinum weighing boat which had been weighed on our Salvioni balance. The sample was dried and ignited to form the plutonium oxide and the boat was again weighed. By subtraction the weight of the oxide was found to be 2.77 micrograms.

This was the first weighing of pure plutonium, in fact the first weighing of any synthetic element, making this a historic day. I intend to preserve this sample, for posterity, even though it means removing a precious quantity of plutonium from our experimental program. [This sample was later photographed by Covey (see Figure 4). It has been preserved and is now on display in the Lawrence Hall of Science on the Berkeley campus of the University of California.] I am glad that I was present to keep in touch with today's dramatic events. The alpha activity of the sample was roughly determined to be about 263,000 disintegrations per minute, which corresponds to a disintegration rate of about 110,000 alpha particle disintegrations per minute per microgram of plutonium element, assuming the formula of the oxide to be Pu_2O_5 and the molecular weight of plutonium to be 239. (We assume the counting efficiency of our "inside" alpha-particle counter, used to measure the alpha-particle emission rate of an aliquot sample, is 45%.)

We have now seen pure compounds of 94 (plutonium) and weighed a compound of plutonium, results which should give great impetus to the Met Lab's program of producing and separating gram and kilogram quantities of this treasured element.

War front reports are all depressing today. The Nazis claim they have driven to the edge of Stalingrad. At the same time the Japanese have broken through a mountain range in Guinea and are only 44 miles from Port Moresby, keystone of New Guinea defenses.

The descriptions of the first isolation and first weighing of plutonium that appeared in Metallurgical Laboratory Reports at that time have been reproduced in a Benchmark Book of reprints (Seaborg, 1978).

The work of Cunningham and Werner continued the next day:

Friday, September 11, 1942. Today Cunningham and Werner worked on the remaining plutonous nitrate solution of yesterday. They converted the plutonium to the hydroxide

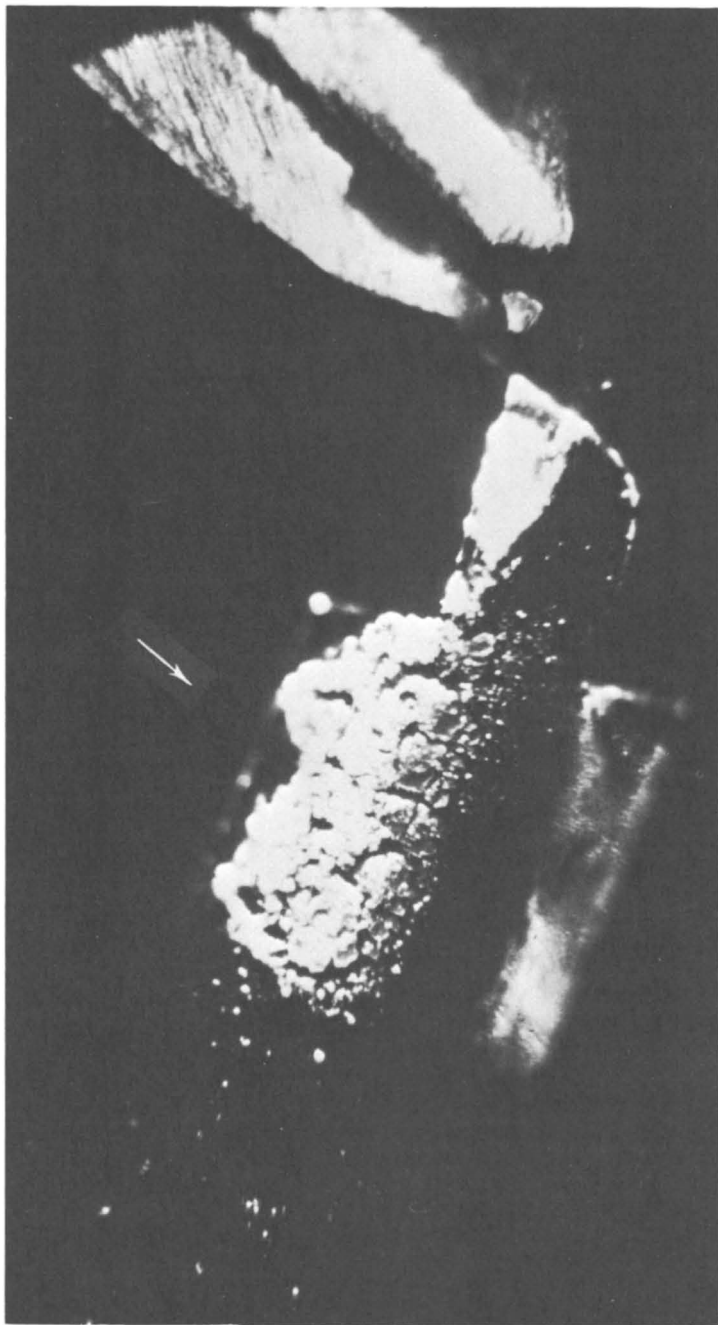


Figure 4. Plutonium oxide (2.77 micrograms) weighed on September 10, 1942. It is shown on a platinum weighing boat magnified approximately 40-fold. The Pu oxide appears as a crusty deposit (indicated by the arrow) near the end of the platinum weighing boat, which is held with forceps that grip a small handle.

by the addition of NH_4OH , dissolved this in HNO_3 and precipitated the iodate by the addition of saturated KIO_3 solution. After washing, this precipitate was converted to the hydroxide by the addition of concentrated ammonium hydroxide, washed, dissolved in acid and then reprecipitated as the hydroxide. As Cunningham and Werner's notebook states at this time, this hydroxide precipitation was made "for the purpose of displaying the pure material to certain interested persons. After this material was returned..." You can imagine how interested we were in showing off and photographing this pure compound. After this digression for the benefit of display purposes, the hydroxide was converted to the nitrate by solution in nitric acid and evaporation to dryness. An aqueous solution of this was placed on a weighed platinum boat, evaporated and ignited and found to weigh 4.45 micrograms, corresponding to 4.02 micrograms of plutonium on the more reasonable assumption that the formula of the oxide is PuO_2 . The oxide dissolved fairly readily in hot concentrated H_2SO_4 , presumably due to the formation of the stable soluble complex of Pu^{+4} with sulfate ion for which we have previous evidence. An alpha particle count on an aliquot of this indicates that the total alpha activity in the sample is 672,000 alpha disintegrations per minute. This corresponds to a specific activity of 167,000 alpha disintegrations per minute per microgram, which leads to a half-life value of $20,000 \pm 2,000$ years for 94^{239} .

Other Investigations

The group in Berkeley with W. M. Latimer also contributed to this ultramicrochemical program of investigation. During the summer of 1942, A. C. Wahl was also processing cyclotron-irradiated uranium in order to isolate pure plutonium. He isolated 200 micrograms of chemically pure plutonium in 92 per cent yield from 45 kilograms of uranium that had been irradiated for two months with neutrons from the Berkeley 60-inch cyclotron. He employed lanthanum fluoride precipitations from reduced and oxidized solutions and measured yields and decontamination factors at every step, collecting data which proved very valuable in evaluation of this separations process, then the only practical method for isolation of plutonium. The chemical procedure was started in July, but progress was slow because of the care exercised in evaluation of the separations process, and a pure compound of plutonium (IV) hydroxide, was not isolated until September 29, 1942. Wahl was very pleased to show the 0.2 milligram plutonium sample, easily visible to the naked eye, to E. O. Lawrence, whose cyclotron had produced the plutonium. This plutonium was used in an ultramicrochemical program of investigation at Berkeley. Among other accomplishments, the Berkeley chemists were able to

establish in 1943 that the oxidation number of the highest state is VI (Connick and co-workers, 1949).

Some continuing ultramicrochemical investigations of Cunningham and Werner are described in my journal.

Monday, September 28, 1942. Upon returning to Jones Laboratory this morning, I found that my group has been extremely active all week during my absence.

Cunningham, Werner, and Cefola have spent the last two weeks doing experiments and recovering the 94 from the various fractions and residues following their experiments using 94 from Perlman's, Kohman's, and Jaffey's batches. Cunningham and Werner have prepared a "stock solution" of pure 94 nitrate containing about 2 γ (micrograms) of 94 per λ (cubic millimeter) of solution. This they plan to use to test the solubilities of a number of 94 compounds to give information that might be useful in developing a procedure for the separation of 94 from uranium and fission products in neutron-bombarded uranium from a pile. They have perfected methods for the determination of solubility of 94 compounds.

In their experiments a small amount of 94 nitrate (containing approximately 0.1 γ 94) is placed in 2 λ of solution, the appropriate precipitating agent added, the mixture centrifuged, the supernatant liquid removed and replaced by about 5 λ of the medium in which the solubility of the compound is to be measured. The two phases are mixed by vigorous stirring, allowed to stand overnight or longer at room temperature ($25^{\circ}\text{C} \pm 5^{\circ}\text{C}$). Then a measured volume of the supernatant is withdrawn and its alpha activity determined. Solubilities of 94 (plutonium) are calculated in terms of the concentration of the element, assuming the specific activity to be 167,000 alpha disintegrations per microgram of plutonium per minute (half-life of 20,000 years).

On Saturday, upon measuring the supernatants of the various precipitations performed the day before, Cunningham and Werner found the following solubilities:

<u>Precipitant</u>	<u>Compound</u>	<u>Medium</u>	<u>Solubility (mg Pu/liter)</u>
KIO ₃	plutonous iodate	sat'd KIO ₃ soln	2.1
"	" "	1/2-sat'd KIO ₃	1.8
"	" "	sat'd KIO ₃	4.8
"	" "	3 M HNO ₃	
"	" "	sat'd KIO ₃	6.2
		6 M HNO ₃	
HF	plutonous fluoride	H ₂ O	10.8
		3 M HF	12.3

<u>Precipitant</u>	<u>Compound</u>	<u>Medium</u>	<u>Solubility (mg Pu/liter)</u>
HF	plutinous fluoroide	6 M HF	44.8
NH ₄ OH	plutinous hydroxide	H ₂ O	1.8
"	"	conc. NH ₄ OH	0.24

Also on Saturday Cunningham and Werner received Goldschmidt's one-fourth portion of 94^{239} (batch No. 4) from the large St. Louis neutron bombardment of uranium. This consists of about 8×10^6 alpha-particle disintegrations per minute, corresponding to about 70 micrograms of 94^{239} in a volume of 25 cc. To this they added about 3×10^6 alpha-particle disintegrations per minute that they have recovered from the residues of Kohman's and Jaffey's portion during the last couple of weeks.

An important experiment was the establishment of the +4 oxidation state of plutonium:

Tuesday, October 13, 1942. Cunningham and Werner prepared a sample of plutonium iodate from a small portion of their stock plutonium nitrate solution by the addition of excess HIO₃ in 4 M HNO₃. The precipitate was removed by centrifugation, washed with H₂O, transferred to a platinum weighing boat, dried for four hours at 100°C, then weighed with the Salvioni balance. The precipitate was then dissolved and the dried platinum boat was weighed again giving a weight of 1.70 micrograms for the plutonium iodate. The alpha-particle activity of the dissolved iodate was determined and found to be 73,000 alpha disintegrations per minute. Using a specific activity for plutonium of 165,000 alpha disintegrations per minute per microgram, this corresponds to 0.44 micrograms of plutonium element. From this we can calculate the mole ratio of iodate to plutonium to be 3.89, pointing strongly to a valence charge of +4 for the plutonium in plutinous iodate. This is the first instance in which the formula for a plutonium compound has been established. The formula, Pu(IO₃)₄, agrees with our expectations.

Move to New Chemistry Building

By October 1942, my research group had grown to about 25 members, completely saturating the laboratory space that had been allotted to us on the fourth floor of George Herbert Jones Laboratory (Figure 5). In anticipation of this, construction of a new building was nearing completion to house my group and other chemists on the Plutonium Project, at a site on Ingleside Avenue (between 56th St. and 57th St.) at the edge of the University of Chicago campus. We moved into this building--the New Chemistry

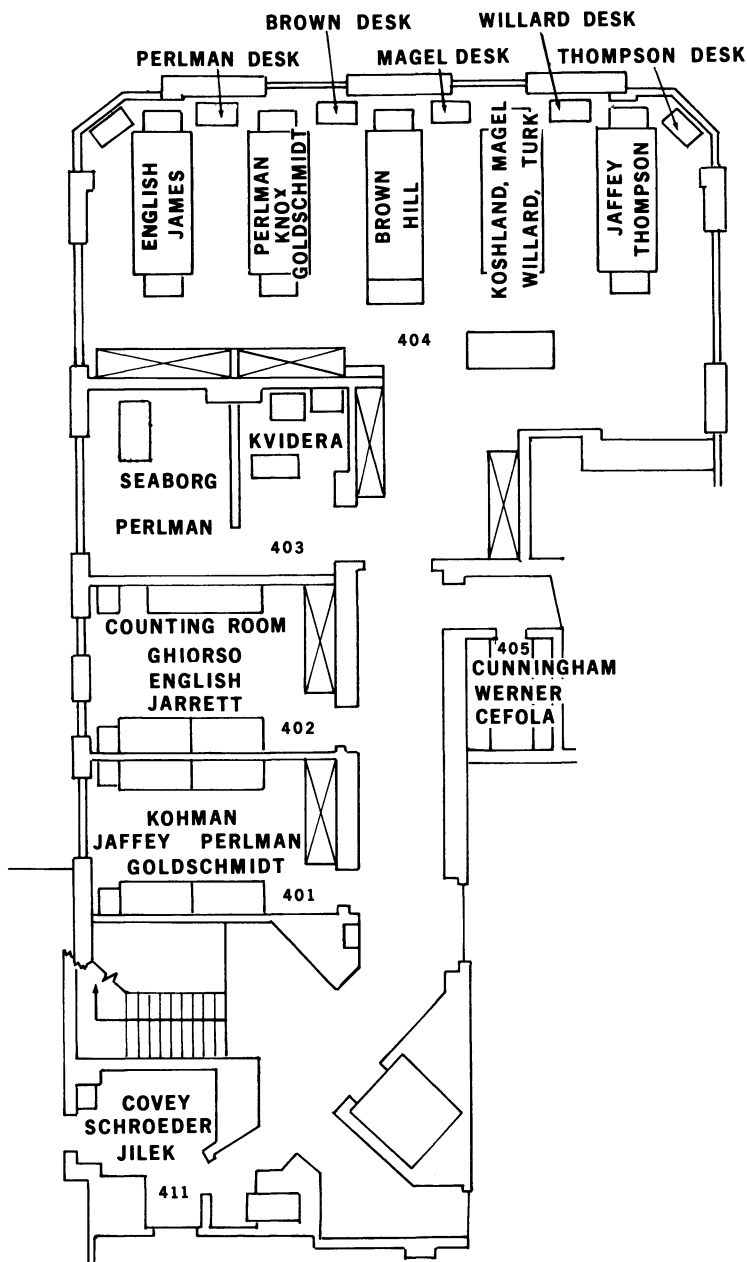


Figure 5. Space occupied by individual members of our group, early October 1942, on fourth floor of Jones Laboratory.

Building--during December and by the following April (1943) our group (now called Section C-I) had doubled in number to about 50 people (Figure 6).

The Bismuth Phosphate Process

Stanley G. Thompson joined my group on October 1, 1942 and it fell to his lot to discover the process that was chosen for use at Clinton Laboratories (in Tennessee) and the Hanford Engineer Works (in the state of Washington) for the separation of plutonium from uranium and the immense intensity of radioactive fission products with which it was produced in the nuclear chain reactors. Again I turn to my journal to tell the story:

Saturday, December 19, 1942. Today Thompson tested the use of bismuth phosphate as a carrier for 94 in its reduced state with rather encouraging results. Upon precipitating relatively high concentrations of bismuth (15-25 mg per 10 cc) as bismuth phosphate from 20% UNH solution, he finds the 94 to be carried to the extent of more than 85%. The bismuth phosphate precipitates are slow in forming and require digestion at temperatures of the order of 75°C . He finds that the bismuth phosphate precipitate is very dense and crystalline, which are desirable properties, and dissolves readily in HCl.

In view of Thompson's results on the carrying of Pu^{+4} by bismuth phosphate, Cunningham and Werner made an immediate test today to see whether it is carried at a ratio of $\text{Bi}^{+3}:\text{Pu}^{+4}$ of about 100:1. Their results indicate that under conditions similar to those of Thompson's experiment, the Pu^{+4} is carried to the extent of 98%. This was fast work and illustrates the pace at which our group is now working. They also made a test of the carrying of Pu^{+4} by hafnium phosphate at a ratio of Hf:Pu of 100:1 and they find that about 90% of the Pu is carried.

The reason for the ultramicrochemical test was to establish whether the bismuth phosphate would carry the plutonium at the concentrations that would exist at the Hanford extraction plant. This test was necessary because it did not seem logical that tri-positive bismuth should be so efficient in carrying tetrapositive plutonium. In subsequent months there was much skepticism on this point and the ultramicrochemists were forced to make repeated tests to prove this point. Thompson soon showed that $\text{Pu}(\text{VI})$ was not carried by bismuth phosphate, thus establishing that an oxidation-reduction cycle would be feasible. All the various parts of the bismuth-phosphate oxidation-reduction procedure, bulk reduction via cross-over to a rare earth fluoride oxidation-reduction step and final isolation by precipitation of plutonium (IV) peroxide were tested at the Hanford concentrations of

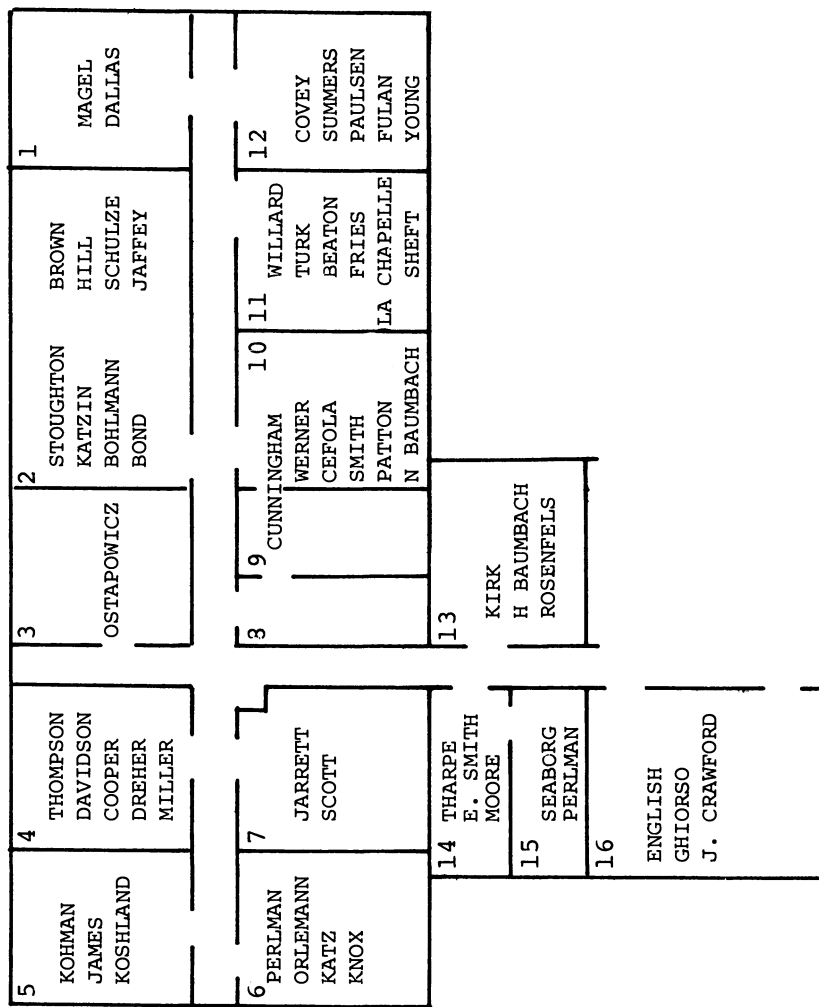


Figure 6. Room assignments of members of Section C-I, late April 1943. in New Chemistry Building.

plutonium in careful and crucial experiments performed by Cunningham, Werner, Perlman, Daniel R. Miller, and others. Without the possibility of these tests early in 1943, I believe that this process, which went into production at Hanford in the state of Washington, and which performed exceedingly well, would not have been chosen. Several alternative processes, including solvent extraction, volatility, adsorption and other precipitation methods were also under investigation, but these either were beset with problems or could very well have delayed the date of obtaining the final product plutonium in the required quantities.

Discovery of Other Fundamental Chemical Properties

The first definite production of plutonium metal was made in November, 1943 by Baumbach and coworkers (1958). Approximately 35 micrograms of PuF_4 in a small thoria crucible in a high vacuum was reacted with barium metal at 1400°C to yield plutonium metal. The metal was found to have a silvery lustre, a density of about 16 grams per cubic centimeter and it rapidly absorbed hydrogen at about 210°C to form a black powder subsequently identified as PuH_3 (a proof that metal had been produced).

The successful operation of the reactor and plutonium extraction plant at Oak Ridge, Tennessee led to the availability of first milligram, and then gram, amounts of plutonium starting early in 1944. The availability of milligram amounts of plutonium led to the immediate discovery of the III oxidation state. As mentioned above, early tracer work at the University of California in 1941 had established the existence of a lower oxidation state (IV and/or III state) and a higher state (VI and/or higher state), and the ultramicrochemical work late in 1942 and in 1943 had defined the existence of the IV and VI states. The III oxidation state was discovered early in 1944 by Connick and coworkers (1949), who actually worked with about 0.25 milligram of cyclotron-produced plutonium, at the University of California, Berkeley, and, essentially simultaneously, by Hindman and coworkers (1949) at the Metallurgical Laboratory and Mastick and Wahl (1944) at the Los Alamos Laboratory; the latter two groups utilized the milligram amounts of plutonium made available at the time through the operation of the reactor and chemical separation plant at the Clinton Laboratories in Tennessee. The existence of the V oxidation state was established in the summer of 1944, through the use of plutonium obtained from the Clinton Laboratories, by Connick and coworkers (1949), at the University of California, Berkeley.

Although a number of solid compounds of plutonium were synthesized by ultramicrochemical techniques during our first year and a half at the Metallurgical Laboratory, it was not until November, 1943 that a positive identification of a crystal structure was made. W. H. Zachariasen joined the project in the fall of 1943 and very soon began to make definitive identifi-

cations of compounds on the microgram scale using the x-ray diffraction technique. The first positive result was obtained on plutonium dioxide:

Monday, November 8, 1943. In the course of their attempts to produce powdered plutonium metal suitable for study by the x-ray diffraction method, Kirk and Baumbach submitted a sample that turned out to be plutonium dioxide weighing 10 micrograms which they gave to Zachariasen last Wednesday; he succeeded in obtaining a satisfactory x-ray diffraction pattern, enabling him to determine its crystal structure. This is a tremendous accomplishment! This probably means that it is possible, even on a microgram scale, to obtain the structure of numerous plutonium compounds. This would be a tremendous boost to our program. Consider the following results. The oxide has the fluorite structure. There are four molecules in the unit cube which has an edge equal to $5.370 \pm 0.005 \text{ \AA}$. The density of the oxide is 11.54 gm/cm^3 . For comparison, the edge of the unit cube of thorium oxide and uranium oxide is 5.58 and 5.47 \AA , respectively. All of this information was obtained with 10 micrograms!

The ingenuity and experimental skill displayed by the microchemists in devising methods for conducting dry-chemical reactions in tiny, thin-walled capillary tubes, and the astonishing ability of Zachariasen in securing and interpreting x-ray diffraction patterns on products so prepared, led to the identification of a large number of plutonium compounds. Although the first such work was performed with the small (microgram) quantities of cyclotron-produced plutonium, more progress was made when the larger amounts became available from the operation of the pilot production plant at Clinton Laboratories in Tennessee (first milligram and then gram amounts) early in 1944, and when the still larger amounts became available from the production plant at the Hanford Engineer Works in the state of Washington early in 1945. During this period all of the binary halides as well as the oxides and oxyhalides and several other compounds of plutonium were synthesized and identified. It was also possible to obtain basic thermodynamic data on a number of these compounds by direct thermochemical methods or by observations of the temperature coefficients of equilibrium constants or, as rough estimates, by noting the presence or absence of reactions under chosen experimental conditions to establish lower or upper limits of stability.

A good deal was learned about plutonium metal, including the determination of its density by both capillary displacement and x-ray diffraction methods, its melting point and vapor pressure.

Much was also learned at the Metallurgical Laboratory about the solution chemistry of plutonium during these first few years of investigation. This included elucidation of the ionic species present in aqueous solutions of different acids and determination

of the nature of various complex ions. The group at Berkeley made notable contributions to measuring the oxidation potentials relating the various oxidation states and toward understanding the kinetics of reactions involving these states. The group at Los Alamos also added much to this knowledge, especially about methods for production of the metallic state and the properties of the metal.

Thus, a large amount of information about the chemical properties of plutonium, working with macroscopic or weighable amounts, was obtained during those first few years, i.e., 1942 to 1945. Until the fall of 1943, cyclotron bombardments were the sole source of plutonium and a total of about 2000 micrograms, or 2 milligrams, were prepared. When the larger amounts became available from Clinton Laboratories early in 1944 and still larger amounts from the Hanford Engineer Works early in 1945, the amounts available to the chemists were still relatively small and the investigations continued on the microchemical scale.

Subsequent Investigations

Investigations of the chemical properties of plutonium have continued in many laboratories throughout the world as it has become available. This has led to the situation where the chemistry of this relative newcomer is as well understood as is that of most of the well-studied elements. The four oxidation states of plutonium--III, IV, V, and VI--lead to a chemistry which is as complex as that of any other element. It is unique among the elements in that these four oxidation states can all exist simultaneously in aqueous solution at appreciable concentration. As a metal, also, its properties are unique. Metallic plutonium has six allotropic forms, in the temperature range from room temperature to its melting point (640°C), and some of these have properties not found in any other known metal.

This account of the beginnings and early days of the forty years of plutonium chemistry should serve as a background for the following papers which illuminate many of the accomplishments of the intervening years and emphasize the high level of the present status of information on the chemical properties of this remarkable synthetic element.

Acknowledgments

This work was supported by the Director, Office of Energy Research, Division of Nuclear Physics of the Office of High Energy and Nuclear Physics of the U.S. Department of Energy under Contract DE-AC03-76SF00098.

Literature Cited

1. Connick, R. E.; Gofman, J. W., McVey, W. H.; and Sheline, G. E.; 1949. Determination of the oxidation number of plutonium(VI). Seaborg, G. T.; Katz, J. J.; and Manning, W. M. (Ed.), "The Transuranium Elements: Research Papers, Part I." McGraw-Hill Book Co., Inc., New York. Paper 3.140, pp. 336-344.
2. Connick, R. E., Kasha, M.; McVey, W. H.; and Sheline, G. E.; 1949. The pentapositive oxidation state of plutonium. Seaborg, G. T.; Katz, J. J.; and Manning, W. M. (Ed.), "The Transuranium Elements: Research Papers, Part I." McGraw-Hill Book Co., Inc., New York. Paper 3.15 pp. 227-240.
3. Connick, R. E.; McVey, W. H.; and Sheline, G. E.; 1949. The tri-positive oxidation state of plutonium. Seaborg, G. T.; Katz, J. J.; and Manning, W. M. (Ed.), "The Transuranium Elements: Research Papers, Part I." McGraw-Hill Book Co., Inc., New York. Paper 3.12, pp. 175-179.
4. Fried, S.; Westrum, E. F., Jr.; Baumbach, H. L.; and Kirk, P. L.; 1958. The microscale preparation and micrometallurgy of plutonium metal. J. Inorg. Nucl. Chem. 5, 182-189.
5. Hindman, J. C.; Kraus, K. A.; Howland, J. J., Jr.; and Cunningham, B. B.; 1949. Determination of the tripositive oxidation state of plutonium and notes on the spectrophotometry of plutonium and uranium. Seaborg, G. T.; Katz, J. J.; and Manning, W. M., (Ed.), "The Transuranium Elements: Research Papers Part I." McGraw-Hill Book Co., Inc., New York. Paper 3.2, pp. 121-132.
6. Mastick, D. F.; and Wahl, A. C.; 1944. Los Alamos Report, LA-63, Feb. 22, 1944.
7. Seaborg, G. T.; "The Transuranium Elements: Products of Modern Alchemy," Dowden, Hutchinson and Ross, Inc., Stroudsburg, Pennsylvania, 1978, 488 pp.

RECEIVED January 19, 1983

Magnetic Properties of Organometallic and Coordination Compounds of Plutonium

B. KANELLAKOPOULOS and R. KLENZE

Kernforschungszentrum Karlsruhe, Institut für Heisse Chemie,
Postfach 3640, D-7500 Karlsruhe, Federal Republic of Germany

The magnetic properties of Pu compounds in different oxidation states are reviewed. New measurements on $\text{Pu}(\text{C}_8\text{H}_8)_2$, PuF_4 , $[(\text{C}_2\text{H}_5)_4\text{N}]_2\text{PuCl}_6$, and $[(\text{C}_2\text{H}_5)_4\text{N}]_4\text{Pu}(\text{NCS})_8$ are presented. The interpretation of the data is based on intermediate, j-j mixed crystal field states and orbital reduction due to covalency. Especially in the case of the organometallic compounds a large orbital reduction is found.

The known oxidation states of plutonium present a $5f^q$ -series, starting from f^1 [Pu(VII)] up to f^5 [Pu(III)]. But contrary to the $4f^q$ - and $5f^q$ series across the period table, where the properties can be described by some smooth varying parameters, changing of the oxidation states influences the electronic properties drastically. Due to the large range of available oxidation states plutonium represents a favorable element among the actinides to study these effects.

The interpretation of the electronic and especially of the magnetic properties of the actinides is much more complicated than in the lanthanides for the following reasons:

1. Mixing of LS-states by spin orbit coupling will be stronger with an increasing number of f-electrons. As a consequence, intermediate values of Landé g factor and reduced crystal field matrix elements must be used.
2. Crystal field effects are of the order of the free ion interaction; thus they cannot be treated as a small perturbation as in the lanthanides. Whereas the crystal field splitting in the oxidation state +3 is comparable to that for the lanthanides, it is significantly increased in the progression to higher oxidation states. On the other hand the energy gap between ground state and excited multiplets decreases with rising number of f-electrons. Thus the effect of j-j mixing is important for all oxidation states of plutonium.

0097-6156/83/0216-0025\$06.00/0
© 1983 American Chemical Society

3. Covalency directly influences the magnetic properties by lowering the Landé g value. It is expected to be larger for the higher oxidation states but the influence on reducing the g value is much more pronounced for the f^4 (Pu(IV))- and f^5 (Pu(III))-systems with low g values. This is seen in Table I, where the reduction of $g^2(J)$ due to Steven's overlap reduction factor k is given assuming $k=0.90$.

Pu(VII) $5f^1$

Magnetic measurements of Li_5PuO_6 in the temperature range from 4.2 to 300 K were interpreted by taking into account the optical spectrum of $[\text{PuO}_4(\text{OH})_2]^{3-}$ solution and using a model similar to that of Pryce and Eisenstein including a tetragonal distortion of the O_h -symmetry (1,2). The following results were obtained: spin-orbit coupling constant $\zeta = 1900 \text{ cm}^{-1}$, which is not much higher than for other f^1 -systems with lower oxidation states of the central ion; $\Delta = 8967$ and $\Theta = 4201 \text{ cm}^{-1}$, corresponding to the cubic field parameters $A_4^0 \langle r^4 \rangle = 2862$, $A_6^0 \langle r^6 \rangle = -129 \text{ cm}^{-1}$; a tetragonal distortion $\delta = -625 \text{ cm}^{-1}$ and orbital reduction factor $k = 0.8$ (Γ_5) and $k' = 1.0$ (Γ_4). To account for the high temperature magnetism an empirical correction of 120×10^{-6} emu for the temperature independent paramagnetism (TIP) must be included.

The $1/\chi$ -vs- T plot is shown in Fig. 1. It should be noted that the same set of parameters fits all six expected transitions of the optical spectrum. For Pu(VII) this is the only known magnetic measurement in the temperature range between 4 and 300 K.

Pu(VI) $5f^2$

The magnetic susceptibility of $\text{Na}[\text{PuO}_2(\text{CH}_3\text{COO})_3]$ was measured by Dawson between 90 and 333 K (3). The resulting magnetic moment, $\mu_{\text{eff}}^2 = 8.0 \mu_B^2$, is temperature independent and corresponds to $\mu_{\text{eff}}^2 = 8.70 \mu_B^2$, which is calculated from EPR measurements on a diluted sample (4). The interpretation was based on a strong axial field of the PuO_2^{2+} ion.

The poor data on PuF_6 are probably best interpreted as a very small TIP of about 150×10^{-6} emu indicating a singlet ground state and a large crystal field splitting of the octahedral compound (5).

Pu(V) $5f^3$

No magnetic measurements for compounds of pentavalent plutonium have been reported so far.

Pu(IV) $5f^4$

The most information on the electronic structure of Pu ions is available for Pu(IV) compounds. As far as our own results are

Table I. g -values and μ_{eff}^2 of ground states in Russell-Saunders and intermediate coupling for different configurations.

El. conf.	f^1	f^2	f^3	f^4	f^5
Ox. state	VII	VI	V	IV	III
R-S term	$2F_{5/2}$	$3H_4$	$4I_{9/2}$	$5I_4$	$6H_{5/2}$
g_J	6/7	4/5	8/11	3/5	2/7
μ_{eff}^2 (μ_B^2)	6.429	12.800	13.091	7.200	0.714
interm. coupling	100% $2F_{5/2}$	84% $3H_4$	78% $4I_{9/2}$	78% $5I_4$	66% $6H_{5/2}$
g_J	0.8571	0.8358	0.7720	0.6508	0.4211
μ_{eff}^2 (μ_B^2)	6.429	13.971	14.751	8.471	1.5516
q_{red}^2	0.751	0.741	0.707	0.628	0.391
$q_{\text{red}}^2 = g_J(k=0.9)/g_J(k=1.0)$.					

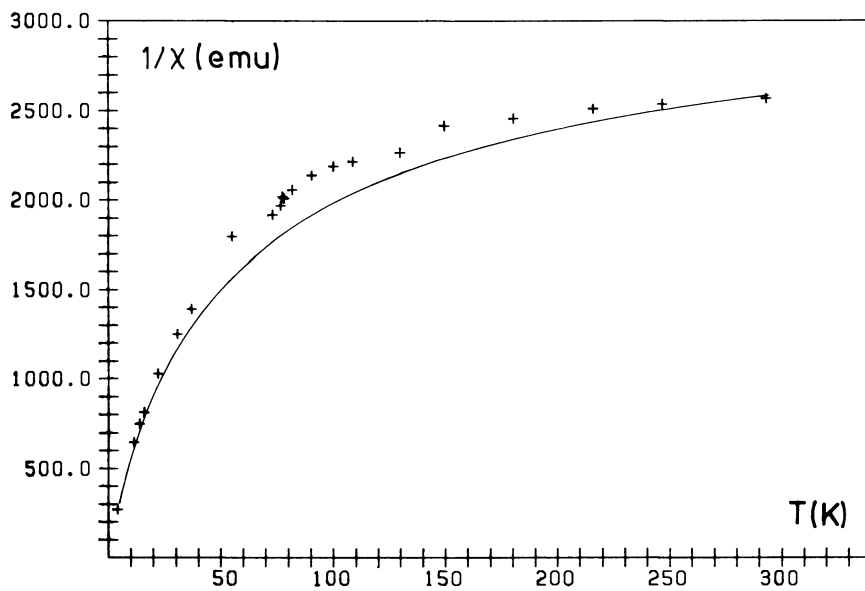


Figure 1. Reciprocal molar susceptibility vs. temperature of Li_5PuO_6 .

presented we used for our calculations a free ion parameter set extrapolated from spectroscopic studies on the octothiocyanato-complexes of uranium and neptunium (6). It is similar to other parameter sets determined for Pu(IV) but includes the Tree's parameters α, β, γ , with ($E_1 = 3592$, $E_2 = 17.95$, $E_3 = 319.8$, $\zeta = 2420$, $\alpha = 20$, $\beta = -500$, $\gamma = 1200 \text{ cm}^{-1}$). j-j mixing was included for the lowest 12 J-states corresponding to $17,000 \text{ cm}^{-1}$, which is sufficient to describe the ground state properties.

PuO₂

In order to demonstrate the importance of simultaneously diagonalizing the free ion and crystal field interactions (j-j mixing) we may focus on PuO₂. The magnetism was measured by Raphael et al. (7). Up to 1000 K a pure TIP of $536 \times 10^{-6} \text{ emu}$ was found without any indication of population of higher states. Applying the Lee, Leask, Wolf diagram (8) for cubic coordination, a Γ_1 state was predicted as ground state. The energy gap to the first Γ_4 was calculated to be 2290 cm^{-1} from the magnetic interaction between these levels. Thus it is evident that j-j mixing with higher states cannot be neglected. It is interesting that this large energy gap is not easy to produce. The j-j mixing will compensate the splitting for larger crystal field parameters, and for ratios $A_6^0 \langle r^6 \rangle / A_4^0 \langle r^4 \rangle < 0.3$ the maximum splitting is lower than 1000 cm^{-1} . This can be rationalized by the fact that in the low energy region of $5f^4$ there is more crowding of Γ_4 than of Γ_1 levels, thus a stronger repulsion of Γ_4 levels yields a Γ_1 - Γ_4 crossing. To reproduce the observed TIP the crystal field parameters must be of the order $A_4^0 \langle r^4 \rangle < -4,000$ and $A_6^0 \langle r^6 \rangle \approx 2,600$ - $3,500 \text{ cm}^{-1}$. It should be emphasized that the ratio of the parameters is larger than in any other known actinide compound. For comparison the estimated values for UO₂ (9) are: $A_4^0 \langle r^4 \rangle = -3,300$ and $A_6^0 \langle r^6 \rangle = 200 \text{ cm}^{-1}$.

PuF₄

Magnetic measurements of PuF₄ between 4.2 and 300 K are consistent at high temperatures with older measurements (10-12). The large temperature dependent diamagnetism observed earlier was not found. Up to 100 K the susceptibility is nearly temperature independent with a value of $\chi_{\text{TIP}} \approx 2940 \times 10^{-6} \text{ emu}$. The Curie-Weiss behavior near room temperature indicates population of a higher first excited state. The structure of PuF₄ is isomorphic with that of UF₄ (13), where two different sets of actinide atoms are 8-fold coordinated by a distorted antiprism.

If we apply the Mulak model of a pseudoaxial, D_{4d} symmetry (14), using a ratio $c/a = 0.95$, we find indeed a singlet ground state $|0\rangle$ and a first excited state $|\pm 1\rangle$ causing the observed TIP. Deviation from D_{4d} symmetry will affect to first order only the excited degenerate states and will not alter this simple

model. Using the parameters $A_2^0 \langle r^2 \rangle = -63$, $A_4^0 \langle r^4 \rangle = -1290$, and $A_6^0 \langle r^6 \rangle = 564 \text{ cm}^{-1}$, calculated from a point charge model and scaled down to fit the magnetic properties, we calculate the following energy levels:

0>:	0 cm^{-1}
±1>:	575
±4>:	1184
±3>:	1241
±2>:	2373

As seen from Fig. 2(a) the energy gap between |0> and |±1> is too large to allow the observed population of the first excited state. Thus we assume some orbital reduction to fit the observed behavior. The values found are $k = 0.91$ and $E(|±1>) = 424 \text{ cm}^{-1}$ and yield the curve (b).

$[(\text{C}_2\text{H}_5)_4\text{N}]_2\text{PuCl}_6$

The magnetic properties of some R_2PuCl_6 complexes ($\text{R}=(\text{CH}_3)_4\text{N}$, $(\text{C}_2\text{H}_5)_4\text{N}$, Cs) were measured between 3 and 50 K by Karraker (15). The interpretation was based on a Γ_1 or alternatively a split Γ_5 ground state. In both cases a small total splitting of the $^5\text{I}_4$ state was proposed, contradictory to the small magnetic moment found at room temperature (11,16) and to the extrapolated values found for similar complexes of other actinides. In Fig. 3 our measurement of $[(\text{C}_2\text{H}_5)_4\text{N}]_2\text{PuCl}_6$ is shown. We assume that the only state involved is the Γ_5 and that a distortion of the cubic symmetry will produce a splitting of about 200 cm^{-1} . The low temperature magnetism is due to a further splitting of about 18 cm^{-1} . Details of the calculation depend of course on the nature of the distortion. But it was found that the general picture will not be changed for different kinds of distortions.

As the room temperature value of the magnetic moment is considerably lower than the expected value for a Γ_5 state ($\mu_{\text{eff}}^2 \approx 5.45 \mu_B^2$), considerable lowering of the g value must be expected.

$[(\text{C}_2\text{H}_5\text{N})_4\text{Pu}(\text{NCS})_8]$

That magnetic measurements often raise more problems than they solve, is demonstrated for the indicated compound. We prepared a series of $[(\text{C}_2\text{H}_5\text{N})_4\text{An}(\text{NSC})_8]$ compounds ($\text{An} = \text{Th}, \text{U}, \text{Np}, \text{Pu}$) with cubic coordination of the actinide ion. We derived a consistent interpretation of the magnetic and optical properties of the uranium and the neptunium compounds (6). In the case of Pu we expect an isolated Γ_1 ground state and a first excited state at about 728 cm^{-1} . To our surprise we found a magnetic ground state much more pronounced than in the case of the hexachloro-complex, Fig. 4.

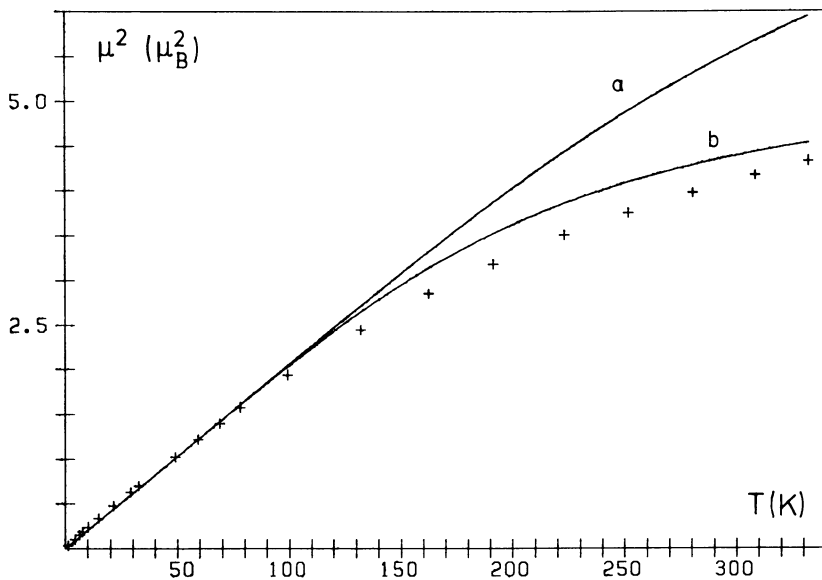


Figure 2. μ_{eff}^2 vs. temperature diagram of PuF_4 .

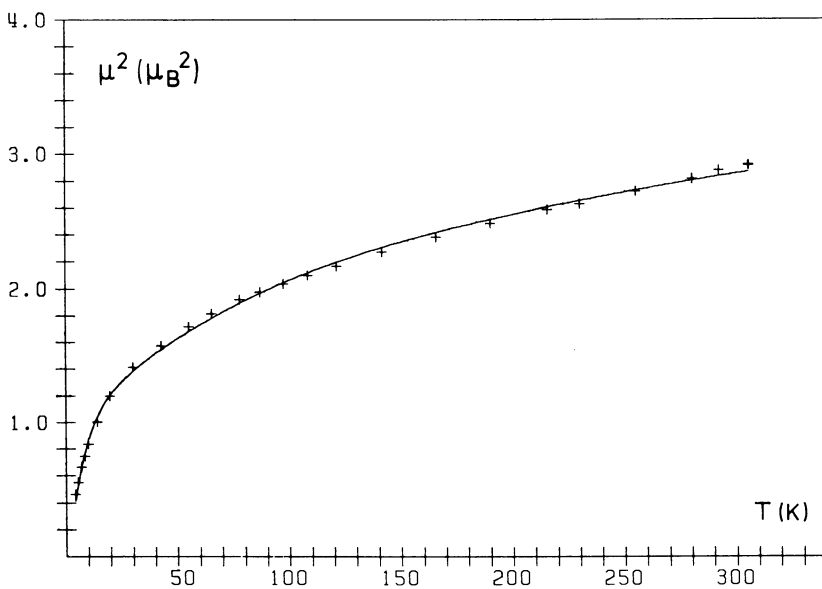


Figure 3. μ_{eff}^2 vs. temperature diagram of $[(\text{C}_2\text{H}_5)_4\text{N}]_2\text{PuCl}_6$.

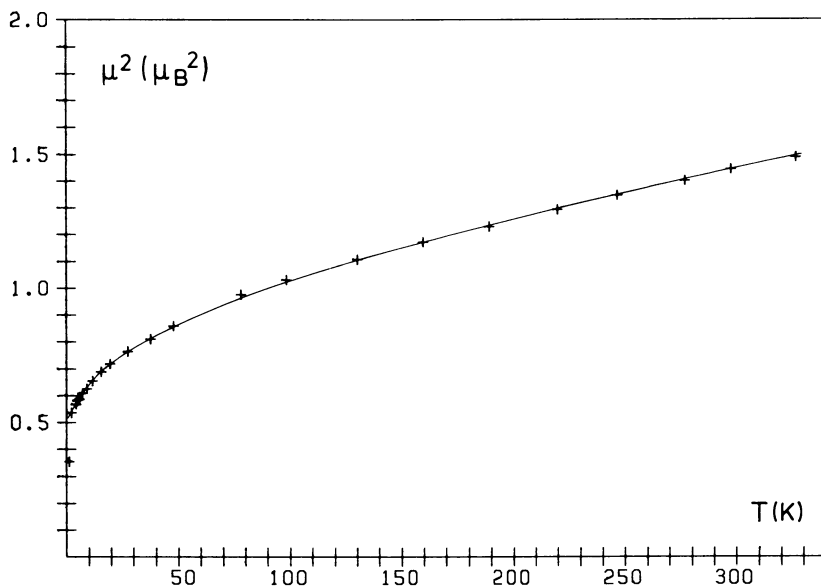


Figure 4. μ_{eff}^2 vs. temperature diagram of $[(\text{C}_2\text{H}_5)_4\text{N}]_4\text{Pu}(\text{NCS})_8$.

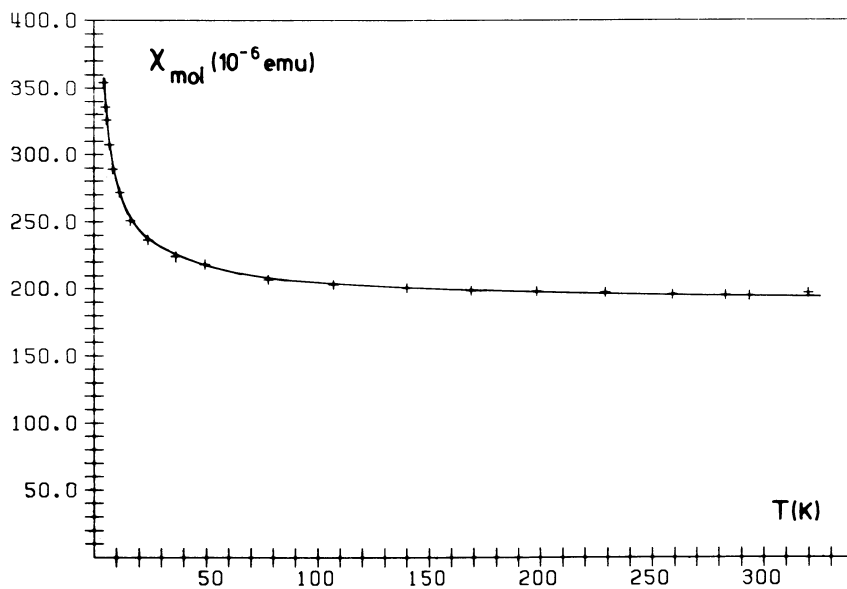


Figure 5. χ_{mol} vs temperature diagram of $\text{Pu}(\text{C}_8\text{H}_8)_2 \cdot 2\text{as}$ as function of k .

Pu(C₈H₈)₂

The magnetic properties of Pu(C₈H₈)₂ (=Pu(COT)₂), Pu(C₂H₅COT)₂ and Pu(C₄H₉COT)₂ were measured by Karraker (17,18). All compounds proved to be diamagnetic at room temperature near the theoretically calculated diamagnetic value. At low temperature they showed strong temperature dependent diamagnetism from -5,000 x 10⁻⁶ emu at 4 K to -900 x 10⁻⁶ emu at 45 K.

Our new measurements within the temperature range 4.2 to 300 K shows that Pu(COT)₂ is temperature independent paramagnetic, Fig. 5. A small paramagnetic impurity was found which corresponded to $\mu_{\text{eff}}^2 = 0.01 \mu_B^2$. Extrapolation for 1/T → 0 yielded $\chi_{\text{TIP}} = (191 \pm 10) \times 10^{-6}$ emu. The diamagnetic correction used, $\chi^{\text{dia}} = -209 \times 10^{-6}$ emu, was obtained from Th(COT)₂.

The "diamagnetism" or better the nonmagnetic ground state of Pu(COT)₂, was a specific test of different models for the electronic structure of the An(COT)₂ compounds. It has been explained by a |0> ground state in a pseudoaxial D_{8h} symmetry, interacting with the excited |±1> state giving rise to the observed

$$\chi_{\text{TIP}} = \frac{3.477}{\Delta E(|\pm 1\rangle - |0\rangle)} g_J^2(k) \times 10^{-6} \text{ emu } (\Delta E \text{ in cm}^{-1}),$$

where the Landé $g_J(k)$ factor depends on the orbital reduction factor k . It is seen from Fig. 6 that the calculated energy gap is extremely large ($\approx 7,700 \text{ cm}^{-1}$ for $k = 1.0$). If we take a large amount of orbital reduction into account, as was found empirically for organometallic compounds of the tetravalent actinides, this energy gap still remains remarkably large, compared to the estimated values by different authors (19-21), which are lower than 1000 cm^{-1} .

Pu(III) 5f⁵

Contrary to other oxidation states most of the compounds of trivalent plutonium that have been investigated show magnetic ordering at low temperatures.

β-Pu₂O₃

This is one of the best investigated plutonium compounds. Specific heat and magnetic measurements show an antiferromagnetic transition at 17.6 K (22,23). From neutron diffraction measurements a pseudo spiral magnetic structure like that in the heavy lanthanide metals was deduced. There are two magnetic components, both with $0.6 \mu_B$ perpendicular to the c -axis with a modulation of c and $2.5c$ respectively. The saturation moment of $0.85 \mu_B$ corresponds to a $\mu_{\text{eff}}^2 = 1.01 \mu_B^2$. Below 6 K the magnetic moments are expected to align parallel to the c -axis without change of the entropy of the system. No attempt was made to interpret the

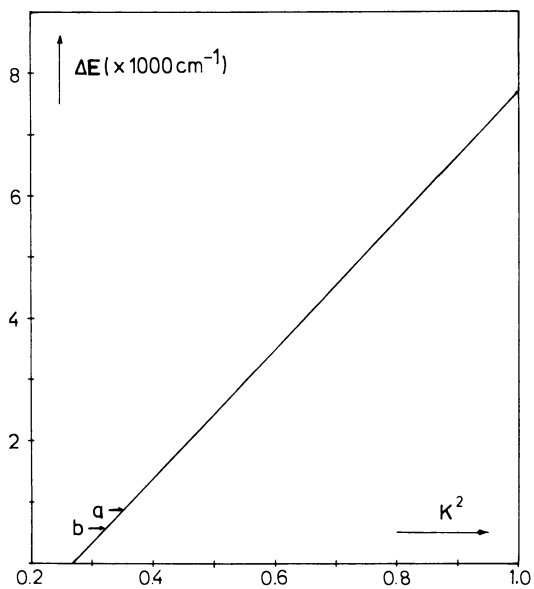


Figure 6. Calculated energy gap $\Delta E(+1 \rightarrow |0\rangle)$ as function of k . Predicted gaps: a, Ref. 19; and b, Ref. 20.

paramagnetic properties. Using the formula $(1/\chi)_{\text{exp}} = (1/\chi)_{\text{coop}} + (1/\chi)_{\text{para}}$ and extrapolating $(1/\chi)_{\text{coop}} = 460 \times 10^{-6} \text{ emu}$ the calculated moment is $\mu_{\text{eff}}^2 = 0.95$ at 25 K and $1.7 \mu_{\text{B}}^2$ at 300 K. From specific heat measurements one excited energy level of the ${}^6\text{H}_{5/2}$ ground state was estimated to be at about 50 and the other between 160 and 300 cm^{-1} .

Cubic Compounds

Due to the intermediate coupling the sign of the crystal field matrix element β is reversed compared to the pure Russell-Saunders state. Thus for 8-fold cubic coordination a Γ_7 ground state was found. From EPR measurements on Pu^{3+} diluted in fluorite host lattices, a magnetic moment at $T=0 \text{ K}$ can be calculated, ranging from $\mu_{\text{eff}}^2 = 1.333$ (in CeO_2) to $\mu_{\text{eff}}^2 = 0.942 \mu_{\text{B}}^2$ (in SrCl_2) (24, 25). The large deviation from the expected value $\mu_{\text{eff}}^2 = 0.370 \mu_{\text{B}}^2$ points up the strong crystal field interaction with the higher state ${}^6\text{H}_{7/2}$. The energy of the Γ_8 state is about 85 (in CeO_2) or 50 cm^{-1} (in SrCl_2) above the ground state.

From magnetic measurements on the elpasolite $\text{Cs}_2\text{NaPuCl}_6$ a Γ_8 ground state and a low lying Γ_7 state was deduced (26). The magnetic moment varies from 0.65 at 3 K to $1.1 \mu_{\text{B}}^2$ at 50 K.

Halides

For PuF_3 only high temperature measurements of magnetism are available (27). The magnetic moment between 90 and 300 K is about $\mu_{\text{eff}}^2 = 1.6 \mu_{\text{B}}^2$ and decreases at higher temperature.

An antiferromagnetic transition was found for PuCl_3 at 4.5 K, whereas PuI_3 orders ferromagnetically at 4.75 K (28). PuBr_3 shows a pure Curie behavior (28). The magnetism of PuCl_3 was fitted by using the van Vleck formula assuming the energy levels of Pu^{3+} in LaCl_3 , $E_1 = 13$ and $E_2 = 77 \text{ cm}^{-1}$. A TIP contribution of $236 \times 10^{-6} \text{ emu}$ for the ${}^6\text{H}_{7/2}$ was also included (21,28).

Organometallics

The magnetic susceptibility of $\text{K}[\text{Pu}(\text{COT})_2] \cdot 2\text{THF}$ was measured in the temperature range from 4.2 to 50 K (30). The magnetic moment was found to be $\mu_{\text{eff}}^2 = 1.56 \mu_{\text{B}}^2$ using $\bar{O} = 3.7 \text{ K}$.

$\text{Pu}(\text{C}_5\text{H}_5)_3$ and $(\text{C}_5\text{H}_5)_3\text{Pu} \cdot \text{C}\equiv\text{NC}_6\text{H}_{11}$ (Fig. 7) show a similar temperature dependence to that of PuCl_3 . The lower magnetic moments indicate some reduction of the g-factor (21,31).

Conclusions

Although magnetic properties of a number of plutonium compounds are known, it seems from the above discussion that the knowledge of the electronic ground state properties is very limited. Each compound represents a system of its own which has to be

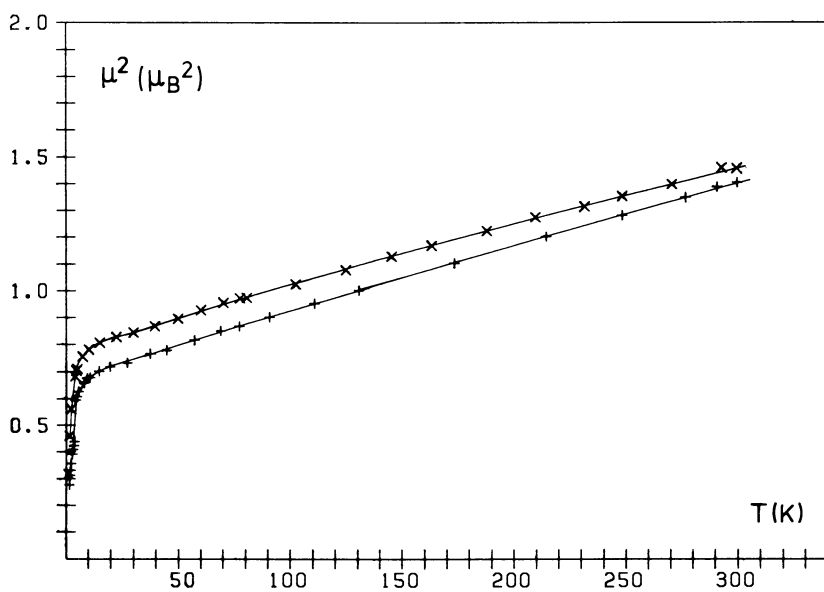


Figure 7. μ_{eff}^2 vs. temperature diagram of $\text{Pu}(\text{C}_5\text{H}_5)_3$ (+) and $(\text{C}_5\text{H}_5)_3\text{Pu}\cdot\text{C}\equiv\text{NC}_6\text{H}_{11}$ (x).

analyzed carefully before any comparison with others is possible. As seen in Fig. 8 the experimentally determined magnetic moments at room temperature are in general much lower than the free ion values. To extract the contribution of orbital reduction, the influence of intermediate coupling, crystal field effects and j-j mixing must be considered.

Especially for low symmetry compounds the information from measurement of the susceptibility is often not enough to describe the ground state unambiguously. Spectroscopic, EPR and other techniques should be combined with more magnetic investigations to firmly establish the interpretation.

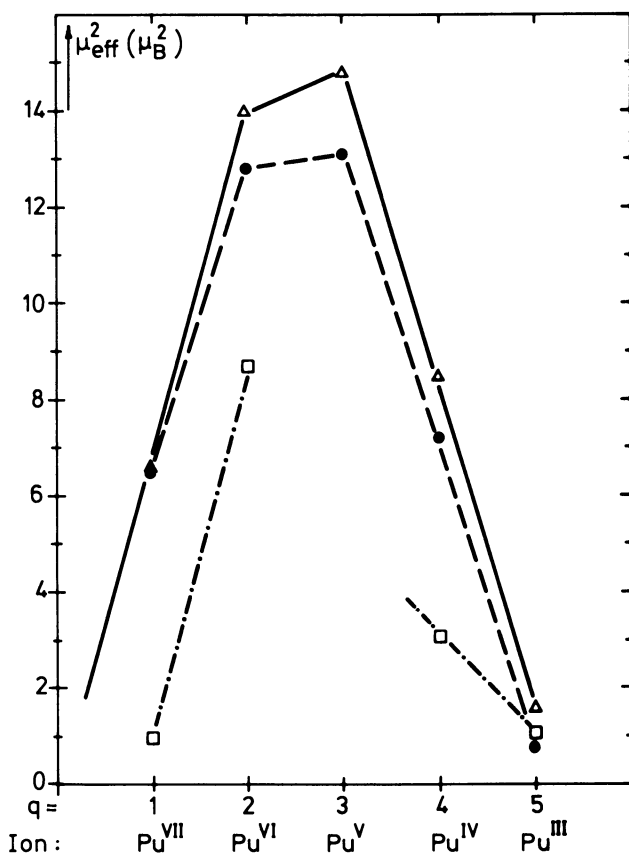


Figure 8. Calculated and experimentally measured μ_{eff}^2 values of Pu compounds in different oxidation states.

Literature Cited

1. Henrich, E. Thesis, University of Heidelberg, 1971.
2. Kanellakopulos, B.; Henrich, E.; Keller, C.; Baumgärtner, F.; König, E.; Desai, V. P. Chem. Phys. 1980, 53, 197-213.
3. Dawson, J. K. J. Chem. Soc. 1952, 2705-7.
4. Hutchison, C. A., Jr.; Lewis, W. B. Phys. Rev. 1954, 95, 1096.
5. Gruen, D. M.; Malm, J. G.; Weinstock, B. J. Chem. Phys. 1956, 24, 905-6.
6. Carnall, W. T.; Kanellakopulos, B.; Klenze, R., Stollenwerk, A. H. Journées des Actinides, Stockholm, May 27-28, 1980, Johanson, B.; Rosengren, A.; Eds., pp. 201-11.
7. Raphael, G.; Lallement, R. Solid State Comm. 1968, 6, 383-5.
8. Lee, K. R.; Leask, M. J. M.; Wolf, W. P. J. Phys. Chem. Solids 1962, 23, 1381-1405.
9. Rahman, H. U.; Runciman, W. A. J. Phys. Chem. Solids 1966, 27, 1833-5.
10. Dawson, J. K. J. Chem. Soc. 1952, 1882.
11. Lewis, W. B.; Elliot, N. J. Chem. Phys. 1957, 27, 904-8.
12. Hendricks, M. E. Ph.D. Thesis, Aiken, South Carolina, 1971.
13. Larson, A. C.; Roof, R. B., Jr.; Cromer, D. T. Acta Cryst. 1964, 17, 555-8.
14. Mulak, J. J. Solid State Chem. 1978, 25, 355-66.
15. Karraker, D. G. Inorg. Chem. 1971, 10, 1564-6.
16. Candela, G. A.; Hutchison, C. A., Jr.; Lewis, W. B. J. Chem. Phys. 1959, 30, 246-50.
17. Karraker, D. G.; Stone, J. A.; Jones, E. R.; Edelstein, N. J. Amer. Chem. Soc. 1970, 92, 4841-5.
18. Karraker, D. G. Inorg. Chem. 1973, 12, 1105-8.
19. Hayes, R. G.; Edelstein, N. J. Amer. Chem. Soc. 1972, 94, 8688-91.
20. Warren, K. D. Inorg. Chem. 1975, 14, 3095-103.
21. Aderhold, C. M. Thesis, University of Heidelberg, 1975.
22. McCart, B.; Lander, G. H.; Aldred, A. T. J. Chem. Phys. 1981, 74, 5263-8.
23. Flotow, H. E.; Tetenbaum, M. J. Chem. Phys. 1981, 74, 5269-77.
24. Edelstein, N.; Mollet, H. F.; Easley, W. C.; Mehlhorn, R. J. J. Chem. Phys. 1969, 51, 3281-4.
25. Kolbe, W.; Edelstein, N.; Finch, C. B.; Abraham, M. M. J. Chem. Phys. 1974, 60, 607-9.
26. Hendricks, M. E.; Jones, E. R., Jr.; Stone, J. A.; Karraker, D. G. J. Chem. Phys. 1974, 60, 2095-103.
27. Dawson, J. K.; Mandlberg, C. J.; Davies, D. J. Chem. Soc. 1951, 2047-50.
28. Jones, E. R.; Hendricks, M. E.; Stone, J. A.; Karraker, D. G. J. Chem. Phys. 1974, 60, 2088-94.

29. Laubereau, P. G. Thesis, Techn. University of Munich, 1967.
30. Karraker, D. G.; Stone, J. A. J. Amer. Chem. Soc. 1974, 96, 6885-8.
31. Kanellakopoulos, B. "Organometallics of the f-elements", Marks, T. J.; Fischer, R. D. Eds., D. Reidel, Dordrecht, Holland, 1979, pp. 1-35.

RECEIVED December 21, 1982

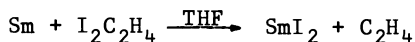
Reaction of Plutonium Metal with Diiodoethane

DAVID G. KARRAKER

E. I. du Pont de Nemours & Company, Inc., Savannah River Laboratory,
Aiken, SC 29808

The reaction of alpha plutonium metal with diiodoethane yielded a product analyzed to be $\text{PuI}_3\text{C}_2\text{H}_4 \cdot 4\text{THF}$. Heating this compound to 140°C for one hour yielded a green product, $\text{PuI}_2\text{C}_2\text{H}_3$. Ir spectra of both compounds showed the presence of ethylenic double bonds, and magnetic susceptibility showed that both were Pu^{+3} compounds. From this evidence, tentative compositions for these compounds were deduced as $\text{PuI}_3(\text{CH}_2=\text{CH}_2) \cdot 4\text{THF}$ and $\text{PuI}_2(\text{CH}=\text{CH}_2)$. The large, polarizable iodide ion is considered to be an important factor in stabilizing the Pu^{+3} -ethylenic bonds.

Samarium and ytterbium metals dissolve in tetrahydrofuran (THF) solutions of diiodoethane to yield solutions of their diiodides, (1) as



The blue samarium diiodide solutions are stable indefinitely in the absence of water and oxygen, and SmI_2 and YbI_2 solutions have been employed as reducing agents in organic synthesis.

The chemical similarity between lanthanide and actinide metals suggests that $\text{C}_2\text{H}_4\text{I}_2$ might also react with actinide metals. Preliminary experiments found no reaction between thorium or uranium metals and a THF solution of $\text{C}_2\text{H}_4\text{I}_2$. Plutonium and neptunium metals reacted, but not in the same manner as samarium and ytterbium metals. This paper reports studies on the products of the reaction between plutonium metal and THF solutions of $\text{C}_2\text{H}_4\text{I}_2$.

0097-6156/83/0216-0041\$06.00/0
© 1983 American Chemical Society

Experimental

Materials. THF and ethyl ether were purified by distillation from LiAlH_4 in an argon atmosphere. Toluene and petroleum ether (b.p., 20–40°C) were stirred overnight with CaH_2 and filtered before use. Alpha-phase plutonium metal pieces, prepared at Rocky Flats (Rockwell International, Golden, Colorado), were cleaned with a THF solution of $\text{C}_2\text{H}_4\text{I}_2$ before use.

Diiodoethane was purified from iodine by dissolving in ether and washing the ether solution with an aqueous solution of sodium thiosulfate. The ether phase was dried with anhydrous sodium sulfate and vacuum evaporated to recover pure $\text{C}_2\text{H}_4\text{I}_2$.

Analyses. Plutonium was determined radiometrically. A weighed sample of a compound was dissolved in 2M H_2SO_4 with a few drops of 90% HNO_3 to oxidize organic material, and an aliquot of this solution counted for alpha activity.

Carbon was estimated by a variation of the Van Slyke method.(2) A 30–100 mg sample was heated for 30 minutes with 0.5 g $\text{K}_2\text{Cr}_2\text{O}_7$, 1g KIO_3 , 10 mL 20% fuming H_2SO_4 and 5 mL H_3PO_4 in a closed flask swept by a purified N_2 stream. The N_2 stream carried the evolved CO_2 to an absorption solution of 0.5M NaOH –0.3M N_2H_4 . After the wet combustion, the absorbed CO_2 was released from an aliquot of the NaOH solution with lactic acid in a manometric apparatus. Corrections were applied for the vapor pressure of water and for reagent blank.

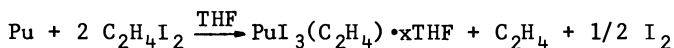
Iodine was determined by an iodometric titration adapted from White and Secor.(3) Instead of the normal Carius combustion, iodide was separated from the samples either by slurring in 6M NaOH , or by stirring the sample with liquid sodium-potassium (NaK) alloy, followed by dissolving excess NaK in ethanol. Precipitated plutonium hydroxides were filtered. Iodine was determined in the filtrate by bromine oxidation to iodate in an acetate buffer solution, destruction of the excess bromine with formic acid, acidifying with H_2SO_4 , addition of excess KI solution, and titrating the liberated iodine with standard sodium thiosulfate. The precision of the iodine determination is estimated to be about 5% of the measured value, principally due to incomplete extraction of iodine from the sample.

Measurements. Infra-red spectra for the region 600–4000 cm^{-1} were measured with a Perkin-Elmer Model 710B spectrometer on samples pressed in KBr pellets. Magnetic susceptibilities were measured with a vibrating sample magnetometer (Princeton Applied Physics) as previously described.(4)

Preparations. All preparations, purifications, etc. were performed in a purified argon atmosphere. The plutonium metal and a THF solution of $\text{C}_2\text{H}_4\text{I}_2$ were stirred together at room temperature in the dark, to minimize $\text{C}_2\text{H}_4\text{I}_2$ decomposition. In a typical preparation, a 3.0 g piece of alpha-plutonium metal was stirred for three days with a solution of 2.1g $\text{C}_2\text{H}_4\text{I}_2$ in 50 mL THF. An

off-white precipitate formed in the solution; 1.90 g of unreacted Pu metal was recovered. The precipitate was filtered, washed with pet. ether, and dried over night at 80°C in vacuum. The recovered product weighed 3.70 g. The filtrate from the reaction contained 15 mg Pu. Analyses found 25±2% Pu, 41 ± 2% I and 23±2% C, consistent with the empirical formula $\text{PuI}_3\text{C}_{18}\text{H}_{36}\text{O}_4$, (Pu, 25.53%; I, 40.70%; C, 23.08%). Assuming four molecules of solvated THF, the empirical formula is $\text{PuI}_3\text{C}_2\text{H}_4 \cdot 4\text{THF}$. Attempts to react Pu metal with $\text{C}_2\text{H}_4\text{I}_2$ in toluene and ethyl ether solutions were unsuccessful.

The stoichiometry of the reaction was measured by reacting Pu metal with a THF solution of $\text{C}_2\text{H}_4\text{I}_2$ in a sealed, evacuated flask. After 24 hours, volume and pressure measurements showed that 1.46 mm of gas was evolved, after correction for the vapor pressure of THF; 1.54 mm of Pu was consumed, and titration of the THF filtrate found 1.8 mm of iodine. The gas composition was not determined, but assuming that the evolved gas was C_2H_4 , these data indicate that the reaction is:



Heating the white reaction product to 140°C for one hour in vacuum caused a visible iodine evolution and approximately 40% weight loss. No further weight loss was observed up to 250°C. The gaseous products from the pyrolysis were not collected. The green product from pyrolysis analyzed Pu, 43±3%; I, 50 ± 2%; C, 4.9 ± 1%. The empirical formula $\text{PuI}_2\text{C}_2\text{H}_3$ has the calculated composition Pu, 45.88%; I, 48.75%; C, 4.79%.

Both empirical formulae have hydrogen compositions assigned to agree with the composition chosen based on other evidence.

Results

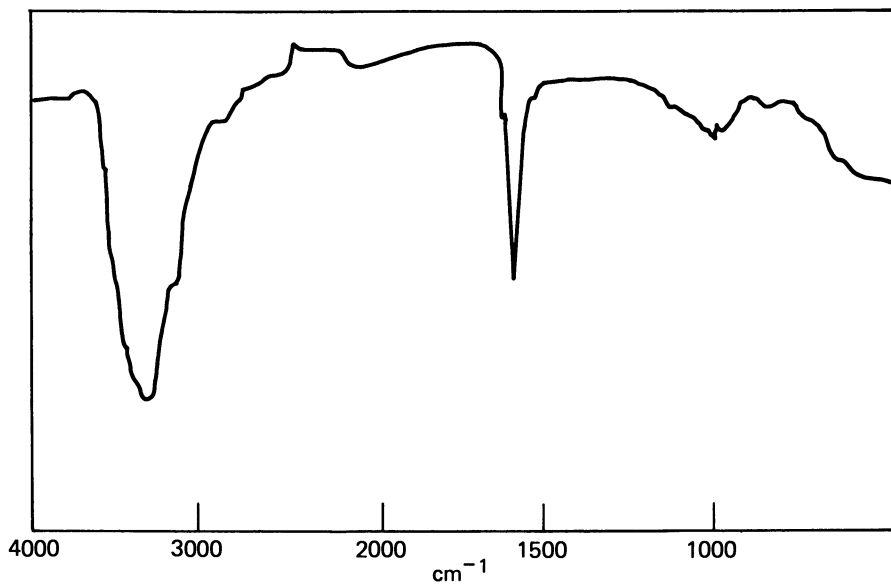
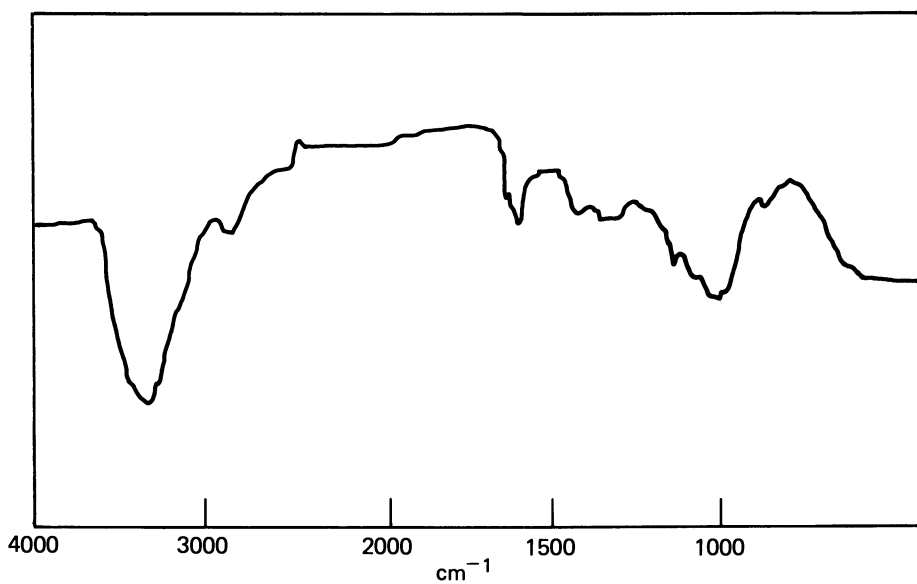
IR Spectra. The infrared absorption bands of $\text{C}_2\text{H}_4\text{I}_2$, $\text{PuI}_3\text{C}_2\text{H}_4 \cdot 4\text{THF}$ (referred to below as "R") and $\text{PuI}_2\text{C}_2\text{H}_3$ (P) are listed in Table I, and the spectra are shown in Figures 1 and 2. The spectra of both plutonium compounds have strong absorption bands at 3400 cm^{-1} and 1600 cm^{-1} that are interpreted as due to C-H and C=C stretching frequencies. The IR spectrum of $\text{C}_2\text{H}_4\text{I}_2$ has a broad complex absorption from 2800-4000 cm^{-1} and a sharp, strong band at 1128 cm^{-1} . Absorption in the 3000 cm^{-1} region is normally associated with CH stretching vibrations.(5) The normal CH_2 stretch is found at higher frequencies in $\text{C}=\text{CH}_2$ and $\text{C}\equiv\text{CH}$ groupings.

The absorption at 1600 cm^{-1} in the plutonium compounds is slightly lower than that expected for a C=C stretching vibration.(5) The C-C vibration in $\text{C}_2\text{H}_4\text{I}_2$ is found at 1128 cm^{-1} , and coordination or bonding of a $\text{C}_2\text{H}_4\text{I}$ moiety would be expected to lower this value.(6) However, coordination or bonding of a C=C linkage would be expected to both lower the frequency and increase the intensity

TABLE I
Infrared Absorption Bands (cm^{-1})

$\text{C}_2\text{H}_4\text{I}_2$	$\text{PuI}_3\text{C}_2\text{H}_4 \cdot 4\text{THF}$	$\text{PuI}_2\text{C}_2\text{H}_3$
2800-4000 S, bd	3400 S 2900 sh 2200 W, bd 1600 S, sp	3400 S 2880 W, bd 1600 sp
1150 S, sp		1150 W 1100 sh
1050 sh	1000 W, bd	1050 M, bd 1000 sh 890 W

S, strong; M, medium; W, weak; bd, broad; sp, sharp; sh, shoulder.

Figure 1. Infrared spectrum of $\text{PuI}_3\text{C}_2\text{H}_4 \cdot 4\text{THF}$.Figure 2. Infrared spectrum of $\text{PuI}_2\text{C}_2\text{H}_3$.

of this band. The presence of a C=C vibration is consistent with the shift of a CH₂ stretch from 2900 cm⁻¹ to greater frequencies.

The spectrum of R has absorption bands in the 1000 cm⁻¹ region that can be attributed to coordinated THF.(7, 8) The broad absorption in the spectrum of P in the 1000-1150 cm⁻¹ region is probably due to skeletal and deformation vibrations.(5) The absence of absorption at 1200-1350 cm⁻¹ indicates that there are probably no hydride hydrogens.(8)

Magnetic Susceptibilities. The magnetic susceptibilities of both plutonium compounds (Figure 3) show a weak Curie-Weiss paramagnetism; for R, $\mu_{\text{eff}}=0.87\mu_{\text{B}}$, $\Theta=2.6^{\circ}\text{K}^9$ and for P, $\mu_{\text{eff}}=0.52\mu_{\text{B}}$, $\Theta=1.4^{\circ}\text{K}$ over the temperature range 6 to 40°K. Below 6°K, the deviation of the data from the straight line indicates lower crystal field levels. At higher temperatures, the magnetism becomes too weak to measure by the magnetometer.

These magnetic measurements indicate that plutonium is present as the +3 valence in these compounds. Pu³⁺ has a 5f⁵ configuration, and ⁶H_{5/2} ground state, and would show Curie-Weiss paramagnetism similar to the paramagnetism found for the compounds studied here.(10) Pu⁴⁺ has a 5f⁴ configuration and a ⁵I₄ ground state. In a crystal field of low enough symmetry to remove any degeneracy, the lowest crystal field level would be a singlet state, which could only show temperature-independent (Van Vleck) paramagnetism.(11) Pu²⁺ would be expected to have a 5f⁶ configuration, and a ⁷F₀ ground state, like Am³⁺. The magnetic susceptibility for a ⁷F₀ ground state can only be temperature-independent, in any crystal field symmetry.

Discussion

To review the available evidence, the plutonium in both compounds is trivalent, the compounds have coordinated or bonded ethylenic groups, and the empirical formulae are PuI₃C₂H₄·4THF (the reaction product) and PuI₂C₂H₃ (the pyrolytic product). Formulae that are consistent with this evidence are PuI₃(CH₂=CH₂)·4THF for the reaction product, and PuI₂(CH=CH₂) for the pyrolytic product. The evidence is only sufficient to propose these compositions, and until corroborative measurements can be made, these formulae should be considered tentative.

Other possibilities considered were that a C₂H₄I moiety was bonding to the Pu³⁺ ion, and that the pyrolytic product could be a Pu²⁺ compound. The former is incompatible with the ir spectra, the latter with the magnetic susceptibility results. No evidence was found for a hydride ion in the ir spectra. The pyrolytic product

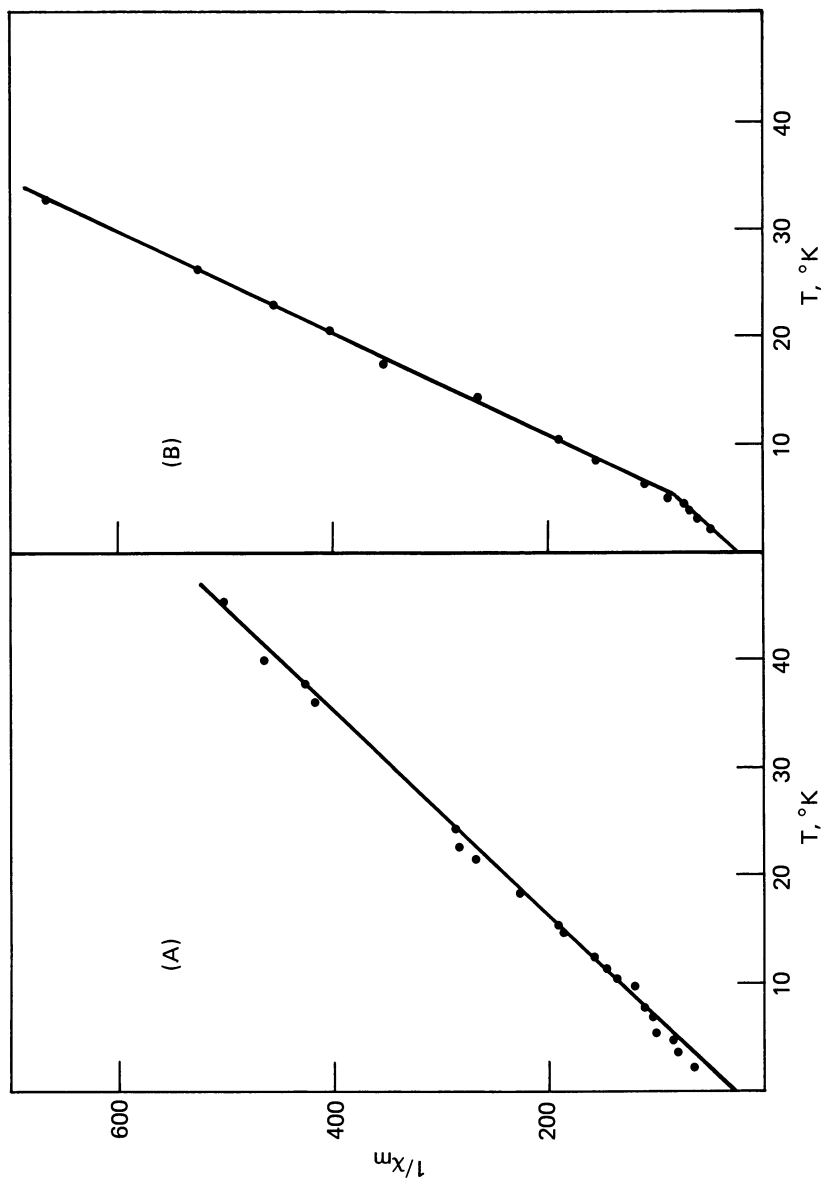


Figure 3. Inverse magnetic susceptibilities of (A) $\text{PuI}_3\text{C}_2\text{H}_4$ and (B) $\text{PuI}_2\text{C}_2\text{H}_3$.

American Chemical
Society Library
1155 16th St., N.W.
Washington, D. C. 20036

certainly has a polymeric structure, since otherwise the Pu^{3+} ion would be only 3-coordinate. The structure of the pyrolytic product probably involves extensive iodide bridging.

Some speculation may be entertained on the series of reactions involved in the oxidation of Pu metal by $\text{C}_2\text{H}_4\text{I}_2$. An initial step could be the attack on Pu metal by $\text{C}_2\text{H}_4\text{I}_2$ producing a Pu^{2+} species, such as $\text{PuI}_2 \cdot x\text{THF}$. Comparison with SmI_2 or YbI_2 indicates that a PuI_2 species would be soluble in THF. Once in solution, the PuI_2 species would be oxidized by $\text{C}_2\text{H}_4\text{I}_2$, liberating I_2 and precipitating $\text{PuI}_3(\text{C}_2\text{H}_4) \cdot x\text{THFF}$. The low concentration of Pu in the THF solution suggests that the oxidation of Pu^{2+} to Pu^{3+} is a rapid reaction. SmI_2 is not oxidized in the presence of excess Sm metal. In a similar reaction, Yb metal is oxidized first to Yb^{2+} species, then to a Yb^{+3} species by Me_5CpI .(12).

Assuming confirmation by further work, these compounds are the first Pu compounds to show Pu-ethylene bonding. The nature of this bonding is unknown, but participation of 5f orbitals with π orbitals of the ethylene double bond, though unlikely, should be considered. The large and easily polarizable iodide ions could be the key factor in stabilizing the proposed Pu^{+3} -ethylene bonds.

Acknowledgment

This paper was prepared in connection with work done under Contract No. DE-AC09-76SR00001 with the U.S. Department of Energy.

Literature Cited

1. Girard, P.; Namy, J. L.; Kagan, H. B. J. Am. Chem. Soc. **1980**, 102, 2693.
2. Steyermark, A. "Quantitative Organic Microanalysis", 2nd Ed. Academic Press, N.Y., **1961**. p 454 et. Seq.
3. White, L. M.; Secor, G. E., Anal. Chem. **1950**, 22, 1047.
4. Hoehn, M. V.; Karraker, D. G. J. Chem. Phys. **1974**, 60, 393.
5. Bellamy, L. J. "The Infra-red Spectra of Complex Molecules", 2nd Ed. John Wiley and Sons, Inc., N.Y., **1958**. Chapters 2, 3, 4 and 6.
6. Wu, T.-Y. J. Chem. Phys. **1939**, 7, 965.
7. Barrow, G. M.; Searles, S. J. Am. Chem. Soc. **1953**, 76, 1175.
8. Evans, W. J.; Meadows, J. H.; Wayda, A. L.; Hunter, W. E.; Atwood, J. L. J. Am. Chem. Soc. **1982**, 104, 2015.
9. The Curie-Weiss expression used here is $\chi_m = C/(T+\theta)$.
10. Hendricks, M. E.; Jones, E. R., Jr.; Stone, J. A.; Karraker, D. G. J. Chem. Phys. **1974**, 60, 2095.
11. Lea, K. R.; Leask, M. J. M.; Wolf, W. P. J. Phys. Chem. Solids, **1962**, 23, 1381.
12. Watson, P. L.; Whitney, J. F.; Harlow, R. L. Inorg. Chem. **1981**, 20, 3271.

RECEIVED January 10, 1983

Bis(μ -hydroxo)tetraaquadiplutonium(IV) Sulfate

Its Relation to Other Tetravalent Hydroxysulfates and to the Plutonium(IV) Polymer

DENNIS W. WESTER

Argonne National Laboratory, Chemistry Division, Argonne, IL 60439

$\text{Pu}_2(\text{OH})_2(\text{SO}_4)_3(\text{H}_2\text{O})_4$, (I) is a hydroxysulfate which is unique among the actinides. Other members of the series form hydroxysulfates of different composition. The conditions leading to I are compared to conditions by which hydroxysulfates of other tetravalent actinide, lanthanide and Group IVB elements are produced. The crystal structure of I is described and compared to other known hydroxysulfate structures. Hydroxysulfates of Zr, Hf and Ce are isomorphous to I. A common feature of all hydroxysulfates is shown to be the presence of double hydroxide bridges. Infrared, visible and near-IR spectroscopic results are compared to those for Pu(IV) polymer and indicate a close similarity between I and the polymer.

Hydrothermal hydrolysis of metal ions is useful in producing crystalline phases which contain metals in a state of partial hydrolysis, i.e., a state intermediate between that of the hydrated metal ion and that of the hydrous hydroxide. Such reactions have been used to produce numerous crystalline phases of actinides (1-4), Group IV metal ions (5-14) and lanthanides (15-21).

Previous studies of the hydrothermal hydrolysis of tetravalent Th, U and Np (1-4) have shown a remarkable similarity in the behavior of these elements. In each case compounds of stoichiometry $\text{M}(\text{OH})_2\text{SO}_4$ represent the major product. In order to extend our knowledge of the hydrolytic behavior of the actinides and to elucidate similarities and differences among this group of elements, we have investigated the behavior of tetravalent plutonium under similar conditions. The relationships between the major product of the hydrothermal hydrolysis of Pu(IV), $\text{Pu}_2(\text{OH})_2(\text{SO}_4)_3(\text{H}_2\text{O})_4$, (I), and other tetravalent actinide, lanthanide and Group IVB hydroxysulfates are the subject of this re-

0097-6156/83/0216-0049\$06.00/0
© 1983 American Chemical Society

port. The compounds are compared with respect to synthesis, structure and spectral properties.

Discussion

$\text{Pu}_2(\text{OH})_2(\text{SO}_4)_3(\text{H}_2\text{O})_4$, (I), is an extremely stable phase in the $\text{PuO}_2 \cdot \text{SO}_3 \cdot \text{H}_2\text{O}$ system. The synthesis and characterization of I have been described previously (22). The red crystals of the compound were observed to be stable in air for at least sixteen months.

Synthetic Studies. Table 1 presents the results of several hydrothermal hydrolysis reactions involving various concentrations of Pu(IV) and sulfate. These results suggest that the pH of the solution may be an important factor leading to the formation of I. If the amorphous product is assumed to be an extensively hydrolyzed compound, its formation at lower pH values would be inhibited so that the Pu(IV) ions would remain in solution and be available for formation of I. Such behavior is observed since at sulfuric acid concentrations less than 0.20 M only the amorphous product is observed. The pH values for sulfuric acid of 0.20–0.25 M are in the borderline region where temperature and concentration of Pu(IV) can have large effects. For instance, at a concentration of Pu(IV) equal to 0.325 M in 0.20 M sulfuric acid, both I and the amorphous product are observed at 140°C. However, raising the temperature to 180°C, which increases the degree of hydrolysis, causes only the amorphous product to appear. In another case, both products are observed at a Pu(IV) concentration of 0.166 M and a sulfuric acid concentration of 0.25 M. Presumably, an increase in the concentration of Pu(IV) would lead to a larger proportion of I due to the necessity of forming dimers. Sulfate concentration unfortunately paralleled that of hydrogen ion so that the effects of changing sulfate concentration were obscured. However, the following observations can be made. At the lowest sulfate concentration the amorphous product was the only product observed. As the concentration of sulfate (sulfuric acid) was raised, the only other product which was observed was red crystalline I. Although the green powdery amorphous product was observed up to sulfate concentrations of 0.25 M, by the time the sulfate concentration reached 0.50 M, I was the only product observed at 140°C. However, since the formation of the hydroxysulfates is intimately related to the hydrolysis of the cation, we feel that the pH is the controlling factor.

Comparison of these results for plutonium with those for other tetravalent metals reveals some interesting facts. Thorium(IV), uranium(IV) and neptunium(IV) sulfates have been investigated under hydrothermal hydrolytic conditions. For uranium, the stable phases which have been reported include $\text{U}(\text{OH})_2\text{SO}_4$ (2), $\text{U}_6\text{O}_4(\text{OH})_4(\text{SO}_4)_6$ (3), $\text{U}(\text{SO}_4)_2 \cdot 4\text{H}_2\text{O}$ (23) and $\text{U}(\text{SO}_4)_2$ (24). For thorium (1) and neptunium (4), the hydroxysulfates $\text{M}(\text{OH})_2\text{SO}_4$ are known. The conditions for formation of these hydroxysulfates

TABLE 1

Hydrothermal Hydrolysis Reactions in the PuO ₂ ·SO ₃ ·H ₂ O System			
[Pu(IV)]	[SO ₄ ⁻²]	T, K	Products
0.138	0.125	140	amorphous (12Pu ₂ ·2SO ₃ ·7H ₂ O)
0.325	0.20	140	amorphous + I
0.325	0.20	180	amorphous
0.166	0.25	140	amorphous + I
0.238	0.50	200	I
0.552	0.50	140	I

are nearly identical to those for formation of I. For instance, from uranium-containing solutions of 0.1-0.5 M sulfuric acid at 100-150°C, $U(OH)_2SO_4$ is the predominant product (2). Unfortunately, the exact concentrations of uranium which were used are not given. At somewhat higher uranium concentrations in 0.5 M sulfuric acid at 200°C, $U_6O_4(OH)_4(SO_4)_6$ is the predominant phase (3). $U(SO_4)_2$ forms from 0.3 M U(IV) in 0.3 M sulfuric acid at 140°C (24). $Np(OH)_2SO_4$ forms from a solution of 0.08 M Np(IV) in 0.5 M sulfuric acid at 140°C (4). $Th(OH)_2SO_4$, along with other phases (one of which may be $Th(SO_4)_2 \cdot 4H_2O$), is prepared in a similar manner (1). It is remarkable that in view of the many different phases observed in the actinide-sulfate systems, to this date the only crystalline phase which has been observed in the plutonium sulfate system is one which is entirely different from all the other actinide phases. The reasons for this distinctive behavior of plutonium are as yet unclear especially in view of the similarity of the first hydrolysis constants for U, Np and Pu. Experiments involving further variations of the conditions are in progress.

Although the phase which appears to be very stable for plutonium has not been observed in other $AnO_2 \cdot SO_3 \cdot H_2O$ systems, phases of identical composition have been observed for Zr, Hf and Ce. The crystal structure of the zirconium compound $Zr_2(OH)_2(SO_4)_3(H_2O)_4$, is well known (5). One very interesting feature of the $MO_2 \cdot SO_3 \cdot H_2O$ systems for Zr, Hf and Co is that there are a large number of phases which have been observed. Some of these correspond to phases which are known for Th, U and Np. For zirconium, a series of basic sulfates is known to include $Zr_2(OH)_2(SO_4)_3(H_2O)_4$ and two modifications of $Zr(OH)_2SO_4$ as the major constituents (5). Other basic sulfates such as $Zr(OH)_2SO_4 \cdot H_2O$, $Zr_4(OH)_{10}(SO_4)_3(H_2O)_{10}$, $Zr_3(OH)_8(SO_4)_2(H_2O)_8$ and some basic sulfates of less definite composition are known (7), but these at present bear little relation to the basic actinide sulfates. In addition, the compounds $Zr(SO_4)_2 \cdot 4H_2O$, $Zr(SO_4)_2 \cdot 1.5H_2O$, $Zr(SO_4)_2 \cdot H_2O$, $Zr(SO_4)_2$ and $Zr(SO_4)_2 \cdot H_2SO_4$ are observed at 100°C. (6).

The $HfO_2 \cdot SO_3 \cdot H_2O$ system also has been extensively studied. The basic sulfates which are well known include $Hf_2(OH)_2(SO_4)_3(H_2O)_4$ (10), $Hf(OH)_2SO_4$ (13), $Hf(OH)_2SO_4 \cdot H_2O$ (12), and $Hf(OH)_2SO_4 \cdot 2H_2O$ (11), although the last compound also has been described as $Hf_4O_5(SO_4)_3 \cdot 9H_2O$ (14). In addition, the compounds $Hf(SO_4)_2 \cdot XH_2O$, $X=0.5, 1.5$ and 4.0 are known (10). The phases which occur in the $CeO_2 \cdot SO_3 \cdot H_2O$ system are more numerous and less well-defined than any of the above metals; however, once again compounds corresponding to $Ce(OH)_2SO_4$, $Ce_6O_4(OH)_4(SO_4)_6$ and $Ce_2(OH)_2(SO_4)_3(H_2O)_4$ are observed (15,16).

The conditions under which the basic sulfates of tetravalent, Zr, Hf and Ce form provide analogies on which to base speculation about the hydrothermal hydrolysis of tetravalent plutonium. In the zirconium system at 100°C, the only basic sulfate observed is $Zr_2(OH)_2(SO_4)_3(H_2O)_4$, i.e., the zirconium analog of

I. However, as the temperature of the hydrothermal hydrolysis is raised, two forms of $\text{Zr}(\text{OH})_2\text{SO}_4$ are formed. In addition, $\text{Zr}(\text{OH})_2\text{SO}_4 \cdot \text{H}_2\text{O}$ forms from solutions more concentrated in zirconium than solutions which produce $\text{Zr}_2(\text{OH})_2(\text{SO}_4)_3(\text{H}_2\text{O})_4$. Thus, it would seem that either higher temperatures or solutions more concentrated in plutonium would produce $\text{Pu}(\text{OH})_2\text{SO}_4$ or $\text{Pu}(\text{OH})_2\text{SO}_4 \cdot \text{H}_2\text{O}$. This trend seems to continue for the $\text{HfO}_2 \cdot \text{SO}_3 \cdot \text{H}_2\text{O}$ system. For hafnium, the basic sulfates $\text{Hf}(\text{OH})_2\text{SO}_4 \cdot 2\text{H}_2\text{O}$, $\text{Hf}(\text{OH})_2\text{SO}_4 \cdot \text{H}_2\text{O}$ and $\text{Hf}(\text{OH})_2\text{SO}_4$ are formed at 100, 200 and 300°C, respectively. In addition, $\text{Hf}_2(\text{OH})_2(\text{SO}_4)_3(\text{H}_2\text{O})_4$ is observed at least up to 200°C. However, for hafnium it appears that $\text{Hf}(\text{OH})_2(\text{SO}_4)_3(\text{H}_2\text{O})_4$ becomes more stable at 200°C than $\text{Hf}(\text{OH})_2\text{SO}_4 \cdot \text{H}_2\text{O}$. In fact, the published solubility diagram for the $\text{HfO}_2 \cdot \text{SO}_3 \cdot \text{H}_2\text{O}$ system does not predict the existence of $\text{Hf}(\text{OH})_2\text{SO}_4 \cdot \text{H}_2\text{O}$ at 200°C, so that the results for the hafnium system must be interpreted with caution. Fortunately, for the $\text{CeO}_2 \cdot \text{SO}_3 \cdot \text{H}_2\text{O}$ system the results are in concordance with the trend observed for the zirconium system. At temperatures up to 100°C, the principal phases are $6\text{CeO}_2 \cdot 5\text{SO}_3 \cdot 12\text{H}_2\text{O}$, $2\text{CeO}_2 \cdot 3\text{SO}_3 \cdot 4\text{H}_2\text{O}$, $3\text{CeO}_2 \cdot 2\text{SO}_3 \cdot 3\text{H}_2\text{O}$, $\text{CeO}_2 \cdot \text{SO}_3 \cdot \text{H}_2\text{O}$, $\text{Ce}(\text{SO}_4)_2 \cdot 4\text{H}_2\text{O}$ and $\text{Ce}(\text{SO}_4)_2$. As the temperature of the system is raised, phases begin to disappear from the solubility diagram until at 175°C, only $\text{CeO}_2 \cdot \text{SO}_3 \cdot \text{H}_2\text{O}$ and $\text{Ce}(\text{SO}_4)_2$ remain. This behavior is similar to that of zirconium and the same conclusions with respect to plutonium can be drawn.

Structural Studies. X-ray powder diffraction patterns for I indicate that the crystal structure is isomorphous to $\text{Zr}_2(\text{OH})_2(\text{SO}_4)_3(\text{H}_2\text{O})_4$. Figure 1 depicts the structure of the zirconium compound (5). The structure of I is identical to that of the zirconium analog except for variations in bond distances and angles which do not affect the overall structure. We have as yet been unable to obtain single crystals of I which are suitable for X-ray diffraction studies.

By analogy to the Zr compound, the structure of I can be described as being composed of $\text{Pu}_2(\text{OH})_2^{6+}$ moieties to which are coordinated water molecules and bridging sulfate groups. Each plutonium is coordinated to eight oxygens (two hydroxide oxygens, four sulfate oxygens and two water oxygens). The geometry of the coordination sphere is dodecahedral. In the absence of data obtained from a single crystal structural analysis, more detailed discussion of the coordination sphere is not possible.

The crystal structures of $\text{Hf}_2(\text{OH})_2(\text{SO}_4)_3(\text{H}_2\text{O})_4$ (14) and $\text{Ce}_2(\text{OH})_2(\text{SO}_4)_3(\text{H}_2\text{O})_4$ (14) also have been determined and found to be isomorphous to the zirconium compound. The cell constants for this series of four isomorphous compounds reflect the effect of the ionic radii on the dimensions of the unit cell. The values for these cell constants are in Table II. Thus, the cell constants for the zirconium and hafnium compounds are nearly identical and smaller than the cell constants for the cerium and plutonium compounds which are also nearly identical. This trend is exactly that followed by the ionic radii of these elements.

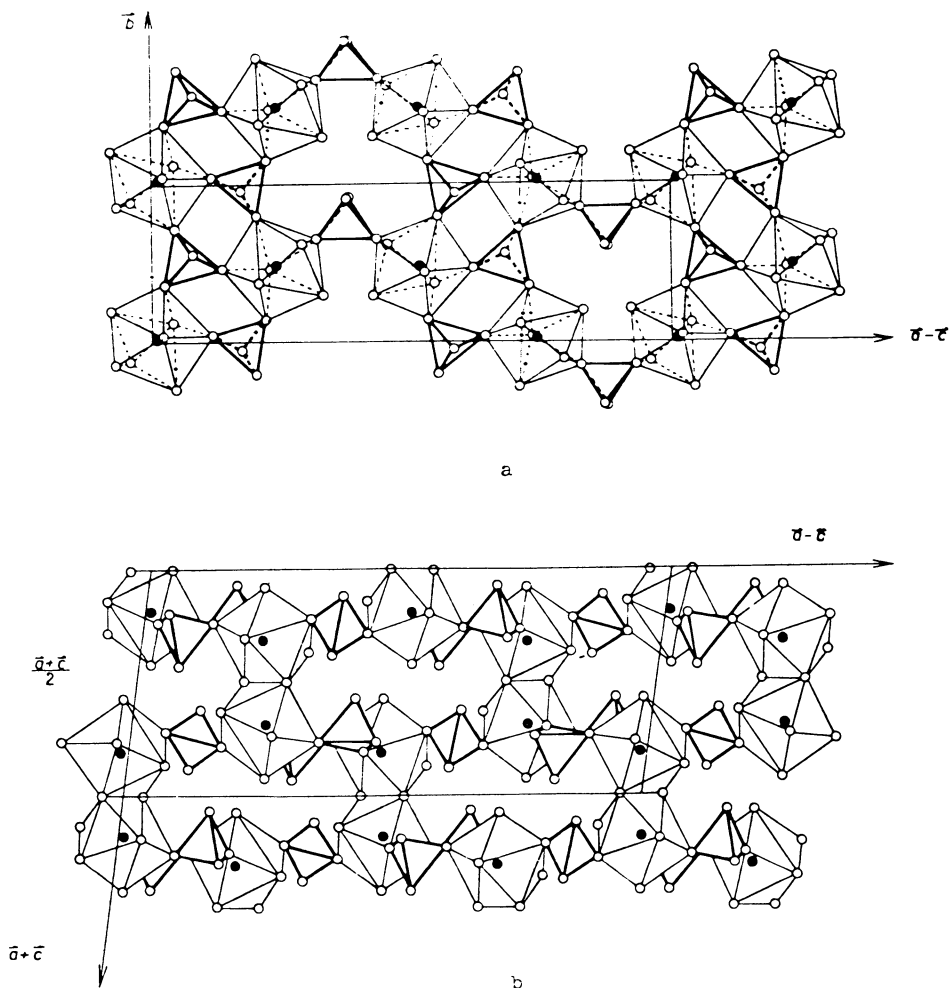


Figure 1. The crystal structure of $Zr_2(OH)_2(SO_4)_3(H_2O)_4$, reprinted with permission from Ref. 5, copyright 1966, American Chemical Society. Zirconium atoms are shown as solid circles, oxygen atoms as open circles. The Pu compound is isomorphous, Zr being replaced by Pu. 1a shows the manner in which the bridging sulfates link Pu atoms to form layers. 1b shows the manner in which layers are linked through the double hydroxide bridges.

TABLE II

Cell Constants for $M_2(OH)_2(SO_4)_3 \cdot 4H_2O$				
M =	Zr	Hf	Ce	Pu
a (Å)	13.056	13.1	13.5	13.51
b (Å)	6.5075	6.5	6.7	6.71
c (Å)	15.092	15.1	15.8	15.52
β (°)	96.35	96.5	91	95.7

Comparison of the crystal structure for the $M_2(OH)_2(SO_4)_3 \cdot (H_2O)_4$ series of compounds ($M=Zr, Hf, Ce, Pu$) with the crystal structure of other hydroxysulfate compounds reveals a common structural feature which pervades the chemistry of these hydrolyzed species. The existence of $-M(OH)_2M^{6+}$ moieties in nearly all of the hydroxysulfate structures which have been determined is indeed very striking. For the series of compounds $M(OH)_2SO_4$, where $M=Zr$ (14), Hf (13), Th (1), U (2) and Np (4), the metal atoms are linked into chains through the bridging hydroxides. Figure 2 shows the structure of the compound $Th(OH)_2SO_4$ from several viewpoints. The metal atoms form zigzag arrays, with two hydroxide ligands separating one metal from the next. Thus, the stoichiometry of the chains is $[M(OH)_2]_n^{2n+}$. Crystal structures for $M(OH)_2SO_4 \cdot H_2O$ where $M=Zr$ (8), Hf (12) also have been determined and reveal the presence of almost planar zigzag chains of metal atoms joined by double hydroxide bridges. The single exception to this trend toward formation of double hydroxy-bridged metal dimers or chains is the compound which is best described as $CeOSO_4 \cdot H_2O$ (17). However, even in this structure the cerium ions form chains which are linked by bridging oxide ions.

Accommodation of metal atoms of widely differing ionic radii into the same overall structure creates interesting possibilities for the doping of metal ions into a common matrix for spectroscopic examination under nearly constant crystal field effects. For instance, observation of identical phases for zirconium and plutonium indicate that the zirconium compound would serve as a suitable matrix in which to isolate plutonium. Similarly, the appearance of identical phases for Th , U and Np makes possible the doping of uranium or neptunium into a thorium matrix.

Hydrolysis of tetravalent plutonium leads ultimately to a species described as $Pu(IV)$ polymer (25-27). Although this species is soluble, its structure has eluded detection. Due to the predominance of double hydroxy-bridged dimeric metal clusters in the structural chemistry of tetravalent Zr , Hf , Ce , Th , U , Np and Pu ; it is plausible to suggest that the initial step in the formation of the $Pu(IV)$ polymer may be the hydrolysis of aqueous $Pu(IV)$ to form hydroxy-bridged dimers. Further steps may be related to those observed in zirconium hydrolysis. As mentioned previously, species such as $Zr_4(OH)_{10}(SO_4)_3(H_2O)_{10}$ containing cyclic tetramers of oxide-bridged zirconium atoms have been assigned to these slowly hydrolyzed species, but final confirmation of the structures of both the zirconium and plutonium polymers is lacking. However, using typical interatomic distances from crystallographic structure determinations, the radius of such tetrameric clusters would be on the order of 14 Å, a dimension which agrees remarkably well with the dimension of the primary particles of $Pu(IV)$ polymer as determined from electron micrographs (25).

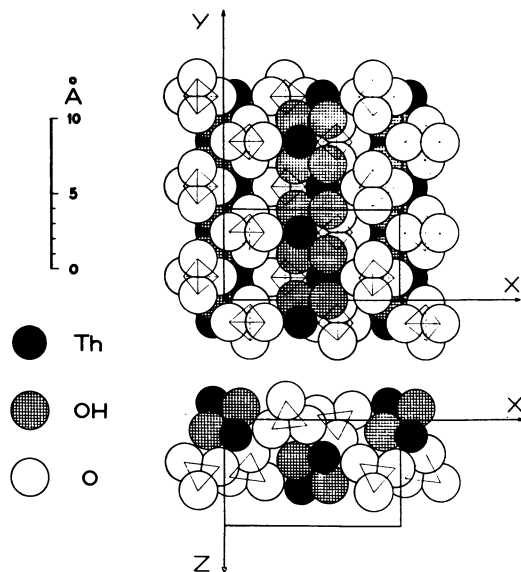
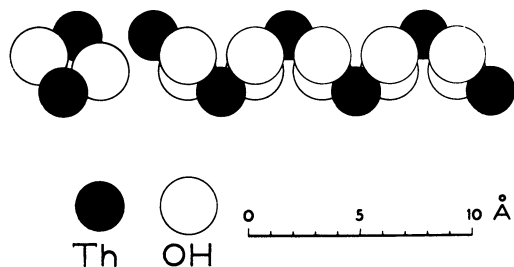


Figure 2. The crystal structure of $\text{Th}(\text{OH})_2\text{SO}_4$, reprinted with permission from Ref. 1, copyright 1950, Royal Swedish Academy of Science. The $-\text{M}(\text{OH})_2\text{M}-$ moiety is shown in the upper left. The $[\text{M}(\text{OH})_2]_2^{2n+}$ zigzag chain is illustrated in the upper right. The bottom views show how the zigzag chains are linked by bridging sulfate groups.

Spectroscopic Studies. Comparison of the infrared spectrum of I with that for the $M(OH)_2SO_4$ compounds, where $M=U,Np$, reveals the expected differences and similarities. The infrared spectrum of I is shown in Figure 3. The presence of water of coordination in the structure of I gives rise to bands at $\sim 3200\text{ cm}^{-1}$ and 1600 cm^{-1} . Since such water molecules are absent in the structure of the $M(OH)_2SO_4$ compounds, these bands also are absent in the infrared spectrum of the $M(OH)_2SO_4$ compounds. On the other hand, bridging sulfate groups are common to both structures and the sulfate region of the infrared spectrum, $\sim 1300\text{--}1000\text{ cm}^{-1}$, is surprisingly similar for both types of compounds.

Plutonium(IV) polymer has been examined by infrared spectroscopy (26). One of the prominent features in the infrared spectrum of the polymer is an intense band in the OH stretching region at $\sim 3400\text{ cm}^{-1}$. Upon deuteration, this band shifts to $\sim 2400\text{ cm}^{-1}$. However, it could not be positively assigned to OH vibrations in the polymer due to absorption of water by the KBr pellet. In view of the broad band observed in this same region for I, it now seems likely that the bands observed previously for Pu(IV) polymer are actually due to OH in the polymer. Indeed, we have observed a similar shift in the sharp absorption of $U(OH)_2SO_4$ upon deuteration (28). This absorption shifts from $\sim 3500\text{ cm}^{-1}$ to $\sim 2600\text{ cm}^{-1}$.

Visible and near-IR spectra of I are shown in Figures 4 and 5, respectively. Both regions of the spectra are distinctive due to the sharpness and abundance of absorptions. At this time a detailed analysis of the spectrum of I has not been carried out. However, qualitative comparison with some spectra of Pu(IV) compounds does reveal some interesting relationships.

The visible spectrum of $Pu(SO_4)_2 \cdot 4H_2O$ at $-92^\circ C$ (29) also shows numerous sharp absorptions between $\sim 700\text{--}400\text{ nm}$. Although $Pu(SO_4)_2 \cdot 4H_2O$ exists in two polymorphic forms, both forms contain eight coordinate plutonium in a site symmetry similar to the D_{4d} site of plutonium in I. Thus, even though the form of $Pu(SO_4)_2 \cdot 4H_2O$ which was used for the spectroscopic study is not specified, we can assume that the site symmetry of plutonium is similar to that in I. In the region $600\text{--}700\text{ nm}$, both spectra are characterized by a series of three absorptions. In addition, an absorption occurs at $\sim 710\text{--}720\text{ nm}$ for each compound, but that for I shows much more fine structure in this region. Each spectrum has two very sharp absorptions near 575 nm which are followed by broad absorptions near 540 nm . Features of the spectra at higher energies are also very similar and may be indicative of Pu(IV) in site symmetry approaching D_{4d} , i.e., an Archimedean antiprism.

Near-IR and visible spectra of the Pu(IV) polymer have been published (27). Although the spectra generally are very broad, the absorptions correspond well to the families of peaks seen for I. Especially notable are features between $1000\text{--}1200\text{ nm}$ and $600\text{--}700\text{ nm}$. In each case, the spectrum of I resembles that of

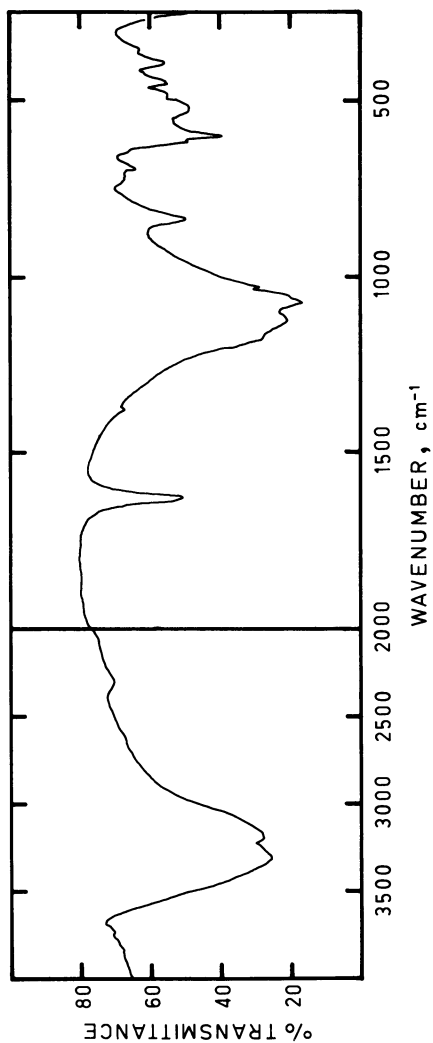


Figure 3. Infrared spectrum of I, reprinted with permission from Ref. 22, copyright 1982, American Chemical Society.

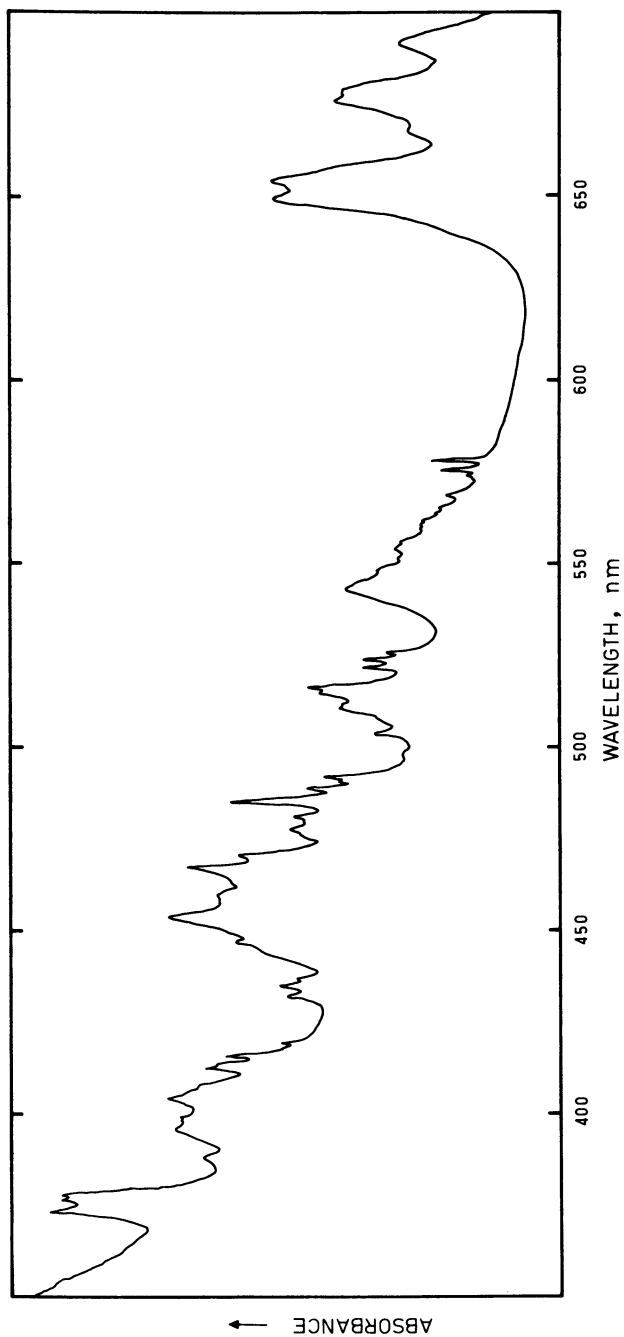


Figure 4. Visible spectrum of I, reprinted with permission from Ref. 22, copyright 1982, American Chemical Society.

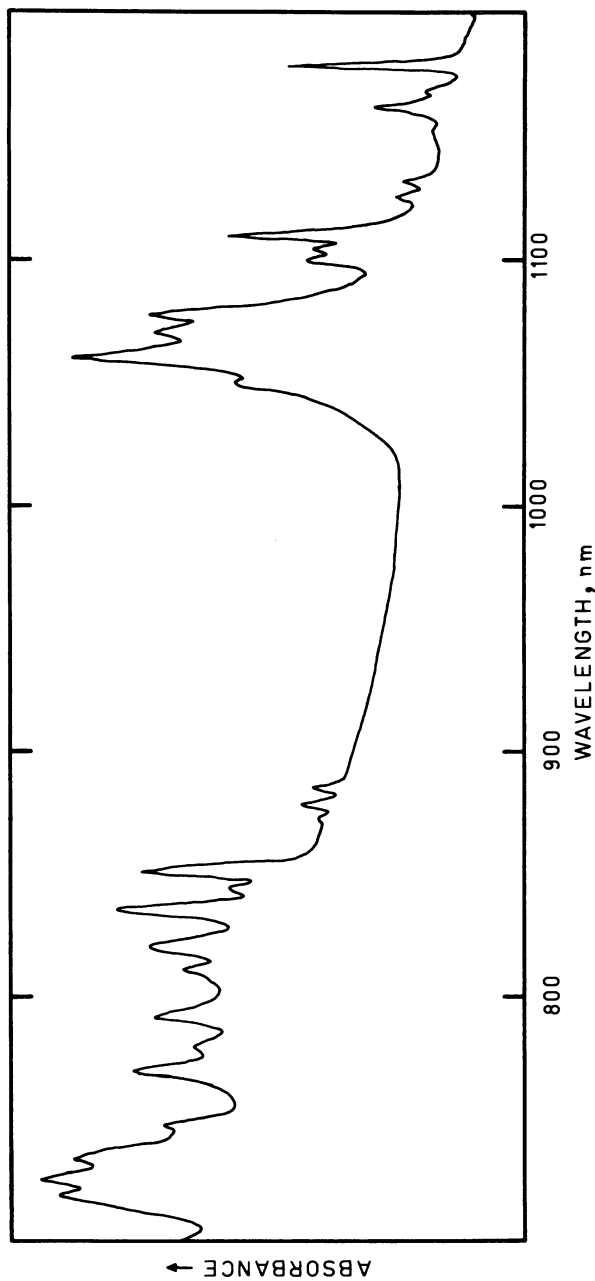


Figure 5. Near-IR spectrum of I, reprinted with permission from Ref. 22, copyright 1982, American Chemical Society.

the polymer, except that numerous sharp peaks are superimposed on what would correspond to the broad absorptions of the polymer.

Gaseous PuCl_4 at 928°C has been examined spectroscopically (30). Comparison of its spectrum with that of I once again shows similarities although the relatively broad peaks in the spectrum of PuCl_4 which correspond to the families of peaks in the spectrum of I are shifted to lower energies. The fact that the spectra of Pu(IV) are similar under such widely differing conditions suggests that these transitions may be insensitive to the environment of the central atom.

Conclusions

We have investigated the hydrothermal hydrolytic behavior of Pu(IV) sulfate solutions in the temperature range $140\text{--}200^\circ\text{C}$. The only crystalline phase which has been isolated has the formula $\text{Pu}_2(\text{OH})_2(\text{SO}_4)_3(\text{H}_2\text{O})_4$. The appearance of this phase is quite remarkable because under similar conditions the other actinides which have been examined form phases of different composition ($\text{M}(\text{OH})_2\text{SO}_4$, $\text{M}=\text{Th}, \text{U}, \text{Np}$). Thus, plutonium apparently lies at that point in the actinide series where the actinide contraction influences the chemistry such that elements in identical oxidation states will behave differently. The chemistry of plutonium in this system resembles that of zirconium and hafnium more than that of the lighter tetravalent actinides. Structural studies do reveal a common feature among the various hydroxysulfate compounds, however, i.e., the existence of double hydroxide bridges between metal atoms. This structural feature persists from zirconium through plutonium for compounds of stoichiometry $\text{M}(\text{OH})_2\text{SO}_4$ to $\text{M}_2(\text{OH})_2(\text{SO}_4)_3(\text{H}_2\text{O})_4$. Spectroscopic studies show similarities between $\text{Pu}_2(\text{OH})_2(\text{SO}_4)_3(\text{H}_2\text{O})_4$ and the Pu(IV) polymer and suggest that common structural features may be present.

Acknowledgment

This work was performed under the auspices of the Office of Basic Energy Sciences, Division of Nuclear Sciences, U. S. Department of Energy under contract number W-31-109-ENG-38.

Literature Cited

1. Lundgren, G. Ark. Kemi 1950, 2, 535.
2. Lundgren, G. Ark. Kemi 1952, 4, 421.
3. Lundgren, G. Ark. Kemi 1953, 5, 349.
4. Wester, D.W.; Mulak, J.; Banks, R.; Carnall, W.T. in press.
5. McWhan, D. B.; Lundgren, G. Inorg. Chem. 1966, 5, 284.
6. Motov, D.L.; Ritter, M.P. Russ. J. Inorg. Chem. 1968, 13, 1339.
7. Chekmarev, A.M.; Molokanova, L.G.; Kharlambus, L.P.; Yagodin, G.A. Russ. J. Inorg. Chem. 1978, 23, 1474.

8. Hansson, M. Acta Chem. Scand. 1973, 27, 2614.
9. Vinarov, I.V.; Kovaleva, E.I. Russ. J. Inorg. Chem. 1968, 13, 1024.
10. Motov, D.L.; Ritter, M.P. Russ. J. Inorg. Chem. 1968, 13, 879.
11. Hansson, M.; Lundgren, G. Acta Chem. Scand. 1968, 22, 1683.
12. Hansson, M. Acta Chem. Scand. 1969, 23, 3541.
13. Hansson, M. Acta Chem. Scand. 1973, 27, 2455.
14. Rogachev, D.L.; Antsyshkina, A.S.; Porai-Koshits, M.A. Zh. Strukt. Khim. 1972, 13, 260.
15. Trofimov, G.V.; Belokoskov, V.I. Russ. J. Inorg. Chem. 1968, 13, 135.
16. Trofimov, G.V. Russ. J. Inorg. Chem. 1968, 13, 1457.
17. Lundgren, G. Ark. Kemi 1954, 6, 59.
18. Fahey, J.A.; Williams, G.J.B.; Haschke, J.M. "The Rare Earths in Modern Science and Technology"; McCarthy, G.J., Rhyne, J.J., Silber, H.B. Eds.; Plenum: New York, 1980, Vol. 2, 181.
19. Lance-Gomez, E.T.; Haschke, J.M.; Butler, W.; Peacor, D.R. Acta Crystallogr. 1978, B34, 758.
20. Lance-Gomez, E.T.; Haschke, J.M. J. Solid State Chem. 1978, 23, 275.
21. Haschke, J.M.; Eyring, L. Inorg. Chem. 1971, 10, 2267.
22. Wester, D.W. Inorg. Chem. 1982, 21, 3382.
23. Kierkegaard, P. Acta Chem. Scand. 1956, 10, 599.
24. Aldred, A.T.; Koprowicz, L.; Mulak, J.; Weglowski, S.; Wrobel, B. Proc. 11th Journees des Actinides 1981, p. 169.
25. Lloyd, M.H.; Haire, R.G. Radiochim. Acta 1978, 25, 139.
26. Toth, L.M.; Friedman, H.A. J. Inorg. Nucl. Chem. 1978, 40, 807.
27. Costanzo, D.A.; Biggers, R.E.; Bell, J.T. J. Inorg. Nucl. Chem. 1973, 35, 609.
28. Baran, B.; Wester, D.W., personal communication.
29. Leontovich, A.M. Opt. Spektrosk. 1957, 2, 695.
30. Gruen, D.M.; DeKock, C.W. J. Inorg. Nucl. Chem. 1967, 29, 2569.

RECEIVED December 21, 1982

Superconductivity and Magnetism in Metallic Plutonium Systems

J. L. SMITH, Z. FISK, and J. O. WILLIS

Los Alamos National Laboratory, Center for Materials Science,
Los Alamos, NM 87545

R. G. HAIRE

Oak Ridge National Laboratory, Oak Ridge, TN 37830

Within the general trend in the behavior across the actinide series, their alloys, and their metallic compounds from superconductors to local moment magnets, the only serious irregularity occurs in some plutonium compounds. These compounds should be magnetic but turn out to be temperature independent paramagnets. The explanation appears to be related to current work on mixed-valent cerium compounds. Plutonium-ameridium alloys also show this behavior. Considerations based upon the plutonium atomic volume in the solids show the greatest promise of explaining this irregularity.

The f-electrons in plutonium metal participate in the metallic bonding and yet are almost localized electrons. This makes plutonium the most complex elemental metal and the most difficult to understand. Most metals become either superconducting or magnetic at low temperatures. Because these phenomena are relatively well understood theoretically, low temperature measurements usually provide a wealth of information on the electronic properties of metals. Plutonium materials have never yielded to such simplification except for a few magnetic compounds. Behavior similar to plutonium also occurs for cerium, manganese, and iron because they possess the same property: electrons that are almost non-conducting and hence almost magnetic. These other elements are still much studied because of this, but even elementary experimental studies of many metallic plutonium systems are still lacking because of its radioactivity.

We shall discuss the role of f-electron bonding in pure plutonium and in its neighboring actinides, the usefulness of the size of the atoms in solids for predicting behavior, and the general trends in superconductivity and magnetism in the periodic table. Then we shall show that within this framework there are many problems remaining in describing the onset of magnetism in

0097-6156/83/0216-0065\$07.00/0
© 1983 American Chemical Society

plutonium materials, yet not for its neighboring actinides. Finally we shall describe our recent efforts to find simple behavior in PuAm alloys.

Plutonium Metal

Figure 1 shows the monoclinic crystal structure of the room temperature α -phase of plutonium (1) with bonds drawn in one plane to emphasize the pseudo-hexagonal layers, that is, the planar six-fold coordination. Each of the eight types of atoms also makes six to ten bonds with atoms in adjacent planes. Figure 1 is a very unusual structure for a metal and deserves some discussion. The fact that the original structure report (2) refers to "covalent" bonds can be taken as a suggestion that this metal demonstrates the continuum between covalent and so-called metallic bonding. Both types involve sharing electrons, and in plutonium, the atomic parentage of the 5f-wavefunction bonding shows itself in the solid. This f-electron bonding is from the spatially extended 5f electrons and is unique to the actinides. (The same situation also occurs in the 4f element cerium under applied pressure (3)). It is the symmetry of the f-electron orbitals which disfavors the traditional close packed structures (fcc, face-centered-cubic, and hcp, hexagonal-close-packed) and distorts α -Pu from an hcp crystal structure.

In fact this covalent-like structure does not make a particularly good metal. Its room-temperature resistance is high, and it is very brittle. The bond lengths fall into a bimodal distribution with short bonds of 2.57-2.78 Å and long bonds of 3.19-3.71 Å with the short bonds of atoms numbered 2 through 7 all falling within one hemisphere (1). It is as though f-electron bonding must predominate in the short bonds. Simple models have been made that estimate atomic volumes in the actinide metals with and without an f-contribution (4). It seems likely that this approach could be extended to predict bond lengths with and without an f-contribution to check if this is the cause for the hemispherical division that occurs in most of the α -Pu atoms. It is clear that f-electrons profoundly influence the plutonium crystal structure.

f-Character in Actinides

The idea of f-bonding was not, to our knowledge, firmly established theoretically until energy band calculations that were both self-consistent and relativistic were available about a decade ago (5,6). Earlier thinking about crystal structures (7,8) and melting points (8) tended to refer to the presence of f-character in the valence bands (9). However the most obvious way to demonstrate the presence and effects of an f-electron energy band is to consider the connected binary alloy phase diagrams shown in Figure 2 (10). The figure begins and ends with ordinary behavior for metals. The middle is marked by the transit of an

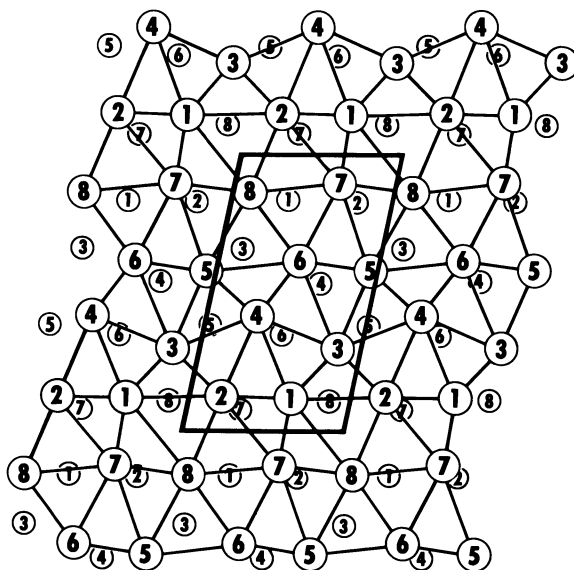


Figure 1. The crystal structure of α -Pu. The large numbered circles represent the eight different types of atoms in one plane of the structure. The smaller circles show the next plane below. The third plane down repeats the first one. The unit cell contains 16 atoms and is indicated by the heavy parallelogram.

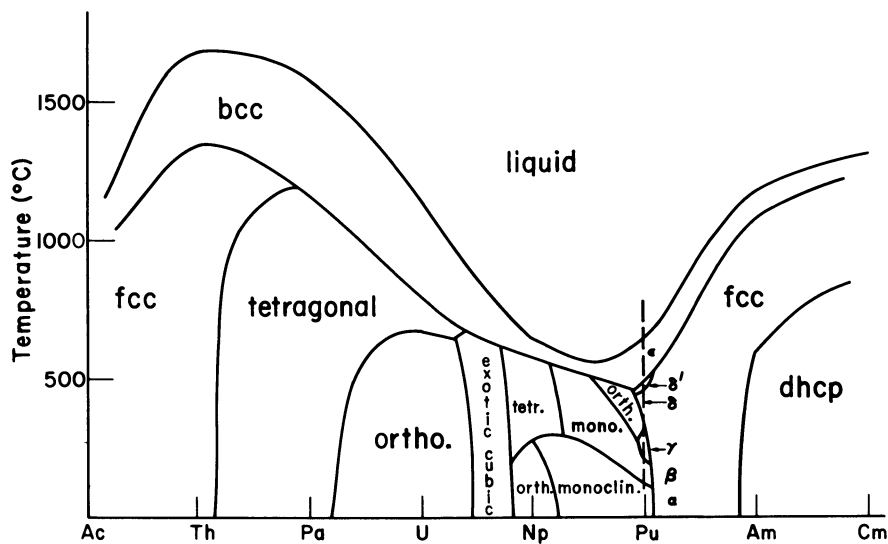


Figure 2. The connected schematic binary alloy phase diagrams for the light actinides. The diagrams for Ac through U and for AmCm are estimates based upon the pure elements. The crystal structures are indicated on the figure, including the standard designations for pure plutonium.

f-band down through the Fermi energy E_F . An f-band simply means that the f-electrons are conducting and bonding; this is an itinerant electron state. So as part of the f-band is clearly occupied a crystallographic distortion sets in at Pa and as the band moves down the crystal structures get more complex until the f-band drops below E_F just past Pu where the fcc structure returns. The melting point is depressed by the f-band (8,9) which also shows its transit. Since at pure plutonium there are six crystallographic allotropes in a 600°C temperature range, the details of the f-band are most subtle just as it drops below E_F . As we shall show later, this is the most difficult behavior in metallic actinide materials to understand. The point of lowest symmetry crystal structures can be shifted to heavier elements with applied pressure because f-electron bonding is enhanced by increased wave function overlap (11). Similarly, diluting the actinide atoms with other atoms in compounds or alloys often simply shifts the interesting region to lighter actinides (12). So pressure and dilution (negative pressure) can be thought of as a third axis to be added in Figure 2.

To be more general, since this discussion is confined to metallic materials there are always spd-electron conduction bands present near E_F . So f-electron bands can be formed by hybridization with these bands as well by direct f-electron wavefunction overlap. This is why dilution with other elements can act like negative pressure even when direct 5f-wave function overlap is nil. Note that cerium is the element that sees the 4f-band transit through the Fermi level (10,12) and manganese and iron see the 3d-band transit (10). The low symmetry structures and low melting points of course occur only in f- and p-band metals because of the parity of the wave functions where the sign of the wave function changes on going through zero (9,10).

Volume Considerations

The presence of f-bands indicates a contribution to bonding which means that the volume of the atoms in the solid is decreased, or equivalently, that the valence increases. By valence in metals, we mean the number of electrons outside the inert gas core minus any localized electrons (which we find by their magnetic moments). There is then a one-to-one correspondence between the size of the atom in the metal and the valence. These have been tabulated by Zachariasen although his counting of f-electrons should be reconsidered (13). Figure 3 shows the metallic radii for the light actinide elements where the departure from the tri-valent line is due to f-electron overlap. A similar plot for a family of compounds shows the same departure due to hybridization where the minimum in size is shifted to the lighter actinides as mentioned earlier. Since both the lanthanides and actinides would be trivalent if there were no f-bands and only localized f-electrons, the departure of sizes is a measure of the band formation (as are the low-symmetry structures and low melting points of Figure 2).

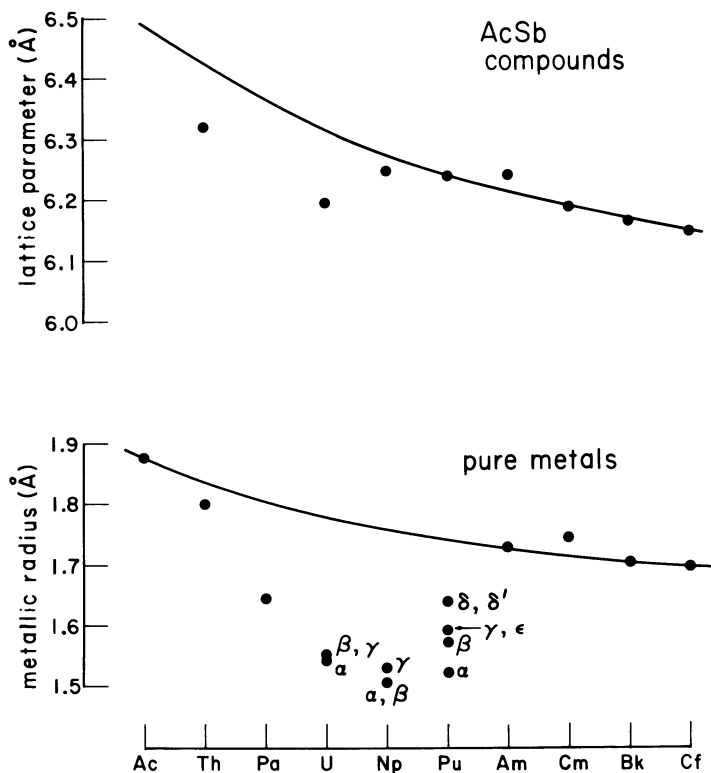


Figure 3. The lattice parameter for the family of rock-salt structure actinide-antimonide compounds is shown where the line is for the corresponding lanthanide compounds. The metallic radii for the light actinide elements are plotted. The smooth line simply connects Ac to the heavy actinides. In both cases the smooth line represents the ideal tri-valent behavior.

Thus the rather easily obtained atomic sizes are the best indicator of what the f-electrons are doing. It has been noted that for all metallic compounds in the literature where an f-band is believed not to occur, that the lanthanide and actinide lattice parameters appear to be identical within experimental error (12). This actually raises the question as to why the lanthanide and actinide contractions (no f-bands) for the pure elements are different. Analogies to the compounds and to the identical sizes of the 4d- and 5d- electron metals would suggest otherwise. The useful point here is that since the 4f- and 5f-compounds have the same lattice parameters when f-bands are not present, it simplifies following the systematics and clearly demonstrates that actinides are worthy of that name.

Figure 3 also shows the metallic radii for the various allotropic crystal structures. The scatter in those sizes increases slowly, is the widest at plutonium, and collapses at americium. This shows that plutonium, with increasing temperature, has the greatest instability towards going tri-valent. It is δ which is the lowest density phase (including the liquid) that must have the least f-bonding. Interestingly its fcc structure is the only one that is called a close-packed-structure and yet it is the loosest packed among the plutonium allotropes. Figure 2 shows that this δ -phase is the tip of the fcc iceberg that should mark the turning off of f-bonding. This bonding is obviously gone in americium because it is clearly tri-valent as it must be to have an exactly nonmagnetic, $J=0$ ground state which is compatible with its superconductivity (14). However, as Figure 2 shows δ -Pu still has an f-band because its radius is still below the tri-valent line. So within the continuous fcc phase field from plutonium to americium, the f-band must slowly disappear. The new experiments described later are the beginning of an effort to investigate the alloys to see if low temperature experiments can track the f-band disappearance. (Room temperature x-rays did not see any features in this alloy system that could demonstrate an f-band except for a modest departure from Vegard's law (15).)

Superconductivity and Magnetism

Across all d- and f-electron transition metal series there is a contraction of the relevant d- or f- wavefunctions. In metallic systems this can cause a crossover from itinerant, bonding electron behavior to localized electron, magnetic moment behavior some where along the series. The position of the crossover allows these five series to be ordered as 4f, 5f, 3d, 4d, and 5d in decreasing ability to form magnetic moments (10). In general, cerium the first element in the 4f series is often magnetic, while no elements in the 4d and 5d series ever make it. When the relevant d- or f-electron is clearly bonding, the elements, compounds, or alloys are usually superconducting. If the electrons are

clearly localized, magnetic moments appear and long range magnetic order often occurs. In between these two cases is an intermediate region where many interesting phenomena occur (10) (including materials that make sparks), but for our purposes here it can be called a nearly magnetic region where spin fluctuations occur as well as concurrent volume (valence) instabilities. The simplest point of view is that the spin fluctuations suppress superconductivity but do not yield magnetic moments.

The pure actinide metals follow this pattern nicely. Protactinium and uranium are superconductors; neptunium and plutonium are spin fluctuation materials; americium has localized f-electrons but happens to be a superconductor because its magnetic moment is identically zero; and the remaining actinides continue to be found to have local moments (12). The actinide metallic compounds also follow this general trend. Brodsky (16) reviewed their magnetic properties most recently. The only serious irregularity in compounds often occurs at plutonium. For example, in $AuCu_3$ -type compounds: URh_3 is a temperature independent paramagnet; $NpRh_3$ has a moment but does not order magnetically; $PuRh_3$ is an antiferromagnet; USn_3 has a moment but does not order; $NpSn_3$ is an antiferromagnet; but $PuSn_3$ is a temperature independent paramagnet. The point is that plutonium compounds that ought to be magnetic, often are not (12). These compounds are clearly extremely intriguing, and the interest is similar to that in the current intense efforts on cerium compounds that are equally puzzling.

The first caveat is that if a plutonium compound has fully localized f-electrons it will resemble its lanthanide analog samarium which never shows simple magnetic behavior. That is, crystal field splitting of the magnetic ground state may make the properties seem unusual. Nonetheless, at low temperatures magnetism should still always be observed. It seems likely that the real answer is that the f-electron moments are compensated by the spins of the spd-conduction electrons as has been discussed for cerium compounds (17). The details of compensating spin and orbital contributions even for cerium with only one f-electron remain uncertain; so it certainly seems possible that the rather small moment of $0.84 \mu_B$ expected for the five f-electrons in plutonium from Russell-Saunders coupling could be similarly compensated. Indeed, there no longer seems to be any doubt that such a phenomenon must be invoked in uranium compounds (18,19) where of course the moment is larger and cannot be completely compensated.

The problem could be stated from another point of view. In an isostructural series the uranium and neptunium compounds tend to be itinerant electron magnets or band magnets (like iron) and their orbital contribution is at least partially quenched. For much heavier actinides we know that the compounds will make local moment magnets with orbital contributions. It is quite possible that in between these two clear cut forms of magnetism that the intermediate case could be dominated by fluctuations, and no recognizable form of magnetism would occur. To state that the

lack of magnetism in many plutonium compounds could be either a compensation or fluctuation does not expose the real problem which is that there is a great deal of experimental work to be done. This is the most intriguing current question for metallic plutonium compounds and it parallels the current effort on cerium compounds.

PuAm Alloys

The presence of the fcc phase field running from spin-fluctuating plutonium to superconducting americium had, until the recent thinking described above, seemed to be a reasonable candidate for superconductivity. The δ -Pu phase has the highest electronic heat capacity (and electronic density of states) of any allotrope of any element (20). This is favorable for superconductivity. On the other hand, americium has an extremely low electronic heat capacity (21) but is a superconductor (presumably from strong electron phonon interactions). Measurements of the superconducting transition temperatures would show how the competition goes between spin-fluctuations and electronic density of states.

We prepared several alloys across the PuAm system by helium arc-melting of pre-weighed milligram quantities of the endpoints. Compositions determined from starting weights usually agreed within a few per cent with compositions determined from the fcc lattice parameter. The X-rays on the unannealed (and sometimes mechanically worked) samples yielded parameters good to $\pm 0.01 \text{ \AA}$ because of line broadening. Faint lines of other phases were seen in most specimens. Low temperature ac susceptibility measurements using the techniques of Smith and Haire (14) down to a temperature of 0.05 K show a rather slow depression of the americium superconducting transition temperature of approximately 0.07 K/% Pu. No sign of any local moment behavior is seen. The alloys were uniformly slightly paramagnetic. Further work is in progress near the pure americium end. The suggestion presented earlier, that on a microscopic scale, plutonium atoms can have their magnetic moments compensated by conduction electrons would be a situation that would inhibit superconductivity. So our results are consistent in that no magnetism or superconductivity was observed. We are planning electrical resistivity measurements on the alloys to attempt to demonstrate the validity of our explanation. The difficulty is that the samples are quite tiny. Nonetheless, it is clear from our preliminary results that the plutonium in the alloys does possess an unusual magnetic character in that superconductivity is suppressed without the appearance of magnetic moments.

Conclusions

There remain three regions of the periodic table where there is no successful theoretical treatment of the onset of magnetism.

They are centered on the elements manganese, cerium, and plutonium. There is much theoretical work underway on all of these elements. The only inadequacy in the experimental side is that there remains a tremendous shortage of even fundamental data on plutonium metallic compounds. The reasons for the shortage are known to all plutonium scientists, but there is also no doubt that there is still a lot of science to be done.

Acknowledgments

This work was performed under the auspices of the U.S.DOE. We are indebted to D. T. Cromer for assistance with Figure 1 and to the late E. A. Kmetko for many discussions.

Literature Cited

1. Zachariasen, W. H.; Ellinger, F. H. Acta Cryst. 1963, 16, 777.
2. Zachariasen, W. H.; Ellinger, F. H. J. Chem. Phys. 1957, 27, 811.
3. Zachariasen, W. H. Proc. Nat. Acad. Sci. 1978, 75, 1066.
4. Johansson, B.; Skriver, H. L. J. Magnetism Mag. Mater., in press.
5. Kmetko, E. A.; Hill, H. H. "Plutonium 1970 and Other Actinides"; Miner, W.N., Ed., AIME, 1970, p. 233.
6. Freeman, A. J.; Koelling, D. D., "The Actinides: Electronic and Related Properties"; Freeman, A. J.; Darby, J. B., Eds., Academic, 1974, Vol. I, p. 51.
7. Friedel, J. J. Phys. Rad. 1958, 19, 573.
8. Matthias, B. T.; Zachariasen, W. H.; Webb, G. W.; Engelhardt, J. J. Phys. Rev. Lett. 1967, 18, 781.
9. Kmetko, E. A.; Hill, H. H. J. Phys. F 1976, 6, 1025.
10. Smith, J. L.; Kmetko, E. A. J. Less Common Metals, in press.
11. Roof, R. B.; Haire, R. G.; Schiferl, D.; Schwalbe, L. A.; Kmetko, E. A.; Smith, J. L. Science 1980, 207, 1353.
12. Smith, J. L.; Fisk, Z. J. Appl. Phys., in press.
13. Zachariasen, W. H. J. Inorg. Nucl. Chem. 1973, 35, 3485.
14. Smith, J. L.; Haire, R. G. Science 1978, 200, 535.
15. Ellinger, F. H.; Johnson K. A.; Struebing, V. O. J. Nucl. Mat. 1966, 20, 83.
16. Brodsky, M. B. Rep. Prog. Phys. 1978, 41, 103.
17. Lawrence, Jon J. Appl. Phys. 1982, 53 (3), 2117.
18. Holden, T. M.; Buyers, W. J. L.; Svensson, E. C.; Jackman, J. A.; Murray, A. F.; Vogt, O.; DuPlessis, P. De V. J. Appl. Phys. 1982, 53 (3), 1967.
19. Reihl, B.; Martensson, N.; Vogt, O. J. Appl. Phys. 1982, 53 (3), 2008.
20. Stewart, G. R.; Elliott, R. O. "Actinides-1981", LBL Report 12441, 1981, p. 206.
21. Smith, J. L.; Stewart, G. R.; Huang, C. Y.; Haire, R. G. J. de Phys. 1979, 40 (C-4), 138.

RECEIVED December 29, 1982

Thermodynamics of Plutonium Halides and Halogeno Complexes in the Solid State and in Aqueous Media

J. FUGER

University of Liège (Sart Tilman), Laboratory of Analytical Chemistry and Radiochemistry, B-4000 Liège, Belgium

The thermodynamic data on the binary halides, oxyhalides and halogeno-complexes of plutonium in the solid state as well as halide complexes in aqueous solutions are critically reviewed and areas which require further studies are identified. For a number of compounds that lack experimental data, thermodynamic parameters are estimated, in connection with existing results for other actinides. Thermodynamic relationships with other actinides are also used to predict the stability for a number of compounds which have not yet been prepared. Our information concerning the aqueous halogeno-complex species contrasts with the rather satisfactory situation prevailing in the case of solid halides. A thorough literature survey indicates that experimental data on halide complexes in aqueous solution are limited in number and sometimes are contradictory; in addition, the results are scattered over a wide range of media and ionic strengths. However, in a number of instances, extrapolation to standard conditions appears to be feasible. The enthalpy of formation data that can be derived from temperature dependence measurements of the stability constants are discussed and the thermodynamic parameters associated with the formation of the plutonium complexes are compared with the corresponding data for other actinides.

A critical assessment of the chemical thermodynamic properties of the actinides and their compounds is presently being prepared by an international team of scientists under the auspices of the International Atomic Energy Agency (Vienna). As a result of this effort, four publications (1, 2, 3, 5) have already become available and a further ten (4, 6-14), including the halides (8) and aqueous complexes with inorganic ligands (12),

0097-6156/83/0216-0075\$07.00/0
© 1983 American Chemical Society

are in various stages of preparation. The present discussion will therefore be carried out in a manner that preserves the consistency with the published IAEA data and will reflect the actual status of the assessment work which is under way. Unless otherwise mentioned, auxiliary thermodynamic data are taken from CODATA-1977 (15) Recommended Key Values for Thermodynamics or compatible with the CODATA selection (16). Throughout the various tables in this paper the sign X refers to a known compound for which the author feels that no thermodynamic result can be reported with sufficient confidence. In the Tables, values in square brackets are new estimates. For the inorganic aqueous ions all available experimental data are tabulated; the presently recommended values are boxed. Unless otherwise specified all data are reported for 298 K.

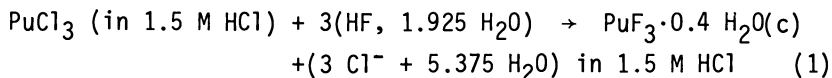
Solid Compounds

Compounds with Fluorine. The available data on plutonium fluorides and related species are listed in Table I.

Table I
Thermodynamic data associated with the solid
plutonium fluorides and oxyfluorides at 298 K.

	$-\Delta H_f^\circ$ kJ.mol ⁻¹	S° J.K ⁻¹ .mol ⁻¹		$-\Delta H_f^\circ$ kJ.mol ⁻¹	S° J.K ⁻¹ .mol ⁻¹
PuF ₃	1585.7(2.9)	126.11(0.38)	PuOF	[1139(20)]	[88(21)]
PuF ₄	1846(21)	147.23(.38)			
PuF ₆	1862(29)	221(17)	PuO ₂ F ₂	X	X
			PuOF ₄	X	X

The enthalpy of formation of PuF₃(c) is based on the measurements by Westrum and Eyring (17) of the enthalpy of precipitation according to reaction (1)

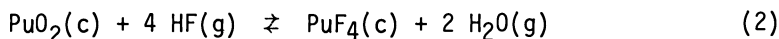


knowing $\Delta H_f^\circ(\text{PuCl}_3, \text{c})$, and the enthalpy of solution of this compound in 1.5 M HCl, $-123.4 + 0.4 \text{ kJ.mol}^{-1}$ (18). The enthalpy for reaction (1) was reported as $-30.1 + 1.3 \text{ kJ.mol}^{-1}$ when the enthalpy of solution of the excess HF used to precipitate the fluoride had been subtracted. In their original study Westrum and Eyring (17) had assumed that the precipitate was anhydrous but a subsequent detailed study by Jones (19) indicated that indeed the precipitate should have contained 0.4 H₂O. To obtain $\Delta H_f^\circ(\text{PuF}_3, \text{c})$, the

enthalpy of dehydration of $\text{PuF}_3 \cdot 0.4 \text{H}_2\text{O}(\text{c})$ has to be taken in account. This can be done using a value of $-3.8 + 2.1 \text{ kJ.mol}^{-1}$ estimated by analogy with recent data (20) on the dehydration of lanthanide trifluorides containing 0.4 to 1 H_2O , instead of the value of $14.2 + 2.1 \text{ kJ.mol}^{-1}$ taken from Rand (21) by analogy with the corresponding uranium and thorium tetrafluoride hydrates. The obtained value $\Delta H_f^\circ(\text{PuF}_3, \text{c}) = -1585.7 + 2.9 \text{ kJ.mol}^{-1}$ cannot be considered as entirely satisfactory as the reliability of the adopted value for the enthalpy of dehydration is not demonstrated. The only experimentally known enthalpies of formation for the actinide trifluorides are $\Delta H_f^\circ(\text{PuF}_3, \text{c})$ and $\Delta H_f^\circ(\text{UF}_3, \text{c})$: accuracy is therefore essential if these two data are used to estimate the enthalpies of formation of the other trifluorides. The low temperature heat capacity measurements of Osborne et al. (22) using $^{242}\text{PuF}_3(\text{c})$ yield $S^\circ(\text{PuF}_3, \text{c}) = 126.11 + 0.38 \text{ J.K}^{-1}.\text{mol}^{-1}$.

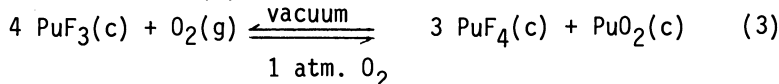
Our information on $\Delta H_f^\circ(\text{PuF}_4, \text{c})$ is based on high temperature reactions (600-900 K) already assessed in 1966 by Rand (21) and on extrapolation of uranium and thorium tetrafluoride data. Thus we have

a) the equilibrium described by reaction (2)



studied by Johns (23) leading to $\Delta H_f^\circ(\text{PuF}_4, \text{c}) = -1843 + 21 \text{ kJ.mol}^{-1}$ through the use of appropriate entropy and ΔG values.

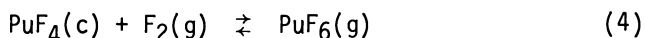
b) the equilibrium (3) at 873 K



studied by Fried and Davidson (24) yielding $\Delta H_f^\circ(\text{PuF}_4, \text{c}) = -1826 \pm 21 \text{ kJ.mol}^{-1}$.

c) the consideration of the difference $\{\Delta H_f^\circ(\text{MF}_4, \text{c}) - \Delta H_f^\circ(\text{M}^{4+}, \text{aq})\}$ as a function of the ionic radii of the quadrivalent actinide ion (25). Knowing experimentally $\{\Delta H_f^\circ(\text{ThF}_4, \text{c}) - \Delta H_f^\circ(\text{Th}^{4+}, \text{aq})\} = -1328.8 + 8.8 \text{ kJ.mol}^{-1}$, $\{\Delta H_f^\circ(\text{UF}_4, \text{c}) - \Delta H_f^\circ(\text{U}^{4+}, \text{aq})\} = -1323.0 + 5.4 \text{ kJ.mol}^{-1}$ (2, 8) and the ionic radii $r(\text{Th}^{4+}) = 0.94 \text{ \AA}$, $r(\text{U}^{4+}) = 0.89 \text{ \AA}$ and $r(\text{Pu}^{4+}) = 0.86 \text{ \AA}$, one obtains $\{\Delta H_f^\circ(\text{PuF}_4, \text{c}) - \Delta H_f^\circ(\text{Pu}^{4+}, \text{aq})\} = -1319.6 + 13.0 \text{ kJ.mol}^{-1}$ from a linear extrapolation. With $\Delta H_f^\circ(\text{Pu}^{4+}, \text{aq}) = -536.4 + 3.3 \text{ kJ.mol}^{-1}$ (2) one obtains $\Delta H_f^\circ(\text{PuF}_4, \text{c}) = -1856 + 13 \text{ kJ.mol}^{-1}$.

The value listed in Table I is a weighted average of the three above paths. Thus $\Delta H_f^\circ(\text{PuF}_4, \text{c}) = -1846 + 21 \text{ kJ.mol}^{-1}$. These large uncertainty limits are unsatisfactory in view of the technological importance of $\text{PuF}_4(\text{c})$. The entropy of $\text{PuF}_4(\text{c})$, $147.23 + 0.38 \text{ J.K}^{-1}.\text{mol}^{-1}$, is based on the low temperature heat capacity measurements of Osborne et al. (26) using the long-lived isotope ^{242}Pu . This value is in rather sharp disagreement with the value of $161.9 + 2.1$ deduced by Rand (21) from the thermodynamic parameters associated with equilibrium (4)



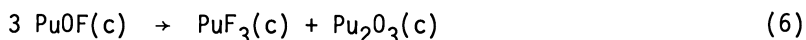
measured by Trevorrow et al. (27) and, in less detail, by Weinstock and Malm (28) and Florin et al. (29). This observation stresses once more the need of the low temperature measurements for the determination of accurate entropy data at 298 K as opposed to the use of indirect methods such as temperature equilibria. Yet, $\text{PuF}_3(\text{c})$ and $\text{PuF}_4(\text{c})$ are the only halogen-containing plutonium compounds for which such low temperature heat capacity data are available. In the particular case of $\text{PuF}_4(\text{c})$ these results cast some doubt on the accuracy of the thermodynamic parameters associated with the formation of $\text{PuF}_6(\text{c})$. The data of Trevorrow et al. (27) yield $\Delta H_4 = 29 \text{ kJ}\cdot\text{mol}^{-1}$ by second law analysis and $37 \text{ kJ}\cdot\text{mol}^{-1}$ by third law treatment. Although the agreement is poor, the average of these two data yield $\Delta H_f^\circ(\text{PuF}_6, \text{g}) = -1813 + 29 \text{ kJ}\cdot\text{mol}^{-1}$. These large uncertainty limits also take in account the uncertainty in the knowledge of $\Delta H_f^\circ(\text{PuF}_4, \text{c})$. The vapor pressure data of both crystalline and liquid PuF_6 have thoroughly been assessed by Rand (21). He reports for relation (5) between 260 and 325 K

$$\text{PuF}_6(\text{c}) \rightarrow \text{PuF}_6(\text{g}) \quad \Delta G_5 = 62760 - 456.1 T + 105.9 T \log T \quad (5)$$

(kJ·mol⁻¹)

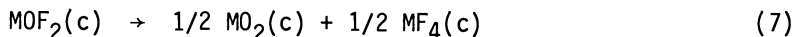
from which, with a $\Delta C_p = -46 \text{ J}\cdot\text{K}^{-1}\cdot\text{mol}^{-1}$, he deduces $\Delta H_5(298) = 49.0 \text{ kJ}\cdot\text{mol}^{-1}$ and $\Delta S_5(298) = 148.1 \text{ J}\cdot\text{K}^{-1}\cdot\text{mol}^{-1}$. From these data, $\Delta H_f^\circ(\text{PuF}_6, \text{c})$ reported above and $S^\circ(\text{PuF}_6, \text{g}) = 369.0 + 0.8 \text{ J}\cdot\text{K}^{-1}\cdot\text{mol}^{-1}$ obtained from calculations of the thermodynamic functions of PuF_6 as an ideal gas (30) one deduces $\Delta H_f^\circ(\text{PuF}_6, \text{c}) = -1862 + 29 \text{ kJ}\cdot\text{mol}^{-1}$ and $S^\circ(\text{PuF}_6, \text{c}) = 221 + 17 \text{ J}\cdot\text{K}^{-1}\cdot\text{mol}^{-1}$. It is worth noting that PuF_6 is the only hexavalent plutonium compound for which thermodynamic data are known experimentally.

Although a number of oxyfluorides of plutonium are known, no experimentally based thermodynamic data are available for these compounds. $\text{PuOF}(\text{c})$ was only obtained accidentally during the attempted reduction of $\text{PuF}_3(\text{c})$ by atomic hydrogen (31) and also during an attempted measurement of the melting point of plutonium metal. An estimate of its enthalpy of formation can be obtained by analogy with the $\text{PuCl}_3\text{-PuOCl}$ and $\text{PuBr}_3\text{-PuOBr}$ systems: using the relationship $\{\Delta H_f^\circ(\text{PuOX}, \text{c}) - \Delta H_f^\circ(\text{PuX}_3, \text{c})/3\}$, with $X = \text{Cl}$ or Br , we obtain $-611.0 + 1.7 \text{ kJ}\cdot\text{mol}^{-1}$ and $-608.5 + 4.2 \text{ kJ}\cdot\text{mol}^{-1}$ for the chloride and the bromide systems, respectively. Accepting a value of $-610 + 20 \text{ kJ}\cdot\text{mol}^{-1}$ for the fluoride system and using the above value for $\Delta H_f^\circ(\text{PuF}_3, \text{c})$, we obtain $\Delta H_f^\circ(\text{PuOF}, \text{c}) = -1139 + 20 \text{ kJ}\cdot\text{mol}^{-1}$. Taking an estimate of $S^\circ(\text{PuOF}, \text{c}) = 88 + 21$ based on accepted entropy data for $\text{PuCl}_3(\text{c})$, $\text{PuOCl}(\text{c})$, $\text{PuBr}_3(\text{c})$ and $\text{PuOBr}(\text{c})$ and using $\Delta H_f^\circ(\text{Pu}_2\text{O}_3, \text{hex}) = -1710 + 13 \text{ kJ}\cdot\text{mol}^{-1}$ (10, 32) and $S^\circ(\text{Pu}_2\text{O}_3, \text{hex}) = 163.02 + 0.65 \text{ J}\cdot\text{K}^{-1}\cdot\text{mol}^{-1}$ (33) we calculate for reaction (6):



$\Delta G_6 = + 113 + 60 \text{ kJ.mol}^{-1}$, a value which accounts for the stability of PuOF towards decomposition into $\text{PuF}_3(\text{c})$ and $\text{Pu}_2\text{O}_3(\text{c})$.

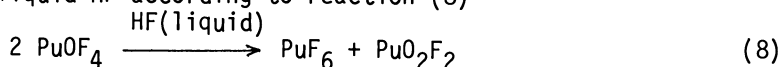
$\text{PuOF}_2(\text{c})$ has not been stabilized so far and only the thorium and uranium analogs have been reported. These compounds are of marginal stability towards decomposition according to reaction (7)



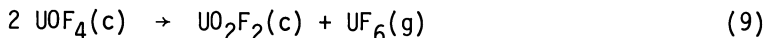
since the available thermodynamic data (8) yield $\Delta G_7 = + 6.5 + 3.5 \text{ kJ.mol}^{-1}$ and $\Delta G_7 = + 6.6 + 7.5 \text{ kJ.mol}^{-1}$ for the thorium and uranium system, respectively. The limited accuracy of the available data for $\text{ThOCl}_2(\text{c})$ and especially $\text{UOCl}_2(\text{c})$ precludes quantitative prediction of the stability of $\text{PuOF}_2(\text{c})$. However, the equilibrium (3) reported above indicates that, most probably, $\text{PuOF}_2(\text{c})$ should have a very narrow range of stability, if any.

$\text{PuO}_2\text{F}_2(\text{c})$ is well characterized as are its uranium to americium homologues (34). Unfortunately, thermodynamic data are available for $\text{UO}_2\text{F}_2(\text{c})$ only (8) and therefore the estimates of the thermodynamic parameters associated with the formation of $\text{PuO}_2\text{F}_2(\text{c})$ would involve large uncertainty limits. Although $\text{PuO}_2\text{F}_2(\text{c})$ formation has initially been observed upon controlled hydrolysis of $\text{UF}_6(\text{c})$, the fluorination of $\text{PuO}_3 \cdot 0.8 \text{H}_2\text{O}(\text{c})$ has been suggested as a better preparative method (34).

Another oxyfluoride, $\text{PuOF}_4(\text{c})$, has recently been reported (35) as a product of controlled hydrolysis of PuF_6 dissolved in anhydrous HF and precipitation from the solution. Again, no thermodynamic data are available but it appears that the compound is of very limited stability: although stable in the solid state at room temperature, it is reported to decompose in the presence of liquid HF according to reaction (8)



when no excess of PuF_6 is initially present. This behaviour may be compared to that of the corresponding neptunium and uranium compounds which remain stable in anhydrous HF. NpOF_4 is reported (36) to decompose into $\text{NpF}_6(\text{g})$ and $\text{NpO}_2\text{F}_2(\text{c})$ above 373 K while $\text{UOF}_4(\text{c})$ undergoes the same reaction at 523 K (37) or 473 K (38) and at lower temperatures yields $\text{U}_2\text{O}_3\text{F}_6(\text{c})$ and $\text{UF}_6(\text{g})$ (39). A recent solution calorimetric study by O'Hare and Malm (40) indicates that the enthalpy change at 298 K for reaction (9)

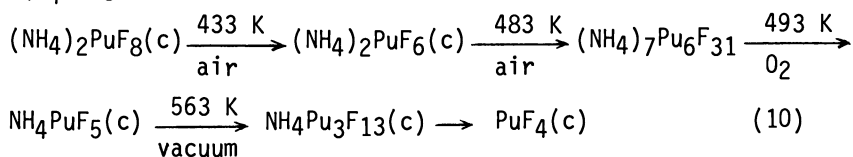


is $\Delta H_9 = 46.3 + 5.5 \text{ kJ.mol}^{-1}$. This value is very close to the enthalpy of sublimation of UF_6 at that temperature. O'Hare and Malm conclude that, on the thermochemical point of view, $\text{UOF}_4(\text{c})$ behaves as a loosely bound 1:1 complex of $\text{UO}_2\text{F}_2(\text{c})$ and $\text{UF}_6(\text{c})$. If this is the case, a similar situation should prevail for $\text{PuOF}_4(\text{c})$.

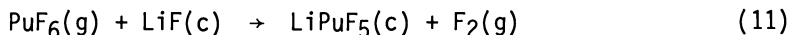
There is a wealth of information concerning preparative and structural aspects of the fluoro- and oxyfluorocomplexes of

plutonium with alkali metal, ammonium and alkaline earth metal ions, containing plutonium in the +3 to +6 valency state (34, 41). $M(I)Pu(III)F_4$, $M(I)Pu(III)_2F_7$, $M(I)Pu(IV)F_5$, $M(I)_2Pu(IV)F_6$, $M(I)_3Pu(IV)F_7$, $M(I)_4Pu(IV)F_8$, $M(I)Pu(IV)_2F_9$, $M(I)_3Pu(IV)_3F_{13}$, $M(I)_7Pu(IV)_6F_{31}$, $M(II)Pu(IV)F_6$, $M(I)Pu(V)F_6$, $M(I)_2Pu(V)F_7$, $M(I)Pu(V)O_2F_2$, $M(I)Pu(VI)O_2F_4$ and various hydrates are examples of such compounds.

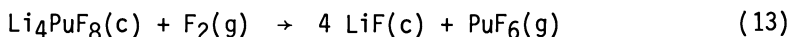
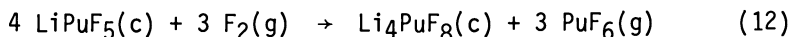
It is worth noting that although $PuF_5(c)$ has not been characterized pentavalent fluorocomplexes are well known. In the hexavalent state only oxyfluorocomplexes are known. However, thermodynamic data on these species are almost completely lacking. The thermal decomposition study (42) of the quadrivalent complex $(NH_4)_4PuF_8$ according to scheme (10)



is quite similar to that observed by the same authors for the corresponding uranium salt. These experiments, however, do not yield quantitative information concerning the thermodynamic stability of the various observed species. It is also interesting to note that, when contacted with $LiF(c)$ between 373 and 973 K, $PuF_6(g)$ reduces to the quadrivalent state (43, 44). The most extensive study is that of Trevorrow et al. (44) who indicate that, at 573 K, the observed reaction is described by relation (11)



In the temperature range 623–723 K, the process is reported to be reversible with the intermediate formation of $Li_4PuF_8(c)$ according to reactions (12) and (13)



For reaction (13), at 673 K, constants $[P(UF_6)/P(F_2)]$ between 10^{-3} and 6.25×10^{-5} (44) or between 2.5×10^{-5} and 6.7×10^{-5} (43) were reported. When contacted with $NaF(c)$, $PuF_6(g)$ is also reported to reduce to the quadrivalent state with formation of $Na_3PuF_7(c)$ (45).

Compounds with Chlorine. The available thermodynamic data on plutonium chlorides and related species are listed in Table II.

The enthalpy of formation of $PuCl_3(c)$ is derived from the measurement of the enthalpy of solution of this compound in 6 M HCl according to reaction (14)

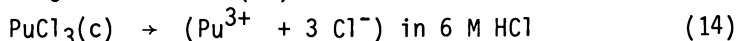


Table II

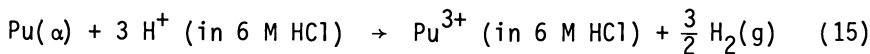
Thermodynamic data associated with the solid plutonium chlorides, oxychlorides and chlorocomplexes at 298 K.

	$-\Delta H_f^\circ$ kJ.mol ⁻¹	S° J.K ⁻¹ .mol ⁻¹		$-\Delta H_f^\circ$ kJ.mol ⁻¹	S° J.K ⁻¹ .mol ⁻¹
PuCl ₃	959.8 (1.7)	163.6 (4.2)	PuOCl	930.9 (1.7)	104.2 (5.4)
PuCl ₃ .6H ₂ O	2773.6 (2.1)	420.1 (5.9)			
Cs ₂ NaPuCl ₆	2294.9 (2.5)	X			

PuCl ₄ (unstable)	963.6 (7.5)				
Cs ₂ PuCl ₆	1978.6 (8.4)	X			

Cs ₂ PuO ₂ Cl ₄	X	X	PuO ₂ Cl ₂ .6H ₂ O	X	X

obtained by Robinson and Westrum (18) as $\Delta H_{14} = -92.68 + 0.42$ kJ.mol⁻¹. Use, as additional data, of the enthalpy of solution of α -Pu in 6 M HCl according to reaction (15)



assessed (2) as $\Delta H_{15} = -592.0 + 1.7$ kJ.mol⁻¹ and of the partial molar enthalpy of formation of hydrochloric acid in 6 M HCl ($-153.43 + 0.042$ kJ.mol⁻¹) (16) leads to $\Delta H_f^\circ(\text{PuCl}_3, \text{c}) = -959.8 + 1.7$ kJ.mol⁻¹. The entropy of PuCl₃(c) at 298 K is based on three consistent estimation paths given by Rand (21) :

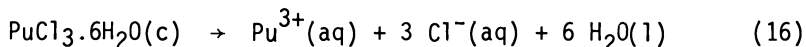
a) Latimer's method (46) with the entropy of the plutonium atom in the compound taken as 75.7 J.K⁻¹.mol⁻¹ and the entropy of each chloride being taken as 28.9 J.K⁻¹.mol⁻¹, yields $S^\circ(\text{PuCl}_3, \text{c}, 298) = 162.3$ J.K⁻¹.mol⁻¹. The value chosen for the entropy of the plutonium atom is obtained from the only experimentally known entropy of a trivalent plutonium halide, PuF₃, (126.11 + 0.38) J.K⁻¹.mol⁻¹ using a value of 16.7 J.K⁻¹.mol⁻¹ for the entropy of each fluorine atom.

b) Assuming that the entropy of formation of PuCl₃ and UCl₃ are identical, with $S^\circ(\text{U}, \alpha, 298) = (50.21 + 0.13)$ J.K⁻¹.mol⁻¹ and $S^\circ(\text{Pu}, \alpha, 298) = (56.15 + 0.42)$ J.K⁻¹.mol⁻¹ (1) and $S^\circ(\text{UCl}_3, \text{c}, 298) = (159.0 + 0.8)$ J.K⁻¹.mol⁻¹ (8), one obtains $S^\circ(\text{PuCl}_3, \text{c}, 298) = 164.8$ J.K⁻¹.mol⁻¹.

c) Assuming that the entropy difference between PuCl_3 and UCl_3 is due to the spin only contribution of the additional electrons gives $S^\circ(\text{PuCl}_3, \text{c}, 298) = 163.2 \text{ J.K}^{-1}.\text{mol}^{-1}$.

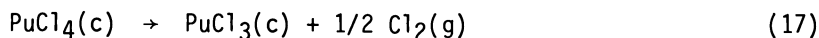
The average of these three estimates yields the accepted value $S^\circ(\text{PuCl}_3, \text{c}, 298) = (163.6 + 4.2) \text{ J.K}^{-1}.\text{mol}^{-1}$. An experimental datum is nevertheless desirable.

The enthalpy of formation of $\text{PuCl}_3.6\text{H}_2\text{O}(\text{c})$ is based on the enthalpy of solution in water according to reaction (16)



for which Hinchey and Cobble (47) report a value of $-34.56 \pm 0.84 \text{ kJ.mol}^{-1}$ (the uncertainty limits being increased compared to the original paper). Using auxiliary data, this value leads to $\Delta H_f^\circ(\text{PuCl}_3.6\text{H}_2\text{O}, \text{c}) = -2773.6 + 2.1 \text{ kJ.mol}^{-1}$. Hinchey and Cobble also measured the solubility of the hexahydrate in water. They used activity coefficients for the solute and activity values for the water which were estimated by analogy with existing data on the isomorphous samarium chloride hexahydrate (48). From these data Hinchey and Cobble (47) report $\Delta G_{16}^\circ = 30.1 + 0.8 \text{ kJ.mol}^{-1}$ (uncertainty limits being ours). $S^\circ(\text{PuCl}_3.6\text{H}_2\text{O}, \text{c})$ can be estimated as $420.1 + 5.9 \text{ J.K}^{-1}.\text{mol}^{-1}$ from the entropy value of the corresponding isoelectronic samarium salt $S^\circ(\text{SmCl}_3.6\text{H}_2\text{O}, \text{c}) = 414.2 \text{ J.K}^{-1}.\text{mol}^{-1}$ (49) by including a contribution (50) of $5.8 \text{ J.K}^{-1}.\text{mol}^{-1}$ for the greater mass of plutonium. Use of various auxiliary data for $S^\circ(\text{Cl}^{-}, \text{aq})$, $S^\circ(\text{H}_2\text{O}, \text{l})$ (16) leads to $S^\circ(\text{Pu}^{3+}, \text{aq}) = -184.5 + 8.4 \text{ J.K}^{-1}.\text{mol}^{-1}$. This value, adopted in the IAEA assessment (2), serves as basis for the estimation of the entropy of the other trivalent actinide ions. In view of its importance, the assumptions made in its determination should be reduced through additional experiments: in particular, the low temperature heat capacity determination of $\text{PuCl}_3.6\text{H}_2\text{O}(\text{c})$ leading to the entropy of this salts would be of prime interest.

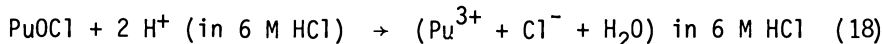
Although PuCl_4 has been well characterized in the gas phase (51) in the temperature range 670-1025 K, all attempts to obtain this compound in the solid state have failed. Use of a plot of the difference $\{\Delta H_f^\circ(\text{MCl}_4, \text{c}) - \Delta H_f^\circ(\text{M}^{4+}, \text{aq})\}$ (2, 8) as a function of the actinide ionic radii (25) (as done above for PuF_4) in the case of thorium, protactinium, uranium and neptunium yields a first path leading to $\Delta H_f^\circ(\text{PuCl}_4, \text{c})$. A second path involves the extrapolation to the plutonium system of the difference $\{\Delta H_{\text{soln}}^\circ(\text{MCl}_4, \text{c}) - \Delta H_{\text{soln}}^\circ(\text{MCl}_3, \text{c})\}$ for the uranium and neptunium systems (2, 8). These two paths give constant values, leading to $\Delta H_f^\circ(\text{PuCl}_4, \text{c}) = -963.6 + 7.5 \text{ kJ.mol}^{-1}$. With this value, knowing $\Delta H_f^\circ(\text{PuCl}_3, \text{c}) = -959.8 \pm 1.7 \text{ kJ.mol}^{-1}$ and assuming for the theoretical reaction (17)



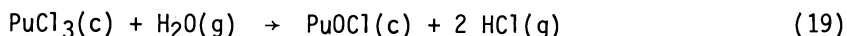
an entropy change $\Delta S_{17} = 73.4 \pm 1.5 \text{ J.K}^{-1}.\text{mol}^{-1}$ identical to that of the corresponding uranium reaction (8), we obtain $\Delta G_{18} = -18.1 \pm 7.7 \text{ kJ.mol}^{-1}$. All data thus indicate that $\text{PuCl}_4(\text{c})$ is

unstable at room temperature towards chlorine evolution. Its synthesis as a solid remains therefore a challenging experiment.

The enthalpy of formation of $\text{PuOCl}(c)$ is based on the determination by Westrum and Robinson (52) of its enthalpy of solution in 6 M HCl according to reaction (18)



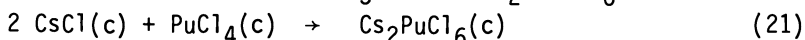
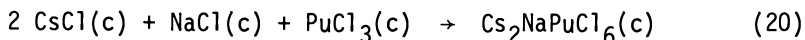
yielding $\Delta H_{18} = -101.13 + 0.42 \text{ kJ}\cdot\text{mol}^{-1}$. This result leads to $\Delta H_f^\circ(\text{PuOCl}, c) = -930.9 + 1.7 \text{ kJ}\cdot\text{mol}^{-1}$. The enthalpy of formation of PuOCl has also been derived from high temperature hydrolysis of $\text{PuCl}_3(c)$ according to reaction (19)



as measured by Sheft and Davidson (53) and Weigel et al. (54). Corrected to 298 K, these results are in excellent agreement (within $4 \text{ kJ}\cdot\text{mol}^{-1}$) with the solution calorimetry result. However, these corrections involve estimated heat capacity data and therefore the solution calorimetry result is preferred. The standard entropy of $\text{PuOCl}(c)$ is derived from the equilibrium constant for reaction (19) above as a function of temperature in the range 814-969 K (53) and 733-893 K (54). With a ΔC_p of $6.3 \text{ J}\cdot\text{K}^{-1}\cdot\text{mol}^{-1}$, as suggested by Rand (21), one obtains $\Delta S_{19} = 125.5 + 3.3 \text{ J}\cdot\text{K}^{-1}\cdot\text{mol}^{-1}$ as average of the two sets of consistent data leading to $S^\circ(\text{PuOCl}, c) = 104.2 + 5.4 \text{ J}\cdot\text{K}^{-1}\cdot\text{mol}^{-1}$.

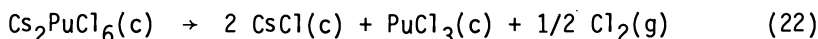
Plutonyl(VI) chloride has only been reported as the hydrate $\text{PuO}_2\text{Cl}_2\cdot 6\text{H}_2\text{O}(c)$ but no thermodynamic data are available on this compound.

Complex chlorides of plutonium (34, 41) do not present such a wide range of formulae as the complex fluorides but we have at hand thermodynamic information on two important species which have also been characterized with other actinides. In table II we have disregarded the complex halides for which no thermodynamic data are available. The enthalpy of formation of $\text{Cs}_2\text{NaPuCl}_6(c)$ (55) and $\text{Cs}_2\text{PuCl}_6(c)$ (56) have been obtained from enthalpy of solution measurements. The selected (8) values are $\Delta H_f^\circ(\text{Cs}_2\text{NaPuCl}_6, c) = -2294.9 + 2.5 \text{ kJ}\cdot\text{mol}^{-1}$ and $\Delta H_f^\circ(\text{Cs}_2\text{PuCl}_6, c) = -1978.6 + 8.4 \text{ kJ}\cdot\text{mol}^{-1}$. For the enthalpy of formation from the binary salts ($\Delta H_{\text{complex}}$) according to reactions (20) and (21)



the above enthalpies of formation yield, respectively, $\Delta H_{20} = -38.5 + 1.7 \text{ kJ}\cdot\text{mol}^{-1}$ and $\Delta H_{21} = -129.7 + 11.3 \text{ kJ}\cdot\text{mol}^{-1}$. There is no value available for another actinide compound of the type $\text{Cs}_2\text{NaAnCl}_6(c)$ although the uranium, neptunium (57), americium (58) and berkelium (59) compounds are known. It is, however, to be expected that $\Delta H_{\text{complex}}$ should increase in magnitude with the

decreasing ionic radii of the actinide, as in the case of the lanthanide series $\Delta H_{\text{complex}}$ varies from $-15.1 \text{ kJ.mol}^{-1}$ for the lanthanum compound to $-106.3 \text{ kJ.mol}^{-1}$ for the lutecium compound (55). Our information is more complete for the $\text{Cs}_2\text{MCl}_6(\text{c})$ compounds as thermodynamic data are available for all the compounds from thorium to plutonium: $\Delta H_{\text{complex}}$ for $\text{Cs}_2\text{ThCl}_6(\text{c})$ is $-76.1 + 1.3 \text{ kJ.mol}^{-1}$ and increases in magnitude to $-129.7 + 11.3 \text{ kJ.mol}^{-1}$ for $\text{Cs}_2\text{PuCl}_6(\text{c})$ as given above. There are no thermodynamic data on $\text{Cs}_2\text{BkCl}_6(\text{c})$ which is not isomorphous with the other compounds of the series (59). The magnitude of $\Delta H_{\text{complex}}$ in the case of $\text{Cs}_2\text{PuCl}_6(\text{c})$ is responsible for the stabilization of quadrivalent plutonium in a chloride environment while $\text{PuCl}_4(\text{c})$ has been shown to be unstable. This is easily shown: if, for reaction (21) above, we take $\Delta S_{21} \geq -30 \text{ J.K}^{-1}.\text{mol}^{-1}$ from the data of Latimer (46) on the entropies of related salts such as $\text{K}_2\text{PtCl}_6(\text{c})$, $\text{K}_2\text{PtBr}_6(\text{c})$, $\text{K}_3\text{IrCl}_6(\text{c})$, ... and use $\Delta S_{17} = 73.4 + 1.5 \text{ J.K}^{-1}.\text{mol}^{-1}$ accepted above, we obtain for the hypothetical reaction (22)



$\Delta S_{22} \leq 103 \text{ J.K}^{-1}.\text{mol}^{-1}$. With the accepted enthalpies of formation we have $\Delta H_{22} = 133.5 + 8.5$ and $\Delta G_{22} \geq 103 \text{ kJ.mol}^{-1}$. Other alkali metal complex chlorides of quadrivalent plutonium have not been unambiguously characterized but, as observed for the thorium (60) and uranium salts (61, 62), one should expect $\Delta H_{\text{complex}}$ to decrease drastically with the decreasing size of the alkali metal cation (63): therefore the difficulty of stabilizing quadrivalent plutonium in such salts should increase with the decreasing ionic size of the alkali metal cation.

Although we have available thermodynamic data for $\text{Cs}_2\text{MO}_2\text{Cl}_4(\text{c})$ compounds with $\text{M} = \text{U}, \text{Np}$ (63) and that $\text{Cs}_2\text{AmO}_2\text{Cl}_4(\text{c})$ has been reported (58, 64), the corresponding plutonium has not been studied, although it is capable of existence (65); as for a number of other plutonium complex halides, analogues containing bulky organic cations (tetramethylammonium, tetraethylammonium, ...) have been reported (34, 41).

Compounds with Bromine and Iodine. The available thermodynamic data on these compounds are listed in Table III.

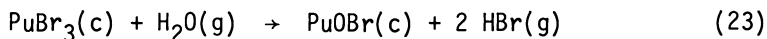
The enthalpy of formation of $\text{PuBr}_3(\text{c})$ rests on three concordant sets of data for the enthalpy of solution of this compound in O_2 -free 6 M HCl (66), 1 M HCl and 0.1 M HCl (67) and comparison with the enthalpy of solution of $\text{PuCl}_3(\text{c})$ in the same media (18). These data yield virtually identical values for the enthalpy of formation of $\text{PuBr}_3(\text{c})$ and can be averaged as $\Delta H_f^\circ(\text{PuBr}_3, \text{c}) = -792.9 + 2.1 \text{ kJ.mol}^{-1}$. The entropy of this compound is an estimate (8) from the value for $S^\circ(\text{UBr}_3, \text{c}) = 192.5 + 8.4 \text{ J.K}^{-1}.\text{mol}^{-1}$ taking in account the increment in entropy when going from $\text{UF}_3(\text{c})$ and $\text{UCl}_3(\text{c})$ to $\text{PuF}_3(\text{c})$ and $\text{PuCl}_3(\text{c})$, respectively and allowing larger uncertainty limits. Thus, $S^\circ(\text{PuBr}_3, \text{c}) = 201 \pm 17 \text{ J.K}^{-1}.\text{mol}^{-1}$.

Table III

Thermodynamic data associated with the solid plutonium, bromides, iodides, and related species at 298 K.

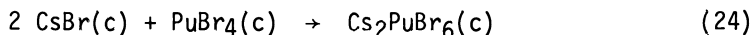
	$-\Delta H_f^\circ$ kJ.mol ⁻¹	S° J.K ⁻¹ .mol ⁻¹	$-\Delta H_f^\circ$ kJ.mol ⁻¹	S° J.K ⁻¹ .mol ⁻¹
PuBr ₃	792.9(2.1)	201(17)	PuOBr	872.8(4.6) 121(13)
Cs ₂ PuBr ₆	1694.1(4.2)	X		
PuI ₃	579.9(2.5)	230(17)	PuOI	[803(20)] [137(21)]

The enthalpy of formation of PuOBr(c) is derived from the vapor phase equilibrium measurements of Sheft and Davidson (68) and very recently of Weigel et al. (69) for reaction (23)



The two sets of data can be represented by $\Delta G_{23} = 95400 - 138.9 T$ J.mol⁻¹ (68) in the temperature range 800-900 K and $\Delta G_{23} = 89100 - 132.2 T$ J.mol⁻¹ (69) in the temperature range 728-877 K. Using a $\Delta C_p = 6.3 \text{ J.K}^{-1}.\text{mol}^{-1}$ as suggested by Rand (21) we calculate $\Delta H_{23}(298) = 92.0 + 2.9 \text{ kJ.mol}^{-1}$ from (68) and $\Delta H_{23}(298) = 85.9 + 2.9 \text{ kJ.mol}^{-1}$ from (69). The average of these marginally concordant data $\Delta H_{23} = 89.1 + 4.2 \text{ kJ.mol}^{-1}$ leads to $\Delta H_f^\circ(\text{PuOBr}, \text{c}) = -872.8 + 4.6 \text{ kJ.mol}^{-1}$ through the use of $\Delta H_f^\circ(\text{PuBr}_3, \text{c})$, given above, and of auxiliary data. The standard entropy of PuOBr(c) is also derived from the thermodynamic parameters associated with equation (23). With $\Delta C_p = 6.3 \text{ J.K}^{-1}.\text{mol}^{-1}$, we obtain an average of $\Delta S_{23}(298) = 128.9 + 6.3 \text{ J.K}^{-1}.\text{mol}^{-1}$ leading to $S^\circ(\text{PuOBr}, \text{c}) = 121 + 13 \text{ J.K}^{-1}.\text{mol}^{-1}$.

Bromocomplexes of plutonium are limited in number: tri- and tetravalent complexes with organic cations, namely $[(\text{C}_6\text{H}_5)_3\text{PH}]_3 \text{PuBr}_6(\text{c})$ (70) and $[(\text{C}_2\text{H}_5)_4\text{N}]_2 \text{PuBr}_6(\text{c})$ (71) have been reported. Also, adducts of the type $\text{PuBr}_4 \cdot 2\text{L}$ (with L = hexamethylphosphoramide and triphenylphosphine oxide) are known (72). No thermodynamic information are available on these species. More recently, however, the compound $\text{Cs}_2\text{PuBr}_6(\text{c})$ has been prepared (63) and its enthalpy of solution in 1 M HCl was measured as $-75.6 + 0.21 \text{ kJ.mol}^{-1}$. This measurement leads to a value of $\Delta H_f^\circ(\text{Cs}_2\text{PuBr}_6, \text{c}) = -1694.1 + 4.2 \text{ kJ.mol}^{-1}$. Using a procedure similar to that employed in the case of $\text{PuCl}_4(\text{c})$, we can estimate the enthalpy of formation of the hypothetical $\text{PuBr}_4(\text{c})$ as $\Delta H_f^\circ(\text{PuBr}_4, \text{c}) = -755.0 + 7.0 \text{ kJ.mol}^{-1}$ and $\Delta H_{\text{complex}}$ according to reaction (24)



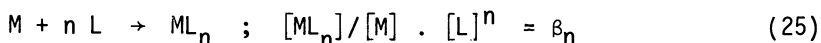
as $\Delta H_{24} = -127.6 + 8.0 \text{ kJ}\cdot\text{mol}^{-1}$. As $\Delta H_f^\circ(\text{PuBr}_3, \text{c})$ is given above as $-792.9 + 2.1 \text{ kJ}\cdot\text{mol}^{-1}$, ΔH_{24} largely accounts for the stabilization of quadrivalent plutonium in the complex. In the case of $\text{Cs}_2\text{UBr}_6(\text{c})$ and $\text{Cs}_2\text{NpBr}_6(\text{c})$ $\Delta H_{\text{complex}}$ values of $-96.1 + 0.6 \text{ kJ}\cdot\text{mol}^{-1}$ and $-100.4 + 0.7 \text{ kJ}\cdot\text{mol}^{-1}$ can be deduced (8) from the data of Vdovenko et al. (73), and Magette and Fuger (74), respectively.

Measurement of the enthalpy of solution of $\text{PuI}_3(\text{c})$ in O_2 -free 1 M HCl yielded a value of $-180.2 + 2.0 \text{ kJ}\cdot\text{mol}^{-1}$ (67) which, upon combination with the enthalpy of solution of PuCl_3 in the same medium (18), gives $\Delta H_f^\circ(\text{PuI}_3, \text{c}) = -579.9 + 2.5 \text{ kJ}\cdot\text{mol}^{-1}$. $S^\circ(\text{PuI}_3, \text{c}) = 230 + 17 \text{ J}\cdot\text{K}^{-1}\cdot\text{mol}^{-1}$ is estimated from the value for $\text{UI}_3(\text{c})$, $221.8 + 8.4 \text{ J}\cdot\text{K}^{-1}\cdot\text{mol}^{-1}$, assuming that the same entropy difference exists between $\text{UI}_3(\text{c})$ and $\text{PuI}_3(\text{c})$ as between $\text{UBr}_3(\text{c})$ and $\text{PuBr}_3(\text{c})$.

$\text{PuOI}(\text{c})$ is a well-characterized compound first observed as a by-product of the preparation of $\text{PuI}_3(\text{c})$ (75) but more conveniently obtained (67) by reaction of stoichiometric amounts of $\text{Sb}_2\text{O}_3(\text{c})$ on $\text{PuI}_3(\text{c})$. Incidentally, the latter method is a rather general way to obtain oxyhalides. Taking by analogy with the chloride and bromide compounds, as done for $\text{PuOF}(\text{c})$, a value of $-610 + 20 \text{ kJ}\cdot\text{mol}^{-1}$ for $\{\Delta H_f^\circ(\text{PuOI}, \text{c}) - (\Delta H_f^\circ(\text{PuI}_3, \text{c})/3)\}$ we obtain $\Delta H_f^\circ(\text{PuOI}, \text{c}) = -803 + 20 \text{ kJ}\cdot\text{mol}^{-1}$. The entropy of this compound can be estimated as $137 + 21 \text{ J}\cdot\text{K}^{-1}\cdot\text{mol}^{-1}$ from the accepted values for $\text{PuOCl}(\text{c})$, $\text{PuOBr}(\text{c})$, $\text{AmOCl}(\text{c})$ and $\text{AmOBr}(\text{c})$ (8). No iodo-complexes of plutonium have been reported to date.

Complexes in Aqueous Solutions

In this part we shall use the nomenclature of Sillen and Martell (76) to define stability constants, medium and experimental techniques. We shall only deal with overall stability constants of the cation M with the ligand L according to reaction (25)



with $n = 1, 2, 3, \dots$ When needed to avoid confusion, we shall represent the thermodynamic parameters associated with reaction (25) by $\beta_n(\text{ML}_n)$, $\Delta H_n(\text{ML}_n)$, $\Delta G_n(\text{ML}_n)$ and $\Delta S_n(\text{ML}_n)$. Few enthalpy and entropy data are available, however. In the case of plutonium halides no species containing more than one plutonium have been identified. For the medium the following abbreviations are used :

- 0.1 : ionic strength, μ , of 0.1 ($\text{mole}\cdot\text{litre}^{-1}$).
- 2 NaClO_4 : constant concentration of the substance stated (2 $\text{mole}\cdot\text{litre}^{-1}$).
- 2(NaClO_4) : ionic strength held constant at the value stated (2 $\text{mole}\cdot\text{litre}^{-1}$) by addition of the species in parentheses.
- 2(Na) ClO_4 : concentration of the anion held constant at the value stated (2 $\text{mole}\cdot\text{litre}^{-1}$) with the ion shown in parentheses as inert species.

The abbreviations for the investigation methods are also taken from the nomenclature of Sillen and Martell (76) : aiex = anion exchange ; cal = calorimetry ; ciex = cation exchange ; dis = distribution between two phases ; est = estimate ; red = e.m.f. with redox electrode ; sp = spectrophotometry. Our selected data, rather limited in number, arise from the present status of the IAEA assessment of inorganic complexes of the actinides (12). For these selected data the medium is assumed to be perchloric acid or sodium perchlorate.

Complexes with the Fluoride Ion. For the compilation of stability constants (Table IV) of complexes with F^- , we have used, when needed, thermodynamic parameters (K , ΔH) pertaining to the dissociation of hydrofluoric acid as given by Smith and Martell (77) or extrapolated from their selection.

In the case of trivalent plutonium, the literature does not reveal any experimental result. However, a rather extensive study by Choppin and Unrein (85) on the monofluorocomplexes of Am^{3+} to Cf^{3+} in 1.0 M $NaClO_4$, using solvent extraction over the temperature range 283-328 K yields, upon recalculation from the original data, $\Delta H_1(AMF^{2+}) = 12.3$, $\Delta H_1(CmF^{2+}) = 11.8$, $\Delta H_1(BkF^{2+}) = 12.0$ and $\Delta H_1(CfF^{2+}) = 11.8$ $kJ.mol^{-1}$. As these data show no distinct trend, we shall adopt $\Delta H_1(PuF^{2+}) = 12.0 + 4$ $kJ.mol^{-1}$. The values of the stability constants given by Choppin and Unrein at 298 K, $\log \beta_1(AMF^{2+}) = 2.49 + 0.02$, $\log \beta_1(CmF^{2+}) = 2.99 + 0.13$, $\log \beta_1(BkF^{2+}) = 2.77 + 0.04$ and $\log \beta_1(CfF^{2+}) = 2.99 + 0.13$, are somewhat lower than the values reported by other authors (86) using the same technique : $\log \beta_1(AMF^{2+}) = 3.39 + 0.01$ and $\log \beta_1(CmF^{2+}) = 3.34$ in 0.5 M $NaClO_4$. In addition the stability constants given by the latter authors are more in line with the corresponding values obtained by others for the lanthanide elements (87, 88). We therefore suggest for an ionic strength of 0.5 a value of $\log \beta_1(PuF^{2+}) = 3.3 + 0.3$, thus $\Delta G_1(PuF^{2+}) = -18.8 + 1.7$ $kJ.mol^{-1}$. Accepting for that medium the enthalpy values from Choppin and Unrein, $\Delta H_1(PuF^{2+}) = 12.0 + 4.0$ $kJ.mol^{-1}$, we obtain $\Delta S_1(PuF^{2+}) = 103 + 15$ $J.K^{-1}.mol^{-1}$. This entropy value is not incompatible with the values reported for the light lanthanides. Estimation of data for the trivalent fluorocomplexes containing more than one fluoride is still more difficult.

In the case of the monofluorocomplexes of quadrivalent plutonium, it is obvious that the lower values obtained in chloride and nitrate media are due to complexing by these ions ; these results will not be discussed further. In $HClO_4$ media the data for the first two fluoride complexes are quite self-consistent and well within the same order of magnitude as these reported for the other quadrivalent actinides (12, 89). An extensive comparison would extend beyond the scope of this paper. In the case of PuF^{3+} , extrapolation of β_1 to zero ionic strength is not warranted as such in view of the limited number of data. However, in the case of ThF^{3+} where the data extend over a very wide range of ionic

Table IV
Stability constants of the fluoride complexes of Plutonium

Ion	T	μ , medium	log β_1	log β_2	log β_3	log β_4	Method	Ref.
Pu ³⁺	298	0.5	3.3(.3)				Our selection	
	283	2(HClO ₄)	7.72(.02)	13.91(0.03)			dis	78
		293	2H(1.98 ClO ₄ + 0.02 NO ₃)	7.54(.02)				ciex
	293	1H(0.98 ClO ₄ + 0.02 NO ₃)	7.12(.08)				ciex	80
		298	2(HCl)	7.11(.05) ⁺			red	81
	298	2(HClO ₄)	7.77(.02)	13.87(0.02)			dis	79
	298	2(HNO ₃)	6.91(.02)				ciex	82
	298	1(HNO ₃)	7.00(.04)				ciex	82
	298	1(HNO ₃)	6.76(.30) ⁺				sp	81
	PuO ₂ ²⁺	298	2	7.8(.1)				Our selection
298		1	7.6(.1)					
298		0	8.8(.3)					
PuO ₂ ²⁺	298	2(HClO ₄)	5.13(.05)	10.08(.06)	14.91(.12)	19.20(.17)	ciex	83
	298	2(HClO ₄)	4.04				dis	84
	298	1(HClO ₄)	5.07(.05)	10.07(.07)	14.96(.08)	18.14(.13)	ciex	83
PuO ₂ ²⁺	298	2	5.13(.05)				Our selection	
	298	1	5.07(.05)					
	298	0	5.7(.2)					

+ Uncertainty limits being ours.

strengths such an extrapolation has been reported (81) using a modification of a Debye-Hückel relation proposed by Vasil'ev (90) as relation (26)

$$\log \beta^\circ = \log \beta - (\Delta Z^2 A \mu^{1/2}) / (1 + 1.6 \mu^{1/2}) - b\mu \quad (26)$$

in which A is the Debye-Hückel constant (0.5115 at 298 K), ΔZ^2 is the variation of the sum of the squares of the ionic charges in the reaction under consideration, b is an empirical parameter and 1.6 is a constant valid for all systems, taken instead of the more classical 0.33 (a being the distance of closest approach of the ions). It is obvious that the selection of 1.6 as constant for all systems is too simple for a rigorous treatment of the problem but it may be used for practical calculations of stability constants since the uncertainties of the data are usually far greater than those arising from the activity coefficients of the electrolytes. In any case Vasil'ev's equation has been shown to account for the variation of stability constants of multicharged complexes over a wide range of ionic strengths. Thus, a plot of $\log \beta - (\Delta Z^2 A \mu^{1/2}) / (1 + 1.6 \mu^{1/2})$ versus μ should yield a straight line. The treatment of ThF^{3+} data has been quite satisfactory (89) yielding at $\mu = 0$ $\log \beta_1^\circ(\text{ThF}^{3+}) = 8.58 + 0.15$ and $b = 0.32 + 0.04$ with $\log \beta(\text{ThF}^{3+}) = 7.56 + 0.03$ in 2 M HClO_4 . With $\log \beta(\text{PuF}^{3+}) = 7.8$ in the same medium, we suggest, for $\mu = 0$, $\log \beta^\circ(\text{PuF}^{3+}) = 8.8 + 0.3$, assuming the same functional dependence as for Th^{3+} and using conservative uncertainty limits to account for the scatter of the PuF^{3+} data. From the measurements on PuF^{3+} at 283 K and 298 K (78, 79) in 2 M HClO_4 a value of $\Delta H_1(\text{PuF}^{3+}) = 5.0 + 1.3$ kJ. mol^{-1} has been reported. With $\log \beta_1(\text{PuF}^{3+}) = 7.77 + 0.02$ or $\Delta G_1(\text{PuF}^{3+}) = -44.4 + 0.1$ kJ. mol^{-1} one obtains $\Delta S_1(\text{PuF}^{3+}) = 165.7 + 4.4$ J. K^{-1} . mol^{-1} . Although temperature dependence data with only two results over such a narrow temperature range may be of limited accuracy, the above results are not incompatible with $\Delta H_1(\text{ThF}^{3+}) = 3.0 + 0.6$ kJ. mol^{-1} (calorimetry), $\Delta S_1(\text{ThF}^{3+}) = 150.6 + 6.3$ J. K^{-1} . mol^{-1} (potentiometry), $\Delta H_1(\text{UF}^{3+}) = 0.8 + 3.0$ kJ. mol^{-1} , $\Delta S_1(\text{UF}^{3+}) = 151 + 13$ J. K^{-1} . mol^{-1} (potentiometry), $\Delta H_1(\text{NpF}^{3+}) = 3.2 + 1.8$ kJ. mol^{-1} and $\Delta S_1(\text{NpF}^{3+}) = 154.8 + 6.3$ J. mol^{-1} . K^{-1} (distribution coefficient) reported by Choppin and Unrein (45) for 1.0 M HClO_4 . However, Baumann (91) reports for $\mu = 0$ $\Delta H_f^\circ(\text{ThF}^{3+}) = -5.0$ kJ. mol^{-1} and $\Delta S_1^\circ(\text{ThF}^{3+}) = 163$ J. K^{-1} . mol^{-1} .

The stability constant of the monofluorocomplex of PuO_2^{2+} given by Krylov et al. (83) are $0.50 + 0.05$ log unit larger than the very consistent results obtained by others (84, 92-95) for UO_2F^+ in the same media. In fact, UO_2F^+ has been studied over a wide range of ionic strengths down to 0.05 M NaClO_4 . A plot using Vasil'ev's equation yields $\log \beta_1(\text{UO}_2\text{F}^+) = 5.19 + 0.10$. Similarly, we shall accept $\log \beta_1(\text{PuO}_2\text{F}^+) = 5.70 + 0.20$ in agreement with the value of 5.63 used by Lemire and Tremaine (96). The value reported for the monofluorocomplex by Patil and RamaKrishna (84) seems to be an order of magnitude too low. For the plutonium complexes

containing 2 or more fluorides the data of Krylov et al. (83) are several orders of magnitude larger than the data obtained for the uranyl (92, 94, 95) or the neptunyl (97, 98) complexes.

Complexes with the Chloride Ion. Table V summarizes the existing data on the stability of these complexes showing the large variety of techniques used. For all the valency states of plutonium the complexes are weak ($\log \beta < 1$) and the data are rather scattered with $\log \beta_2$ always smaller than $\log \beta_1$. In the case of PuCl_2^{2+} the most consistent set of data is obtained from the cation exchange measurements of Ward and Welch (99) at ionic strength between 1 and 0.2. An extrapolation of these data to $\mu = 0$ using Vasil'ev's equation yields a value of $\log \beta_1^\circ(\text{PuCl}_2^{2+}) = 1.2 \pm 0.1$. This value is identical within its uncertainty limits to that we obtain by combining and extrapolating the results of various authors for AcCl_2^{2+} (115, 116), AmCl_2^{2+} (94, 117-121) and CmCl_2^{2+} (99). It can therefore be accepted without much reservation. There is only one value reported for the enthalpy of formation of a trivalent actinide chlorocomplex. It has been obtained by Martin and White (102) and pertains to PuCl_2^{2+} . It is based on the difference in enthalpy of solution of PuCl_3 in 0.1 M HCl (18) and 0.1 M HClO_4 (102). From these data and using a $\log \beta_1(\text{PuCl}_2^{2+}) = + 0.57$ based on the results of Ward and Welch (99), Martin and White report $\Delta H_1(\text{PuCl}_2^{2+}) = + 19.2 \text{ kJ}\cdot\text{mol}^{-1}$ and $\Delta S_1 = 78 \text{ J}\cdot\text{K}^{-1}\cdot\text{mol}^{-1}$. These results call however for some caution as the enthalpy of solution of PuCl_3 in 0.1 M HClO_4 reported by Martin and White is $5.9 \text{ kJ}\cdot\text{mol}^{-1}$ more negative than that reported by Fuger and Cunningham (122) for a perchlorate medium of the same ionic strength (10^{-3} M HClO_4 - $0.099 \text{ M NH}_4\text{ClO}_4$), the latter value being nearly identical with that obtained by Robinson and Westrum (18) in 0.1 M HCl. In addition, the data of Martin and White contrast with the results of the temperature dependence measurements of the stability constant of EuCl_2^{2+} obtained by Choppin and Unrein (123) who report at $\mu = 1$ (HClO_4) and 298 K enthalpy and entropy changes not significantly different from zero ($\Delta H(\text{EuCl}_2^{2+}) = - 0.21 \pm 0.13 \text{ kJ}\cdot\text{mol}^{-1}$, $\Delta S_1(\text{EuCl}_2^{2+}) = + 13 \pm 13 \text{ J}\cdot\text{K}^{-1}\cdot\text{mol}^{-1}$) or of those on LaCl_2^{2+} reported by Mattern (124) also at $\mu = 1$ (NaClO_4) and 298 K who gives $\Delta H_1(\text{LaCl}_2^{2+}) = 5.9 \pm 4.2 \text{ kJ}\cdot\text{mol}^{-1}$, $\Delta S_1(\text{LaCl}_2^{2+}) = 17 \pm 17 \text{ J}\cdot\text{K}^{-1}\cdot\text{mol}^{-1}$. The stability constants (100) reported in 3-13 M $[\text{LiCl}]$ cannot directly be compared with the other data as the water activity in these media is drastically modified and therefore the hydration sphere is highly affected with the probable occurrence of closer contact between the actinide cation and the halide anion.

Although quadrivalent plutonium forms complexes up to PuCl_6^{2-} with the increasing HCl concentration, quantitative data only exist for the cationic species. In fact, for complexes containing more than two chlorides only two results have been reported: $\log \beta_3(\text{PuCl}_3^+) = - 0.8$ and $- 1$ in 4 M HClO_4 (103) and 1 to 5 M (HClO_4 -KCl) (104), respectively. As these data are isolated, they

Table V
Stability constants of the chloride complexes of plutonium.

Ion	T	μ , medium	$\log \beta_1$	$\log \beta_2$	Method	Ref.
Pu^{3+}	294	1 HCl	-0.04		ciex	99
	294	0.5 HCl	0.24		ciex	99
	294	0.5 H(0.2 Cl, 0.3 ClO ₄)	0.35		ciex	99
	294	0.207 HCl	0.35		ciex	99
	298	3-13 LiCl	-2.4(0.1)	-5.00(.06)	sp	100
	298	1(HClO ₄)	\sim -0.15		est	101
	298	0.1 H(ClO ₄)	0.57		est	102
	298	1	-0.1+0.05		our selection	
298	0	1.2+0.1				
Pu^{+4}	293	4 H(ClO ₄)	0.15(.06)	0.08(.08)	ciex	103
	298	1-5(HClO ₄ -KCl)	-0.1	-0.3	red	104
	298	4 H(ClO ₄)	0.30(.01)	-0.80(.08)	dis	105
	298	2 HNO ₃	-0.42		sp	106
	298	2 H(ClO ₄)	0.15(.01)	-0.64(.10)	dis	79
	298	2 H(ClO ₄)	-0.23(.01)		red	107
	298	1 H(ClO ₄)	-0.24		red	108
	298	1 H(ClO ₄)	0.14		red	109
	298	0.2-1.2 HCl	+0.36		ciex	110
	298	4	0.22(.05)		our selection	
	298	2	0.15(.05)			
	298	1	0.23(.05)			
	298	0	1.67(.10)			
PuO_2^+	?		-0.17		sp	111
PuO_2^{2+}	?	4.1 X(ClO ₄) pH = 1.15	0.02	-0.8 ?	dis	112
	298	2 H(ClO ₄)	0.10	-0.46	sp	113
	275.55	2 H(ClO ₄)	-0.04	-0.68	sp	114
	283.35	2 H(ClO ₄)	0.0	-0.60	sp	114
	288.15	2 H(ClO ₄)	0.03	-0.55	sp	114
	293.35	2 H(ClO ₄)	0.06	-0.48	sp	114
	302.75	2 H(ClO ₄)	0.11	-0.37	sp	114
	298	2	0.09(.05)	-0.45(.10)	our selection	

have been discarded from Table V. The ion exchange data in 4 M HClO₄ of Grenthe and Noren (103), the solvent extraction data of Danesi et al. (105) in the same medium and of Bagawde et al. (79) in 2 M HClO₄, together with the potentiometric data of Rabideau et al. (109) in 1 M HClO₄, provide the basis for our selection leading to $\log \beta^\circ(\text{PuCl}_3^+) = 1.67 + 0.10$, thus $\Delta G_1(\text{PuCl}_3^+) = -9.5 + 0.6 \text{ kJ.mol}^{-1}$. Earlier values (107, 108) did not take into account the nitrate or the chloride complexing of Pu³⁺. For the same reason the $\Delta H_1(\text{PuCl}_3^+) = 7.9 \text{ kJ.mol}^{-1}$ and $\Delta S_1(\text{PuCl}_3^+) = 21 \text{ J.K}^{-1}.\text{mol}^{-1}$ reported by Rabideau and Cowan (108) from the temperature dependence of the Pu⁴⁺/Pu³⁺ couple in HCl and HClO₄ will only be mentioned. The spectrometric value of Hindman (106), as noted by the author himself, should only be regarded as approximative in view of the importance of nitrate complexing of Pu⁴⁺. Although detailed comparison of our selection for $\log \beta^\circ(\text{PuCl}_3^+)$ with the data for other quadrivalent actinide cannot be made here, it is clear that our value fits well the general pattern: for instance, we obtain $\log \beta^\circ(\text{ThCl}_3^+) = 1.64 + 0.10$ from numerous data (125-128) covering ionic strengths ranging from 6 to 0.5.

Of all plutonium species, PuO₂²⁺ should have the lowest tendency to form complexes. The only reported value, $\log \beta_1(\text{PuO}_2\text{Cl}) = -0.17$ appears high compared to the data reported for NpO₂Cl: absence of complexing (129) at $\mu = 4$ (1 H, Na, ClO₄), -0.30 ± 0.05 (130) in 2 M HClO₄, -0.42 (131) in 2 M NaClO₄.

The spectrophotometric data as a function of temperature in 2 M HClO₄ by Rabideau and Masters (114) are said by these authors to be equally well interpreted on the basis of the existence of both PuO₂Cl⁺ and PuO₂Cl₂, or of PuO₂Cl⁺ only. However, evidence for the presence of both species is definitely found at $\mu = 4$ (112) and $\mu = 2$ (113). At $\mu = 2$ values of $\log \beta_1(\text{PuO}_2\text{Cl}^+) = 0.09 + 0.05$, thus $\Delta G_1(\text{PuO}_2\text{Cl}^+) = -0.48 + 0.30 \text{ kJ.mol}^{-1}$, and $\log \beta_2(\text{PuO}_2\text{Cl}_2) = -0.45 + 0.1$, thus $\Delta G_2(\text{PuO}_2\text{Cl}_2) = 2.4 + 0.6 \text{ kJ.mol}^{-1}$, can be selected from the concordant spectrophotometric measurements of Newton and Baker (113) and Rabideau and Masters (114). Calculation of the enthalpy changes from the data of Rabideau and Masters yield, at $\mu = 2$, $\Delta H_1(\text{PuO}_2\text{Cl}^+) = 9.0 + 4.2 \text{ kJ.mol}^{-1}$ and $\Delta H_2(\text{PuO}_2\text{Cl}_2) = 18.3 + 4.2 \text{ kJ.mol}^{-1}$. These values lead to $\Delta S_1(\text{PuO}_2\text{Cl}^+) = 32 + 15 \text{ J.K}^{-1}.\text{mol}^{-1}$ and $\Delta S_2(\text{PuO}_2\text{Cl}_2) = 53 + 15 \text{ J.K}^{-1}.\text{mol}^{-1}$, results which are not unreasonable. Comparison of these results (β , ΔH ...) with the numerous data existing on the uranyl and neptunyl complexes does not reveal smooth trends so that discussion of this topic cannot be carried out here.

Complexes with the Bromide and Iodide Ions. The few existing data on bromide complexes are assembled in Table VI. Data on iodide complexes are completely lacking.

The values for PuBr²⁺ and PuBr₂⁺ deduced by Shiloh and Marcus (100) from absorption spectra of concentrated LiBr solutions are one order of magnitude lower than the values observed by the same authors for the chloride complexes in LiCl solutions at

Table VI
 Stability constants of the bromide complexes of plutonium.

Ion	T	μ , medium	$\log \beta_1$	$\log \beta_2$	Method	Ref.
Pu ³⁺	298	9.3-11.5 LiBr	3.45(.08)	6.54(.10)	sp	100
Pu ⁴⁺	298	4 H(Cl)	1.00(.02)	0.64(.07)	dis	105
	298	2.0 HClO ₄	0.33(.01)		dis	132

comparable concentrations : this observation confirms the expected lower stability of the bromocomplexes. The same authors have shown that, as for the chlorocomplexes, the stability of these species increases slightly (< 1 order of magnitude) when going from uranium to americium.

The two sets of data for the tetravalent bromocomplexes are not in good agreement. In addition, compared to the value obtained for the first chloride complex at $\mu = 4$, $0.22 + 0.05$, the values for the bromocomplexes appear high, the results of Danesi et al. (105) being definitely out of line.

Conclusion

In spite of well identified deficiencies, the status of the existing thermodynamic data on solid halides and related compounds is rather satisfactory. By contrast, the data on aqueous halogeno-complexes are fragmentary, sometimes contradictory and in most cases limited to stability constants : in such a context, recommendation of best values can be made for a few species only.

Literature Cited

1. Medvedev, V.A.; Rand, M.H.; Westrum, E.F., Jr. (Eds.); Oetting, F.L. (Exec. Ed.); "The Chemical Thermodynamics of Actinide Elements and Compounds", I.A.E.A.-Vienna. STI/PUB/424, Part 1- Oetting, F.L.; Rand, M.H.; Ackermann, R.J. : "The Actinide Elements", 1976.
2. Idem, Part 2 - Fuger, J.; Oetting, F.L. : "The Actinide Aqueous Ions", 1976.
3. Idem, Part 3 - Cordfunke, E.H.P.; O'Hare, P.A.G. : "The Actinide Miscellaneous Compounds", 1978.
4. Idem, Part 5 - Chiotti, P.; Akhachinskij, V.V.; Ansara, I.; Rand, M.H. : "The Actinide Binary Alloys", 1981.
5. Idem, Part 4 - Grønvold, F.; Drowart, J.; Westrum, E.F., Jr. : "The Actinide Chalcogenides", in preparation.
6. Idem, Part 6 - Holley, C.E., Jr.; Rand, M.H.; Storms, E.K. : "The Actinide Carbides", in preparation.
7. Idem, Part 7 - Potter, P.E.; Mills, K.C.; Takahashi, Y. : "The Actinide Pnictides", in preparation.

8. Idem, Part 8 - Fuger, J.; Parker, V.B.; Hubbard, W.N.; Oetting, F.L. : "The Actinide Halides", in the press.
9. Idem, Part 9 - Flotow, H.E.; Yamauchi, S. : "The Actinide Hydrides", in preparation.
10. Idem, Part 10 - Rand, M.H.; Ackermann, R.J.; Grønvold, F.; Oetting, F.L.; Pattoret, A. : "The Actinide Oxides", in preparation.
11. Idem, Part 11 - Potter, P.; Holleck, H.; Spear, K.E. : "Selected Actinide Ternary Systems", in preparation.
12. Idem, Part 12 - Fuger, J.; Khodakovskij, I.L.; Medvedev, V.A.; Navratil, J.D. : "The Actinide Complex Ions with Inorganic Ligands", in preparation.
13. Idem, Part 13 - Hildenbrand, D.L.; Gurvich, L.V.; Yungman, V.S.; Fred, M. : "The Actinide Gaseous Ions", in preparation.
14. Idem, Part 14 - Baisden, P.; Choppin, G.R.; Myasoedov, B.; Navratil, J.D. : "The Actinide Complex Ions with Organic Ligands", in preparation.
15. CODATA Recommended (1977) Key Values for Thermodynamics. J. Chem. Thermodynamics 1978, 10, 903.
16. Parker, V.B.; Wagman, D.D.; Garvin, D. "Selected Thermochemical Data Compatible with the CODATA Selection", NBSIR 75-968.
17. Westrum, E.F., Jr.; Eyring, L. In Seaborg, G.T.; Katz, J.J.; Manning, W.M. (Eds.) ; "The Transuranium Elements", McGraw-Hill, New York 1949, 14B, p. 908.
18. Robinson, H.P.; Westrum, E.F., Jr. Idem, p. 922.
19. Jones, M.M. 1953, Report HW-30384.
20. Storozhenko, T.P.; Khanaev, E., Afanas'ev, Yu.A. Russ. J. Phys. Chem. 1975, 49, 1241.
21. Rand, M.H. in "Plutonium : Physico-Chemical Properties of Its Compounds and Alloys" ; Atomic Energy Review 1966, 4, Special Issue n° 1, I.A.E.A. Vienna, p. 7.
22. Osborne, D.W.; Flotow, H.E.; Fried, S.M.; Malm, J.G. J. Chem. Phys. 1974, 61, 1463.
23. Johns, I.B. 1945, Rep. USAEC-LA-381.
24. Fried, S.M.; Davidson, N.R.; In Seaborg, G.T.; Katz, J.J.; Manning, W.M. (Eds.) ; "The Transuranium Elements", McGraw-Hill, New York 1949, 14B, 784.
25. Shannon, R.D. Acta Cryst. 1976, A32, 751.
26. Osborne, D.W.; Flotow, H.E.; Fried, S.M.; Malm, J.G. J. Chem. Phys. 1975, 63, 4613.
27. Trevorrow, L.E.; Shinn, W.A.; Steunenberg, R.K. J. Phys. Chem. 1961, 65, 398.
28. Weinstock, B.; Malm, J.G. J. Inorg. Nucl. Chem. 1956, 2, 380.
29. Florin, A.E.; Tannenbaum, I.R.; Lemons, J.F. J. Inorg. Nucl. Chem. 1956, 2, 368.
30. Nagarajan, K.; Brinkley, D.C. Z. Natforsch. 1971, 26a, 1958.
31. Cunningham, B.B. In Seaborg, G.T.; Katz, J.J. (Eds.) "The Actinide Elements", McGraw-Hill, New York, 1954, 14A, 371.
32. I.A.E.A. "Panel on Thermodynamics of Plutonium Oxides", Technical Report, Series n° 79, 1967.

33. Flotow, H.E.; Tetenbaum, M. J. Chem. Phys. 1981, 74, 5269.
34. Brown, D. "Halides of the Lanthanides and Actinides"; Wiley-Interscience, London-New York-Sydney, 1968.
35. Burns, R.C.; O'Donnell, T.A. Inorg. Nucl. Chem. Letters 1977, 13, 657.
36. Dobryshevskii, Yu.V.; Serik, V.F.; Sokolov, V.B. Dokl. Akad. Nauk. SSSR 1975, 225, 1079.
37. Jacob, E.; Polligkeit, W. Z. Natforsch. Teil B 1973, 28, 120.
38. Paine, R.T.; Ryan, R.R.; Asprey, L.B. Inorg. Chem. 1975, 14, 1113.
39. Wilson, P.W. J. Inorg. Nucl. Chem. 1974, 36, 1783.
40. O'Hare, P.A.G.; Malm, J.G. J. Chem. Thermodynamics 1982, 14, 331.
41. Brown, D. In Gmelins Handbuch der anorganischen Chemie Band 4 - Transurane, Teil C, Verlag Chemie, Weinheim, 1972.
42. Benz, R.; Douglass, R.M.; Kruse, F.H.; Penneman, R.A. Inorg. Chem. 1963, 2, 799.
43. Katz, S.; Cathers, G.I. Nucl. Appl. 1968, 5, 5.
44. Trevorrow, L.E.; Riha, J.G.; Steindler, M.J. J. Inorg. Nucl. Chem. 1971, 33, 2875.
45. Anonym. 1966 Report ANL 7279 ; Riha, J.; Trevorrow, L.E. Report 7425.
46. Latimer, W.M. "Oxidation Potentials", 2nd Ed. ; Prentice Hall, Englewood Cliffs, N.H., 1952.
47. Hinchey, R.J.; Cobble, J.W. Inorg. Chem. 1970, 9, 922.
48. Saeger, V.W.; Spedding, F.H. 1960, Report 1S-338.
49. Schumm, R.H.; Wagemann, D.D.; Bailey, S.; Evans, W.H.; Parker, V.B. "Selected Values of Chemical Thermodynamic Properties" - Table for Lanthanide Elements", NBS-Technical Note 270-7, U.S. Govt. Printing Office, 1973.
50. Lewis, C.N.; Randall, M. "Thermodynamics" 2nd Ed. revised by Pitzer, K.S. and Brewer, L.; McGraw-Hill, New York, 1961.
51. Benz, R. J. Inorg. Nucl. Chem. 1962, 24, 1191.
52. Westrum, E.F., Jr.; Robinson, H.P. In Seaborg, G.T.; Katz, J.J.; Manning, W.M. (Eds.) ; "The Transuranium Elements"; McGraw-Hill, New York 1949, 14B, 930.
53. Sheft, I.; Davidson, N.R. Idem, p. 841.
54. Weigel, F.; Wishnevsky, V.; Hauske, H. J. Less-Common Metals 1977, 56, 113.
55. Morss, L.R. J. Phys. Chem. 1971, 75, 392.
56. Fuger, J.; Brown, D. J. Chem. Soc. A, 1971, 841.
57. Hendricks, M.E.; Jones, E.R., Jr.; Stone, J.A.; Karracker, D.G. J. Chem. Phys. 1974, 60, 2095.
58. Bagnall, K.W.; Laidler, B.J.; Stewart, M.A.A. J. Chem. Soc. A 1968, 133.
59. Morss, L.R.; Fuger, J. Inorg. Chem. 1969, 8, 1433.
60. Chauvenet, E. Ann. Chim. Phys. 1911, 23, 425.
61. Martynova, N.S.; Kudryashova, Z.P.; Vasil'kova, I.V. Soviet At. Energ. 1968, 25, 1000.

62. Vdovenko, V.M.; Suglobova, I.G.; Chirkst, D.E. Sov. Radiochem. 1974, 16, 364.
63. Fuger, J. J. Phys. Colloque C4 1979, 40, Suppl. n° 4, 207.
64. Bagnall, K.W.; Laidler, B.J.; Stewart, M.A.A. Chem. Comm. 1967, 24.
65. Brown, D. unpublished results.
66. Westrum, E.F., Jr. In Seaborg, G.T.; Katz, J.J.; Manning, W.M. (Eds.); "The Transuranium Elements", McGraw-Hill, New York 1949, 14B, 926.
67. Brown, D.; Hurtgen, C.; Fuger, J. Rev. Chimie Minérale 1977, 14, 189.
68. Sheft, I.; Davidson, N.R. In Seaborg, G.T.; Katz, J.J.; Manning, W.M. (Eds.); "The Transuranium Elements", McGraw-Hill, New York 1949, 14B, 831.
69. Weigel, F.; Wishnevsky, V.; Güldner, R. J. Less-Common Metals 1982, 84, 147.
70. Ryan, J.L. In Fields, P.R.; Moeller, T. (Eds.); "Lanthanide and Actinide Chemistry"; American Chemical Society, Washington, 1967, 71, 331.
71. Ryan, J.L.; Jørgensen, C.K. Mol. Physics 1963, 7, 17.
72. Brown, D.; Holah, H.; Rickard, C.E.F. Chem. Comm. 1968, 651.
73. Vdovenko, V.M.; Suglobova, I.G.; Chirkst, D.E. Soviet Radiochem. 1973, 16, 56.
74. Magette, M.; Fuger, J. Inorg. Nucl. Chem. Letters 1977, 13, 529.
75. Hagemann, F.; Abraham, B.N.; Davidson, N.R.; Katz, J.J.; Sheft, I. In Seaborg, G.T.; Katz, J.J.; Manning, W.M. (Eds.); "The Transuranium Elements", McGraw-Hill, New York 1949, 14B, 957.
76. Sillen, L.G.; Martell, A.E. "Stability Constants of Metal Complexes"; Special Publication n° 17. The Chemical Society, London, 1964.
77. Smith, R.M.; Martell, A.E. "Critical Stability Constants" volume 4 : Inorganic Complexes, Plenum Press, New York, 1976.
78. Bagawde, S.V.; Ramakrishna, V.V.; Patil, S.K. Radiochem. Radioanal. Letters 1977, 31, 56.
79. Bagawde, S.V.; Ramakrishna, V.V.; Patil, S.K. J. Inorg. Nucl. Chem. 1976, 38, 1339.
80. Krylov, V.N.; Komarov, E.V. Soviet Radiochem. 1969, 11, 94.
81. McLane, C.K. In Seaborg, G.T.; Katz, J.J.; Manning, W.M. (Eds.) "The Transuranium Elements", McGraw-Hill, New York 1949, 14B, 414.
82. Krylov, V.N.; Komarov, E.V.; Pushlenkov, M.F. Soviet Radiochem. 1969, 11, 97.
83. Krylov, V.N.; Komarov, E.V.; Pushlenkov, M.F. Soviet Radiochem. 1968, 10, 705.
84. Patil, S.K.; Ramakrishna, V.V. J. Inorg. Nucl. Chem. 1976, 38, 1075.

85. Choppin, G.R.; Unrein, P.J. In Müller, W.; Lindner, R. (Eds.); "Transplutonium Elements", North Holland Elsevier, Amsterdam, 1976, 97.
86. Aziz, A.; Lyle, S.J. J. Inorg. Nucl. Chem. 1969, 34, 347.
87. Kury, J.W.; Hugus, Z.Z.; Latimer, W.M. J. Phys. Chem. 1957, 61, 1021.
88. Walker, J.B.; Choppin, G.R. In Fields, P.R.; Moeller, T. (Eds.) "Lanthanide and Actinide Chemistry"; American Chemical Society, Washington, 1967, 71, 127.
89. Fuger, J.; Khodakovskij, I.L.; Medvedev, V.A.; Navratil, J.D. in "Thermodynamics of Nuclear Materials 1979", I.A.E.A., Vienna, 1980, 59.
90. Vasil'ev, V.P. Russ. J. Inorg. Chem. 1962, 7, 924.
91. Baumann, E.W. J. Inorg. Nucl. Chem. 1970, 32, 3823.
92. Ahrland, S.; Larsson, R. Acta Chem. Scand. 1954, 8, 354.
93. Day, R.A.; Powers, R.M. J. Amer. Chem. Soc. 1954, 76, 3895.
94. Ahrland, S.; Larsson, R.; Rosengren, K. Acta Chem. Scand. 1956, 10, 705.
95. Ahrland, S.; Kullberg, L. Acta Chem. Scand. 1971, 25, 3471.
96. Lemire, R.; Tremaine, P.R. J. Chem. Eng. Data 1980, 25, 361.
97. Ahrland, S.; Brandt, L. Acta Chem. Scand. 1968, 22, 1579.
98. Al-Niaimi, N.S.; Wain, A.G.; McKay, H.A.C. J. Inorg. Nucl. Chem. 1970, 32, 2331.
99. Ward, M.; Welch, G.R. J. Inorg. Nucl. Chem. 1956, 2, 395.
100. Shiloh, M.; Marcus, Y. J. Inorg. Nucl. Chem. 1966, 28, 2725.
101. Conninck, R.E.; McVey, W.H. J. Amer. Chem. Soc. 1953, 75, 474.
102. Martin, P.E.; White, A.G. J. Chem. Soc. 1958, 2490.
103. Grenthe, I.; Noren, B. Acta Chem. Scand. 1960, 14, 2216.
104. Kabanova, O.L.; Palei, P.N. Russ. J. Inorg. Chem. 1960, 5, 15.
105. Danesi, P.R.; Orlandini, F.; Scibona, G. J. Inorg. Nucl. Chem. 1966, 28, 1047.
106. Hindman, C.E. In Seaborg, G.T.; Katz, J.J.; Manning, W.M. (Eds.); "The Transuranium Elements"; McGraw-Hill, New York 1949, 14B, 405.
107. Rabideau, S.W.; Cowan, H.D. J. Amer. Chem. Soc. 1955, 77, 6145.
108. Rabideau, S.W.; Lemons, J.F. J. Amer. Chem. Soc. 1951, 73, 2895.
109. Rabideau, S.W.; Asprey, L.B.; Keeman, T.K.; Newton, T.W. Proc. 2nd Geneva Conference on Peaceful Uses of At. Energy. United Nations, 1958, 28, 361.
110. Souka, N.; Shabana, R.; Farah, K. J. Radioanal. Chem. 1976, 33, 215.
111. Newton, T.W. Unpublished work cited in Katz, J.J.; Seaborg, G.T. "The Chemistry of the Actinide Elements"; Methuen, London, 1957, 313.
112. Mazumdar, A.S.G.; Sivaramakrishnan, C.K. J. Inorg. Nucl. Chem. 1965, 27, 2423.
113. Newton, T.S.; Baker, F.B. J. Phys. Chem. 1957, 61, 934.
114. Rabideau, S.W.; Masters, B.J. J. Phys. Chem. 1961, 65, 1256.

115. Shahani, C.J.; Mathew, K.A.; Rao, C.L.; Ramaniah, M.V. Radioch. Acta 1968, 10, 165.
116. Sekine, T.; Sakairi, M. Bull. Chem. Soc. Japan 1969, 42, 2712.
117. Grenthe, I. Acta Chem. Scand. 1962, 16, 2300.
118. Peppard, D.F.; Mason, G.W.; Hucher, I. J. Inorg. Nucl. Chem. 1962, 24, 881.
119. Bansal, B.M.L.; Patil, S.K.; Sharma, M.D. J. Inorg. Nucl. Chem. 1964, 26, 993.
120. Sekine, T. J. Inorg. Nucl. Chem. 1964, 26, 1463.
121. Sekine, T. Acta Chem. Scand. 1965, 19, 1435.
122. Fuger, J.; Cunningham, B.B. J. Inorg. Nucl. Chem. 1963, 25, 1423.
123. Choppin, G.R.; Unrein, P.J. J. Inorg. Nucl. Chem. 1963, 25, 387.
124. Mattern, K.L. 1951, Report UCRL-1407.
125. Zebroski, E.L.; Alter, H.W.; Heumann, F.K. J. Amer. Chem. Soc. 1951, 73, 5646.
126. Waggner, W.C.; Stoughton, R.W. J. Phys. Chem. 1952, 56, 1.
127. Patil, S.K.; Ramakrishna, V.V. Inorg. Nucl. Chem. Letters 1975, 11, 421.
128. Nabivanets, B.I.; Kudritskaya, L.N. Ukrain. Khim. Zhur. 1964, 30, 1007.
129. Danesi, P.R.; Chiarizia, R.; Scibona, E.; D'Alessandro, G. J. Inorg. Nucl. Chem. 1974, 36, 2396.
130. Gainer, I.; Sykes, K.W. J. Chem. Soc. 1964, 6452.
131. Vasudeva Rao, P.R.; Gudi, N.M.; Bagawde, S.V.; Patil, S.K. J. Inorg. Nucl. Chem. 1981, 41, 235.
132. Raghavan, R.; Ramakrishna, V.V.; Patil, S.K. J. Inorg. Nucl. Chem. 1975, 37, 1540.

RECEIVED December 21, 1982

Thermodynamics of Plutonium–Noble Metal Compounds

DEAN E. PETERSON

Los Alamos National Laboratory, Materials Science and Technology Division,
Los Alamos, NM 87545

Plutonium–noble metal compounds have both technological and theoretical importance. Modeling of nuclear fuel interactions with refractory containers and extension of alloy bonding theories to include actinides require accurate thermodynamic properties of these materials. Plutonium was shown to react with noble metals such as platinum, rhodium, iridium, ruthenium, and osmium to form highly stable intermetallics. Vapor pressures of phases in these systems were measured by the Knudsen effusion technique. Use of mass spectrometer–target collection apparatus to perform thermodynamic studies is discussed. The prominent sublimation reactions for these phases below 2000 K was shown to involve formation of elemental plutonium vapor. Thermodynamic properties determined in this study were correlated with corresponding values obtained from theoretical predictions and from previous measurements on analogous intermetallics.

Thermodynamic properties of actinide intermetallics have both technological and theoretical importance. Analyses of the phase behavior, fuel-cladding interactions, and vapor transport in radioisotopic generators, nuclear reactors, and nuclear fuel reprocessing facilities require a knowledge of free energies and heats of formation of these materials. Verification and extension of intermetallic bonding theories such as the Engel–Brewer correlation⁽¹⁾ or Miedema model⁽²⁾ to include the

0097-6156/83/0216-0099\$06.00/0
© 1983 American Chemical Society

actinides depends upon measurement of accurate thermodynamic properties of these materials.

Relatively few thermodynamic studies have been performed on compounds involving Th, U and Pu with noble metals. Most of the previous work has involved electrochemical cell determinations of free energies of formation, hence little has been published concerning the sublimation behavior of actinide intermetallics.

Equilibrium vapor pressures were measured in this study by means of a mass spectrometer/target collection apparatus. Analysis of the temperature dependence of the pressure of each intermetallic yielded heats and entropies of sublimation. Combination of these measured values with corresponding parameters for sublimation of elemental Pu enabled calculation of thermodynamic properties of formation of each condensed phase. Previously reported results on the sublimation of the PuRu₂ phase⁽³⁾ and the Pu-Pt and Pu-Ru systems⁽⁴⁾ are correlated with current research on the PuOs₂ and PuIr₂ compounds. Thermodynamic properties determined for these Pu-intermetallics are compared to analogous parameters of other actinide compounds in order to establish bonding trends and to test theoretical predictions.

EXPERIMENTAL APPROACH

The phases studied in this work were PuPt₅, PuPt₄, PuPt₃, PuPt₂, URh₃, PuRh₂, PuRu₂, and PuOs₂. All samples were prepared by arc-melting weighed foils of ²³⁹Pu and the respective noble metal. Less than a 0.1 wt.% mass loss occurred during preparation of each sample. Spectroscopic analyses of the sample buttons revealed no impurity levels higher than 100 ppm. Individual samples were also characterized by x-ray diffraction, metallography, and electron microprobe. The sample preparation and characterization is more fully discussed in the phase studies of the Pu-Pt and Pu-Rh systems by Land, Peterson, and Roof.⁽⁵⁾

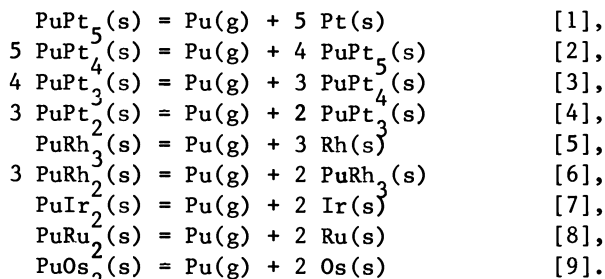
Sample cells were fabricated from tungsten. Additional crucibles composed of a Pt-40 w/o Rh-8 w/o W alloy were also used in experiments on the PuPt₂ phase. Each tungsten cell was vacuum outgassed at 1800° for 1 h before an experiment. The cell temperature was determined during the measurements by sighting with a pyrometer (Pyrometer Instrument Co.) onto a blackbody hole in each cell base. The pyrometer and sight glasses were calibrated with an NBS standard lamp.

Vapor pressures⁽⁶⁾ were determined by using the Knudsen effusion technique. Effusion rates through and orifice contained in each sample cell were measured as a function of temperature by use of a mass spectrometer/target collection

apparatus. The equipment design and techniques have been previously⁽⁷⁾ discussed in detail by Edwards, Starzynski, and Peterson. The unit enabled concurrent measurements of the vapor composition and total pressure. Selected targets on the copper ribbon were exposed to the effusate for a given time period and radioanalyzed by alpha counting to determine the condensate level. The effusate was also mass spectrometrically analyzed to determine the composition of the vapor as a function of temperature. An extranuclear quadrupole was used to scan the mass spectrum over the range 5-800 amu. The spectrometer was calibrated by simultaneously evaporating Ag metal with several samples and normalizing the Pu (239) and Ag (109) intensities. The vapor pressure of Ag as a function of temperature was obtained from Hultgren and coworkers.⁽⁸⁾ A vacuum of 10^{-6} torr was maintained in the apparatus throughout the sublimation experiments.

DATA TREATMENT

The predominant reaction associated with the sublimation of each intermetallic studied was assumed to involve gaseous Pu and the associated noble metal rich adjacent phase as products. The equilibrium sublimation reactions are as follows:



Total vapor pressures associated with each of the above reactions were calculated by use of the Knudsen equation

$$P = 3.760 \times 10^{-8} \frac{G}{AWt} \left(\frac{T}{M} \right)^{1/2} \quad [10]$$

where P = vapor pressure (atm), G = mass collected on target (μg), t = exposure time (min), A = orifice area (mm^2), W = transmission probability, T = temperature (K), and M = molecular weight of vapor (239).

The vapor pressure of $\text{Pu}(\text{g})$ in equilibrium with various phases was also determined from ion intensity measurements with the mass spectrometer. The pressure was calculated from the equation

$$P = CIT / \sigma \gamma f \quad [11]$$

where C is the machine constant, I is the ion intensity, σ is the ionization cross section, γ is the multiplier gain, and f is the isotopic fraction.

Linear least squares treatments of plots of the logarithm of the vapor pressure versus the reciprocal temperature were performed. The second-law enthalpy and entropy of sublimation at the median temperature are proportioned to the slope and intercept respectively. The enthalpy of sublimation at 298 K, $\Delta H^{\circ}(298)$ was obtained from a third law treatment which used the Gibbs free energy function,

$$\Delta \phi^{\circ}(T) = [\Delta G^{\circ}(T) - \Delta H^{\circ}(298)]/T. \quad [12]$$

Values of $\Delta \phi^{\circ}(T)$ were obtained by using simulant elements which have the same number of bonding electrons as each intermetallic phase. Second law values of $\Delta H^{\circ}(298)$ were also obtained by use of heat capacities of the same simulant and constituent elements.

RESULTS

Sample analyses by metallography, x-ray diffraction and spectroscopy confirmed the desired solid compositions. These analyses revealed that only the small compositional variations expected due to the sublimation were encountered during the studies.

Mass spectrometric examination of the effusate in equilibrium with each solid intermetallic showed only the presence of the $^{239}\text{Pu}^{+}$ ion. Ionization efficiency curve measurements conducted on the Pu^{+} species yielded an appearance potential of 6.5 ± 0.5 eV based on a calibration of the energy scale with $^{202}\text{Hg}^{+}$ ions. Due to the lack of molecular ions derivable from the effusate, the sublimation reactions were assumed to proceed by dissociation to elemental Pu and the adjoining noble metal rich phase. A second law plot of the temperature dependence of the Pu vapor pressure over each phase as measured by target collection is shown in Figure 1. The absolute values and temperature dependence of the pressures determined by mass spectrometry are concurrent with these target collection results. The thermodynamic properties associated with the sublimation and formation of each intermetallic are summarized in Table I.

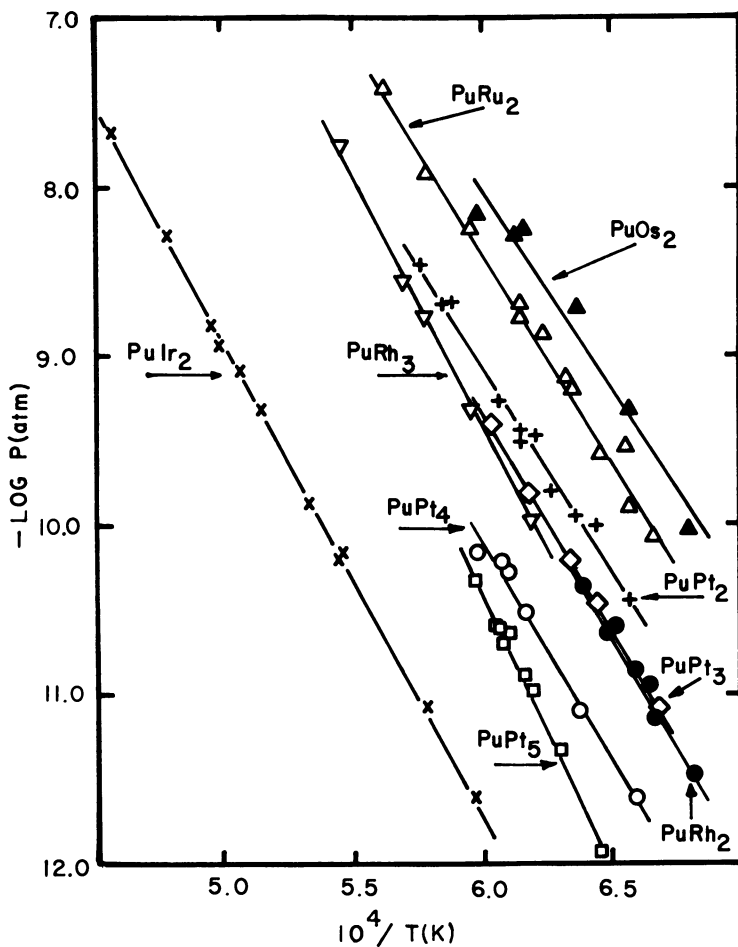


Figure 1. Temperature dependence of plutonium vapor pressure over intermetallics as measured by target collection.

TABLE I
Heats and entropies of sublimation and formation
of Pu-intermetallics at median temperature and 298 K.

Phase	Median T(K)	$\Delta H_s^o(T)$ (kJ/mol)	Second Law $\Delta S_s^o(T)$ (J/K/mol)	$\Delta H_s^o(298)$ (kJ/mol)	Third Law $\Delta H_f^o(T)$ (kJ/g atom)	$\Delta S_f^o(T)$ (J/K/g atom)	$\Delta H_f^o(298)$ (kJ/g atom)
PuRu ₂	1640	477.2±18.8	126.0±12.1	474.2	-49.0	-11.3	-41.3
PuOs ₂	1553	455.9±45.2	121.0±28.9	432.0	-42.0	-9.8	-34.7
PuIr ₂	1929	537.1±5.9	98.4±2.9	547.1	-69.2	-2.23	-65.0
PuRh ₂	1519	499.8±33.1	121.4±21.8	491.9	-74.2	-20.0	-60.7
PuRh ₃	1725	578.1±15.1	166.6±8.8	545.0	-62.2	-18.7	-49.9
PuPt ₂	1629	467.6±18.0	107.6±10.9	481.0	-69.7	-15.0	-64.0
PuPt ₃	1579	496.0±12.6	119.3±8.0	490.6	-61.0	-14.9	-55.2
PuPt ₄	1596	492.3±30.6	102.1±18.8	514.0	-54.1	-19.1	-49.1
PuPt ₅	1614	626.6±27.2	177.1±16.7	610.3	-49.5	-14.2	-44.2

DISCUSSION

Measurement of the very low pressures associated with many of the Pu-intermetallics requires the high sensitivity afforded by target collection. To identify the gas phase species which are in the effusates, a mass spectrometer is needed. The excellent agreement between the mass spectrometric and target collection results confirms the predominance of the Pu gaseous species in the sublimation of these intermetallics.

Free energies of formation for Pu-noble metal compounds are compared in Figure 2 with corresponding values for other actinide compounds over their respective temperature ranges of measurement. The following work is presented. URu₃-Edwards, Starzynski, Peterson; (7) ThOs₂, ThIr₃, URh₃, UIr, UOs₂, ThRu₂, ThRh-Kleykamp, coworkers; (9) UPt, UPd-Schmidt; (10) UPd₃-Lorenzelli, Marcon. (11) The magnitudes of the free energies of formation on the Pu intermetallics compare favorably with the other actinide systems, although corresponding Th and U phases appear to be more thermodynamically stable.

Using a Wigner-Seitz approximation, Miedema (2) has developed a bonding model which appears useful for predicting enthalpies of formation. Experimental enthalpies at 298 K for Pu intermetallics are plotted versus corresponding calculated values in Figure 3. Overall agreement is very good for most of the compounds studied.

Entropies of formation measured for the Pu-intermetallics ranged from -2 to -20 JK⁻¹·g atom⁻¹. Normally solid state reactions have values falling in the range -8 to -9 JK⁻¹·g atom⁻¹; however, due to the formation reactions involving liquid Pu and the large negative enthalpies of formation, more negative entropies might be expected.

It would be interesting to further examine the vaporization of Pu-intermetallics at higher temperatures in order to search for molecular vapor species involving Pu and the noble metals. Due to the directional nature of 5f electrons in Pu, they may not be involved in the bonding of the solid intermetallics, but could contribute to the stability of a gas phase molecule. Additional measurements of the thermodynamic stabilities of Np- and Am-noble metal intermetallics corresponding to the Pu phases considered in this work would also assist in establishing bonding trends.

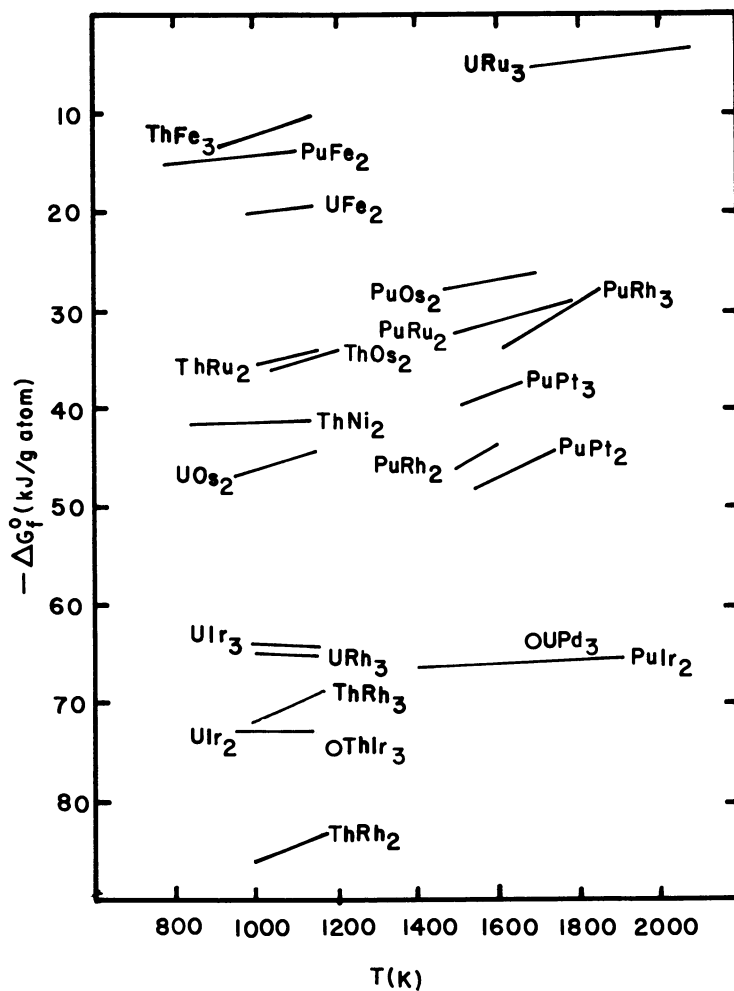


Figure 2. Temperature dependence of free energy of formation, ΔG_f^0 , of actinide intermetallics.

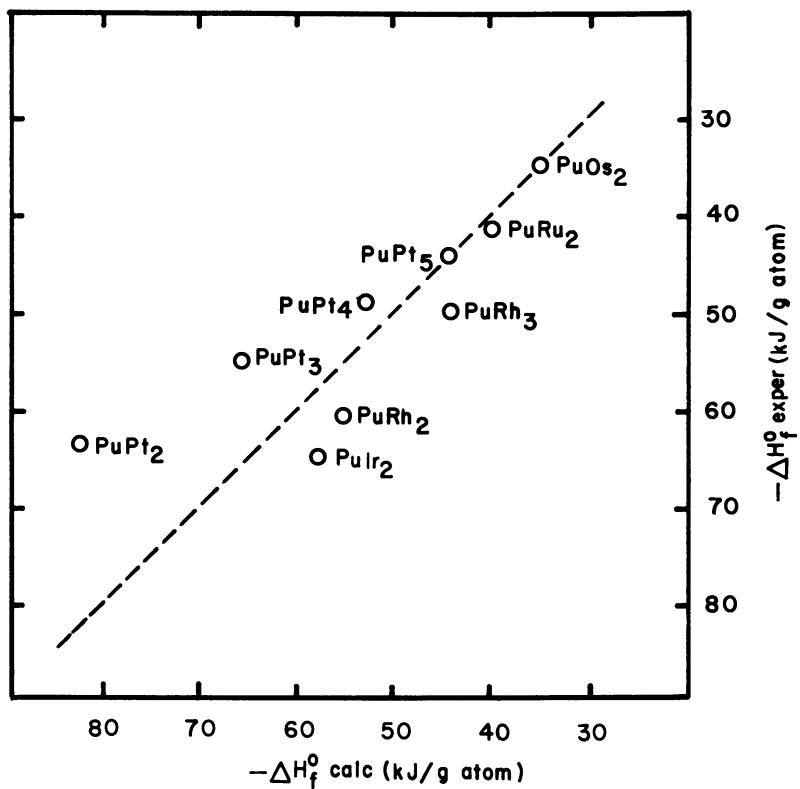


Figure 3. Experimental heats of formation of plutonium intermetallics versus corresponding heats calculated from Miedema⁽²⁾ model.

LITERATURE CITED

1. Brewer, L. "Plutonium 1970 and Other Actinides" (Proc. 4th Int. Conf. Plutonium and Other Actinides, Santa Fe, NM 1970), Amer. Inst. Mining NY 1970, p. 650; J. Opt. Soc. Amer. 1971, 61, 1101; J. Nucl. Mater. 1974, 51, 2; Wengert, P. R. Met. Trans. 1973, 4, 83.
2. Miedema, A. R. "Plutonium 1975 and Other Actinides" (Proc. 5th Int. Conf. Plutonium and Other Actinides, Baden Baden, 1975) Amsterdam 1976, p. 3.
3. Peterson, D. E. J. Nucl. Mater. 1980, 91, 306.
4. Peterson, D. E. Submitted to J. Nucl. Mater. (Sept. 1982).
5. Land, C. C., Peterson, D. E., Roof, R. B. J. Nucl. Mater. 1978, 75, 262.
6. Kennard, E. H. "Kinetic Theory of Gases" McGraw-Hill, NY, 1938, p. 68.
7. Edwards, J. G., Starzynski, J. S.; Peterson, D. E. J. Nucl. Mater. 1980, 73, 908.
8. Hultgren, R.; Desai, P. D.; Hawkins, D. T.; Gleiser, M.; Kelley, K. K.; Wagman, D. D. "Selected Values of the Thermodynamic Properties of the Elements" Amer. Soc. for Metals, Metals Park, OH 1973.
9. Kleykamp, H. J. Less Common Metals 1979, 63, 25; Holleck, H. J. Nucl. Mater. 1972/73, 45, 47; Holleck, H.; France, J. I. J. Nucl. Mater. 1975, 66, 298; Murabayaski, M. J. Less Common Metals 1974, 35, 227.
10. Schmidt, N. Kernforschungszentrum Karlsruhe report KFK1987 (July 1974).
11. Lorenzelli, N.; Marcon, J. P. J. Nucl. Mater. 1972, 44, 57.

RECEIVED December 21, 1982

Thermodynamic Aspects of the Plutonium-Oxygen System

MARVIN TETENBAUM

Argonne National Laboratory, Chemical Technology Division, Argonne, IL 60439

This paper reviews data on certain thermodynamic aspects of the nonstoichiometric Pu-O system, which may serve as a basis for use in reactor safety analysis. Emphasis is placed on phase relationships, vaporization behavior, oxygen-potential measurements, and evaluation of pertinent thermodynamic quantities. Limited high temperature oxygen potential data obtained above the fluorite, diphasic, and sesquioxide phases in the Pu-O system are presented.

Reliable data on the thermodynamic and phase relationships of actinide oxide systems are essential for reactor safety analysis. This paper reviews certain aspects of thermodynamic data currently available on the nonstoichiometric Pu-O system, which may serve as a basis for use in reactor safety analysis. Emphasis is placed on phase relationships, vaporization behavior, oxygen-potential measurements, and evaluation of pertinent thermodynamic quantities. It should be emphasized that very little is quantitatively known about how the total pressures of plutonium-bearing species vary with oxygen potential, stoichiometry, and temperature in the bi-variant region of oxygen-deficient plutonia between the phase limits at very high temperatures. New (though limited) oxygen potential data have been obtained in our laboratory above the fluorite, diphasic, and sesquioxide phases in the Pu-O system at 1750, 2050, and 2250 K.

Phase Relationships

It is generally agreed that the four known oxide phases in the Pu-O system are Pu₂O₃ (hexagonal, La₂O₃ type), PuO_{1.52} (bcc), PuO_{1.61} (fcc, tentative), and PuO₂ (fcc, fluorite type). Above

0097-6156/83/0216-0109\$06.00/0
© 1983 American Chemical Society

At 925 K the PuO_{2-x} phase exhibits a wide range of composition homogeneity, varying from the stoichiometric composition, $\text{O}/\text{Pu} = 2.00$ to $\text{O}/\text{Pu} = 1.61$. The tentative phase diagram of the Pu-O system reported by the 1966 IAEA Panel (1) is shown in Figure 1; it is based primarily on the high temperature X-ray studies of Gardner et al. (2) and Chikalla et al. (3), the galvanic cell study of Markin and Rand (4), as well as via electrical resistivity and thermal expansion measurements. (5, 6, 7) According to a recent assessment of Potter and Rand (8) which was based on suggestions by Sari et al. (9) and X-ray studies by Boivenau (10), the lower phase boundary of the PuO_{2-x} fluorite phase below 1000 K has a composition of $\text{O}/\text{Pu} = 1.72$. Around this composition there is a narrow diphasic region with fcc PuO_{2-x} and a bcc phase which exists from $\text{O}/\text{Pu} = 1.70$ down to $\text{O}/\text{Pu} = 1.61$. It should be emphasized that lower phase boundary compositions shown as line compounds even at high temperatures in Figure 1 have not been critically defined as a function of temperature. For example, the hexagonal sesquioxide phase shown as a line compound on the phase diagram has been found to exhibit a significant range of homogeneity (11) (see below). Finally, it should be noted that unlike the urania system, hyperstoichiometric plutonia (PuO_{2+x}) has not been found to exist.

Vaporization Behavior

The vaporization behavior of the bivariant PuO_{2-x} phase has been investigated by means of mass effusion, mass spectrometry, and transpiration. With tungsten, rhenium, and iridium effusion cells, the agreement between the vapor pressure measurements (i.e., total pressure of plutonium-bearing species) of Mulford and Lamar (12) (2000-2400 K), Pascard (13) (1670-2270 K), Messier (14) (2070-2380 K), Battles et al. (15) (1937-2342 K), and Ackermann et al. (16) (1650-2150 K) is within a factor of two. The measurements of Ohse and Ciani (17) (1800-2200 K) gave vapor pressure values that were somewhat higher than those obtained by the above investigators. The results of transpiration measurements of Pardue and Keller (18) (1730-2000 K), which were obtained with carrier gas streams of oxygen, air, and argon, were not of sufficient accuracy to be quantitative.

With tantalum effusion cells, the results of Ackermann et al. (16) are virtually identical with the earlier work of Phipps et al. (19) (1593-2063 K) and yielded total vapor pressure values of plutonium-bearing species which were considerably higher (by approximately a factor of ten) than those obtained with the less reducing tungsten (as well as Re and Ir) cells. Ackermann et al. (16) correlated the vapor pressure results obtained with tantalum effusion cells with the univariant diphasic system consisting of $\text{Pu}_2\text{O}_3(\text{s})$ - $\text{PuO}_{1.61}(\text{s})$ as the condensed phases and $\text{PuO}(\text{g})$ as the primary gaseous species.

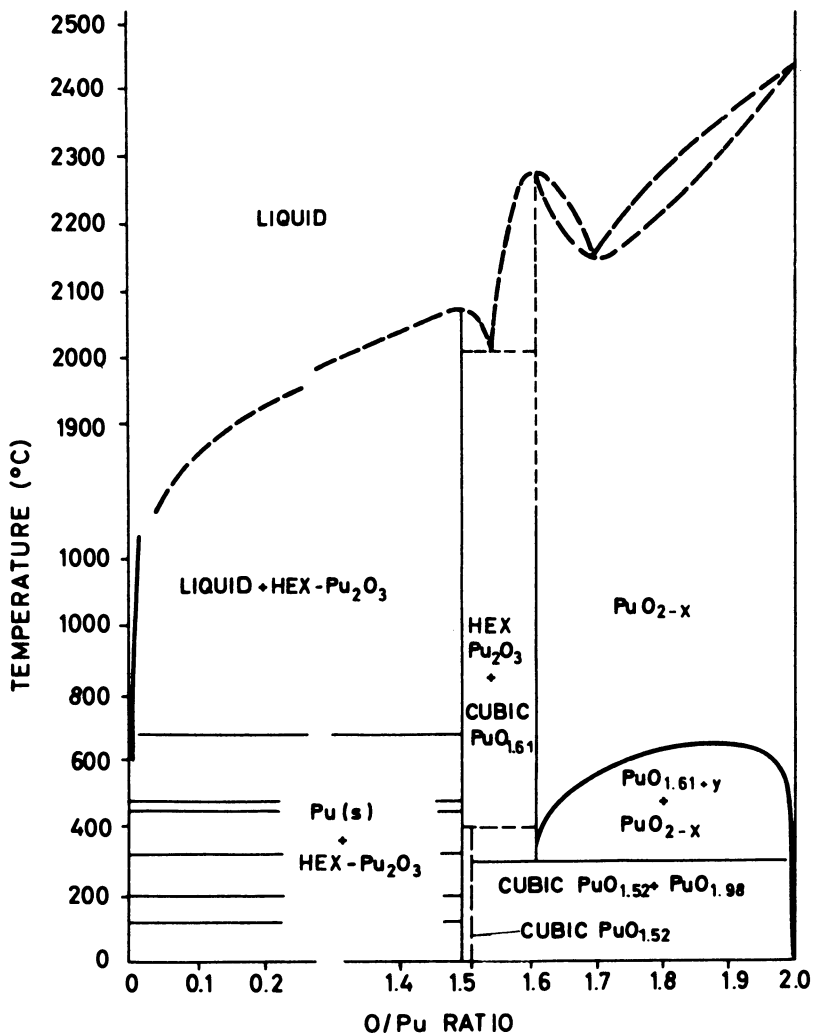
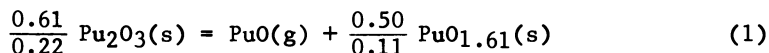


Figure 1. Tentative plutonium-oxygen phase diagram.

It should be emphasized that a survey of the vapor pressure measurements of plutonium-bearing species above bivariant $\text{PuO}_{2-x}(\text{s})$ revealed that in general these measurements suffer from a lack of knowledge of the composition of the condensed phase. Over the composition range, $\text{O}/\text{Pu} = 1.82$ to 1.93 , the measured pressures appear to be insensitive to the composition. This accounts for the general agreement in vapor pressure measurements above bivariant PuO_{2-x} of varying composition obtained by various investigators with tungsten effusion cells. However, Ackermann *et al.* (16) rigorously established the temperature dependency of plutonium-bearing species above the bivariant composition of $\text{O}/\text{Pu} = 1.92 \pm 0.01$. As a consequence of these measurements and the results obtained at the lower phase boundary with Ta effusion cells, meaningful thermodynamic analysis can be made.

Evaluation of Pertinent Thermodynamic Quantities

The principal mode of vaporization at the lower phase boundary based on the thermodynamic analysis of Ackermann *et al.* (16, 20) can be represented by the equation



From a knowledge of the temperature dependency of oxygen potentials above PuO_{2-x} compositions derived from the galvanic cell measurements of Markin and Rand (4), a knowledge of the standard free energy of formation of $\text{PuO}_2(\text{s})$ (21, 22), the standard free energy of formation of PuO_{2-x} compositions can be estimated. The results are given in Table I. It should be emphasized that these calculations involve extrapolations in temperature of the order of 500 K. From the estimated free energy of formation values of Pu_2O_3 and $\text{PuO}_{1.61}$ (16), and the temperature dependency of the partial pressure of $\text{PuO}(\text{g})$ given by

$$\log p_{\text{PuO}/\text{atm}} = - \frac{(27800 \pm 500)}{T} + (8.09 \pm 0.27) \quad (2)$$

the standard free energy of formation of $\text{PuO}(\text{g})$ (20) can be readily obtained

$$\Delta G_f^\circ (\text{PuO}, \text{g}) = -28500 - 9.7T \quad (1600-2150 \text{ K}) \quad (3)$$

Ackermann *et al.* (16, 20) calculated the free energy of formation of $\text{PuO}_2(\text{g})$ based on the reaction

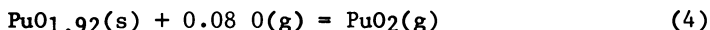


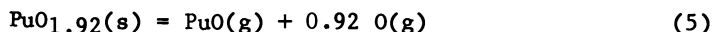
Table 1

Equations for the Standard Free Energy of Formation
and Partial Molar Free Energies of Atomic Oxygen
for Plutonium Oxides (1600-2150 K), cal/mol

O/Pu (s)	$\Delta G_f^\circ = A + BT$		$\bar{\Delta G}_O = A + BT$	
	A	B	A	B
2.00	-249000	42.6	(-204750) ^a	(87.7) ^a
1.98	-246200	41.3	-181750	63.4
1.95	-242600	39.9	-178000	59.0
1.92	-239200	38.7	-173750	54.1
1.90	-237000	38.0	-171150	50.8
1.85	-231600	36.4	-164250	43.4
1.80	-226600	35.2	-157500	36.1
1.75	-222000	34.4	-151500	29.5
1.70	-217500	33.8	-149250	26.5
1.65	-213100	33.3	-150250	26.1
1.61	-209500	32.9	-153000	26.9
1.50	-199800	31.9	-153000	26.9

^aEstimated.
(1 cal = 4.184 J)

The contribution of $\text{PuO}(\text{g})$ to the measured vapor pressure of $\text{PuO}_{1.92}(\text{s})$ can be estimated via the reaction



and subtracted from the measured vapor pressure to yield the temperature dependency of the partial pressure of $\text{PuO}_2(\text{g})$ (16)

$$\log p_{\text{PuO}_2/\text{atm}} = 7.67 - \frac{29640}{T}$$

and, therefore, via equation (4)

$$\Delta G_f^\circ(\text{PuO}_2, \text{g}) = -112600 + 6.6T \quad (1600-2150 \text{ K}) \quad (6)$$

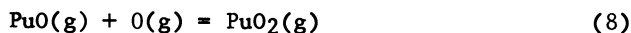
For comparison, Battles et al. (15) determined the partial heats of sublimation of $\text{PuO}_2(\text{g})$ and $\text{PuO}(\text{g})$ above $\text{PuO}_{1.83}$ over the temperature range 1937 to 2342 K by means of mass spectrometric measurements with iridium effusion cells. The absence of iridium oxides or iridium species in the vapor phase indicated that iridium was nonreducing toward plutonia. The partial heats of sublimation calculated from the slopes of the temperature dependency data yielded values of 127.1 ± 1.2 and 138.8 ± 1.6 kcal/mol for $\text{PuO}(\text{g})$ and $\text{PuO}_2(\text{g})$.

From the vapor phase composition and the rate of effusion at 2219 K, Battles et al. (14) calculated the following partial pressures (atm): $\text{PuO}(\text{g}) = 1.50 \times 10^{-6}$, $\text{PuO}_2(\text{g}) = 1.19 \times 10^{-6}$, $\text{Pu}(\text{g}) = 2.6 \times 10^{-9}$, and $\text{O}(\text{g}) = 2.60 \times 10^{-7}$. It should be noted that the vapor phase composition was based on ionization cross section values given by Otvos and Stevenson (23) for O^+ , Pu^+ , PuO^+ , and PuO_2^+ .

Battles et al. calculated the free energies of formation of $\text{PuO}(\text{g})$ and $\text{PuO}_2(\text{g})$ via the equations



and



Combination of the partial pressures of $\text{PuO}(\text{g})$ and $\text{PuO}_2(\text{g})$ at 2219 K with the corresponding partial heats of sublimation yields the following equations for the temperature dependence of $\text{PuO}(\text{g})$ and $\text{PuO}_2(\text{g})$ for $\text{O}/\text{Pu} = 1.83$:

$$\log p_{\text{PuO}/\text{atm}} = - \frac{(27770 \pm 270)}{T} + (6.69 \pm 0.14) \quad (9)$$

and

$$\log p_{\text{PuO}_2/\text{atm}} = - \frac{(30330 \pm 340)}{T} + (7.76 \pm 0.17) \quad (10)$$

An expression for the temperature dependency of the partial pressure of O(g) was derived by Battles *et al.* (15) by using the O(g) pressure measured at 2219 K, and the value of 2.92×10^{-21} atm at 1200 K estimated from the oxygen-potential data of Markin and Rand (4) for PuO_{1.83}

$$\log p_{\text{O}/\text{atm}} = - \frac{36500}{T} + 9.88 \quad (11)$$

For the temperature dependency of Pu(g), Battles *et al.* (15) combined the partial pressure of Pu(g) determined at 2219 K and an assumed partial enthalpy of vaporization value of 118 kcal/mol, leading to the expression

$$\log p_{\text{Pu}/\text{atm}} = - \frac{25800}{T} + 3.04 \quad (12)$$

From equations (9), (10), (11), and (12) and the free energy of formation of O(g), the free energies of formation of PuO(g) and PuO₂(g) can be obtained via the vaporization processes given by equations (3) and (4). Therefore,

$$\Delta G_f^\circ (\text{PuO}, \text{g}) = -16840 - 10.25T \quad (13)$$

and

$$\Delta G_f^\circ (\text{PuO}_2, \text{g}) = -111590 + 14.23T \quad (14)$$

The free energy of formation relationships derived by Ackermann *et al.* (20) for PuO(g) and PuO₂(g) are not in agreement with the corresponding equations obtained by Battles *et al.* At 2000 K, the relationships derived by Ackermann *et al.* yield values for the free energy of formation of PuO(g) and PuO₂(g) of -47.9 and -99.4 kcal/mol, respectively, compared to values of -37.3 and -83.1 kcal/mol based on the equations of Battles *et al.*

The major source of error in calculating the free energies of PuO(g) and PuO₂(g) from Battles *et al.* probably results from the derived equations for the partial pressures of O(g) and Pu(g) as a consequence of uncertainties in ionization cross sections. The thermodynamic assessments of Ackermann *et al.* involve extrapolations of oxygen potentials reported by Markin and Rand (4) in temperature of the order of 500 K. However, a second and third

law assessment carried out by Green (24) has shown that the equations derived by Ackermann et al. are more accurate than those derived by Battles et al.

Based on the thermodynamic assessment of Ackermann et al. (16, 20) the detailed vaporization behavior of the PuO_{2-x} phase is summarized in Figure 2, in which the partial pressures of the various vapor species are given as a function of the composition of the solid phase at 1970 K. It is apparent that the partial pressures of $\text{PuO}(\text{g})$, $\text{Pu}(\text{g})$, $\text{O}(\text{g})$, and $\text{O}_2(\text{g})$ depend on the O/Pu ratio of the condensed phase whereas the partial pressure of $\text{PuO}_2(\text{g})$ is rather insensitive to the composition. It should be noted that the minimum total pressure of the system occurs for the congruently vaporizing composition of O/Pu \approx 1.87. The congruently vaporizing composition has been calculated by Ackermann et al. (16) to vary from O/Pu = 1.92 at 1600 K to 1.84 at 2400 K. For comparison, Ohse and Ciani (17) estimate congruent vaporizing composition values of O/Pu = 1.84, 1.86, and 1.89 (based on the minimum total pressures obtained for the vapor pressure isotherms at 1800, 2000, and 2200 K).

Region of Homogeneity of Pu_2O_3 Phase

As indicated previously, the tentative phase diagram of the Pu-O system shows plutonium sesquioxide as a line compound from room temperature up to its melting point. During the course of the preparation of $\beta\text{-}^{242}\text{Pu}_2\text{O}_3$ for low temperature heat capacity measurements (11), a procedure was established which can serve as a basis for mapping out the region of homogeneity of the sesquioxide phase as well as other phase boundary compositions in the PuO_{2-x} system.

The single phase $\beta\text{-}^{242}\text{Pu}_2\text{O}_3$ sample was prepared by high-temperature reduction of $^{242}\text{PuO}_2$. The reduction was carried out in the high-temperature transpiration apparatus previously used to investigate the vaporization behavior of various actinide oxide systems (25, 26). Because of the limited amount of $^{242}\text{PuO}_2$ available and the lack of well-defined methods for the preparation of $\beta\text{-Pu}_2\text{O}_3$, the synthesis was made batchwise with one gram portions of $^{242}\text{PuO}_2$ in order to minimize the possibility of large amounts of sample loss due to unforeseen preparative failures.

The reduction of the sample was made at 2250 K in a flowing stream of hydrogen carrier gas ($\sqrt{280}$ cm³/min). The total pressure of the carrier gas was approximately 1 atm. The water vapor produced during the reduction was swept by the carrier gas into an electrolytic-type (P₂O₅) moisture monitor and a continuous recorder trace of the water concentration as a function of time was obtained. A typical plot of the moisture content of the carrier gas as a function of time is shown in Figure 3. The region on the left side of this figure where the moisture content

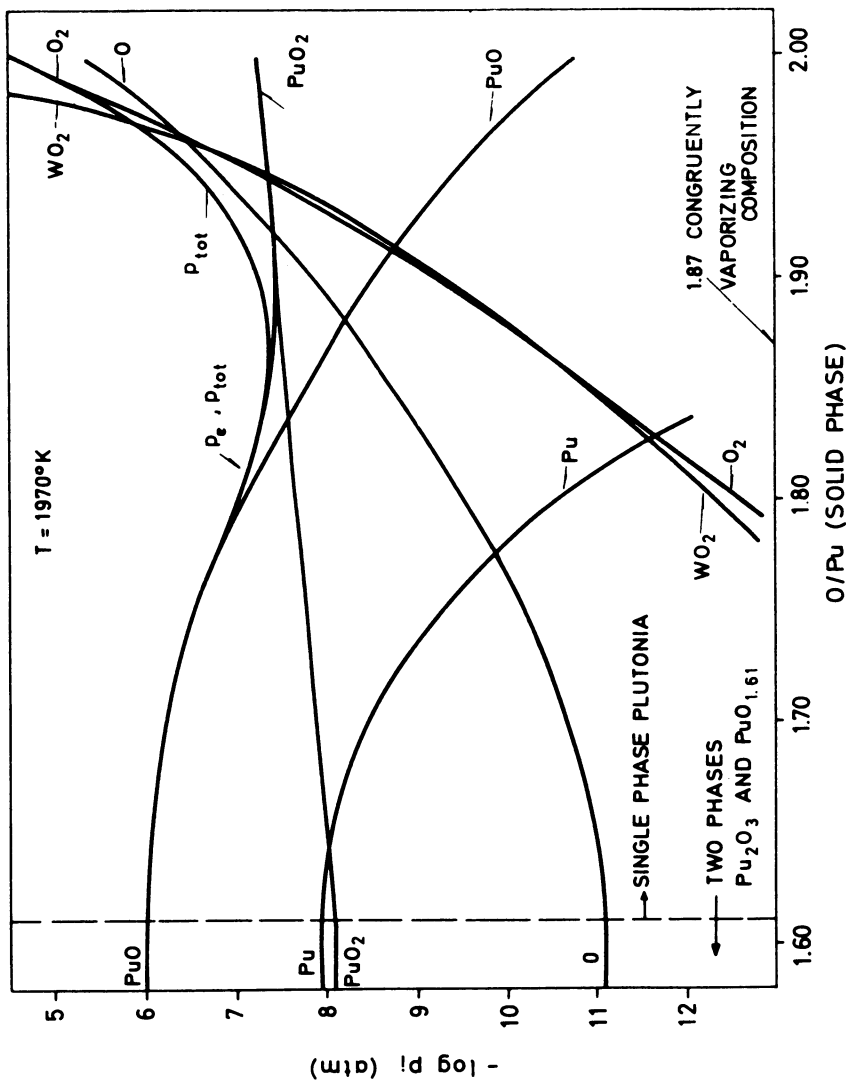


Figure 2. Partial pressures of vapor species versus composition of the substoichiometric plutonium dioxide phase at 1970 K.

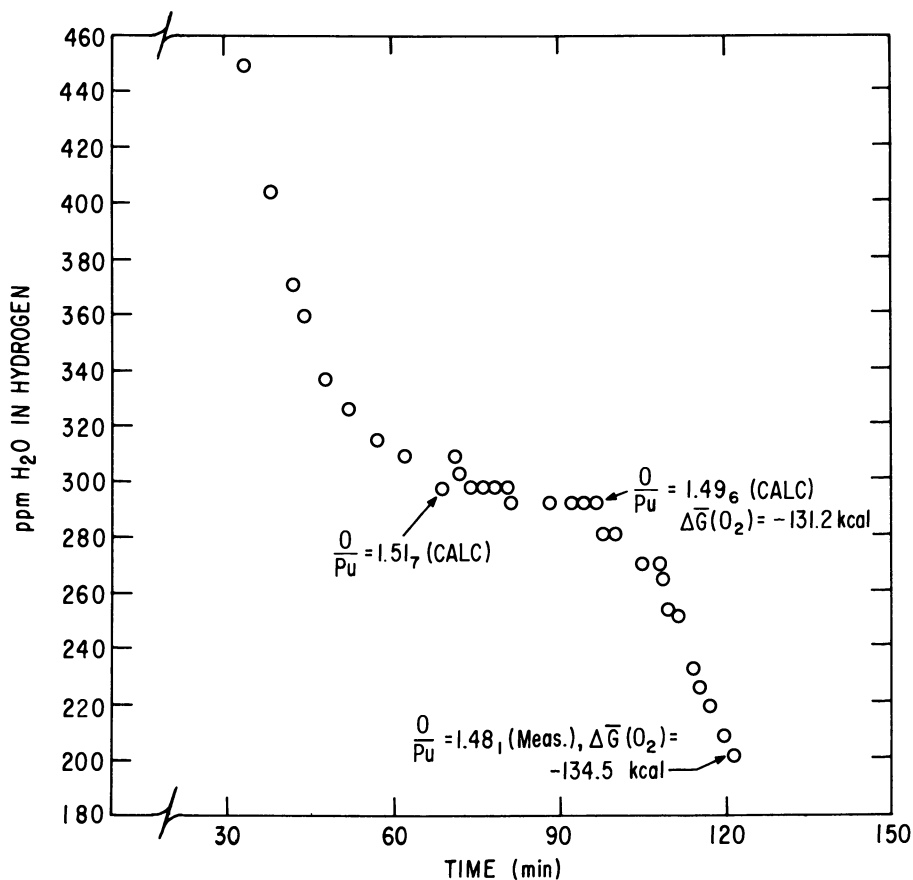


Figure 3. Moisture concentration (ppm H₂O) in the hydrogen carrier gas as a function of time during the preparation of the plutonium sesquioxide sample by hydrogen reduction at 2250 K.

decreases with time is interpreted as a single phase region, (namely fluorite PuO_{2-x}), the plateau region is a diphasic region, and the final rapid decrease of the plateau is interpreted as indicating single-phase plutonium sesquioxide. In contrast to the phase diagram, the present result indicates a considerable range of composition homogeneity of the plutonium sesquioxide phase at 2250 K.

The reduction was terminated following the plateau region when the moisture content was approximately 200 ppm. The reduced product was analyzed for oxygen content by heating it in air at approximately 1023 K to produce stoichiometric PuO_2 . From the increase in mass upon oxidation to PuO_2 , the O/Pu ratio was found to be 1.481 ± 0.005 . The oxygen potential for this composition was calculated to be $\Delta G_{\text{O}_2} = -134.6$ kcal/mol at 2250 K. X-ray analysis of a portion of a 10⁻²-gram sample prepared batchwise by the above procedure showed the presence of only β -²⁴²Pu₂O₃ phase. The lattice constants were determined to be $a = 3.837$ and $c = 5.948$ Å ($a/c = 0.6451$); these parameters are in excellent agreement with those of Gardner *et al.* (2) who reported $a = 3.8388 \pm 0.0002$ Å and $c = 5.9594 \pm 0.0006$ Å for a sample with a O/Pu ratio of 1.498.

From the water concentration in the hydrogen carrier gas as a function of time, flow rate, and the measured composition O/Pu = 1.481, one can make a rough estimate of the initial and terminal compositions of the diphasic region and the corresponding oxygen potential. The results are given in Figure 3. For comparison, based on the galvanic cell measurements of Markin and Rand, $\Delta G_{\text{O}_2} = -135.8$ kcal/mol for the diphasic region $\text{Pu}_2\text{O}_3 + \text{Pu}_{0.61}$. The agreement is reasonable, considering the long temperature extrapolation required for the calculation of the oxygen potential based on the measurements of Markin and Rand.

"High-Temperature" Oxygen-Potential Measurements

A scarcity of high-temperature oxygen-potential measurements above well-defined condensed phase compositions exists for the Pu-O system. Reliable high-temperature data combined with free energy of formation values of the known vapor species and condensed phase compositions are essential for estimating the vaporization behavior of plutonia. To date, extrapolated values of oxygen potentials derived from the galvanic cell measurements of Markin and Rand (4) have been used to estimate the vaporization behavior of oxygen-deficient plutonia with a reasonable degree of success over a restricted temperature range.

During the course of exploratory experimentation involved in the preparation of β -²⁴²Pu₂O₃, some limited oxygen potential measurements over PuO_{2-x} fluorite phase were made at 1750 and 2050 K. The transpiration method was used for this study because, for a given temperature, the composition of the condensed phase can be fixed by appropriate choice of oxygen potential (via H₂/

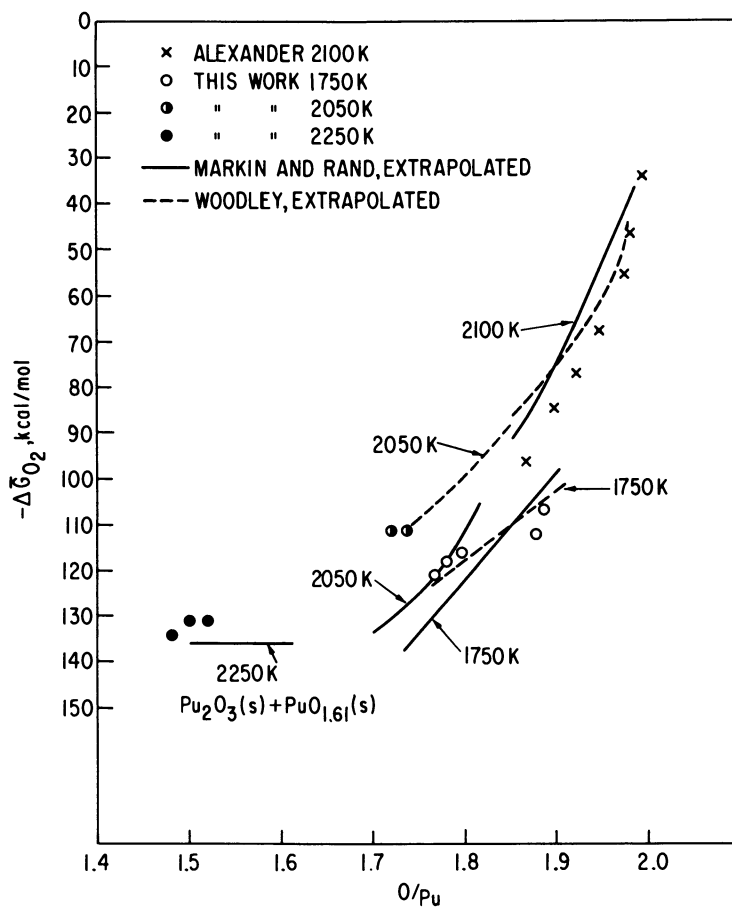


Figure 4. "High temperature" oxygen potentials above the PuO_{2-x} system.

H₂O ratios) of the carrier gas. This is consistent with the requirements based on the phase rule for a bivariant system.

The results of limited oxygen potential measurements at 1750 and 2050 K are shown in Figure 4. Included in Figure 4 are measurements at 2100 K reported by Alexander *et al.* (27) as well as our measurements with the sesquioxide phase and the diphasic region (O/Pu = 1.50 - 1.52) at 2250 K. The extrapolated oxygen-potential values of Markin and Rand are in fair agreement with the measurements obtained at 1750 and 2100 K (and the diphasic region at 2250 K), but deviate considerably from the limited measurements obtained at 2050 K. The extrapolated values of oxygen potentials derived from Woodley's (28) recent TGA and limited emf oxygen-potential measurements at 1273, 1373, and 1473 K over the composition range, $\sqrt{1.8}$ to 1.98, appears to be in better agreement with the high-temperature experimental measurements than the extrapolated oxygen potentials of Markin and Rand.

Some Recommendations for Future Studies on the Pu-O System

(1) Measurements of oxygen potentials and vapor pressure of plutonium-bearing species above a wide range of Pu-O compositions, including the difficult region close to stoichiometric plutonia, should be made at high temperatures, particularly above 3000°C, for purpose of safety analysis.

(2) The temperature dependence of lower phases boundary compositions needs to be established.

(3) Measurements of solidus and liquidus temperatures need to be established.

(4) There is a scarcity of oxygen-transport data for oxygen-deficient actinide oxide systems. Because of this, our understanding and predictive capabilities of the effect of the defect solid state on the properties of reactor fuel systems, as well as on the chemical state of fission products in these systems, are limited.

Acknowledgments

The author is grateful to Drs. P. Potter (AERE), D. W. Green (ANL), J. K. Fink (ANL), and L. Leibowitz (ANL) for helpful discussions concerning the Pu-O system. The author is particularly grateful to Dr. J. E. Battles (ANL) for providing this writer with his unpublished manuscript and permission to quote the results of a mass spectrometric study of the volatilization of plutonia.

Literature Cited

1. "The Plutonia-Oxygen and Uranium-Plutonium-Oxygen Systems: A Thermochemical Assessment", Technical Reports No. 79, International Atomic Energy Agency, Vienna (1967).

2. Gardner, E. R.; Markin, T. L.; Street, T. L. *J. Inorg. Nucl. Chem.* 1965, 27, 541.
3. Chikalla, T. D.; McNeilly, C. E.; Skadvahl, R. E. *J. Nucl. Mater.* 1964, 12, 131.
4. Markin, T. L.; Rand, M. H. "Thermodynamics"; IAEA, Vienna, 1966, Vol. I, p. 145.
5. Blanc, J. M.; Andriessen, H. EURAEC-434, 1962.
6. Brett, N. H.; Russell, L. E. "Plutonium 1960", Cleaver Hume Press, London, 1961, p. 397.
7. McNeilley, C. E. *J. Nucl. Mater.* 1964, 11, 53.
8. Potter, P. E.; Rand, M. H., *High Temp. Sci.* 1980, 13, 315.
9. Sari, C.; Benedict, U.; Blank, H. *Thermodynamics of Nuclear Materials*, IAEA, Vienna 1968, p. 587.
10. Boivineau, J. C. *J. Nucl. Mat.* 1976, 60, 31.
11. Flotow, H. E.; Tetenbaum, M. *J. Chem. Phys.* 1981, 74, 5269.
12. Mulford, R. N. R.; Lamar, L. E. "The Volatility of Plutonium Oxide", *Plutonium 1960*, Cleaver-Hume Press, Ltd., London 1961, p. 411.
13. Pascard, R. reported in reference 1.
14. Messier, D. R. *J. Am. Ceram. Soc.* 1968, 51, 710.
15. Battles, J. E.; Shinn, W. A.; Reishus, J. W. ANL-7575, p. 77.
16. Ackermann, R. J.; Faircloth, L. J.; Rand, M. H. *J. Phys. Chem.* 1966, 70, 3698.
17. Ohse, R. W.; Ciani, C. "Thermodynamics of Nuclear Materials", IAEA, Vienna 1967, p. 545.
18. Pardue, W. M.; Keller, D. L. *J. Am. Ceram. Soc.* 1964, 47, 610.
19. Phipps, T. E.; Sears, G. W.; Simpson, O. C. *J. Chem. Phys.* 1950, 18, 724.
20. Ackermann, R. J.; Chandrasekhariah, M. S. "Thermodynamics of Nuclear Materials 1974", IAEA, Vienna, 1975, p. 3.
21. Kruger, O. L.; Savage, H. *J. chem. Phys.* 1968, 49, 4540.
22. Ogard, A. E. "Plutonium 1970 and Other Actinides", W. N. Miner, ed., Part I, 1970, p. 78.
23. Otvos, J. W.; Stevenson, D. P. *J. Amer. Chem. Soc.* 1956, 78, 546.
24. Green, D. W. personal communication.
25. Tetenbaum, M.; Hunt, P. D. *J. Chem. Phys.* 1968, 49, 4739.
26. Tetenbaum, M. "Thermodynamics of Nuclear Materials 1974", IAEA, Vienna, 1975, Vol. II, p. 305.
27. Alexander, C. A. (Battelle Memorial Institute, Columbus, Ohio) data presented at the Libby-Cockcraft Exchange Meeting on Phase Diagrams and Thermodynamics of Fuel Materials, May 20-22, 1968.
28. Woodley, R. E. *J. Nucl. Mater.* 1981, 96, 5.

RECEIVED December 21, 1982

Vapor Pressures and Vapor Compositions in Equilibrium with Hypostoichiometric Plutonium Dioxide at High Temperatures

D. W. GREEN, J. K. FINK, and L. LEIBOWITZ

Argonne National Laboratory, Chemical Technology Division, Argonne, IL 60439

Vapor pressures and vapor compositions in equilibrium with a hypostoichiometric plutonium dioxide condensed phase have been calculated for the temperature range $1500 \leq T \leq 4000$ K. Thermodynamic functions for the condensed phase and for each of the gaseous species were combined with an oxygen-potential model, which we extended from the solid into the liquid region to obtain the partial pressures of O_2 , O, Pu, PuO and PuO₂ as functions of temperature and of condensed phase composition. The calculated oxygen pressures increase rapidly as stoichiometry is approached. At least part of this increase is a consequence of the exclusion of Pu⁶⁺ (or other high oxidation state) from the oxygen-potential model. No reliable method was found to estimate the importance of this ion, whose existence has not been established in the oxide system and whose effects might be expected to increase greatly with temperature, similar to the effects due to U⁶⁺ in the uranium/oxygen system. As a result of large oxygen potentials at high temperatures, extremely high total pressures that produced unreasonably high vapor densities were calculated. Results were limited to temperatures below 4000 K and oxygen-to-metal ratios of 1.994 to 1.70. These calculations show that the vapor in equilibrium with hypostoichiometric plutonium dioxide is poorly approximated as PuO₂ for most of the temperature and composition range of interest. In addition, the vapor is much more oxygen-rich than the condensed phase with which it is in equilibrium. The limitations of this approach and the implications of these calculations for the technologically important (U,Pu)O_{2-x} system are also discussed.

0097-6156/83/0216-0123\$06.25/0
© 1983 American Chemical Society

One of the most important thermophysical properties of reactor fuel in reactor safety analysis is vapor pressure, for which data are needed for temperatures above 3000 K. We have recently completed an analysis of the vapor pressure and vapor composition in equilibrium with the hypostoichiometric uranium dioxide condensed phase (1), and we present here a similar analysis for the plutonium/oxygen (Pu/O) system.

The process we have followed is identical with the one we used previously for the uranium/oxygen (U/O) system (1-2) and is summarized by the procedure that is shown in Figure 1. Thermodynamic functions for the gas-phase molecules were obtained previously (3) from experimental spectroscopic data and estimates of molecular parameters. The functions for the condensed phase have been calculated from an assessment of the available data, including the heat capacity as a function of temperature (4). The oxygen potential is found from extension into the liquid phase of a model that was derived for the solid phase. Thus, we have all the information needed to apply the procedure outlined in Figure 1.

In this paper we describe: (1) the gas-phase thermodynamic functions; (2) the condensed-phase thermodynamic functions; (3) the oxygen potential (and the phase boundaries that are consistent with it); and (4) the resulting vapor pressure and composition as functions of temperature and composition of the condensed phase.

Methods

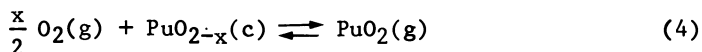
General. The methods we have used to calculate the vapor pressures and vapor compositions at high temperatures are the same as those used previously (1-2) for the U/O system. The total pressure, $p(\text{total})$, in equilibrium with a PuO_{2-x} condensed phase is

$$p(\text{total}) = p(\text{O}) + p(\text{O}_2) + p(\text{Pu}) + p(\text{PuO}) + p(\text{PuO}_2) \quad (1)$$

where only the neutral species are considered. The oxygen-to-plutonium molar ratio in the gas phase, $R(\text{gas})$, is

$$R(\text{gas}) = \frac{p(\text{O}) + 2p(\text{O}_2) + p(\text{PuO}) + 2p(\text{PuO}_2)}{p(\text{Pu}) + p(\text{PuO}) + p(\text{PuO}_2)} \quad (2)$$

The set of partial pressures given by Eq. (1) must satisfy equilibria among themselves and with the condensed phase. Of the several possible choices of independent equilibria, the following set is a convenient one:



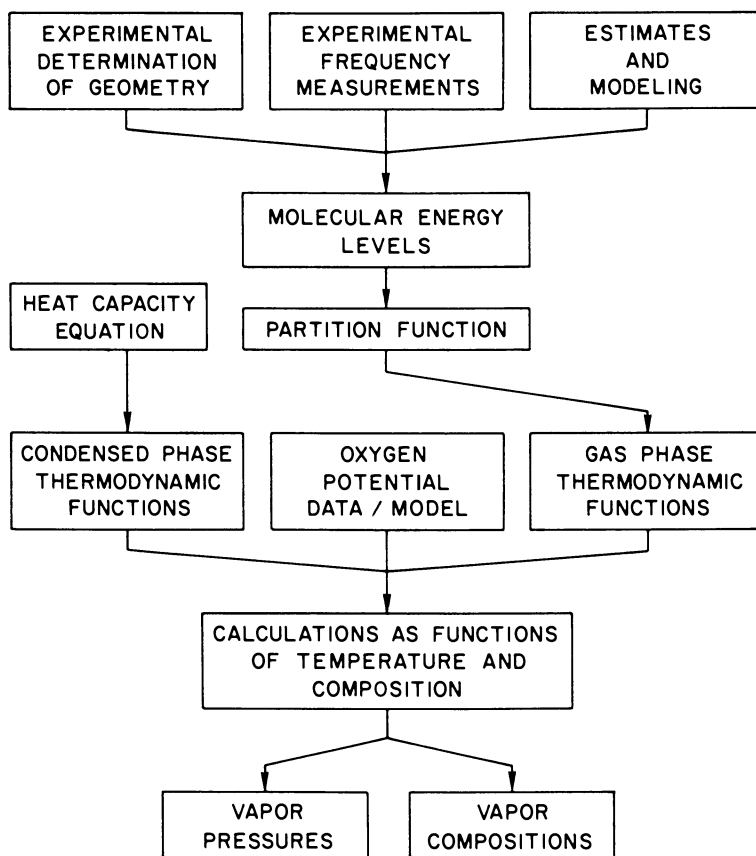
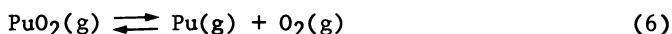
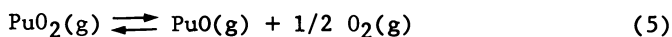


Figure 1.
Procedure for calculation of vapor pressures from spectroscopic data.



where c represents the condensed phase and g represents the gas phase.

If we know the oxygen pressure, $p(\text{O}_2)$, from the oxygen potential, the required partial pressures may be obtained from Eqs. (3-6), in sequence, using the following relationships:

$$\ln p(\text{O}) = 1/2 \ln p(\text{O}_2) - \Delta G_f^\circ(\text{O})/RT \quad (7)$$

$$\ln p(\text{PuO}_2) = \frac{x}{2} \ln p(\text{O}_2) + [\Delta G_f^\circ(\text{PuO}_{2-x}, \text{c}) - \Delta G_f^\circ(\text{PuO}_2, \text{g})]/RT \quad (8)$$

$$\ln p(\text{PuO}) = [\Delta G_f^\circ(\text{PuO}_2, \text{g}) - \Delta G_f^\circ(\text{PuO}, \text{g})]/RT - 1/2 \ln p(\text{O}_2) + \ln p(\text{PuO}_2) \quad (9)$$

$$\ln p(\text{Pu}) = [\Delta G_f^\circ(\text{PuO}_2, \text{g}) - \Delta G_f^\circ(\text{Pu}, \text{g})]/RT - \ln p(\text{O}_2) + \ln p(\text{PuO}_2) \quad (10)$$

Thermodynamic Functions of the Gases. To apply Eqs. (1-10), the free energies of formation, ΔG_f° , for all gaseous species as a function of temperature are required. Tabulated data were fit by a least-squares procedure to derive an analytical equation for ΔG_f° of each vapor species. For the plutonium oxide vapor species, the data calculated from spectroscopic data (3) were used; for $\text{O}(\text{g})$ and $\text{O}_2(\text{g})$, the JANAF data (5) were used; and for $\text{Pu}(\text{g})$, data from the compilation of Oetting et al. (6) were used. The coefficients of the equations for ΔG_f° of the gaseous species are included in Table I.

Oxygen Potential for Solid PuO_2 . Considerable attention has been devoted to the temperature and composition dependence of the oxygen potential, $\Delta G^\circ(\text{O}_2)$, for the solids PuO_{2-x} and $(\text{U}, \text{Pu})\text{O}_{2-x}$ (7) and many models of the oxygen potential have been proposed (8-20). The model devised by Blackburn (12-14) has been used for solid PuO_{2-x} for three reasons: (1) it fits the available experimental data reasonably well (12-14), (2) it has a small number of adjustable parameters for which a physical basis can be provided, and (3) it is analogous to the one that has been successfully applied to the UO_{2-x} system (1-2). This model for the solid phase assumes the following equilibrium between oxygen gas and the ions in the lattice:

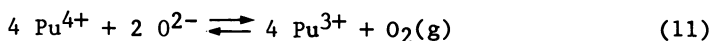


Table I. Coefficients of ΔG_f° (in $\text{kJ}\cdot\text{mol}^{-1}$) = $A + BT + CT^2 + DT^3 + E/T + F\cdot\ln(T)$. (T represents 298.15 K.)

Species	T-range, K	A	B	C	D	E	F
O (g)	2-1400	252.36	-6.2747×10^{-2}	-1.3294×10^{-6}	---	-527.69	---
	1400-6000	259.03	-6.7710×10^{-2}	-1.6525×10^{-8}	---	-3747.4	---
Pu (g)	1000-3605	260.58	-7.9957×10^{-2}	-2.4343×10^{-6}	---	12715	6.8126
	3605-6000	0.0	---	---	---	---	---
PuO (g)	1000-3605	-106.88	-6.4867×10^{-2}	3.4979×10^{-6}	---	---	---
	3605-6000	-452.62	3.0418×10^{-2}	3.6209×10^{-6}	---	---	---
PuO ₂ (g)	1000-3605	-481.09	2.1026×10^{-2}	2.3283×10^{-6}	---	---	---
	3605-6000	-783.92	8.9630×10^{-2}	7.6581×10^{-6}	-2.9487×10^{-10}	---	---
PuO ₂ (c)	913-2701	-1060.9	2.0521×10^{-1}	-6.0130×10^{-6}	---	---	---
	2701-3605	-918.62	1.3644×10^{-1}	---	---	---	---
	3605-6000	-1241.0	2.1943×10^{-1}	-2.0882×10^{-6}	-8.9622×10^{-11}	---	---

From this equilibrium the oxygen pressure may be determined:

$$\ln p(\text{O}_2) = 4 \ln (\text{Pu}^{4+})/(\text{Pu}^{3+}) + 2 \ln (\text{O}^{2-}) + \ln K_S \quad (12)$$

where the parentheses indicate ionic concentration (in moles per mole of Pu) and K_S is the equilibrium constant for Eq. (11):

$$K_S = \frac{(\text{Pu}^{3+})^4 p(\text{O}_2)}{(\text{Pu}^{4+})^4 (\text{O}^{2-})^2} \quad (13)$$

Blackburn also included in his model an equilibrium between trivalent and divalent plutonium. Because our interest lies principally in the region for which $x < 0.1$, the divalent ion concentration is relatively unimportant (21).

If we consider conservation of plutonium and charge, where $(\text{O}^{2-}) = 2 - x$, $(\text{Pu}^{4+}) = 1 - 2x$ and $(\text{Pu}^{3+}) = 2x$; Eq. (12) becomes

$$\ln p(\text{O}_2) = 4 \ln [(1 - 2x)/2x] + 2 \ln (2 - x) + \ln K_S \quad (14)$$

To evaluate K_S , Blackburn assumed $\ln K_S = A_S + B_S/T$, where T is the absolute temperature, and A_S and B_S are constants characteristic of $\text{PuO}_{2-x}(\text{s})$ which were found from an examination of available oxygen potential data [Alexander (22), Atlas and Schlehman (8), Markin and McIver (23), Woodley (24), Javed (25), Tetenbaum (26-27), and Blackburn (28)]. This evaluation gave $B_S = -101600$ and $A_S = 20.8$. We have compared the oxygen potentials calculated using Eq. (14) and these parameter values with more recent unpublished data of Tetenbaum (27) and have found reasonable agreement.

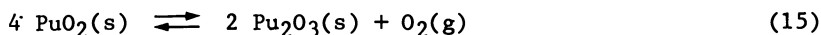
The substitution of $(\text{Pu}^{3+}) = 2x$ into Eq. (14) creates a mathematical problem in the first term for the special case of $x = 0$ and a physical problem for all small values of x . We considered this problem in detail elsewhere (21). Because of this problem at $x = 0$, we limit our discussion and numerical calculations to cases with $x > 0.005$.

In the oxygen-potential model that was used for the U/O system (1-2), two equilibria for the solid were considered. One of these equilibria is analogous to Eq. (11) and the other involved the U^{6+} ion. We are unaware of evidence for the existence of the Pu^{6+} ion in the oxide system. No PuO_3 molecule was identified in the matrix-isolation studies (29) although, with similar experimental methods, the UO_3 molecule was easily observed (30). No evidence for PuO_3 has been reported in mass spectrometric studies (31). However, the existence of the Pu^{6+} ion has been established by the observation of the hexafluoride (32). We have not included any Pu^{6+} in our calculations.

Oxygen Potential for Liquid PuO_2 . To extend the oxygen-potential model from the solid to the liquid phase, we assume that Eqs. (11-14) apply to the liquid with new values of the model parameters.

Therefore, we must find a new equilibrium constant, K_ℓ , that is analogous to K_s . We have considered (21) several methods of evaluating the model parameters (the equation that gives K_ℓ as a function of temperature) from the available data.

The model for the liquid phase may be obtained by analogy with the solid phase. Equation (11) is the ionic model reaction for



The equilibrium constant for this reaction is given by

$$-RT \ln K = \Delta G^\circ = \Delta H^\circ - T \Delta S^\circ \quad (16)$$

An analogous equation may be written for the liquid counterpart of Eq. (15) so that an equation like Eq. (16) is valid for the liquid as well. The difference between ΔG° in Eq. (16) and ΔG° for its liquid analog becomes

$$\Delta(\Delta G^\circ) = 2 \Delta H_m^\circ(\text{Pu}_2\text{O}_3) - 4 \Delta H_m^\circ(\text{PuO}_2) - T [2 \Delta S_m^\circ(\text{Pu}_2\text{O}_3) - 4 \Delta S_m^\circ(\text{PuO}_2)] \quad (17)$$

where ΔH_m° and ΔS_m° are the enthalpy and entropy of fusion, respectively of the indicated compound.

If we assume $\ln K = A + B/T$ for the liquid as well as for the solid, then:

$$(A_\ell - A_s) + (B_\ell - B_s)/T = -\Delta(\Delta G^\circ)/RT \quad (18)$$

If the enthalpy and entropy of fusion are assumed to be independent of temperature, Eq. (17) with Eq. (18) to obtain

$$\Delta A = A_\ell - A_s = [2 \Delta S_m^\circ(\text{Pu}_2\text{O}_3) - 4 \Delta S_m^\circ(\text{PuO}_2)]/R \quad (19)$$

$$\text{and } \Delta B = B_\ell - B_s = -[2\Delta H_m^\circ(\text{Pu}_2\text{O}_3) - 4 \Delta H_m^\circ(\text{PuO}_2)]/R \quad (20)$$

The enthalpies and entropies of fusion that are required for evaluation of Eqs. (19) and (20) may be estimated for PuO_2 and Pu_2O_3 in a manner analogous to that for UO_2 (1). An estimate of the entropy of fusion was obtained (1) from the available data in JANAF (5), for which the average value of R_m [$R_m = \Delta S_m^\circ T_m/R \cdot m$] is 1.4. Thus, we obtain $\Delta A = -2.8$. The value of ΔB depends on the melting points.

The Phase Boundaries. Our interest in the phase diagram is solely to define the method by which the calculation of the partial pressures should be done. Because (1) there are only small

effects on the total pressure and vapor composition as a result of small changes in the phase boundaries and (2) the range of T and x values for which the method of calculation will be affected is small, there is little need to have an accurate phase diagram. It is more important for our purpose to use a phase diagram that is consistent with our method and choice of parameter values.

The solidus, the liquidus, the oxygen-potential model for the solid Pu/O system, and the oxygen-potential model for the liquid Pu/O system each depend upon the temperature and composition. Because the oxygen-potential model has a greater effect on the vapor pressure and composition at high temperature than do the solidus and liquidus, we have fixed the functional forms and the parameter values for the oxygen-potential model. We choose the IAEA solidus (32) and determine the liquidus that is consistent with it and with the two parts of the oxygen-potential model. The calculated liquidus, which is based on the liquid model parameters, is very close to the IAEA liquidus (33).

The phase diagram that we shall use to define the method of calculation is given in Figure 2. The regions are defined by:

Region I: One-phase solid; $T < 2416$ K; $0.005 < x < 0.30$

Region II: One-phase solid; $2416 < T < 2701$;
 $0.005 < x < x_s$

Region III: Solid and liquid phases: $2416 < T < 2701$;
 $x_s < x < x_l$

Region IV: One liquid phase; $T < 2701$; $x_l < x < 0.30$

Region V: One liquid phase: $2701 < T < 5000$;
 $0.005 < x < 0.3$

The solidus, which is the one recommended by the IAEA (32), may be represented by the following equation for $2416 < T < 2701$ K:

$$x_s = 9.577 - 6.333 \times 10^{-3} T + 1.032 \times 10^{-6} T^2 \quad (21)$$

The liquidus, which is consistent with Eq. (21) and the two parts of the oxygen-potential model, may be represented by the following equation for $2416 < T < 2701$ K:

$$x_l = 5.108 - 2.534 \times 10^{-3} T + 2.378 \times 10^{-7} T^2 \quad (22)$$

Thermodynamic Functions of the Condensed Phases. Tabulated thermodynamic functions for the condensed phases of plutonium dioxide and a detailed description of their calculation are given elsewhere (21). The $\Delta G_f^\circ(\text{PuO}_2, c)$ is represented by the equation given in Table I. The ΔG_f° values were calculated using standard thermodynamic relations and the data given below.

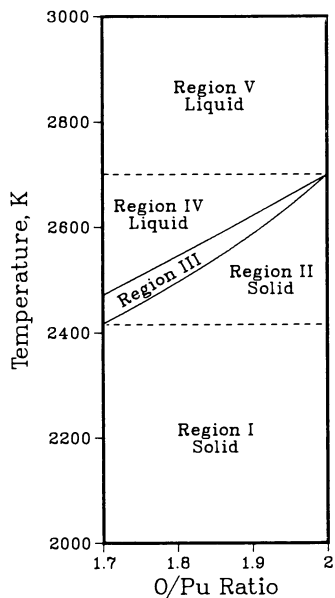


Figure 2.
Phase diagram of the plutonium/oxygen system.

The phase-transition temperatures for Pu and PuO₂, that were used, are given in Table II.

Table II. Important Transition Temperatures for the Plutonium Dioxide Condensed Phase

T, K	Phase Transition	Reference
395	Pu(α)--Pu(β)	Oetting <i>et al.</i> (6)
480	Pu(β)--Pu(γ)	Oetting <i>et al.</i> (6)
588	Pu(γ)--Pu(δ)	Oetting <i>et al.</i> (6)
730	Pu(δ)--Pu(δ')	Oetting <i>et al.</i> (6)
752	Pu(δ')--Pu(ε)	Oetting <i>et al.</i> (6)
913	Pu(ε)--Pu(ℓ)	Oetting <i>et al.</i> (6)
2701	PuO ₂ (s)--PuO ₂ (ℓ)	Aitkin and Evans (34)
3605	Pu(ℓ)--Pu(g)	Calculated from data in (6)

The heat capacity function for the solid phase is from Fink (4). Fink points out that although (U,Pu)O₂, UO₂, and ThO₂ have solid-solid phase transitions, the available data (4) make it impossible to determine the existence of a similar phase transition for PuO₂. If additional high-temperature measurements indicate the presence of a solid-solid phase transition, the heat capacity of PuO₂ between the phase transition and 2701 K may be significantly higher.

The heat capacity for liquid PuO₂ has been estimated (21) as 96 J·mol⁻¹·K⁻¹ assuming no electronic contribution. If an electronic contribution is found by experiment to be present, the liquid heat capacity would be increased.

The free energy of formation of the hypostoichiometric condensed phase ΔG_f^o(PuO_{2-x},c), can be calculated at any temperature from the free energy of formation of PuO₂(c) and the oxygen potential using the following relationship:

$$\Delta G_f^o(\text{PuO}_{2-x}, c) = \Delta G_f^o(\text{PuO}_2, c) - \frac{RT}{2} \int_0^x \ln p(\text{O}_2) dx' \quad (23)$$

This relationship, which is applicable provided that no phase boundaries are crossed at T between x = 0 and x = x', arises from

the Gibbs-Duhem equation and has been successfully used for the U/O system (1).

The evaluation of the integral in Eq. (23) differs from the corresponding integral for the U/O system because of the differences in the oxygen-potential models. In particular, the neglect of Pu^{6+} , but not U^{6+} , leads to the problem that $\ln p(\text{O}_2)$ for the Pu/O system becomes infinite as x goes to zero. However, the integral in Eq. (23) remains finite and has been evaluated (21).

The model we have used and the parameter values in the model are consistent with the available experimental data (insofar as consistency is possible). It is not possible to determine without additional data whether the difficulties at small x and at high temperature are attributable to inadequacies in the model or inadequacies in the available experimental data, which have been used to evaluate the model parameters.

Ions. The ionization potentials of each vapor species given in Table III are similar to their counterparts in the U/O system (1). Ionization was shown to be of minor importance for the U/O system in the temperature and composition ranges of interest. Furthermore, the results obtained from the oxygen-potential model alone indicate that the vapor composition for the Pu/O system will be as oxygen-rich or more oxygen-rich than that for the U/O system. A very oxygen-rich equilibrium vapor gives less ionization because of the relatively high ionization potentials of O and O_2 . Thus, we conclude that ionization may be neglected for the temperature and composition ranges of interest and have not included ionization effects in our calculations.

Table III. Ionization Potentials (IP) of the Molecules and Atoms in Equilibrium with a Plutonium Dioxide Condensed Phase ($1 \text{ eV} \cdot \text{molecule}^{-1} = 23.06 \text{ kcal} \cdot \text{mol}^{-1} = 96.48 \text{ kJ} \cdot \text{mol}^{-1}$)

Species	IP, eV	Reference
Pu	5.83	Moore (35)
PuO	6.2 ± 0.5	Blackburn <i>et al.</i> (36)
PuO ₂	9.4 ± 0.5	Blackburn <i>et al.</i> (36)
O	13.61	Moore (37)
O ₂	12.07	Huber and Herzberg (38)

Results

The partial pressures of O, O₂, Pu, PuO, and PuO₂ were calculated as functions of T (1500 ≤ T ≤ 4000 K) and x (0.005 ≤ x ≤ 0.30), with particular emphasis on 0.005 ≤ x ≤ 0.10. Preliminary calculations at 5000 K yielded unreasonably high oxygen pressures and vapor densities such that an upper temperature limit of 4000 K was selected. Tables presenting selected results are given in ANL-CEN-RSD-82-1 (21).

The calculated composition of the vapor in equilibrium with a PuO_{1.96} condensed phase, which is a typical composition for a reactor fuel, is shown in Figure 3. Below 2652 K, which is the temperature at which PuO_{1.96} begins to melt, the vapor is PuO₂ with varying amounts of PuO, O, and O₂. Above 2668 K, which is the liquidus temperature for PuO_{1.96}, the vapor is almost entirely O₂ with some O. None of the plutonium-containing species makes an appreciable contribution to the total pressure at high temperatures. Even the vapor in equilibrium with PuO_{1.90}, which is shown in the bottom part of Figure 3, is largely O₂ and O at temperatures above 3000 K.

An alternative way to view the oxygen enrichment of the vapor relative to the condensed phase is to calculate the oxygen-to-plutonium ratio of the gas, R(gas), with Eq. (2). The value of R(gas) exceeds that of the condensed phase with which it is in equilibrium by a large amount. Like the U/O system, this oxygen enrichment of the vapor relative to the condensed phase is increasing with temperature. One implication of these results is that the condensed-phase and vapor-phase compositions will depend upon the extent of vaporization of a sample with overall composition given by O/Pu = 2 - x.

The temperature dependences of the total pressures in equilibrium with the condensed-phase composition PuO_{1.90}, PuO_{1.96}, and PuO_{1.994} are compared in Figure 4. The differences shown in Figure 4 are due to the differences in oxygen pressures for the different compositions.

Discussion and Conclusions

Comparison to the U/O System. Comparison of the results of these calculations with those for the corresponding U/O system shows that the major difference is the very high oxygen pressures calculated for the plutonium oxides. Some of these data are compared in Table IV for T = 2100 and 4000 K. The oxygen pressures in equilibrium with PuO_{2-x} at 4000 K are higher than those in equilibrium with UO_{2-x} by factors ranging from about 10⁶ to 10³ for oxygen-to-metal ratios ranging from 1.98 to 1.90. Although these ratios are quite large, an examination of comparable data at 2100 K, where experimental oxygen potentials are available, shows ratios over the same composition range that vary by 10¹⁰ to 10⁸. Thus, the oxygen potentials for the two materials are actually

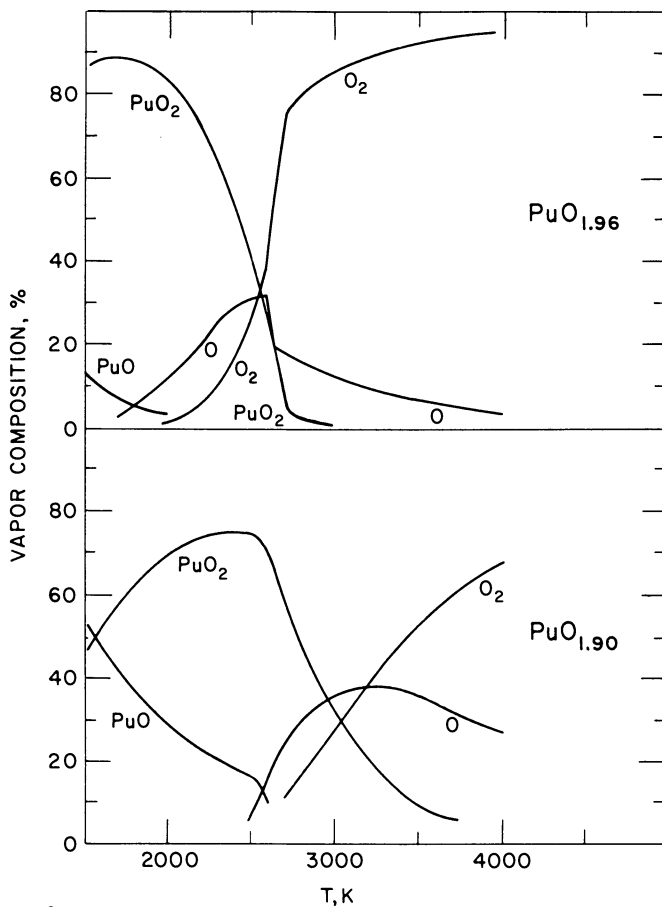


Figure 3.
Vapor compositions in equilibrium with a $\text{PuO}_{1.96}$ condensed phase (top) and a $\text{PuO}_{1.90}$ condensed phase (bottom).

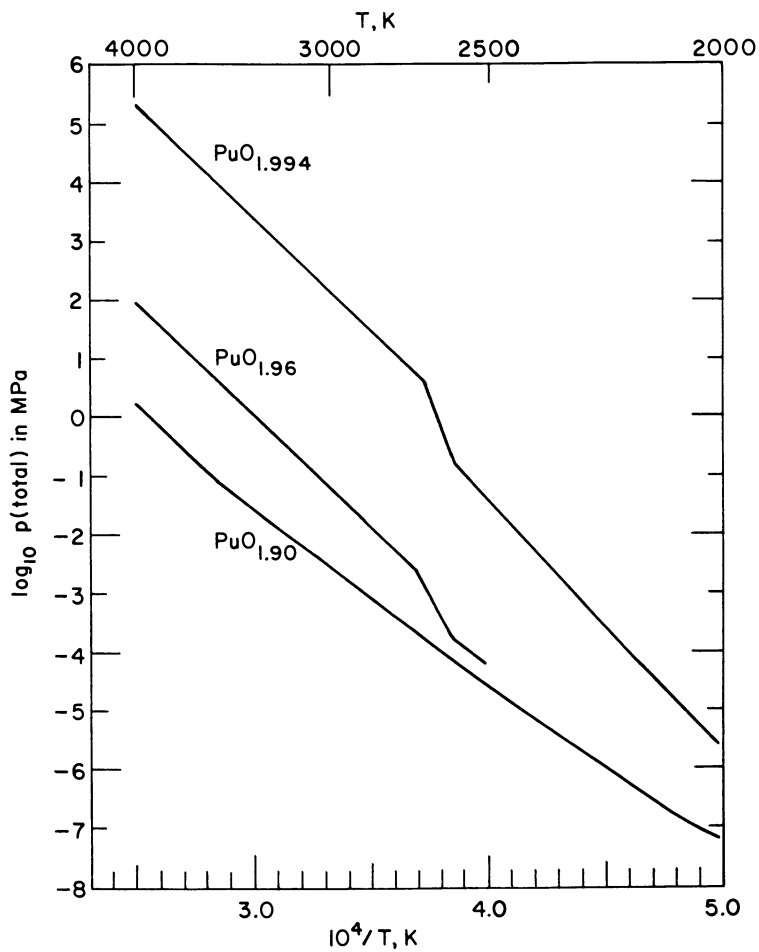


Figure 4.
Log of total pressure (MPa) in equilibrium with $\text{PuO}_{1.994}$, $\text{PuO}_{1.96}$, and $\text{PuO}_{1.90}$.

Table IV. Calculated Partial Pressures (in MPa) of O₂ at 2100 K and 4000 K for the U/O and Pu/O Systems

T, K	System	x = 0.02	x = 0.04	x = 0.06	x = 0.08	x = 0.10
2100	UO _{2-x}	3.4x10 ⁻¹⁸	8.0x10 ⁻¹⁹	3.3x10 ⁻¹⁹	1.8x10 ⁻¹⁹	1.3x10 ⁻¹⁰
	PuO _{2-x}	1.2x10 ⁻⁸	7.2x10 ⁻⁹	1.2x10 ⁻⁹	3.0x10 ⁻¹⁰	9.8x10 ⁻¹¹
4000	UO _{2-x}	3.5x10 ⁻³	1.9x10 ⁻³	1.1x10 ⁻³	7.1x10 ⁻⁴	4.7x10 ⁻⁴
	PuO _{2-x}	1.8x10 ³	92	15	3.9	1.3

getting closer as the temperature increases. The high oxygen pressures for equilibrium with PuO_{2-x} at 4000 K relative to those at UO_{2-x} should not be at all surprising when compared with available experimental data.

Another significant comparison between the two systems concerns the partial pressures of the metal dioxide molecules. These pressures are relatively insensitive to the condensed-phase composition and are quite similar in the plutonia and urania systems. Calculated metal dioxide vapor pressures are compared in Table V for $O/M = 1.96$.

Table V. Partial Pressures (in MPa) of the Dioxides in Equilibrium with the Hypostoichiometric ($O/M = 1.96$) Dioxides of Plutonium and Uranium

T, K	$p(\text{PuO}_2)$	$p(\text{UO}_2)$
2000	3.8×10^{-8}	1.2×10^{-8}
3000	1.0×10^{-3}	1.0×10^{-3}
4000	6.2×10^{-2}	7.8×10^{-2}

A consequence of the extreme sensitivity of oxygen pressure to stoichiometry for small values of x in PuO_{2-x} is that the total pressures change by a factor of about 10^3 in going from $\text{PuO}_{1.98}$ to $\text{PuO}_{1.90}$ at 4000 K. In contrast, the corresponding factor for the U/O system is approximately 2.

It is important to consider the complex nature of the vapors in both oxide systems. Any analysis which considers only the dioxide partial pressures, or approximates the total pressures as a dioxide pressure, will be seriously in error.

Implications for Mixed Oxides

Because the oxygen potentials for the liquid plutonium oxide were so high, some preliminary calculations were performed and have now been confirmed for the mixed $(\text{U,Pu})\text{O}_{2-x}$ system (39). Calculations were done by simultaneously solving the equations for the oxygen potentials of the Pu/O and U/O systems as described by Blackburn (11). These results showed that, even though the Pu/O system has an oxygen pressure larger than that for the comparable U/O system (same composition and temperature) by a factor of 10^4 or 10^5 , the mixed oxide containing 20% plutonium has oxygen pressures only slightly greater than those for urania. Moreover, the pressure differences between the urania and mixed-oxide systems decreased as the temperature increased.

It appears that the presence of U^{6+} , for which there is no counterpart in the Pu/O system, is responsible for preventing the oxygen pressures from increasing as rapidly in the mixed-oxide system as in the plutonia system. These results (39) indicate that the oxygen partial pressures in equilibrium with the mixed oxide will not differ drastically from those in equilibrium with urania.

Uncertainties and Limitations

Numerical evaluation of the uncertainties in calculated results has been discussed more completely elsewhere (21). Uncertainties in the gas phase thermodynamic functions have been discussed in detail previously (3, 40) and are smaller than other uncertainties in these calculations. Not all experimental thermodynamic data for PuO and PuO₂ are consistent and further data are needed (40). The use of alternative equations recommended by Ackermann and Chandrasekhariah (41) for ΔG_f° of PuO and PuO₂ lead to larger (less negative) values for $\Delta H_f^\circ(298.15\text{ K})$ for both PuO and PuO₂, which will result in higher calculated vapor pressures of PuO₂ (60% larger at 4000 K and 146% at 2000 K). However, the choice of these equations for ΔG_f° , which improves the consistency of the derived Second- and Third Law-values of $\Delta H_f^\circ(\text{PuO}_2, g, 298.15\text{ K})$, leads to serious inconsistencies for PuO. Some resolution of these inconsistencies would further reduce the uncertainties in the gas-phase thermodynamic functions.

The uncertainties in the condensed-phase thermodynamic functions arise from (1) the possible existence of a solid-solid phase transition in the temperature range 2160 to 2370 K and (2) the uncertainty in the estimated value of the liquid heat capacity which is on the order of 40%. While these uncertainties affect the partial pressures of plutonium oxides by a factor of 10 at 4000 K, they are not limiting because, at that temperature, the total pressure is due essentially entirely to O₂ and O.

The limitation of our calculations to temperatures less than 4000 K is a consequence of excessive oxygen partial pressures, which are, in turn, the result of the oxygen-potential model or the model parameters that are used. Approximations in that model include: neglect of Pu²⁺, neglect of Pu⁶⁺, entropy estimates, phase diagram uncertainties, and uncertainties in evaluation of the model parameters of the liquid. Neglect of Pu²⁺ is not a major contributor to uncertainty in the region of application of the model. Calculations showed that the use of 1.4nR rather than nR for the heat of fusion resulted in differences at the most of 8% at 3000 K and 4% at 4000 K. These differences are small compared to other uncertainties. Because the phase diagram is used solely to determine limits of integration, changes in it would have small effects on total pressures calculated. Comparison of the method used in the evaluation of liquid model parameters with methods used for the U/O system gave differences of

8%. Changes in the method used here would tend to increase the oxygen pressures not decrease them. The unrealistically high oxygen pressures may be partially attributable to the absence of a Pu^{6+} state (or other higher valence states). The lack of any evidence of a hexavalent state in the Pu/O low-temperature data implies that the hexavalent state would have a steep concentration gradient if it is important at 4000 K. Examination of the role of a hexavalent state in the mixed-oxide system clearly shows its importance in limiting the oxygen partial pressures. Thus, the lack of experimental data on Pu^{6+} creates a major uncertainty in the oxygen-potential model. Furthermore, high-temperature experimental data are required to test the model employed here and, if necessary, modify it. If this problem with the oxygen-potential model is solved, then the limiting source of error would be the condensed-phase thermodynamic functions.

Needed Measurements

Throughout this paper, the limitations of the calculations due to the lack of experimental data have been emphasized. Each of the major uncertainties discussed above could be reduced by additional measurements. The following list includes some specific areas where further experiments may be feasible and useful:

- (1) Measurement of the oxygen pressure or oxygen potential near stoichiometry.
- (2) Measurement of the equilibrium oxygen pressure as functions of both x and T at higher temperatures than are currently available.
- (3) Measurement of the O/Pu ratio of the vapor in equilibrium with plutonium dioxide liquid.
- (4) Measurement of the partial pressures over PuO_2 .
- (5) Measurement of the heat capacities of both solid and liquid.
- (6) Measurement of a more reliable phase diagram for the Pu/O system, particularly near the melting point.

With the currently available information, the largest uncertainty is in the oxygen-potential model and the parameter values within the model. A recent assessment of the Pu/O system (42) has indicated that the values of the parameters used in the Blackburn model yield slightly smaller oxygen potentials than those of Alexander (22), those of Tetenbaum (22-42) and those extrapolated from the data of Woodley (43). A reevaluation of the model parameters would allow a better fit to these experimental data;

however, this revision would not significantly alter the results at higher temperatures. As more data become available, a revision of the present calculations to include new parameter values may be in order. Additional work in other areas is of little value to the calculations at high temperature unless it contributes to reducing the uncertainty in the oxygen pressure at high temperature.

Acknowledgments

We gratefully acknowledge helpful discussions with Drs. P. E. Blackburn, M. Tetenbaum, and M.-L. Saboungi. Valuable comments on the oxygen potential model by Dr. R. E. Woodley are also gratefully acknowledged.

Literature Cited

1. Green, D. W.; Leibowitz, L. Argonne National Laboratory Report ANL-CEN-RSD-81-1, 1981.
2. Green, D. W.; Leibowitz, L. *J. Nucl. Mater.* 1982 **105**, 184.
3. Green, D. W. Argonne National Laboratory Report ANL-CEN-RSD-80-2, 1980.
4. J. K. Fink, *Int. J. Thermophysics* 1982 **3**, 165.
5. "JANAF Thermochemical Tables," 2nd Ed. Nat. Bur. of Std. Rept. NSRDS-NBS 37, 1971; 1974 Suppl. *J. Phys. Chem. Ref. Data* 1974 **3**, 311; 1975 Suppl. *J. Phys. Chem. Ref. Data* 1975 **4**, 1; 1978 Suppl. *J. Phys. Chem. Ref. Data* 1978 **7**, 793.
6. Oetting, F. L.; Rand, M. H.; Ackermann, R. J. "The Chemical Thermodynamics of Actinide Elements and Their Compounds," International Atomic Energy Agency, Vienna, 1976.
7. Potter, P. E.; Rand, M. H. *High Temp. Sci.* 1980 **13**, 315.
8. Atlas, L. M.; Schlehman, G. J. "Thermodynamics of Nuclear Materials," International Atomic Energy Agency, Vienna, 1966; p. 407.
9. Manes, L.; Manes-Pozzi, B. "Plutonium 1975 and Other Actinides," Blank, H.; Linder, R., Eds., North Holland, Amsterdam, 1976; p. 145.
10. Browning, P.; Gillan, M. J.; Potter, P. E. *Rev. Int. Hautes Temp. Refract.* 1978 **15**, 333.
11. Manes, L.; Mari, C. M.; Ray, I.; Sørensen, O. T. "Thermodynamics of Nuclear Materials," International Atomic Energy Agency, Vienna, 1979, p. 405.
12. Blackburn, P. E. Argonne National Laboratory Report ANL-79-77, 1972; p. 12.
13. Blackburn, P. E. Argonne National Laboratory Report ANL-75-48, 1975; p. 5.
14. Blackburn, P. E.; Johnson, C. E. "Thermodynamics of Nuclear Materials," International Atomic Energy Agency, Vienna, 1974; p. 17.

15. Schmitz, F. J. J. Nucl. Mater. 1975 58, 357.
16. Schmitz, F.; Marajofski, A. "Thermodynamics of Nuclear Materials," International Atomic Energy Agency, Vienna, 1974; p. 457.
17. Breitung, W. Kernforschungszentrum Karlsruhe Report KFK-2363, 1976.
18. de Franco, M.; Gatsoupe, J. P. "Plutonium 1975 and Other Actinides," Blank, H.; Linder, R., Ed., North Holland, Amsterdam, 1978; p. 133.
19. Catlow, C. R. A. J. Nucl. Mater. 1977 67, 236.
20. Catlow, C. R. A. J. Nucl. Mater. 1978 74, 172.
21. Green, D. W.; Fink, J. K.; Leibowitz, L. Argonne National Laboratory Report ANL-CEN-RSD-82-1, 1982.
22. Alexander, C. A. (Batelle Memorial Institute, Columbus Laboratories) data presented at the Libby-Cockcroft Exchange Meeting on Phase Diagrams and Thermodynamics of Fuel Materials, May 20-22, 1968.
23. Markin, T. L.; McIver, E. J. "Plutonium 1965," Kay, A. E.; Waldron, M. B., Ed., Chapman and Hall, London, 1967; p. 845.
24. Woodley, R. E. J. Amer. Ceram. Soc. 1973 56, 116.
25. Javed, N. A. J. Nucl. Mater. 1973, 47, 336.
26. Tetenbaum, M. "Thermodynamics of Nuclear Materials," Vol. II, International Atomic Energy Agency, Vienna, 1974; p. 305.
27. Tetenbaum, M. personal communication.
28. Blackburn, P. E. "Proc. Panel on Behavior and Chemical State of Irradiated Ceramic Fuels," International Atomic Energy Agency, Vienna, 1974; p. 393.
29. Green D. W.; Reedy, G. T. J. Chem. Phys. 1978 69, 544.
30. Green, D. W.; Reedy, G. T. unpublished results.
31. Battles, J. E.; Reishus, J. W.; Shinn, W. A. Argonne National Laboratory Report ANL-7575, 1968; p. 77.
32. Rand, M. "Plutonium: Physico-Chemical Properties of Its Compounds and Alloys, Kubaschewski, O., Ed., Atomic Energy Review, Vol. 4, Special Issue No. 1, International Atomic Energy Agency, Vienna, 1966; p. 7.
33. Livey, D. T.; Feschotte, P. "Plutonium: Physico-Chemical Properties of Its Compounds and Alloys," Kubaschewski, O., Ed., Atomic Energy Review, Vol. 4, Special Issue No. 1, International Atomic Energy Agency, Vienna, 1966; p. 53.
34. Aitken, E. A.; Evans, S. K. General Electric Reports GEAP-5672, 1968.
35. Moore, C. E. National Bureau of Standards (U.S.) Report NSRDS-NBS 34, 1978.
36. Blackburn, P. E.; Battles, J. E.; Reushus, J. W.; Shinn, W. A. Argonne National Laboratory Report ANL-7575, 1968; p. 79.
37. Moore, C. E. "Atomic Energy Levels," National Bureau of Standards, Circular 467, Washington, D.C., 1949.

38. Huber, K. P.; Herzberg, G. "Molecular Spectra and Molecular Structure. IV. Constants of Diatomic Molecules," Van Nostrand Reinhold, New York, 1979.
39. Green, D. W.; Fink, J. K.; Leibowitz, L. "Vapor Pressures and Vapor Compositions in Equilibrium with Hypostoichiometric Uranium-Plutonium Dioxide at High Temperatures," presented at the 8th European Conference on Thermophysical Properties, Baden-Baden, September 27 - October 1, 1982; to be published in *High Temperatures-High Pressures*.
40. Green, D. W. *Int. J. Thermophysics* 1980 1, 61.
41. Ackermann, R. J.; Chandrasekhariah, M. S. "Thermodynamic of Nuclear Materials 1974," International Atomic Energy Agency, Vienna, 1975; p. 3-26.
42. Tetenbaum, M.; "Some Thermodynamic Aspects of the Pu-O System" presented at the ACS Symposium on the Chemistry of Plutonium, Kansas City, September 13-15, 1982.
43. Woodley, R. E.; *J. Nucl. Mater.* 1981, 96, 5.

RECEIVED January 24, 1983

x-Ray Photoemission Spectroscopy (XPS) Study of Uranium, Neptunium, and Plutonium Oxides in Silicate-Based Glasses

D. J. LAM, B. W. VEAL, and A. P. PAULIKAS

Argonne National Laboratory, Materials Science and Technology Division,
Argonne, IL 60439

Using XPS as the principal investigative tool, we are in the process of examining the bonding properties of selected metal oxides added to silicate glass. In this paper, we present results of XPS studies of uranium, neptunium, and plutonium in binary and multi-component silicate-based glasses. Models are proposed to account for the very diverse bonding properties of 6+ and 4+ actinide ions in the glasses.

Silicate glasses are being considered as possible media for long term storage of radioactive wastes. Actinide elements are among those active species which must be isolated from the biosphere for many centuries. Thus it is important to understand bonding properties of actinides in the glasses in order to formulate the most effective storage medium and to discover potential failure modes.

As part of a more extensive study of metal oxides dissolved in simple glasses (1-5), we report results for U, Np, and Pu oxides dissolved in sodium silicate glass. For this work, we rely primarily on XPS data. Valence states of the incorporated ions can be quite reliably determined through a careful examination of binding energy shifts, 5f electron intensities, and the satellite structure associated with core level excitation (1). For suitably concentrated samples, the actinyl structure can be recognized in the splitting of the An (actinide) $6p_{3/2}$ level (2). (Data for hexavalent Np oxides are similar to results reported for U^{6+} compounds (6)). These (actinyl) results can also be tested with EXAFS spectra where the An-O separation can be directly measured (7). The spectral analyses, solubility data, and observed property changes associated with addition of actinide elements to glasses have enabled us to suggest bonding models of An 4+ and 6+ ions in silicate glasses.

0097-6156/83/0216-0145\$06.00/0
© 1983 American Chemical Society

Experimental

The samples were prepared by melting appropriate amounts of constituent oxides with powdered sodium trisilicate glass. To minimize the compositional variation of the samples, a large batch of sodium-trisilicate glass was prepared. This glass was then used to prepare the Np and Pu glasses as well as the multicomponent glass samples. The glasses were melted in an atmosphere of flowing oxygen or in a reducing atmosphere of controlled CO/CO₂ ratio, at 1250°C in platinum crucibles for several hours. The samples were crushed, thoroughly mixed and remelted several times to insure homogeneity. X-ray powder diffraction patterns were taken for several randomly selected samples to check for the presence of crystalline phases. After the final melting, the samples were visually examined for gross nonuniformity of color distribution. If found, the sample was crushed and remelted. Most of the samples studied were furnace cooled from 1250°C to room temperature. To check the effect of cooling rate on the XPS spectra, several samples were air quenched and reannealed at 400°C. No apparent differences were found between the furnace cooled and reannealed specimens. Two bar shaped samples measuring approximately 3x3x15 mm were cut from the ingots with a diamond wafering saw using methanol as coolant. The bars were scored and were subsequently fractured in the ultra-high (6×10^{-10} Torr) vacuum chamber of the spectrometer to expose clean surfaces of the bulk glass composition for examination with XPS.

The spectrometer was a Physical Electronics Model 548 modified for emplacement in a glovebox so that actinide samples could be examined. Spectra were taken using AlK_α radiation (1486.6 eV). The overall energy resolution of the spectrometer was ~1.2 eV using an analyzer pass energy of 25 eV. The spectrometer control was interfaced to a Nicolet 1180 minicomputer providing automatic data acquisition and analysis capability.

Experimental Results

We have previously reported that dissolution of UO₂ or UO₃ in sodium silicate glasses in an atmosphere of oxygen or air produces a glass in which uranium appears only in the hexavalent state (2). In order to obtain dissolved tetravalent uranium ions, it is necessary to melt the glass in very reducing conditions. In contrast, the melting of NpO₂ and PuO₂ into silicate glass in flowing oxygen will not oxidize the Np or Pu to a higher valence state. The solubility of NpO₂ and PuO₂ in sodium trisilicate glass at 1250°C is three and two mole percent, respectively. When attempts were made to dissolve higher concentrations of Np or Pu oxide, nonglassy residues were obtained. For UO₂ dissolved into the same glass

at 1250°C, the solubility is five (for U⁴⁺) and twenty (for U⁶⁺) mole percent when melted in atmospheres of CO/CO₂ = 7 and in air, respectively. The large difference in solubility between hexavalent and tetravalent uranium in these glasses will be discussed below.

The valence states of Pu and Np ions in complex borosilicate glasses (designated 76101 and 7668, glasses prepared by Battelle Pacific Northwest Laboratories for waste form simulation) were previously investigated with XPS (1). Nominal compositions of these glasses are given in ref. 1. Both trivalent and tetravalent states of Pu were readily observed in the glasses but Np was present essentially in a single valence state (+4), in both glasses. Similar results are seen in Fig. 1, which shows an XPS spectrum that includes actinide 4f core levels for the 76101 glass into which one mole percent each of UO₃, NpO₂, and PuO₂ has been added. Two valence states for Pu (+4 and +3) and U (+6 and +4) are discernable while Np appears only in the 4+ state.

The Ti 2p doublet appears on the extreme left side of Fig. 1. TiO₂ was added to the glass because it is present in nuclear waste and also because it is useful as an internal reference for binding energy determinations (1). The sodium trisilicate glasses with various additive oxides, listed in Table I, were studied by XPS.

Although multiple valence states were frequently observed with XPS, caution should be exercised in associating these valence states with the unperturbed bulk glass. Particularly for Pu⁴⁺, a significant amount of reduction (to Pu³⁺) occurred during the XPS data accumulation time. This is particularly troublesome for dilute samples where long data acquisition times are needed to obtain an adequate signal-to-noise ratio. The effect is illustrated in Fig. 2 which shows progressive changes of Pu 4f spectra for glass I (see Table I) as a function of data acquisition time. Spectrum (a) is a 10 minute scan acquired immediately after fracture. Each successive spectrum, run for an additional ten minutes, was acquired immediately after the previous spectrum. The spectra were then smoothed, using a 5 point Savitsky-Golay routine supplied by Nicolet. After extended X-ray exposure (several hours), the relative concentrations of 4+ and 3+ ions became approximately equal. Since the photoelectron escape depth is ~20-30 Å, it appears that Pu ions in the top ~15 Å layer were reduced. A low energy electron beam was used during measurement to maintain charge neutralization at the sample surface. To test for possible reduction resulting from the neutralization beam, the sample was exposed overnight to the beam. No reduction from this source was detectable. (This source also produces more sample heating than the X-ray beam so we rule out thermal decomposition.) Thus reduction of tetravalent Pu and hexa-

American Chemical
Society Library

1155 16th St., N.W.

Washington, D. C. 20036

In Plutonium Chemistry; Carnall, W., et al.;

ACS Symposium Series; American Chemical Society: Washington, DC, 1983.

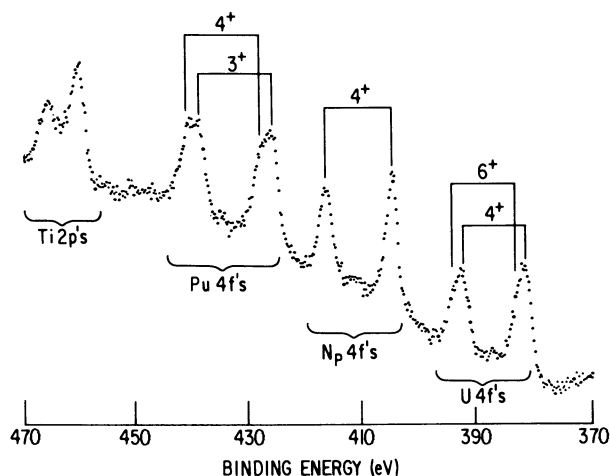


Figure 1. XPS 4f core level spectra for glass 76101 containing dissolved UO_3 , NpO_2 and PuO_2 . Multiple valence states appear for U and Pu. Intensities of the low valence states are enhanced by in-situ reduction during the XPS measurement.

Table I. Composition of Various Samples Studied

<u>Glass Samples</u>	<u>Composition (mole fraction)</u>
A	$0.25 \text{ Na}_2\text{O} \cdot 0.75 \text{ SiO}_2$
B	$(0.25 \text{ Na}_2\text{O} \cdot 0.75 \text{ SiO}_2)_{0.964} (\text{TiO}_2)_{0.036}$
C	$(0.25 \text{ Na}_2\text{O} \cdot 0.75 \text{ SiO}_2)_{0.985} (\text{PuO}_2)_{0.015}$
D	$(0.25 \text{ Na}_2\text{O} \cdot 0.75 \text{ SiO}_2)_{0.914} (\text{TiO}_2)_{0.036} (\text{UO}_3)_{0.050}$
E	$(0.25 \text{ Na}_2\text{O} \cdot 0.75 \text{ SiO}_2)_{0.944} (\text{TiO}_2)_{0.036} (\text{NpO}_2)_{0.020}$
F	$(0.25 \text{ Na}_2\text{O} \cdot 0.75 \text{ SiO}_2)_{0.949} (\text{TiO}_2)_{0.036} (\text{PuO}_2)_{0.015}$
G	$(0.25 \text{ Na}_2\text{O} \cdot 0.75 \text{ SiO}_2)_{0.909} (\text{TiO}_2)_{0.036} (\text{PuO}_2)_{0.015}$ $(\text{CaO})_{0.040}$
H	$(0.25 \text{ Na}_2\text{O} \cdot 0.75 \text{ SiO}_2)_{0.889} (\text{TiO}_2)_{0.036} (\text{PuO}_2)_{0.015}$ $(\text{ZnO})_{0.060}$
I	$(0.25 \text{ Na}_2\text{O} \cdot 0.75 \text{ SiO}_2)_{0.809} (\text{TiO}_2)_{0.036} (\text{PuO}_2)_{0.015}$ $(\text{B}_2\text{O}_3)_{0.140}$

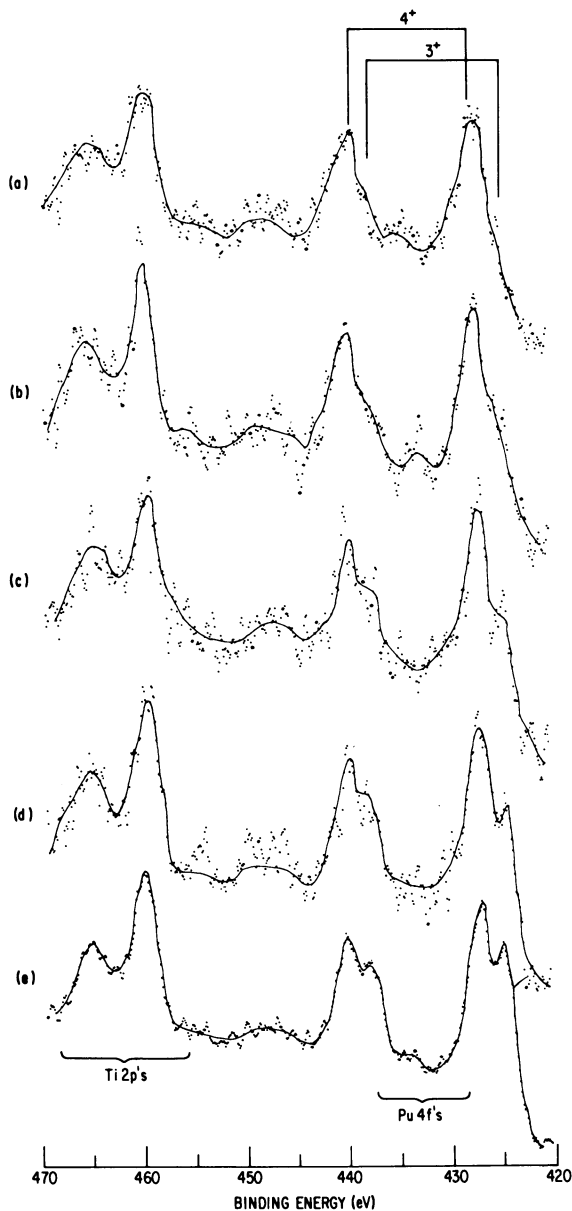


Figure 2. 4f core level spectra for glass I (Table I) demonstrating the strong tendency of the Pu^{4+} ions to reduce in the XPS spectrometer. Spectra (a) through (e) are short (10 min) sequential runs showing accumulative reduction of Pu^{4+} to Pu^{3+} .

valent U was caused by the X-ray flux under UHV conditions. Probably, oxygen desorption was stimulated by photons or secondary electrons. It is not known whether those oxygen atoms in the vicinity of actinide ions are preferentially removed or if O atoms come from the surface randomly. (We note, however, that similar reduction behavior often occurs from simple uranate salts where the U^{6+} ions always have a relatively close association with all oxygen atoms.)

The ease of reduction of the Pu 4+ ions apparently can be affected by inclusion in the glass of additional additives. Whereas the addition of TiO_2 apparently does not affect in-situ reduction, the addition of CaO, ZnO, or B_2O_3 appreciably accelerated reduction of the Pu 4+ ions. This effect is demonstrated with 4f core level spectra of glasses F, G, H, and I shown in Fig. 3. Each sample was subjected to the same X-ray exposure, i.e., the same number of scans at the same flux. (Note that the concentrations of additive oxides differ. No attempt has been made to scale this effect with additive concentration). This curious reduction effect is not easily understood but emphasizes the complex nature of the glasses including the possible cooperative involvement of the multiple components. Similarly complex phenomena might influence leaching behavior in the complex, multicomponent glasses of interest for radioactive waste storage.

Discussion

A consideration of the structure of silicate glasses provides a useful starting point for examining bonding properties of elements incorporated into the glasses. It is commonly believed that added metal ions are randomly situated in large interstitial spaces or holes of the amorphous SiO_2 network. Variation of the bond angles between SiO_4 tetrahedra give rise to the holes of irregular shape and size. This model of glass structure, developed by Zachariasen (8) and Warren (9), would imply that solubilities of incorporated elements should be determined, in large part, by the ionic size of the added element. With this view, it is surprising that the difference in the solubility of hexavalent (ionic radius, $r_c = 0.8 \text{ \AA}$) and tetravalent ($r_c = 0.97 \text{ \AA}$) uranium is so large, i.e., 20 versus 5 mole percent. In contrast to experimental observation, it would also be expected that the solubility of tetravalent Np ions ($r_c = 0.95 \text{ \AA}$) and Pu ions ($r_c = 0.93 \text{ \AA}$) should be larger or at least equal to that of the tetravalent U in the same glass. Previous studies of hexavalent U in silicate glasses have indicated that U appears in the uranyl structure (2, 7, 10). If both the U^{+4} ions and the UO_2^{++} ions are situated in the interstitial holes of the glass network, then the solubility of UO_2^{++} should be smaller, instead of much larger than the U^{+4} ion.

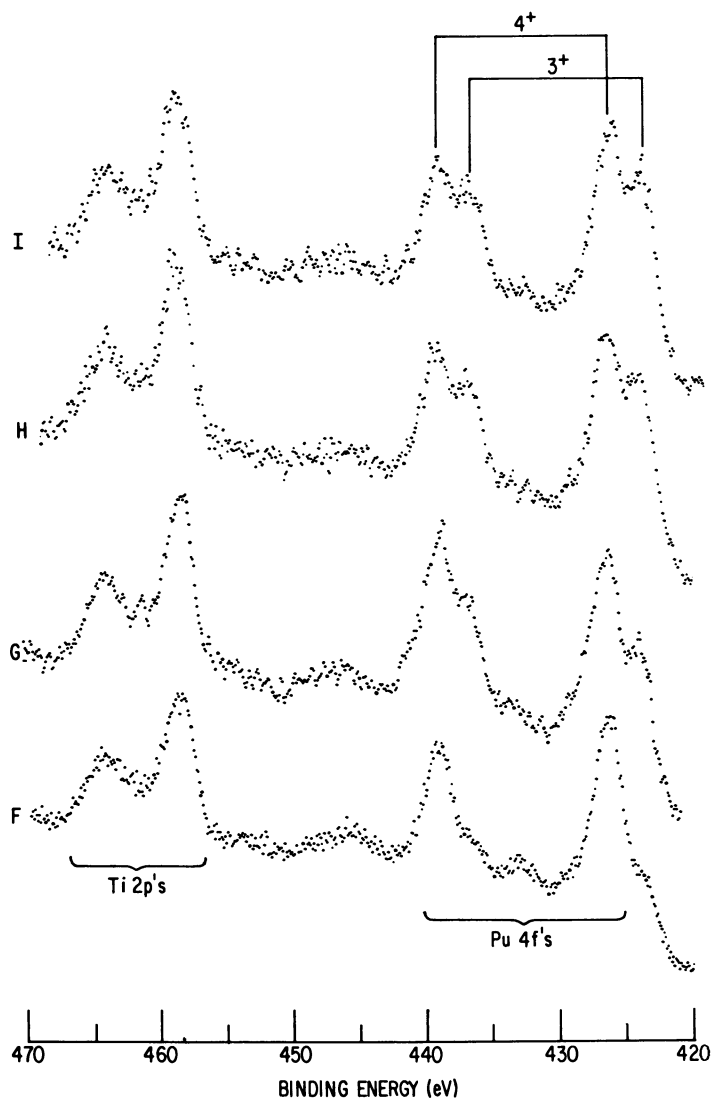


Figure 3. 4f core level spectra for a series of glasses containing Ca, Zn, or B oxide additives (glass sample F, G, H, and I of Table I). The rate of reduction of Pu⁴⁺ to Pu³⁺ during XPS measurement is apparently influenced by the choice of additive (see text).

For our purposes, we use a crystal chemistry approach and consider crystal structures of silicates with chemical compositions approximating the glasses of interest. Structural features of these crystal forms should be preserved in varying degrees in the glasses. For example, the SiO_4 tetrahedron is a structural element common to all of the silicate glasses. Of comparable importance, but more difficult to demonstrate, is the possibility that extended range chains or sheets, readily observable in the crystalline forms, may also appear in the glasses and play an important role in determining the physical properties of a particular glass.

Consider the $\alpha\text{-Na}_2\text{O}\cdot 2\text{SiO}_2$ crystalline form (11). This silicate consists of identifiable sheets that are assembled from SiO_4 tetrahedra. Three "bridging" oxygen bonds join the tetrahedra with bond strengths comparable to those found in pure SiO_2 . A single "nonbridging" oxygen (joining an alkali atom) on each tetrahedron provides a termination layer of alkali atoms on the sheet surface. Thus, the sheets, which contain strong internal bonds, are weakly joined through ionically bonded, monovalent alkali atoms. However, if metal atoms of higher valence were added to the compound and adjacent sheets were bonded (cross linked) through these polyvalent additives, one might expect to find profound changes in the physical properties of the glass.

An example of this contrast in bonding conditions for crystals silicates is provided by the compound $\text{Li}_2\text{O}\cdot 2\text{SiO}_2$ (12) which displays very weak intersheet bonding and the mineral petalite (13), which has the composition $\text{Li}_2\text{O}\cdot \text{Al}_2\text{O}_3\cdot 8\text{SiO}_2$. To convert the disilicate to petalite requires the replacement of three Li atoms with one Al, a process that is accomplished entirely within the intersheet region without significantly perturbing the sheet structure of the parent disilicate. The Al thus cross links the silica sheets with a strong bond and profoundly alters the physical properties.

It is our view that similar phenomena occur in glassy silicates. Probably, chains or sheets of silica with strong internal bonds form in the melt at an early stage of cooling. Additive elements that form strong cross links between these sheets will then be expected to significantly affect the glass rigidity. Such hardening (analogous to the cross linking of chains in polymers) is commonly observed in glasses. One manifestation of the cross linking is increased viscosity, often apparent when polyvalent metals are added to simple silicate glasses (14).

Utilizing this description of silicate glass formation, we suggest models to explain the incorporation of 4+ and 6+ actinide ions in sodium disilicate glass. During cooldown, SiO_4 tetrahedra link together to form a sheet-like structure

with, on average, one nonbridging oxygen per tetrahedron. The sodium ions, being completely ionized (5) and relatively large, are situated in the interstitial spaces between the sheets, weakly bonding those sheets together. Presumably, the tetravalent actinide ions are also located in the "intersheet" regions but they bond with greater strength than alkalis to oxygens of the tetrahedra, thus crosslinking the distorted silica layers. This glassy structure will be frozen in as the sample is cooled. This "strong cross linking" model is consistent with the (qualitative) observation that, with addition of actinide 4+ ions, the glass viscosity increases.

It would appear that a rather different picture is needed to explain the bonding of U 6+ in silicate glasses. Strong evidence is now available to support the assertion that U 6+ appears in a uranyl configuration (2,7,10). In the glasses, the UO_2^{++} ion has a linear structure with U-O separation of about 1.8 Å (7). Alkali uranates containing hexavalent uranium in the uranyl structure form easily and in considerable variety. They often display sheet structures (sometimes distorted) with sheets separated by alkali or alkaline earth atoms. These same features, sheets separated by alkalis, are characteristic of crystalline alkali disilicates. It thus appears likely that, during cooldown of U 6+ glasses, uranyl structures form and bond into the interstices regions between silica sheets. This dissolution mode permits a large U 6+ solubility. Since alkalis play the role of delineating silica or uranate sheets, structural rigidity should be weak. The relatively low viscosity of U 6+ silicate glasses (again a qualitative observation) supports this picture. Uranates are not stable at 1250°C where the samples were melted so we do not expect macroscopic phase separated regions of U 6+ uranate. (Furthermore, X-ray diffraction data do not show the presence of crystalline second phase regions.) Rather, it appears that a thin uranate layer is formed between silica sheets and held in place by layers of alkali atoms.

The different bonding characteristics of U^{+4} and U^{+6} in alkali silicate glasses may have important implications to the leaching properties of high level waste glasses. In the UO_3 glasses, the uranyl structures probably occur in association with alkalis (similar to alkali uranates), an association that dramatically increases bonding of the sodium ions in the glass. This conclusion is supported by qualitative leaching studies of sodium disilicate glass containing UO_3 (15). It was observed that the glass maintained its structural integrity and no significant change in the leachant pH was detected after (static) leaching in distilled water for 180 days at room temperature.

In contrast, disilicate glasses containing U 4+ showed much less leach resistance. The 4+ glass was only slightly more leach resistant than pure sodium disilicate glass which is water soluble. For 4+ glasses, the pH of the leach solution

rose to 10.7 under the same leaching conditions used for the U 6+ glass. The U 4+ ions, which are soluble in low concentration, apparently cross link silica sheets to produce significant physical property changes. However, this cross linking process would not appear to significantly affect the bonding of alkali ions in the glass, so that the ability of a simple silicate glass to withstand leach attack is not appreciably increased by adding U 4+ ions.

More quantitative leaching data is needed for well characterized sodium silicate glasses containing U⁺⁴ and U⁺⁶ ions. It is clear, however, that the general practice of using air-melted uranium glass (U⁶⁺) to simulate leaching behavior of transuranic actinides in waste glasses should be discarded. Since transuranics in silicates do not, in general, appear in the 6+ valence state, this is not a reliable simulation. Also U 6+ ions appear to have bonding properties (associated with a strong tendency to form the uranyl structure) in glasses that are not typical of transuranic ions.

Acknowledgment

Work supported by the U. S. Department of Energy.

Literature Cited

1. Karim, D. P.; Lam, D. J.; Diamond, H.; Friedman, A. M.; Coles, D. G.; Bazan, F.; McVay, G. L., Proc. of Materials Res. Soc. Symp. 1982, p. 67.
2. Lam, D. J.; Veal, B. W.; Chen, H; Knapp, G. S. "Scientific Basis for Nuclear Waste Management;" McCarthy, G. J., Ed.; Plenum Publ. Co., New York, 1979, Vol. I, p. 97.
3. Veal, B. W.; Lam, D. J., Proc. Int. Conf. on Physics of SiO₂ and its Interfaces 1978, p. 299.
4. Lam, D. J.; Paulikas, A. P.; Veal, B. W. J. Non-Cryst. Solids 1980, 42, 41.
5. Veal, B. W.; Lam, D. J.; Paulikas, A. P.; Ching, W. Y. J. Non-Cryst. Solids 1982, 49, 309.
6. Banks, R., Carnall, W. T., Veal, B. W., Lam, D. J., and Paulikas, A. P., to be published.
7. Detailed x-ray absorption experimental results will be published elsewhere.
8. Zachariasen, W. H. J. Am. Chem. Soc. 1932, 54, 3841.
9. Warren, B. E. J. Am. Ceram. Soc. 1934, 19, 249; J. Am. Ceram. Soc. 1941, 24, 256; J. Appl. Phys. 1942, 13, 602.
10. Karraker, D. G. J. Am. Ceram. Soc. 1982, 62, 53.
11. Pant, A. K., Cruickshank, D. W. J., Acta Cryst., 1968, B24, 13.
12. Liebau, F., Acta Cryst., 1961, 14, 389.
13. Liebau, F., Acta Cryst., 1961, 14, 309
14. Morey, G. W., "The Properties of Glass"; Reinhold Publ. Co., New York, 1954.
15. Veal, B. W., Lam, D. J., Paulikas, A. P., and Karim, D. P., Nucl. Tech. 51, 136-142 (1980).

RECEIVED January 21, 1983

Plutonium Hexafluoride Gas Photophysics and Photochemistry

JAMES V. BEITZ, CLAYTON W. WILLIAMS, and W. T. CARNALL

Argonne National Laboratory, Chemistry Division, Argonne, IL 60439

Little has been published concerning the photodynamics of PuF_6 gas, although this compound was first synthesized in 1942. We recently reported the first observation of fluorescence from electronically excited PuF_6 and found its behavior to differ significantly from that of UF_6 or NpF_6 . The photophysics of PuF_6 excited at 532 nm and at 1064 nm has now been observed in detail using laser-induced fluorescence techniques. The fluorescence emission spectra recorded are the same at both excitation wavelengths with the fluorescence intensity peaking at about 2300 nm. The fluorescence decay of PuF_6 gas excited at 532 nm was found to be laser-fluence dependent and a mechanism is proposed which accounts for this observation. Net photodecomposition of PuF_6 was rapid at a fluence of 5 J/cm^2 at 532 nm (7 ns pulse width).

Our recent observation (1) of electronic state fluorescence from laser-excited $\text{PuF}_6(\text{g})$ and $\text{NpF}_6(\text{g})$ has marked the beginning of systematic studies of the photophysics and photochemistry of transuranic hexafluorides and has provided the key to further exploration of the complex vibronic structure characteristic of these compounds. While the photochemistry of UF_6 has been the object of numerous investigations, only a few remarks are found in the literature concerning the electronic state photochemistry of the transuranic hexafluorides. Given the dense electronic energy level structures of PuF_6 and NpF_6 and their relative instability in comparison with UF_6 , we can anticipate that their photochemistry will involve a rich and complex set of interactions. The work we report here deals primarily with $\text{PuF}_6(\text{g})$. We turn first to a very brief review of PuF_6 studies

0097-6156/83/0216-0155\$06.00/0
© 1983 American Chemical Society

related to its synthesis, energy levels, thermodynamics, photophysics and photochemistry.

Review of Related PuF₆ Studies

In light of the subject of this Symposium it is particularly appropriate to note that PuF₆ was first synthesized in 1942 on a microgram scale as part of the Manhattan Project although it was not isolated as a pure compound (2). Steindler (3,4) has reviewed early PuF₆ studies. By 1950 Florin had synthesized PuF₆ on a gram scale and it was no longer a laboratory curiosity. Many of the physical properties of PuF₆ were measured by Weinstock, Malm and co-workers in the 1950's. These workers were unable to record the Raman spectrum of PuF₆ due to photodecomposition (5). They noted that "light of the intensity of ordinary room illumination" decomposed PuF₆, and they reasonably assumed that the products were PuF₄(s) and F₂(g) (6). Steindler and coworkers found that PuF₆ could be synthesized using ultraviolet irradiation of PuF₄(s) and F₂(g) (7). The key to this seeming contradiction probably lies in the thermodynamic stability of PuF₅(s), a compound often postulated to exist but whose synthesis has never been reported. Other more general reviews which deal in part with PuF₆ properties include those of Rand (8), Oetting (9), D. Brown (10) and Keller (11). Brown's (12) and Cleveland's (13) books also contain useful information concerning PuF₆. O'Donnell and co-workers have recently compared the chemical reactivity of PuF₆ in anhydrous HF to that of other hexafluorides in the same medium (14). Little can be gleaned from the literature concerning gas phase chemical reactions of PuF₆.

Electronic Energy Levels and Thermodynamics

Absorption band structure due to electronic states of PuF₆ extends from the infrared into the vacuum ultraviolet and contains contributions from 5f electron states, charge transfer and dissociative states. Its complex vibronic structure has long challenged spectroscopists. M. Fred recorded the optical absorption spectrum of PuF₆ in 1954, noting the presence of vibronic structure (15). Steindler and Gunther published accurate molar absorptivity data for PuF₆ in 1963 (16). Kugel et al. discovered resolvable isotope shifts in the electronic absorption spectra of PuF₆ gas at room temperature in 1976 and described a theoretical model used to predict the energy level structure of its 5f electron states (15). A theoretical model for this structure has also been presented by Boring and Hecht (17). Relativistic calculations concerning PuF₆ have been carried out by Koelling, Ellis and Bartlett (18) and, concerning Pu⁺⁶, by Desclaux and Freeman (19). These theoretical assignments of the electronic energy level structure of PuF₆

have yet to be confirmed experimentally. No theory has been reported which successfully predicts the occurrence of the isotope shifts found by Kugel *et al.* (15).

Fuger has briefly reviewed the current state of critical assessments of actinide thermodynamics (20). He largely follows Rand's earlier assessment in determining the enthalpy of formation of PuF₄ and PuF₆. As Fuger noted, it is surprising that the heat of formation of such a technologically important compound as PuF₆ should be based solely on values for the equilibrium between PuF₆, PuF₄ and F₂. While PuF₆(g) at room temperature is thermodynamically unstable with respect to PuF₄(s) and F₂(g), it is quite stable at room temperature with respect to forming PuF₄(g) and F₂(g). From a photochemical point of view, the lack of thermodynamic information concerning PuF₅ is particularly unfortunate since it is likely that the first dissociation limit of PuF₆(g) corresponds to forming PuF₅(g) and an F atom.

In Figure 1 the electronic energy level structures of UF₆, NpF₆ and PuF₆ gases are shown together with the regions in which these compounds show continuous optical absorption and their known or estimated thermodynamic dissociation limits for gas phase products. The data in Figure 1 are presented in terms of the traditional spectroscopic unit of energy, the cm⁻¹ (1 cm⁻¹ = 19.86484 × 10⁻²⁴ J per molecule or atoms). Since UF₆ is a 5f⁰ system it has no low-lying electronic states. Continuous optical absorption in UF₆, beginning in the near-ultraviolet, is believed to arise from charge transfer bands. The first of these bands has an origin at about 24647 cm⁻¹ based on Andrews and co-workers' matrix isolation studies (21). The UF₆ dissociation limit shown is based on Hildenbrand's work (22).

The regions in which NpF₆ shows continuous absorption are shown in Figure 1 and are based largely on Steindler and Gerding's measurements (23) with preference given in setting the lowest energy at which electronic state absorption occurs to unpublished NpF₆ fluorescence work by Beitz. There is no thermodynamic information concerning the first dissociation limit of NpF₆. The value shown is a rough interpolation of the measured UF₆ value and our crude estimate of the first dissociation limit of PuF₆. The positions of the 5f states of NpF₆ are based on the work of Goodman and Fred (24) and of Hutchinson and Weinstock (25).

The regions in which PuF₆ shows continuous absorption as well as the 5f state energies shown in Figure 1 are based primarily on Steindler and Gunther's measurements (16). For a current theoretical interpretation of the 5f state structure of PuF₆ see J. Blaise *et al.* (this volume). The first dissociation limit of PuF₆ is crudely estimated based on the extremely small PuF₆ gas fluorescence photon yield but long fluorescence lifetime we have found (see below). In addition, the fact that PuF₆ is a better fluorinating agent than molecular fluorine

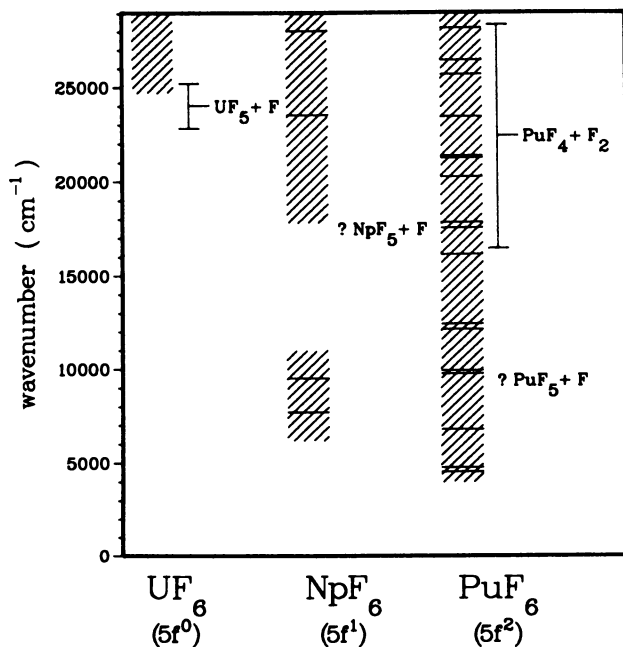


Figure 1. Electronic energy level diagram for gas phase actinide hexafluorides. The regions in which a given hexafluoride exhibits continuous absorption are shown shaded with diagonal lines. 5f electron states are shown as short horizontal lines. The thermodynamic dissociation limits and resultant gas phase products are shown to the right of the energy level diagram for each hexafluoride. UF₆(g), a 5f⁰ system, has no low-lying electronic levels and is thermodynamically more stable than NpF₆(g) or PuF₆(g). For these reasons UF₆ is unlikely to be a good model compound for transuranic hexafluoride photochemistry studies.

suggests that the first dissociation limit of PuF₆ lies below the dissociation limit of molecular fluorine (12800 cm⁻¹). The second dissociation limit, corresponding to molecular products, is based on Rand's analysis (8) of the enthalpies of formation of PuF₄(g) and PuF₆(g).

The striking feature of Figure 1 is the dissimilarity of UF₆ and either NpF₆ or PuF₆. UF₆, possessing greater thermodynamic stability and no low-lying electronic states, is likely to be a poor model compound for transuranic hexafluoride photophysics and photochemistry.

Experimental Methods

A Q-switched Nd:YAG laser (7 ns pulse duration, Quanta-Ray DRC-1A) operated at 10 Hz was used as a light source. The 1064 nm fundamental was frequency doubled to 532 nm for some experiments. In all experiments reported here a geometry was used which focused the laser beam in front of the entrance window of the sample cell such that the laser beam was diverging as it passed through the sample cell. In this geometry the laser beam was about 3 mm in diameter at the region viewed by the light detection system.

PuF₆ was synthesized using ²⁴²PuO₂ from ANL stocks in an apparatus similar to that described by Steindler *et al.* (26) with the addition of a fluorine gas recirculation system. Prior to filling a sample cell the PuF₆ was purified as described by Malm and Weinstock (27). The all quartz sample cells were constructed with cylindrical bodies made of 8 mm i.d. "water-free" quartz (GE 214) to minimize optical absorbance at 2700 nm. The laser beam passed coaxially through the cylinder. The sample cells were baked out under vacuum and were passivated using small amounts of PuF₆ prior to being filled and sealed off. The temperature of a side arm on the sample cell was varied to obtain the desired PuF₆ pressure based on the vapor pressure-temperature relationship given by Weinstock, Weaver and Malm (28). The side arm was also used to condense out all the PuF₆ in the cell when background fluorescence was being checked. Typically the main body of the sample cell was held at 300 K.

Fluorescence was collected perpendicular to the laser beam propagation direction (i.e. 90 degree light collection) using calcium fluoride lenses. Infrared fluorescence was monitored using a 3 mm diameter Infrared Associates InSb photovoltaic detector cooled to 77 K and a current mode preamplifier which provided an overall 1/e response time of 1 microsecond. A gallium arsenide photomultiplier (RCA 31034) was used in the spectral region between 560 nm and 920 nm and a cooled S-1 photomultiplier (RCA 7102) was used from 920 nm to 1100 nm. Circular variable interference filters (CVF) were installed in a housing equipped with a synchronous motor drive and were used as

a scanning monochromator for wavelengths from 1370 nm to 4600 nm. The OCLI CV-1.3/2.5 and CV-2.3/4.6 CVF's provided a spectral bandpass which varied over the range of 1% to 3% of the wavelength selected. The CVF's made possible 1:1 imaging at f/1.4 light collection thereby improving fluorescence light collection efficiency by a factor of 9 in comparison with the 20 cm f.l., f/4.2, holographic grating monochromator used. The grating monochromator (ISA H20FIR) was used between 560 nm and 1400 nm at typically 32 nm spectral bandpass.

Fluorescence lifetimes were measured using a 2048 channel digital transient recorder (AEL PTR-9200) which was connected to a multichannel analyzer (Tracor Northern 570A). This provided "add-to-memory" signal averaging with a best time resolution of 10 ns per channel. Typically 2048 laser shots were averaged together. The multichannel analyzer output was fed to a computer where a linear least squares analysis was carried out to obtain the lifetime of the fluorescing state. Fluorescence emission spectra were recorded using a boxcar integrator (PAR 162/164) with typically a 5 microsecond gate width delayed 25 microseconds from the laser pulse and an output time constant of 100 seconds. The pump laser intensity was simultaneously recorded and was used to correct the recorded fluorescence intensity for the small changes in laser intensity which occurred during a fluorescence emission scan.

Experimental Results

Fluorescence Emission Spectra. We recently reported the first observation of fluorescence from electronically excited PuF₆ gas noting that the observed fluorescence peaked at about 2300 nm (1). We have now measured the fluorescence emission spectrum of PuF₆ excited both at 1064 nm and at 532 nm. The spectrum shown in Figure 2 was corrected for the wavelength dependence of the infrared detection system described above by recording the spectrum of a tungsten lamp whose filament temperature was measured with an optical pyrometer. From this data the spectral response function (29) of the detection system was determined and the fluorescence spectrum accordingly corrected. The emission spectrum of a low pressure mercury arc was recorded to obtain a wavelength calibration.

To within the intensity uncertainty shown in Figure 2, the fluorescence emission spectrum of PuF₆ is unchanged in switching from 1064 nm excitation to low fluence 532 nm excitation (circa 0.3 J/cm²). Laser fluence is a measure of the laser pulse energy per unit cross-sectional area of the laser beam. The laser energy was measured using a calibrated volume absorber calorimeter and the laser beam diameter was estimated from "burn" patterns on thermally sensitive paper. The wavelength range of 1370 nm to 4600 nm was searched when using 1064 nm excitation and the range 560 nm to 4600 nm was searched when

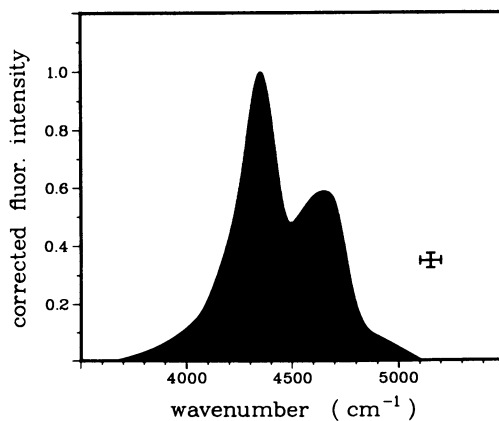


Figure 2. The fluorescence intensity of $\text{PuF}_6(\text{g})$ excited at 1064 nm is shown as a function of the energy of the emitted photons. The spectral bandpass and intensity uncertainty are indicated. To within experimental error, the same emission spectrum is found when 532 nm excitation is used.

using 532 nm excitation. The only PuF₆ fluorescence emission found was in the 4500 cm⁻¹ region as shown in Figure 2. When 532 nm excitation was used, scattered laser light was found to give rise to weak fluorescence from some of the long pass optical filters used to separate grating orders.

Photodecomposition. A greyish-white film of solid material slowly formed along the bottom of the sample cell in PuF₆ cells irradiated at 1064 nm. A similar film formed considerably faster in sample cells irradiated at 532 nm with the film forming on the entrance face of the cells as well as along the walls of the cell. Film formation was evident after less than a minute of irradiation at a laser fluence of 5 J/cm² at 532 nm. The exact chemical composition of the film has not yet been determined. It is known that it contains plutonium and fluorine. Most likely it is amorphous PuF₄. At present we can not rule out the possibility that the film contains other plutonium fluorides such as Pu₄F₁₇, Pu₂F₉ or PuF₅. It is evident that net photodecomposition of PuF₆ occurs using light of a photon energy less than the first dissociation limit of UF₆.

Fluorescence Lifetimes. We recently reported the first measurement of the fluorescence lifetimes of electronically excited PuF₆, using 1064 nm and 532 nm excitation (1). We have extended our measurements using 532 nm light to higher laser fluence and have found that the fluorescence decay of PuF₆ excited at 532 nm is not single exponential. This "non-exponential" behavior is evident at lower laser fluence only in a slight curvature in plots of the residuals that result from fitting the data to a single exponential decay model. Plots were made of the observed fluorescence decays as log [fluor. intensity] versus time following the 532 nm laser pulse. The plots significantly departed from the straight line behavior expected for a single exponential decay as laser fluence was increased. Fluorescence intensity decayed most rapidly at short times. Even at these higher fluences, the near-infrared fluorescence intensity of PuF₆ was so weak that the lifetimes had to be measured using the InSb detector and only a long pass filter to block scattered 532 nm laser light. The observed fluorescence risetimes corresponded to the detection system response time.

At 1064 nm, laser fluences in the range of 0.15-1.4 J/cm² were used during the course of this work. At 1064 nm, the observed fluorescence decays were well-fit in all cases by assuming a single exponential decay. As we previously reported (1), the fluorescence lifetime of PuF₆ gas at 300 K excited by 1064 nm light is 204 ± 12 microseconds independent of PuF₆ gas pressure over the range studied (18 to 109 torr, 1 torr = 133.322 pascal). At the highest PuF₆ pressure used about

120,000 hard sphere collisions occur during the lifetime of the emitting PuF₆ excited electronic state. The emitting state, assigned as a 5f electron excited state (see below), is remarkably metastable with respect to collisionally induced energy transfer.

At 532 nm, the range of laser fluences used was 0.1-5.0 J/cm². As previously reported (1), excitation at 532 nm resulted in a shorter lifetime (86 ± 4 microseconds) even at the lowest fluence used (0.1 J/cm²), where, with extensive signal averaging, a final signal-to-noise ratio of about 20 was obtained. As noted above the observed fluorescence decays at 532 nm became increasing non-exponential with increasing laser fluence.

The significantly faster PuF₆(g) fluorescence decay rate found using 532 nm excitation is unlikely to be due to a thermally induced effect (e.g. pyrolysis). The optical absorption coefficients of PuF₆(g) at 532 nm is at most twice as large as at 1064 nm (15). Assuming the 1064 nm absorption coefficient remains independent of laser fluence, then use of 1.4 J/cm² laser fluence at 1064 nm would result in deposition of about 7 times as much energy per unit sample volume as would be deposited by 0.1 J/cm² laser fluence at 532 nm. While different energy degrading processes may occur at these two wavelengths, shorter wavelength excitation will more strongly favor dissociation of PuF₆ and hence may even result in a smaller immediate heating effect per absorbed photon. The net result is that any sample heating effect present at 532 nm excitation at 0.1 J/cm² laser fluence should be substantially larger at 1.4 J/cm² laser fluence using 1064 nm excitation. The observation that the measured fluorescence lifetime using 1064 nm excitation was independent of laser fluence therefore provides evidence that thermal effects are unimportant in this work.

The "add-to-memory" signal averaging method currently available to us distorts fluorescence intensity versus time plots when the fluorescence intensity is a non-linear function of incident laser energy and the laser energy varies from shot to shot. For this reason we have not attempted detailed kinetic modelling of the observed fluorescence intensity decay curves recorded at high 532 nm laser fluence.

Fluorescence Photon Yields. We previously estimated the experimental fluorescence photon yield of PuF₆ excited at 1064 nm as well as at 532 nm as being $10^{-(4 \pm 1)}$ (1). We define the experimental fluorescence photon yield (FPY) as:

$$\text{FPY} = (\text{fluor. photons emitted})/(\text{pump laser photons absorbed}) \quad (1)$$

This estimated FPY was based on the reported molar absorptivity of PuF₆ at the pump laser wavelength, the pressure of PuF₆ in

the optical region of the sample cell, the geometrical fluorescence light collection solid angle, the transmission of the optical filters used, the estimated quantum efficiency of the InSb detector, the gain of the amplifiers used and an integration of the observed fluorescence intensity signal as a function of time. Although the uncertainty in the estimated FPY is large, this estimate is valuable in assessing the photophysics and photochemistry of $\text{PuF}_6(\text{g})$.

Discussion

We will first consider possible assignments for the fluorescing states in laser-excited $\text{PuF}_6(\text{g})$ based on available energy level structure and thermodynamic information. We will then consider some of the implications of the long-lived PuF_6 fluorescence we have observed in terms of potential photochemical separation processes.

Emission Spectrum Assignment - 1064 nm Excitation. The fluorescence emission spectrum observed using 1064 nm excitation is shown in Figure 2. We note that the largest energy gap between PuF_6 electronic states energetically accessible using this excitation wavelength occurs between the ground state and the 5f state at about 4550 cm^{-1} (see Figure 1). The observed emission spectrum corresponds well to that expected for the 4550 cm^{-1} state and its vibrational levels fluorescing to the ground state and its vibrational levels if one assumes that the next higher 5f state contributes little to the observed fluorescence spectrum.

The fluorescence spectrum shown in Figure 2 confirms the vibronic nature of the 4550 cm^{-1} transition since the peak separation corresponds well to $2\nu_6$ as would be expected from Steindler and Gunther's absorption measurements (16). Based on calculations of Kugel *et al.* (15) of PuF_6 energy level structure and their state assignments, $\text{PuF}_6(\text{g})$ fluoresces from its lowest lying $^3\Gamma_4$ state. It should be noted again, however, that the state assignments given by Kugel *et al.* have not yet been systematically confirmed.

The different relative intensities of the vibronic components of the fluorescence emission spectrum shown in Figure 2 in comparison with the intensities of the corresponding peaks in Steindler and Gunther's absorption spectrum are readily understood in terms of the arguments presented by Eisenstein and Pryce (30) concerning the 7540 cm^{-1} absorption band of $\text{NpF}_6(\text{g})$. The argument in essence is that the weaker band in each case can be interpreted as a "hot" band. The small shoulder evident at 4550 cm^{-1} in Steindler and Gunther's $\text{PuF}_6(\text{g})$ absorption spectrum, which might be interpreted as a direct, magnetic dipole allowed, transition, is not evident in the fluorescence spectrum shown in Figure 2. This probably results

from the lower spectral resolution of the fluorescence spectrum which would tend to obscure such a feature.

An alternate assignment of the emitting state in PuF₆ following 1064 nm excitation would be the 5f state at about 9755 cm⁻¹. Fluorescence from this state to lower lying levels would be expected to occur centered around 9755, 5205, 4970 and 3960 cm⁻¹, in poor agreement with the single observed band centered at about 4550 cm⁻¹. This alternate assignment is therefore rejected.

Non-Radiative Decay Channels - 1064 nm Excitation. We turn now to a comparison of the observed fluorescence photon yield defined by Equation 1 and the expected fluorescence quantum yield of the 4550 cm⁻¹ state which indicates that several non-radiative decay channels may be open following 1064 nm excitation of PuF₆(g). The following relationship between fluorescence quantum yield (FQY), observed fluorescence lifetime and the 4550 cm⁻¹ state's radiative or spontaneous emission lifetime is expected to hold (31):

$$\text{FQY} = (\text{observed fluor. lifetime})/(\text{radiative lifetime}) \quad (2)$$

Since the 4550 cm⁻¹ state is the first excited state of PuF₆, its radiative lifetime can be determined to be a reasonable approximation by integrating the optical absorption spectrum of PuF₆ over the wavelength range where absorption due to the 4550 cm⁻¹ state occurs. Some uncertainty arises since optical absorption from the next higher state undoubtedly overlaps that due to the 4550 cm⁻¹ state.

Using Steindler and Gunther's quantitative PuF₆ absorption spectrum (16), the observed PuF₆ fluorescence emission band half width as found from Figure 2, and initial and final state degeneracies based on the PuF₆ state assignments of Kugel *et al.* (15), the radiative lifetime of the 4550 cm⁻¹ state is estimated to be 120 milliseconds. Using this value and the observed lifetime (204 microseconds) in Equation 2 requires that the 4550 cm⁻¹ state's fluorescence quantum yield be about 1.7×10^{-3} . Since the upper limit of the experimental fluorescence photon yield ($1 \times 10^{-(4 \pm 1)}$) differs little from the value required by Equation 2, it may be that most initially excited PuF₆ molecules non-radiatively decay to the 4550 cm⁻¹ state. If the true fluorescence photon yield lies near the middle range or lower limit of the experimental fluorescence photon yield then other non-radiative decay processes must occur which result in only a small fraction of the absorbed pump laser photons giving rise to population of the emitting state. As shown schematically in Figure 3 one such non-radiative process may be dissociation of PuF₆ into the radicals PuF₅ and F atom.

A further consequence of assigning the emitting state as the 4550 cm⁻¹ state is that this state then must be assumed to

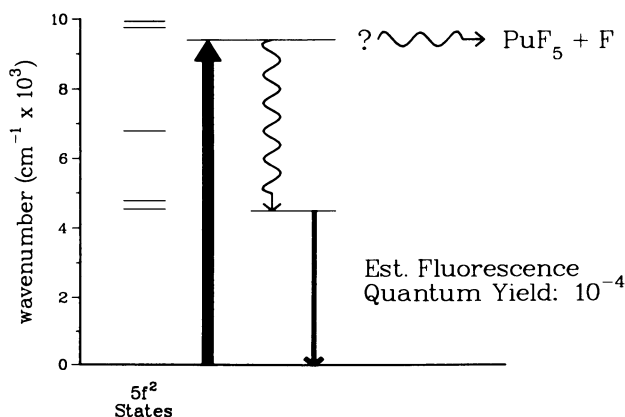


Figure 3. Energy diagram for 1064 nm excitation of $\text{PuF}_6(\text{g})$. The 5f electron states of PuF_6 are shown at the left. The solid arrows indicate photon absorption or emission processes. The wavy arrows indicate nonradiative processes by which excited states of PuF_6 are lost. Comparison of observed fluorescence photon yields versus the fluorescence quantum yield expected for the 4550 cm^{-1} state indicate that the PuF_6 state initially populated following 1064 nm excitation may dissociate as shown.

undergo efficient non-radiative decay in light of its evidently small fluorescence quantum yield. It is not known whether the primary non-radiative decay process is collisionless conversion of 5f electronic energy into internal energy or a "unimolecular" reaction (32) involving bimolecular collisions activating excited PuF₆ molecules to a dissociative state. If such a "unimolecular" reaction is occurring then even 18 torr pressure must be sufficient to reach the high pressure limit in which the "unimolecular" reaction becomes pseudo-first order since even at 18 torr the observed fluorescence decays were single exponential.

Emission Spectrum Assignment - 532 nm Excitation. Since the same PuF₆(g) fluorescence emission spectrum is found using 1064 nm or 532 nm excitation, we begin by assuming that the emitting state following 532 nm excitation of PuF₆ is the same state as when PuF₆ is excited at 1064 nm (i.e. the 4550 cm⁻¹ state). The principal difficulty with this assignment is the fact that the observed fluorescence decay rate is over a factor of 2 faster when 532 nm rather than 1064 nm excitation is used (1). In addition the observed fluorescence decay rate is non-exponential and laser-fluence dependent at 532 nm excitation. Figure 4 shows schematically some of the radiative and non-radiative processes which may occur when PuF₆ is excited at 532 nm. If the processes shown in Figure 4 with a "?" do occur, then the faster fluorescence decay rate as well as its non-exponential character and laser-fluence dependence can be understood in terms of the photochemical mechanism described below. Since the proposed photochemical mechanism qualitatively accounts the observations found using 532 nm excitation, we tentatively assign the fluorescence emission spectrum observed following 532 nm excitation as arising from the first excited state of PuF₆, the state around 4550 cm⁻¹.

Non-Radiative Decay Channels - 532 nm Excitation. A mechanism in which the emitting state of PuF₆ undergoes a bimolecular reaction with a photodecomposition product would account for the fluorescence decay behavior found when PuF₆(g) is excited at 532 nm. The significantly increased net photodecomposition observed on switching from 1064 nm to 532 nm excitation also argues that an additional non-radiative decay channel has been opened when using the shorter wavelength excitation. Since fluorescence is observed when using 532 nm excitation, it is likely that the initially populated PuF₆ state branches to several non-radiative decay channels such as dissociation and collisionless degradation of electronic energy into vibrational and rotational energy. One or more of these channels would lead to population of the emitting PuF₆ state.

If PuF₄(g) is formed via dissociation of the PuF₆ state initially populated, then a bimolecular reaction between PuF₆

and $\text{PuF}_4(\text{g})$ to produce $\text{PuF}_5(\text{g})$ would account for the non-exponential and laser-fluence dependent fluorescence intensity decay observed. Here PuF_6^* denotes $\text{PuF}_6(\text{g})$ in its 4550 cm^{-1} state. The reaction between $\text{PuF}_6(\text{g})$ in its ground electronic state and ground state $\text{PuF}_4(\text{g})$ would be expected to be exothermic both in comparison with the known thermodynamics of the corresponding uranium species (22,23) and from the PuF_6 dissociation limits shown in Figure 1. However such a bimolecular reaction involving non-radical reactants in their ground electronic states would be expected to have a significant activation energy.

The activation energy for the $\text{PuF}_6(\text{g}) + \text{PuF}_4(\text{g})$ reaction would most likely be a considerable fraction of the energy required to break a Pu-F bond in PuF_6 . Therefore the reaction of $\text{PuF}_6(\text{g}) + \text{PuF}_4(\text{g})$ in their ground states would be expected to proceed relatively slowly at room temperature. If the electronic energy of PuF_6^* is available to overcome this activation energy barrier, then the reaction of $\text{PuF}_6^* + \text{PuF}_4$ would become sufficiently rapid to largely account for the laser-fluence dependent fluorescence decays we have observed following 532 nm excitation of $\text{PuF}_6(\text{g})$. In the proposed mechanism, the measured fluorescence lifetime of PuF_6 following 532 nm excitation would be expected to be shortened in comparison with 1064 nm excitation and to become non-exponential with increasing laser fluence due to the increasing rapid removal of PuF_6^* via reaction with $\text{PuF}_4(\text{g})$. Dimerization of sub-hexavalent plutonium fluorides, subsequent formation of higher aggregates and possibly disproportionation reactions are processes which may contribute to formation of the solid photodecomposition product.

The proposed photochemical reaction mechanism shown in Figure 4 accounts for the observations we have reported and is in accord with presently available thermodynamic and spectroscopic data. However, this mechanism must be regarded as subject to revision as more information becomes available concerning the properties of plutonium fluorides in gas and solid phases. We have excluded bimolecular energy transfer reactions such as $\text{PuF}_6^*(\text{g}) + \text{PuF}_5(\text{g}) \rightarrow \text{PuF}_6(\text{g}) + \text{PuF}_5(\text{g})$ from consideration as important non-radiative decay channels since energy transfer between 5f states seem unlikely to be facile during the short time span of a gas phase collision.

Research Opportunities. The presence of a long-lived fluorescing state following either 532 nm or 1064 nm excitation of $\text{PuF}_6(\text{g})$ provides a valuable opportunity to study the extent to which electronic energy in a 5f electron state is available in photochemical and energy transfer reactions. Such gas phase bimolecular reactions would occur in a weak interaction limit governed by van der Waals' forces. Seen from the perspective of potential photochemical separations in fluoride volatility

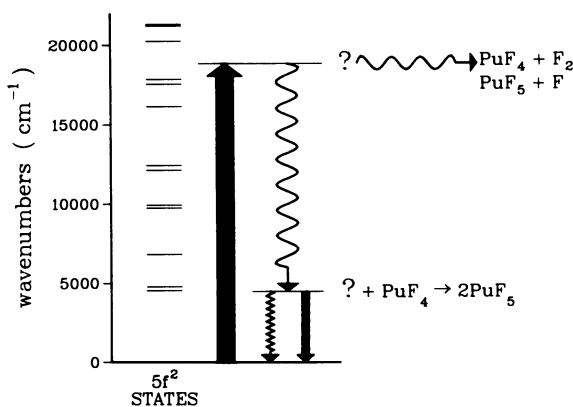


Figure 4. Energy diagram for 532 nm excitation of $\text{PuF}_6(\text{g})$. The $5f$ electron states of PuF_6 are shown at the left. The solid arrows indicate photon absorption or emission processes. The wavy arrows indicate nonradiative processes by which excited states of PuF_6 may be lost. The laser-fluence dependent fluorescence decay found at this excitation wavelength can be explained in terms of a bimolecular reaction between $\text{PuF}_6(\text{g})$ in its 4550 cm^{-1} state and $\text{PuF}_4(\text{g})$ to form $\text{PuF}_5(\text{g})$. It is assumed that $\text{PuF}_4(\text{g})$ is formed via dissociation of the initially populated PuF state.

processing, for example, the long-lived excited electronic states found in both $\text{NpF}_6(\text{g})$ and $\text{PuF}_6(\text{g})$ may pose significant problems.

Conclusions

Laser-induced fluorescence has proven to be the key to these pioneering studies of transuranic hexafluoride electronic state photophysics and photochemistry. This is a research area of unique opportunity in which fundamental and technical research interests strongly converge.

As we have noted many of the properties of PuF_6 and NpF_6 are poorly understood and should be the subject of further fundamental investigation. Little is known concerning the gas phase reaction rates and mechanisms of mixtures containing transuranic hexafluorides. The thermodynamic dissociation limits of $\text{PuF}_6(\text{g})$ are not well-established which is only in part due to the present lack of a synthesis for PuF_5 . There is no thermodynamic information concerning NpF_6 . While $\text{NpF}_6(\text{g})$ and $\text{PuF}_6(\text{g})$ have been the subject of several spectroscopic investigations, our work again points up the lack of proven electronic state assignments and the difficulty in making such assignments posed by the predominantly vibronic nature of their 5f transitions.

Given the powerful techniques that can now be brought to bear on these problems, we stand on the threshold of a new era and confidently look forward to achieving a systematic and predictive understanding of the electronic state properties of all the actinide hexafluorides.

Acknowledgment

We wish to thank one of our reviewers for his informed and constructive criticism. This work was performed under the auspices of the Office of Basic Energy Sciences, Division of Nuclear Sciences, U. S. Department of Energy under contract number W-31-109-ENG-38.

Literature Cited

1. Beitz, J. V.; Williams, C. W.; Carnall, W. T. J. Chem. Phys. 1982, 76, 2757-2758.
2. Seaborg, G. T. Univ. of Chicago Met. Lab. Report CN-125 (1942).
3. Steindler, M. J. Argonne Nat. Lab. Report ANL-6753 (1963).
4. Steindler, M. J. U.S. AEC Div. Tech. Info. Report CONF-680610 (1968); pp. 2-17.
5. Malm, J. G.; Weinstock, B. and Claassen, H. H. J. Chem. Phys., 1955, 23, 2192-2193.

6. Malm, J. G.; Weinstock, B.; Weaver, E. E. J. Phys. Chem. 1958, 62, 1506-1508.
7. Trevorrow, L. E.; Gerding, T. J.; Steindler, M. J. Inorg. Nucl. Chem. Let. 1969, 5, 837-839.
8. Rand, M. H. Atomic Energy Review 1966, 4 (Special Issue 1), 7-51.
9. Oetting, F. L. Chem. Rev. 1967, 67, 261-297.
10. Brown, D. "Gemlins Handbuch der Anorganischen Chemie, Transurane, Teil C: Die Verbindungen", G. Koch, ed.; Verlag Chemie: Weinheim, 1972; pp. 100-128.
11. Keller, C.; Chemiker-Zeitung 1982, 106, 137-142.
12. Brown, D. "Halides of the Lanthanides and Actinides"; John Wiley and Sons: London, 1968.
13. Cleveland, J. M. "The Chemistry of Plutonium"; Gordon and Breach: New York, 1970.
14. Burns, R. C.; O'Donnell, T. A.; Randall, C. H. J. Inorg. Nucl. Chem. 1981, 43, 1231-1238.
15. Kugel, R.; Williams, C.; Fred, M.; Malm, J. G.; Carnall, W. T.; Childs, W. J.; Goodman, L. S. J. Chem. Phys. 1976, 65, 3486-3492.
16. Steindler, M. J.; Gunther, W. H. Spectrochim. Acta 1964, 20, 1319-1322.
17. Boring, M.; Hecht, H. G. J. Chem. Phys. 1978, 69, 112-116.
18. Koelling, D. D.; Ellis, D. E.; Bartlett, J. J. Chem. Phys. 1976, 65, 3331-3340.
19. Desclaux, J. P.; Freeman, A. J. J. Magn. Magn. Mater. 1978, 8, 119-129.
20. Fuger, J. in "Actinides in Perspective" N. M. Edelstein, ed.; Pergamon press: Oxford, 1982; pp. 409-431.
21. Miller, J. C.; Allison, S. W.; Andrews, L. J. Chem. Phys. 1979, 70, 3524-3530.
22. Hildenbrand, D. L. J. Chem. Phys. 1977, 65, 4788-4794.
23. Steindler, M. J.; Gerding, T. J. Spectrochim. Acta 1966, 22, 1197-1200.
24. Goodman, G. L.; Fred, M. J. Chem. Phys. 1959, 30, 849-850.
25. Hutchison Jr., C. A.; Weinstock, B. J. Chem. Phys. 1960, 32, 56-61.
26. Steindler, M. J.; Steidl, D. V.; Steunenbeg, R. K. Nuclear Sci. and Eng. 1959, 6, 333-340.
27. Weinstock, B.; Malm, J. G. J. Inorg. Nucl. Chem. 1956, 2, 380-394.
28. Weinstock, B.; Weaver, E. E.; Malm, J. G. J. Inorg. Nucl. Chem. 1959, 11, 104-114.
29. Rutgers, G. A. W. J. Res. Natl. Bur. Stand. Sec. A 1972, 76A, 427-436.
30. Eisenstein, J. C.; Pryce, M. H. L. Proc. Roy. Soc. (London) 1960, A255, 181-198.
31. Carnall, W. T. in "Organometallics of the f-Elements" T. J. Marks and R. D. Fischer, eds.; D. Reidel Pub. Co.: Dordrecht, 1979; pp. 281-307.

32. Robinson, R. J.; Holbrook, K. A. "Unimolecular Reactions"; John Wiley and Sons: London, 1972; pp. 13-27.
33. Hildenbrand, D. L. Lawrence Berkeley Lab. Report LBL-12441 (1981); pp. 256-257.

RECEIVED December 21, 1982

Measurement and Interpretation of Plutonium Spectra

J. BLAISE

Laboratoire Aimé Cotton, Centre de la Recherche Scientifique,
Bat. 505, 91405 Orsay Cedex, France

M. S. FRED, W. T. CARNALL, H. M. CROSSWHITE, and
H. CROSSWHITE

Argonne National Laboratory, Chemistry Division, Argonne, IL 60439

The atomic spectroscopic data available for plutonium are among the richest of any in the periodic system. They include high-resolution grating and Fourier-transform spectra as well as extensive Zeeman and isotope-shift studies. We summarize the present status of the term analysis and cite the configurations that have been identified. A least-squares adjustment of a parametric Hamiltonian for configurations of both Pu I and Pu II has shown that almost all of the expected low levels are now known. The use of a model Hamiltonian applicable to both lanthanide and actinide atomic species has been applied to the low configurations of Pu I and Pu II making use of trends predicted by *ab initio* calculations. This same model has been used to describe the energy levels of Pu³⁺ in LaCl₃, and an extension has permitted preliminary calculations of the spectra of other valence states.

In the fifteen years since publication of an earlier status report on the atomic spectra of plutonium and other actinide elements (1) there has been steady progress, especially in the parametric interpretation of the energy levels. The analogy to lanthanide electronic structure has been more firmly established, the relationships among all the elements of the actinide series have been clarified, and a detailed theory of the lanthanide/actinide crystal spectra has been developed. The most thoroughly advanced of the actinide atomic spectroscopic studies are probably those for plutonium, so it is particularly appropriate that in this 40th anniversary year we look again at where we stand. Because of the close relationship between ionic energy levels in the free state and

0097-6156/83/0216-0173\$07.50/0
© 1983 American Chemical Society

in crystalline environments, the current status of both experimental approaches is presented, along with a brief summary of the generalized parametric theory. A more thorough discussion of the results of the term analysis for neutral plutonium (Pu I) will be given elsewhere (2); a complete listing of spectrum lines and energy levels for Pu I and Pu II will be made available as an Argonne National Laboratory Report (3). Abbreviated line lists were recently published by Conway and coworkers (4), and some independent work has also been reported by Striganov (5). Less progress has been made in interpreting the spectra of the higher valence states of plutonium in condensed phases. The summary of studies published up to ~1970 (6) is still a relevant description of the status of this work.

Free-Ion Spectra

The spectrum of Pu was first photographed in 1943 by Rollefson and Dodgen (7), who measured the wavelengths (and intensities) of about 125 lines. However, the first energy level analysis did not come until 1959, when McNally and Griffin (8), using a low-current dc arc loaded with ^{239}Pu in a magnetic field of 2.447 teslas, found 7 out of the 13 levels of the ground terms $5f^6 7s^8 F$ and $6F$ in Pu II and also reported 84 high odd levels. (Only 73 of these levels have been confirmed).

The ground multiplet of Pu I was subsequently established by Bovey and Gerstenkorn (9). Combining Harwell Zeeman spectra (from an electrodeless discharge tube containing ^{239}Pu in a magnetic field of 3 teslas (10), with the hyperfine structure and isotope shift measurements made at Laboratoire Aimé Cotton (LAC) from a hollow cathode with a photoelectric Fabry-Perot interferometer, these authors found the lowest five levels of $5f^6 7s^2 7F$, as well as 25 upper odd levels (9, 11). Beginning in 1961, the analysis of the plutonium spectra became a joint project carried out by spectroscopists from three laboratories: Argonne National Laboratory (ANL), Lawrence Livermore National Laboratory (LLNL) and LAC. In the early stages of the term analysis, when separated isotopes became available in sufficient quantity for spectroscopic use, special electrodeless tubes were prepared for particular experiments. One, prepared by E. Worden of LLNL, contained 88% ^{240}Pu for use with the ANL 30-foot Paschen-Runge spectrograph and the 2.4 tesla magnet. The thousands of Zeeman patterns (an example is shown in Fig. 1), obtained with this tube were essential for further progress in the analysis. The small residual amount of ^{239}Pu also permitted isotope-shift measurements to supplement the more accurate interferometric measurements of Gerstenkorn (11) and Striganov and Korostyleva (12, 13, 14). Subsequent spectrograms taken with tubes prepared by F. S. Tomkins at ANL

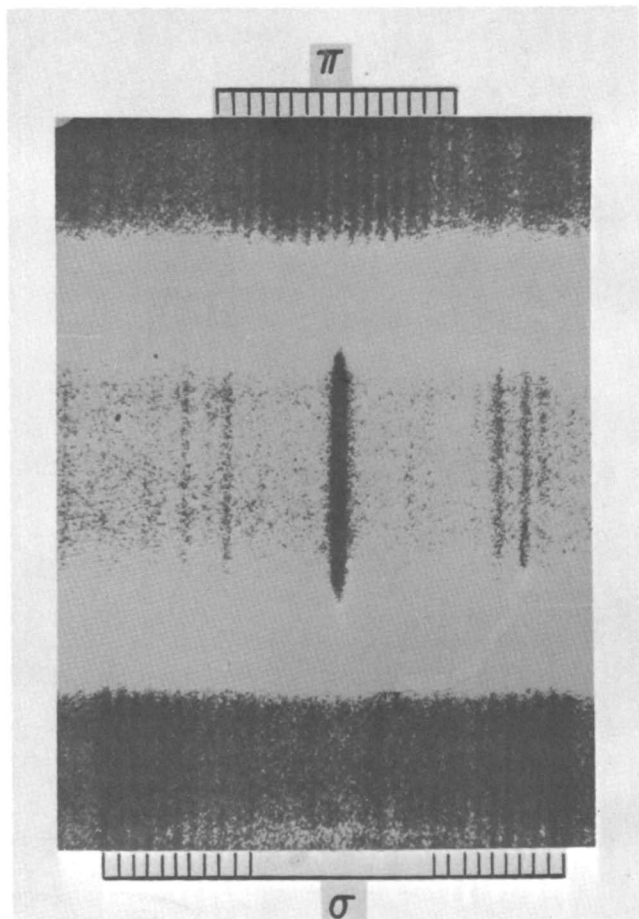


Figure 1.
Zeeman pattern for Pu I at 8534 Å photographed at 2.4 teslas.

with mixtures of ^{239}Pu and even isotopes 238-244 (as they became available as separated species) were measured by Gerstenkorn at LAC. In 1970 the spectra of ^{240}Pu and of a mixture of the 240, 242, and 244 isotopes were recorded by Fourier-transform spectroscopy at LAC up to $3.59\ \mu\text{m}$. A portion of one of these recordings is shown in Fig. 2. The higher resolution made available by these experiments and the connections between low levels made possible by this extension into the infrared greatly advanced the analysis.

For easier reference to earlier work the shift for (239-240) was adopted as the reference for tabulation and where necessary derived from the (240-244) isotope shift by dividing the latter by 2.531, a constant factor determined by Blaise *et al.* (15). Over 9500 isotope shifts have now been measured, 50% of them in the infrared.

The number of energy levels found to date, with the aid of the Zeeman effect and the isotope shift data, is 605 even and 586 odd levels for Pu I and 252 even and 746 odd for Pu II. The quantum number J has been determined for all these levels, the Lande g -factor for most of them, and the isotope shift for almost all of the Pu I levels and for half of those of Pu II. Over 31000 lines have been observed of which 52% have been classified as transitions between pairs of the above levels. These represent 23 distinct electron configurations.

The main problems in these very complex spectra are (1) to find the levels, and (2) to assign the levels to the proper configuration. In the absence of configuration interaction one can estimate the isotope shift for various configurations, taking into account the screening of the $7s$ electron charge density at the nucleus by the $5f$, $6d$, and $7p$ electrons (16). Comparison of these estimates with experimental observations is an important first step in identifying numerical energy levels with their quantum mechanical counterparts. Computations of the central electron density, $[4\pi\psi_S^2(0)]$ have been reported using both the non-relativistic (17) and relativistic (18) Hartree-Fock procedures. When the isotope shift characteristic of the lines belonging to a particular configuration is plotted against the relativistic value for $4\pi\psi_S^2(0)$, the resulting relationship is seen to be a linear function, Fig. 3 (18).

Thus far, we have identified levels belonging to 14 different configurations of Pu I and to 9 configurations in Pu II. The lowest levels of these configurations are given in Table I along with Landé g -factors and the experimental isotope shifts. The latter values are averages and have changed in magnitude somewhat as more experimental data has been analyzed. This can be seen by comparison of values in Table I with earlier tabulations such as shown in Fig. 7 of reference 1. Several levels showing anomalous isotope shifts are perturbed by nearby levels with the same J but which however belong to another configuration. For a more detailed

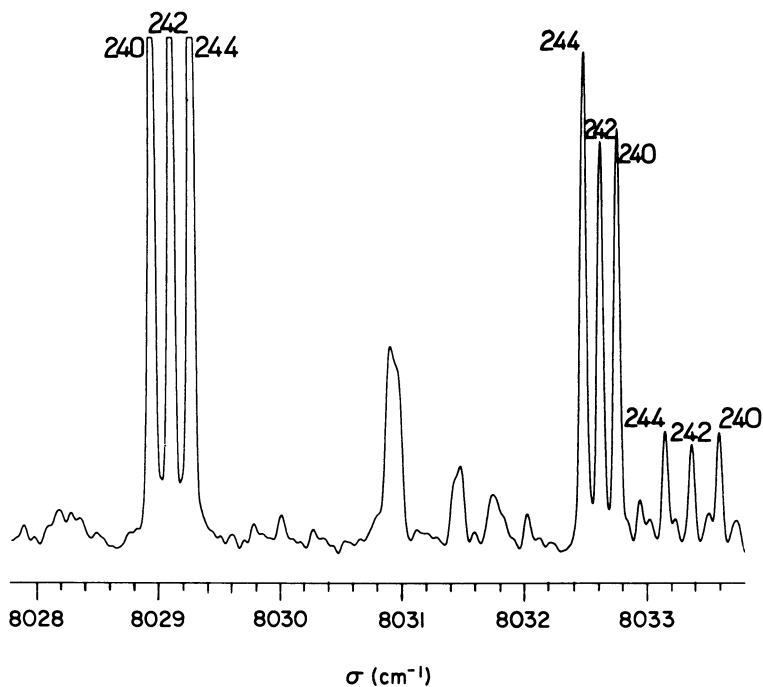


Figure 2.
Spectra of a mixture of $^{240}, ^{242}, ^{244}\text{Pu}$ isotopes recorded by Fourier-transform spectroscopy.

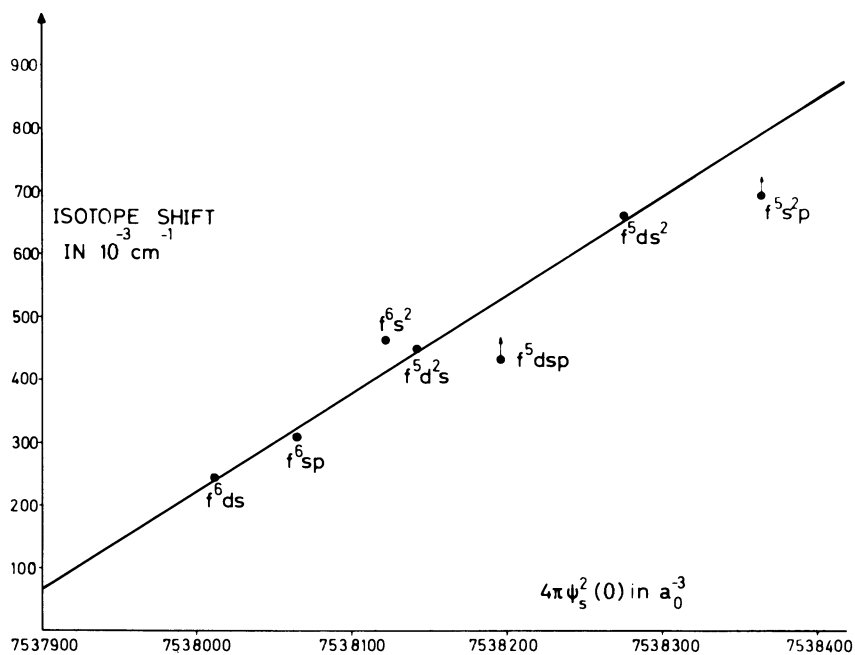


Figure 3.

Isotope shift for various configurations in Pu I plotted as a function of the central electron density, $4\pi\psi_s^2(0)$.

Table I. The Lowest Level of Each Configuration of Pu I and Pu II with their Corresponding Landé g-Values and Experimental Isotope Shifts (E in cm⁻¹ and IS in 10⁻³ cm⁻¹).

Pu I	E	g	IS	E	g	IS
5f ⁶ 7s ²	0	-	465	6314	0.487	653
5f ⁶ 6d7s	13528	-0.590	253	14912	0.496	488
5f ⁶ 6d ²	31711	0.200	115	?		
5f ⁶ 7s7p	15449	-	336	17898	0.450	698
5f ⁶ 6d7p	33071	0.673	293	20828	0.352	467
5f ⁶ 7s8s	31573	2.403	446	37415	0.980	403
5f ⁷ 7s	25192	1.768	273	39618	0.270	503
<hr/>						
Pu II						
5f ⁶ 7s	0	3.150	381	8199	0.414	896
5f ⁶ 6d	12008	-0.019	77	8710	0.308	555
5f ⁶ 7p	22039	0.344	287	17297	0.494	242
5f ⁷	?		(0)	30956	0.646	424
				33793	0.800	208
				37641	0.70	813

discussion of the dependence of isotope shifts on the electron configuration occupancy, see Reference (18). According to the systematic relationships developed by Brewer (19), the still-missing f^5d^3 configuration in Pu I should begin around $27000 \pm 5000 \text{ cm}^{-1}$, and the level $5f^7(^8S_{7/2})$ of Pu II is predicted to occur at $14000 \pm 8000 \text{ cm}^{-1}$.

A further check on the configuration assignments made to date can be obtained by systematically comparing those given in Table I for the lowest levels with analogous ones for other elements, as in Figs. 4 and 5 for all the known actinide configurations. To better see the trends across the series for given configuration types we have changed the energy reference from the experimental zero (ground state) to the lowest level of a particular configuration type. In the left half of Fig. 4, we have chosen $5f^N7s^2$ as the reference. Configurations with two valence electrons then tend to show a flatter, less irregular display than if referenced against a ground state with variable configuration type. Configurations with three or four valence electrons show a steep, but also more regular, rise as the f-shell collapse progresses. In the alternate display on the right, $5f^{N-1}6d7s^2$ lowest levels were taken as the reference. Trivalent configurations are now relatively flat, with the former reference $5f^N7s^2$ configurations showing a steep fall and $5f^{N-2}6d^27s^2$ a less steep rise. Not all configuration types are plotted in both diagrams. Similar displays of Pu II lowest levels are plotted in Fig. 5, with $5f^N7s$ and $5f^{N-1}7s^2$ being chosen for alternative references. All the assignments given in Table I are consistent with these diagrams.

The first and second spectra of plutonium are probably the most thoroughly studied of any in the periodic table insofar as experimental description of the observed spectra and the term analysis is concerned, but a detailed quantum mechanical treatment has been handicapped by their great complexity. Fortunately, the lowest odd and lowest even configurations for both Pu I and Pu II are relatively simple, and parametric studies of the lowest levels of the $5f^67s^2$, $5f^56d7s^2$ and $5f^67s8s$ configurations in Pu I (20, 21) and $5f^67s$ in Pu II (21) were performed at an early stage. A "generalized" parametric study (22) of the $5f^N7s^2$ and $5f^N7s$ configurations in the first and second spectra of the actinides has shown a smooth variation of all the usual parameters of the core $5f^N$. The only missing level below 20000 cm^{-1} in $5f^67s^2$ of Pu I has now been found, 107 cm^{-1} lower than predicted.

Some rather heavily-truncated versions of the more complex configurations have been used at ANL to assist in level identifications. A summary of the fitted parametric results for the lowest configurations of Pu I and Pu II is given in Table II. In some cases configuration mixing has been included. The numbers enclosed in parentheses following the

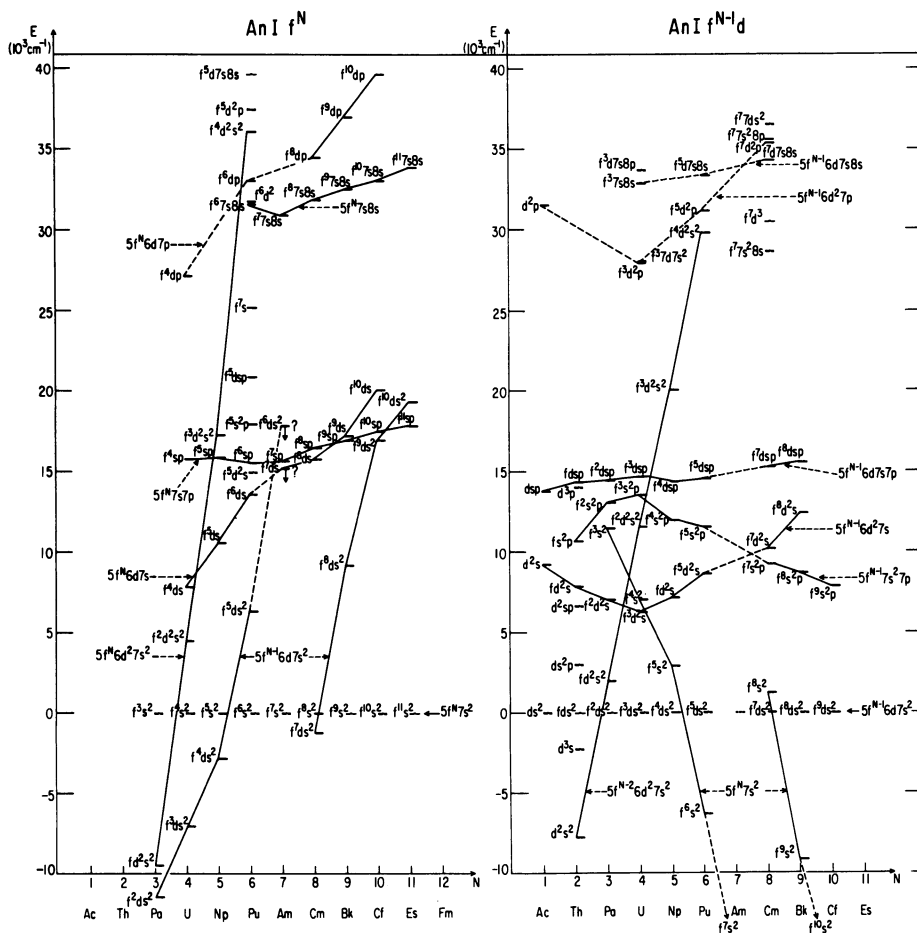


Figure 4.
 Systematic variation of the lowest-energy levels in a given configuration for An I plotted as a function of N, where $N = Z - 88$.

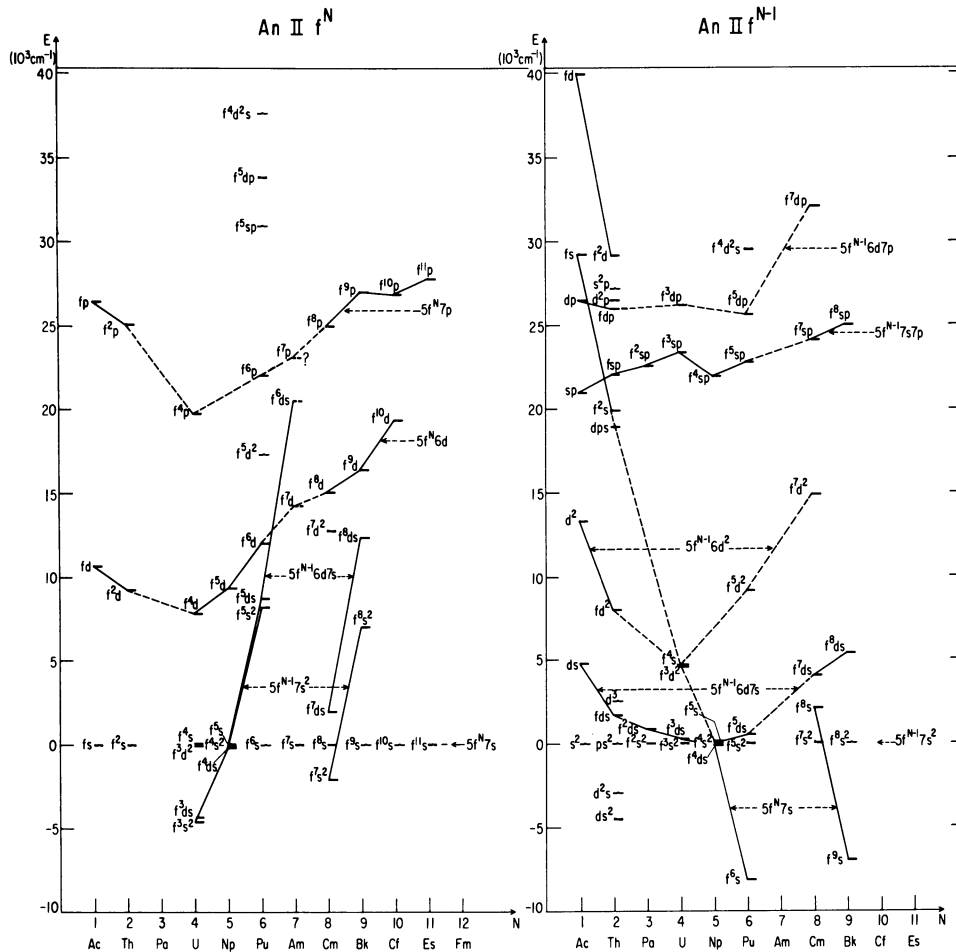


Figure 5.

Systematic variation of the lowest-energy levels in a given configuration for An II plotted as a function of N , where $N = Z - 88$.

Table II. Parameter Values for Low Plutonium Configurations in cm^{-1} .

	Pu I			Pu II			
	$f^6 s^2 \alpha$	$f^6 ds \alpha$	$f^5 ds^2 \alpha$	$f^6 s^2 b$	$f^6 d \alpha$	$f^5 s^2 \alpha$	$f^5 ds \alpha$
EAV	45122(189)	65466(1076)	52342(1115)	-	60844(169)	48696(215)	57794(328)
F ²	45114(624)	47578(1373)	[49300]	43311(221)	[43500]	49066(770)	49230(1243)
F ⁴	31656(1174)	[36164]	[39500]	32103(536)	[34000]	39640(719)	37215(1468)
F ⁶	[24452]	[27124]	27460(739)	23201(297)	[24000]	26946(785)	[27918]
α	[32.55]	[32.55]	[35]	53.5(1.5)	[31.5]	[32.55]	[32.55]
β	[-652]	[-750]	[-900]	-1261(84)	[-750]	[-652]	[-652]
γ	[1200]	[1300]	[1100]	2035(140)	[1300]	[1200]	[1200]
ζf	2063(20)	2100(26)	2233(12)	2079(11)	2084(26)	2275(27)	2263(11)
ζd		897(42)	1412(28)		1429(82)		1677(39)
F ² (fd)		9469(593)	14973(335)		18805(635)		20468(445)
F ⁴		11108(987)	[11000]		[12000]		14251(1090)
G ¹		3977(202)	6357(113)		2266(594)		9027(159)
G ²		[902]	614(355)		[1000]		387(932)
G ³		9148(638)	8293(304)		10840(823)		9452(528)
G ⁴		[1000]	[2000]		[1000]		1903(808)
G ⁵		985(549)	6081(307)		[7500]		8515(661)
G ³ (fs)		2819(93)		2498(45)			2353(93)
G ² (ds)		3684(549)					7838(386)
R ² (fd,fs)		-8260(1715) ^c					
R ³ (fd,sf)		-3782(1291)					

^aAlso: $T^2 = 200$, $T^3 = 30$, $T^4 = 11$, $T^6 = -368$, $T^7 = 389$, $T^8 = 352$, $M^0 = 0.75$, $M^2 = 0.41$, $M^4 = 0.29$,
 $P^2 = 1334$, $P^4 = 1000$, $P^6 = 667$, all fixed.

^bFrom Reference 22.

^cConfiguration mixing between $f^6 s^2$ and $f^6 ds$.

tabulated values represent the statistical errors associated with that particular parameter value. A number enclosed by square brackets is one for which that parameter was held fixed during the least-squares fitting procedure. Calculations such as these have been invaluable in defining the quantum-electronic nature of the empirical levels; the derived eigenvectors are used to compute g-values and isotope shifts for direct comparison with experimental measurements as well as for more indirect analyses of hyperfine structure parameters (23). Because of the stability of the f-orbitals it is possible to draw a strong parallel among their atomic parameters and analogous parameters from studies of other actinide and lanthanide cases. In fact, Hartree-Fock calculations of the associated radial integrals shown in Tables IIIA and B for some cases of interest here, together with appropriate systematic corrections deduced from empirical studies, can be used as the basis of a parametric model which embraces all of the actinide and lanthanide spectra so far subjected to detailed study. These corrections take two forms: (1) a numerical correction to the Hartree-Fock estimates, partially accounting for the masking of parameters which is one consequence of the breakdown of the single-configuration approximation and (2) introduction of additional (effective) Hamiltonian operators which have no meaning in a single-configuration approximation but which to a large extent mimic the effects of interactions with other configurations without increasing the sizes of the matrices involved. Because these corrections to the Hartree-Fock estimates, and the empirical parameters associated with effective operators, are nearly independent of the particular ion under study, it is possible to make reasonably accurate estimates of plutonium parameters in advance of the detailed analysis. Indeed, as nearly as we have been able to determine, none of the effective-operator parameters are significantly different in analogous crystal/free-ion comparisons. As a consequence, we have used the general parametric model to give estimates where empirical data are insufficient, in attempts to interpret both crystal and free-ion cases. In spite of the complications brought about by the effects of the crystal-field interaction, the fact that in crystal spectra only transitions between levels of $5f^N$ itself are encountered at low energies has led to a great simplification of the problems of identification and interpretation. The condensed-phase spectra of plutonium in the tetravalent, (IV), through (VII) oxidation states are known, but theoretical interpretation of the observed transitions is not as highly developed as that characteristic of Pu^{3+} . However, several general statements regarding the electronic structure of Pu in condensed phase can be made as a result of recent work. The subsequent discussion, therefore, represents a continuation of that of Pu I and Pu II spectra,

Table III(A). HFR^a Values for 5f^N Cores of Pu Configurations.

Spectrum	Configuration	F ²	F ⁴	F ⁶	ζ	M ⁰
I	5f ⁶ 7s ²	71461	46094	33638	2230	0.75
	5f ⁵ 6d7s ²	76279	49543	36268	2422	0.84
	5f ⁶ 6d7s	70790	45619	33280	2215	0.74
II	5f ⁶ 7s	71900	46400	33867	2239	0.76
	5f ⁵ 7s ²	77274	50260	36815	2249	0.86
	5f ⁵ 6d7s	76452	49664	36360	2426	0.85
	5f ⁶ 6d	70980	45747	33374	2217	0.74
III	5f ⁶	72563	46868	34220	2255	0.77
	5f ⁵ 6d	76820	49926	36558	2436	0.85
IV	5f ⁵	78223	50942	37335	2479	0.88
V	5f ⁴	82908	54356	39965	2679	0.98
VI	5f ³	86982	57347	42285	2914	1.09
VII	5f ²	90625	60037	44381	3130	1.19

^aComputed using Hartree-Fock methods and including an approximate relativistic correction (24).

Table III(B). HFR^a Values for Inequivalent-Electron Interactions

Parameter	Pu I	Pu I	Pu II	Pu II	Pu III
	5f ⁵ 6d7s ²	5f ⁶ 6d7s	5f ⁵ 6d7s	5f ⁶ 6d	5f ⁵ 6d
ζ _d	1695	985	1976	1418	2255
F ² (fd) ^d	24469	17687	27225	22959	29649
F ⁴ (fd)	12649	8871	14292	11913	15773
G ¹ (fd)	14187	11109	15918	14713	17378
G ³ (fd)	10326	7588	11701	10257	12918
G ³ (fs)		2995	3696		
G ² (ds)		19822	21708		

^aComputed using Hartree-Fock methods and including an approximate relativistic correction (24).

beginning with consideration of divalent plutonium, and addressing the condensed-phase spectra at increasing stages of ionization.

Crystal Spectra

In what follows we briefly review some of the previous attempts to analyze the available spectra of plutonium (6). In addition, we estimate energy level parameters that identify at least the gross features characteristic of the spectra of plutonium in various valence states in the lower energy range where in most cases, several isolated absorption bands can be discerned. The method used was based on our interpretation of trivalent actinide and lanthanide spectra, and the generalized model referred to earlier in the discussion of free-ion spectra.

As was the case with lanthanide crystal spectra (25), we found that a systematic analysis could be developed by examining differences, ΔP , between experimentally-established actinide parameter values and those computed using Hartree-Fock methods with the inclusion of relativistic corrections (24), as illustrated in Table IV for An^{3+} . Crystal-field effects were approximated based on selected published results. By forming tabulations similar to Table IV for 2^+ , 4^+ , 5^+ and 6^+ spectra, to the extent that any experimental data were available to test the predictions, we found that the ΔP -values for Pu^{3+} provided a good starting point for approximating the structure of plutonium spectra in other valence states. However, adjustments were required for each individual oxidation state.

In addition to transitions within the $5f^N$ configuration which characterize the lower energy states in the following discussion, the energy of onset of $f \rightarrow d$ transitions is an important variable which strongly influences the nature of the spectra. For example, intense absorption bands characteristic of $f \rightarrow d$ transitions in the ultraviolet range of the $Pu^{3+}(\text{aquo})$ spectrum, Fig. 6, completely mask the presence of weaker $f \rightarrow f$ transitions. The first $f \rightarrow d$ transition is shifted toward higher energies with increasing valency, and with increasing atomic number within a single oxidation state.

Prediction of the energy level structure for $Pu^{2+} (5f^6)$ is of particular interest since no spectra for this valence state of Pu have been reported. On the basis of what is known of the spectra of Am^{2+} (26), Cf^{2+} (27), and Es^{2+} (28), there appears to be evidence for a very small crystal-field splitting of the free-ion levels. Such evidence encourages use of a free-ion calculation in this particular case. The parameter values selected are indicated in Table V. Based on the systematics given by Brewer (19), the first $f \rightarrow d$ transition should occur near 11000 cm^{-1} , so the $f \rightarrow f$ transitions at higher energies would be expected to be at least partially obscured. A

Table IV. Comparison of Energy Level Parameters Computed Using Hartree-Fock Methods and Those Evaluated from Fitting Experimental Data for An^{3+} (all in cm^{-1}).

	U	Np	Pu	Am
F^2 (HFR) ^a	71442	74944	78223	81346
F^2 (FIT) ^b	<u>39715</u>	<u>44907</u>	<u>48670</u>	<u>51800</u>
ΔP	31727	30037	29553	29546
F^4 (HFR)	46370	48733	50942	53044
F^4 (FIT)	<u>33537</u>	<u>36918</u>	<u>39188</u>	<u>41440</u>
ΔP	12833	11815	11754	11604
F^6 (HFR)	33981	35684	37335	38905
F^6 (FIT)	<u>23670</u>	<u>25766</u>	<u>27493</u>	<u>30050</u>
ΔP	10248	9918	9842	8855
ζ (HFR)	1898	2182	2479	2792
ζ (FIT)	<u>1623</u>	<u>1938</u>	<u>2241</u>	<u>2580</u>
ΔP	275	244	238	212

^aComputed using Hartree-Fock methods and including an approximate relativistic correction (24).

^bComputed by fitting to experimental data.

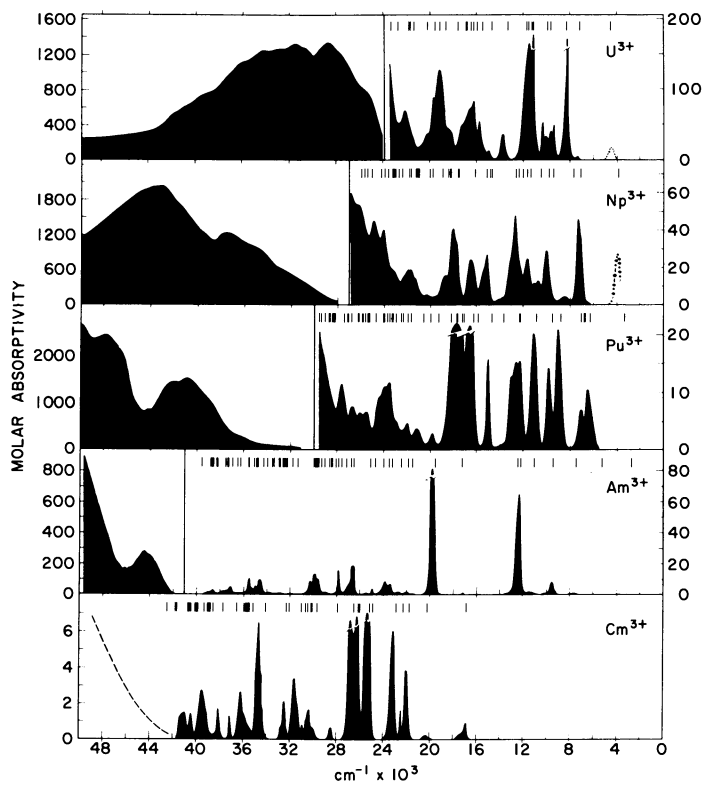


Figure 6.
Solution absorption spectra of $U^{3+}(\text{aq})$ through $Am^{3+}(\text{aq})$ in the region 0-50000 cm^{-1} .

Table V. Estimated Values of $\Delta F = F^k(\text{or } \zeta)_{\text{HFR}}^a - F^k(\text{or } \zeta)_{\text{EXPT}}^b$ for Pu (all in cm^{-1}).

	Pu ²⁺	Pu ⁴⁺	Pu ⁵⁺	Pu ⁶⁺
ΔF^2	26500	28000	30000	30000
ΔF^4	14000	13000	15000	16000
ΔF^6	10000	9200	10000	11000
$\Delta \zeta$	200	350	350	350

^aThe values of $F^k(\text{or } \zeta)_{\text{HFR}}$ are given in Table IIIA.

^bIn each case the following additional free-ion parameters were included in the calculation, (25): $\alpha = 35$, $\beta = -1000$, $\gamma = 1200$, $T^2 = 200$, $T^3 = 50$, $T^4 = 100$, $T^6 = -300$, $T^7 = 400$, $T^8 = 350$, $P^2 = 1200$, $P^4 = 900$, $P^6 = 600$, $M^0 = .767$, $M^2 = .423$, $M^4 = .293$, all in cm^{-1} .

predicted energy level scheme is given in Fig. 7. The group of bands computed to lie near 10000 cm^{-1} may be useful in any effort to characterize compounds in which this valence state is stabilized.

The spectra of $\text{Pu}^{3+}:\text{LaCl}_3$ (29) and isostructural PuCl_3 (30) have been examined and the energy-level analysis has been refined using extensive crystal-field data. Consequently, the results included in Table IV are well established. As already indicated, they serve as one basis for estimating parameters for higher-valent species.

Attempts have been made to analyze the energy level structure of Pu^{4+} compounds in terms of a free-ion model, but, with increasing metal-ion valence the crystal-field splitting also increases significantly. Frequent overlap in energies of crystal-field levels belonging to several different parent free-ion states is predicted. For a realistic calculation, the crystal-field must be diagonalized simultaneously with the free-ion parts of the interaction. In addition, many Pu^{4+} compounds exhibit an inversion symmetry at the Pu^{4+} site. In such cases the spectrum is dominated by vibronic transitions. The zero-phonon transitions are forbidden in the limit of inversion symmetry but may appear weakly if there is any significant distortion away from the symmetry. Thus, not only must the effects of the crystal-field interaction be treated simultaneously with the free-ion interactions, but the analysis can be exceedingly complex.

There is an interesting similarity in the character of the solution absorption spectra of the isoelectronic ions Np^{3+} and Pu^{4+} even though the absorption bands in Pu^{4+} are all shifted toward higher energies due to increases in both the electrostatic (F^k) and spin-orbit (ζ) parameters, Table VI. We have also examined the spectra of complex alkali-metal: $\text{Pu}(\text{IV})$

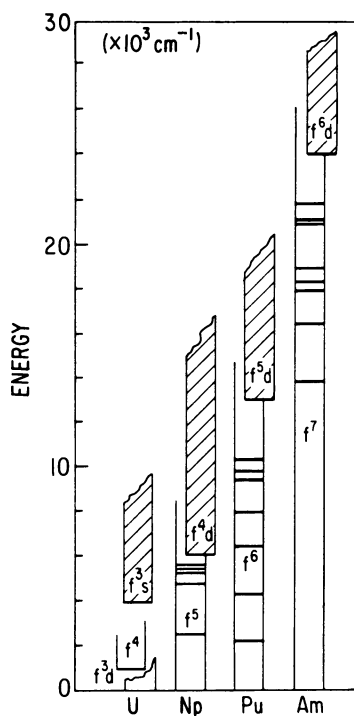


Figure 7.
 Predicted free-ion energy levels in the $5f^N$ -configuration of U^{2+} through Am^{2+} and the overlapping range of the $5f^N, 5f^{N-1}d$ transitions.

fluorides (31), and find a strong similarity in the energies at which many of the absorption bands are observed compared to those for $\text{Pu}^{4+}(\text{aq})$. Thus, while the crystal-field interaction of An^{4+} is larger than that in An^{3+} , some of the characteristics of the latter structure still remain.

Table VI. Estimated Values of Energy Level Parameters for Parametric Model, in cm^{-1} .

	Np^{3+}	Pu^{4+}	Increase
F^2	44900	55000	+22%
F^4	36900	41300	+12%
F^6	25770	30800	+20%
ζ	1938	2350	+21%

The electrostatic and spin-orbit parameters for Pu^{4+} which we have deduced are similar to those proposed by Conway some years ago (32). However, inclusion of the crystal-field interaction in the computation of the energy level structure, which was not done earlier, significantly modifies previous predictions. As an approximation, we have chosen to use the crystal-field parameters derived for Cs_2UCl_6 (33), Table VII, which together with the free-ion parameters lead to the prediction of a distinct group of levels near 1100 cm^{-1} . Of course a weaker field would lead to crystal-field levels intermediate between 0 and 1000 cm^{-1} . Similar model calculations have been indicated in Fig. 8 for Np^{4+} , Pu^{4+} and Am^{4+} compared to the solution spectra of the ions. For Am^{4+} the reference is Am^{4+} in 15 M NH_4F solution (34).

Table VII. Crystal-Field Parameters for Hexahalide $5f^1$ -Actinide Ions.

	$\text{Cs}_2\text{UCl}_6(5f^2)^a$	$\text{CsUF}_6(5f^1)^b$	$\text{NpF}_6(5f^1)^c$
B_0^4	7200 cm^{-1}	22500 cm^{-1}	44550 cm^{-1}
B_0^6	1300 cm^{-1}	3500 cm^{-1}	8000 cm^{-1}

^aCrystal-field parameters are from Reference 33, consistent with those for $\text{Pa}^{4+}:\text{Cs}_2\text{ZrCl}_6(5f^1)$ (43).

^bReference 40.

^cPresent work.

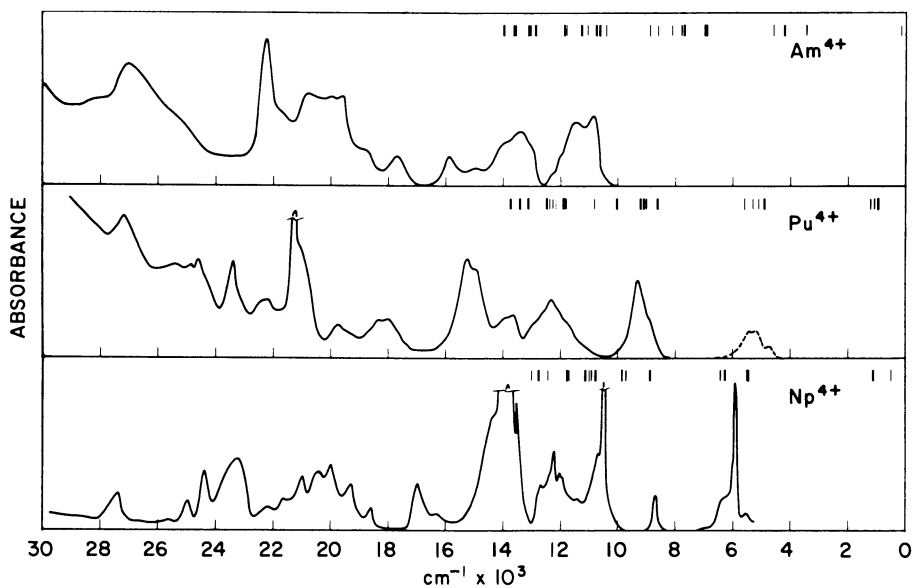


Figure 8.

Solution absorption spectra for Np^{4+} , Pu^{4+} , and Am^{4+} in the range $0\text{--}30000\text{ cm}^{-1}$ with predicted energy level structure indicated.

It should be emphasized that whereas the theoretical modelling of An^{3+} spectra in the condensed phase has reached a high degree of sophistication, the type of modelling of electronic structure of the (IV) and higher-valent actinides discussed here is restricted to very basic interactions and is in an initial state of development. The use of independent experimental methods for establishing the symmetry character of observed transitions is essential to further theoretical interpretation just as it was in the trivalent ion case.

For valence states higher than (IV), two types of Pu compounds are known: the simple and complex halides, such as PuF_6 and $CsPuF_6$, and the plutonyl species, PuO_2^+ or PuO_2^{++} . The oxygenated species are encountered in aqueous solutions. However, definitive analyses of the latter type spectra including that characteristic of Pu(VII) have yet to be proposed. The difficulty in analyzing the spectra of plutonyl compounds (35), is not unique; some degree of controversy still surrounds the interpretation of the spectra of UO_2^{2+} (36). In the spirit of the present paper, our interests were to explore some of the consequences of a predictive model for energy level structures. At present such model calculations are best suited for the spectra of the halides.

Spectroscopic analysis of Pu^{5+} and Pu^{6+} halides is in its initial stages. No low-temperature single-crystal spectra have been reported. A 25°C mull spectrum of the compound Rb_2PuF_7 was described earlier (37), and is now supplemented by the results for $CsPuF_6$ (31); PuF_6 gas-phase spectra have been reported by several different groups at ANL (38-39).

One of the methods of estimating the energy level parameters for Pu^{5+} in compounds such as $CsPuF_6$ is to examine the magnitude of the free-ion and crystal-field parameters in other similar An^{5+} compounds. Although there are problems with some of the assumptions that have been made in analyzing the spectra of compounds such as $CsUF_6(5f^1)$ (40-41) and $CsNpF_6(5f^2)$ (42), we tentatively conclude that the approximate crystal field parameters for $CsUF_6$ represent a reasonable step in the progression of $5f^1$ parameters indicated in Table VII. The actual crystal field in $CsPuF_6$ may be smaller than in $CsUF_6$, and consistent with results reported for $CsNpF_6$. It may also be of lower symmetry. We choose here to use what we believe to be a limiting case for illustration.

The assumption of a large crystal-field interaction for Pu^{5+} spectra makes it necessary to conclude that while certain aspects of earlier free-ion estimates (37) are valid, the "assignment" of free-ion states to observed absorption bands was premature. Much of the structure must be due to crystal-field components of many free-ion groups that overlap in energy or to vibronic satellites similar to those encountered in Cs_2UCl_6 (33). Thus, while the present computations would agree with earlier work in interpreting the levels observed in

Rb₂PuF₇ as well as in CsPuF₆ in the range 6000–7000 cm⁻¹ as belonging to a somewhat isolated first excited state, a more detailed calculation including the CsUF₆ crystal-field gives the results shown in Fig. 9. It predicts an essentially continuous level structure at energies >8800 cm⁻¹. Extensive detailed analysis will be required before firm assignments can be made. However, it should be somewhat more straight-forward to uniquely establish the crystal field splitting of the ground state by observation of fluorescence from the first excited state (~7000 cm⁻¹).

Finally, the highest valence state reported for plutonium in a non-oxygen-containing compound is exemplified in PuF₆, whose optical spectrum has been shown to be extremely complex (39). Estimated free-ion, Table V, and ligand-field parameters used in the present analysis are consistent with those reported earlier (44), but differ considerably from the free-ion parameters developed by Boring and Hecht (45) whose values for F⁴ and F⁶ would appear to us to be distorted. The crystal-field parameters characteristic of NpF₆, Table VII, should represent a good basis for estimating the similar interaction in PuF₆. Our results are summarized in Fig. 10.

Recent observations of fluorescence in NpF₆ and PuF₆ (46) are consistent with the energy-level scheme proposed. However, comparison of the calculated level structure with high-resolution spectra of PuF₆ (44) confirms that much of the observed structure is vibronic in character, built on electronic transitions that are forbidden by the inversion symmetry at the Pu site.

Conclusion

The investigation of Pu free-ion spectra has reached a point at which further progress is slow because of the time-consuming analysis required and incompleteness of the data. In one sense the first phase of this work is complete and rests on the existing extensive experimental data base (3). The possibilities now exist for taking much higher resolution spectra using Fourier-transform methods, but the earlier spectra obtained photographically using high dispersion spectrographs will continue to be an essential building block. The complexity of the interpretive problem, given the many interacting configurations, insures that challenging problems in theory as well as experiment remain to be addressed.

It is also apparent that there remains much to be done in developing our understanding of the model interactions that best characterize the spectra of higher-valent Pu compounds and indeed of the actinides in general. The synthesis of new compounds with a variety of different site symmetries could be of particular value in developing more detailed crystal-field

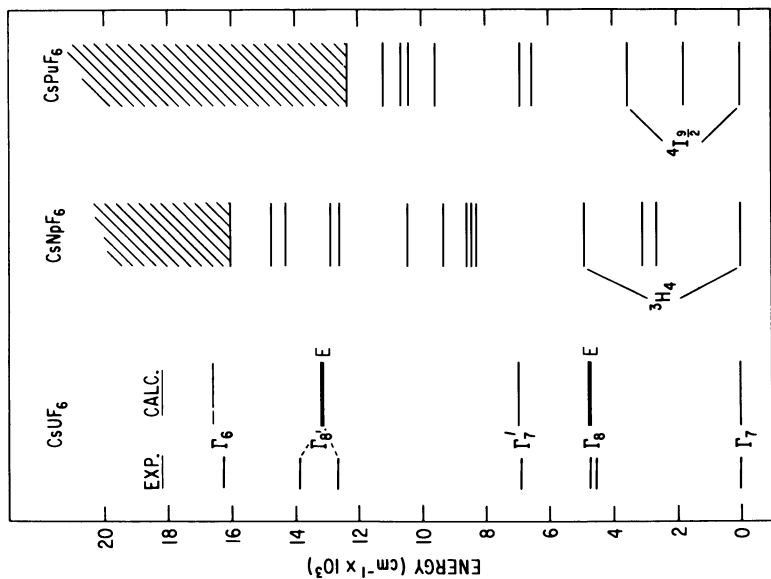


Figure 9. Predicted energy-level structure for CsUF_6 , CsNpF_6 , and CsPuF_6 in the range 0-20000 cm^{-1} .

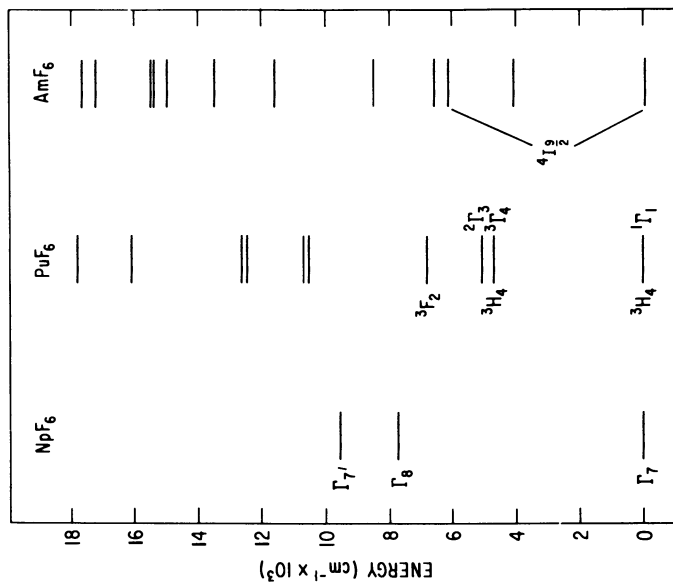


Figure 10. Predicted energy-level structure for NpF_6 , PuF_6 , and AmF_6 in the range 0-18000 cm^{-1} .

models. Of equal importance with the theoretical tools is the acquisition of high-resolution spectra under conditions that permit the independent experimental definition of properties that will help characterize the observed transitions. It is the lack of a solid experimental basis that has inhibited more widespread interest in the theoretical modelling.

Literature Cited

1. Fred, M. Adv. Chem. Ser. 1967, 71, 180-202.
2. Blaise, J.; Fred, M.; Gutmacher, R. J. Opt. Soc. Am. (to be submitted).
3. Fred, M.; Blaise, J. Argonne National Laboratory Report, 1983, in preparation.
4. Conway, J. G.; Blaise, J.; Verges, J. Spectrochimica Acta 1976, 31B, 31-47; Conway, J. G. "Handbook of Chemistry and Physics", Weast, R. C.; Astle, M. J., Eds. CRC Press, Boca Raton, 1980, pp. E-290-1.
5. Striganov, A. R., Report IAE-2965, Kurchatov Institute of Atomic Energy, Moscow, 1978 (in Russian). Translated by G. V. Shalimoff, Lawrence Berkeley Laboratory.
6. Carnall, W. T. "Gmelin Handbook of Inorganic Chemistry", Transurane A-2 (Erg.-Werk Band 8) Verlag Chemie, Weinheim/Bergstr., 1973, 35-79.
7. Rollefson, G. K.; Dodgen, H. W. "Report on Spectrographic Analysis Work CK-812", July 1943 (Declassified 29 December 1954).
8. McNally Jr., J. R.; Griffin, P. M. J. Opt. Soc. Am. 1959, 49, 162-6.
9. Bovey, L.; Gerstenkorn, S. J. Opt. Soc. Am. 1961, 51, 522-5.
10. Bovey, L.; Ridgeley, A. "The Zeeman Effect of Pu I", A.E.R.E.-R3393, Harwell, 1960.
11. Gerstenkorn, S. Ann Physique (Paris) 1962, 7, 367-404.
12. Striganov, A. R.; Korostyleva, L. A.; Dontsov, Yu, P. Zh. Eksp. Teor. Fiz. 1955, 28, 480; Sov. Phys. JETP 1955, 1, 354.
13. Korostyleva, L. A. Opt. i. Spektroskopiya 1963, 14, 177; Opt. Spectrosc. (USSR) 1963, 14, 93.
14. Korostyleva, L. A.; Striganov, A. R. Opt. i. Spektroskopiya 1966, 20, 545-53; Opt. Spectrosc. (USSR) 1966, 20, 309-17.
15. Blaise, J.; Fred, M.; Gerstenkorn, S.; Tomkins, F. S. 2nd E.G.A.S. Conference, Hanover, 14-17 July 1970.
16. Blaise, J.; Steudel, A. Z. Physik 1968, 209, 311-28.
17. Wilson, M. Phys. Rev. 1968, 176, 58-63.
18. Rajnak, K.; Fred, M. J. Opt. Soc. Am. 1977, 67, 1314-23.
19. Brewer, L. J. Opt. Soc. Am. 1971, 61, 1101-11, 1666-82.
20. Blaise, J.; Fred, M.; Gerstenkorn, S.; Judd, B. R. C. R. Acad. Sci. Paris 1962, 255, 2403-5.

21. Bauche, J.; Blaise, J.; Fred, M. C. R. Acad. Sci. Paris 1963, 256, 5091-93; 257, 2260-63.
22. Blaise, J.; Wyart, J. F.; Conway, J. G.; Worden, E. F. Physica Scripta 1980, 22, 224-30.
23. Bauche-Arnoult, C.; Gerstenkorn, S.; Verges, J.; Tomkins, F. S. J. Opt. Soc. Am. 1973, 63, 1199-1203.
24. Cowan, R. D.; Griffin, C. D. J. Opt. Soc. Am. 1976, 66, 1010-14.
25. Crosswhite, H. M. Colloques Internationaux du C.N.R.S., Spectroscopie des Elements de Transition et des Elements Lourds des Solids, 28 Juin - 3 Juillet 1976, Editions du C.N.R.S., Paris 1977, 65-69.
26. Edelstein, N.; Easley, W.; McLaughlin, R. Adv. Chem. Ser. 1967, 71, 203-10.
27. Peterson, J. R.; Fellows, R. L.; Young, J. P.; Haire, R. G. Radiochem. Radioanal. Letters 1977, 31, 277-82.
28. Fellows, R. L.; Peterson, J. R.; Young, J. P.; Haire, R. G. "The Rare Earths in Modern Science and Technology", McCarthy, G. J.; Rhyne, J. J., Eds. Plenum Corp., New York 1978, 493-99.
29. Conway, J. G.; Rajnak K. J. Chem. Phys. 1966, 44, 348-54; Hessler, J. P.; Carnall, W. T. ACS Sympos. Ser. 1980, 131, 349-68.
30. Carnall, W. T.; Fields, P. R.; Pappalardo, R. G. J. Chem. Phys. 1970, 53, 2922-38.
31. Morss, L. R.; Williams, C. W.; Carnall, W. T. Chapter _____ in this book.
32. Conway, J. G. J. Chem. Phys. 1964, 41, 904-5.
33. Johnston, D. R.; Satten, R. A.; Schreiber, C. L.; Wong, E. Y. J. Chem. Phys. 1966, 44, 3141-3.
34. Asprey, L. B.; Penneman, R. A. Inorg. Chem. 1962, 1, 134-36.
35. Einstein, J. C.; Pryce, M. H. L. Proc. Roy. Soc. 1956, A238, 31-45; J. Res. Natl. Bureau Stds. 1966, 70A, 165-73.
36. Carnall, W. T. "Gmelin Handbook of Inorganic Chemistry", 8th Ed., System 55, Springer-Verlag, Berlin, 1982, 147-57.
37. Varga, L. P.; Reisfeld, M. J.; Asprey, L. B. J. Chem. Phys. 1970, 53, 250-55.
38. Weinstock, B.; Malm, J. G. J. Inorg. Nucl. Chem. 1956, 2, 380-94.
39. Steindler, M. J.; Gunther, W. H. Spectrochim. Acta 1964, 20, 1319-22.
40. Reisfeld, M. J.; Crosby, G. A. Inorg. Chem. 1965, 4, 65-70.
41. Leung, A. F. J. Phys. Chem. Solids 1977, 38, 529-32.
42. Hecht, H. G.; Varga, L. P.; Lewis, W. B.; Boring, A. M. J. Chem. Phys. 1979, 70, 101-108; Poon, Y. M.; Newman, D. J. J. Chem. Phys. 1982, 77, 1077-79.

43. Axe, J. D. "Electronic Structure of Octahedrally Coordinated Protactinium(IV) in Cs_2ZrCl_6 ", UCRL-9293, Berkeley, 1960.
44. Kugel, R.; Williams, C.; Fred, M.; Malm, J. G.; Carnall, W. T.; Hindman, J. C.; Childs, W. J; Goodman, L. S. J. Chem. Phys. 1976, 65, 3486-92.
45. Boring, M.; Hecht, H. G. J. Chem. Phys. 1978, 69, 112-16.
46. Beitz, J. V.; Williams, C. W.; Carnall, W. T., Chapter _____ in this book.

RECEIVED January 7, 1983

Stability and Electronic Spectrum of Cesium Plutonium Hexafluoride

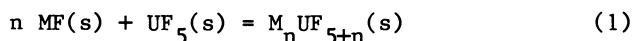
L. R. MORSS, C. W. WILLIAMS, and W. T. CARNALL

Argonne National Laboratory, Chemistry Division, Argonne, IL 60439

CsPuF₆ was prepared and verified to be isostructural with corresponding compounds of uranium and neptunium. Its decomposition was studied in an inert gas atmosphere and in vacuum. Its spectrum has been measured in the region 400–2000 nm. The energy level structure of Pu⁵⁺ in the trigonally distorted octahedral CsPuF₆ site was computed from a predictive model and compared with the observed spectrum.

Only two complex fluorides of pentavalent plutonium are known, both having been prepared by Penneman et al. (1). One of these, Rb₂PuF₇, appeared to be stable; its crystal structure (1) and its electronic spectrum (2) have been reported. The other, CsPuF₆, appeared to decompose after a few days (1) and only its crystal structure was reported. Our interest in the bonding and electronic structure of Pu(V) and particularly in Pu(V) fluorides prompted the present study of CsPuF₆.

Recently Suglobova et al. (3,4,5) reported structural data, phase diagrams, and enthalpies of reaction of several complex fluorides of uranium(V) with alkali metals. Their observations indicate that the enthalpy of stabilization represented by the equation



becomes more negative as n increases and as M changes from sodium to cesium (Table I). We expect similar stabilization behavior for complex fluorides of neptunium(V) and plutonium(V); this paper represents an initial effort in a comprehensive study of the Pu(V)-fluoride system.

We attempted to prepare Pu(V) stabilized as K₂PuF₇, Rb₂PuF₇, and CsPuF₆, but were only successful in repeating the preparation of CsPuF₆ (1). Since there is a paucity of information concerning syntheses of this sort, we cite possible grounds for our unsuccessful as well as our successful efforts.

0097-6156/83/0216-0199\$06.00/0
© 1983 American Chemical Society

Table I. Stabilization Enthalpies of Alkali Fluorouranates(V).^a

LiUF_6 ^b			
NaUF_6		Na_3UF_8	
-26		-70	
KUF_6	K_2UF_7	K_3UF_8	K_4UF_9
-56	-92	-170	-179
RbUF_6	Rb_2UF_7	Rb_3UF_8	Rb_4UF_9
-75	-135	-198	-222
CsUF_6	$\alpha\text{-Cs}_2\text{UF}_7$	Cs_3UF_8	Cs_4UF_9
-94	-175	-258	
	$\beta\text{-Cs}_2\text{UF}_7$		
	-163		

^aNumber under each compound is ΔH in kJ mol^{-1} for the reaction $n\text{MF}(s) + \text{UF}_5(s) = \text{M}_n\text{UF}_{5+n}(s)$. These enthalpies were calculated from reaction enthalpies of References 4 and 5 and recently assessed auxiliary thermodynamic data (U. S. National Bureau of Standards Technical Notes 270-3, 270-4, 270-5, and 270-8).

^bCompound reported to exist but thermodynamic data are not available.

Experimental

A solution of 104 mg of $^{239}\text{Pu}(\text{IV})$ (0.435 mmol), and an equimolar amount of CsCl in 2M hydrochloric acid, were mixed in a platinum crucible. Concentrated hydrofluoric acid (24 mmol) was added dropwise with stirring. The pink precipitate that formed immediately was allowed to settle and the supernatant liquid was evaporated gently. The dry product was a fine pink powder with traces of yellow color at the edges of the crucible. This mixture was ground thoroughly in an agate mortar, transferred to a nickel boat, evacuated to 5×10^{-5} mmHg at 100°C , then fluorinated overnight (950 mmHg F_2 pressure) at 350°C . The product, handled only in a dry box, was a pale blue powder whose x-ray powder pattern (Table II) showed it to be isostructural with CsUF_6 (6) and CsNpF_6 (7).

A sample of CsPuF_6 in a Pyrex x-ray capillary tube, sealed in dry-box N_2 , was heated in 100°C increments to 400°C and x-rayed after each heating period of 2-16 hours. Only the few strongest lines of CsPuF_6 were visible after heating at 100°C . The material was essentially amorphous after heating at 200 and 300°C . After heating at 400°C , weak but well resolved PuO_2 lines were observed. Oxygen or H_2O may have been present in trace amounts in the capillary or adsorbed on the capillary walls, setting up reactions leading to formation of PuO_2 .

To ascertain the oxidation state of the product, a sample (13.910 mg) was weighed into a Pt crucible on a Cahn 27 microbalance in the dry box. After evacuation (10^{-5} mmHg) and heating to 315°C , the sample lost 0.464 mg. A test for volatilization of Pu (possibly as PuF_6) was negative. This weight loss to a residue of CsPuF_5 represents an initial formula of $\text{CsPuF}_{5.85}$. Further heating in a thermogravimetric apparatus in flowing N_2 resulted in decomposition to PuO_2 (as identified by its powder x-ray pattern) at 400 - 500°C , apparently caused by traces of O_2 in the TGA stream.

We note one difference between the behavior of our preparation of CsPuF_6 and that of Penneman et al. (1). Our samples did not decompose (in sealed x-ray capillaries) after 3 months. Three weeks in a dry-box atmosphere (ca. 10 ppm H_2O in N_2) did leave a product with weaker, more diffuse CsPuF_6 lines.

Because of the stabilization of U(V) in K_2UF_7 and Rb_2UF_7 (Table I), and because we hoped that K_2PuF_7 might be isostructural with K_2TaF_7 , K_2UF_7 , Rb_2UF_7 , Rb_2NpF_7 , and Rb_2PuF_7 (1,8), we attempted preparations of K_2PuF_7 and Rb_2PuF_7 . Concentrated hydrofluoric acid was added to a mixture of $2\text{KF} + \text{Pu}(\text{OH})_4$. The product was dried, ground, and fluorinated at 400°C . Despite repeated grinding and fluorination, the product remained pink and its spectrum was that of $\text{Pu}(\text{IV})$. Although not identifiable by x-ray diffraction, we refer to this product as K_2PuF_6 . Three mixtures of (2 Rb):(1 Pu) were precipitated with concentrated hydrofluoric acid. They were dried, ground,

Table II. X-Ray Powder Pattern for CsPuF₆.

\bar{R}_3 (hexagonal axes): $a_0 = 8.000 \pm 0.008 \text{ \AA}$, $c_0 = 8.366 \pm 0.016 \text{ \AA}$.^a

d(obsd)	d(calc)	hkl	I(obsd) ^b	I(calc) ^c
5.35	5.34	101	20	7
4.01	4.00	110	100	100
3.59	3.58	012	90	95
2.667	2.668	202	60	65
2.307	2.309	300	50	40
2.218	2.220	122, 21 $\bar{2}$	60	54
2.000	{ 2.002 2.000 }	{ 104 220 }	40	43
1.798	1.790	024	30	16
1.744	1.746	312, 13 $\bar{2}$	30	25
1.636	1.634	214, 124	30	25
1.513	1.512	410, 140	20	17
1.487	1.486	232, 32 $\bar{2}$	20	20
1.411	1.415	134, 314	10	14
1.330	{ 1.334 1.333 }	{ 404 330 }	10	11
1.317	{ 1.315 1.317 }	{ 502 116, 11 $\bar{6}$ }	10	20
1.263	1.266	324, 234	10	10
1.252	1.250	422, 24 $\bar{2}$	10	8
1.193	{ 1.194 1.193 }	{ 306, 036 152, 512 }	10	15
0.9988	{ 1.000 1.001 1.000 0.9985 }	{ 434, 344 208 440 155, 515 }	10	11
0.8721	{ 0.8730 0.8736 0.8729 }	{ 624, 264 238, 328 630, 360 }	10	18
0.8686	{ 0.8681 0.8678 0.8678 }	{ 526, 256 452, 542 256, 256 }	10	18

^aTwo standard deviations, using least-squares refinement with Nelson-Riley absorption correction (Williams, D. E., Ames Laboratory Report IS-1052, 1964).

^bVisually estimated from film.

^cUsing program LAZY PULVERIX (Yvon, K.; Jeitschko, W.; Parthé, E. J. *Appl. Cryst.* 1977, 10, 73-74) and F atomic positions from CsUF₆ (6).

and fluorinated at 300–400°C, with repeated fluorinations and slow or rapid cooling in F₂. Two of these preparations resulted in Rb₂PuF₆ and one in predominately Rb₇Pu₆F₃₁, identified by x-ray powder patterns, although they all were varying degrees of green in color. Clearly Pu(IV) is stabilized in compounds such as K₂PuF₆ and Rb₂PuF₆ and if these double salts form they may be resistant to oxidation. A slight excess of alkali metal over the 2:1 ratio may have facilitated the initial preparation of Rb₂PuF₇ (1,9).

For spectroscopic study, samples of CsPuF₆, Rb₂PuF₆, and K₂PuF₆ were thoroughly mixed in the dry box with vacuum dried Teflon powder and pressed into thin pellets (10). When pellets containing CsPuF₆ were prepared at a pressure of 6800 atm, some of the blue CsPuF₆ in the pellet decomposed to pink Pu(IV), but when pellets were pressed at 1700 atm, only pink traces at the pellet edges were seen. Optical spectra of sample pellets and of blank Teflon pellets were taken in the wavelength region 400–2000 nm with a Cary 17 spectrophotometer at 298 and 77 K, using blank pellets or neutral density filters in the reference beam.

Results and Discussion

Assuming that CsPuF₆(s) is in equilibrium with CsF(s) + PuF₄(s) + 1/2F₂(g) at 600 K at an estimated F₂ pressure of 0.1 atm, we estimate ΔG° for the above equilibrium as +6 ± 6 kJ mol⁻¹. From data of the uranium(V) system in Table I, we estimate $\Delta G^\circ = -94 \pm 15$ kJ mol⁻¹ for the reaction CsF(s) + PuF₅(s) = CsPuF₆(s). ($\Delta G^\circ = \Delta H^\circ$ since all reactions and products are solids.) Therefore we estimate $\Delta G^\circ = +88 \pm 16$ kJ mol⁻¹ at 600 K for the reaction PuF₄(s) + 1/2F₂(g) = PuF₅(s). Compounds such as K₃PuF₈, Rb₃PuF₈, Cs₂PuF₇, etc., should be stable if the results of Suglobova et al. hold for the PuF₅-MF systems. We note, however, that a report of absorption of PuF₆ onto CsF at 100°C appeared to produce only CsPuF₆; fluorination of Cs₂PuF₆ at 250–500°C did not produce any Pu(V) or Pu(VI) (11).

The absorption spectrum of CsPuF₆ at 298 K in a Teflon pellet in the range 400–1500 nm is shown in Figures 1–3 in comparison with spectra of Pu(IV) fluorides. Cooling to 77 K resulted in some absorption bands becoming somewhat narrower and more intense than those shown, but none became significantly weaker. Some additional structure was observed in the broad band near 620 nm. No absorption attributable to CsPuF₆ was evident in the 1500–2400 nm range, but a band near 2000 nm characteristic of Pu(IV) (12,13) appeared in partially reduced samples (Figure 3).

The spectrum of CsPuF₆ shown in Figures 1 and 2, both of which refer to the same sample, shows only marginal resemblance to that of Rb₂PuF₇ in a fluorolube mull (2). However, this

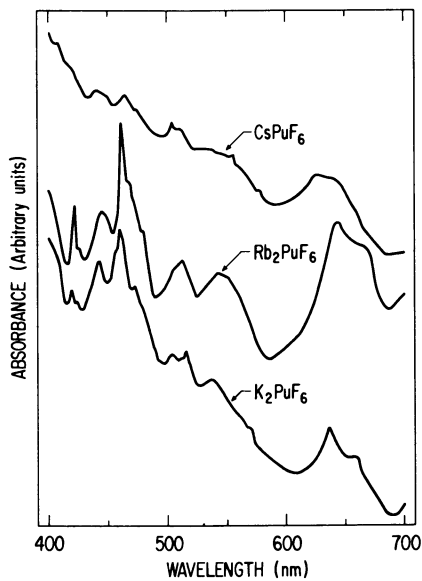


Figure 1. Absorption spectra of K_2PuF_6 , Rb_2PuF_6 and CsPuF_6 in Teflon pellets at 298 K (400–700 nm).

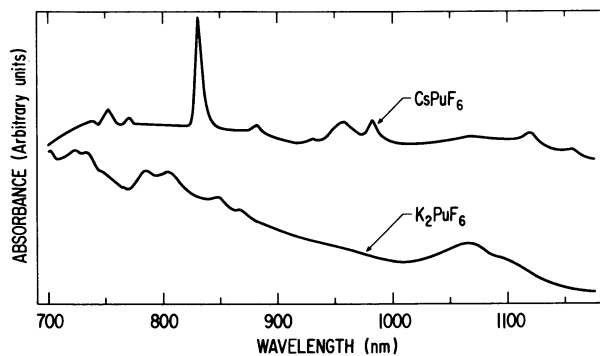


Figure 2. Absorption spectra of K_2PuF_6 and $CsPuF_6$ in Teflon pellets at 298 K (700–1150 nm).

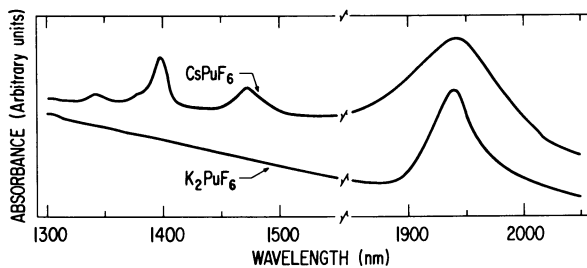


Figure 3. Absorption spectra of K_2PuF_6 and $CsPuF_6$ in Teflon pellets at 298 K (1300–2050 nm).

lack of resemblance is not surprising, considering the different Pu(V) site symmetries in the two compounds.

Spectra of K_2PuF_6 and Rb_2PuF_6 , which were handled in the same manner as $CsPuF_6$ and pressed into Teflon pellets, are also shown in Figure 1. While x-ray powder patterns of $CsPuF_6$ samples showed no extraneous lines, it is clear that in the 400-700 nm region of the spectrum the correlation with Pu(IV) absorption spectra strongly suggests the presence of Pu(IV) in the Cs compound. When partially decomposed to Pu(IV), the Cs compound developed bands very similar to those shown for K_2PuF_6 . We conclude that the absorption spectrum is more sensitive to small amounts of Pu(IV) than the x-ray pattern. Some Pu(IV) in $CsPuF_6$ probably remained from incomplete fluorination and some Pu(IV) may have been produced when the pellets were pressed. In any case the Pu(V) bands in Figure 2 are distinct from the structural features attributed to Pu(IV). The latter did not show much variation from one compound to another and they are indeed quite similar in many respects to those found in the spectrum of aqueous Pu(IV) (14).

The absorption features uniquely characteristic of Pu(V) and shown in Figures 2 and 3 occur in the region 800-1500 nm, where little absorption was found in K_2PuF_6 . The spectra of K_2PuF_6 in Figures 1-3 are from the same sample, whereas the absorption bands of Pu(V) in Figure 3 are from a more concentrated sample of $CsPuF_6$ than that used for Figures 1 and 2. The concentrated sample of $CsPuF_6$ in Figure 3 shows obvious evidence of Pu(IV) as indicated by the characteristic Pu(IV) band near 1950 nm. The intensity scale for the Pu(V) spectrum in Figure 3 is approximately 1/10 that of Figures 1 and 2.

To develop a detailed interpretation of the $CsPuF_6$ spectrum at this point would be premature. However, some modeling of the expected electronic structure is possible following the procedure outlined by Blaise et al. (15) to estimate the appropriate free-ion parameters. An earlier attempt to make assignments to Pu(V) spectra (2) treated the problem solely in terms of a free-ion model. If we consider the magnitude of the splitting of crystal-field levels in the spectrum of isostructural $CsUF_6$ (16,17) we see that such effects cannot be neglected. By combining the octahedral field that approximates the structure observed in $CsUF_6$ with free-ion parameters for Pu^{5+} assuming a Hartree-Fock related model (15), we compute the set of energy levels shown in Figure 4(A).

Electronic structure parameters have also been deduced in an analysis of the spectrum of $CsNpF_6$ (18), and recently some modification of the original values was proposed (19). On the basis of the latter set, including the ligand-field parameters, a second prediction of the energy levels of $CsPuF_6$ has been made, Figure 4(B). Comparison of results for Rb_2PuF_7 (2) and $CsPuF_6$, Figure 3, shows that indeed there are observed bands in the 6600-7100 cm^{-1} range consistent with the calculations. The differences between the two predictions, Table III, stem

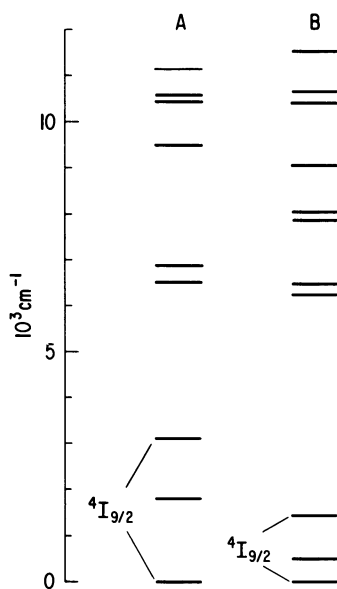


Figure 4. Calculated energy levels of Pu^{5+} in CsPuF_6 : (A) using CsUF_6 ligand-field parameters; (B) using CsNpF_6 ligand-field parameters.

TABLE III. Energy Level Parameters (in cm^{-1}) Estimated for CsPuF_6 .^a

	A	B
F^2	57000 ^b	47841 ^d
F^4	42350 ^b	34572 ^d
F^6	32300 ^b	23505 ^d
ζ	2541 ^b	2406 ^d
α	35	35
β	-700	-700
γ	500	500
T^2	200	200
T^3	50	50
T^4	100	100
T^6	-300	-300
T^7	400	400
T^8	350	350
P^2	400	400
B_0^4	22500 ^c	12000 ^e
B_6^6	3500 ^c	1200 ^e

^aA and B correspond to designations given in Figure 4. The symbols are defined in Reference 20.

^bReference 15.

^cReference 16 and 17.

^dExtrapolated from results for CsNpF_6 (19).

^eReference 19.

primarily from a difference of approximately a factor of two in the magnitude of the ligand field parameters derived from CsUF₆ and CsNpF₆ and these differences are evident in the splitting expected from the ground state. The differences in the free-ion parameters appear to be of lesser importance in the energy range shown in Figure 4.

The predicted structure of the ⁴I_{9/2} ground state levels in Figure 4 can in principle be tested by observation of fluorescence such as that expected to originate in the 1500 nm state. We have performed preliminary experiments at 77 K using as an excitation source a nitrogen laser (337.1 nm, 6000 kW pulses of 8 nsec duration). No fluorescence was observed at >500 nm. If excitation involved charge transfer bands, which is highly probable, then rapid non-radiative relaxation of the excitation energy might occur.

It remains for future investigations to explore the fate of selective excitation into lower energy absorption bands, an area of considerable interest. Our expectations are that fluorescence from the ≈1500 nm band in CsPuF₆ should be detectable, whereas in the isostructural U and Np compounds fluorescence may be more difficult to observe because there are few energy gaps large enough to hinder non-radiative relaxation processes. Thus for Pu(V) fluorides we have a particularly good opportunity to explore excited state relaxation processes but also to assess the validity of the predicted crystal field splitting based on two different models of precursor electronic structures. Extensive studies of the properties of complex Pu(V) fluorides are planned.

Acknowledgments

We thank J. V. Beitz, P. G. Eller, J. P. Hessler, J. G. Malm, R. A. Penneman, J. C. Sullivan and D. W. Wester for experimental collaborations and fruitful discussions. This work was performed under the auspices of the Office of Basic Energy Sciences, Division of Chemical Sciences, U. S. Department of Energy under contract number W-31-109-ENG-38.

Literature Cited

1. Penneman, R. A.; Sturgeon, G. D.; Asprey, L. B.; Kruse, F. H. J. Am. Chem. Soc. 1965, 87, 5803-5804.
2. Varga, L. P.; Reinfeld, M. J.; Asprey, L. B. J. Chem. Phys. 1970, 53, 250-255.
3. Suglobova, I. G.; Fedorov, V. L.; Chirkst, D. E. Inorg. Materials 1980, 16, 452-459.
4. Kudryashov, V. L.; Suglobova, I. G.; Chirkst, D. E. Sov. Radiochem. 1978, 20, 320-323.

5. Suglobova, I. E.; Fedorov, V. L.; Chirkst, D. E. Inorg. Materials 1981, 17, 482-487.
6. Rosenzweig, A.; Cromer, D. T. Acta Crystallogr. 1967, 23, 865-867.
7. Asprey, L. B.; Keenan, T. K.; Penneman, R. A.; Sturgeon, G. D. Inorg. Nucl. Chem. Lett. 1966, 2, 19-21.
8. Penneman, R. A.; Ryan, R. R.; Rosenweig, A. Structure and Bonding 1973, 13, 1-52.
9. P. G. Eller and R. A. Penneman, personal communication.
10. Schmieder, H.; Dornberger, E.; Kanellakopulos, B. Appl. Spectrosc. 1970, 24, 499-505.
11. Riha, J. in ANL-7375 (1967) pp. 54-56.
12. Swanson, J. L. J. Phys. Chem. 1964, 68, 438-439.
13. Conway, J. G. J. Chem. Phys., 1964, 41, 904-905.
14. Cohen, D. J. Inorg. Nucl. Chem. 1961, 18, 211-218.
15. Blaise, J.; Fred, M. S.; Carnall, W. T.; Crosswhite, H. M.; Crosswhite, H., Chapter ___ in this book.
16. Reisfeld, M. J.; Crosby, G. A. Inorg. Chem. 1965, 4, 65-70.
17. Leung, A. F. J. Phys. Chem. Solids 1977, 38, 529-532.
18. Hecht, H. G.; Varga, L. P.; Lewis, W. B.; Boring, A. M. J. Chem. Phys. 1979, 70, 101-108.
19. Poon, Y. M.; Newman, D. J. J. Chem. Phys. 1982, 77, 1077-1079.
20. Hessler, J. P.; Carnall, W. T. American Chemical Society Symposium Series 1980, 131, 349-368.

RECEIVED January 7, 1983

Aspects of Plutonium Solution Chemistry

GREGORY R. CHOPPIN

The Florida State University, Department of Chemistry, Tallahassee, FL 32306

The effect of pH and complexation on the relative stabilities of the oxidation states of Pu is discussed. A set of ionic radii are presented for Pu in different oxidation states and different coordination numbers. A model for Pu hydration is presented and the relation between hydrolysis and oxidation state evaluated, including the problem of hydrous polymerization.

Complexation of Pu is discussed in terms of the relative stabilities of different oxidation states and the "effective" ionic charge of PuO_2^+ and PuO_2^{+2} . An equation is proposed for calculating stability constants of Pu complexes and its correlation with experimental values demonstrated. The competition between inner vs outer sphere complexation as affected by the oxidation state of Pu and the pKa of the ligand is reviewed. Two examples of uses of specific complexing agents for Pu indicate a useful direction for future studies.

The investigation of plutonium chemistry in aqueous solutions provides unique challenges due in large part to the fact that plutonium exhibits an unusually broad range of oxidation states - from 3 to 7- and in many systems several of these oxidation states can coexist in equilibrium. Following the normal pattern for polyvalent cations, lower oxidation states of plutonium are stabilized by more acidic conditions while higher oxidation states become more stable as the basicity increases.

As with all such generalizations, this one can be negated by other factors such as complexing which can even reverse the trends and the relative stability of the different oxidation states. For example, the greater strength of complexation of

0097-6156/83/0216-0213\$06.00/0
© 1983 American Chemical Society

Pu(IV) cations relative to that of Pu(III) increases the stability of the (IV) species compared to (III). While Pu(III) is stable to air and warm water in acidic solutions, in the presence of acetate or EDTA (pH 3.5), it partially oxidizes to Pu(IV) (1). This increased stabilization of the IV state is reflected in the variation in the standard potential (E°) for the (III)/(IV) couple which is -0.98v in 1M HClO_4 compared to $+0.63\text{v}$ at pH 7 (2). The change in the E° value is due to the much more extensive hydrolysis at pH 7 of the Pu(IV) compared to Pu(III).

Disproportionation reactions, which lead to several oxidation states simultaneously in solution, are also a significant aspect of plutonium chemistry, particularly for the IV and V species.

Plutonium cations in whatever oxidation state can be described as hard acids and interact with anionic species by ionic bonding. As a result certain generalizations can be made about the relative complexing tendencies of the different oxidation states.

In this review the nature of the various oxidation species in solution are reviewed and generalizations drawn about their complexing behavior.

Oxidation States

Pu(III) can be rather easily formed and maintained in acid solutions using a reducing agent such as N_2H_4 and NH_2OH . Pu(IV) is also stable in concentrated acid solutions but undergoes strong hydrolysis even at relatively low pH's and is removed from the solution phase by adsorption to suspended particles and to the walls of the reaction vessels. PuO_2^+ increases in stability as the pH of an aqueous solution is increased to about 7 after which the stability again decreases. This oxidation state has a strong tendency to disproportionate but there is some evidence that it may be the predominant plutonium species at ultratrace concentrations in solution and some natural waters where the probability of two PuO_2^+ ions interacting is very small (3). PuO_2^{+2} ions in aqueous solution have a stability between that of the UO_2^{+2} and NpO_2^{+2} species. The VI oxidation state can be achieved in solution by the use of oxidants such as bromate and persulfate. Pu(VII) is reduced rapidly by water in acid solutions but the reduction is considerably slower in basic solution. In such basic solutions the Pu(VII) species seems to be trinegative, corresponding most simply to PuO_5^{-3} , although it has been proposed that a more likely formulation is $\text{PuO}_2(\text{OH})_6^{-3}$ (4).

The oxidation potentials for plutonium at pH 0, 8 and 14 are given in Figure 1. The values for pH 8 and 14 are those estimated by Allard et al. (5).

Coordination Numbers and Radii. In the transition metal ions, the interaction of the ligand orbitals with the d orbitals of the metal ions generally determines the coordination number and geometry of the coordination sphere about the metal. The

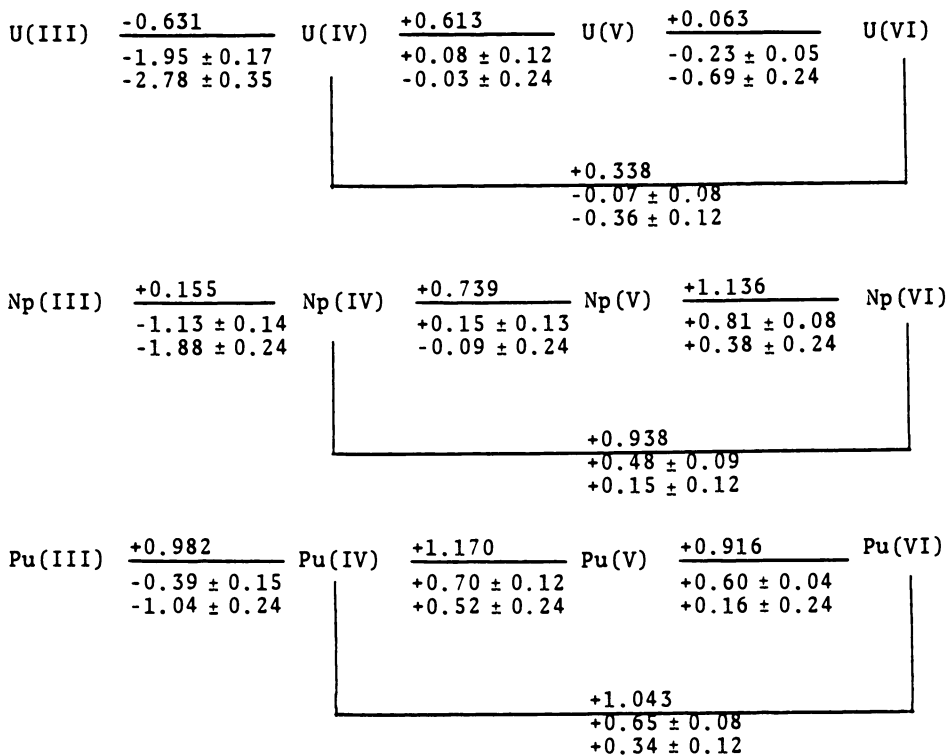


Figure 1. Redox potential diagram for U, Np, and Pu. The reduction potentials as listed are for the pH values:

$\frac{\text{pH} = 0}{\text{-----}}$

pH = 8

pH = 14

bonding in plutonium complexes is strongly ionic and the number of ligands as well as their geometric arrangement about the plutonium cations is determined primarily by steric and electrostatic factors. The result is a range of coordination numbers - from 6 to 12 for the simple III and IV cations and 2 to 8 for the dioxygenated V and VI cations. Coordination numbers of 8 and 9 seem to be the most common for Pu(III) in solution. For example, PuEDTA⁻¹_(aq) probably has 3 to 4 hydration waters in the coordination sphere even though EDTA is hexadentate. For Pu(IV), the smaller cationic radius may result in somewhat lower 'most probable' coordination numbers - e.g. 7 and 8.

The uncertainty of the proper coordination number of any particular plutonium species in solution leads to a corresponding uncertainty in the correct cationic radius. Shannon has evaluated much of the available data and obtained sets of "effective ionic radii" for metal ions in different oxidation states and coordination numbers (6). Unfortunately, the data for plutonium is quite sparse. By using Shannon's radii for other actinides (e.g., Th(IV), U(VI)) and for Ln(III) ions, the values listed in Table I have been obtained for plutonium. These radii are estimated to have an uncertainty of $\pm 0.02 \text{ \AA}$.

Hydration and Hydrolysis. The various oxidation states of plutonium form strong ion-dipole bonds with water to become strongly hydrated in aqueous solution. To a first approximation, we can expect the hydration numbers of the first coordination sphere to be the same as the most probable coordination numbers suggested in the preceding section. This means values of 8 or 9 for Pu(III), 7 or 8 for Pu(VI), and, perhaps, 4 for PuO₂⁺¹ and 6 for PuO₂⁺². However, the polarization of the water dipoles of the primary hydration layer leads to attraction of additional waters of hydration. Estimates of the total number of waters of hydration for trivalent lanthanides and actinides have been given as 12 - 15 (7,8,9) based on a model of a small number of tightly bound waters.

A more complete description of the hydration is suggested by the correlation of the entropy of hydrated cations with the cationic charge density Z^2/r , as shown in Figure 2 (10). The increasing curve of S_{aq} from Na⁺_(aq) to Pu⁺⁴_(aq) indicates that the orienting effect of the cations on the hydration waters steadily increases with the charge density. Perhaps a better hydration model, then, is one of a primary layer of water molecules about the plutonium cations with a weaker orienting effect extending some distance into the solvent beyond that first layer. Figure 2 indicates that the total hydrational ordering of Pu⁺⁴ is about twice that of Pu⁺³ while that of PuO₂⁺² is comparable to that of Ca⁺². An estimate of the extent of the hydrational ordering by Pu⁺³ can be obtained from a recent study of ${}^0\text{Gd}^{+3}$ which indicated that the hydration effect extends about 50Å from the Gd⁺³ cation (12).

Table I
Estimated Effective Ionic Radii⁺ for Plutonium

<u>Coordination Number</u>	<u>Oxidation State</u>			
	<u>III</u>	<u>IV</u>	<u>V</u>	<u>VI</u>
4	0.79	0.65	0.53	0.50
6	<u>1.00</u> [†]	<u>0.86</u>	<u>0.74</u>	<u>0.71</u>
7	1.06	0.92	0.80	0.77
8	1.10	<u>0.96</u>	0.84	0.81
9	1.15	1.01	0.89	0.86
10	1.21	1.01	0.95	0.92
12	1.26	1.12	1.00	0.97

+ The radii are in Å (= 10⁻⁸cm) units

† The underlined values are from reference 6.

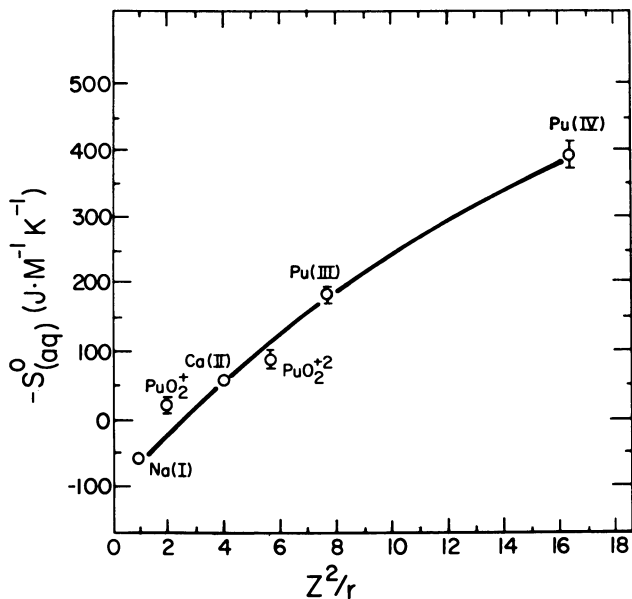
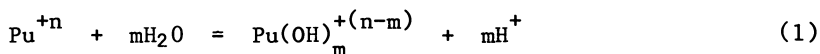
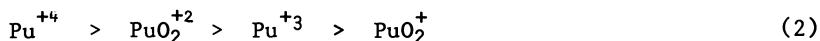


Figure 2. The correlation between $-S_{aq}^\circ$ and Z^2/r ; for the radius, r , the C.N. = 6 values are used for Na(I), Ca(II) and PuO_2^{+2} , that of C.N. = 8 for Pu(IV), that of C.N. = 9 for Pu(III) and that of C.N. = 4 for PuO_2^{+1} . The S_{aq}° values are from reference 11.

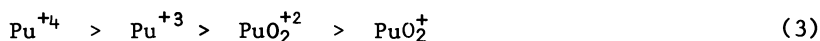
A significant aspect of plutonium hydration is the increase with pH of hydrolysis reactions such as:



The order of hydrolysis (i.e., order of increasing pH for onset of hydrolysis) follows the sequence



which differs from that in Figure 2 for the hydration entropies which is,



The difference in these patterns probably reflects that the hydrate entropies are related simply to the net positive charge on the cationic species (i.e., +2 for PuO_2^{+2}) while the hydrolysis reaction is the result of interaction of a water molecule with the metal atom itself -- i.e., Pu in PuO_2^{+2} . If this is a valid explanation, the hydrolysis order indicates that the charge on Pu in PuO_2^{+2} is actually between +3 and +4 and probably about +3.3.

The variation of the concentration of the free (non-hydrolyzed) cations with pH is shown for the oxidation states of III to VI in Figure 3. These curves are based on estimated values of the hydrolysis constants but are of sufficient accuracy to indicate the pH values at which hydrolysis becomes significant (e.g., ~6-8 for Pu^{+3} , < 0 for Pu^{+4} , 9-10 for PuO_2^+ and 4-5 for PuO_2^{+2}). Values of the hydrolysis constants are listed in Table II and represent the "best" values (experimental or estimated) from various laboratories.

The study of plutonium hydrolysis is complicated by the formation of oligomers and polymers once the simple mononuclear hydrolysis species start forming. The relative mono-oligomer concentrations are dependent on the plutonium concentration - e.g. the ratio of Pu present as $(\text{PuO}_2)_2(\text{OH})_2^{+2}$ to that as $\text{PuO}_2(\text{OH})^+$ is 200 for $[\text{Pu}]_T = 0.1$ M, 5.6 for 10^{-4} M and 0.05 for 10^{-8} M.

The hydrolysis of Pu^{+4} can result in the formation of polymers which are rather intractable to reversal to simpler species. Generally such polymerization requires $[\text{Pu}]_T > 10^{-6}$ M but, due to the irreversibility, dilution of more concentrated hydrolysis solutions below this value would not destroy the polymers. The rate of polymerization has been found to be third order in Pu concentrations and has a value of 5.4×10^{-5} moles/hr at 50°C and $[\text{Pu}^{+4}]_T \approx 0.006$ M, $[\text{HNO}_3] \approx 0.25$ M (13). Soon after formation, such polymers can be decomposed readily to simple species in solution by acidification or by oxidation to Pu(VI). However, as the polymers age, the decomposition process requires increasingly rigorous treatment. The rate of such irreversible aging varies with temperature, Pu(IV) concentration, the nature of

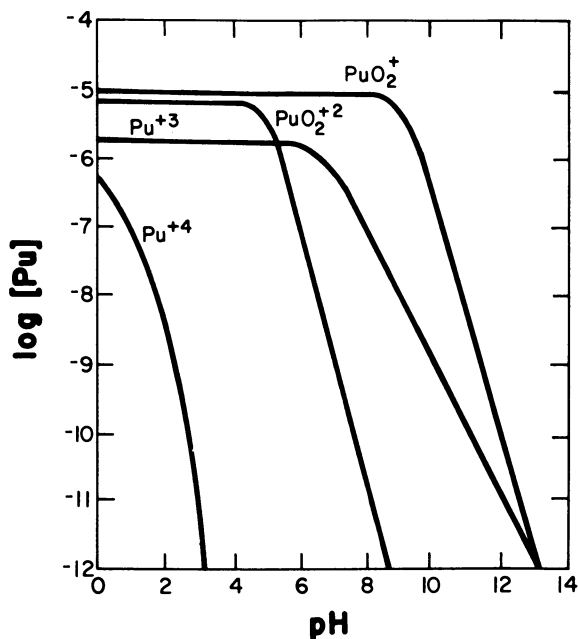


Figure 3. The effect of hydrolysis, as a function of pH, on the concentration of hydrated Pu cationic species. The initial ($\log [Pu]$ at $pH = 0$) concentrations are those at $pH \geq 8$ which correspond to the k_{sp} values of the hydroxide precipitate of each species.

Table II
Hydrolysis Constants for Plutonium

$$\log * \beta_{ij} = [M_i(OH)_j] [H]^j / [M]^i$$

$$T = 25^\circ\text{C}, I = 1.0 \text{ M}(\text{ClO}_4^-), pK_w = 13.8$$

<u>M</u>	<u>log *β_{11}</u>	<u>log *β_{12}</u>	<u>log *β_{13}</u>	<u>log *β_{14}</u>	<u>log *β_{22}</u>	<u>log *β_{35}</u>
Pu ⁺³	-7.8 (-7.84) [†]	-16.6	-25.9	-36.2	-12.8	-32
Pu ⁺⁴	-0.3 (-1.5)	-2.3 (-2.7)	-5.4 (-6.6)	-9.7 (-10.8)		
PuO ₂ ⁺	-9.2 (-9.9)					
PuO ₂ ⁺²	-5.5 (-6.0)	-11.6			-5.1 (-8.59)	-14.5 (-22.1)

Value in () are from reference 28, except ()[†] which is from reference 10 (for Am⁺³). The other values are from reference 29.

anions present in solution, etc. A reasonable model of the aging involves initial formation of aggregates with hydroxy bridging which convert with time to structures with oxygen bridging. The relative percentage of oxygen bridges presumably determines the relative inertness of the polymer.

The polymers apparently increase in aggregate size as the pH increases. At pH 4, 99% is still suspended in solution after 6 days but at pH 5 this has fallen to 7.4% and at pH 6, to 0.1% (14).

Complexation

In studies where different oxidation states of plutonium have been complexed by the same ligand, the sequence of complexing strength most commonly observed is that described for the hydrolysis reactions: i.e.:



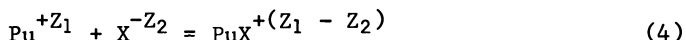
The sequence $\text{Pu}^{+4} > \text{Pu}^{+3}$ is expected from the ionic nature of the $\text{Pu}^{+n} - \text{X}^{m-}$ interaction which should increase with n for constant m . The observation that the complexing strength of the PuO_2^{+2} cations is greater than the Pu^{+3} cations can be understood by assuming that the central metal atom, Pu, in the linear $[\text{O}-\text{Pu}-\text{O}]^{+2}$ cation has an effective charge that is greater than +3. It is this effective charge that determines the strength of complexing since the ligands bind in the equatorial positions about the linear PuO_2^{+2} . Wadt (15) recently analyzed UO_2^{+2} by the relativistic core potential method and obtained a value of +2.4 for the atomic charge on the uranium. However, the effective charge in the equatorial plane would be expected to exceed this value and an estimate of an effective charge of $+3.3(\pm 0.1)$ was obtained from analysis of complexation by F^- anions (16). Similar evaluation of the stability constants for NpO_2F and $\text{NpO}_2\text{SO}_4^{-1}$ lead to an estimated effective charge on the Np atom in the linear species of 2.3 ± 0.2 (17). Effective charges for Pu of +3.3 in PuO_2^{+2} and +2.3 in PuO_2^{+1} are consistent with the complexation stability constants of these species.

Measurement of the stability constants of plutonium complexes is hampered by difficulties of maintaining a particular oxidation state. Formation of complexes of Pu^{+3} , except in very acid solutions, is accompanied and often obscured by complexation catalyzed oxidation to Pu^{+4} . Study of complexation of Pu^{+4} is often confused by competition with hydrolysis above pH 1-2. Except in tracer level solutions where its concentration is often difficult to ascertain, PuO_2^+ is normally present in a mixture of Pu oxidation states in which that of PuO_2^+ is much lower than PuO_2^{+2} and Pu^{+4} . PuO_2^{+2} can be formed in good yield and maintained with a holding oxidant (which may be a complexor itself). Conversely, PuO_2^{+2} may be reduced by many complexing agents, (18), leading to calculation of erroneous stability constants if the extent of reduction is not taken into account. Photochemical

redox reactions can be a further complication in plutonium systems (19). A compilation of the reported stability constants is available (20) and the paucity of data reflects the difficulties in studying plutonium complexation.

Despite the problems of direct experimental evaluation of plutonium stability constants, they are needed in modeling of the behavior of plutonium in reprocessing systems in waste repositories and in geological and environmental media. Actinide analogs such as Am^{+3} , Th^{+4} , NpO_2^+ and UO_2^{+2} can be used with caution for plutonium in the corresponding oxidation states and values for stability constants of these analogues are to be found also in reference 20.

It is possible to obtain fairly reliable values for many complexes of 1:1 (metal:ligand) stoichiometry by using an extended empirical equation in which the dielectric constant is dependent on the cationic charge (21). For the complexation reaction:



at 25°C, the equation (ΔG in $\text{kJ}\cdot\text{m}^{-1}$) is:

$$\Delta G = - \frac{(1.387 \times 10^3) Z_1 \cdot Z_2}{D_e d_{12}} + 9.952 + 2.478 \Sigma \ln f \quad (5)$$

where D_e is the dielectric constant, d_{12} the internuclear cation-anion distance in Å ($= r_1 + r_2$), Z_1 , Z_2 , the ionic charges. Also

$$\Sigma \ln f = -(0.30 \Delta Z^2 + 0.75) I^{\frac{1}{2}} + 0.015 I \quad (6)$$

and

$$\Delta Z_2 = Z_{\text{PuX}}^2 - (Z_{\text{Pu}}^2 - Z_{\text{X}}^2) \quad (7)$$

This equation provides values in good agreement with experiment for inner sphere complexation by both inorganic and organic ligands. In organic ligands, the value of Z_2 is assumed to be proportional to the acid constant, pK_a , of the bonding group (or to $\Sigma \text{K}_{\text{an}}$ for polydentate ligands). Figure 4 is the relation between Z_2 and $\Sigma \text{pK}_{\text{an}}$ which was obtained by using equation (5) with experimental free energies of protonation, holding all values constant except Z_2 (10). These values of Z_2 , in turn, were used with equation (5) to estimate the ΔG of complexation of $\text{Am}(\text{III})$ and $\text{Np}(\text{IV})$ by aminocarboxylate ligands, of $\text{Am}(\text{III})$ and $\text{Th}(\text{IV})$ by acetate and the $\text{Th}(\text{IV})$ by malonate. The comparison of experimental and calculated values is shown in Figure 5. The value used for D_e was 57 for $\text{Am}(\text{III})$ and 50 for $\text{Th}(\text{IV})$ and $\text{Np}(\text{IV})$; for all the ligands, $r_2 = 1.55$ Å while r_1 was obtained from Table I ($\text{CN} = 8$). The calculated and experimental values for UO_2^{+2} with acetate and malonate show similar agreement when $Z_1(\text{UO}_2^{+2}) = 3.2$ and $D_e = 55$. For $\text{NpO}_2\text{Mal}^{-1}$ when $Z_1(\text{NpO}_2^+) = 2.3$ and $D_e = 65$, the calculated ΔG agreed with the experimental value.

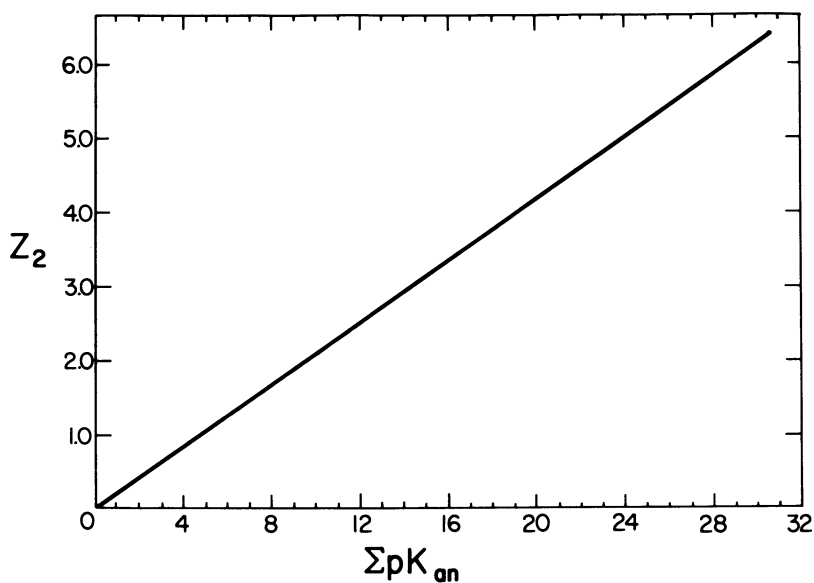


Figure 4. The variation of Z_2 and ΣpK_{an} for organic ligands used in equation (5).

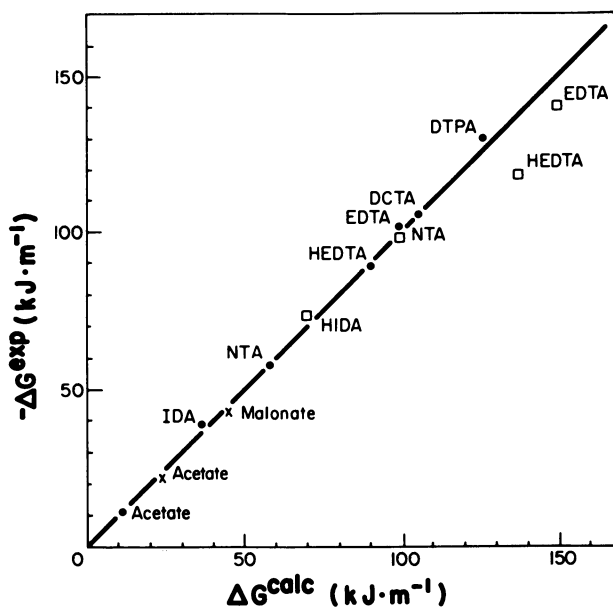
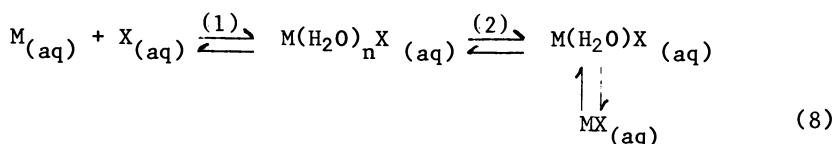


Figure 5. Comparison of the ΔG calculated by equation (5) and the ΔG from experiment: • = Am(III); x = Th (IV); □ = Np(IV). The solid line represents $\Delta G(\text{calc}) - \Delta G(\text{exper.})$.

All of the polydentate ligand systems which showed agreement between experimental and calculated ΔG values involved 5 or 6 membered chelate rings. The experimental values for complexes of chelate rings of 7 or more members were progressively lower than the calculated values as the ring size increased. By that criterion, poor agreement between the calculated and experimental value for $\text{UO}_2\text{NTA}^{-1}$ (5-membered rings) indicates that the experimental value is probably incorrect.

Unfortunately, for ligands of strong acids, this equation may underestimate the stability constant as it calculates values for inner sphere formation only. Eigen (22) has proposed that the formation of complexes proceeds sequentially as follows:



The first step is diffusion controlled while the second represents the formation of an outer sphere complex in which the metal ion and the ligand are separated by at least one molecule of water. In the final step, this outer sphere complex ejects the water and forms an inner sphere complex in which the metal and ligand are directly associated. Some ligands cannot displace the water and complexation apparently terminates with the formation of the outer sphere complex. Plutonium cations form both inner and outer sphere complexes, depending on the ligand pK_a . For trivalent plutonium, we can assign a predominant outer sphere character to the halide, nitrate, sulfonate and trichloroacetate complexes and an inner sphere character to the fluoride, iodate, sulfate and acetate complexes (23). A study of Am^{+3} , Th^{+4} and UO_2^{+2} complexation by chloroacetate ligands ($\text{Cl}_n\text{H}_3-n\text{CCO}_2^-$, $n = 0-3$) (24) leads to assignment of complexation character for different oxidation states of plutonium as given in Table III.

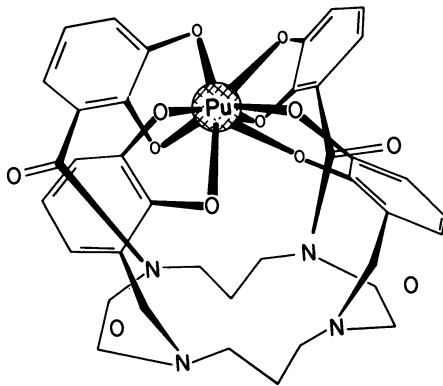
Some attention has been given to the complexation of actinides by macrocyclics and similar multidentate ligands. Generally, the strength of the interaction of the metal-functional group is too weak to displace the metal-water bonds if the functional group is an ether or a phenol. Amine groups are protonated below pH 6 to 8, preventing Pu-N interaction through the repulsion of the positively charged plutonium and amine groups. As a result, hydrolysis usually completes successfully at lower pH's with actinide-amine interaction. By contrast, in aminopolycarboxylates, the amine group does bind to plutonium, increasing the stability of the complexation (10).

Raymond's group has studied the complexation of Pu^{+4} by linear and cyclic catechoylamide ligands in which the plutonium has CN = 8 through interaction with phenolate groups (Figure 6). The ligands were designed to be specific complexing agents for Pu^{+4} from biological systems (25). Another specific complexing

Table III

Relationship of Complexation Character
of Plutonium and Ligand pKa

<u>Cation</u>	<u>Complexation Character</u>		
Pu^{+3}	$i/o < 1$	$2.0 \lesssim \text{pKa} \gtrsim 2.0$	$i/o > 1$
Pu^{+4}	$i/o < 1$	$1.0 \lesssim \text{pKa} \gtrsim 1.0$	$i/o > 1$
PuO_2^{+2}	$i/o < 1$	$1.7 \lesssim \text{pKa} \gtrsim 1.7$	$i/o > 1$

Figure 6. The Pu^{+4} - tetracatechoylamide complex.

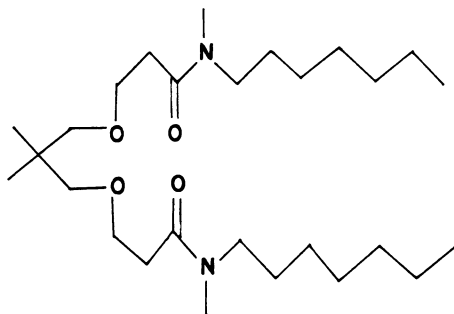


Figure 7. N,N' - diheptyl - N,N' , 6,6-tetramethyl -4,8-dioxaundecane used in the PuO_2^{+2} CWE.

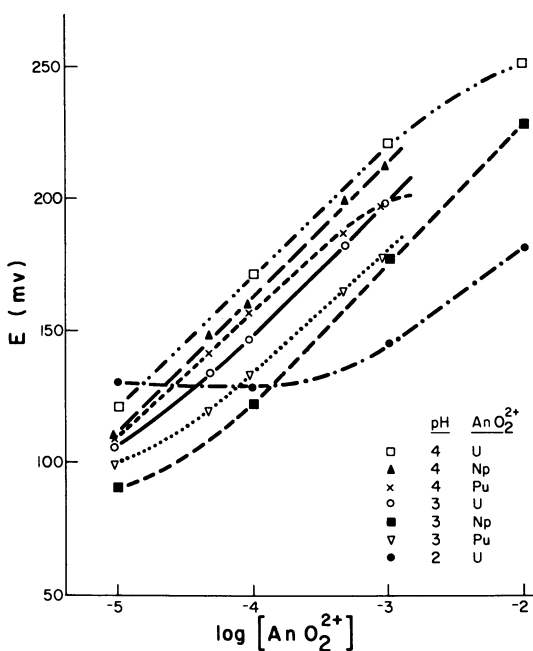


Figure 8. Response of the actinyl(VI) CWE to concentrations of UO_2^{+2} (—), NpO_2^{+2} (---) and PuO_2^{+2} (···) at pH 2 (x), 3 (o, ●, ◆) and 4 (□, ▲, △).

agent, N,N' - diheptyl-N,N', 6,6-tetramethyl- 4,8-dioxaundecane diamide (Figure 7), for UO_2^{+2} was shown to provide the basis for a uranyl specific ion electrode (26). We have used this ligand to develop a simple coated wire type electrode for PuO_2^{+2} which reacts rapidly and reproducibly (27). It has very good specificity for PuO_2^{+2} against a greater than 10 fold excess of +2 and +3 cations and a 100 fold excess of NpO_2^{+2} but does show interference by Th^{+4} as its concentration exceeds that of the PuO_2^{+2} . The electrode operates well between pH 2 and 5 and for PuO_2^{+2} concentrations from 10^{-5} to 10^{-2} M (Figure 8) and has been found useful in redox and complexation studies as it responds to the concentration of "free" plutonyl, not the total.

Conclusion

Studies of ligands which might provide specificity in binding to various oxidation states of plutonium seems a particularly promising area for further research. If specific ion electrodes could be developed for the other oxidation states, study of redox reactions would be much facilitated. Fast separation schemes which do not change the redox equilibria and function at neutral pH values would be helpful in studies of behavior of tracer levels of plutonium in environmental conditions. A particularly important question in this area is the role of PuO_2^{+2} which has been reported to be the dominant soluble form of plutonium in some studies of natural waters (3,14).

The research from F.S.U. described in this review was conducted under contracts with the Offices of Basic Energy Science and of Health and Environmental Research of the U.S.D.O.E.

Literature Cited

- (1). Foreman, J.K. and Smith, T.D., *J. Chem. Soc.*, 1957, 1752.
- (2). Connick, R.E., The Actinide Elements, Ch. 8, ed. G.T. Seaborg and J.J. Katz, McGraw Hill, New York, 1954.
- (3). "Transuranics in the Environment", ed. H.D. Hanson, DOE/TIC-22800, U.S.D.O.E., 1980.
- (4). Ahrlund, S., private communication.
- (5). Allard, B., Kipatsi, H., and Liljensin, J.O., *J. Inorg. Nucl. Chem.*, 1980, 42, 1015.
- (6). Shannon, R.D., *Acta Cryst.*, 1976, A32, 751.
- (7). Choppin, G.R., *Pure Appl. Chem.*, 1971, 27, 23.
- (8). Choppin, G.R. and Strazik, W.F., *Inorg. Chem.*, 1965, 4, 1250.
- (9). Lundquist, R., Hulet, E. K. and Baisden, P. A., *Acta Chem. Scand.*, 1981, A35, 653.
- (10). Choppin, G. R., *Radiochim. Acta*, in press.
- (11). Fuger, J., and Oetting, F. L., The Chemical Thermodynamics of Actinide Elements and Compounds; Part 2. The Actinide Aqueous Ions., *Inter. At. Ener. Agen.*, Vienna, 1976.
- (12). Svoronos, D. R., Antic-Fidancev, E., Lamaitre-Blaise, M., and Caro, P., *Nouveau J. Chim.*, 1981, 5, 547.

- (13). Toth, L. M., Friedman, H. A., and Osborne, M. M., *J. Inorg. Nucl. Chem.*, 1981, 43, 2929.
- (14). Rai, D. and Swanson, J. L., *Nucl. Tech.*, 1981, 54, 107.
- (15). Wadt, W. R., *J. Am. Chem. Soc.*, 1981, 103, 6053.
- (16). Choppin, G. R., and Unrein, P. J., *Transplutonium Elements*, W. Muller and R. Lindner, eds., North-Holland, Amsterdam, 1976, p. 97
- (17). Rao, L. F., and Choppin, G. R., unpublished data.
- (18). Bertrand, P. A. and Choppin, G. R., to be published.
- (19). Toth, T. M., Bell, J. T., and Friedman, H. A., *Actinide Separations*, J. D. Navratil and W. W. Schultz, eds., ACS Symposium Series 117, Washington, D. C., 1980, pp. 253-266.
- (20). Martell, A. E., and Smith R. M., Critical Stability Constants, Vol. 1-5., Plenum Press, New York, 1974-81.
- (21). Munze, R., *J. Inorg. Nucl. Chem.*, 1972, 34, 661.
- (22). Eigen, M., and Wilkins, R., *Adv. Chem. Ser. No. 49*, 1965, p. 55.
- (23). Choppin, G. R., and Bertha, S. L., *J. Inorg. Nucl. Chem.*, 1973, 35, 1309.
- (24). Khalili, F. I., and Choppin, G. R., to be published.
- (25). Raymond, K. N., Kappel, N. J., Pecoraro, V. L., Harris, W. R., Carrano, C. J., Weith, F. L., and Durbin, P. W., Actinides in Perspective, Edelstein, N. M., ed., Pergamon, New York, 1982, p. 491.
- (26). Senkyr, J., Ammann, D., Meier, P. C., Morf, W. E., Pretsch, E., and Simon, W., *Anal. Chem.*, 1979, 51, 786.
- (27). Bertrand, P. A., Choppin, G. R., Rao, L. F., and Bunzli, J. C., submitted for publication.
- (28). Baes, C. F., and Mesmer, R. E., The Hydrolysis of Cations, Wiley-Interscience, New York, 1976.
- (29). Allard, B., Actinides in Perspective, N. Edelstein, ed., Pergamon Press, 1982, p. 553.

RECEIVED December 21, 1982

Aspects of Plutonium(IV) Hydrous Polymer Chemistry

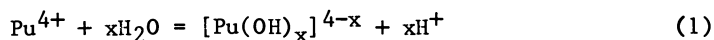
L. M. TOTH, H. A. FRIEDMAN, and M. M. OSBORNE

Oak Ridge National Laboratory, Chemical Technology Division,
Oak Ridge, TN 37830

The polymerization of Pu(IV) hydrolysis products in aqueous nitric acid solutions containing uranyl nitrate has been examined as a function of pH, temperature, and concentration. Even in the absence of the uranyl solute, an induction period usually follows the polymer growth stage during which time formation of primary hydrolysis products occurs. Uranyl nitrate retards the polymerization rate by approximately 35% in spite of the counteracting influence of the nitrate ions associated with this solute; evidence is given to demonstrate that the uranyl ion attaches through hydroxyl bridges to active sites in the polymer network and functions as a chain-terminating unit. The rate of polymer growth has been shown to be third order with respect to Pu(IV).

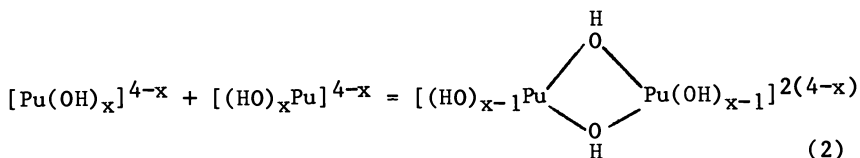
The reflux of aqueous Pu(IV) solutions containing $\leq 6 \text{ M HNO}_3$ produces polymer precipitates that are resistant to subsequent dissociation and dissolution in nitric acid. Rapid aging of the Pu(IV) polymer to form a PuO_2 -like structure is responsible for the unusually stable polymer. Comparative studies under nonreflux conditions show that polymer does not form at concentrations of $\text{HNO}_3 > 3 \text{ M}$.

The hydrolysis of Pu(IV)



and subsequent aggregation of hydrolysis products

0097-6156/83/0216-0231\$06.00/0
© 1983 American Chemical Society



has been a subject of considerable study over the past four decades. Since this strongly acid dependent chemistry is not unusual when compared with that of other metal cations, the experimental techniques are typical of those used in studies of other hydrolysis and aggregation reactions. These include (1) the electrochemistry and spectroscopy of the elementary hydrolysis reactions, light scattering and ultracentrifuge examination of the size of the hydrous polymeric aggregates, diffraction and microscopy experiments on the nature of the aggregates, and general chemical studies on the reactivity of Pu(IV) and its polymeric products. Although the results from these previous plutonium investigations may appear to be sufficient for an understanding of the chemistry involved in the hydrolysis reactions, there still remain uncertainties that must be worked out to ensure reliable performance in the aqueous reprocessing of nuclear fuels.

The need for additional work stems in part from several deficiencies. One of these, which is characteristic of all actinides, is that much of the work has only been documented, at best, in unrefereed laboratory publications and, at worst, in the notebooks or recollections of that generation of actinide researchers. In addition, the earlier research was focused mainly on providing basic information about isolated Pu(IV) systems; and while this has been necessary as a first step, the realization that most real situations involve plutonium in the presence of many interactive ions dictates the design of more complicated and extensive experiments. The recent interests in Pu(IV) hydrolysis chemistry have arisen from a desire to define its behavior in these realistic situations, e.g., in the presence of large amounts of accompanying solutes, namely uranyl nitrate. This work has led to the revelation of some very interesting aspects of interaction between uranyl ions and plutonium polymer. Structural aspects of the polymer network gleaned through the usage of infrared and Raman spectroscopy have revealed the exact nature of these interactions with other ions; these techniques have great promise of providing further insights into the interactions between plutonium and the medium in which it resides.

The general goal in the recent efforts has been very practical — to ensure better control of Pu(IV) in low acid reprocessing streams through quantitative measurements of the parameters that determine polymer formation. Admittedly, similar studies have been conducted to some degree already, but

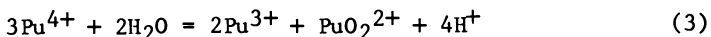
with better techniques we can offer refinements that more accurately guide the design engineer away from situations where plutonium(IV) hydrolysis will prevail. An example of this parametric study will be given toward the end of this presentation.

The techniques used in the work have generally been spectroscopic; visible-uv for quantitative determinations of species concentrations and infrared-Raman for structural aspects of the polymer. Although the former has often been used in the study of plutonium systems, there has been considerably less usage made of the latter in the actinide hydrolysis mechanisms.

Nature of the Hydrous Polymer Reaction

If the growth of Pu(IV) hydrous polymer is monitored spectrophotometrically at 400 nm as a function of time, it is observed under many circumstances (cf., Fig. 1) (2) that the polymer growth in nitric acid solution often proceeds after an induction period which is determined by the purity of the system. The subsequent growth stage of the polymer in nitric acid solution occurs through a reaction that is third order with respect to Pu(IV) concentration as demonstrated by the plot of rate constants as a function of Pu(IV) concentration shown in Fig. 2 (2). Shown here are several sets of data that all have a slope of 3. Included on the plot is a single point for a HNO₃ concentration of 0.12 M to indicate where other data at this acidity would fall under the assumption that the third order relationship was still valid. These characteristics of hydrous polymer formation are typical of many hydrolytic systems, e.g., Si(OH)₄, and lend confidence in extrapolating these data to more extreme and difficult to measure conditions.

Uranyl Nitrate Influence on Polymer Growth. The effect of a solute such as uranyl nitrate on this polymer formation is so complex that the net effect on the polymer growth rate cannot be predicted. Experimentally, it is observed that the rates of growth at given initial HNO₃ concentration are always slower in the presence of UO₂(NO₃)₂ as indicated by the solid curve in Fig. 1. This occurs in spite of an observed back-shift in the Pu(IV) disproportionation equilibrium,



and the accompanying decrease in the acidity of the solution when uranyl nitrate is added. Thus the presence of UO₂(NO₃)₂ in the solution causes two phenomena to occur.

- (1) the increase in nitrate ion concentration causes the stabilization of Pu(IV) through nitrate complexation

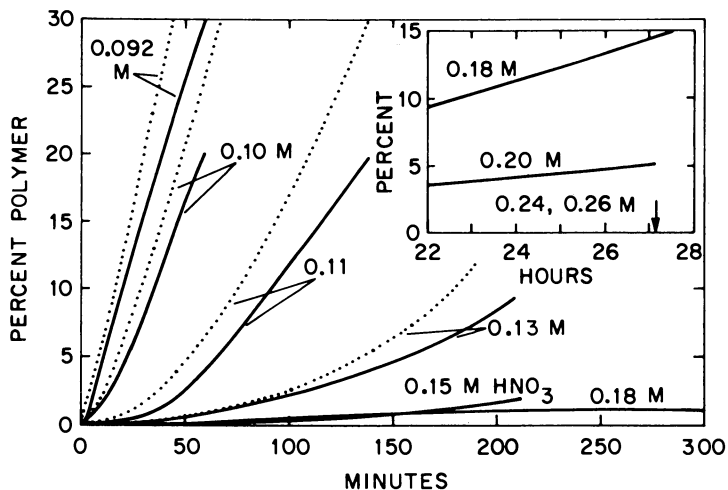


Figure 1. Percent Pu(IV) polymer vs. time for 0.05 M Pu solutions at 50°C. Solid/dashed lines--solutions with/without 0.05 M $\text{UO}_2(\text{NO}_3)_2$ added. Makeup HNO_3 concentrations for solutions are indicated. (Reprinted with permission from Ref. 2.)

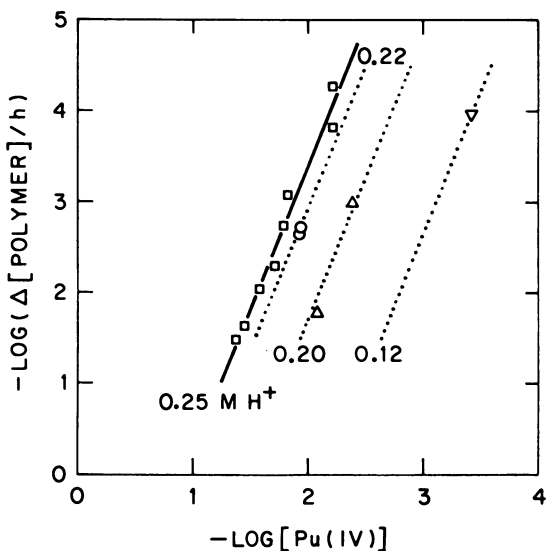


Figure 2. Determination of reaction order for Pu(IV) polymer growth stage at 50°C. Slope ≈ 3 for all HNO_3 concentrations indicated. (Reprinted with permission from Ref. 2.)

which shifts the above equilibrium to the left. (The same shift in the equilibrium is obtained by adding NaNO_3 or $\text{Ca}(\text{NO}_3)_2$.) This shift causes a lower acidity and hence an increased rate of polymerization.

- (2) The presence of UO_2^{2+} causes a net decrease in the rate of polymerization which means that it must overcome the nitrate ion effect that accompanies it.

Chemical analyses reveal that measurable amounts of uranyl ion are actually present in Pu(IV) polymers grown in mixtures of Pu(IV) and uranyl nitrate suggesting that uranyl ion is being taken up in the polymer network and consequently hampers the growth through a chain termination process as suggested in Fig. 3. The uranyl serves to terminate active sites because it does not typically form extensive polymeric aggregates as does Pu(IV); instead it tends only to dimerize and, at most, trimerize (4).

The proof of the chain terminating function of UO_2^{2+} could be obtained by the identification of a uranyl-to-polymer bond through the usage of Raman spectroscopy. However, Raman spectra of plutonium solutions are difficult to measure since the solutions must be kept in alpha-containment boxes; we, therefore, have turned to polymer solutions of Th(IV) in place of Pu(IV) for the initial studies. It is through the decrease in the frequency of the UO_2^{2+} symmetric stretching vibration that the attachment of UO_2^{2+} to the Th(IV) polymer network is demonstrated, for when uranyl dimerizes in pure solutions a similar shift occurs. (One observes separate symmetric stretching vibrations due to monomeric unhydrolyzed uranyl, dimeric and trimeric hydroxyl-bridged uranyl each at progressively lower vibrational frequencies (5).) In uranyl-thorium(IV) mixtures that are adjusted to pH = 3.1, the appearance of the uranyl symmetric stretching vibration attributable to a dimeric species appears quite readily (in addition to that of the monomeric species) even though the pH is not high enough for uranyl to hydrolyze and aggregate on its own. It is for this reason that we believe UO_2^{2+} chemically attaches to the polymeric network through hydroxyl bridges.

Carbon Dioxide Adsorption on Dried Polymer. Other unexpected interactions of these hydrolytic polymers have been noted previously during the measurement of infrared spectra of dried Pu(IV) polymers (like those used for diffraction studies). Vibrational bands first attributed to nitrate ion were observed in samples exposed to room air; however, these bands were not present in samples prepared under nitrogen atmospheres (see Fig. 4) (6). Chemical analyses established enough carbon in the exposed samples to confirm the assignment of the extraneous bands to the carbonate functional group

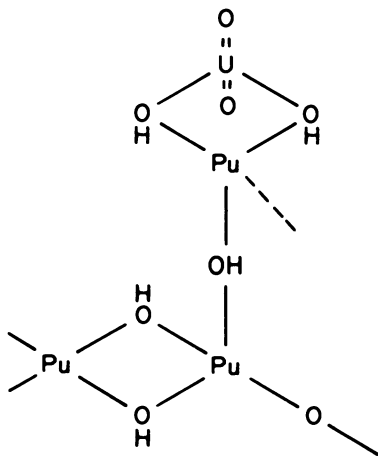


Figure 3. Termination of Pu(IV) polymer network propagation by attachment of UO_2^{2+} to active $-\text{OH}$ sites.

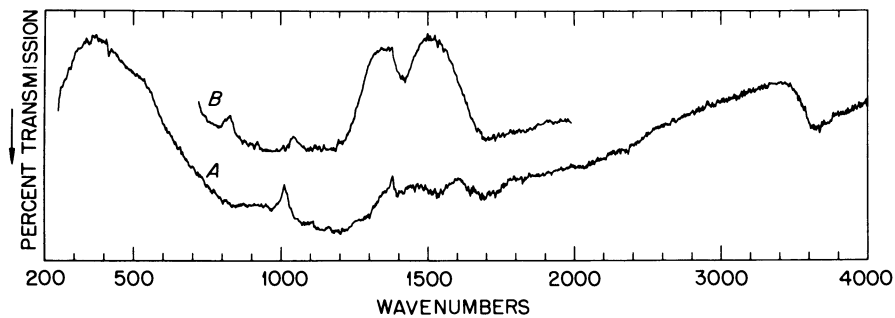


Figure 4. Infrared spectra of KBr pellets containing Pu(IV) polymer precipitates, (A) prepared in N_2 -purged glove bag free of CO_2 ; (B) prepared in laboratory atmosphere. (Reprinted with permission from Ref. 6.)

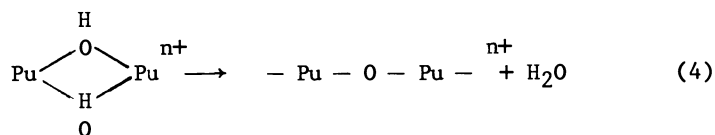
formed by the rapid adsorption of atmospheric CO₂. Although the affinity of the polymer for CO₂ is not unusual, it has not often been considered in previous diffraction studies and could have compromised some of the earlier results.

The implication of these two examples is that the medium in which the Pu(IV) hydrolysis chemistry is studied has a strong bearing on the outcome of the results. In the past, we were content to treat the pure systems and either ignore external interferences (such as the atmosphere) or infer the behavior of mixtures (such as Pu⁴⁺ and UO₂²⁺) based on the known chemistries of the individual species. The example of UO₂²⁺ interactions with Pu(IV) polymer demonstrates that neither of these approaches is accurate. Therefore, future research efforts will necessarily have to consider plutonium hydrolysis reactions in more detail than has previously been done.

Parametric Studies

Reflux Experiments. More recent efforts have been directed at a quantitative evaluation of those parameters that affect polymer growth, namely acidity, plutonium concentration, temperature, and reflux action. The last is an interesting example to illustrate since the admission of low acid condensates or diluents to a Pu(IV) solution causes some polymer formation even when the bulk solution is otherwise acidic enough to prevent any measurable degree of hydrolysis.

This untimely polymer formation is understood to be caused by the very rapid hydrolysis and aggregation of monomeric Pu(IV) species (at the region of condensate reentry into the hot plutonium solution) to produce hydrous polymers that are not readily depolymerized. At high temperatures such as found under reflux conditions, the polymer rapidly ages through the conversion of hydroxyl- to oxo-bridges:



and thus becomes highly resistant to redissolution.

Although the effect of reflux on polymer formation has been recognized for many years, little detailed information is available concerning the extent to which changes in temperature, acidity, and plutonium concentration affect it. Recent work in this laboratory has sought to provide some of this information. Unfortunately, absorption spectrophotometry is not suitable for monitoring the formation of Pu(IV) polymer

under reflux conditions, because the aged polymer formed at about 100°C does not remain suspended in the solution. Instead it precipitates and produces extensive light scatter. More qualitative techniques which involve simply refluxing the solutions until precipitates are visually observed have therefore been used. Reflux rates of approximately 0.3 ml/min in these experiments produce a turnover of the 10 ml samples in 0.5 h. Refluxed samples were compared with nonrefluxed samples held isothermally in an oil bath. The length of time until polymer was observed in 0.05 M Pu solutions is shown in Table 1. It is seen that above 2 M HNO₃ no polymer formed in the nonreflux control samples, whereas polymer formed under all conditions tested at reflux. Furthermore, the polymer that formed was resistant to all attempts at redissolution in nitric acid, thus suggesting a very aged state of the polymer.

Table 1. Formation of aged polymer under reflux and nonreflux conditions with 0.05 M Pu at 105°C

HNO ₃ concentration (M)	Hours to form observable polymer ^a	
	Reflux	Nonreflux
1	1.5 [0.013]	18 [0.049]
2	2.0 [0.029]	191 [0.049]
3	4.0 [0.050]	b [0.050]
4	22.0 [0.013] ^c	b [0.050]
6	48.0 [0.007] ^d	b [0.045]

^aValues in brackets are the Pu(IV) molar concentrations at the end of the experiment.

^bNo polymer formation was observed, even after a total of 596 h.

^cDecrease in acidity noted at end of experiment; final [HNO₃] = 3.5 M.

^dDecrease in acidity noted at end of experiment; final [HNO₃] = 5.0 M.

Table 2 shows the effect of reflux on high concentrations of plutonium (up to 0.55 M) in comparison to nonreflux situations of comparable acidities. Again, the nonreflux solutions did not polymerize above a fixed acid concentration (in this case 3M) whereas all solutions that were refluxed showed the formation of polymer.

If one takes the 4 or 6 M HNO₃ data under reflux conditions and evaluates the increase in rates with increasing concentration of Pu(IV), he would find that the time to form observable polymer is inversely proportional to the first power (1.1 ± .4) of the Pu(IV) concentration. At first glance this might seem to contradict earlier findings (7) that showed the

polymer growth rate to follow a third power dependency on Pu(IV) concentration; but the former case was for the growth rate after polymer was observed and the present case is for the appearance or initiation of polymer. The initiation of polymer involves a mechanism that has not yet been elucidated and, therefore, the first order kinetics found here are not in contradiction with the previous study. (If the time to form observable polymer followed third order kinetics, a 1000-fold increase in rate would be expected for a 10-fold increase in concentration.)

Table 2. Formation of aged polymer under reflux and nonreflux conditions with 0.27 and 0.55 M Pu at 105°C

HNO ₃ concentration	Pu concentration	Hours to perform observable parameters	
		Reflux	Nonreflux
3	0.55		97 [0.493]
4	0.27	7.6 [0.093]	
	0.55	1.5 [0.261]	b [0.455]
6	0.55	3.0 [0.357]	b [0.348]

^aValues in brackets are the Pu(IV) molar concentrations at the end of the experiment.

^bNo polymer formation observed, even after a total of 596 h.

Conclusions

Many reports on the hydrolysis of Pu(IV) and polymerization (aggregation) of the primary hydrolysis products exist in one form or another. The validity of some of the earlier data may be subject to question because the experimental conditions were not properly controlled. Therefore, these systems deserve further consideration for the sake of refinements. Nevertheless, the major area of interest for the future will remain with interactions between Pu(IV) hydrolysis products and other reactive species present in the solution. There is not only considerable promise of elucidating novel chemical interactions, but there is also a great practical need to fully understand the extent of these interactions in order to ensure the most complete control of plutonium in reprocessing operations.

Acknowledgments

Research sponsored by the Office of Spent Fuel Management and Reprocessing Systems, U.S. Department of Energy under contract W-7405-eng-26 with the Union Carbide Corporation.

Literature Cited

1. Johnson, G. L.; Toth, L. M. "Pu(IV) and Th(IV) Hydrous Polymer Chemistry" ORNL/TM-6365, May 1978.
2. Figure taken from Toth, L.M.; Friedman, H. A.; Osborne, M. M. J. Inorg. Nucl. Chem. 1981, 43 (11) 2929.
3. Harvey, W. W.; Turner, M. J.; Slaughter, J.; Makridges, A. C. "Study of Silica Scaling from Geothermal Brines," EIC Corp. Prog. Rep. March-September 1976, C00-2607-3.
4. Baes, C. F.; Mesmer, R. E. "The Hydrolysis of Cations"; Wiley, New York, 1976, pp. 177-182.
5. Toth, L. M.; Begun, G. M. J. Phys. Chem. 1981, 85, 547.
6. Figure taken from Toth, L. M.; Friedman, H. A. J. Inorg. Nucl. Chem. 1978, 40, 807.
7. Toth, L. M.; Friedman, H. A.; Osborne, M. M. J. Inorg. Nucl. Chem., 1981 43 (11) 2929.

RECEIVED December 21, 1982

Reactions of Plutonium Ions with the Products of Water Radiolysis

J. C. SULLIVAN

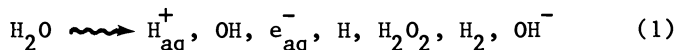
Argonne National Laboratory, Chemistry Division, Argonne, IL 60439

The free radicals produced in the radiolysis of H₂O range from the powerful reductant e⁻(aq) to the oxidant OH. The reactions of the hydrated electron with Pu(VI) are reviewed. The effect of absorption on a SiO₂ colloid markedly reduces the rate k(e⁻(aq) + Pu(VI)). The reactions of OH with CO₃⁼ and subsequent reaction with Pu(V) are discussed. Salient problems in the process and waste disposal chemistry of Pu are outlined.

The gifted chemists who worked on the "Manhattan Project" recognized and attempted to quantitatively describe the effects of α self-radiolysis soon after the preparation of macroscopic quantities of ²³⁹Pu. The present symposium provides an appropriate time and place to cite a number of these individuals for their contributions to an important aspect of Pu solution chemistry.

The authors of reports referred to in Vol. 14-B (2) who participated in these early investigations under the direction of Professor R. E. Connick are (in alphabetical order) S. C. Carniglia, M. Kasha, W. H. McVey, G. E. Moore, G. E. Sheline and W. K. Wilmarth. These early studies were carried out in HClO₄ and HCl solutions and the net effect was a reduction to Pu(III).

To provide an appropriate background for a discussion of the title reactions note that ~10⁻⁹ secs after irradiation the water decomposition (products) can be expressed as:



The amounts of these primary products per 100 eV adsorbed (G values) are respectively; 2.9, 2.75, 2.65, 0.65, 0.70., 0.45 and 0.25. These values are for neutral water and a ⁶⁰Co-γ source. The G values may vary somewhat with energy and type of particle

0097-6156/83/0216-0241\$06.00/0
© 1983 American Chemical Society

used for the irradiation, but not markedly over a wide range of particles and energies.

The thermodynamically powerful oxidant(OH) and reductant $e^-(aq)$ are produced. Estimates have been made of the values for the potentials of some of the characteristic reactions of the so-called primary products of radiolysis. These values are presented in Table I. It is of importance to note that the H atom can act as either an oxidant or reductant

Table I. Half-Cell Potentials^(a)

Reactions	E_0, V
$OH + H^+ + e^- = H_2O$	2.65
$H + H^+ + e^- = H_2$	2.30
$OH + e^- = OH^-$	1.83
$O_2 + 2H^+ + e^- = H_2O_2$	1.73
$H + H_2O + e^- = H_2 + OH^-$	1.47
$H^+ + HO_2 + e^- = H_2O_2$	1.44
$O_2 + e^- = O_2^-$	-0.33
$H^+ + e^- = H$	-2.30
$e^- = e^-_{aq}$	-2.87

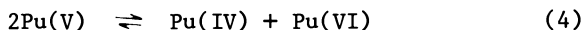
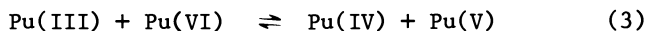
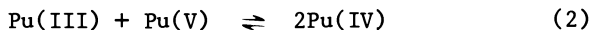
(a) $H_2O(lig), H_2(g, 1 \text{ atm } 25^\circ), (O_2g, 1 \text{ atm } 25^\circ)$ as standard states. Schwartz H. A., *J. Chem. Ed.* 1981, 58, 101.

The development of pulse radiolysis techniques have led to the determination of a number of the important kinetic processes of the species produced by the irradiation of H_2O . The results that have been obtained for a number of the most important reactions are presented in Table II. These results demonstrate that the net effect of radiation is H_2O decomposition in the absence of any reactive substrate.

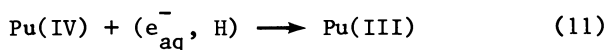
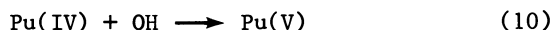
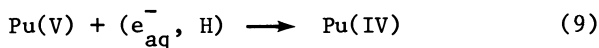
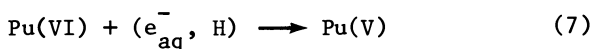
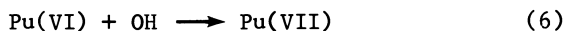
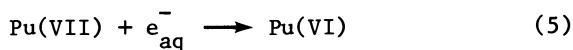
Table II. Reactions of the Radicals

Reaction	Rate Constant $\times 10^9$ $M^{-1}s^{-1}$
$e^-(aq) + e^-(aq) + 2H_2O_2 \longrightarrow H_2 + 2OH^-$	6.0
$e^-(aq) + H_3O^+ \longrightarrow H + H_2O$	23.5
$e^-(aq) + OH \longrightarrow OH^-$	3.0
$OH + OH \longrightarrow H_2O_2$	5.0
$OH + H \longrightarrow H_2O$	20.0
$H + H \longrightarrow H_2$	10.0
$H^+ + OH^- \longrightarrow H_2O$	100.0

The solution chemistry of Pu is unique in that it is possible for all four of the common oxidation states to be present in the same solution. The well-known relations are presented in equations 2, 3 and 4.



The reactions to be expected between the radicals produced by the radiation of H₂O with the plutonium ions in aqueous solution are:



There is in addition to the pulse radiolysis technique the classical continuous radiation method. This later procedure uses either the ⁶⁰Co-γ sources or in the case of Pu the self α irradiation due to the radioactive decay.

The vast majority of the studies on the reactions such as 5-12 have been the classical type in acidic solutions, predominantly in nitric acid solutions for obvious process related interests. The results of such studies have been summarized by Newton (4) so only a very brief recapitulation is warranted.

1. The predominant reactions in perchloric acid tend to reduce Pu to a "steady state" mixture of Pu(III) and Pu(IV).
2. In sulfuric acid solutions Pu(VI) is reduced only to Pu(IV).
3. In HCl solutions there are conflicting observations as to whether reduction of Pu(VI) and Pu(IV) occurs.

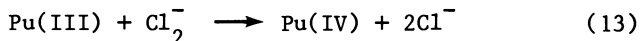
4. The vast amount of work carried out in nitric acid solutions can not be adequately summarized. Suffice it to say results in these solutions are plagued with irreproducibility and induction periods, but the general pattern is reduction of Pu(VI).

There are a limited number of such "steady radiolysis" studies of Pu in neutral or basic solutions that have been reported. Here too, the results are not unambiguous. For example, in a series of studies (5) with ~20 mM Pu and added ^{244}Cm (1.8×10^9 D/mM/ml) the Pu(III) decreased over periods of days in solutions containing Cl^- (i.e., artificial sea water and WIPP Brine) as well as in triply distilled water. The most striking result was the growth and disappearance of Pu(VI) in distilled H_2O over some 300 days.

In a different set of experiments solutions of Pu(III) or Pu(VI) in H_2O (Ar saturated, pH adjusted to 7, 2×10^{-5} M in Pu) were irradiated in the ANL ^{60}Co - γ source at a position where the dose was 1 megarad/hr (6) ~1 mM H_2O_2 produced/hr. Cation exchange column behavior was used in an attempt to identify Pu oxidation states, see Table III. The results obtained after an irradiation of 1 hr. were indistinguishable from the "blank", i.e. a solution not subjected to irradiation. The irradiation for a 24 hr. period failed to demonstrate a marked increase in the amount of Pu(IV) produced that could be ascribed to the effects of radiolysis.

When a solution of Pu(VI) is subjected to the 24 hr. irradiation the bulk of the Pu has been reduced to the Pu(III) oxidation state. There exists the ambiguity that residence on the column may cause some reduction of Pu(VI) to Pu(V) and Pu(IV) to Pu(III). The general conclusion is still valid that under these conditions the effect of radiation is to reduce the Pu. It is apparent that steady radiolysis experiments in the near neutral pH regime are subject to the same type of problems of interpretation as are those studies carried out in strong acid.

There is an additional problem that arises in continuous radiolysis studies. If the solutions contain, Cl^- , SO_4^{2-} , NO_3^- or CO_3^{2-} ions the products of H_2O radiolysis can react to produce the corresponding radicals. These radicals, Cl_2^- , SO_4^- , or CO_3^- can then undergo redox reactions with the Pu ions such as



The application of techniques of pulse radiolysis offers the potential to determine rates of primary radiolysis induced reaction processes. This knowledge can be of great value in the determination of redox processes of Pu ions occurring in a wide variety of aqueous solutions. As a matter of fact, such information is essential to a prediction of the Pu oxidation states to be expected in breached repository scenarios. For an

Table III. Distribution of Oxidation States*

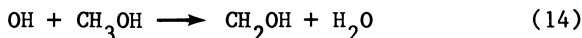
	3xDW	Pu(V) 0.5 M HClO ₄	Pu(VI) 2.0 M HClO ₄	Pu(III) 3 M HCl	Pu(IV) 6 M HCl	?
Pu(III) 1 hour blank	0.7	0.6	0.3	60.0	25.9	12.4
Pu(III) 1 hour blank acid wash	0.04	0.3	0.01	95.4	4.2	0.00
Pu(III) 1 hour irradiated	7.5	1.7	0.7	58.2	22.5	9.5
Pu(III) 1 hour irradiated acid wash	0.00	0.6	0.01	93.7	5.1	0.6
Pu(III) 24 hour blank	0.06	0.3	0.2	79.3	10.3	9.8
Pu(III) 24 hour blank acid wash	0.18	0.2	0.2	98.3	0.3	0.7
Pu(III) 24 hour irradiated	1.3	0.4	1.0	62.2	17.4	17.6
Pu(III) 24 hour irradiated acid wash	0.3	0.4	0.2	97.5	0.9	0.6
Pu(VI) 24 hour blank	0.1	31.5	60.6	6.1	0.6	1.0
Pu(VI) 24 hour blank acid wash	7.5	51.4	18.5	22.6	0.00	0.00
Pu(VI) 24 hour irradiated	1.1	0.1	0.3	86.1	5.6	6.8
Pu(VI) 24 hour irradiated acid wash	0.00	0.2	0.02	98.0	0.4	1.3

* % Oxidation State = $\frac{(\text{cmp/ml}) \sum \text{volume of fraction}}{\sum \text{cmp of all fractions}}$

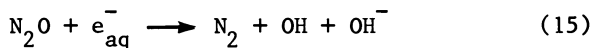
Note: The final pH of all solutions showed little change. However, the solutions irradiated for 24 hours changed the most, pH ~6.2, as compared to initial pH = 7.

understanding of the effects of radiolysis in process streams the Edisonian (steady radiolysis) approach can provide adequate information.

In pulse radiolysis studies it is feasible to eliminate undesired radical reactions by the use of "scavengers". For example, to produce a totally reducing system simple aliphatic alcohols are added and the ensuing reaction



produces a radical which is slow to react on the pulse radiolysis time scale. To eliminate $e^-(\text{aq})$ the solution is saturated with N_2O and the reaction



insures that the system is predominantly an oxidizing system.

The rate parameters for the reactions of $e^-(\text{aq})$ with substrates are generally determined by monitoring the disappearance of the hydrated electron at 600-700 nm. The first order rate parameters are generally determined over a range of substrate concentrations and the second order rate parameter calculated from the resulting linear relation. The data available for such studies with Pu ions are presented in Table IV.

Table IV. Reaction Rates of $e^-(\text{aq})$ with Pu

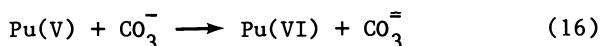
[Pu]	[M] $\times 10^{-4}$	Solution	$k(10^{10} \text{ M}^{-1}\text{s}^{-1})$
VI	0.12-1.0	pH 5.6 (HClO_4)	6.4 ± 0.4 (b)
VI	0.09-1.08	pH 6.1 (HClO_4)	5.8 ± 0.3 (b)
VI	0.2-0.8	0.05 M Na_2CO_3	2.3 ± 0.3 (c)
VI	0.26	2 M NaOH	1.9 ± 0.3 (d)
VII	0.2	2 M NaOH	4.2 ± 0.8 (d)

- (a) Ambient temperature, 25°C for (b) and (c), 20-22°C for (d).
 (b) Sullivan, J. C.; Gordon, S.; Cohen, D.; Mulac, W. and Schmidt, K. H., *J. Phys. Chem.* 1976, 80, 1684.
 (c) Mulac, W. and Sullivan, J. C., unpublished results.
 (d) Pakaev, A. K.; Mefad'eva, M. P.; Knot, N. N. and Spitsyn, V. I., *High Energy Chem.* 1973, 7, 448.

The amazing feature of these results is the fact that the reaction occurs at essentially the diffusion controlled limit over a wide range of solution composition. In particular in 0.05 M Na_2CO_3 solutions the Pu(VI) exists predominantly as the

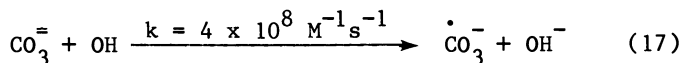
tris-carbonato complex. Yet there is no marked effect in the rate of the reaction despite the fact that simple electrostatic considerations would predict a priori that the formal negative charge on the Pu(VI) would be a kinetic barrier for the reaction with $e^-(aq)$. The data in this table are sufficient to provide a basis for the prediction that in homogeneous solutions the rate of the reaction of $e^-(aq)$ with Pu(VI) will not be influenced markedly by any complexing of the Pu(VI).

There are two additional pulse radiolysis investigations of Pu(VI) reactions that are of importance. These are the rate of reaction of $e^-(aq)$ with Pu(VI) adsorbed on SiO_2 colloids and the rate of the reaction between Pu(V) and the carbonate ion radical

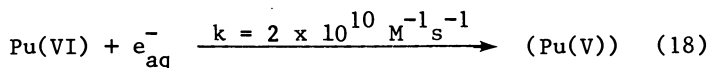


The former investigation was motivated, in part by the fact that in a previous study (7) there had been a marked difference on the rates of reactions of $e^-(aq)$ and U(VI) between homogeneous solutions and those containing micellar material. When the rate of disappearance of the hydrated electron is measured over a range of concentrations from 2×10^{-5} M to 8×10^{-4} M at pH = 9.7 in solutions formally 0.003 M SiO_2 , the calculated second order rate parameter is 1.4×10^9 $M^{-1}s^{-1}$. This is a marked decrease from any of the previous measurements and emphasizes the point that the prediction of Pu chemistry in a natural water system must take cognizance of factors that are not usually deemed significant.

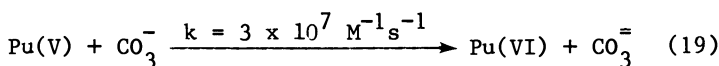
The point has previously been made that common anions can react with the products of water radiolysis to produce reactive species. One such well documented (8) reaction is



The product $\cdot CO_3^-$ radical can react with a variety of inorganic ions including the carbonato complex of Pu(V). Thus, in a pulse radiolysis experiment, Pu(VI) in 0.05 M Na_2CO_3 , He saturated, there are the parallel reactions (17) and (18)



followed by



Thus Pu(VI) in carbonate media will not suffer a net reduction due to radiolysis.

**American Chemical
Society Library
1155 16th St., N.W.
Washington, D. C. 20036**

Future Trends

It has been noted that results of steady radiolysis experiments provide adequate data for separations related problems. The difficulty is that in the absence of kinetic data for the primary process it becomes necessary to repeat this type of experiment for each particular set of concentrations and times.

One problem that should be of particular interest for separation processes is the identification and kinetic characterization of the reactive radicals that occur when strong nitric acid solutions are subject to ionizing radiation. The important reducing radical in such solutions is the H atom. There are presently no direct measurements of the rate of reduction of H atoms with any Pu oxidation state.

In marked contrast there exists a voluminous literature on pulse radiolysis studies of nitric acid solutions (9). The NO₃ radical has been identified as a major product although the mechanism of formation is still a matter of debate. While a number of reactions of this radical have been reported (10) there has evidently not been any pulse radiolysis studies of reactions with Pu ions.

For reactions in the near neutral or slightly basic pH regime - which are of interest in environmental chemistry and waste disposal problems - the presence of the common anions Cl⁻, SO₄⁻ and CO₃⁻ can introduce additional complications.

We have already discussed the reactions of Pu(VI) in carbonate solutions but there is no information available on reactions of Cl₂⁻ or SO₄⁻ radicals with any of the Pu species which may be postulated to be present. The published data on the reactivity of these radicals indicates that they are both oxidants and could therefore be expected to provide important paths for the distribution of Pu oxidation states.

While there have been only a limited number of reactions of e⁻(aq) and Pu ions in near neutral or basic solutions, apparently systematic reactivity patterns provide some additional insight. For example, it has been noted that the second order rate parameters (M⁻¹s⁻¹) for the reactions of Np(VI) and Np(V) (11) (pH=6) are respectively $(5.4 \pm 0.2) \times 10^{10}$ and $(2.13 \pm 0.03) \times 10^{10}$. The values of the second order rate parameters when Am(VI) and Am(V) are the oxidants (12) are $(3.9 \pm 0.9) \times 10^{10}$ and $(3.18 \pm 0.08) \times 1810$. So one can predict that the value for $k(e^-(aq) + Pu(V))$ at pH=6 would be $3 \pm 1 \times 10^{10} \text{ M}^{-1}\text{s}^{-1}$.

The conclusion to be drawn is that the data set of kinetic information on reactions of Pu ions in solution with primary products of H₂O radiolysis needs to be substantially augmented. The steady radiolysis studies that have been and are currently out are of immediate pragmatic value. It is imperative that selected rate data for reactions in aqueous

systems that can be used to model the aquatic reservoir be obtained.

Acknowledgment

The skillful and dedicated collaborative efforts of members of the ANL Chemistry Division Radiation Chemistry Group, S. Gordon, W. Mulac and K. H. Schmidt have provided not only the technical expertise but also continuing intellectual stimulation which has made the pulse radiolysis studies possible.

Literature Cited

1. This work was performed under the auspices of the Office of Basic Energy Sciences, Division of Chemical Sciences, U. S. Department of Energy, under contract number W-31-109-ENG-38.
2. Transuranium Elements, NNES, IV-14-B, 1944, p. 334.
3. Draganic, I. G. and Draganic, Z. D. "The Radiation Chemistry of H₂O"; Academic Press: New York, 1941.
4. (a) Newton, T. W. "The Kinetics of the Oxidation-Reduction Reactions of Uranium, Neptunium, Plutonium and Americium in Aqueous Solutions"; National Technical Information Service, U. S. Department of Commerce: Springfield, Virginia, 1975. (b) Buxton, G. V. and Sellers, R. M. "The Radiation Chemistry of Metal Ions in Aqueous Solutions" in *Coordination Chemistry Reviews*, A. B. P. Lever, Ed., 1977, Vol. 22, pp. 195-274. (c) Miner, F. J. and Seed, J. R. Chem. Rev. 1967, 67, 299.
5. Fried, S.; Friedman, A.; Sullivan, J. C.; Nash, K.; Cohen, D. and Sjoblom, K. "Scientific Basis for Waste Management", Ed. Northrup, Jr, C. J. M., Plenum Publ. Co.: New York, 1980.
6. Soldano, J. E., Report of ANL Student Research Participation Program, Fall, 1981.
7. Meisel, D.; Mulac, W. and Sullivan, J. C., Inorg. Chem. 1981, 20, 4247.
8. Dorfman, L. M. and Adams, G. E., "Reactivity of the Hydroxyl Radical in Aqueous Solutions", NSRDS-NBS46, U. S. Government Printing Office: Washington, D.C., 1973.
9. See for example, Brosckiewicz, R. K.; Kozlaraska-Milner, E. and Blum, A., J. Phys. Chem. 1981, 85, 2258 and references therein.
10. Ross, A. B. and Neta, P. "Rate Constants for Reactions of Inorganic Radicals in Aqueous Solutions", NSRDS-NBS65, U. S. Government Printing Office, Washington, D.C., 1979.
11. Sullivan, J. C.; Gordon, S.; Cohen, D.; Mulac, W. and Schmidt, K., J. Phys. Chem. 1976, 80 1684.
12. Gordon, S.; Mulac W.; Schmidt, K. H.; Sjoblom R. K. and Sullivan, J. C., Inorg. Chem. 1978, 17, 294.

RECEIVED December 27, 1982

Stability Constants, Enthalpies, and Entropies of Plutonium(III) and Plutonium(IV) Sulfate Complexes

K. L. NASH and J. M. CLEVELAND

U.S. Geological Survey, Denver, CO 80225

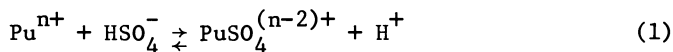
The physical nature of the sulfate complexes formed by plutonium(III) and plutonium(IV) in 1 M acid 2 M ionic strength perchlorate media has been inferred from thermodynamic parameters for complexation reactions and acid dependence of stability constants. The stability constants of 1:1 and 1:2 complexes were determined by solvent extraction and ion-exchange techniques, and the thermodynamic parameters calculated from the temperature dependence of the stability constants. The data are consistent with the formation of complexes of the form $\text{PuSO}_4^{(n-2)+}$ for the 1:1 complexes of both plutonium(III) and plutonium(IV). The second HSO_4^- ligand appears to be added without deprotonation in both systems to form complexes of the form $\text{PuSO}_4\text{HSO}_4^{(n-3)+}$.

Prediction of the chemistry of plutonium in near-neutral aqueous media is highly dependent on understanding reactions that may be occurring in such media. One of the most important parameters is the stability and nature of complexes formed by plutonium in its four common oxidation states. Because Pu(III), Pu(IV), and Pu(VI) are readily hydrolysed, complexation reactions generally are studied in mildly to strongly acidic media. Data determined in acid media (and frequently at high concentrations of plutonium) then are used to predict the chemical speciation of plutonium at near-neutral pH and low concentrations of the metal ion.

Several potentially important ground-water complexing ligands exist predominantly as protonated species in acidic media, while they are completely ionized at pH 7. An example of one such system is the sulfate-bisulfate system. At pH <2, the predominant species in aqueous solution is HSO_4^- , while above this pH, SO_4^{2-} is the dominant form of the ligand. Previous investigations of Pu(III) and Pu(IV) complexation by sulfate all have been in 0.5 to 2.0 M acid media (1-6). Interpretation of the data generally includes the assumption that complexation of plutonium by HSO_4^- is

This chapter not subject to U.S. copyright.
Published 1983, American Chemical Society

accompanied by ionization of HSO_4^- , according to the generic reaction:



In an attempt to verify (or refute) this assumption, we have determined the thermodynamic parameters (ΔH , ΔS) for the complexes formed between Pu(III), Pu(IV), and HSO_4^- in 1 M acid media utilizing cation-exchange and solvent extraction procedures.

Experimental

Reagents. All reagents used in this study were of reagent grade or better and were purified further by the following procedures. Thenoyltrifluoroacetone (TTA) was recrystallized twice from cyclohexane and protected from light and air after recrystallization. Hydroquinone (holding reductant for plutonium(III)) was purified by vacuum sublimation and also protected from light and air after sublimation. Stock solutions of H_2SO_4 and HClO_4 were prepared from Ultrex (7) ultrapure reagents. Both Na_2SO_4 and NaClO_4 were recrystallized from deionized water. Toluene used in the solvent extraction work was distilled prior to use, and all aqueous solutions were prepared in triply-distilled water. In the cation-exchange study of Pu(III) complexation, Dowex AG50X2 (20 to 50 mesh) cation-exchange resin was used, after being subjected to an extensive cleaning procedure, including washing with 15% H_2O_2 in 1 M NaOH, acetone, and 6 M HCl. Following a distilled-water wash to remove all traces of acid, the resin was dried at room temperature under mild vacuum and stored in a desiccator.

Procedures

Stability constants of the complexes formed between Pu(III), Pu(IV), and HSO_4^- were determined in 1 M acid media by measuring the decrease in extraction (either into TTA-toluene or ion-exchange resin) with increasing concentration of HSO_4^- in the aqueous solution. Because of very different degrees of extraction for Pu(III) and Pu(IV) and the imposed requirement of 1 M acidity, Pu(IV)- HSO_4^- complexation was studied by TTA extraction, while the Pu(III)- HSO_4^- system was studied by cation exchange.

Stock solutions of Na_2SO_4 and NaClO_4 were prepared by weight and standardized by passing several aliquots through a bed of Dowex AG50X8 (H^+ form) resin and titrating the generated acid with standardized NaOH. Stock solutions of H_2SO_4 and HClO_4 were standardized by titration with NaOH. In the solvent extraction study, TTA solutions were prepared by weight and pre-equilibrated with 1.0 M HClO_4 for at least 24 hours prior to use.

The plutonium stock solutions were prepared by dissolving 99.1% pure $^{239}\text{PuO}_2$ (0.9% $^{240}\text{PuO}_2$) in HNO_3 -HF solution. Aliquots of this stock were repeatedly taken to near-dryness in HClO_4 and

finally dissolved in 0.5 M HClO₄. This solution then was electrolytically reduced to Pu(III) and made chemically pure by loading onto a column of AG50X2 resin and washing with 0.5 M HClO₄. To prepare Pu(III) stocks, the plutonium was eluted from the column with 3 M HCl. For the preparation of Pu(IV) stocks, elution was performed with 8 M HNO₃. This elutriant then was made up to 0.1 M in NaNO₂ and allowed to equilibrate overnight. Oxidation-state purity was greater than 99% in each case, as determined by 0.5 M TTA extraction from 1.0 M HClO₄.

The Pu(III)-HSO₄⁻ stability constants were determined at 2.7, 10.0, 16.5, and 25.0°C using the following procedure. Approximately 1 gram of AG50X2 resin was introduced into each of 22 polyethylene vials. Five mL (milliliters) of 1.0 M HClO₄ (2 M ionic strength) solutions containing 0.0 to 1.0 M H₂SO₄ were pipetted into each of the vials (two blank vials and 20 different concentrations of H₂SO₄). Five hundred μ L (microliters) of 0.1 M hydroquinone were added to each, with enough Pu(III) for a total concentration of 3.3×10^{-8} M. These vials were capped and mixed on a rotating mixer in a water bath for 24 to 48 hours. After equilibrium was achieved, duplicate 1.0-mL samples of the aqueous phase were taken and counted by liquid scintillation. Replicate determinations were done at each temperature. In addition, one experiment was conducted using the same procedure with solutions at 2.0 M acidity.

In the Pu(IV) distribution experiments, 1.0 mL of each phase was contacted in a glass culture tube. Ten μ L of 1.0 M NaNO₂ and 10 μ L of the Pu(IV) stock were added to the aqueous phase to give total concentrations of 0.01 M NaNO₂, 0.074 M HNO₃, and 1.8×10^{-7} M plutonium. The phases were mixed vigorously for 2 minutes, centrifuged, and allowed to equilibrate in a constant-temperature (10.0, 25.0, and 35.0°C) water bath overnight; at 0.0°C, equilibration was for 5 days. Preliminary experiments indicated that equilibrium was achieved in this time. Two hundred microliter samples were taken from each phase and counted by liquid scintillation, to an average counting error of 1 to 3%. At the TTA concentrations used in these experiments (0.01 to 0.05 M), no quenching of the liquid scintillation by TTA was observed. Two sets of experiments were conducted at each temperature. The first set was to determine the solvent extraction equilibrium for the Pu(IV)-TTA system. In the second set of experiments, a constant concentration of TTA was equilibrated with a series of aqueous solutions at 1 M acidity, 2 M ionic strength, containing varying sulfate concentrations between 0.002 and 0.1 M. In all instances, duplicate experiments were run with good agreement between the sets. Mass balance (that is, plutonium accounted for in each vial) generally was greater than 95%.

Results and Discussion

Stability constants in each system were determined by measuring the distribution coefficient as a function of HSO₄⁻ concen-

tration. Mathematical treatment of the data is based on the method of Schubert (8), which has been described many times previously. In each system, data were represented adequately by considering the formation of only a 1:1 and 1:2 complex. The expression used to fit the data is given in equation 2.

$$1/D = 1/D_o + \beta_1/D_o \frac{[\text{HSO}_4^-]}{[\text{H}^+]^n} + \beta_2/D_o \frac{[\text{HSO}_4^-]^2}{[\text{H}^+]^m} \quad (2)$$

Data reduction was accomplished via non-linear regression formulae. Coefficients of the regression analysis are $A_0 = 1/D_o$, $A_1 = \beta_1/(D_o[\text{H}^+]^n)$, and $A_2 = \beta_2/(D_o[\text{H}^+]^m)$; where $n = m = 0$, if $\text{Pu}(\text{HSO}_4)_x^{(4-x)+}$ complexes are formed; $n = 1$ for PuSO_4^{2+} ; $m = 1$ for $\text{PuSO}_4\text{HSO}_4^+$; and $m = 2$ for $\text{Pu}(\text{SO}_4)_2$. The values for n and m are determined experimentally by repetition of complexation experiments as a function of acidity. The value of K_2 is determined as the ratio of A_2/A_1 , with appropriate correction for acidity ($K_2 = (A_2[\text{H}^+]^m)/(A_1[\text{H}^+]^n)$). A sample of the data for the $\text{Pu}(\text{III})\text{-HSO}_4^-$ and $\text{Pu}(\text{IV})\text{-HSO}_4^-$ systems is given in Table I.

The $\text{Pu}(\text{III})\text{-HSO}_4^-$ System. Data reduction in the $\text{Pu}(\text{III})\text{-HSO}_4^-$ system is complicated by the possibility that sulfate complexes of $\text{Pu}(\text{III})$ could be adsorbed by the resin. Because the mathematical treatment in the case of formation of a 1:1 complex is simpler, and any adsorption of the 1:2 complex is likely to be less than that for the 1:1 complex, equations applying to the limit $[\text{HSO}_4^-] \rightarrow 0$ (i.e., predominantly 1:1 complex in solution) were derived and applied to the appropriate data to evaluate the possibility of adsorption of the 1:1 complex. Assuming the 1:1 complex is PuSO_4^+ , the distribution coefficient in the limit of low $[\text{HSO}_4^-]$ is:

$$D = \frac{[\text{Pu}^{3+}]_r + [\text{PuSO}_4^+]_r}{[\text{Pu}^{3+}]_a + [\text{PuSO}_4^+]_a} \quad (3)$$

where the r subscript denotes species in the resin phase, and the a subscript denotes aqueous species. If we define $A = [\text{PuSO}_4^+]_r/[\text{PuSO}_4^+]_a$, and

$$\beta_1 = \frac{[\text{PuSO}_4^+][\text{H}^+]}{[\text{Pu}^{3+}]_a[\text{HSO}_4^-]} \quad (4)$$

equation 3 can be rewritten:

$$D = \frac{[\text{Pu}^{3+}]_r + (A\beta_1/[\text{H}^+]) [\text{Pu}^{3+}]_a[\text{HSO}_4^-]}{[\text{Pu}^{3+}]_a (1 + (\beta_1/[\text{H}^+])[\text{HSO}_4^-])} \quad (5)$$

Table I Sample data for stability constant determination

Pu(IV)-HSO ₄ ⁻		Pu(III)-HSO ₄ ⁻		Pu(III)-HSO ₄ ⁻	
[HSO ₄ ⁻]	1/D	[HSO ₄ ⁻]	1/D	[HSO ₄ ⁻]	1/D
0.0	0.0508	0.0	0.0608	0.0	0.0681
.002	.0784	.045	.0706	.045	.0758
.004	.1046	.091	.0820	.091	.0824
.006	.1570	.136	.0915	.136	.0867
.008	.2004	.182	.1000	.182	.0977
.010	.2490	.227	.1080	.227	.1034
.015	.3857	.273	.1224	.273	.1110
.020	.5949	.318	.1294	.318	.1196
.025	.8776	.364	.1420	.364	.1304
.030	1.012	.409	.1698	.409	.1379
.035	1.186	.454	.1832	.454	.1500
.040	1.594	.500	.1869	.500	.1514
.045	2.004	.545	.2050	.545	.1668
.050	2.544	.591	.2160	.591	.1860
.055	3.196	.636	.2331	.636	.1929
.060	3.823	.682	.2344	.682	.1935
.065	4.276	.727	.2484	.727	.2014
.070	4.616	.773	.2694	.773	.2067
.075	4.926	.818	.2769	.818	.2344
.080	5.612	.864	.3179	.864	.2389
.085	6.309			.909	.2500
.091	7.337				
.096	7.695				
.100	7.719				
HTTA = 0.050 <u>M</u>		HClO ₄ = 1.00 <u>M</u>		HClO ₄ = 2.00 <u>M</u>	
HClO ₄ = 1.00 <u>M</u>		I = 2.00 <u>M</u>		I = 2.00 <u>M</u>	
T = 25.0°C		T = 25.0°C		T = 25.0°C	
I = 2.00 <u>M</u>					

Define $D_o = [Pu^{3+}]_r/[Pu^{3+}]_a$ and $C = A/D_o$, separate the variables, and invert to get equation 6:

$$D_o/D = \frac{1 + (\beta_1/[H^+])[HSO_4^-]}{1 + (C\beta_1/[H^+])[HSO_4^-]} \quad (6)$$

Subtracting 1 from both sides of equation 6 yields:

$$(D_o/D - 1) = \frac{(\beta_1/[H^+])[HSO_4^-] - (C\beta_1/[H^+])[HSO_4^-]}{1 + (C\beta_1/[H^+])[HSO_4^-]} \quad (7)$$

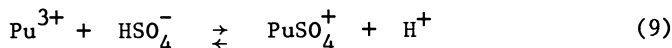
Removal of $[HSO_4^-]$ to the left side of equation 7 and inversion results in an equation having the general form of a straight line:

$$[HSO_4^-]/(D_o/D - 1) = \frac{[H^+]}{\beta_1(1-C)} + \frac{C}{1-C} [HSO_4^-] \quad (8)$$

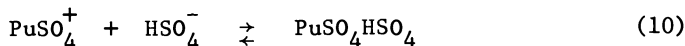
The coefficients can be determined by a plot of $[HSO_4^-]/(D_o/D - 1)$ vs. $[HSO_4^-]$.

Application of equation 10 to the experimental D vs. $[HSO_4^-]$ data determined at 25°C and both 1 and 2 M acidity yielded straight line plots with slopes indistinguishable from zero and reproduced the β_1 values determined in a non-linear regression fit of the data. This result implies no adsorption of $PuSO_4^+$ by the resin and justifies use of the simpler data treatment represented by equation 2. A similar analysis of the Th(IV)- HSO_4^- system done by Zielen (9) likewise produced results consistent with no adsorption of $ThSO_4^{2+}$ by Dowex AG50X12 resin.

Stability constants as a function of temperature and the calculated complexation enthalpies and entropies of the associated reactions are given in Table II. The results of duplicate experiments at 2.0 M acidity and ionic strength are shown as the last entry in the table. Comparison of the results at 25°C, and 1.0 and 2.0 M acidity indicate an approximate inverse first order stoichiometry in $[H^+]$ for the K_1 and acid independence for K_2 . The postulated reactions in this medium are given in equations 9 and 10.



and



DeCarvalho and Choppin (10, 11) previously have reported the stability constants, complexation enthalpies, and entropies for a series of trivalent lanthanide and actinide sulfates. As their work was conducted a pH 3, the dominant sulfate species was SO_4^{2-} and the measured reaction was as in equation 12.

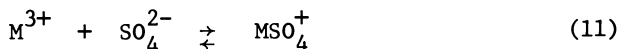


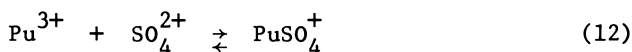
Table II Pu(III)-HSO₄⁻ stability constants, enthalpies, and entropies, for the reactions represented by equations 9 and 10, (I = 2.00 M; [HClO₄] = 1.00 M)

Temperature (degrees Celsius)	K ₁	K ₂
2.7	4.25 (+ 0.33)	0.92 (+ 0.10)
10.0	4.06 (+ 0.47)	0.80 (+ 0.14)
16.5	3.92 (+ 0.54)	0.67 (+ 0.14)
25.0	3.57 (+ 0.26)	0.36 (+ 0.08)
25.0*	2.17 (+ 0.26)	0.41 (+ 0.12)

*HClO₄ = 2.00 M.

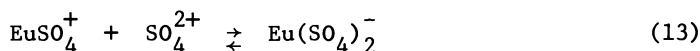
$$\begin{array}{ll} \Delta G_1 = -3.15 (\pm 0.18) \text{ kJ/m} & \Delta G_2 = +2.53 (\pm 0.62) \text{ kJ/m} \\ \Delta H_1 = -5.2 (\pm 1.0) \text{ kJ/m} & \Delta H_2 = -28.1 (\pm 6.4) \text{ kJ/m} \\ \Delta S_1 = -6.8 (\pm 1.4) \text{ J/m}^\circ\text{K} & \Delta S_2 = -102 (\pm 34) \text{ J/m}^\circ\text{K} \end{array}$$

To compare the present results with those of DeCarvalho and Choppin, our results in 1 M acid must be corrected for the heat and entropy of HSO₄⁻ ionization. Zebroski et al. (12) determined K_a = 0.084, while Zielen (9) gives the heat of ionization as ΔH_a = +23.2 kJ/m. The calculated entropy is ΔS_a = +98 J/m-°K. The thermodynamic parameters for the reaction



calculated from our results are K₁ = 42.5 (+ 13.2), ΔH₁ = +18 (+ 1.7) kJ/m, and ΔS₁ = +91 (+ 13) J/m-°K. The corresponding parameters determined by DeCarvalho and Choppin are in the range: K₁ = 12.2(Lu) - 27(Am), ΔH₁ = +15.5 - 18.8 kJ/m, ΔS₁ = +77 - 88 J/m-°K. The agreement, particularly in the enthalpies and entropies, is quite good and tends to support our interpretation of the equilibrium represented in equation 9.

DeCarvalho and Choppin report the values K₂ = 4 (+ 1), ΔH₂ = 10.0 (+ 1.0) kJ/m, and ΔS₂ = 47 (+ 7) for the reaction



If we assume a similar reaction for the formation of Pu(SO₄)₂⁻ the corresponding parameters are K₂ = 4.3 (± 2), ΔH₂ = -4.9 (+ 1.2) kJ/m, and ΔS₂ = -4.0 (+ 1.6) J/m-°K. While the calculated value of K₂ agrees with the Eu(SO₄)₂⁻ results, the enthalpy and entropy are of opposite sign, indicating that Eu(SO₄)₂⁻ is not a good model for the 1:2 Pu³⁺ - sulfate complex formed in 1 - 2 M acid media. This result we interpret as support for the conclusion represented by equation 10.

Previous investigations of the Pu(III)-sulfate system in 1 - 2 M acid media have produced results in which the authors do not agree on either the nature of the complexes or the magnitude of the stability constants (4-6). Both Fardy and Buchanan (4) and Vasudeva Rao et al. (5) interpret their data in terms of the complexes PuSO_4^+ and $\text{Pu}(\text{SO}_4)_2^-$. Fardy and Buchanan report $K_1 = 3.65$ (± 0.21) and $K_2 = 3.3$ (± 0.39), while Vasudeva Rao et al. find $K_1 = 6.64$ (± 0.14) and $K_2 = 0.79$ (± 0.08). The former results give a K_1/K_2 ratio of 1.1, which is much lower than normally is observed for stepwise addition of the same ligand (DeCarvalho and Choppin found $K_1/K_2 \sim 6$ in the Ln^{3+} , $\text{An}^{3+}-\text{SO}_4^{2-}$ system). While the K_1/K_2 ratio found by Vasudeva Rao et al. ($K_1/K_2 = 8.4$) is in reasonable agreement with that of DeCarvalho and Choppin, the calculated stability constant for the reaction represented by equation 12 is 79, a factor of 3 higher than that of AmSO_4^+ .

The interpretation of both of these papers requires the existence of an anionic complex. The authors attempted to confirm this possibility by electromigration, anion exchange, and amine extraction. Fardy and Buchanan found in their anion exchange and electromigration experiments that the existence of anionic Pu(III)-sulfate species could not be confirmed by either method. Vasudeva Rao et al., attempted to establish the existence of anionic species in their experiments by performing a series of amine extractions. For the extraction of Pu(III) by Primene JM-T, they observed an increase in the distribution coefficient of $\sim 1.3 \times 10^6$ for 0.1 M H_2SO_4 over the extraction from 0.1 M HClO_4 . While this increase indeed implies the existence of anionic Pu(III)-sulfate complexes, their existence almost certainly is promoted by the presence of the amine. A calculation of the speciation of Pu(III) in 0.1 M H_2SO_4 (using their stability constants) indicates 59% Pu^{3+} , 38% PuSO_4^+ , and only 3% $\text{Pu}(\text{SO}_4)_2^-$. In both instances, the existence of $\text{Pu}(\text{SO}_4)_2^-$ must be viewed with some skepticism.

Nair et al. (6) investigated this system by cation exchange (at 1 M ionic strength and acidity) and interpreted the results in terms of the species PuSO_4^+ and $\text{Pu}(\text{HSO}_4)_2^+$ with $K_1 = 18.13$ (± 0.44) and $K_2 = 9.94$ (± 0.24). The assignment of these two species is based on a computer fit of the data (at 1 M acidity) and the observation of no anionic species in electromigration and anion exchange studies. An analysis of our data (at two different acidities) assuming the formation of $\text{Pu}(\text{HSO}_4)_2^+$ in addition to PuSO_4^+ and $\text{PuSO}_4\text{HSO}_4$, indicates the possible existence of $\text{Pu}(\text{HSO}_4)_2^+$ ($\beta_2 \sim 0.25$). However, the uncertainty in this assignment is great due to the error associated with K_2 and the fact that only two acidities are used in the investigation. Pending further experimentation, we conclude that the dominant form of the 1:2 complex in this medium is $\text{PuSO}_4\text{HSO}_4$.

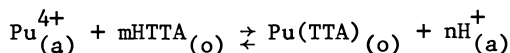
The Pu(IV)-HSO₄⁻ System. In the Pu(IV)-HSO₄⁻ system, a series of preliminary experiments was necessary to establish the stoichiometry of the TTA extraction process with respect to $[\text{H}^+]$ and

[HTTA]. This was done by varying the concentration of each independently. Results of this investigation are given in Table III. With the exception of the acid dependence at 10.0°C and the TTA dependence at 35.0°C, the slope of the Log K vs. Log [H⁺] or Log [HTTA] plots are within 3% of the theoretical value of 4.0. The low TTA dependence at 35.0°C probably is attributable to dissolution of TTA in the aqueous phase. Observation of fourth-power dependence on acidity argues against any change in the extraction mechanism (e.g., Pu(IV) reduction or NO₃⁻ involvement). An aqueous Pu(TTA)₃⁺ complex has been reported (14, 15) and this possibility has been considered in the error analysis of the Pu(IV)-sulfate stability constants.

To verify the integrity of the extraction system in the presence of bisulfate, an experiment was run in which the TTA stoichiometry was determined at constant acidity and two different concentrations of HSO₄⁻. At 0.015 M HSO₄⁻, the Pu(IV)-TTA stoichiometry was 3.79 (+ 0.25); while at 0.07 M HSO₄⁻, the stoichiometry was 3.84 (+ 0.33). Both values are in agreement with observed stoichiometries in the absence of HSO₄⁻.

Stability constants, enthalpies, and entropies determined in the Pu(IV)-HSO₄⁻ system are presented in Table IV. The enthalpy and entropy for each of the complexation steps were determined by a van't Hoff plot of the stability constant data. These stability constants include a correction for nitrate complexing of Pu(IV) [(K₁ = 2.88 (13)): [NO₃⁻] = 0.074 M]. Error limits of the stability constants are 2σ values and reflect the uncertainty in K_{ex}, and the nitrate complex formation constant and any contribution due to the aqueous Pu(TTA)₃⁺ complex.

Table III Extraction equilibria for the reaction



Temperature (degrees Celsius)	n	m	Log K _{ex} [*]
0.0	4.04 (+ 0.13)	3.87 (+ 0.05)	6.992 (+ 0.047)
10.0	3.73 (+ 0.04)	3.89 (+ 0.08)	6.813 (+ 0.048)
25.0	3.99 (+ 0.09)	3.84 (+ 0.07)	6.622 (+ 0.097)
35.0	3.94 (+ 0.02)	3.45 (+ 0.03)	6.449 (+ 0.107)

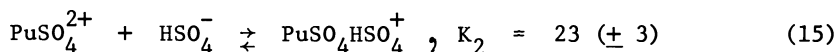
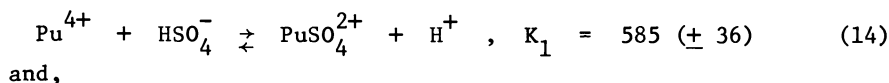
$$*K_{\text{ex}} = \frac{[\text{Pu}(\text{TTA})_4] [\text{H}^+]^4}{[\text{Pu}^{4+}] [\text{HTTA}]^4}$$

Table IV Pu(IV)-HSO₄⁻ stability constants, enthalpies, and entropies, (I = 2.00 M; [HClO₄] = 1.00 M)

Temperature (degrees Celsius)	K ₁	K ₂
0.0	285 (+ 46)	44 (+ 6)
10.0	385 (+ 35)	30 (+ 4)
25.0	585 (+ 36)	23 (+ 3)
35.0	713 (+ 76)	18 (+ 3)

$$\begin{aligned} \Delta G_1 &= -15.8 (+ 0.2) & \Delta G_2 &= -7.8 (+ 0.3) \text{ kJ/m} \\ \Delta H_1 &= 18.5 (+ 0.6) \text{ kJ/m} & \Delta H_2 &= -17.6 (+ 3.1) \text{ kJ/m} \\ \Delta S_1 &= 115 (+ 23) \text{ J/m-}^\circ\text{K} & \Delta S_2 &= -33 (+ 7) \text{ J/m-}^\circ\text{K} \end{aligned}$$

One of several studies of this system shows remarkable agreement with the present results. Fardy and Pearson (3) investigated this system by cation exchange at 2 M acidity and ionic strength and reported uncorrected stability constants $\beta_1 = 278 (+ 8)$ and $\beta_2 = 6.8 (+ 0.2) \times 10^3$ ($K_2 = 24$). Assuming the difference in the medium (2 M HClO₄ vs. 1 M NaClO₄, 1.0 M HClO₄) has a minimal effect on the activities of the various complexes, Pu⁴⁺, and HSO₄⁻, this result combined with our results at 1 M acidity indicates an inverse first power stoichiometry in [H⁺] for the 1:1 complex, and acid independence in the formation of the second complex. If we assume $n = m = 1$ in equation 2, the equilibria and associated stability constants in this system are given in equations 14 and 15.



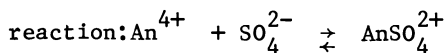
In addition to the results of Fardy and Pearson, at least two previous investigations of the Pu(IV)-sulfate system have produced stability constants in substantial agreement with our results. Rabideau and Lemons (1) determined potentiometrically the association constant for Pu⁴⁺ and SO₄²⁻ as $K_1 = 4.61 (+ 0.09) \times 10^3$ (assuming $K_a = 0.24$) in 1 M HCl. The calculated stability constant for Pu⁴⁺ and HSO₄⁻ is 1.1×10^3 . Bagawde et al. (2) determined by TTA extraction the values (I = 2 M NaClO₄) $\beta_1 = 676 (+ 29)$ and $\beta_2 = 4.77 (+ 0.10) \times 10^4$ (assuming both the 1:1 and 1:2 complexes are deprotonated on complex formation). If we assume that the second complex is monoprotonated, the values

$K_1 = 676 (+ 29)$ and $K_2 = 35.2 (+ 3.0)$ are calculated. While these are somewhat higher than our results, the K_1/K_2 ratio of 19 is in reasonable agreement with that of our study ($K_1/K_2 = 25$).

Stability constants, enthalpies, and entropies have been published for both the 1:1 and 1:2 sulfate complexes of the Th^{4+} (9, 12), U^{4+} (16), and Np^{4+} (17) (Table IV). Only in the thorium system have stability constants been determined as a function of acidity. Zebroski et al., (12) found that the 1:2 complex had the form $\text{Th}(\text{SO}_4)_2$ at 0.5 M and 1.0 M acidity but suggested a contribution from the monoprotonated, bis-sulfato complex in 2 M acid. However, Zielen (9) found no evidence for such a species. The K_1/K_2 ratio found in the latter study (~ 8) compares favorably with the $\text{Am(III)}-\text{SO}_4^{2-}$ data of DeCarvalho and Choppin (10) ($K_1/K_2 \sim 7$) and suggests Zielen's interpretation is correct in the thorium sulfate system. The increasing K_1/K_2 ratio for U^{4+} (~ 15) Np^{4+} (~ 24), and Pu^{4+} (~ 25) is consistent with our interpretation of the existence of the complex $\text{AnSO}_4\text{HSO}_4^+$. Why this species should become increasingly important with increasing atomic number is not understood.

In contrast to the situation observed in the trivalent lanthanide and actinide sulfates, the enthalpies and entropies of complexation for the 1:1 complexes are not constant across this series of tetravalent actinide sulfates. In order to compare these results, the thermodynamic parameters for the reaction between the tetravalent actinide ions and HSO_4^- were corrected for the ionization of HSO_4^- as was done above in the discussion of the trivalent complexes. The corrected results are tabulated in Table V. The enthalpies are found to vary from +9.8 to +41.7 kJ/m and the entropies from +101 to +213 J/m²K. Both the enthalpy and entropy increase from U^{4+} to Pu^{4+} with the ThSO_4^{2+} parameters being similar to those of NpSO_4^{2+} . Complex stability is derived from a very favorable entropy contribution implying (not surprisingly) that these complexes are inner sphere in nature.

Table V Stability constants, enthalpies, and entropies for the



An	β_1	ΔH_1	ΔS_1
Th	1.98×10^3	20.9	133
U	3.93×10^3	9.8	101
Np	3.21×10^3	18.3	128
Pu	6.96×10^3	41.7	213

Literature Cited

1. Rabideau, S. W.; Lemons, J. F. J. Am. Chem. Soc. 1951, 73, 2895.
2. Bagawde, S. V.; Ramakrishna, V. V.; Patil, S. K. J. Inorg. Nucl. Chem. 1976, 38, 1339.
3. Fardy, J. J.; Pearson, J. M. J. Inorg. Nucl. Chem. 1974, 36, 671.
4. Fardy, J. J.; Buchanan, J. M., J. Inorg. Nucl. Chem. 1976, 38, 579.
5. Vasudeva Rao, P. R.; Bagawde, S. V.; Ramakrishna, V. V.; Patil, S. K. J. Inorg. Nucl. Chem. 1978, 40, 123.
6. Nair, G. M.; Rao, C. L.; Welch, G. A. Radiochim. Acta 1967, 7, 77.
7. Use of trade names is for descriptive purposes only and does not imply endorsement by the U.S. Geological Survey.
8. Schubert, J. J. J. Phys. Coll. Chem. 1948, 52, 340.
9. Zielen, A. J. J. Am. Chem. Soc. 1959, 81, 5022.
10. DeCarvalho, R. G.; Choppin, G. R. J. Inorg. Nucl. Chem. 1967, 29, 725.
11. DeCarvalho, R. G.; Choppin, G. R. J. Inorg. Nucl. Chem. 1967, 29, 737.
12. Zebroski, E. L.; Alter, H. W.; Heumann, F. K. J. Am. Chem. Soc. 1951, 73, 5646.
13. Martell, A. E.; Smith, R. M. "Critical Stability Constants, Volume 4--Inorganic Ligands"; Plenum Press: New York, 1977, p. 49.
14. Poskanzer, A. M.; Foreman, B. M., Jr. J. Inorg. Nucl. Chem. 1961, 16, 323.
15. Badawde, S. V.; Ramakrishna, V. V.; Patil, S. K. J. Inorg. Nucl. Chem. 1976, 38, 2085.
16. Day, R. A., Jr.; Wilhite, R. N.; Hamilton, F. D. J. Am. Chem. Soc. 1955, 77, 3180.
17. Sullivan, J. C.; Hindman, J. C. J. Am. Chem. Soc. 1954, 76, 5931.

RECEIVED December 21, 1982

Photochemistry of Aqueous Plutonium Solutions

J. T. BELL, L. M. TOTH, and H. A. FRIEDMAN

Oak Ridge National Laboratory, Chemical Technology Division,
Oak Ridge, TN 37830

Aqueous plutonium photochemistry is briefly reviewed. Photochemical reactions of plutonium in several acid media have been indicated, and detailed information for such reactions has been reported for perchlorate systems. Photochemical reductions of Pu(VI) to Pu(V) and Pu(IV) to Pu(III) are discussed and are compared to the U(VI)/(V) and Ce(IV)/(III) systems respectively. The reversible photoshift in the Pu(IV) disproportionation reaction is highlighted, and the unique features of this reaction are stressed. The results for photoenhancement of Pu(IV) polymer degradation are presented and an explanation of the post-irradiation effect is offered.

The authoritative documents on plutonium (1,2) do not include photo-chemical reactions of plutonium in aqueous systems. The first papers in Western world literature on studies that were dedicated to aqueous plutonium photochemistry appeared in 1976 (3,4), even though photochemical changes in oxidation states were indicated as early as 1952 (5,6,7). Other reasons for investigating plutonium photochemistry in the mid-seventies included the widely known uranyl photochemistry and the similarities of the actinyl species, the exciting possibilities of isotope separation or enrichment, the potential for chemical separation or interference in separation processes for nuclear fuel reprocessing, the possible photoredox effects on plutonium in the environment, and the desire to expand the fundamental knowledge of plutonium chemistry.

0097-6156/83/0216-0263\$06.00/0

© 1983 American Chemical Society

Burger and coworkers (5) in 1952 reported that some distribution coefficients for PuO_2^{2+} in organic-aqueous systems at lighted conditions were different from those observed for dark conditions, and those authors believed that some PuO_2^{2+} had been photochemically reduced. That reduction was confirmed by others (6) in 1965, and in 1969 a report suggested that most aqueous plutonium reactions were affected by light (7).

Studies of actinide photochemistry are always dominated by the reactions that photochemically reduce the uranyl, U(VI) , species. Almost any UV-visible light will excite the uranyl species such that the long-lived, $\sim 10^{-4}$ seconds, excited-state species will react with most reductants, and the quantum yield for this reduction of UO_2^{2+} to UO_2^+ is very near unity (8). Because of the continued high level of interest in uranyl photochemistry and the similarities in the actinyl species, one wonders why aqueous plutonium photochemistry was not investigated earlier.

Isotope photoseparation techniques for actinides probably will include only gaseous systems, hexafluorides and metal vapors. Hence, aqueous actinide photochemistry is not likely to influence isotope separations. However, the intense interest in laser separation techniques for the gaseous systems promotes interest in the aqueous systems.

The possible application of aqueous plutonium photochemistry to nuclear fuel reprocessing probably has been the best-received justification for investigating this subject. The necessary controls of and changes in Pu oxidation states could possibly be improved by plutonium photochemical reactions that were comparable to the uranyl photochemistry.

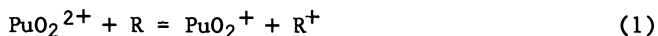
The primary reason for studying aqueous plutonium photochemistry has been the scientific value. No other aqueous metal system has such a wide range of chemistry; four oxidation states can co-exist (III, IV, V, and VI), and the Pu(IV) state can form polymer material. Cation charges on these species range from 1 to 4, and there are molecular as well as metallic ions. A wide variety of anion and chelating complex chemistry applies to the respective oxidation states. Finally, all of this aqueous plutonium chemistry could be affected by the absorption of light, and perhaps new plutonium species could be discovered by photon excitation.

Visible and UV spectrophotometric techniques are most convenient for studying the polymer and various oxidation states of plutonium. The spectra of the plutonium states and the procedure for resolution of the concentrations were previously described (9). Changes in the relative concentrations of the oxidation states and of the polymer generally are determined from corresponding changes in the spectra and a comparison of the changes to standard spectra of the various states. These techniques have been used exclusively for studying the photochemistry of aqueous plutonium.

Only the obvious studies of aqueous plutonium photochemistry have been completed, and the results are summarized below. The course of discussion will follow the particular photochemical reactions that have been observed, beginning with the higher oxidation states. This discussion will consider primarily those studies of aqueous plutonium in perchloric acid media but will include one reaction in nitric acid media. Aqueous systems other than perchlorate may affect particular plutonium states by redox reactions and complex formation and could obscure photochemical changes. Detailed experimental studies of plutonium photochemistry in other aqueous systems should also be conducted.

Photochemical Reduction of Aqueous Plutonium (VI)

Plutonium VI exists in solution as the molecular plutonyl ion, PuO_2^{2+} . The structure of this ion is essentially the same as that of the uranyl ion, but the plutonyl ion is much less stable than the uranyl ion. The greater stability of the uranyl species results from its having only 12 bonding electrons which exactly fill the bonding orbitals of the actinyl molecular orbital model, while the plutonyl ion has the 12 bonding electrons plus two non-bonding electrons (10). The two extra electrons in the plutonyl system are energetically favored as unpaired in the two lowest nonbonding orbitals, and the ground state for the plutonyl ion is a triplet state. From theoretical considerations, one would predict that Pu(VI) would be reduced to Pu(V) when excited by light and reacted with a mild reducing agent such as ethanol. Stronger reducing agents such as nitrous acid would directly reduce Pu(VI), and the stronger agents should be avoided in the photochemical experiments. The reaction



where R is an agent with reducing potential similar to ethanol, does not proceed in dark conditions. However, the reaction was observed when the aqueous perchlorate system was exposed to UV light [3]. Both PuO_2^+ and Pu^{4+} were observed after the UV irradiation, (Fig. 1), and the spectra showed that PuO_2^+ was initially formed and then disproportionated to form Pu^{4+} . A quantum yield of 0.02 was determined for reaction 1 and was reported to be a low value, perhaps by as much as a factor of 10, because of interfering reactions. The low quantum yield relative to that for the similar UO_2^{2+} reaction is likely related to the short life-time of the excited-state PuO_2^{2+} . The lowest-level, excited triplet state of UO_2^{2+} has an unusually long lifetime of $\sim 10^{-4}$, which is ample time for reaction with a reductant that is either associated with the UO_2^{2+} ion or that is an unassociated species in the same solution. One

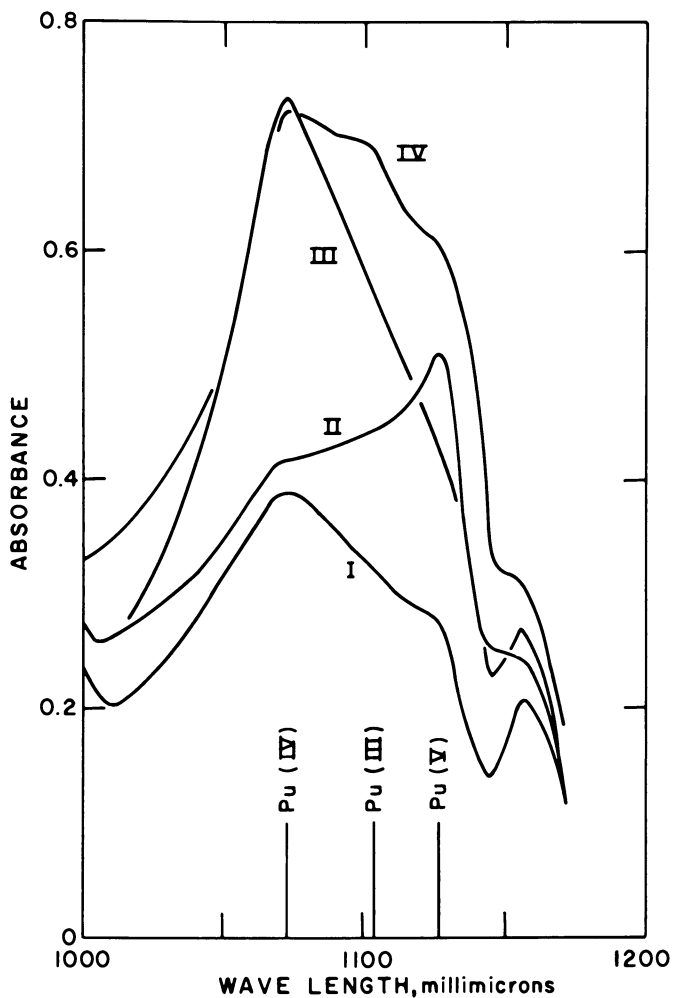


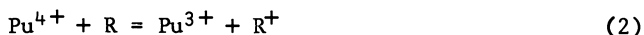
Figure 1.

Plutonium spectra showing the photoreduction of plutonyl. (I) 0.385 M PuO_2^{2+} , some Pu^{4+} and 1.5 M ethanol in 1.32 M HClO_4 . (II) Immediately after the first UV irradiation. (III) Twenty-four hours after the first UV irradiation. (IV) Immediately after the second and 25 h after the first UV irradiations (3).

can speculate on the basis of continuities in the actinyl spectra (10) that the UV absorption by PuO_2^{2+} involves the excitation of a bonding electron to a non-bonding level, producing an excited-state species with two or four unpaired electrons that would have a very short lifetime. Thus only a low fraction of the excited-state species would react with other solution components. This theory is supported only by the similarities to the actinyl ions and is subject to correction by experimental efforts.

Photochemical Reduction of Aqueous Plutonium(IV)

Plutonium(IV), in perchloric acid with ethanol present, is stable under dark conditions but produces Pu(III) when the solution is exposed to UV light. A quantum yield of 0.03 was reported (3) for the reaction,



where R^{\dagger} was an intermediate oxidized ethanol species. When the reductant is ethanol, formic acid, or formate, there is no dark-state reaction. When a stronger reductant is used, such that the dark state reaction progresses slowly, the addition of UV light increases the reaction rate. For example, hydrazine will slowly reduce Pu(IV), and the addition of UV photons will appreciably increase the reaction rate.

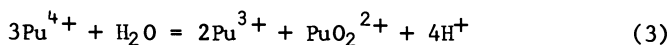
Some unpublished and more recent work by these authors examined the photoreduction of Pu(IV) in nitric acid solution that contained hydrazine. That reduction was shown to occur with or after the formation of a Pu(IV) peroxy complex. This complex is responsible for the enhanced rates of Pu(IV) reduction in dark periods following the photolysis. The photolysis of HNO_3 in the presence of N_2H_4 produces H_2O_2 , which then complexes with Pu(IV); it is known that H_2O_2 does not appear in the photolysis of pure HNO_3 solutions, and its formation in the presence of N_2H_4 demonstrates some of the complex chemistry associated with N_2H_4 solutions. This may have useful application, because the peroxy complex of Pu(IV) is reduced at a faster rate with N_2H_4 than is the uncomplexed Pu ion.

The Pu(IV) to (III) aqueous photolysis can be compared to the Ce(IV) to (III) light-sensitive reactions, although Pu(IV) is a much weaker oxidizing agent than Ce(IV). The Ce(IV)/Ce(III) couple has a standard reduction potential of 1.7 V in HClO_4 , while the comparable potential for the Pu(IV)/Pu(III) couple is 0.98 V. In HClO_4 solutions, UV light and Ce(IV) will oxidize H_2O with a quantum yield of 0.14, but the similar reaction with Pu(IV) has not been reported. With the low reduction potential, it is not likely to occur. An interesting feature of the photoreduction of Ce(IV) to Ce(III) is the stability of Ce(III), which

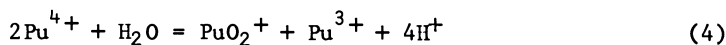
enables the Ce(IV)-(III) equilibrium to be easily studied. Conversely, Pu(III) is relatively unstable and generally requires a holding reductant, making the Pu(IV)-(III) equilibrium more difficult to study, even without considering the experimental problems associated with radioactivity. Therefore, even though Pu(IV) has a more interesting solution chemistry because of more interactions with ligands and aqueous media, it is unlikely that the photochemical reduction of Pu(IV) to Pu(III) will ever receive the attention already given to the cerium system.

Photo Shift in the Pu(IV) Disproportionation

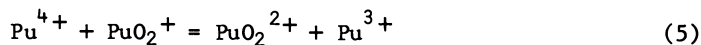
The disproportionation reaction of Pu(IV) is generally written as



This overall reaction was shown more than three decades ago (11) to include at least two separate reactions: the relatively slow reaction,



and the fast electron-exchange reaction,



After observing the photochemical reduction of Pu(VI) and Pu(IV), it seems obvious that reaction (3) should be light-sensitive. However, it is not obvious how photons would affect the equilibrium concentrations of the plutonium species. The experimental results [3,4] are very interesting and are described below, but a complete explanation is yet to be developed.

The UV illumination of carefully selected solutions of 10^{-2} M Pu(IV) in 0.5 M HClO₄ significantly increased the disproportionation rate and shifted the equilibrium in favor of Pu³⁺, PuO₂²⁺, and acid. Those effects are shown in Fig. 2. The reaction proceeded at 22°C for 27 h in dark conditions and was not near equilibrium. The sample was exposed several times for 1 h periods. After each exposure, there was a significant decrease in the Pu(IV) concentration and stoichiometrically equal increases in the Pu(III) and Pu(VI) concentrations. After dark-condition equilibrium was established, as indicated by the visible spectra, the photo-shift in equilibrium was observed to be completely reversed when the illumination ceased. This photogalvanic effect maintained a mass balance in the system, with no reagent consumed or generated during the dark-light-dark cycle. This observation suggested that the plutonium system in the proper network of a concentration cell

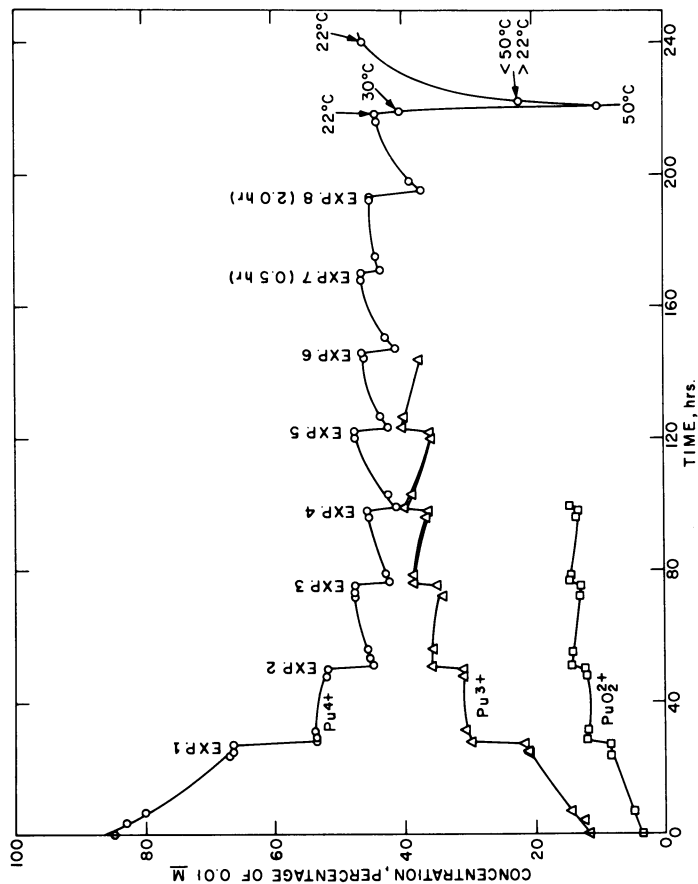


Figure 2.
 The effects of UV light on the disproportionation of Pu(IV) are demonstrated by the rapid decrease in Pu(IV), and corresponding increase in Pu(III) and Pu(IV). A reversible shift in the equilibrium is obvious from the return to dark condition concentrations after each exposure. The effects of increasing temperature are compared (3).

could convert light into an e.m.f. without the expenditure of chemical reactants or the generation of chemical products.

Later experiments (4) were designed to determine a cell e.m.f. for the plutonium disproportionation system with a particular light source. Concentration quotients for the light and dark conditions, Q_e and Q_d , were determined, and an energy difference of 1.65 kcal (32 mV) was calculated by the relation $-RT \ln Q_e/Q_d$. This reversible photochemical shift may be the only single-element system known at this time and certainly is the simplest such system. Even though the radioactive properties could prevent development and utilization of a plutonium photoconversion system, these studies certainly suggest that similar nonradioactive and more acceptable systems could be discovered and developed.

Consideration of where the light effect occurs in the disproportionation mechanism is an interesting exercise. The effect is two-fold in increasing the reaction rate and in reversibly shifting the reaction. Since reaction (4) is rate controlling, and assuming that the rate of reaction (5) is so fast that a photoeffect to increase that rate would not be observed by the mild illumination in the experiments, we suggest that the initial photoeffect is excitation of the Pu(IV) species. Then the rate and the degree of the reaction for the excited-state species are greater than that for the non-excited state species.

Photo Effects on Degradation of Pu(IV) Polymer

Plutonium(IV) polymer is a product of Pu(IV) hydrolysis and is formed in aqueous solutions at low acid concentrations. Depolymerization generally is accomplished by acid reaction to form ionic Pu(IV), but acid degradation of polymer is strongly dependent on the age of the polymer and the conditions under which the polymer was formed (12). Photoenhancement of Pu(IV) depolymerization was first observed with a freshly prepared polymer material in 0.5 M HClO₄, Fig. 3 (3). Depolymerization proceeded in dark conditions until after 140 h, 18% of the polymer remained. Four rather mild 1-h illuminations of identical samples at 5, 25, 52, and 76 h enhanced the depolymerization rates so that only 1% polymer remained after the fourth light exposure (Fig. 3).

An enhancement in depolymerization rate after the light was turned off was also observed. This continued enhancement was very obvious after the exposures at 25 and 52 h, and is believed to represent relatively fast depolymerization of small polymer particles which were fragmented from larger particles during illumination.

Enhancement of depolymerization rates for aged polymer (polymer with high degree of PuO₂ character (13) were observed

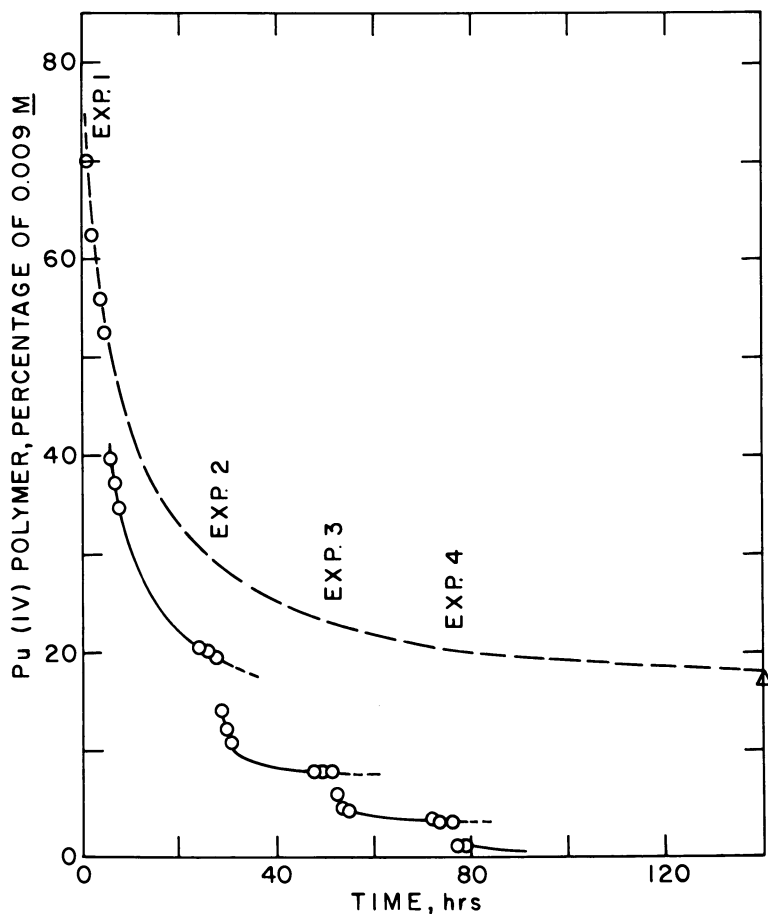


Figure 3.

The effects of four 1 h, low intensity, UV light exposures to enhance the degradation of freshly prepared Pu(IV) polymer. The darkened line represents depolymerization under dark conditions. The solution contained 0.0093 M total Pu and 0.47 M HClO₄ at 22°C (3).

at a later time (4)). Polymer materials which had been age-stabilized by time and temperature were partially depolymerized in three acid solutions and with almost continuous illumination. Plots of percent polymer versus exposure time are shown in Fig. 4, and are there compared with the corresponding amounts of polymer remaining under dark conditions. The photo-enhancement of Pu(IV) depolymerization is clearly established for polymer aged both by time and temperature.

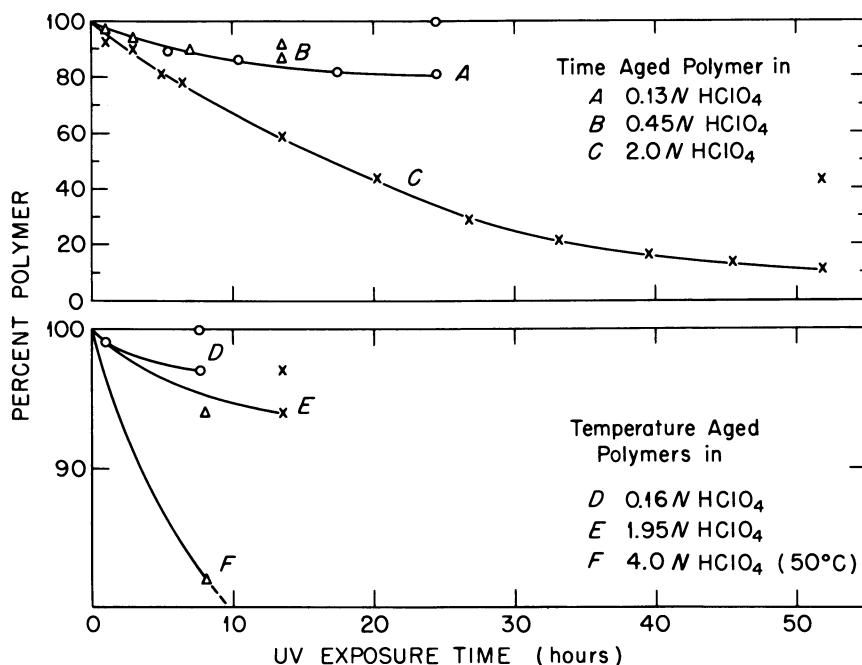


Figure 4:

The effects of UV irradiation to enhance the degradation of aged Pu(IV) polymer in HClO₄. Depolymerization under dark conditions for each experiment is shown by a data point directly above the last light sample point (4).

Concluding Remarks

Several notable photochemical reactions have been observed for aqueous plutonium systems. Only the perchlorate system has been described in detail, and the effects of complexing ligands and various reducing agents are not known. The effects of self radiolysis have not been compared to direct photochemistry of plutonium chemistry. However, these effects generally change the aqueous medium, and the radiolysis products of the medium then react with the plutonium. In studies considered herein, the direct absorption of UV light by plutonium in aqueous media and the subsequent chemistry of this excited state plutonium have overwhelmed the effects of self radiolysis. Application of aqueous plutonium photochemistry probably will remain limited to nuclear fuel processing, as discussed in a recent publication (14). However, the most important consideration of plutonium photochemistry may be with respect to plutonium in the environment, where the transport rates would be dependent on its oxidation states and complexing reactions.

Acknowledgments

Research sponsored by the Division of Material Sciences, Office of Basic Energy Sciences, U.S. Department of Energy under contract W-7405-eng-26 with the Union Carbide Corporation.

Literature Cited

1. Cleveland, J. M. "The Chemistry of Plutonium"; Gordon and Breach: New York; 1970.
2. Wick, O. J. "The Plutonium Handbook"; Vol. I. Gordon and Breach: New York; 1967.
3. Bell, J. T.; Friedman, H. A. J. Inorg. Nucl. Chem. 1976, 38, 83.
4. Friedman, H. A.; Toth, L. M.; Bell, J. T. J. Inorg. Nucl. Chem. 1977, 39.
5. Burger, L. L.; Rehn, I. M.; Slansky, C. M. USAEC Report, HW-19949; 1952.
6. Mazumar, A. S. Ghosh; Sivarmakrishnan, C. K. J. Inorg. Nucl. Chem. 1965, 27, 2423.
7. Palei, P. N.; Nemodruk, A. A.; Berzogova, E. V. Radiochimik 1967, 11, 30.
8. Bell, J. T.; Billings, M. R. J. Inorg. Nucl. Chem. 1975, 37, 2529.
9. Costanzo, D. A.; Biggers, R. E.; Bell, J. T. J. Inorg. Nucl. Chem. 1973, 35, 609.
10. Bell, J. T. J. Inorg. Nucl. Chem. 1969, 31, 703.
11. Connick, R. E. J. Am. Chem. Soc. 1949, 71, 1528.

12. Toth, L. M.; Osborne, M. M. "Further Aspects of Pu(IV) Hydrous Polymer Chemistry," Symposium on the Chemistry of Plutonium, American Chemical Society Meeting, Kansas City, Missouri, September 1982.
13. Johnson, G. L.; Toth, L. M. "Plutonium(IV) and Thorium(IV) Hydrous Polymer Chemistry," ORNL/TM-6365, 1978.
14. Bell, J. T.; Toth, L. M. Radiochimica Acta 1978, 25, 225.

RECEIVED December 21, 1982

Behavior of Plutonium in Natural Waters

BERT ALLARD

Chalmers University of Technology, Department of Nuclear Chemistry,
S-41296 Göteborg, Sweden

JAN RYDBERG¹

Lawrence Livermore National Laboratory, Livermore, CA 94550

The use of nuclear power leads to waste streams containing plutonium. The large scale of plutonium production combined with the high radiotoxicity of this element makes it mandatory to understand how plutonium behaves in nature, particularly how it will migrate in water and be taken up by living species. The paper reviews the plutonium sources, the relevant chemistry of natural waters, and what plutonium species are expected to be formed. Measurements of interaction between natural solid materials (clay, rock, etc) and plutonium dissolved in natural waters are used to show the low environmental risk associated with storage of large amounts of plutonium in repositories located in deep granite bedrock.

The large and widespread production of plutonium in nuclear power stations combined with its high radiotoxicity has caused great public concern about "plutonium poisoning". Consequently, the spread of plutonium in the environment has been extensively studied for several decades. The results have been reported in journals and more recently in a number of monographs and conference proceedings (e.g. 1-7).

Except for large scale accidental releases (e.g. nuclear explosions or catastrophic accidents at nuclear plants), water will be the main transport medium of plutonium to man. Therefore the size and location of plutonium sources, its pathways to man and its behaviour in natural waters are essential knowledge required for the evaluation of its ecological impact. That information, combined with radiological health standards, allows an assessment of the overall risk to the public from plutonium e.g. from a waste repository for spent unprocessed reactor fuel elements in deep granite bedrock (8, 9).

¹ Permanent address: Chalmers University of Technology, Department of Nuclear Chemistry, S-41296 Göteborg, Sweden.

0097-6156/83/0216-0275\$06.25/0
© 1983 American Chemical Society

Plutonium Sources

About 300 tonnes of plutonium (95% ^{239}Pu) are presently stored in nuclear weapons (6). Production figures for weapons grade plutonium are unknown, but they may be estimated to be <10 tonnes annually. Through weapons testing about 4.2 tonnes of plutonium have been injected into the atmosphere. Most of this plutonium has now been deposited on the ground. Further, 1.4 tonnes have been directly deposited in the ground through surface and sub-surface tests (6).

The nuclear power industry (270 nuclear reactors in 25 countries in mid-1982) now has a capacity of 200 GWe, which corresponds to an approximate annual plutonium production of 50 tonnes. The amount of plutonium accumulated from the industry is estimated to be ~ 250 tonnes. The specific activity is 5.3×10^{11} Bq/g Pu for fresh spent fuel, mostly coming from ^{241}Pu (6, 10). It is predicted that by the year 2000, the accumulated plutonium will amount to 2400 tonnes (6).

Reprocessing is now done in about 10 plants in at least 8 countries (11). For an assumed annual reprocessing capacity of 20 tonnes of plutonium, about 100 kg may end up in the waste streams; the true global value may be somewhat higher. The global amount of plutonium entering the sea through low-level effluents is believed to be below 0.1 kg/y (4).

All plutonium produced must be prevented from spreading into the environment. It is presently believed that the safest way is to store plutonium waste in deep underground facilities, and several such are now being constructed (8, 9, 12, 13). In the future, however, releases of various sizes must be anticipated, considering the large amounts of plutonium being handled. The hazards associated with such releases must be reliably assessed.

Plutonium Distribution Coefficients

Plutonium, deposited on soil, moves downwards with a rate which depends on precipitation and soil properties. In dry, sandy areas, the downward rate may be 1 mm/year, while in rainy areas it may be 10 times higher (3). The rate is considerably reduced in clay soil.

The pathway of plutonium dissolved in natural water, from a source such as a nuclear facility, to man, may be quite complicated. During the transport, the plutonium atoms encounter dissolved and particulate inorganic and organic matter, as well as minerals in rocks, sediment and soil, and living organisms which may metabolize the plutonium. Figure 1 depicts some of the more essential routes for plutonium between the point of emission and the plutonium consuming man. The overall effect of these pathways is that plutonium is slowly eliminated from the water, so that only a minor fraction of it reaches man. An example of this is that of the 4.2 tonnes of plutonium deposited on the earth after

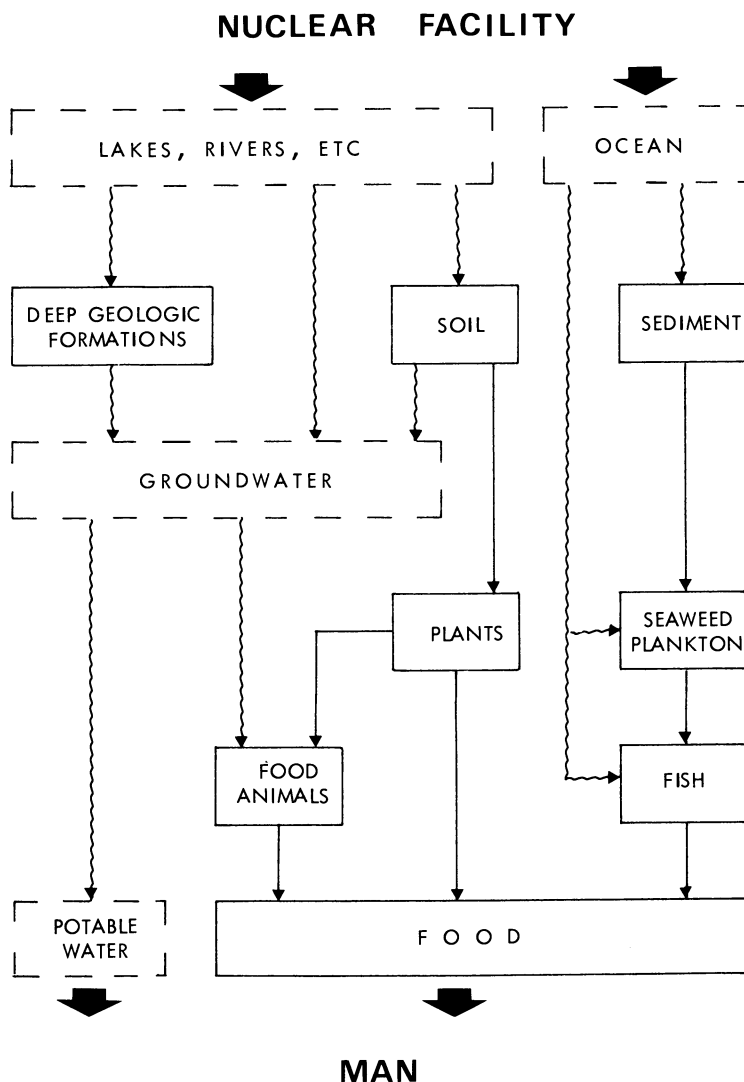


Figure 1.
Pathways of dissolved plutonium from a nuclear facility to man.
Dashed squares and wavy lines refer to predominantly liquid
compartments and flows.

atmospheric nuclear explosions, only 0.25 g of plutonium has found its way into the world population (6).

In Figure 1 dashed squares refer to water bodies, while solid squares refer to solid matter (also containing some water). Plutonium may appear in any of these squares. The ratio of the concentration of plutonium in two adjacent squares is usually referred to as the concentration factor (CF; usually from the water to the solid substance), the transfer coefficient (TC; usually between two biological species), or the sorption ratio (or K_d ; between minerals and water). To avoid ambiguity, we shall use the expression distribution coefficient (abbreviated Kd) with unit dimension (Pu amount per kg product divided by Pu amount per kg source). For the transfer of plutonium from A to B, $\text{Pu}(A) \rightarrow \text{Pu}(B)$, we define

$$Kd = [\text{Pu}]_B / [\text{Pu}]_A$$

Table I summarizes some typical distribution coefficients. Sediments become enriched in plutonium with respect to water, usually with a factor of $\sim 10^5$. Also living organisms enrich plutonium from natural waters, but usually less than sediments; a factor of $10^3 - 10^4$ is common. This indicates that the Kd-value for sediment (and soil) is probably governed by surface sorption phenomena. From the simplest organisms (plankton and plants) to man there is clear evidence of metabolic discrimination against transfer of plutonium. In general, the higher the species is on the trophic level, the smaller is the Kd-value. One may deduce from the Table that the concentration of plutonium accumulated in man in equilibrium with the environment, will not exceed the concentration of plutonium in the ground water, independent of the mode of ingestion.

The Table shows a great spread in Kd-values even at the same location. This is due to the fact that the environmental conditions influence the partition of plutonium species between different valency states and complexes. For the different actinides, it is found that the Kd-values under otherwise identical conditions (e.g. for the uptake of plutonium on geologic materials or in organisms) decrease in the order $\text{Pu} > \text{Am} > \text{U} > \text{Np}$ (15). Because neptunium is usually pentavalent, uranium hexavalent and americium trivalent, while plutonium in natural systems is mainly tetravalent, it is clear from the actinide homologue properties that the oxidation state of plutonium will affect the observed Kd-value. The oxidation state of plutonium depends on the redox potential (Eh-value) of the ground water and its content of oxidants or reductants. It is also found that natural ligands like CO_3^{2-} and fulvic acids, which complex plutonium (see next section), also influence the Kd-value.

Composition of Natural Waters

Water contains dissolved and particulate inorganic and organic matter. To distinguish between dissolved and particulate matter a 0.45 μm pore size filter is often used to separate the fractions.

Table I. Distribution (Kd) of plutonium between different compartments of the ecosystem. Experimental range is indicated by \pm .

Transport from > to	log Kd	Ref.
Water > Sediment		
Pacific Ocean (Enewetak)	5.0 \pm 1.5	29
Irish Sea (Windscale)	4.8 \pm 0.6	29
Lake Michigan	5.5	16
White Oak Lake (Tennessee)	4.7 \pm 0.8	15
Hudson River	4.8	16
Water > Organisms		
White Oak L. (Tenn.) > seaweed	4.3	15
" > sediment species	3	15
Lake Michigan > phytoplankton	4.0	15,30
" > zooplankton	2.5	15,30
" > plant eating fish	1.5	15,30
" > fish eating fish	0.4 \pm 0.6	15,30
White Oak Lake (Tenn.) > fish	0.1 \pm 0.5	15
Irish Sea > fish	0.1	29
Pacific Ocean (Enewetak) > fish	3.7 \pm 2.3	29
Lake Michigan > coastal plants	3.3 \pm 0.4	15,30
" > coastal animals	3.1 \pm 0.2	15,30
Sediments > water organisms (a)		
> algae	2 \pm 2	15
> phytoplankton	-1.5	15
> zooplankton	-3.0	15
> plant eating fish	-2.3 \pm 0.7	15
Sediment, soil, sludge > plants		
Sediment (L. Michigan) > coastal plants	-1.1 \pm 0.3	15
Soil (b) > trees	-4.2	14
" > soybean	-2.7	14
" > tomato	-4.0	14
Soil (California) > wheat grain	-6.2 \pm 0.8	31
Sludge (c) > corn	-5.5	32
" > broccoli	-3.8	32
" > tomato	-4.1	32
Food > animals		
Sediment (L. Mich.) > coastal animals	-1.2 \pm 0.3	15
Vegetation (d) > cotton rats	-0.9	33
Lichen (Lappland) > reindeer	-5.2 \pm 0.3	34
Food (Pu as oxide or hydroxide) > man	-5	35
" (Pu in other common forms) > man	-4	35
" (Pu-citrate) > man	-3	36

(a) Refers to Lake Michigan, where log Kd for water > sediment is 5.5. (b) Western U.S. floodplain. (c) Waste sludge from sewage treatment plant. (d) Savannah River Plant (S. Carolina), where log Kd for soil > rat is -1.9.

The amount of particulate matter varies from very high values in silt carrying rivers (the Mississippi River carries an average of 2600 mg/liter at flood time) to practically zero (0.05 mg/liter; ref. 17) in the ocean. A typical value may be 1-10 mg/liter. The mineral particles often consist of clay with ion exchange properties.

Considering the variety of sources for organic material, a great diversity in the concentration of particulate organic matter occurs; however, it is usually less than a few percent of the total particulate matter, except in areas of excessive human contamination. A typical value for estuarine waters would be 5 mg/liter of particulate organic matter (18). The organic material has the functional groups $-COOH$, $-OH$ and $-NH_2$, which may complex metals at its surface.

When the water becomes stagnant, the particulate matter settles as bottom sediments. In this process it carries with it considerable amounts of plutonium, if any has been dissolved in the water (see Table I).

Table II summarizes analytical data for dissolved inorganic matter in a number of natural water sources (8, 9, 19, 20, 21). Because of the interaction of rainwater with soil and surface minerals, waters in lakes, rivers and shallow wells (<50m) are quite different and vary considerably from one location to another. Nevertheless, the table gives a useful picture of how the composition of natural water changes in the sequence rain → surface water → deep bedrock water in a granitic environment. Changes with depth may be considerable as illustrated by the Stripa mine studies (22) and other recent surveys (23). Typical changes are: an increase in pH and decrease in total carbonate (coupled), a decrease in O_2 and Eh (coupled), and an increase in dissolved inorganic constituents. The total salt concentration can vary by a factor of 10-100 with depth in the same borehole as a consequence of the presence of strata with relict sea water. Pockets with such water seem to be common in Scandinavian granite at >100 m depth.

Rain in equilibrium with atmospheric CO_2 , but uncontaminated by industrial emissions, should have a pH of 5.7. However, atmospheric pollution from burning fossil fuels has resulted in acid rain of pH as low as 3.5 (24). If this condition continues for a long time, it may lead to a change in groundwater composition, which may considerably change the migration of plutonium in nature.

A great diversity in the concentration of dissolved organic matter also occurs in natural water. Commonly, the concentration ranges from 0.5 to 50 mg/liter. Fresh water and seawater typically have values of 0.5-1.5 mg/liter (18).

About half of the dissolved organic carbon may appear in humic or fulvic acids. These are high-molecular weight organic compounds of a composition which is somewhat uncertain. They contain aromatic hydroxyl and carboxyl groups which have the ability to bind to metal ions. Rivers and estuaries typically contain 10 mg/liter of acid with an exchange capacity of 5-10 mmol/g, mainly due to carboxylic

Table II. Composition of natural waters.

Analysis	Units	Rainwater	Surface water (a)	Bedrock water (b)	Ocean
Depth	m	0	0-50	≈500	0-20
Age	years	0	≈10	≈100	
pH		4-6	7.3-8.4 (7.9)	7-10	8.1
Eh	volts	0.9	0.0-0.3	-0.05	0.8
O ₂	mg/liter	10	1-10	<0.1	≈9
Na ⁺	mg/liter	0.3-20	1-20 (12)	10-100 (d)	10,766
K ⁺	mg/liter	0.1-4	0.3-8 (4)	1-5	399
Ca ²⁺	mg/liter	0.5-5	2-100 (25)	20-60	413
Mg ²⁺	mg/liter	0.1-0.5	3-30 (10)	15-30	1292
Fe (total)	mg/liter		0.1-1	5-30	<0.02
F ⁻	mg/liter		≈0.1	0.5-2	1.4
Cl ⁻	mg/liter	0.1-20	0.5-90 (10)	5-50 (d)	19,353
Br ⁻	mg/liter				67
CO ₃ ²⁻ (total) (c)	mg/liter	≈1	60-200	5-400	≈140
NO ₃ ⁻	mg/liter	0.1-4	≈10	<1	<0.7
PO ₄ ³⁻ (total)	mg/liter	0	≈0.1	≈0.1	≈0.1
SO ₄ ²⁻ (total)	mg/liter	≈20 (1-5)	3-300 (20)	1-15	2712
SiO ₂ (total)	mg/liter	0	3-15	5-30	0.01-7
SH ⁻ (e)	mg/liter	0	0	<1	
NH ₃ (e)	mg/liter	≈0.5	<0.1	<0.5	<0.05
Organic carbon	mg/liter		1-50	<1	≈1

(a) Lakes, rivers and shallow wells; values outside this range are not uncommon; typical values within parenthesis, (b) Swedish granite, (c) Mainly as HCO₃⁻ (d) For relict water, the value may be 500-3000 mg/liter, (e) SH⁻ and NH₃ only occur in reducing waters (Eh<0), except for surface waters in industrial areas.

Table III. Selected complex formation constants for plutonium (at 25°C and I=0) (41).

Ligand, L	Species, Pu_xL_y	$\log K_{x,y}$			
		Pu^{3+}	Pu^{4+}	PuO_2^+	PuO_2^{2+}
OH^-	(1,1)	6.0	13.5	4.6	8.3
	(1,2)	11.0	25.5		16.0
	(1,3)	15.5	36.0		
	(1,4)	19.0	45.5		
	(1,5)		50		
	(2,2)	14	27		22.5
	(3,5)	37			54.5
CO_3^{2-}	(1,1)	6.5		(5)	10.0
	(1,2)	11.0		(9)	16.7
	(1,3)	14.5		(14)	23.8
	(1,5)		(37)		
	(2,3)				
	(3,6)				60.5
HPO_4^{2-}	(1,1)	(6)	13.0		8.4
	(1,2)		23.8		18.5
	(1,3)		33.4		
H_2PO_4^-	(1,1)	2.4	4.5		3.0
	(1,2)		8.9		5.5
F^-	(1,1)	4.3	8.6	3.7	5.7
	(1,2)	7.6	14.5		11.1
	(1,3)	10.8	19.1		15.9
	(1,4)		23.6		18.8
	(1,5)		25.3		
SO_4^{2-}	(1,1)	3.5	5.6	2	3.0
	(1,2)	5.2	10.3		4.3

Solubility products ($\log K_s$):

$\text{Pu}(\text{OH})_3$	-23.5	$\text{Pu}(\text{HPO}_4)_2$	-27
PuO_2	-54	PuO_2HPO_4	-12.6
$\text{PuO}_2(\text{OH})$	- 8.8	PuPO_4	-23
$\text{PuO}_2(\text{OH})_2$	-23.0	$(\text{PuO}_2)_3(\text{PO}_4)_2$	-23.5
$\text{Pu}_2(\text{CO}_3)_3$	-31	PuF_3	-10.2
PuO_2CO_3	-13.8	PuF_4	-24

groups (18); thus with respect to binding capacity the acids are 0.05–0.1 mM in the water. Molecular weights of 2000–6000, and values up to 10,000 have been suggested (20, 25), indicating that each molecule may contain 10–100 reactive groups, many probably with chelating ability.

Humic acid precipitates at salt concentrations >0.05 M and pH <4 , while the fulvic acids are still soluble. Thus, humic acid is hardly ever found in salt water (~ 0.5 M). Titration experiments with alkali indicate that there are consecutive steps of deprotonization. A typical average pK_a -value would be 7 (26), and for a selected humic acid values of 4 and 9 are given for pK_{a1} and pK_{a2} (27, 28).

Plutonium Complexes with Natural Complexing Agents

All the oxidation states III, IV, V and VI can exist in aqueous solutions in the Eh-pH-range of environmental interest (37). Strong complexes are formed between plutonium and oxygen containing ligands (O^{2-} , OH^- , CO_3^{2-} , etc.) as well as F^- but not with S^{2-} . The complex strength increases with the effective charge of the acceptor ion, i.e. in the order $Pu^{4+} > PuO_2^{2+} > Pu^{3+} > PuO_2^+$.

Several recent compilations and critical evaluations of data on plutonium redox and complex chemistry are available (e.g. 38–42). However, experimental data on plutonium complexes with e.g. CO_3^{2-} , HPO_4^{2-} , OH^- , etc. are scarce and many of the suggested formation constants are merely extrapolated or even estimated data, e.g. from comparisons with the similar elements thorium, uranium, neptunium and americium. The uncertainty even in measured formation constants is usually a factor of at least 2 to 3, and often up to orders of magnitude for the higher complexes. Moreover, the existence of many of the suggested plutonium species has never been experimentally verified. Still, in any discussion of speciation and solubility in natural systems it is imperative that all relevant species are considered. Thus, it is justified, and necessary, to include estimated or extrapolated data for poorly studied species and even data for non-identified plutonium species that are likely to exist. Some selected complex formation constants which could be valid for plutonium are given in Table III (41), considering the major complexing anions in natural waters (Table II). Selected standard potentials are given in Table IV (41).

Table IV. Selected standard potentials (V) (41)

$Pu^{4+} + e^- = Pu^{3+}$	1.01
$PuO_2^{2+} + 4H^+ + e^- = Pu^{4+} + 2H_2O$	1.10
$PuO_2^{2+} + 4H^+ + 2e^- = Pu^{4+} + 2H_2O$	1.03
$PuO_2^{2+} + e^- = PuO_2^+$	0.96

Little is known about actinide complexation by humic or fulvic acids although $\log \beta_1$ -values for Am^{3+} , Th^{4+} and UO_2^{2+} with humic acid at pH 4.0-4.5 as 6.8, 11.0 and 5.8, respectively, are reported (43).

Plutonium Solubility and Speciation in Natural Waters

Several attempts to calculate plutonium solubility and speciation in environmental systems are given in the literature (e.g. 39, 41, 44-47). Considering the anion concentration ranges in natural waters (Table II) and the magnitude of the corresponding plutonium stability constants (Table III), the chemistry of plutonium, as well as that of uranium and neptunium, is almost entirely dominated by hydroxide and carbonate complexation, considering inorganic complexes only (41, 48, 49).

In Figure 2 the solubility and speciation of plutonium have been calculated, using stability data for the hydroxy and carbonate complexes in Table III and standard potentials from Table IV, for the waters indicated in Figure 2. Here, the various carbonate concentrations would correspond to an open system in equilibrium with air (b) and closed systems with a total carbonate concentration of 30 mg/liter (c,e) and 485 mg/liter (d,f), respectively. The two redox potentials would roughly correspond to water in equilibrium with air (a-d; cf 50) and systems buffered by an $\text{Fe(III)(s)}/\text{Fe(II)(s)}$ -equilibrium (e,f), respectively. Thus, the natural span of carbonate concentrations and redox conditions is illustrated.

Under oxic conditions, the solubility of plutonium is limited by $\text{PuO}_2(\text{s})$ with Pu(OH)_4 as the dominating species in solution in the intermediate pH-range 6-9. At a pH below 5-6 the pentavalent PuO_2^+ would dominate and below pH 3-4, Pu^{3+} would be the major species. At high carbonate concentrations pentavalent carbonate species like $\text{PuO}_2(\text{CO}_3)_3^{5-}$ would dominate in the high pH-range (above 8-9). Hexavalent species would not contribute significantly.

Under reducing conditions the solubility limiting species would still be $\text{PuO}_2(\text{s})$ at high pH (above 7-8) but $\text{Pu}_2(\text{CO}_3)_3(\text{s})$ in the low pH-range. Trivalent species would dominate in the pH-range of environmental interest (up to pH 9-10). The overall solubility of plutonium would be considerably higher under reducing conditions than in oxic systems, in the presence of carbonate. Any of the oxidation states III, IV or V could be obtained.

Previously, it has been suggested (39) that $\text{PuO}_2(\text{s})$ would be comparatively stable in terrestrial waters in most pH and redox potential ranges. Solutions in equilibrium with $\text{PuO}_2(\text{s})$ or $\text{Pu(OH)}_4(\text{s})$ are claimed to contain PuO_2^+ as the dominating species under oxic conditions and at pH below 6-7, according to recent results (50). These experimentally determined solubilities are in general agreement with the calculated curves a-d in Figure 2. Also the possible reduction to the trivalent state in nature by dissolved organic substances (14, 15, 51) at low or intermediate pH-values has been suggested.

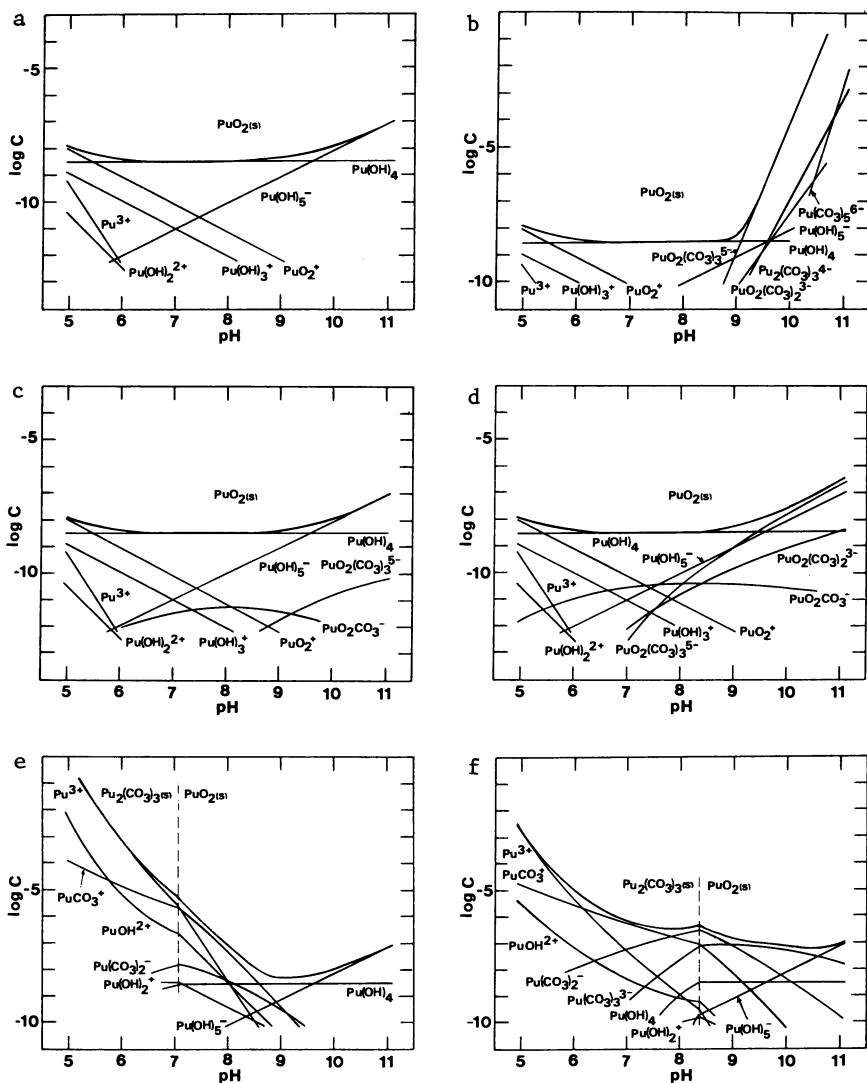


Figure 2.

Plutonium solubilities (M) and species in solution (41). (a) Carbonate free. (b) Equilibrium with atmospheric carbon dioxide; $p(\text{CO}_2) = 10^{-3.5}$ atm. (c,e) Total carbonate 0.5 mM (30 mg/liter). (d, f) Total carbonate 8 mM (485 mg/liter). (a,b, c,d) Aerated systems; $E_h = 0.8 - 0.06\text{pH}$. (e,f) Water containing Fe(II); $E_h = 0.2 - 0.06\text{pH}$.

The existence of plutonium with an oxidation state of V (or VI) in neutral solutions or at high pH and in the presence of carbonate was previously observed (51). It has also been suggested that Pu(V) is the dominant oxidation state in sea-water and that Pu(VI) is rapidly reduced to Pu(V) in these waters (52).

However, it has been concluded from sorption and diffusion experiments that plutonium exists largely in the tetravalent state (53) and clearly not as Pu(V), in the intermediate pH-range under oxic conditions and at low carbonate concentration. This would be representative of many groundwaters and also in agreement with the calculated curves of Figure 2.

The strong plutonium complexing ability of humic acids is illustrated by the uptake of plutonium on Oak Ridge soil, from which it could not be eliminated either by leaching with mild acids or strong complex formers like citrate or EDTA (14). However, considering the reported concentration ranges of humic acid in natural waters and their pK_a -values (see above) and assuming a $\log \beta_1$ -value of <13 for a Pu(IV)-humic acid complex, the maximum possible concentration of plutonium bound to humic acid would be negligible in natural waters of pH above 6-7. At low pH (below 5-6), however, humic complexes may constitute a large, or even dominating, fraction (this is almost certainly true at $pH < 4$). This could be the case in surface waters percolating through organic soil layers.

Plutonium Sorption on Geologic Media

In general, three basic kinds of sorption mechanisms for trace elements in geologic aqueous systems can be distinguished (56). Due to non-specific forces of attraction between sorbent and the solute, a physical adsorption may occur. This sorption mechanism results in the binding of species from the solution in several consecutive layers on exposed solid surfaces. This would be a rapid non-selective and reversible process, fairly independent of nuclide concentration and only little dependent on ion exchange capacity of the solid.

In the case of action of specific chemical forces between sorbent and solute a chemisorption process may result. This process could be regarded as a complex formation reaction and would be specific and selective, concentration dependent, possibly slow and partly irreversible.

The most frequent type of interaction between solid and species in solution would be electrostatic adsorption (ion exchange), due to the action of attractive coulomb forces between charged particles in solution and the solid surfaces. This process would also be concentration dependent.

For plutonium in the tri- and tetravalent state, when hydrolysis would dominate the solution chemistry, most sorption phenomena in geologic systems can be looked upon largely as physical adsorption processes. Ion exchange processes, as defined above, would be

less significant except for non-complexed species (at low pH). The sorption is highly dependent on the degree of hydrolysis, leading to a drastically enhanced sorption when the pH increases into the region where hydrolysis is expected (56, 57, 58). Also neutral or even negatively charged hydroxy species are strongly sorbed e.g. on oxide and silicate surfaces.

In the presence of mineral phases containing anions that would form sparingly soluble compounds (e.g. PO_4^{3-} and F^- for the lower oxidation states) an enhanced plutonium uptake due to chemisorption can be expected (57). For plutonium in the higher oxidation states the formation of anionic carbonate complexes would drastically reduce the sorption on e.g. oxide and silicate surfaces.

The sorption of plutonium on a variety of the common minerals of igneous rocks under groundwater conditions is illustrated in Figure 3 (57, 58, 59). For comparison the sorption of other actinides in discrete oxidation states (Am(III), Th(IV), Np(V), U(IV)) is given in Figure 4, to illustrate the non-existence of a predominant Pu(V) species under these conditions (53).

Plutonium uptake on geologic media under various conditions have been studied extensively during the last few years, and reviewed (e.g. in ref. 60). It should be emphasized that data from various experiments are rarely directly comparable, due to differences in experimental techniques, chemical conditions and other parameters of importance. A detailed discussion of sorption data is outside the scope of this paper.

Formation of Plutonium Colloids

Many highly charged cations have a large tendency to form polymeric hydroxides. This is particularly true for tetravalent actinides (61). Hydroxy colloids may be regarded as highly polymerized species with large residual charges, which due to electrostatic repulsion prevent them from aggregation. Thus, an apparent solubility, which can exceed the solubility product, may be achieved. It has been found that plutonium colloids have a strong tendency to sorb on exposed mineral surfaces (56, 62, 63, 64). However, at high pH stable species can be formed which carry a residual negative charge, leading to a decrease in their sorption.

Natural colloid particles in aqueous systems, such as clay particles, silica, etc. may serve as carriers of ionic species that are being sorbed on the particulates (pseudocolloids). It seems evident that the formation and transport properties of plutonium pseudocolloids can not yet be described in quantitative terms or be well predicted. This is an important area for further studies, since the pseudocolloidal transport might be the dominating plutonium migration mechanism in many environmental waters.

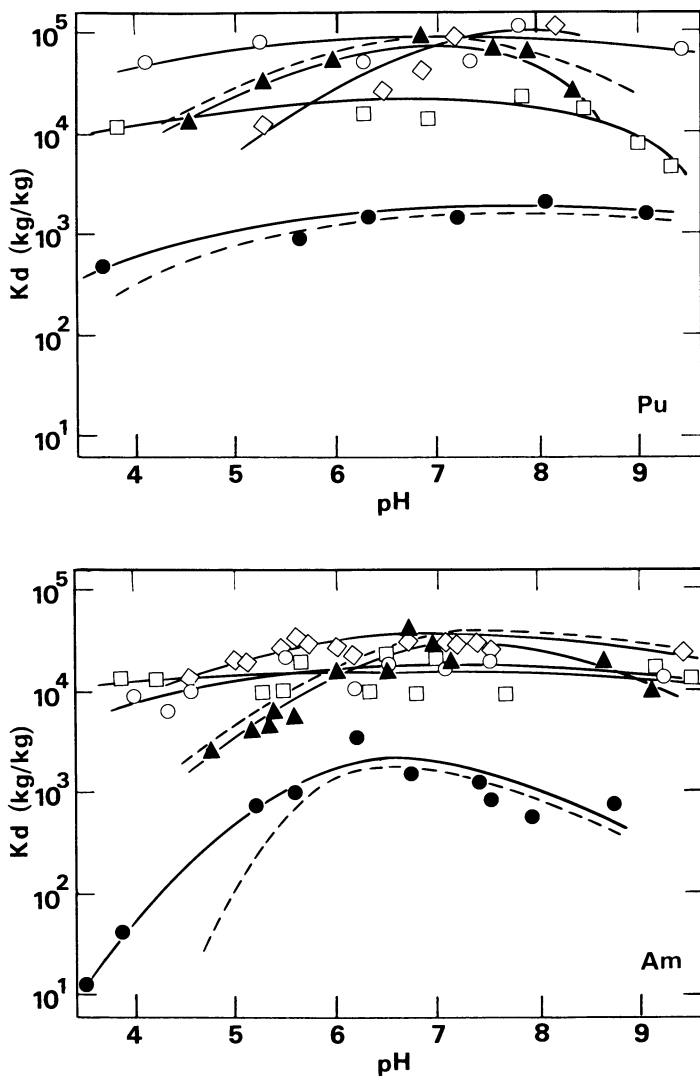


Figure 3.

Sorption of plutonium (1.8×10^{-11} M) and americium (2×10^{-9} M) in artificial groundwater (salt concentration 300 mg/liter; total carbonate 120 mg/liter; Ref. 59) on some geologic minerals. ● quartz, ▲ biotite, ○ apatite, ◇ attapulgite, □ montmorillonite. Dashed lines indicate the range for major minerals in igneous rocks. Experimental conditions: room temperature, particle size 0.04–0.06 mm, solid/liquid ratio 6–10 g/l, aerated system, contact time 6 days.

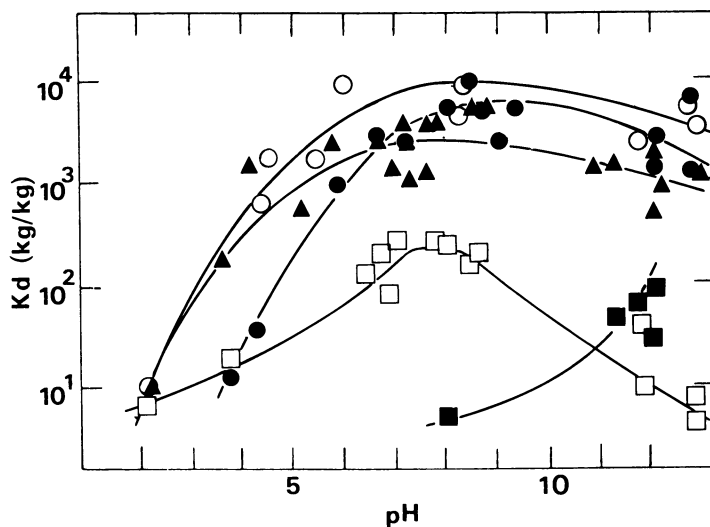


Figure 4.

Coefficients for distribution of Th(IV), U(VI), Np(V), Pu and Am(III) ($0.6\text{--}2.5 \times 10^{-9}$ M) between Al_2O_3 (or SiO_2) and 0.01M NaClO_4 (53). \circ Th(IV), \square U(VI), \blacksquare Np(V), \bullet Am(III) and \blacktriangle Pu. Experimental conditions: 25°C , particle size 0.090–0.125 mm, solid/liquid ratio 20g/l, aerated system, contact time 6 days.

Plutonium Repository in Deep Granite Bedrock

In 1976 the Swedish government stipulated that no new nuclear reactors should be charged until it had been shown how the radioactive waste products could be taken care of in an "absolutely safe manner" (8). Consequently, the nuclear power industry (through their joint Nuclear Fuel Supply Co, SKBF) embarked on a program referred to as the Nuclear Fuel Safety (KBS) Project (8). In one of the schemes (9) a repository for spent nuclear fuel elements in envisaged at a depth of 500 m in granitic bedrock. The repository will ultimately contain 6000 tonnes of uranium and ~ 45 tonnes of plutonium. The spent fuel elements will be stored in copper cylinders (0.8 m in diameter and 4.7 m in length) with a wall thickness of 200 mm; the void will be filled with lead.

A safety analysis (9) has shown that these cylinders should resist the reducing groundwater, which percolates through Swedish bedrock, for about 10^6 years. Still, the Swedish authorities have requested information about the consequences of the groundwater coming into contact with the plutonium.

The maximum concentration of plutonium at the border of the repository is set by Figure 2a-f. Because Swedish groundwater contains small amounts of Fe(II) it is usually reducing, corresponding to Figure 2e and 2f. Analyses of deep groundwater in granitic bedrock from various parts of Sweden have given pH values which are usually in the range 7.0-9.0. Selecting the two highest Pu concentrations, one gets 10^{-5} M at pH 7 (Figure 2e) and 10^{-7} M at pH 9 (Figure 2f); for fresh LWR type plutonium this corresponds to $\sim 10^{12}$ and $\sim 10^{10}$ Bq/m³, respectively. More than 99% of this activity comes from ²⁴¹Pu, (half-life 14.9 y); after 150 years, most of ²⁴¹Pu has decayed, and the corresponding activities will be $\sim 10^9$ and $\sim 10^7$ Bq/m³, respectively. The dominating soluble species are Pu(III) carbonate complexes: PuCO_3^+ , $\text{Pu}(\text{CO}_3)_2^-$ and $\text{Pu}(\text{CO}_3)_3^{3-}$.

In 1959 the International Commission on Radiological Protection (ICRP) recommended a "maximum permissible concentration of plutonium in water (MPC_w) for unlimited public use" of 5×10^{-5} Ci/m³ ($\sim 2 \times 10^6$ Bq/m³) (64). In 1979 ICRP introduced the concept of ALI ("annual limits of intake"). For ²³⁹Pu the value was set at 2×10^6 Bq (or 0.9 mg) per year (35). Because man consumes about 0.5 m^3 water/year, this ALI value corresponds to 4×10^6 Bq/m³ potable water.

The ALI value is based on the assumption that 10^{-5} (0.001%) of all plutonium in the water is taken up by the gastro-intestinal tract. This is valid for plutonium in highly insoluble form, like tetravalent oxide or hydroxide. In a more soluble form, the uptake may increase to 0.01%, and the corresponding ALI-value is then reduced to 2×10^5 Bq/y. For plutonium carbonate complexes, the lower ALI-value, corresponding to 4×10^5 Bq/m³ must be chosen; it could be argued that an even smaller ALI value should be used for the highly soluble carbonate complexes. Thus the maximum theoretical plutonium concentration in groundwater at the border of the repository (considering complexation with hydroxide and carbonate only)

could exceed drinking water limits by a factor of about 2500, when ^{24}Pu has decayed (after 150 years).

Migration of Plutonium through Granite Bedrock

Plutonium is transported by the groundwater in fractures in the rock (usually <1 mm wide). A typical groundwater velocity (v_w) at >100 m depth in Swedish bedrock is 0.1 m/y. The fractures are filled with crushed, weathered, clayish minerals, which have a high capacity to sorb the plutonium. Assuming instantaneous and reversible reactions, the sorption will cause the plutonium to move considerably slower (with velocity v_n) than the groundwater. The ratio between these two velocities is referred to as the retention factor (RF), defined by

$$RF = v_w/v_n = 1 + Kd \rho_r (1-\epsilon) a_f / \rho_w \epsilon a_p$$

This equation has been used for estimating migration velocities of radionuclides (e.g. 66). Here ρ_r is the density of the rock (kg/m^3), ρ_w the density of water, ϵ the fissure porosity, a_f the specific surface of fissures in the bedrock (m^2/m^3) and a_p the specific surface of particles used in the Kd determinations (m^2/m^3). The distribution coefficient Kd represents an equilibrium value for the particular rock under the pertinent conditions.

If, hypothetically, the whole rock was taken to be porous, a_f/a_p would be 1 (volume sorption); this is typical for the migration in a chromatographic column. In reality, only part of the rock matrix could be available for sorption, typically giving $a_f/a_p = 10^{-3}$ (surface sorption) for the conditions used in our studies (66). Other representative values are: $\rho_r = 2500 \text{ kg/m}^3$, $\rho_w = 1000 \text{ kg/m}^3$ and $\epsilon = 0.001$.

Kd-values for plutonium which exactly correspond to the conditions in Figures 2e and f are not available. However, the conditions for Am(III) are very similar to those for plutonium in Figure 2e. This would give a Kd range of 300-30,000, according to Figure 3. Similarly, the conditions for plutonium in Figure 3 correspond fairly well to those of Figure 2f at high pH or of Figure 2c,d; the Kd-range is 1000-80,000.

Introducing the values into the equation, using a minimum Kd-value of >300, gives a retention factor of >750. If this value is combined with a representative water transport time from repository to recipient (>1000 years for a distance >100 m), the transport equation indicates that it will take the plutonium >750,000 years to reach the recipient which is the water man may use. This estimate is supported by findings at the ancient natural reactor site at Oklo in Gabon (67).

The assumptions behind this calculated example are a considerable oversimplification of the real migration behavior. Effects such as diffusion into the rock matrix, dilution with inflowing water, dispersion of the migration front, channeling of the host

rock, irreversible immobilization of plutonium species (yielding a much higher Kd-values than the minimum assessed value of 300), formation of mobile particulates, etc. are neglected. These effects taken together will tend to increase the Kd-value. Thus it seems highly possible that an RF-value of $\gtrsim 10^3$ always will be achievable.

If we consider the radioactive decay of plutonium occurring during a migration time of 750,000 y., one finds that the plutonium concentration reaching the recipient will have decreased to $\lesssim 10^9$ M, or 4×10^4 Bq/m³. This is below the lowest ALI value presently used. Considering the selected conditions -- highest possible plutonium solubility and lowest observed Kd-value for plutonium sorption on rock -- this value contains a considerable safety margin.

In the above analysis we have neglected the plutonium decay products and their associated hazards. All of ²³⁹Pu, ²⁴⁰Pu and ²⁴²Pu decay to much longer lived and less hazardous uranium isotopes. However, ²³⁸Pu (originally present to 1% in reactor plutonium) decays through ²²⁶Ra, and ²⁴¹Pu (originally present to 12%) decays through ²³⁷Np. Both radium and neptunium are of high radiotoxicity and migrate more rapidly in nature than plutonium. They must therefore be considered in a risk analysis (e.g. as in 8, 9, 10) which, however, is outside the scope of this paper.

Conclusion

A general conclusion from the review of the distribution of plutonium between different compartments of the ecosystem was that the enrichment of plutonium from water to food was fairly well compensated for by man's metabolic discrimination against plutonium. Therefore, under the conditions described above, it may be concluded that plutonium from a nuclear waste repository in deep granite bedrock is not likely to reach man in concentrations exceeding permissible levels. However, considering the uncertainties in the input equilibrium constants, the site-specific Kd-values and the very approximate transport equation, the effects of the decay products, etc. -- as well as the crude assumptions in the above example -- extensive research efforts are needed before the safety of a nuclear waste repository can be scientifically proven.

Literature Cited

1. Friedman, A.M., Ed.; "Actinides in the Environment"; ACS Symposium Series No 35; American Chemical Society: Washington, DC, 1976.
2. Fried, S., Ed.; "Radioactive Waste in Geologic Storage"; ACS Symposium Series No 100; American Chemical Society: Washington, DC, 1979.
3. "Transuranium Nuclides in the Environment"; International Atomic Energy Agency: Vienna, 1976.

4. "Techniques for Identifying Transuranic Speciation in Aqueous Environments"; International Atomic Energy Agency: Vienna, 1981.
5. "Environmental Migration of Long-lived Radionuclides"; International Atomic Energy Agency: Vienna, 1982.
6. "The Environmental and Biological Behaviour of Plutonium and Some Other Transuranium Elements"; OECD Nuclear Energy Agency: Paris, 1981.
7. Whicker, F.W.; Schultz, V. "Radioecology: Nuclear Energy and the Environment"; CRC Press: Boca Raton, 1982.
8. "Handling of Spent Nuclear Fuel and Final Storage of Vitriified High Level Reprocessing Waste"; Kärnbränslesäkerhet: Stockholm, 1977.
9. (a) "Handling and Final Storage of Unreprocessed Spent Nuclear Fuel"; Kärnbränslesäkerhet: Stockholm, 1978.
(b) "A Review of the Swedish KBS-II Plan for Disposal of Spent Nuclear Fuel"; NRC, National Academy of Sciences: Washington, DC, 1980.
10. (a) Schneider, K.J.; Platt, A.M., Eds.; "High-level Radioactive Waste Management Alternatives"; BNWL-1900; Battelle Northwest Lab.: Richland, 1974.
(b) "Alternatives for Managing Wastes From Reactors and Post-fission Operations in the LWR Fuel Cycle"; ERDA-76-43; U.S. Energy Research and Development Administration: Washington, DC, 1976.
11. Choppin, G.; Rydberg, J. "Nuclear Chemistry. Theory and Applications"; Pergamon Press: London, 1980.
12. (a) "Planning for Nuclear Power Waste Products"; Svensk Kärnbränsleförsörjning: Stockholm, 1982.
(b) Schultz, G. *IAEA Bulletin* 1982, 24, 20.
13. Geologic Disposal of Radioactive Waste"; OECD Nuclear Energy Agency: Paris, 1982.
14. Dahlman, R.C.; Bondiotti, E.A.; Eyman, L.D.; in Ref. 1, p. 47.
15. Bondiotti, E.A.; Trabalka, J.R.; Arten, C.T.; Killough, G.G.; in Ref. 2, p. 241.
16. Edginton, D.N.; in Ref. 4, p. 3.
17. Riley, J.R.; Skirrow, G. "Chemical Oceanography"; Academic Press: London, 1965.
18. Dyrssen, D.; Wedborg, M. "Chemistry and Biogeochemistry of Estuaries"; Olausson, E., Ed.; John Wiley: New York, 1980.
19. Stumm, W.; Morgan, J.J. "Aquatic Chemistry"; 2nd Ed.; John Wiley: New York, 1981.
20. Freeze, R.A.; Cherry, J.A. "Groundwater"; Prentice-Hall: Englewood Cliffs, 1979.
21. Rydberg, J. "Groundwater Chemistry of a Nuclear Waste Repository in Granite Bedrock"; UCRL-53155; Lawrence Livermore Lab.: Livermore, 1981.
22. Fritz, P.; Barker, J.F.; Gale, J.E. "Geochemistry and Isotope Hydrology of Groundwater in the Stripa Granite"; LBL-8285 (also SAC-12 and UC-70); Lawrence Berkeley Lab.: Berkeley, 1979.

23. Allard, B.; Andersson, K. "The Influence of Groundwater Chemistry on the Leachability of Bitumenized Waste"; Nordisk Kontaktorgan for Atomenergispörmål; in press.
24. Ember, L.R. Chem. Eng. News 1981, Sept. 14.
25. Plechanov, N.; Josefsson, B.; Dyrssen, D.; Lundquist, K. Proc. Symp. Terrestrial and Aquatic Humic Materials, Chapel Hill, 1981.
26. Baudin, G.; personal communication.
27. Choppin, G.; Kullberg, L. J. Inorg. Nucl. Chem. 1978, 40, 651.
28. Nash, K.L.; Choppin, G. J. Inorg. Nucl. Chem. 1980, 42, 1045.
29. Angeletti, L.; in Ref. 4, p. 151.
30. Wahlgren, M.A.; Alberts, J.J.; Nelson, D.M.; Orlandini, K.; in Ref. 3, p. 9.
31. Schulz, R.K.; Tompkins, G.A.; Babcock, K.L.; in Ref. 3, p. 303.
32. Myers, D.S.; Silver, W.J.; Coles, D.G.; Lamson, K.C.; McIntyre, D.R.; Mendoza, B.; in Ref. 3, p. 311.
33. McLendon, H.R.; Stewart, O.M.; Boni, A.L.; Corey, J.C.; McLeod, K.W.; Pinder, J.E.; in Ref. 3, p. 347.
34. Holm, E.; Persson, B.; in Ref. 3, p. 435.
35. "Limits for Intakes of Radionuclides by Workers"; ICRP Publ. 30; Pergamon Press: Oxford, 1979.
36. Baxter, D.W.; Sullivan, M.F. Health Physics 1972, 22, 785.
37. Ahrland, S.; Liljenzin, J.O.; Rydberg, J. "Solution Chemistry (of the Actinides)"; Comprehensive Inorganic Chemistry. Vol. 5; Pergamon Press: Oxford, 1973.
38. Fuger, J.; Oetting, F.L. "The Chemical Thermodynamics of Actinide Elements and Compounds. Part 2. The Actinide Aqueous Ions"; International Atomic Energy Agency: Vienna, 1976.
39. Rai, D.; Serne, R.J. J. Environ. Qual. 1977, 6, 89.
40. Lemire, R.J.; Tremaine, P. "Uranium and Plutonium Equilibria in Aqueous Solutions to 200°C"; AECL-6655; Whiteshell Nucl. Res. Est.: Pinawa, 1980.
41. Allard, B. "Actinides in Perspective"; Edelstein, N., Ed.; Pergamon Press: New York, 1982, p. 553.
42. Phillips, S.L. "Hydrolysis and Formation Constants at 25°C"; LBL-14313; Lawrence Berkeley Lab.: Berkeley, 1982.
43. Choppin, G. Trans. Am. Nucl. Soc. Ann. Meet. 1979, 32, 166.
44. Andelman, J.B.; Rozzell, T.C. "Radionuclides in the Environment"; Gould, R.F., Ed.; Advances in Chemistry Ser. 93; American Chemical Society: Washington, DC, 1970, p. 118.
45. Polzer, W.L. Proc. Rocky Flats Symp. on Safety in Plutonium Handling Facilities, USAEC CONF-710401, 1971.
46. Silver, G.L. "Plutonium in Natural waters"; MLM-1870; Mound Lab., 1971.
47. Ames, L.L.; Rai, D.; Serne, R.J. "A Review of Actinide-Sediment Reactions with Annotated Bibliography"; BNWL-1983; Battelle Northwest Lab.: Richland, 1976.
48. Skytte Jensen, B. "The Geochemistry of Radionuclides with Long Half-Lives"; R-430; Risø Nat. Lab.: Risø, 1980.

49. Grenthe, I.; Ferri, D. Proc. OECD/NEA Workshop on Near-field Phenomena in Geologic Repositories for Radioactive Waste; OECD/NEA: Paris 1981.
50. Rai, D.; Serne, R.J.; Swanson, J.L. J. Environ. Qual. 1980, 9, 417.
51. Bondietti, E.A.; Reynolds, S.A. "Proc. Actinide-Sediment Reactions Working Meeting"; Ames. L.L., Ed.; BNWL-2117; Batelle Northwest Lab.: Richland, 1976.
52. Nelson, D.; statement at Workshop on Environmental Chemistry of Plutonium, Savannah River, 1980.
53. Allard, B.; Olofsson, U.; Torstenfelt, B.; Kipatsi, H.; Andersson, K.; in Ref. 54, in press.
54. Lutze, W., Ed.; "Scientific Management of Radioactive Waste. Vol. 5"; Elsevier: New York, in press.
55. Torstenfelt, B.; Kipatsi, H.; Andersson, K.; Allard, B.; Olofsson, U.; in Ref. 54, in press.
56. Benes, P.; Majer, V. "Trace Chemistry of Aqueous Solutions"; Elsevier: New York, 1980.
57. Allard, B.; Beall, G.W.; Krajewski, T. Nucl. Techn. 1980, 49, 474.
58. Beall, G.W.; Allard, B. "Adsorption from Aqueous Solutions"; Tewari, P.H., Ed.; Plenum Press: New York, 1981, p. 193.
59. Allard, B.; Beall, G.W. "Management of Alpha-Contaminated Wastes"; International Atomic Energy Agency: Vienna, 1981, p. 667.
60. Johnston, H.M.; Gillham, R.W. "A Review of Selected Radionuclide Distribution Coefficients of Geologic Materials"; TR-90; Atomic Energy of Canada Ltd; Univ. of Waterloo, 1980.
61. Johnson, G.L.; Toth, L.M. "Plutonium(IV) and Thorium(IV) Hydrous Polymer Chemistry"; ORNL/TM-6365; Oak Ridge Nat. Lab.: Oak Ridge, 1978.
62. Kepak, F. Chem. Rev. 1971, 71, 357.
63. Olofsson, U.; Allard, B.; Torstenfelt, B.; Andersson, K.; in Ref. 54, in press.
64. Starik, I.E. "Grundlagen der Radiochemie"; Akademie Verlag: Berlin, 1961.
65. "Report of Committee II on Permissible Dose for Internal Radiation"; Publ. 2; ICRP: Oxford, 1959.
66. Neretnieks, I.; in Ref. 5, p. 635.
67. "The Oklo Phenomenon"; International Atomic Energy Agency: Vienna, 1975.

RECEIVED December 22, 1982

Aquatic Chemistry of Plutonium

ROBERT L. WATTERS

U.S. Department of Energy, Ecological Research Division, Washington, DC 20036

Research into the aquatic chemistry of plutonium has produced information showing how this radioelement is mobilized and transported in the environment. Field studies revealed that the sorption of plutonium onto sediments is an equilibrium process which influences the concentration in natural waters. This equilibrium process is modified by the oxidation state of the soluble plutonium and by the presence of dissolved organic carbon (DOC). Higher concentrations of fallout plutonium in natural waters are associated with higher DOC. Laboratory experiments confirm the correlation. In waters low in DOC oxidized plutonium, Pu(V), is the dominant oxidation state while reduced plutonium, Pu(III+IV), is more prevalent where high concentrations of DOC exist. Laboratory and field experiments have provided some information on the possible chemical processes which lead to changes in the oxidation state of plutonium and to its complexation by natural ligands.

Early in our research program, we realized that an understanding of how plutonium may move through the environment to the human population hinged upon a knowledge of its solution chemistry. This was important knowledge for the description of both contemporaneous movement and long-term mobilization, since plutonium's distribution between solid phases (soils and sediments) and aqueous phases (soil solutions and natural water bodies) largely determined its access to food chains(1). Earlier observations had shown that soil and sediment in most environments held the bulk of plutonium, but that a small mobile fraction always seemed to be present. We encouraged the study of the chemistry of this soluble fraction in terms of the identification and

This chapter not subject to U.S. copyright.
Published 1983, American Chemical Society

quantification of its chemical species, the possible reactions that led to speciation, and the sorption-desorption phenomena on solid phases.

The study of the chemistry of soluble plutonium in natural waters seemed almost impossible when first considered. We needed to develop the information in aquatic systems where the range of pH is 4 to 10, Eh is 0.6v to -0.2v(2) and the ionic strength varies from that of the oceans to lakes with conductivities less than 20 μ S/cm. In addition, the range of dissolved organic carbon varies from about 1ppm to greater than 100ppm. To compound the difficulties, the reported concentrations of soluble plutonium in natural waters ranged from 10⁻¹³ to 10⁻¹⁷ moles/liter depending upon their source. These levels were beyond the sensitivity limits of chemical instrumentation. However, by the use of plutonium's radioactivity and several nonisotopic carrier techniques, a considerable amount of information about its environmental chemistry has been accumulated.

Sources of Plutonium for Environmental Research

The major source of plutonium in natural waters is the atmospheric fallout from nuclear weapons tests. Fallout plutonium is ubiquitous in marine and freshwater environments of the world with higher concentrations in the northern hemisphere where the bulk of nuclear weapons testing occurred(3). Much of the research on the aquatic chemistry of plutonium takes place in marine and freshwater systems where only fallout is present.

Fallout plutonium arrives in natural waters either by direct atmospheric deposition or by erosion and/or dissolution from the land. Although in the past, this plutonium was considered to be in a refractory form due to formation within the fire ball, it seems more likely that most of the plutonium originated in the stratosphere by the decay of ²³⁹Np (from ²³⁹U formed during the detonation)(4). Deposition occurs predominantly with one or a few atoms incorporated in a raindrop. Investigations by Fukai indicate that collected rain contains soluble plutonium which has oxidation states that are almost totally Pu(V+VI)(5).

A second source of plutonium, dispersed more locally, is liquid effluent from fuel reprocessing facilities. One such is the fuel reprocessing plant at Windscale, Cumbria in the United Kingdom where liquid waste is released to the Irish Sea(6). Chemical analysis of this effluent shows that about one percent or less of the plutonium is in an oxidized form before it contacts the marine water(7). Approximately 95 percent of the plutonium rapidly adsorbs to particulate matter after discharge and deposits on the seabed while 5 percent is removed from the area as a soluble component(8). Because this source provided concentrations that were readily detected, pioneering field research into plutonium oxidation states in the marine environment was conducted at this location.

A third source of aquatic plutonium is liquid effluent discharged from laboratory operations into ponds and streams. An example of this is a former waste pond at Oak Ridge National Laboratory, Pond 3513, that received liquid wastes with low concentrations of transuranic elements before it was retired. This impoundment has water quality similar to high pH natural ponds. Since the pond is easily accessible and shallow, scientists at ORNL performed several manipulative experiments with caissons to determine the effects of aerobic and anaerobic environments upon the speciation of actinide elements(9).

Correlative Observations

Environmental chemists funded by the Department of Energy have studied these sources to learn as much as they can about the chemistry of plutonium dispersed in freshwater and marine ecosystems. Much of the early work determined the concentrations in various water bodies and the distribution between water and sediment. Table I shows results of various freshwater and marine surveys(10).

Table I. Distribution Coefficients, K_d , For Plutonium in Different Natural Waters(10)

Sampling area	Concentration on particles (pCi·g ⁻¹)	Concentration in solution (pCi·ltr ⁻¹)	K_d (ml·g ⁻¹) X 10 ⁴
Bombay Harbour	0.4-2.9	4.0-20	4.8-13
Enewetak Lagoon	0.1-75	2.0-75	5.0-60 4.0-30
Hudson River	0.02	0.3	6.7
Irish Sea	36	500	7.5
	23-80	370-650	4.6-21
	9.0-29	310-460	1.9-9.3
	0.22	35	0.6
	0.37	50	0.7
Lake Michigan	0.2	0.6	33
Lake Washington	-	-	1.0-8.5
	-	-	6.9-27
Mediterranean Sea	-	-	1.6-9.4
Savannah River	0.014-0.1	0.24-2.4	4.2-41

A number of freshwater lakes were surveyed for concentrations of plutonium, the ratio of its upper to lower oxidation states, pH, and the concentration of dissolved organic carbon (DOC), which are shown in Table II(11).

Table II. Concentrations of Actinides and Dissolved Organic Carbon and Pu Oxidation State Ratios in Filtered Lake Water(11)

Lake	pH	Concentrations in filtered water		$\frac{\text{Pu(V+VI)}}{\text{Pu(III+IV)}}$	Dissolved Organic carbon DOC (ppm)
		Pu(III+IV) (fCi L ⁻¹)	Pu(V+VI)		
Clear Lake	8.0	0.09	0.57	6.5	-
Lake Michigan	8.0	0.06	0.39	6.5	1.6
ELA 302S	6.3	0.13	0.21	1.6	<5
ELA 224	6.4	0.18	0.30	1.6	3.2
ELA 223	5.6	0.19	0.30	1.6	4.6
Last Mountain Lake	8.4	0.28	0.46	1.6	-
GSL, McLeod Bay	7.5	0.34	0.45	1.3	2.5
ELA 161	6.8	0.28	0.35	1.3	1.9
GSL, Main Basin	8.2	0.13	<0.1	0.7	5.0
GSL, Christie Bay	8.5	0.39	0.21	0.5	6.8
ELA 305	6.9	0.81	0.32	0.4	5.1
ELA 227	6.6	0.34	0.13	0.4	11.1
Lake of the Woods	7.1	0.35	0.11	0.33	-
Lake Katherine	8.5	0.31	0.10	0.31	-
AELA-885	8.4	1.0	0.16	0.15	40
ELA-239	6.3	2.6	0.28	0.11	8.3
ELA-661-77	4.8	7.1	<0.15	<0.05	-
ELA-661-78	5.6	3.4	<0.1	<0.01	15.2
Volo Bog	5.5	0.61	<0.1	<0.01	15
Okeefenokee	3.9	1.8	<0.1	<0.02	34.2
ELA 241	5.9	5.5	<0.1	<0.02	-
Little Manito	>8.7	9.6	<0.2	<0.03	115

The results indicated certain correlations and generalities about plutonium that led to further questions regarding its chemical state in aquatic systems. For instance, the concentrations of fallout plutonium in natural waters was strongly dependent upon the concentration of DOC but no correlation to pH was obtained. In systems that receive only fallout plutonium, the lakes with

high DOC have concentrations of soluble plutonium ten to a hundredfold higher than those lakes and marine waters with low dissolved organic carbon. This implied that natural organic molecules might make plutonium ions more soluble by complexation.

At Mono Lake, a closed basin, alkaline, saline lake in California, the concentrations of plutonium in the water column are about two orders of magnitude higher than in Lake Michigan(12). In experiments where Mono Lake water was acidified to remove carbonate and bicarbonate ions and again adjusted to pH 10, more than 90 percent of the soluble plutonium moved to the sediment phase. When carbonate ion concentration was restored, the plutonium returned to solution--strong evidence of the importance of inorganic carbon to solubility in that system(13). Early studies with Lake Michigan water, which has low DOC, had also implicated bicarbonate and carbonate as stabilizing ligands for plutonium at pH 8(14). This latter research characterized the soluble species as mainly anionic in character.

The distribution ratios, K_d , of plutonium defined as

$$K_d = \frac{\text{concentration plutonium on sediment}}{\text{concentration in water}}$$

are remarkably similar in bodies of water with midrange pH and similar low organic content. Table I indicates the K_d 's are within one to two orders of magnitude over a broad geographical range. The results of two investigations from two diverse locations provided evidence that this distribution ratio might be due to reversible sorption-desorption reactions. Scientists at Argonne National Laboratory (ANL) equilibrated filtered Lake Michigan water with sediments that had been contaminated with ^{238}Pu ten years earlier. As many as nine extractions on the same portions of sediment produced essentially identical K_d values(15). Noshkin has observed that the concentrations of plutonium in the waters of Enewetak remain relatively constant although there is a continual replacement of water at an estimated residence time of 144 days (16). The concentration corresponds well with that predicted from the experimental distribution ratio between lagoon sediment and water.

Although the relationship of sediment adsorption to water concentration appears to be a controlling feature of shallow water systems such as lakes and coastal shelf water, the open ocean is more likely to contain soluble plutonium which seems to be unaffected by particulate matter. This is particularly evident in two oceanographic studies. Bowen et al have discovered a stratum of plutonium in the North Pacific at about 500m that has not changed depth appreciably from 1973 to 1980. How it arrived at this depth is subject to conjecture but it appears to be soluble plutonium which is not settling(17). Fukai et al have delineated plutonium maxima in the Mediterranean Sea which seem to be due to soluble species(18). Comparison of americium to plutonium ratios in this

study indicates that americium settles at a rate consistent with the downward movement of marine particulate matter while the plutonium now present in the seawater moves downward more slowly or not at all.

These various broad research observations generated questions about the influence of chemical environments in aquatic systems upon plutonium and what chemical species might be present. The oxidation states of plutonium, its associations with DOC, and its complexation by inorganic ions all seemed interrelated and important to the understanding of environmental transport.

Oxidation State

The ability to identify the oxidation states of plutonium and measure their concentrations in environmental samples has improved markedly in resolution since the start of our research program. The first characterizations employed a rare earth fluoride precipitation to carry down the lower oxidation states, Pu(III+IV), an addition of reducing agent to the supernate to reduce the upper oxidation states, Pu(V+VI), and a subsequent rare earth fluoride precipitation to carry this plutonium(19). The procedure is performed in the presence of two tracers, $^{242}\text{Pu}(\text{IV})$ and $^{236}\text{Pu}(\text{VI})$, with the solution acidified and containing a holding oxidant to stabilize the forms initially present. Table II presents the ratios Pu(V+VI)/Pu(III+IV) determined for various natural waters. The trend of this ratio to decrease with increasing concentrations of DOC is interesting. Those systems such as Lake Michigan and the marine systems, which are considered oligotrophic (low in nutritional materials that encourage biological activity), tend to have high ratios. These are systems which maintain high dissolved oxygen and, therefore, higher redox potentials. Where the dissolved organic concentrations are relatively high, the total concentrations of plutonium are higher, as noted earlier, and the predominant oxidation state is Pu(III+IV). These phenomena seem to be in reasonable agreement with several Eh-pH diagrams, one of which is shown in Figure 1(10). If we infer that increased DOC mediates the reduction of plutonium through electron donation, and/or increases the complexation of Pu(III+IV), then we would expect the formation or stabilization of the lower oxidation states at the expense of Pu(V+VI).

A further resolution of the higher oxidation states in aquatic systems occurred in 1978 when scientists at Argonne National Laboratory(20) and Oak Ridge National Laboratory(21) independently established the capability to identify Pu(V) as the oxidized form that exists in natural waters. Both methods are based upon preferential adsorption on finely divided solids. In the Argonne procedure, adapted from a Japanese method for determining Np(V)(22), Pu(IV) and Pu(VI) adsorb onto silicic acid while Pu(V) does not. The Argonne scientists also have shown that the oxidized form of plutonium in natural waters carries on CaCO_3 when it is formed by

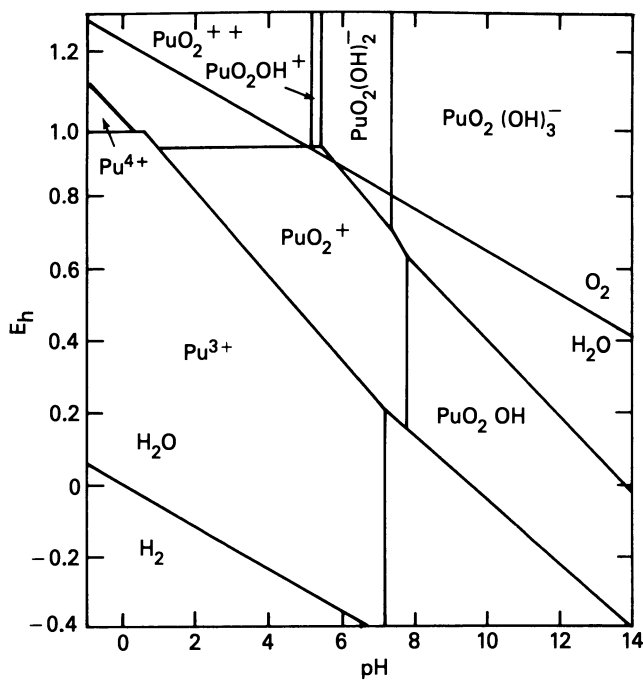


Figure 1.
Eh-pH diagram for the speciation of plutonium in equilibrium with PuO₂ in water (10).

the addition of excess Ca^{++} and adjustment to pH 9, but Pu(VI), formed by the addition of a strong oxidant does not. This precipitate is redissolved and Pu(IV) and Pu(V) are determined by the lanthanum fluoride method. The silicic acid method has confirmed that the oxidized plutonium in Lake Michigan and the Irish Sea is Pu(V). The calcium carbonate method provided additional support to the same conclusion about Lake Michigan water.

The Oak Ridge technique employs TiO_2 powder to adsorb Pu(V). This procedure has been used to characterize the oxidation state of plutonium in Pond 3513 as predominantly Pu(V).

An interesting aspect of the characterization of plutonium as Pu(V) in the Irish Sea, Lake Michigan, and Pond 3513 is that the origins of the radionuclides are different in each system, i.e., fuel reprocessing waste, fallout, and laboratory effluents, respectively.

The mechanisms by which Pu(IV) is oxidized in aquatic environments is not entirely clear. At Oak Ridge, laboratory experiments have shown that oxidation occurs when small volumes of unhydrolyzed Pu(IV) species (i.e., Pu(IV) in strong acid solution as a citric acid complex or in 45 percent Na_2CO_3) are added to large volumes of neutral-to-alkaline solutions(23). In repeated experiments, the ratios of oxidized to reduced species were not reproducible after dilution/hydrolysis, nor did the ratios of the oxidation states come to any equilibrium concentrations after two months of observation. These results indicate that rapid oxidation probably occurs at some step in the hydrolysis of reduced plutonium, but that this oxidation was not experimentally controllable. The subsequent failure of the various experimental solutions to converge to similar high ratios of Pu(V+VI)/Pu(III+IV) demonstrated that the rate of oxidation is extremely slow after Pu(IV) hydrolysis reactions are complete.

These observations contrast with some of the results obtained in natural waters. In the experiments where contaminated sediments were equilibrated with Lake Michigan water for a number of days, the Pu(IV) that was on the sediments and was transferred to the water was oxidized to Pu(V), with the oxidation occurring either during or after desorption (15). The studies in the Irish Sea near Windscale show that although no more than 1 percent of the waste effluent stream is oxidized plutonium, approximately 5 percent of the plutonium released leaves the area in the currents of the Irish Sea as oxidized plutonium. Most of the plutonium, therefore, must be oxidized fairly rapidly in sea water.

Observations of the ratio of oxidized plutonium to reduced plutonium may provide some insight to the observations of erratic formation and lack of equilibration in laboratory solutions at ORNL versus fairly consistent and predictable behavior in oligotrophic lakes and marine systems. In coastal water and the relatively shallow Lake Michigan, Pu(V) is about 90 percent of the soluble plutonium, but in the upper waters of the open ocean, where it does not interact with the seafloor due to the depths,

the oxidized and reduced forms are in about equal concentrations. In the North Pacific, however, at depths close to the ocean floor, about 90 percent of the soluble plutonium is again oxidized. This suggests that contact with bottom sediments may mediate or catalyze the distribution of oxidation states(24). Just what the mechanism might be is not clear.

Two of the study systems, Lake Michigan and Pond 3513, exhibit cyclic behavior in their concentrations of Pu(V) (Figure 2 and 3). The cycle in Lake Michigan seems to be closely coupled with the formation in the summer and dissolution in the winter of calcium carbonate and silica particles, which are related to primary production cycles in the lake(25). The experimental knowledge that both Pu(IV) and Pu(V) adsorb on calcium carbonate precipitates(20) confirms the importance of carbonate formation in the reduction of plutonium concentrations in late summer. Whether oxidation-reduction is important in this process has not been determined.

For Pond 3513, the cycle of ^{238}U and $^{239,240}\text{Pu}$ concentrations in water (filtered with a 0.22μ membrane) is out of phase with the cycle of plutonium concentrations in Lake Michigan. In this shallow pond, the concentrations of the two actinides peak in summer and decline in winter. An explanation for this cycle of plutonium is that photosynthetic activity depletes dissolved CO_2 which results in an increase in pH and this in turn shifts the oxidation state in favor of Pu(V) which is desorbed from the sediments(26).

In April 1982 an experiment was started in Pond 3513 to evaluate the rate at which sediment-bound Pu, when subjected to reducing conditions, would oxidize to the more soluble Pu(V) state after exposure to the atmosphere. Large plastic tanks (127 cm high, 71 cm dia.) were embedded into the pond sediment enclosing about 500 liters of pond water, 1 meter in depth. Two enclosures served as test systems, one where O_2 was excluded by sealing alone, the other by sealing after adding glucose. Both indigenous Pu and added ^{237}Np were studied. The results indicated that solution-phase Pu(V) and Np(V) could be reduced to Pu(III+IV) and Np(IV) by adding glucose and forcing the system anaerobic. When the system was re-aerated, the Np(V) concentration in the overlying water increased rapidly to about 25 percent of its original value. However, the Pu(V) concentration did not increase nearly as rapidly. In fact, in the two covered tanks the response of Pu to aeration was a threefold increase in the Pu(V) concentration over that during anaerobiosis after about three months. These concentrations were still about one fifth of those in the pond itself (but comparable to that in the control enclosure). Although more data are needed, there does appear to be evidence that the reoxidation of Pu is slower than that of Np (as expected). The annual cycle depicted in Figure 3 could, therefore, be due to a redox cycle whose kinetics are controlled by pH, decay processes in the sediment, and temperature.

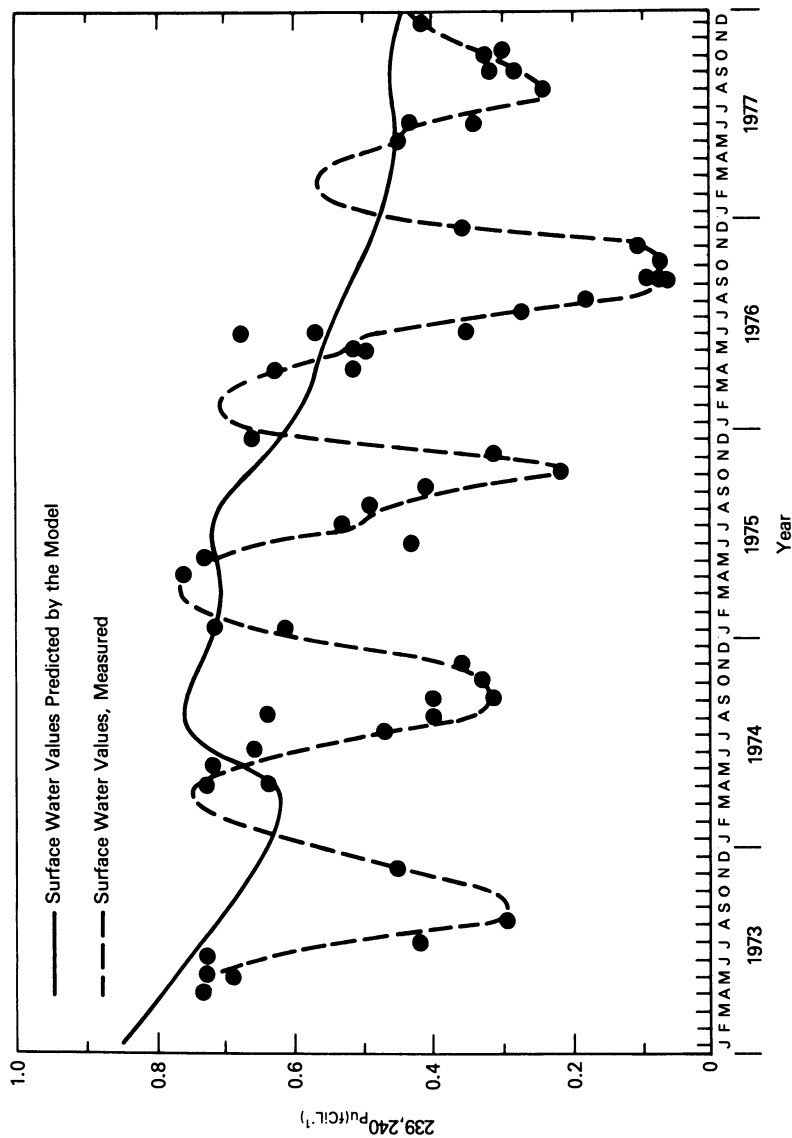


Figure 2.
Experimental measurements of $^{239,240}\text{Pu}$ in Lake Michigan over
a five year time period (25).

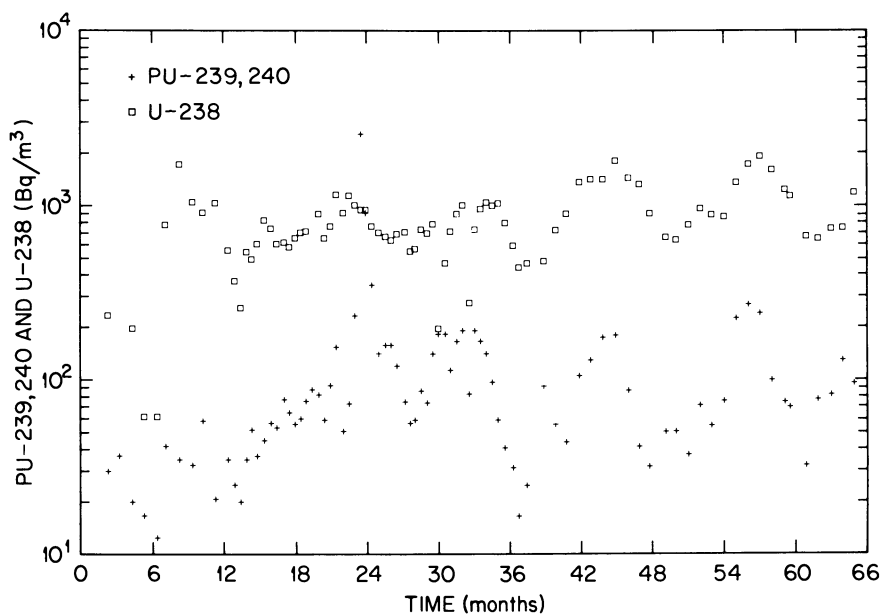


Figure 3.

Behavior of soluble plutonium and uranium in Pond 3513, located at the Oak Ridge National Laboratory. The water concentrations (Bq/m³) represent the period March 1977 through June 1982(26).

The shallow nature of Pond 3513 makes chemical processes occurring in the sediment extremely important. More work will be needed, however, to elucidate the redox cycle.

Influence of Dissolved Organic Carbon (DOC)

The early field studies revealed that elevated concentrations of fallout plutonium correlated with increased concentrations of dissolved organic carbon. Experiments at Argonne National Laboratory corroborate this correlation; the explanation is probably that the organic compounds complex Pu(IV), and, hence, decrease the distribution ratio between water and sediments(27). In these experiments the distribution ratio (K_d) between sediment and natural waters was measured as a function of DOC. Measurements of K_d in both field and laboratory experiments show an unmistakable effect of DOC upon the distribution ratio. Figure 4 shows the inverse correlation between the K_d of plutonium and concentration of DOC.

In other experiments the organic carbon was separated from various swamp and lake waters by ultrafiltration. Portions of these concentrates were combined with aliquots of the ultrafiltered water to produce a series of waters which varied only in their concentration of DOC. A measured amount of $^{237}\text{Pu(IV)}$ was introduced, an aliquot of a sediment that was representative of a range of lakes was added, the samples were shaken for one week, and the K_d 's for reduced plutonium were determined. The effects of increasing concentrations of DOC in the various Okefenokee and Lake Michigan waters is shown in Figure 5a and 5b, respectively. In the swamp waters, the DOC affects the adsorption of plutonium at concentrations far below its ambient concentration of 35 ppm. In Lake Michigan waters, where natural concentrations of DOC are about 1 ppm, the DOC does not affect the distribution ratio for plutonium until the concentration is considerably higher than ambient.

Nelson et al(28) have developed an equation assuming competitive equilibrium between Pu(IV) and soluble complexing ligands and between Pu(IV) and a solid adsorber:

$$\frac{1}{K_d} = \frac{1}{K_d^0} + \frac{K_1}{K_3} (\text{DOC}) + \frac{K_2}{K_3} (\text{DOC})^2$$

where:

K_1 and K_2 are conditional stability constants for the 1:1 and 2:1 complexes of plutonium with organic ligands.

K_d is the observed distribution ratio when organic matter is added.

K_d^0 is the distribution ratio of uncomplexed ions and all low molecular weight inorganic and organic complexes (ultrafiltration cutoff was at a molecular weight of 1000).

K_3 is the conditional stability constant for the association of plutonium with the solid adsorber.

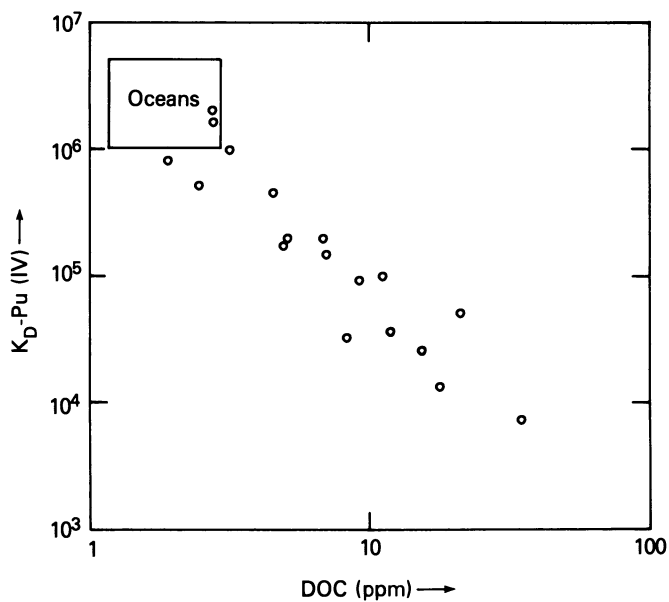


Figure 4.
Variation of K_d as a function of ambient dissolved organic carbon (DOC) for several natural waters (27).

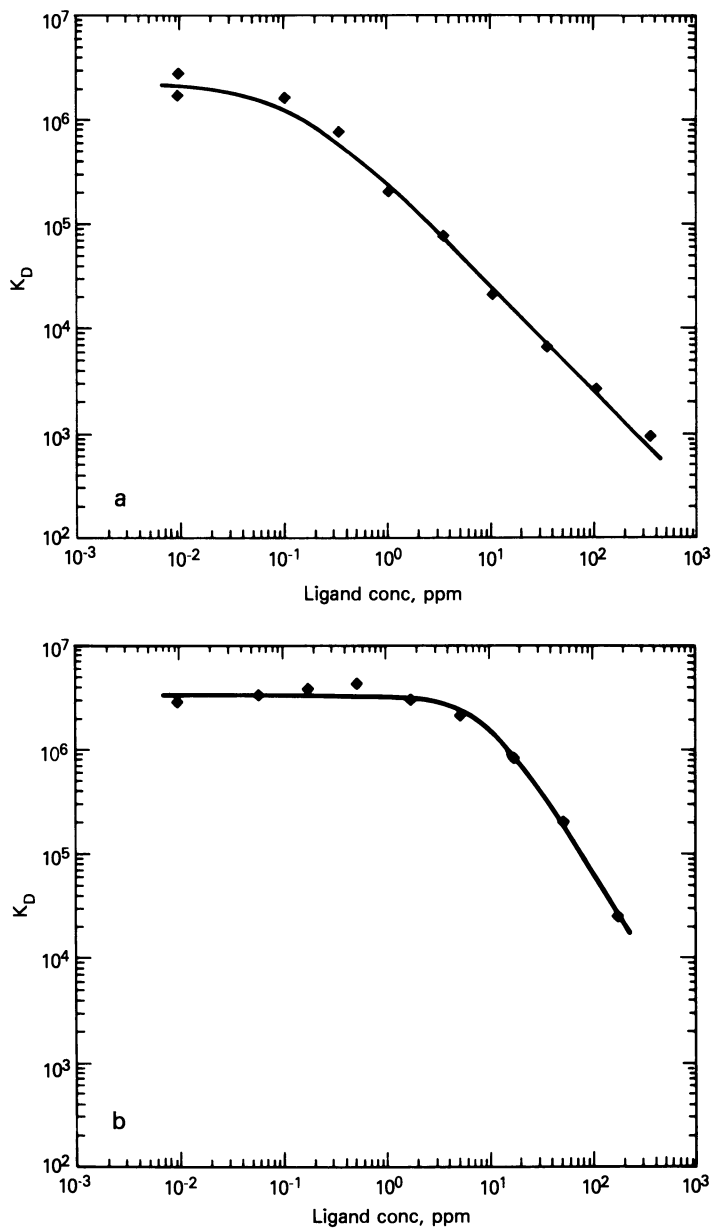


Figure 5. Variation of K_d as a function of DOC for (a) Okefenokee Swamp, and (b) Lake Michigan(27).

The absolute values of the stability constants cannot be deduced from these experiments but the ratios K_1/K_3 and K_2/K_3 can. Table III shows the values of $1/K_d^0$, K_1/K_3 , and K_2/K_3 for the nine equilibration experiments.

Table III. Concentration and Stability Constant Ratios(28)

	$1/K_d^0 \times 10^{6a}$	K_1/K_3^b	K_2/K_3^c
Okeefenokee Swamp	0.35 (40)	3.85 (9)	-0.002 (90)
Volo Bog	2.3 (14)	2.94 (13)	0.003 (50)
Banks Lake	0.98 (16)	0.56 (15)	0.001 (40)
Argonne Pond	0.80 (12)	0.43 (30)	0.027 (5)
Saganashkee Slough	0.72 (12)	0.42 (30)	0.023 (24)
Bay of Fundy	0.85 (15)	0.35 (30)	0.012 (60)
ELA Lake 239	0.81 (11)	0.20 (60)	0.048 (20)
Gulf of Mexico	0.38 (13)	0.16 (30)	-0.002 (110)
Lake Michigan	0.26 (10)	0.03 (40)	0.001 (24)

^aUnits of $\text{kg sediment} \cdot \text{L}^{-1}$ solution.

^bUnits of $\text{kg sediment} \cdot \text{kg}^{-1}$ DOC.

^cUnits of $\text{kg sediment} \cdot \text{kg}^{-2}$ DOC \cdot L solution.

() Estimate of the standard error expressed as percent

The values of K_d^0 seem to confirm the correlations of the earlier field data that the adsorption onto sediments does not vary by more than an order of magnitude in systems with low DOC. No profound effect of pH on K_d^0 was observed for waters which ranged from pH 4 (Okeefenokee Swamp) to pH 8 (Lake Michigan). Nor was there an effect of ionic strength on K_d^0 in the samples which ranged in composition from that of the oceans to that of a lake with a conductivity of less than $20 \mu\text{S}/\text{cm}$.

The K_1/K_3 ratios divide these natural waters into three groups. Okeefenokee Swamp and Volo Bog have ratios of about 3; a group of small lakes and two coastal marine waters show a somewhat weaker binding with K_1/K_3 ranging from 0.16 to 0.56; Lake Michigan exhibits much weaker organic complexes with a K_1/K_3 of 0.03.

The formation of 2:1 complexes as indicated by K_2/K_3 values of 0.01 to 0.05, appears to be important in four of the water bodies, all from the intermediate group.

Both of the ratios of formation constants were dependent on pH. The K_1/K_3 ratio was increased by decreasing the pH while K_2/K_3 increased when pH was increased. When the pH of water from Okeefenokee Swamp was raised from 4 to 8, K_2/K_3 increased from <0.002 to 0.59; when the pH of water from ELA Lake 239 was lowered from 7 to 4 K_2/K_3 decreased from 0.048 to <0.001 .

These studies show the usefulness of relative data for the prediction of plutonium complexation with natural ligands. They

represent the observations for only one type of sediment and one oxidation state, but future experiments will consider other sediment types and the possibility of Pu(V) organic complexes to develop a more comprehensive description of the effect of DOC.

Mathew and Pillai observed a threefold increase in plutonium concentration at low, normal, and high carbonate concentrations when 20mg/liter of organic matter were added to sea water samples (29). Again this indicates the effect of organic complexation upon plutonium solubility in natural waters.

Alberts et al at the Savannah River Ecology Laboratory have performed one set of experiments in an attempt to measure the stability constants for complexes of plutonium with natural organic material that was separated by ultrafiltration from Upper Three Runs Creek, a blackwater stream high in DOC(30). Experiments were run in deionized water at concentrations of plutonium, other elements, organic matter, and hydrogen ion comparable to those found in that southern U.S. environment. The solutions were equilibrated with appropriate ion exchange resins, and concentrations of free and bound elements were determined. Stability constants shown in Table IV were determined by Scatchard plots(31). The K_1 stability constant represents binding at sites that are, probably, carboxylic groups while K_2 may represent binding by dicarboxylic(32) or phenolic groups. Similar types of constants are derived in the study of the binding of other metals by humic acids (note Cu in Table IV). The high values of K_1 and K_2 for Pu are indicative of extremely stable complexes (a thousand times higher than Cu K_1 constants), but the number of sites available for binding (n_1 and n_2) are very low per gram of organic matter as compared to copper. These studies are preliminary and will require further experiments with various natural waters, more characterization of the dissolved organic matter and variations in the oxidation state of the introduced plutonium.

Table IV. Stability Constants of Some Elements When Complexed By Upper Three Runs Organic Matter(30)

	K_1	K_2	n_1	n_2
U	7.3×10^8	1.6×10^7	0.02	0.62
Pu(IV)	3.7×10^9	5.9×10^8	0.0002	0.0011
Cu ^a	4×10^6	1×10^4	0.1	4.1

^aK and n values determined for Aldrich Chemical Co. Humic Acids

Summary

The program of research on the aquatic chemistry of transuranic elements has made important advances in arriving at an understanding of plutonium mobilization and transport in natural systems. This program began with determinations of total plutonium concentrations in a wide variety of terrestrial and water samples to obtain knowledge about geographical distribution, dispersion within water bodies, and correlations with water quality parameters. Inferences from those studies led to other experiments in which the chemical species that are present were identified, as well as their relationship to the key water quality parameters pH and dissolved organic carbon. Two of the important findings from the research are the existence of Pu(V) as a major oxidation state in seawater and oligotrophic lakes, and the importance of dissolved organic matter in the observed solubility in natural waters. These investigations have led in turn to attempts to estimate thermodynamic and kinetic parameters.

All of the information obtained in this research area depends upon indirect evidence through the use of nonisotopic carriers or normalized data in the form of ratios. These are subject to error but the trends and insights that have been obtained are very useful to the description of the behavior of plutonium in the environment. Better thermodynamic data in the range of environmental concentrations would be helpful in further quantification of chemical species, as would phenomenological descriptions of the behavior of plutonium in reasonably good models of the environment.

Acknowledgments

I thank J. J. Alberts, E. A. Bondiotti, W. O. Forster, D. M. Nelson and R. P. Larsen for their reviews of this article and their helpful comments.

Literature Cited

1. Watters R.L.; Edgington, D.N.; Hakonson, T.E.; Hanson, W.C.; Smith, M.E.; Whicker, F.W.; and Wildung, R.E., "Transuranic Elements in the Environment," DOE/TIC 22800; Hanson, W.C., Ed.; National Technical Information Service, Springfield, Va., 1980, pp. 1-44.
2. Bass Becking, L.G.M.; Kaplan, I.R.; and Moore, D., *J. Geol.*, 1960, 68 p. 243.
3. Perkins, R.W. and Thomas, C.W., "Transuranic Elements in the Environment," DOE/TIC 22800; Hanson, W.C., Ed.; National Technical Information Service, Springfield, Va., 1980, pp. 53-82.
4. Joseph, A.B.; Gustafson, P.F.; Russell, L.R.; Schubert, E.A.; Volchok, H.L.; and Tamplin, A., "Radioactivity in the Marine Environment."

5. Fukai, R.; Yamato, A.; Thein, M.; and Bilinski, H., "Techniques for Identifying Transuranic Speciation in Aquatic Environments" STI/PUB/613, International Atomic Energy Agency, Vienna, 1981, pp. 37-41.
6. Hetherington, J.A.; Jeffries, D.E.; Mitchell, N.T.; Pentreath, R.J.; and Woodhead, D.S., "Transuranium Nuclides in the Environment" STI/PUB/410, International Atomic Energy Agency, Vienna, 1976, pp. 139-153.
7. Nelson, D.M. and Lovett, M.B., "Radiological and Environmental Research Division Annual Report," ANL-79-65, Part III; Roland, R.E. and Penrose, W.R., Eds.; National Technical Information Service, Springfield, Va., 1979, pp. 60-61.
8. Nelson, D.M. and Lovett, M.B.; Nature; 1978, 276, No. 5688, pp. 599-601.
9. Auerbach, S.I. and Reichle, D.E., "Environmental Sciences Division Annual Report for Period Ending September 30, 1981," ORNL-5900, National Technical Information Service, Springfield, Va., 1981, p. 75.
10. Edgington, D.N., "Techniques for Identifying Transuranic Speciation in Aquatic Environments" STI/PUB/613, International Atomic Energy Agency, Vienna, 1981, pp. 1-25.
11. Wahlgren, M.A. and Orlandini, K.A., "Environmental Migration of Long-Lived Radionuclides" STI/PUB/597, International Atomic Energy Agency, 1982, pp. 757-774.
12. Simpson, H.J.; Trier, R.M.; Olsen, C.R.; Hammond, D.E.; Ege, A.; Miller, L.; and Melack, J.M., Science; 1980, 207, pp. 1071-1073.
13. Simpson, H.J.; Trier, R.M.; Toggweiler, J.R.; Mathieu, G.; Deck, B.L.; Olsen, C.R.; Hammond, D.E.; Fuller, C.; and Ku, T.L., Science; 1982, 216, pp. 512-514.
14. Alberts, J.J. and Wahlgren, M.A.; Environmental Science and Technology; 1981, 15, pp. 94-98.
15. Edgington, D.N.; Karttunen, J.O.; Nelson, D.M.; and Larsen, R.P., "Radiological and Environmental Research Division Annual Report," ANL-79-65, III, Rowland, R.E. and Penrose, W.R., Eds., National Technical Information Service, Springfield, Va., 1979, pp. 54-56.
16. Noshkin, V.E. and Wong, K.M., Proceedings of Third Nuclear Energy Agency, NEA, "Seminar on Marine Radioecology" Tokyo, October 1-5, 1979, (in press).
17. Bowen, V.T.; Noshkin, V.E.; Livingston, H.D.; and Volchok, H.L., Earth and Planetary Letters, 1980, 49, pp. 411-434.
18. Fukai, R.; Ballestra, S.; and Thein, M., "Techniques for Identifying Transuranic Speciation in Aquatic Environments," STI/PUB/613, International Atomic Energy Agency, Vienna, 1981, pp. 79-87.
19. Lovett, M.B. and Nelson, D.M., "Techniques for Identifying Transuranic Speciation in Aquatic Environments" STI/PUB/613, International Atomic Energy Agency, Vienna, 1981, pp. 27-35.

20. Nelson, D.M. and Orlandini, K.A., "Radiological and Environmental Research Division Annual Report, January-December 1979," ANL-79-65, III, Rowland, R.E. and Penrose, W.R., Eds.; National Technical Information Service, Springfield, Va., 1979, pp. 57-59.
21. Bondiotti, E.A. and Trabalka, J.K., Radiochem. Radioanal. Chem. Lett., 1979, 42(3), p. 169.
22. Inoue, Y. and Tochiyama, O., J. Inorg. Nuc. Chem., 1977, 39, pp. 1443-1447.
23. Auerbach, S.I. and Reichle, D.E., "Environmental Sciences Division Annual Report for Period ending September 30, 1981," ORNL-5900, National Technical Information Service, 1982, pp. 76-77.
24. Nelson, D.M.; Metta, D.N.; and Larsen, R.P., "Radiological and Environmental Research Division Annual Report, January-December 1980," ANL-80-115, III, Rowland, R.E. and Penrose, W.R., Eds., National Technical Information Service, Springfield, Va., 1980, pp. 26-28.
25. Wahlgren, M.A.; Robbins, J.A.; and Edgington, D.N., "Transuranic Elements in the Environment," DOE/TIC 22800, Hanson, W.C., Ed., National Technical Information Service, Springfield, Va., 1980, pp. 659-683.
26. Bondiotti, E.A., personal communication.
27. Nelson, D.M.; Karttunen, J.O.; Orlandini, K.A.; and Larsen, R.P., "Radiological and Environmental Research Division Annual Report, January-December 1980," ANL-80-115, III, Rowland, R.E. and Penrose, W.R., Eds., National Technical Information Service, Springfield, Va., 1981, pp. 19-25.
28. Nelson, D.M.; Karttunen, J.O.; and Mehlhoff, P., "Radiological and Environmental Research Division Annual Report, January-December 1981," ANL-81-85, Rowland, R.E. and Penrose, W.R., Eds., National Technical Information Service, Springfield, Va., 1982, pp. 48-52.
29. Mathew, E. and Pillai, K.C., "Techniques for Identifying Transuranic Speciation in Aquatic Environments," STI/PUB/613, International Atomic Energy Agency, Vienna, 1981, pp. 195-207.
30. Alberts, J.J.; Lutkenhoff, D.; Geiger, R.A.; and Gant, D., "Annual Report of Ecological Research at the Savannah River Ecology Laboratory," Institute of Ecology, University of Georgia, Athens, Ga., 1979, pp. 90-91.
31. Scatchard, G., Ann. N.Y. Acad. Sci., 1949, 51, pp. 660-672.
32. Bertha, E.L. and Choppin, G.R., J. Inorg. Nuc. Chem., 40, 1978, pp. 655-658.

RECEIVED December 22, 1982

Complexation of the Plutonium(IV) Ion in Carbonate–Bicarbonate Solutions

J. I. KIM, CH. LIERSE, and F. BAUMGÄRTNER

Institut für Radiochemie, TU München, 8046 Garching,
Federal Republic of Germany

The complexation of Pu(IV) with carbonate ions is investigated by solubility measurements of $^{238}\text{PuO}_2$ in neutral to alkaline solutions containing sodium carbonate and bicarbonate. The total concentration of carbonate ions and pH are varied at the constant ionic strength ($I = 1.0$), in which the initial pH values are adjusted by altering the ratio of carbonate to bicarbonate ions. The oxidation state of dissolved species in equilibrium solutions are determined by absorption spectrophotometry and differential pulse polarography. The most stable oxidation state of Pu in carbonate solutions is found to be Pu(IV), which is present as hydroxocarbonate or carbonate species. The formation constants of these complexes are calculated on the basis of solubility data which are determined to be a function of two variable parameters: the carbonate concentration and pH. The hydrolysis reactions of Pu(IV) in the present experimental system assessed by using the literature data are taken into account for calculation of the carbonate complexation.

With growing interest in the chemical behaviour of actinide ions in the environment (1), the complexation of these ions with carbonate anions has been recently attracting particular attention (2-10) due to the ubiquitous presence of carbonate ions in nature (11, 12) and their pronounced tendency to form complexes with heavy metal ions (7, 10-14). In spite of the carbonate complexation of actinides being considered important chemical reactions for understanding the chemistry of actinides in natural fluids, not many experiments have been devoted up to now to the quantitative study of the subject, though numerous qualitative observations are discussed in the literature. Although there are a few papers reporting the formation constants of carbonate complexes

0097-6156/83/0216-0317\$06.00/0
© 1983 American Chemical Society

of Pu(III) and Pu(VI) (15, 16), in a critical compilation of stability constants (13) none of these data has been considered worthy of incorporation. To our present knowledge no recorded data have been known for the carbonate complexation of Pu(IV) in the literature except one for the formation of PuCO_3^{2+} species (17).

The study of carbonate complexes of Pu is complicated by various experimental difficulties. The low solubility of many carbonates (7), leaving a very dilute Pu concentration in solution, results in difficulties to the experiments with electrochemical or spectrophotometric methods. However, the radiometric method with solvent extraction or solubility measurement is easily applicable for the purpose. Unlike the solution with anions, like Cl^- , NO_3^- etc., the concentration of which can be varied at a constant pH, the preparation of solutions with varying carbonate concentration accompanies indispensably the change of pH of the solution. As a result, the formation of carbonate complexes involves accordingly the hydrolysis reactions of Pu ions in solutions under investigation. It is therefore prerequisite to know the stability constants of Pu(IV) hydroxides prior to the study of its carbonate complexation.

The present study is conducted under consideration of thus mentioned difficulties. The solubility measurement is applied to the present investigation, selecting the pH range 6 ~ 12 in which the carbonate concentration can be maintained greater than 5×10^{-6} M/l. The carbonate concentration and pH of experimental solutions, both being mutually dependent in a given solution, are taken into account as two variable parameters in the present experiment and hence the final evaluation of formation constants is based on three dimensional functions. For calculation purpose, the hydrolysis constants of Pu(IV) are taken from the literature (18). In order to differentiate the influence of hydrolysis reactions on the carbonate complexation so far as possible, the calculation is based on the solubilities from solutions of carbonate concentration $> 10^{-4}$ M/l and pH > 8 .

Experimental

The $^{238}\text{PuO}_2$ is prepared by precipitation of Pu(IV) hydroxide from nitric acid solution with an addition of conc. NH_4OH , which is followed by washing, filtration, drying and calcination of the hydroxide for 6 hrs at 700 °C. At the time of preparation, the $^{238}\text{PuO}_2$ is found to be in crystalline state with the lattice constant of 5.399 Å and the average crystal size of 225 Å. The isotopic composition of plutonium is known to be 94.84 % ^{238}Pu , 4.89 % ^{239}Pu , 0.24 % ^{240}Pu , 0.024 % ^{241}Pu , 0.004 % ^{242}Pu and 6.2 ppm ^{236}Pu .

About 5 mg of thus prepared $^{238}\text{PuO}_2$ is introduced in each experimental solution of 10 ml, which is prepared with varying the concentration of carbonate ion and pH by changing the $\text{NaHCO}_3/\text{Na}_2\text{CO}_3$ ratio at the constant ionic strength ($I = 1.0$) adjusted

by addition of NaClO_4 . A few solutions prepared with high carbonate concentration, up to 1 M/l, are also included. All samples are placed in glass vials with tightly closed cover and allowed to stand for a long period of time with occasional shaking. Measurements are made after 4, 9 and 12 months contact time.

The sampling of solution for activity measurement is carried out by filtration with 0.22 μm Millex filter (Millipore Co.) which is encapsulated and attached to a syringe for handy operation. The randomly selected filtrates are further passed through Amicon Centriflo membrane filter (CF-25) of 2 nm pore size. The activities measured for the filtrates from the two different pore sizes are observed to be identical within experimental error. Activities are measured by a liquid scintillation counter. For each sample solution, triplicate samplings and activity measurements are undertaken and the average of three values is used for calculation. Absorption spectra of experimental solutions are measured using a Beckman UV 5260 spectrophotometer for the analysis of oxidation states of dissolved Pu ions.

This analysis is further supported by the measurements with differential pulse polarography (Polarecord E 506, Metrohm Co.) using a dropping Hg electrode. To examine the most stable oxidation state of Pu ions in carbonate solutions, the experiment is conducted by combining an electrochemical reaction cell to the absorption spectrophotometry. The Pu solution of different oxidation states prepared electrochemically is continuously circulated between the reaction cell and the cuvette in the spectrophotometer. The original solution of 0.1 M HClO_4 containing 10^{-3} M/l Pu is titrated with Na_2CO_3 solution and the change in oxidation states is observed with gradually varying the pH and carbonate concentration.

At the time of sampling, the total concentration of carbonate ions in each solution and its pH are determined using a CO_2 -electrode (Orion Research Co-Type 95-02) and a glass electrode, respectively. Based on these results, the concentrations of free bicarbonate and carbonate ions in each solution are calculated by taking account of degrees of dissociation of NaHCO_3 , Na_2CO_3 , H_2CO_3 and HCO_3^- , which are taken from the literature (15, 18, 19) or assessed through interpolation or extrapolation of relevant literature data (20, 21).

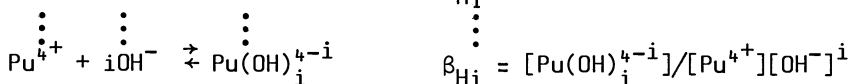
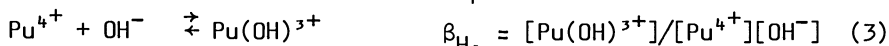
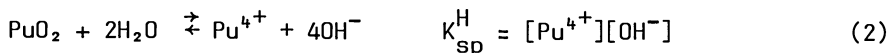
Results and discussion

Hydrolysis reactions. As the system under investigation contains not only carbonate ions but also hydroxide ions of considerable concentration, it is quite plausible that the reactions of hydrolysis and carbonate complex formation compete with each other. Since the hydrolysis reaction is not investigated separately in this experiment, the magnitude of this reaction as a function of pH is evaluated on the basis of the formation constants available in the literature (18), which are reproduced

in Table I, together with the solubility product of PuO_2 taken from the same literature. The dissolved concentration of Plutonium, $[\text{Pu}]_s$, due to hydrolysis reaction is the sum of all hydroxide species:

$$[\text{Pu}]_s = [\text{Pu}^{4+}] + [\text{Pu}(\text{OH})^{3+}] + \dots + [\text{Pu}(\text{OH})_i^{4-i}] \quad (1)$$

which can be written in terms of the solubility product of PuO_2 , K_{sp}^H , and formation constant of each hydroxide species β_{Hi} , such as:



and hence

$$[\text{Pu}]_s = \frac{K_{sp}^H}{[\text{OH}^-]^4} \left(\sum_{i=0}^5 \beta_{Hi} [\text{OH}^-]^i \right) \quad (4)$$

Based on Equation 4, it is possible to evaluate the dissolved concentration of Pu as a function of pH, provided polymer and other complex species are not present. However, the polymerization of hydrolysed species enhances the solubility of PuO_2 , and hence the dissolved Pu concentration is expected to be greater than the quantity calculated by Equation 4. On the other hand, the presence of a strong complexing anion, e.g. carbonate ion, may

Table I. The formation constants of Pu(IV) hydroxides (18) ^{a)}

Species: $\text{Pu}(\text{OH})_i$	$\log \beta_{HiCo}$ ^{b)}
$\text{Pu}(\text{OH})^{3+}$	12.2
$\text{Pu}(\text{OH})_2^{2+}$	24.6
$\text{Pu}(\text{OH})_3^+$	34.7
$\text{Pu}(\text{OH})_4^0$	44.3
$\text{Pu}(\text{OH})_5^-$	52.7
$\text{PuO}_2(s)$	$-\log K_{sp}^H = 52.0$ ^{c)}

a) calculated based on the values in Tables 4.4 and 9.9 in (18)

b) symbol used in this paper (cf. Equation 14)

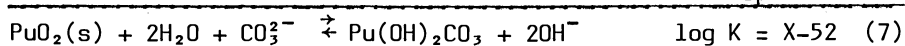
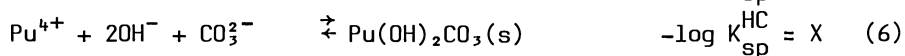
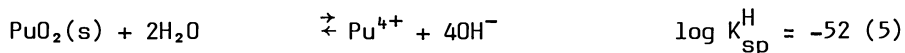
c) the value taken as the average of those given in (7) and (18)

suppress the polymerization and higher degree of hydrolysis reactions through formation of carbonate or hydroxocarbonate species of the Pu(IV) ion.

By the aid of the literature data of hydrolysis constants, the absolute and relative amounts of each hydroxide species of Pu(IV) as a function of pH are calculated and given in Figures 1a and 1b. It is shown in this figure that in the region pH > 8 only the Pu(OH)₅⁻ appears in the solution. By adding the carbonate ion of increasing concentration and thus increasing pH, it is expected that the Pu(OH)₅⁻ ion is transformed to different carbonate complexes and at the same time the solubility pattern of PuO₂ changes.

Complexation of Pu(IV) ion with carbonate anion. The solubilities of PuO₂ are determined to be varying with respect to the carbonate concentration as well as pH simultaneously. The dissolved concentrations of Pu determined after 4 and 12 months contact time are given in Figure 2 as a function of pH, whereas the concentrations of free carbonate and bicarbonate ions determined in each experimental solution are presented in Figure 3. The solubilities measured after 9 and 12 months are found to be almost identical. In Figure 2, it is observed that the solubility of PuO₂ at first decreases slowly with increasing pH until pH = 8.5, then decreases rapidly between pH = 8.5 ~ 10.0, and finally increases steeply above pH = 10.0. This development of solubility with increasing pH does not reflect a monotonous function with single variable as shown by Equation 4 but infers to a function of two variable parameters, i.e. pH and carbonate concentration. The minimum solubility observed at pH = 10 and [CO₃²⁻] = 3 x 10⁻³ M/l implies that there is a transformation of solid species (s) taking place, i.e. from PuO₂(s) to Pu(OH)₂CO₃(s).

The existence of such a process can be indirectly evidenced by the irregular change of decrement observed in free carbonate (also bicarbonate) concentrations near pH = 10 as illustrated in Figure 3. This may be ascribed to the consumption of free carbonate ions for the formation of the plutonium hydroxocarbonate precipitate. The reactions involved in this process are interpreted as follows:



$$\text{where } \log K \text{ can be } X-52 \gtrsim 0 \quad (8)$$

For convenience of illustration and further explanations to be followed later, the free Pu⁴⁺ ion is taken as an intermediate reactant in the formulation of Equations 5 and 6, although this

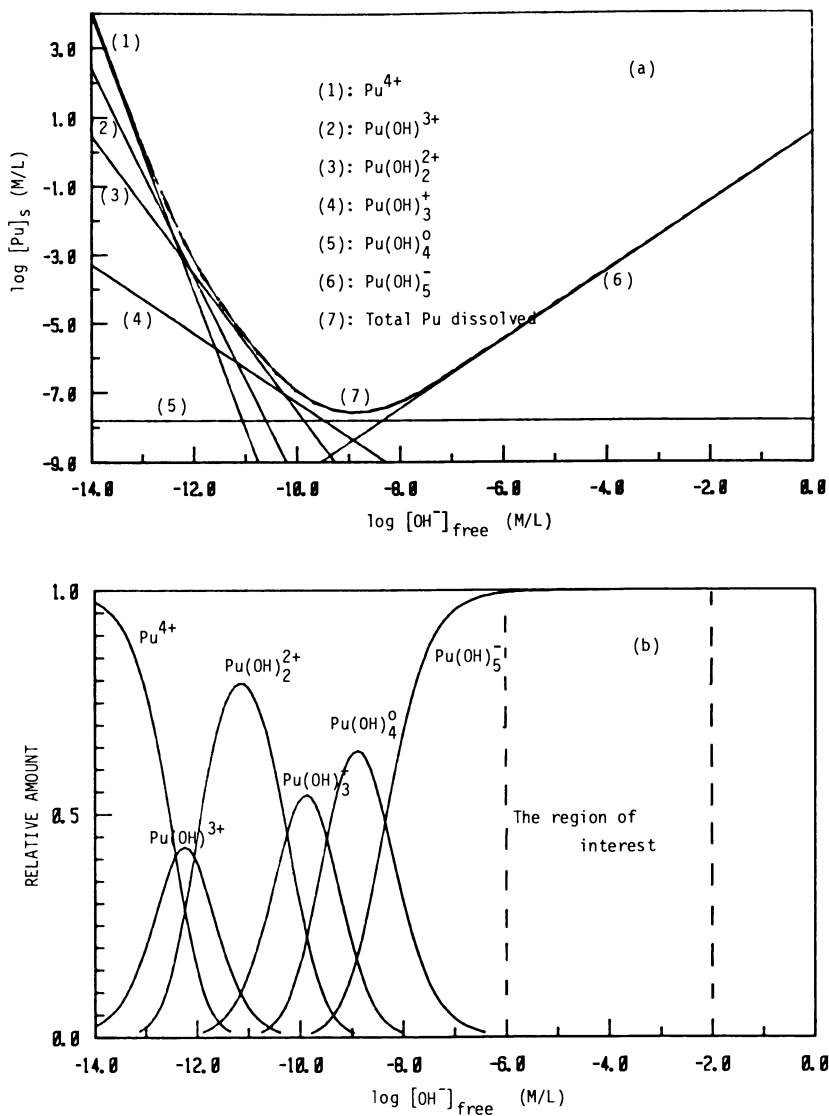


Figure 1.

The absolute (a) and relative (b) amounts of Pu(IV) hydroxide ion concentration (or pH), calculated by Equation 4 based on the data given in Table I. The region of interest for the present investigation is marked by dotted lines.

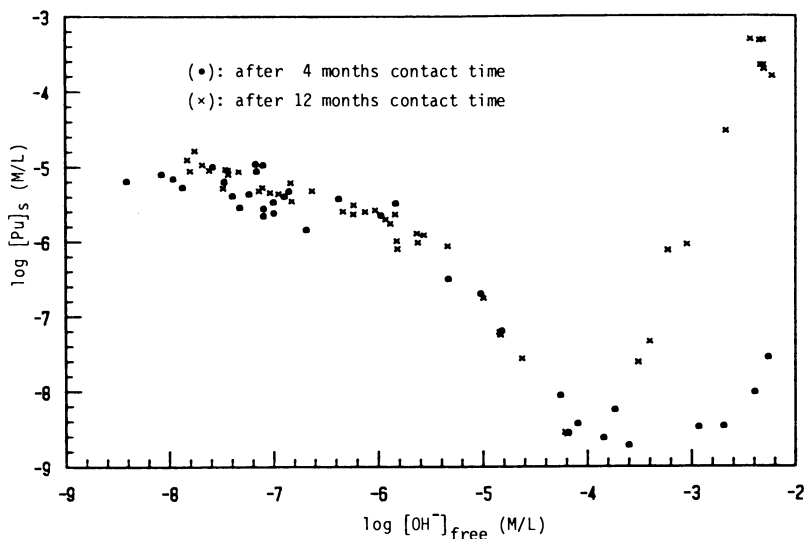


Figure 2.

The solubilities of $^{238}\text{PuO}_2(\text{c})$ as a function of the pH of equilibrium solutions. Up to $\text{pH} = 10$ the solubilities after 4 and 12 months are almost identical, while at $\text{pH} > 10$ the values after 12 months differ from those after 4 months which are not in equilibrium. The values after 12 months and 9 months (not plotted here) are found to be identical.

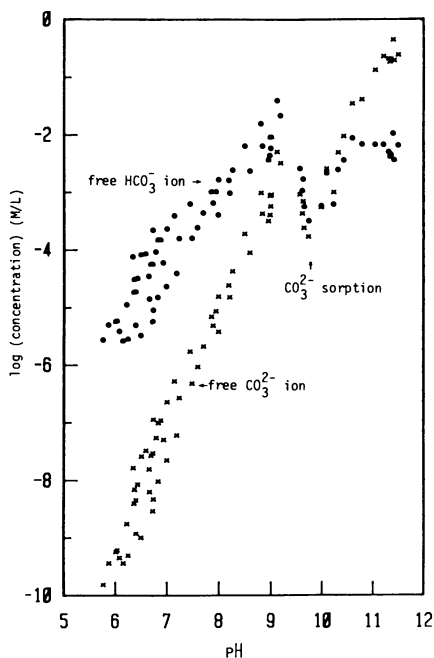
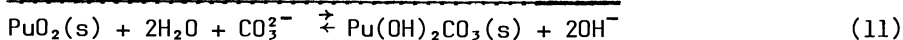
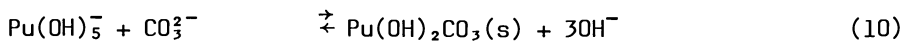
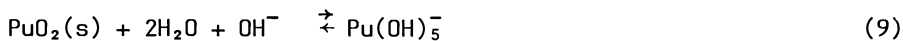


Figure 3.

The concentrations of free carbonate and bicarbonate ions determined at solubility equilibrium as a function of pH. Decrements of the concentration near pH = 10 suggest the formation of the $\text{Pu}(\text{OH})_2\text{CO}_3$ precipitate and hence lowering solubilities of PuO_2 (cf. Figure 2).

ion is not viable species in the solution of pH > 8. The reaction given by Equation 7 can be formulated alternatively with more or less reality relevant reactions:



As is apparent in Figures 1a and 1b, the $\text{Pu}(\text{OH})_5^-$ species is predominant at pH > 8 in the absence of carbonate ions. It appears reasonable to expect that in the presence of carbonate ions in solution the $\text{Pu}(\text{OH})_5^-$ ion undergoes the formation of the $\text{Pu}(\text{OH})_2\text{CO}_3$ precipitate, of which the solubility depends on the carbonate concentration as well as pH. Consideration of $\text{Pu}(\text{OH})_2\text{CO}_3$ as a least soluble species under the present experimental system is attributed to the similar compound, i.e. $\text{ThOCO}_3 \cdot n\text{H}_2\text{O}$, which appears sparingly soluble in alkaline carbonate solutions (22). Equation 8 may result in a positive or negative value; the former indicates $\text{Pu}(\text{OH})_2\text{CO}_3$ less soluble than PuO_2 , while the latter suggesting the reverse.

The dissolved species are considered to be a composite of numerous hydroxides, carbonates, and hydroxocarbonates of Pu(IV), which can be expressed by

$$\begin{aligned} [\text{Pu}]_s = & [\text{Pu}^{4+}] + [\text{Pu}(\text{OH})^{3+}] + \dots + [\text{Pu}(\text{OH})_i^{4-i}] + \\ & + [\text{Pu}(\text{CO}_3)^{2+}] + [\text{Pu}(\text{OH})(\text{CO}_3)^+] + \dots + [\text{Pu}(\text{OH})_i(\text{CO}_3)^{2-i}] + \\ & \vdots \qquad \qquad \qquad \vdots \qquad \qquad \qquad \vdots \\ & + [\text{Pu}(\text{CO}_3)_j^{4-2j}] + [\text{Pu}(\text{OH})(\text{CO}_3)_j^{3-2j}] + \dots + [\text{Pu}(\text{OH})_i(\text{CO}_3)_j^{4-i-2j}] \end{aligned} \quad (12)$$

and in a general form:

$$[\text{Pu}]_s = [\text{Pu}^{4+}] \left[\sum_{i=0}^n \frac{\sum_{j=0}^m \beta_{\text{HiCj}}}{j!} [\text{OH}^-]^i [\text{CO}_3^{2-}]^j \right] \quad (13)$$

where

$$\beta_{\text{HiCj}} = \frac{[\text{Pu}(\text{OH})_i(\text{CO}_3)_j]}{[\text{Pu}^{4+}] [\text{OH}^-]^i [\text{CO}_3^{2-}]^j} \quad (14)$$

The free concentration of Plutonium, $[\text{Pu}^{4+}]$, is controlled by either solubility products, K_{sp}^{H} for PuO_2 or K_{sp}^{C} for $\text{Pu}(\text{OH})_2\text{CO}_3$,

namely

$$[\text{Pu}^{4+}] = \frac{K_{sp}^H}{[\text{OH}^-]^4} \quad \text{or} \quad [\text{Pu}^{4+}] = \frac{K_{sp}^{HC}}{[\text{OH}^-]^2[\text{CO}_3^{2-}]} \quad (15)$$

Which of the two is applicable to the present experiment depends mainly on whether Equation 8 results in a positive or negative value. The solubility changes quite differently in $\text{pH} > 8$ and reaches the minimum ($[\text{Pu}]_s = 2 \times 10^{-9}$ M/l) at $\text{pH} = 10$ and $[\text{CO}_3^{2-}] = 3 \times 10^{-3}$ M/l. Since the minimum is much lower than the value assessed by Equation 4 (cf. Figure 1a), it is plausible that Equation 8 becomes a positive value. As described above, in $\text{pH} < 8$ the carbonate concentrations are relatively small, $< 10^{-4}$ M/l, and it is therefore expected that in that condition different hydroxide species are predominant (cf. Figure 1b). In $\text{pH} > 8$ where $[\text{CO}_3^{2-}] > 10^{-4}$ M/l, the formation of hydroxocarbonate and carbonate complexes may take place. For this reason, evaluation of the final results is mainly based on the experimental data from the solutions of $\text{pH} > 8$ and $[\text{CO}_3^{2-}] > 10^{-4}$ M/l.

For the determination of β_{HiCj} the computational solution of experimental results is carried out by Equation 13. The β_{HiCo} values for hydrolysis reactions are taken into account as given in Table 1. The i and j values are varied from 0 to 5 for the formation of hydroxocarbonate complexes. The input parameters for Equation 13: $[\text{Pu}]_s$, $[\text{OH}^-]$ (or pH), and $[\text{CO}_3^{2-}]$ are all experimental values after 12 months contact time.

Verification of Pu(IV) ion in solution. Whether the dissolved Pu ions are tetravalent is verified by the following experiments. The absorption spectrophotometry of the solutions with higher carbonate concentration (> 0.1 M/l), in which the $[\text{Pu}]_s$ values are greater than 10^{-5} M/l, shows that the dissolved species are Pu(IV) ions. The indirect confirmation of a stable species of Pu ions in carbonate solutions is made by a gradual addition of Na_2CO_3 solution to 0.1 M HClO_4 solution containing Pu ions of different oxidation states. With increasing the carbonate ion concentration in the solution, where pH being also increased accordingly, it is observed that the distinctive absorption peaks of Pu(III), Pu(IV), Pu(VI) in HClO_4 solution disappear gradually and the absorption spectrum of Pu(IV) in carbonate solution is finally observed. Figure 4 manifests the transfer process of different oxidation states of Pu ions from the HClO_4 solution to Pu(IV) in the carbonate solution. The spectrophotometric results are further supported by the measurements with differential pulse polarography, which demonstrates that the most stable Pu oxidation state in carbonate solutions is Pu(IV).

The lowest solubility observed in our experiments is 2×10^{-9} M/l at $\text{pH} = 10$ and $[\text{CO}_3^{2-}] = 3 \times 10^{-3}$ M/l. When the dissolved spe-

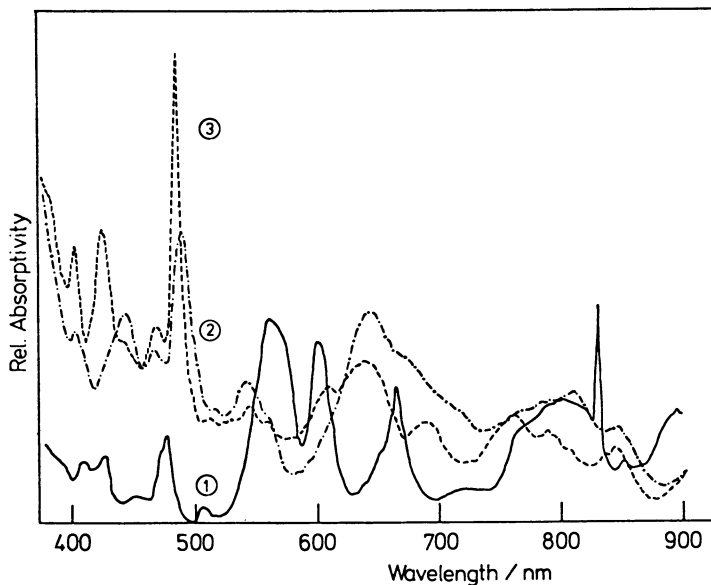


Figure 4.

The absorption spectra of the Pu ions in different solutions. Curve 1: The starting solution containing Pu(III), Pu(IV), Pu(V) and Pu(VI) ions in 0.1 M HClO₄; curve 2: after addition of Na₂CO₃ solution (pH = 6.7; [CO₃²⁻] = 10⁻⁴ M/l); curve 3: after further addition of Na₂CO₃ solution (pH = 10.4; [CO₃²⁻] = 0.3 M/l). The Pu concentration is (1-5) × 10⁻⁵ M/l.

cies may be other than Pu(IV) ion, it is to expect that the solubility under this condition must be higher than the observed value, since the oxidation or reduction enhances the solubility of the least soluble Pu(IV) compound. It is quite well known that the tetravalent actinide compounds are less soluble than the same complex compounds of other oxidation states.

In the literature (3), the possible formation of plutonyl bicarbonate complex is discussed. In order to verify whether we are dealing with bicarbonate or carbonate complexes, the Pu(IV) solutions prepared in NaHCO₃ and Na₂CO₃ solutions are examined by spectrophotometry. The absorption spectra measured up to 900 nm show no visible difference for both solutions. For this reason it is believed that the Pu(IV) ion forms carbonate complexes irrespective of carbonate or bicarbonate ions present in solution.

Formation constants of carbonate complexes. The computational treatment of experimental results by Equation 13 is made by an iteration process. Figures 5 and 6 demonstrate comparisons of computed values with experimental data as a function of two different variable parameters, [OH⁻] and [CO₃²⁻]. Since the experimental error in the measurement of carbonate concentration is relatively large due to small volume of solution available to use, a certain extent of deviation is expected from the comparison of computed values with experimental data. However, Figures 5 and 6 show that reasonable agreements between the two values are attained as a function of pH as well as of the carbonate concentration. Since each solubility point is related with the two parameters simultaneously, the computed points do not follow smooth curves but sensitively fluctuate in accordance with the variation of the conjugate parameter. Because the carbonate concentration and pH are mutually dependent in a given solution and because the OH⁻ and CO₃²⁻ ions are competitive ligands for complexation of the Pu(IV) ion, it is found necessary to investigate the carbonate complexation of Pu(IV) by varying the two parameters simultaneously.

The calculated formation constants of β_{HiCj} are presented in Table 2. Among calculated values for probable complex species, the relative amounts of dominant and less dominant complex species are distinguished by

$$\alpha_{ij} = \frac{\beta_{\text{HaCb}} [\text{OH}^-]^a [\text{CO}_3^{2-}]^b}{\sum_{i=0}^n \sum_{j=0}^m \beta_{\text{HiCj}} [\text{OH}^-]^i [\text{CO}_3^{2-}]^j} \quad (a, b = \text{const.}) \quad (16)$$

The relative amount of dominant species under the experimental condition are shown in Figure 7. Five species are predominant in the solution: Pu(OH)CO₃⁺, Pu(CO₃)₂⁰, Pu(CO₃)₂²⁻, Pu(CO₃)₄⁴⁻, and Pu(CO₃)₅⁶⁻. The species other than those given here are not present in significant amount.

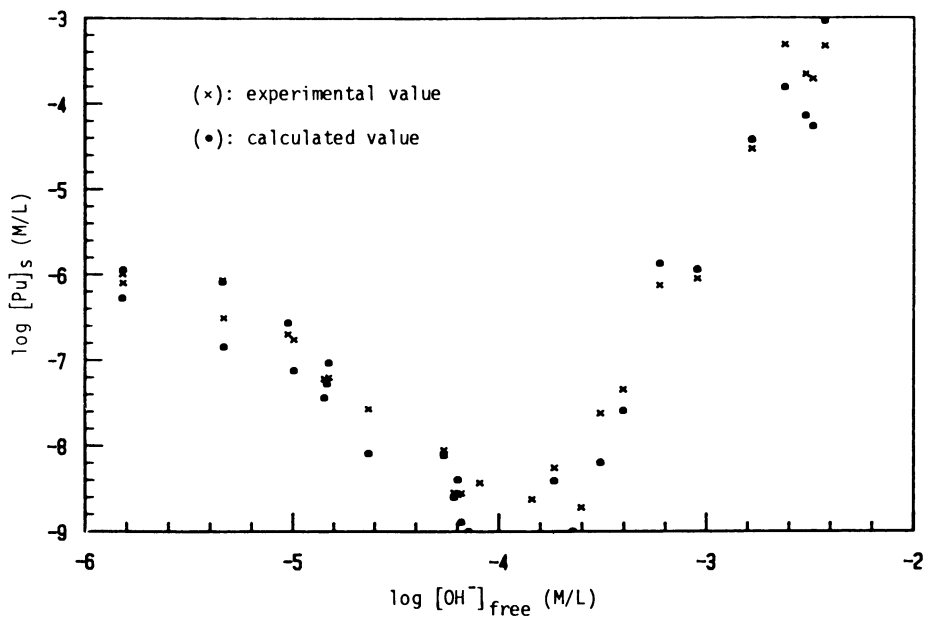


Figure 5.

The comparison of calculated solubilities by Equation 13 with the values from experiment (12 months contact time). The values are plotted as a function of the concentration of free hydroxide ion at solubility equilibria (cf. Figure 6).

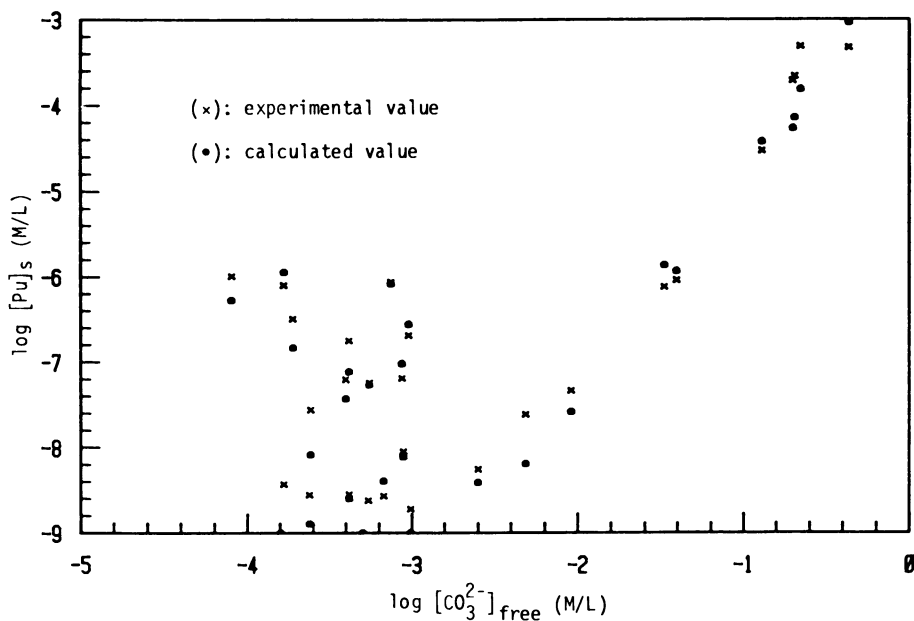


Figure 6.

The comparison of calculated solubilities by Equation 13 with the values from experiment (12 months contact time). The values are plotted as a function of the concentration of free carbonate ion at solubility equilibria (cf. Figure 5).

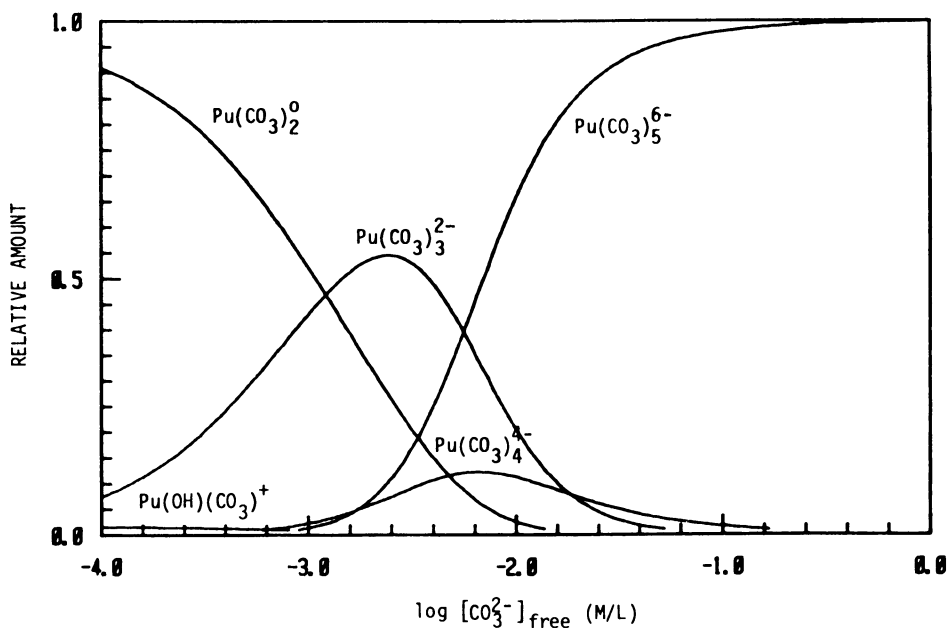


Figure 7.

The relative amounts of predominant hydroxocarbonate and carbonate species of Pu(IV) in the investigated solutions.

The complex formation constants obtained from this experiment are very large in comparison with the complexation of the Pu(IV) ion with other ligands, like OH^- , F^- etc. In view of solubilities observed in higher carbonate concentration ($[\text{Pu}]_s \approx 10^{-3} \text{ M/l}$) it is considered possible that the formation constants of carbonate complexes of the Pu(IV) ion must be relatively large. The postulation made in this work as for the formation of the very insoluble $\text{Pu}(\text{OH})_2\text{CO}_3$ under the present experimental condition is primarily based on the earlier works (22) on $\text{ThOCO}_3 \cdot n\text{H}_2\text{O}$, which is found to be not much soluble in alkaline solution. However, the experimental verification of the postulation is still in progress for the moment. The radiolysis effect due to the ^{238}Pu nuclide used in the present experiment is not investigated separately. The recent paper (23) dealing with the solubility of $^{238}\text{PuO}_2$ in pure water discusses the change of pH due to the radiolysis effect, i.e. decrease of pH on account of the formation of HNO_3 in the solution open to air and hence increasing the solubility of $^{238}\text{PuO}_2$. In our separate experiment made in a system closed to air contact, the solubilities of $^{238}\text{PuO}_2$ after 200 days in water with varying pH = 5 ~ 9 are observed to be identical with the values reported in the literature for $^{239}\text{PuO}_2 \cdot n\text{H}_2\text{O}(\text{am})$ (24) which were measured after 250 days. From experience, it is believed that the radiolysis effect can be of two kinds: the direct effect which changes the crystalline structure of the oxide and thus alters the kinetics of dissolution; the indirect effect which changes the solution and components therein, e.g. producing HNO_3 in case of the solution being in contact with air, and hence leading to a different state of equilibrium, namely higher solubility. However, the thus increased solubility follows the equi-

Table II. The formation constants of Pu(IV) carbonates and hydroxocarbonates

Species: $\text{Pu}(\text{OH})_i(\text{CO}_3)_j$	$\log \beta_{\text{HiCj}}^{\text{a)}$
PuCO_3^{2+}	47.1 ± 3.0
$\text{Pu}(\text{CO}_3)_2^0$	55.0 ± 2.5
$\text{Pu}(\text{CO}_3)_3^{2-}$	57.9 ± 2.7
$\text{Pu}(\text{CO}_3)_4^{4-}$	59.6 ± 2.9
$\text{Pu}(\text{CO}_3)_5^{6-}$	62.4 ± 2.4
$\text{Pu}(\text{OH})\text{CO}_3^+$	55.2 ± 2.3
$\text{Pu}(\text{OH})_2\text{CO}_3(\text{s})$	$-\log K_{\text{sp}}^{\text{HC}} = 68.8 \pm 2.4$

a) symbol used in this paper (cf. Equation 13)

librium function with respect to pH, unless other complexing agents are present in solution. In a carbonate solution, the radiation effect changes pH and therewith the carbonate concentration, and the PuO_2 solubility varies accordingly. The solubility function shown in Figure 2 is not altered after 9 months, not after 4 months at $\text{pH} < 10$, although individual experimental points are shifted to other positions in accordance with new values of pH and the carbonate concentration determined. The primary mechanisms of radiolysis effect on the solubility of PuO_2 are, however, an important subject for separate investigation.

Similar experiments with $^{239}\text{PuO}_2$ are in progress in our laboratory and will be used to verify or to improve the preliminary results presented in this paper.

Acknowledgments

The authors are much indebted to Dr. F. X. Koppold for the computer calculation. Thanks are due to Mr. Y. X. Xia for his help in measuring the absorption spectra and the technical assistance of Miss Ch. Rahner throughout this work is acknowledged.

Literature Cited

1. Hanson, W. C., Ed.; "Transuranic Elements in the Environment"; DOE/TIC-22800, 1980.
2. Billon, A., Ed.; "Techniques for Identifying Transuranic Speciation in Aquatic Environments"; STI/PUB/613, IAEA: Vienna, 1981; p 65.
3. Sullivan, J. C.; Bertrand, P. A.; Choppin, G. R. Radiochim. Acta, in press.
4. Wood, M.; Mitchell, M. L.; Sullivan, J. C. Inorg. Nucl. Chem. Lett. 1978, 14, 465.
5. Rai, D.; Serne, R. J. J. Environ. Qual. 1977, 6, 89.
6. Langmuir, D. Geochim. Cosmochim. Acta 1978, 42, 547.
7. Edelstein, W. M., Ed.; "Actinides in Perspective"; Pergamon Press: New York, 1981; p 553.
8. Bidoglio, G. Radiochem. Radioanal. Lett. 1982, 53, 45.
9. Brückl, N.; Li, G. H.; Kim, J. I. Paper presented in the meeting of German Chemical Society, Nuclear Chemistry: Karlsruhe, Sep. 21-25, 1982.
10. Jensen, B. S. RIS-Report on Critical review of available information on migration phenomena of radionuclides into the geosphere, 1981.
11. Stumm, W.; Morgan, J. J., Eds.; "Aquatic Chemistry"; John Wiley & Sons: New York, 1981.
12. Lindsay, W. L., Ed.; "Chemical Equilibria in Soils"; John Wiley & Sons: New York, 1979.
13. Smith, R. M.; Martell, A. E., Eds.; "Critical Stability Constants"; Plenum Press: New York, 1976.

14. Saltelli, A.; Avogadro, A.; Bertozzi, G. "Proc. Workshop on the Migration of Long-lived Radionuclides in the Geosphere"; OECD/NEA: Paris, 1979; p 147.
15. Sillen, L. G.; Martell, A. E., Eds.; "Stability Constants of Metal Ion Complexes"; The Chemical Society: London, 1964.
16. Cleveland, J. M., Ed.; "The Chemistry of Plutonium"; Gordon & Breach Science, 1970.
17. Moskvina, A. I.; Gel'man, A. D. Russ. J. Inorg. Chem. 1958, 3, 962.
18. Baes, C. F.; Mesmer, R. G., Eds.; "The Hydrolysis of Cations"; John Wiley & Sons: New York, 1976.
19. Walker, J.; Cormack, W. J. Chem. Soc. 1900, 77, 11.
20. Frary, F. C.; Nietz, A. H. J. Am. Soc. 1915, 37, 2271.
21. Seyler, C. A.; Lloyd, P. V. J. Chem. Soc. 1917, 111, 138.
22. Gmelin Handbuch der Anorg. Chem. "Thorium und Isotope"; Sys. Nr. 44, Verlag Chemie: Weinheim, 1955; p 300.
23. Rai, D.; Ryan, L. Radiochim. Acta in press.
24. Rai, D.; Serne, R.; Moore, D. A. Soil Sci. Soc. Am. J. 1980, 44, 490.

RECEIVED December 21, 1982

Ground-Water Composition and Its Relationship to Plutonium Transport Processes

JESS M. CLEVELAND, TERRY F. REES, and KENNETH L. NASH
U.S. Geological Survey, Denver, CO 80225

The degree of plutonium leaching by ground waters from waste glass and its oxidation state distribution in solution were strongly influenced by the chemical composition of the waters. Ground waters from four possible host rock types--basalt, granite, shale, and tuff--as well as deionized water were used in this study. The order of plutonium leachability in the five waters was basalt >> tuff > deionized > granite > shale. High leaching efficiency in the basalt and tuff waters was the result of their high fluoride ion concentrations, whereas the lower leaching ability of granite and shale waters compared to deionized water may result from surface passivation of the glass by dissolved species--possibly sodium or magnesium--present in relatively greater concentrations in these waters. In single-phase speciation experiments with these five waters, plutonium was essentially completely soluble in basalt ground water because of its high fluoride concentration, and almost totally insoluble in shale ground water, probably because of the enhancement of colloid coagulation resulting from the large sulfate concentration in this water. In the single-phase experiments, plutonium(IV) was present in appreciable concentrations only in the basalt ground water, whilst in the leaching studies it was a common component in all of the leachates. Trends were more pronounced at 90°C than at 25°C, probably because of kinetic effects. Because of the large influence of ground-water composition on plutonium leachability and subsequent solubility, we propose that it be included as a radioactive waste repository site-selection criterion.

Transport of plutonium from a geologic repository may be considered to involve three processes:

This chapter not subject to U.S. copyright.
Published 1983, American Chemical Society

1. Leaching from the solid-waste form;
2. Single-phase reactions within the ground water; and
3. Interactions with rock and other matter along the ground water flow path.

These processes do not operate independently; for example, the behavior of plutonium in step 3 will be greatly dependent on the species formed as a result of solution-phase reactions in step 2. However, from a chemical standpoint, we have found that consideration of these processes individually is a useful aid to understanding the transport of plutonium in a ground-water system.

Of these three processes, some have received more study than others. There have been a number of determinations of leach rates (step 1) particularly from borosilicate-glass waste forms (see, for example, 1, 2, 3), but there has been minimal effort to determine species of dissolved plutonium. Sorption of plutonium from ground water onto rock surfaces (step 3) has received extensive investigation (4, 5, 6) in an attempt to bypass a more fundamental chemical approach. Failure to control conditions and to determine the speciation of plutonium in the waters in which the sorption studies were done resulted in plutonium sorption coefficient (K_d) values with standardized rock samples that differed by three orders of magnitude among various laboratories (6). By contrast, the oxidation-state distribution of plutonium in ground water (step 2), which has a strong influence on its solubility and sorption, has received very little study. In an effort to fill these gaps in knowledge and develop a unified chemical understanding of plutonium transport, we have undertaken an investigation of plutonium speciation in actual ground waters taken from host rocks of possible repository sites. The study involved solutions prepared in two different ways: (a) using each of the ground waters for leaching of plutonium-containing borosilicate glass, and (b) by addition of a small volume of dilute plutonium solution to each of the ground waters. We report here the current status of this dual investigation.

Experimental

The four ground waters used in this study were from the following sources: Grand Ronde basalt from the U.S. Department of Energy Hanford Reservation in Washington; tuff and Climax stock granite from the Nevada Test Site; and Cretaceous shale from South Dakota. The first three are or have been considered as possible host rocks for a geologic repository (7); the shale, despite favorable properties (8), has been largely neglected. Chemical compositions of these four ground waters are shown in Table I. In addition, deionized water was also evaluated.

Before starting the plutonium experiments, the influence of dissolved oxygen on the E_h of each ground-water sample was determined by sparging separate samples with oxygen and nitrogen. After a 1-hour sparge with oxygen and standing in closed con-

Table I Ground-Water Compositions (mg/L)

Solute	Basalt	Granite	Shale	Tuff
Alkalinity (as CaCO ₃)	146	140	530	98
Calcium	<0.1	300	100	10
Iron	0.3	0.007	0.01	0.007
Magnesium	<1	3	50	3
Manganese	0.005	0.03	0.3	0.001
Potassium	3.0	2.3	24	4.2
Sodium	300	300	700	50
Strontium	0.01	5	3	0.05
Silica	100	10	10	70
Chloride	140	73	61	7
Fluoride	52	0.8	0.1	2.3
Phosphate	0.1	0.02	0.02	<0.01
Sulfate	75	980	2,000	19
pH	9.3	8.3	8.4	7.8

tainers overnight, the waters had dissolved-oxygen concentrations of about 20 mg/L; after a similar treatment with nitrogen, the dissolved oxygen was about 0.6 mg/L. Despite this great difference, the change in E_h ranged only from 11 mv (deionized water) to 74 mv (shale ground water). On the basis of these results, it was concluded that dissolved-oxygen concentration was not a significant factor in the time scale of this study; this conclusion was corroborated by the general independence of the speciation results from initial oxidation state of the added plutonium.

Leaching speciation studies were accomplished using 5-mm borosilicate glass cubes (Battelle formulation 80-207, whose composition is given in Table II) containing 0.04 weight percent plutonium (93.8% Pu-239, 5.3% Pu-240, 0.4% Pu-241). All leaching experiments were conducted using the Battelle static leach test MCC-1 procedure with two modifications: Only two temperatures, 25°C and 90°C, were used, and the sampling periods were 7, 30, 90, and 180 days. To meet the required surface area/volume ratios of 0.01 mm⁻¹, we used three cubes (each of 150-mm² surface area) and 45 mL of ground water; these were contained in tightly capped Savillex (9) Teflon jars. (Weight losses due to evaporation averaged less than one percent, even after 180 days at 90°C). After the stipulated leaching period, the waters were sampled before and after filtration through 0.05 µm Nuclepore filters and the oxidation-state distribution of plutonium in the filtrates was determined as follows: PrF₃ carrier precipitation for Pu(III) and (IV), PrF₃ precipitation following NaHSO₃ reduction for total plutonium, and thenoyltrifluoroacetone (TTA) extraction

Table II Composition of Borosilicate Glass

Component	Weight Percent
Al ₂ O ₃	3.65
B ₂ O ₃	9.74
BaO	0.14
CaO	10.44
CuO	2.17
Fe ₂ O ₃	10.12
K ₂ O	1.97
Li ₂ O	1.89
MgO	3.18
Na ₂ O	7.27
P ₂ O ₅	2.00
SiO ₂	39.81
SrO	0.07
TiO ₂	4.75
ZnO	0.29
ZrO ₂	1.09
PuO ₂	0.04

for Pu(IV) (10). Plutonium(V) and (IV) concentrations were calculated by subtracting the Pu(III) and (IV) concentrations from the total plutonium concentrations. In addition, the glass cubes in each container were washed with 0.1 M HClO₄ and the resulting solutions were analyzed to determine the amount of sorbed plutonium. Because the plutonium was not isotopically pure the glass contained a small amount of americium, all plutonium analyses required anion-exchange purification followed by radiometric analysis or alpha spectrometry, as described previously (11).

In the single-phase speciation studies, small aliquots of plutonium-239 stock solution in 0.5 M perchloric acid were added to measured volumes of each unfiltered ground water to achieve plutonium concentrations of approximately 10⁻⁹ M. The resulting solutions were placed in Savillex Teflon jars and tightly capped. After periods of 1, 3, 7, 17, and 30 days, the solutions were agitated and samples were withdrawn and analyzed for plutonium both before and after filtration through 0.05-μm Nuclepore polycarbonate filters. The filtered samples were also speciated by PrF₃ carrier precipitation and TTA extraction as described above. All plutonium solutions were analyzed radiometrically by alpha counting. To assess the effect of initial oxidation state, separate sets of experiments were run using plutonium solution in the reduced [(III) and (IV)] and oxidized [(V) and (VI)] states. Also, all experiments were run at 25°C and 90°C to determine the effect of temperature. Thus, there were four sets of runs designed to evaluate the effects of initial oxidation state and temperature;

each was run in duplicate and the results were averaged. The precision of duplicates and the additivity of various fractions suggest that the data are accurate to within about 15 percent.

Glass Leach Speciation Results

Speciation of plutonium leached from the glass cubes is shown in Figure 1. The first bar represents the total amount of insoluble plutonium and is the summation of suspended plutonium (the difference between the values for filtered and unfiltered waters) and sorbed plutonium--viz., the amount removed from the cubes by a 0.1 M perchloric acid wash, normalized to the volumes of leachant solutions so that it is comparable to the other values in the graphs. For simplicity, the insoluble fractions are combined in one bar, whereas the various oxidation states in the soluble fraction are represented by separate bars. It should be noted that the ordinate scale varies among the graphs.

The most striking feature of these results is the much greater leaching of plutonium by the basalt ground water at 90°C compared to any other water at either temperature after 180 days; the concentration of plutonium in basalt water exceeded that in tuff ground water, the second most effective leachant, by a factor of approximately eight. Reference to Table I shows that basalt ground water has by far the highest fluoride concentration, followed by the tuff water, and on this basis we conclude that fluoride has a great influence on the leaching of plutonium from waste glass. This conclusion is not surprising in view of the well-known ability of fluoride to attack glass; in fact, among all the glass cubes used in this study, only those in basalt water were visibly etched. However, it is obvious that other less potent factors are also involved, inasmuch as the third greatest degree of leaching occurred in deionized water, which should have the lowest fluoride concentration of all. Shale ground water had the lowest plutonium concentration after 180 days at 90°C, an observation that is consistent with the inability of this water to solubilize plutonium in the single-phase experiments described below. This water is also unique among those studied in being a more effective leachant at 25°C than at 90°C.

It is instructive to compare the 90°C data after 180 days using as a basis of comparison the results in deionized water, which should contain no complexing agents and no dissolved species that can attack glass. The higher degree of leaching in basalt and tuff ground waters reflects their higher fluoride ion concentrations. The two ground waters containing low fluoride concentrations are less effective leachants than deionized water, suggesting that they may contain dissolved ions capable of passivating the glass surface. The relative leaching effectiveness of shale, granite, and deionized water shows an inverse qualitative dependence on sodium and magnesium concentrations, which could be significant, but the data do not permit a definite

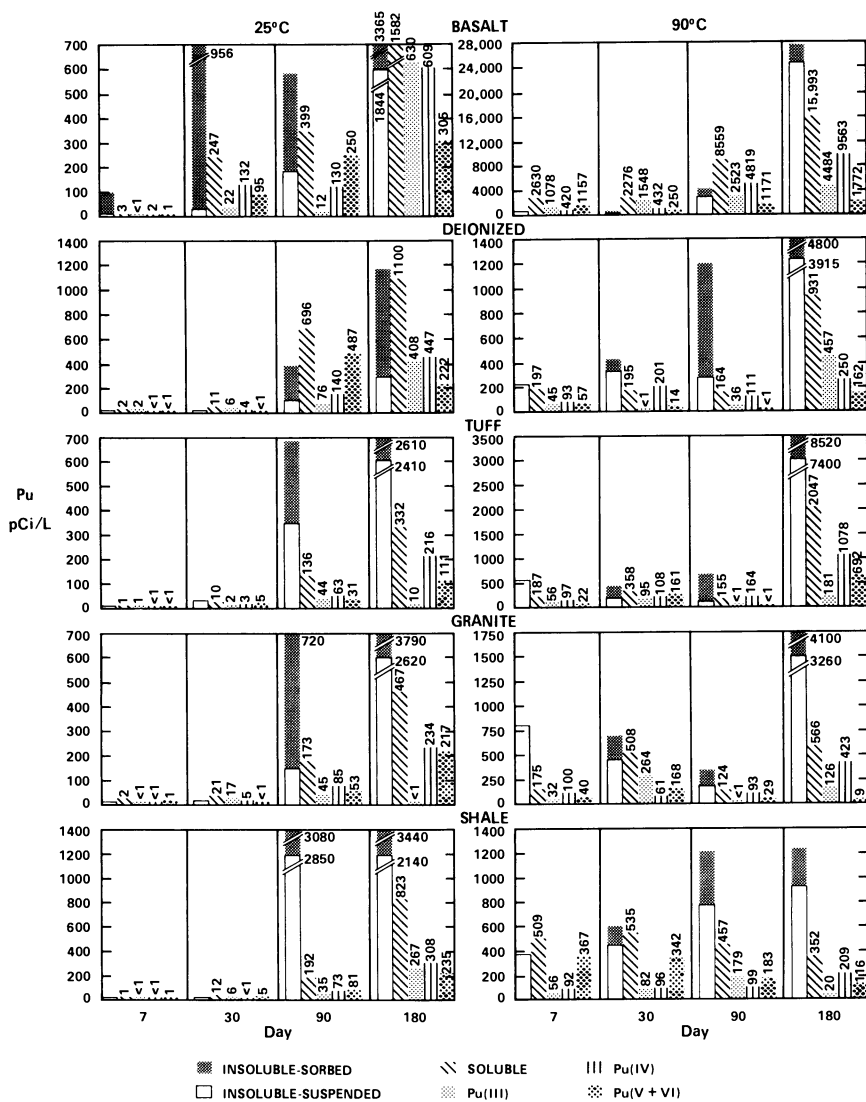


Figure 1. Glass leaching results.

conclusion that these ions inhibit leaching. In any case, the results indicate the hazard of attempting to predict ground water leaching behavior from data obtained with deionized water.

Results of the leaching experiments at 25°C are more difficult to interpret. Basalt ground water is not the most effective leaching agent; nor is shale the least effective. It appears that at the lower temperature fluoride plays a minor role and other, less obvious, factors predominate. Some of the differences could result from kinetic effects. This is a continuing study with further sampling scheduled at still longer time periods, so it is possible that later results will help clarify the 25°C data.

Perusal of the insoluble plutonium concentrations at 90°C indicates that they parallel the soluble concentrations without exception. Moreover, suspended plutonium concentrations greatly exceed the sorbed values in every case. These observations suggest the possibility that the "sorbed" plutonium is actually a partially solubilized species that is intermediate between plutonium in the matrix and that in solution, rather than plutonium that has been dispersed (or dissolved) into the water phase, hydrolyzed, and sorbed onto the glass surface in colloidal form. The next step in this sequence presumably would be dispersal of this "sorbed" plutonium into the water, where some of it would ultimately dissolve. The data obtained in this study do not permit any meaningful conclusions regarding mechanism, but it is interesting that the sorbed plutonium concentration was often relatively greater at the shorter time periods--particularly at 25°C--whereas the suspended fraction predominated at longer times, as would be expected if this mechanism were correct. On the other hand, it is not consistent with the reported plateaus in leach rates after an initial period of relatively rapid leaching, presumably because of formation of a difficultly soluble coating on the glass surface. Perhaps later data will be useful in resolving this question.

Single-Phase Speciation Results

The results for ground waters containing added plutonium solution are described in detail (12) elsewhere, and hence will only be summarized here. Plutonium behavior varied greatly among these waters, with solubility highest in the basalt water and lowest in the shale ground water, and these trends generally prevail regardless of temperature or initial oxidation state of the plutonium. (The behavior of plutonium in the granite, tuff, and deionized waters is intermediate between these extremes, and will not be discussed.) Reference to Table I indicates that the basalt and shale ground waters also have the most highly divergent chemical compositions. The shale ground water had the highest alkalinity, the highest sulfate concentration and the lowest fluoride concentration, while the basalt ground water had the highest fluoride concentration, a much lower sulfate concentration, a

lower alkalinity, and a pH 0.9 unit higher than the shale water. The effects of each of these parameters on plutonium speciation were evaluated in a separate series of experiments. Other possible factors were also investigated.

The similarity of results using unfiltered and pre-filtered (through a 0.05- μ m filter) shale ground water indicated that sorption on pre-existing particulates was not occurring in this water. Several experiments, in which the ionic strengths of deionized water and basalt ground water were increased to that of shale ground water by the addition of NaCl without any appreciable change in plutonium speciation, eliminated ionic strength *per se* as a significant influence.

To determine the effect of the pH difference between the basalt and shale ground waters, the pH of a sample of the latter was increased from its normal value to 9.3 (the pH of the basalt water) with NaOH solution, whereas HCl was used to decrease the basalt water pH to that of the shale ground water. There was no significant change in plutonium solubilities in either water compared to the corresponding unadjusted ground waters; we therefore conclude that pH had no influence within the range encountered in this investigation.

Sulfate and fluoride concentrations were shown to be the prime determinants of plutonium behavior, with sulfate decreasing its solubility and fluoride increasing it. These effects were demonstrated most dramatically in an experiment in which the sulfate concentration of shale ground water was decreased from 2,000 to <5 mg/L by precipitation of BaSO₄, and successive amounts of fluoride were added to attain a final concentration comparable to that in basalt ground water. Plutonium solubility increased with removal of sulfate and with initial addition of fluoride; further additions had little effect, suggesting the existence of a threshold value above which further increases of fluoride have minor influence. Sulfate probably lowers solubility by enhancing coagulation of plutonium colloids. In this experiment, precipitation of BaSO₄ also resulted in a decrease in alkalinity by a factor of three because of the precipitation of BaCO₃. The experiment was repeated with the addition of NaHCO₃ to restore the carbonate concentration to its initial value. Since the results did not change appreciably, we conclude that plutonium speciation in these ground waters is largely independent of carbonate-bicarbonate concentration within the range encountered in this study, although at higher concentrations it could indeed have an influence.

The effect of fluoride was further demonstrated by the increase in plutonium solubility in deionized water from about 11 percent to essentially 100 percent by addition of sufficient NaF to raise the fluoride concentration to that of basalt ground water. It is likely that the enhanced solubility of plutonium in waters containing high fluoride concentrations is the result of stabilization of Pu(IV) in solution by formation of fluoride complexes. Normally Pu(IV) is the least soluble of the four

common oxidation states, but its solubility increases in the presence of strong complexing agents. It is significant that appreciable concentrations of Pu(IV) are found only in the basalt ground water runs.

In the presence of high concentrations of both sulfate and fluoride, the speciation results are somewhat more difficult to interpret. Generally, the effect of fluoride predominates over that of sulfate, but not always. In deionized water containing added fluoride and sulfate to equal the concentrations of these two anions in basalt and shale ground waters, respectively, essentially all the plutonium was soluble--similar to its behavior in deionized water containing only added fluoride. Also, addition of sodium sulfate to basalt ground water to increase its concentration to that of shale ground water had no appreciable effect on plutonium solubility.

On the other hand, increasing the fluoride concentration of shale ground water to that of basalt water increased plutonium solubility by only a negligible amount, leading to the conclusion that another factor besides fluoride and sulfate concentrations was involved. To investigate the influence of alkaline earth ions in lowering the free fluoride ion concentration, an experiment was conducted in which Na_2SO_4 , MgCl_2 , and CaCl_2 were added to basalt ground water to increase its sulfate, magnesium, and calcium concentrations to those of shale ground water. The result was a reduction of plutonium solubility from 100 percent to 70 percent, indicating that alkaline earth ions have an effect, but that they alone cannot account for the observed behavior. It is possible that other polyvalent cations are involved in reducing the free fluoride ion concentration.

Comparison of Results in the Two Systems

Three principal conditions in the leaching studies differed markedly from those in the single-phase studies:

1. A practically unlimited source of plutonium was present, so that its concentration in solution (dissolved or otherwise dispersed) could, at least in theory, increase continuously with time until a steady-state situation was reached.
2. Ground-water composition would be altered by the glass, either by two-phase chemical reactions or, more likely, by leaching of glass components. In particular, relatively high concentrations of dissolved and colloidal silica would be expected.
3. The glass phase furnished an active surface for the possible deposition of dispersed plutonium species.

Because of these differences, it is not surprising that speciation differs significantly in the two systems. The contrast in oxidation-state distributions between the single-phase studies and the leaching experiments is noteworthy. In the latter,

plutonium(IV) was the single most abundant oxidation state, whereas in the single-phase studies its concentration was insignificant in all but the basalt ground water. This observation suggests that species leached from the glass were able to stabilize tetravalent plutonium; reference to the glass composition in Table II suggests that only silica could have this effect. It is possible, therefore, that the coagulation and precipitation of plutonium(IV) polymer was inhibited by its sorption onto sub-colloidal silica particles small enough to pass through a 0.05- μ m filter.

The ability of polyvalent cations leached from the glass to suppress the free-fluoride ion concentration in basalt ground water is difficult to assess. Fluoride definitely enhances leaching and is the primary cause of the high concentrations of dissolved plutonium in the basalt ground-water leachate. Once the plutonium is dissolved, however, it is not possible to determine what fraction is stabilized by fluoride as opposed to other species leached from the glass.

Although there are some obvious differences in plutonium speciation in the single-phase studies and in the leaching studies, there are also significant parallels that can be summarized in several conclusions. The influence of fluoride is obvious in enhancing the glass leaching, and in stabilizing plutonium in solution once it has dissolved. In fact, fluoride seems to be especially important in leaching, as can be seen in the data for tuff ground water. Even though the fluoride in tuff water was insufficient to stabilize plutonium(IV) and enhance its solubility in the single-phase experiments, it did contribute to the relatively high leaching performance of this water. Thus, the necessity for minimizing plutonium mobility mitigates against choosing host rocks whose associated ground water contains even moderate concentrations of fluoride ion.

The effect of sulfate in immobilizing plutonium, so pronounced in the single-phase studies, is more subtle in the leaching experiments, but still appears to be present, particularly at higher temperatures. Hence, presence of this ion in relatively high concentrations in ground water often has the desirable effect of decreasing plutonium solubility. The results also suggest that some dissolved species--possibly sodium and magnesium--can passivate the glass surface and hence retard plutonium leachability.

The wide variation between different ground waters in both sets of experiments emphasizes the necessity of using actual ground waters in all laboratory studies, since the observed plutonium behavior is "ground-water-specific". Moreover, these results reinforce the suggestion made elsewhere (12) that ground-water characterization should be included as a viable repository site-selection criterion.

Acknowledgments

The authors thank Dr. Dana Isherwood of Lawrence Livermore National Laboratory, Ms. Patricia Salter of Rockwell Hanford Operations, and Ms. Kathy Peter and Mr. Eugene Doty of the U.S. Geological Survey for supplying the ground waters for this study. The plutonium-containing glass cubes were provided through the good offices of Mr. Garry Bryan of Battelle Pacific Northwest Laboratory. Water analyses were cheerfully performed by the National Water Quality Laboratory of the U.S. Geological Survey in Denver.

Literature Cited

1. Weed, H.C.; Coles, D.G.; Bradley, D.J.; Mensing, R.W.; Schweiger, J.F.; Rego, J. Nucl. Chem. Waste Mgmt. 1981, 2, 167.
2. Peters, R.D.; Diamond, H. "Actinide Leaching from Waste Glass: Air-Equilibrated versus Deaerated Conditions", Report PNL-3971, Battelle Pacific Northwest Laboratory, 1981.
3. Coles, D.G. "Single-Pass Continuous-Flow Leach Test of Battelle 76-68 Glass: Some Selected Bead Leach I Results", Report UCRL-85405*(Rev, 1), Lawrence Livermore National Laboratory, 1981.
4. Wolfsberg, K.; Aguilar, R.D.; Bayhurst, B.P.; Daniels, W.R.; DeVilliers, S.J.; Erdal, B.R.; Lawrence, F.O.; Maestas, S.; Mitchell, A.J.; Oliver, P.Q.; Raybold, N.A.; Rundberg, R.S.; Thompson, J.L.; Vine, E.N. "Sorption-Desorption Studies on Tuff. III. A Continuation of Studies with Samples from Jackass Flats and Yucca Mountain, Nevada", Report LA-8747-MS, Los Alamos National Laboratory, 1981.
5. Erdal, B.R.; Aguilar, R.D.; Bayhurst, B.P.; Daniels, W.R.; Duffy, C.J.; Lawrence, F.O.; Maestas, S.; Oliver, P.Q.; Wolfsberg, K. "Sorption-Desorption Studies on Granite. I. Initial Studies of Strontium, Technetium, Cesium, Barium, Cerium, Europium, Uranium, Plutonium, and Americium", in "Proceedings of the Task 4 Waste Isolation Safety Assessment Program Second Contractor Information Meeting", Vol. II, Report PNL-SA-7352, Battelle Pacific Northwest Laboratory, 1978, pp. 7-67.
6. Relyea, J.F.; Serne, R.J. "Controlled Sample Program Publication Number 2: Interlaboratory Comparison of Batch K_d Values", Report PNL-2872, Battelle Pacific Northwest Laboratory, 1979.
7. Gonzales, S. Amer. Sci. 1982, 70, 191.
8. Shurr, G.W. "The Pierre Shale, Northern Great Plains; a Potential Isolation Medium for Radioactive Waste", U.S. Geological Survey Open-File Report 77-776, 1977.
9. The use of trade names is for descriptive purposes only and does not constitute endorsement by the U.S. Geological Survey.

10. Bondietti, E.A.; Reynolds, S.A. in "Proceedings of the Actinide-Sediment Reactions Working Meeting, Seattle, Wash., Feb. 10 and 11, 1976", Ames, L.L. (Ed.), Report BNWL-2117, Battelle Pacific Northwest Laboratory, 1976, pp. 505-530.
11. Cleveland, J.M.; Rees, T.F. Science 1981, 212, 1506.
12. Cleveland, J.M.; Rees, T.F.; Nash, K.L. "Plutonium Speciation in Selected Basalt, Granite, Shale, and Tuff Ground Waters", in press.

RECEIVED December 21, 1982

Present Status and Future Directions of Plutonium Process Chemistry

ELDON L. CHRISTENSEN—Los Alamos National Laboratory, Material Science and Technology Division, Los Alamos, NM 87545

LEONARD W. GREY—E. I. du Pont de Nemours & Company, Inc., Savannah River Laboratory, Aiken, SC 29808

JAMES D. NAVRATIL—Rockwell International, Rocky Flats Plant, Golden, CO 80401

WALLACE W. SCHULZ—Rockwell Hanford Operations, Richland, WA 99352

An overview is given of plutonium process chemistry used at the U. S. Department of Energy Hanford, Los Alamos National Laboratory, Rocky Flats, and Savannah River sites, with particular emphasis on solution chemistry involved in recovery, purification, and waste treatment operations. By extrapolating from the present system of processes, this paper also attempts to chart the future direction of plutonium process development and operation. Areas where a better understanding of basic plutonium chemistry will contribute to development of improved processing are indicated.

Large-scale plutonium recovery/processing facilities originated at Los Alamos and Hanford as part of the Manhattan Project in 1943. Hanford Operations separated plutonium from irradiated reactor fuel, whereas Los Alamos purified plutonium, as well as recovered the plutonium from scrap and residues. In the 1950's, similar processing facilities were constructed at Rocky Flats and Savannah River.

A limited overview of the process chemistry used at these sites is presented. This paper will also attempt to bridge, at least partly, the gap between ongoing fundamental plutonium research and development and applied technology needs. We believe it is important to bridge this gap, since a continuous flow of knowledge about plutonium chemistry from academic and government laboratories to the plant is necessary and beneficial

0097-6156/83/0216-0349\$06.00/0
© 1983 American Chemical Society

in motivating and stimulating fundamental research and development studies. The research and development areas indicated in this paper are representative, we feel, of those where fundamental research and development can make a timely and substantial contribution. Our hope is that at least some of our suggestions will be pursued.

Plutonium Processing at Los Alamos

Plutonium metal is prepared by two methods--direct reduction of the oxide by calcium (DOR)(1,2), and reduction of PuF_4 by calcium in our metal preparation line (MPL)(3) (see Figure 1). In the DOR process, the plutonium content of the reduction slag is so low that the slag can be sent to retrievable storage without further processing. Metal buttons that are produced are no purer than the oxide feed and/or the calcium chloride salt. Los Alamos purifies the buttons by electrorefining(4,5), yielding metal rings that are \geq 99.96 percent plutonium.

The Los Alamos MPL can accept either plutonium nitrate solution or plutonium oxide as feed. If the feed is the nitrate solution, then the process steps are: precipitation of plutonium peroxide, hydrofluorination of the peroxide to PuF_4 , and reduction of the PuF_4 to metal. If the feed is oxide, then it is hydrofluorinated to produce PuF_4 , which is then reduced to plutonium metal with calcium metal. This metal usually meets the specifications set by the metal fabrication personnel. This process is well-defined--most parameters are known.

Los Alamos residue processing yields PuO_2 feed that can be easily hydrofluorinated. If the oxide has been prepared by calcination of the oxalate, then that oxide can be easily converted to PuF_4 , whereas other oxides have poor fluorination characteristics.

Los Alamos has been processing unirradiated plutonium scrap since 1944.(6) Scrap processing is presently being done at the new plutonium facility, using the flowsheet shown in Figure 2. Feed to this system comes from the varied research programs at Los Alamos and from other sites through the auspices of the Central Scrap Management Office at Savannah River.

Plutonium Processing at Rocky Flats

Chemical processing activities involve the recovery of plutonium from Rocky Flats Plant scrap, waste materials and residues, and effluent streams. The final product of this recovery and purification effort is high-purity plutonium metal for use in foundry operations.

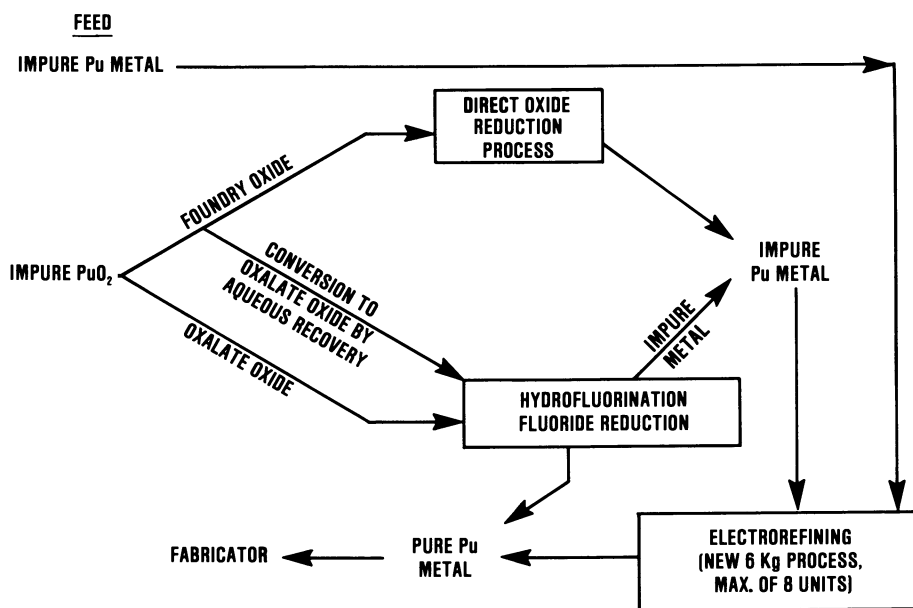


Figure 1. Metal Preparation and Purification at Los Alamos

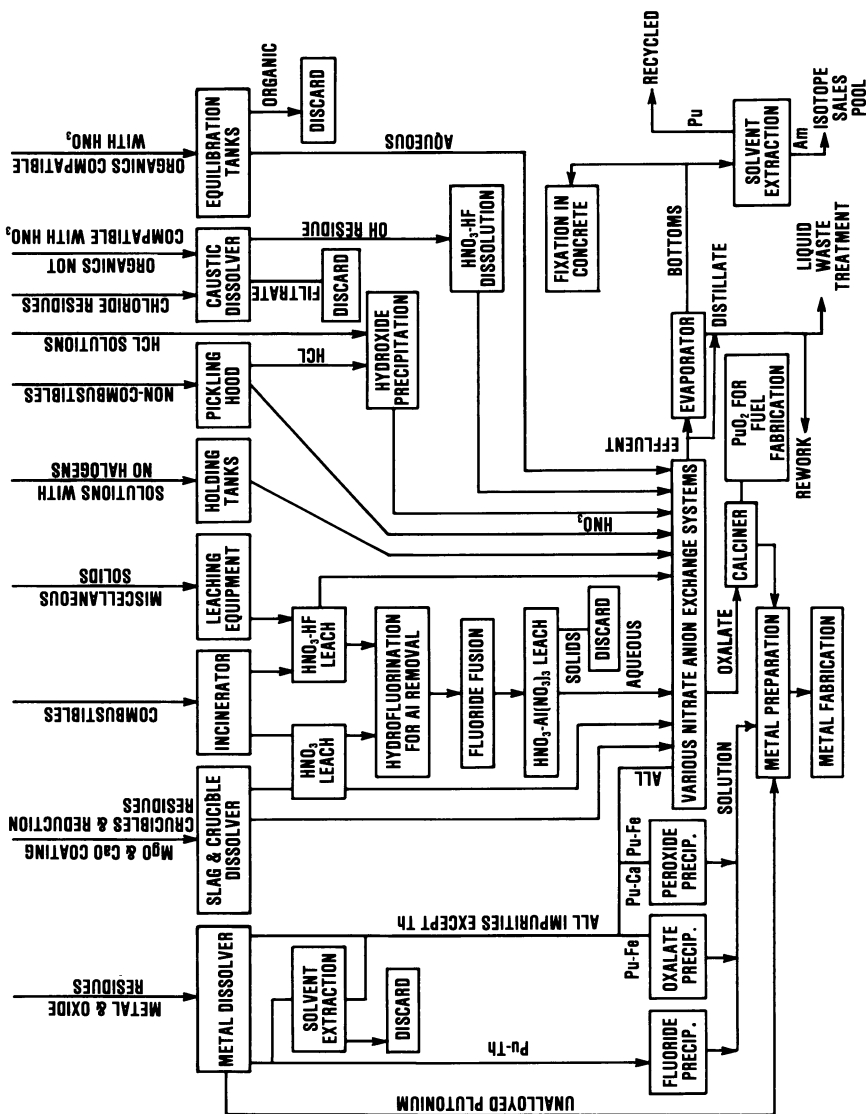


Figure 2. Flow of Material in Scrap Recovery at Los Alamos

The original plutonium recovery and purification processes were adopted from Los Alamos processes in 1950. The processes at Rocky Flats are still similar today, in many respects, to the Los Alamos processes.

Figure 3 shows a flowsheet for plutonium processing at Rocky Flats. Impure plutonium metal is sent through a molten salt extraction (MSE) process to remove americium. The purified plutonium metal is sent to the foundry. Plutonium metal that does not meet foundry requirements is processed further, either through an aqueous or electrorefining process. The waste chloride salt from MSE is dissolved; then the actinides are precipitated with carbonate and redissolved in 7M HNO_3 ; and finally, the plutonium is recovered by an anion exchange process.

Impure plutonium oxide residues are dissolved in 12M HNO_3 -0.1M HF under refluxing conditions, and then the plutonium is recovered and purified by anion exchange. Plutonium is leached from other residues, such as metal and glass, and is also purified by anion exchange. The purified plutonium eluate from the anion exchange process is precipitated with hydrogen peroxide. The plutonium peroxide is calcined to the oxide, and the plutonium oxide is fluorinated. The plutonium tetrafluoride is finally reduced to the metal with calcium.

Acid waste streams are sent through a nitric acid recovery process, and then to a secondary plutonium recovery anion exchange process. The acid waste streams are then sent to waste treatment.

Direct oxide reduction (DOR) is presently being tested on production equipment. Eventually, it is hoped to eliminate the fluorination and bomb reduction processes and replace them with DOR.

Plutonium Processing at Hanford

Irradiated Fuel. A historically important and continuing mission at the Hanford site is to chemically process irradiated reactor fuel to recover and purify weapons-grade plutonium. Over the last 40 years, or so, several processes and plants--Bismuth Phosphate, REDOX, and PUREX--have been operated to accomplish this mission. Presently, only the Hanford PUREX Plant is operational, and although it has not been operated since the fall of 1972, it is scheduled to start up in the early 1980's to process stored and currently produced Hanford-Reactor fuel. Of nine plutonium-production reactors built at the Hanford site, only the N-Reactor is still operating.

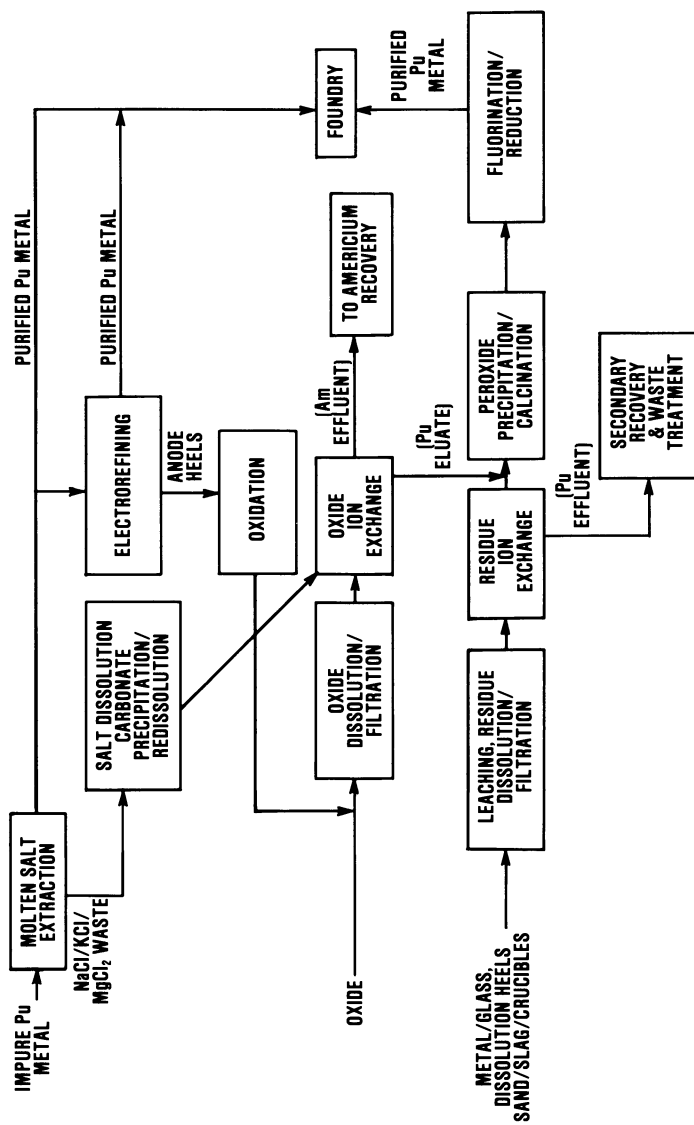


Figure 3. Plutonium Recovery Processes at Rocky Flats

The following, albeit in very brief fashion, outlines the essentials of the technology to be employed in producing pure PuO_2 from irradiated N-Reactor fuel. Following receipt of the fuel in the PUREX Plant, Zircaloy-2 cladding is chemically removed by dissolution with boiling $\text{NH}_4\text{F-NH}_4\text{NO}_3$ solution (Zirflex process). Small amounts of UF_4 resulting from attack of uranium metal core by the Zirflex process reagent are meta-thesized to $\text{Na}_2\text{U}_2\text{O}_7$ and then dissolved along with unattacked uranium metal in HNO_3 . Standard and well-known PUREX process technology is practiced to recover, separate, and purify plutonium. New equipment has been installed in the Hanford PUREX Plant to convert, via plutonium oxalate, the purified $\text{Pu}(\text{NO}_3)_4$ product solution from the third plutonium cycle to PuO_2 for shipment offsite. Following customary Hanford site practice, the denitrated ($\sim 0.5\text{-}1.0\text{M}$ HNO_3) PUREX process high-level waste (HLW) containing small amounts of plutonium and varying amounts of other actinides (Am, Np, and U) will be adjusted to $> \text{pH } 9$ by addition of NaOH , and stored in newly constructed underground double-shell tanks.

Current plans for restart of Hanford PUREX Plant call for storage of neutralized ($\text{pH} > 9$) spent decladding solution in double-shell tanks. Depending upon operating procedures, from two to four such tanks (each costing about \$10,000,000) will be needed to store spent decladdent. (The spent decladdent will not, according to present planning, be mixed with alkaline HLW.) There is an economic incentive to find inexpensive and safe alternative treatment/storage schemes for handling the spent decladding solution. Key to such schemes is, as discussed subsequently, concentration of plutonium and americium, their chemical species in the decladding solution, and a simple method for removing them efficiently.

Plutonium Scrap Processing. In addition to recovering plutonium from irradiated reactor fuel, a Plutonium Reclamation Facility (PRF)(7,8) is operated at the Hanford site to recover, separate, and purify kilogram amounts of plutonium from a wide range of unirradiated scrap materials. A 20 percent TBP-CCl_4 solution is used to extract $\text{Pu}(\text{IV})$ from $\text{HNO}_3\text{-HF-Al}(\text{NO}_3)_3$ solutions of dissolved scrap.

Plutonium Processing at Savannah River

The facilities at Savannah River(9) consist of five heavy-water-moderated and cooled production reactors, two chemical separations areas as a heavy water extraction plant, several test reactors, reactor fuel and target processing facilities, the Savannah River Laboratory, and many other facilities necessary to support the operations. During the 1960's, two of the

production reactors were shut down and placed in standby condition; one of these is scheduled to start up again in the fall of 1983. Two test reactors and the heavy water extraction plant have also been shut down.

Figure 4 illustrates, in very brief fashion, the essentials of the flow of materials from the reactors through the separations area. Depleted uranium targets are processed through the F-Area canyon by well-known PUREX process technology.⁽¹⁰⁻¹³⁾ Enriched uranium fuel elements are processed through the H-Area canyon by a modification of the PUREX process.⁽¹¹⁾ Irradiated neptunium targets are processed through the H-Area canyon by an ion exchange process.⁽¹⁴⁾

Following receipt of the irradiated depleted uranium targets in the F-Area Separations Area, aluminum cladding is chemically removed by dissolution with a NaNO_3 - NaOH solution and sent to waste storage. The bare uranium targets are then dissolved in boiling 10M HNO_3 . PUREX process technology is used to separate and purify both the plutonium and the uranium. The uranium solutions are evaporated by successive evaporation steps, first to $\text{UO}_2(\text{NO}_3)_2 \cdot 6\text{H}_2\text{O}$, and then denitrated to UO_3 . The plutonium solutions are then concentrated by cation exchange and precipitated as PuF_3 . The precipitate is roasted in an oxygen atmosphere to a mixture of ~73 mole % PuF_4 and 27 mole % PuO_2 before undergoing a calciothermic reduction to plutonium metal for shipment offsite. Waste solutions from these processes which contain residual plutonium and small amounts of neptunium are processed through one of two anion exchange systems to recover both the plutonium and neptunium. The waste streams are then evaporated, acid stripped, and adjusted to $\text{pH} > 13$ by addition of NaOH before storage in underground double-shell tanks.

Following receipt of the burned enriched uranium fuel in the H-Area canyon, this aluminum-clad Al-U alloy is dissolved in HNO_3 catalyzed with $\text{Hg}(\text{NO}_3)_2$. The dissolver solution is frequently blended with dissolved offsite fuels, such as university research reactors and HFIR cores from Oak Ridge, before the purified uranium and neptunium are separated and purified by a modification of the PUREX process. The purified $\text{UO}_2(\text{NO}_3)_2$ solution is shipped offsite for conversion to uranium metal. This uranium metal is reprepared into fuel tubes for the SRP reactors. Since this uranium is repeatedly recycled through the reactors, the ^{236}U content has grown over the years. The purified neptunium, produced in the fuel tubes by the irradiation of the ^{236}U , is concentrated by anion exchange, precipitated as an oxalate, and calcined to the oxide. This NpO_2 is then fabricated into Al-clad NpO_2 -Al cement targets and returned to the reactors to produce ^{238}Pu .

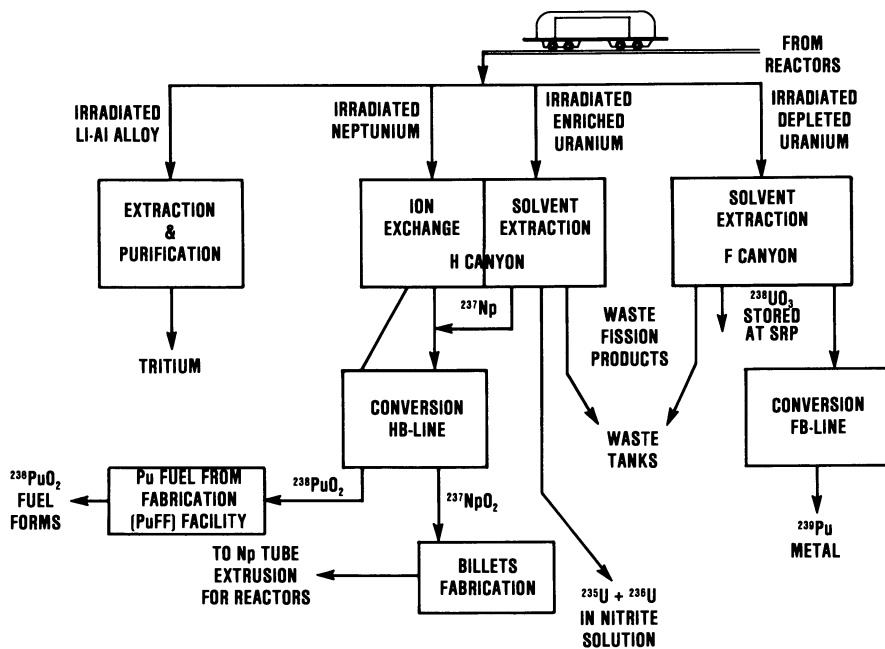


Figure 4. Separation Process at Savannah River Plant

The irradiated neptunium targets are dissolved in HNO_3 catalyzed with $\text{Hg}(\text{NO}_3)_2$. The ^{237}Np and ^{238}Pu are then purified and partitioned from each other by two cycles of anion exchange. Both products are further purified by anion exchange, precipitated as oxalate, and calcined to oxide. The purified PuO_2 is fabricated into heat sources for use in the nation's space program.

The waste streams from the H-Area processes are evaporated, acid-stripped, and adjusted to $\text{pH} > 13$ by addition of NaOH before storage in underground double-shell tanks.

In addition to fuel and targets(15,16) from SRP reactors, SRP also reprocesses a wide variety of fuels from offsite research reactors and a wide range of unirradiated plutonium scrap materials.(17) Following customary Savannah River practice, initial processing of each offsite material is designed to transform the actinides to a solution that is compatible with one of the solvent extraction cycles in either of the separations areas. A major advantage of this practice is that the uranium and plutonium isotopes can be blended over a wide range. Since the actinide can be introduced to the mainline process at several different points, a greater range of contaminants can be handled by routine operations. This simplifies many of the initial purification steps over the steps that would be necessary if only one entry point was available.

Applied Plutonium Technology Needs - Unirradiated Plutonium Scrap and Waste

DOR Processing of High-Grade Plutonium Scrap. Numerous 700-g PuO_2 reductions have been performed at Los Alamos; Rocky Flats is also testing DOR in its production equipment. However, the exact chemical mechanism for the DOR reaction has not yet been fully characterized. Research and development need to be done to transform this from a batch process to a continuous process. Also, the plutonium metal product is contaminated not only with the impurities in the PuO_2 feed, but also with the impurities in the CaCl_2 reaction flux. Research and development need to be done on preparing pure CaCl_2 or recycling the CaO-CaCl_2 slag left after DOR. The CaO possibly could be rechlorinated in an inert atmosphere (no CO_2 , O_2 , or H_2O) and thus have a salt free of carbonate. (The presence of carbonate leads to metal with a high carbon content; the carbon makes the metal have undesirable properties.)

MSE Processing of High-Grade Plutonium Scrap. Americium is removed from plutonium in a liquid-liquid extraction process using molten salt (KCl , NaCl , MgCl_2) and molten plutonium metal

as the immiscible liquid phases. The salt phase, containing most of the americium and some plutonium, is transferred to an aqueous process for recovery of americium and plutonium. The precipitation of Pu(III) and Am(III) carbonates from dissolved MSE residues yields actinide(III) carbonates or hydroxyl carbonates.(18) The physiochemical properties of these compounds are needed, as well as an understanding of the soluble complexes formed in carbonate solution at high pH.

Other Pyrochemical Processes. The chemistry of pyrochemical separation processes is another fertile area of research; e.g., new molten salt systems, scrub alloys, etc.; and the behavior of plutonium in these systems. Studies of liquid plutonium metal processes should also be explored, such as filtration methods to remove impurities. Since Rocky Flats uses plutonium in the metal form, methods to convert plutonium compounds to metal and purify the metal directly are high-priority research projects.

Plutonium Oxide Dissolution. All four sites dissolve impure PuO_2 residues in concentrated HNO_3 (10 to 14M) containing HF (<0.3M). Whereas material calcined at temperatures of <650°C is fairly easy to dissolve, material calcined at higher temperatures (up to 1700°C) becomes an intractable refractory oxide. Better methods, which can be scaled to a production mode, are needed to convert these refractory oxides to a form amenable to reprocessing. Some advances have been made in aqueous dissolution, using an electrolytic assist to fluoride dissolution, but further chemical and engineering data are needed to convert this into a viable production process.(19)

Other aqueous dissolution media, such as H_2SO_4 , H_3PO_4 , and HCl , should also be further investigated. Masking agents which could be used to control the corrosive nature of these alternate dissolution media to stainless steel process equipment should also be studied.

Possible Hydrochloric Acid Processing Plant. The newer processes (e.g., DOR, MSE, electrorefining) for purifying unirradiated plutonium products and scrap are making use of molten chloride salts. These processes generate molten salt residues containing substantial amounts of plutonium. Plutonium in these residues could be recovered using a HCl flowsheet. Other scraps and products, such as PuO_2 residues, could be dissolved in HCl-SnCl_2 solutions. Study of a complete HCl processing plant should include the processing chemistry and chemical engineering of dissolution, separation, purification and waste treatment, and materials of construction (glove boxes and process equipment).

Plutonium Purification Using HNO_3 Solutions. Plutonium from both low-grade scraps and impure high-grade oxides is normally converted into a HNO_3 solution before purification and precipitation. The purification step may be an anion exchange procedure; the precipitation step may use H_2O_2 or HF . These processes are well-defined, that is, most of the parameters are known. However, some work should be done in measuring the decontamination factors for cations and anions frequently found in plutonium nitrate solutions. Ions which are frequently in these solutions include Al, Ca, Mg, Am, U, Th, Np, Pb, Fe, Cr, Ni, sulfate and oxalate. For example, Los Alamos prepares oxide that meets our reactor research technology and approved purity and particle specifications using oxalate and peroxide precipitation. In these processes, the decontamination factors for each of the precipitations need to be determined for the process conditions employed. Leary, et al.(20) reported many decontamination factors for certain peroxide precipitations, but not for these specific conditions and impurities. Less data exist for decontamination factors obtained by oxalate precipitations that are made with present conditions. Fuel fabricators have specified that the oxide feed to their plant must contain less than 15 ppm fluoride, based on plutonium content. This indicates a need to know the behavior of the fluoride ion during peroxide and oxalate precipitation of plutonium from a variety of conditions. The behavior of many cations during these precipitations also needs to be studied.

The complete chemistry of plutonium liquid-to-solid conversion processes, especially peroxide and oxalate precipitation, should be further studied. Research and development of direct thermal denitration methods should also be pursued.

Los Alamos is processing a wide variety of residues, including Pu-Be neutron sources, polystyrene-PuO₂-UO₂ blocks, incinerator ash, Pu-U alloys and oxides, Pu-Zr alloys and oxides, Pu-Np alloys and oxides, Pu-Th alloys and oxides, etc. Processes have been developed for these scrap items (see Figure 2), but we need to know more about: Pu-Np separations; Pu-Th separations; oxalate precipitations for both plus 3 and plus 4 valences; valence stabilization; dissolution methods for high-fired impure oxides; in-line alpha monitors to measure extremely low concentrations of Pu and Am in 7M HNO_3 solutions; and solubility of various mixtures of PuO₂ and UO₂ under a variety of conditions.

Plutonium Purification Using Solvent Extraction. The Hanford Plutonium Reclamation Facility (PRF) uses a 20 percent TBP- CCl_4 solution to extract Pu(IV) from HNO_3 - HF - $\text{Al}(\text{NO}_3)_3$ solutions of dissolved scrap. The final product solution from the

strip column contains, typically, 50 gL⁻¹ plutonium. One of the more troublesome chemical problems encountered from time to time in PRF operations is engendered by disproportionation of Pu(IV) to Pu(III) and Pu(VI). Six-valent plutonium is less well extracted by TBP than is Pu(IV), while Pu(III) is not extracted by TBP. Because of the wide variability in the composition of the aqueous feed to the PRF extraction column, unrecognized Pu(IV) disproportionation can cause undesirably high plutonium losses until necessary empirical flowsheet changes are made. This experience emphasizes a need for research to (a) develop a useful tool (e.g., nomograph, etc.) to predict quickly and reliably the extent of Pu(IV) disproportionation in solvent extraction process feed solutions, and (b) if possible, development of a reliable on-line instrument to measure concentrations of plutonium in (III), (IV), and (VI) oxidation states in feed and raffinate solutions.

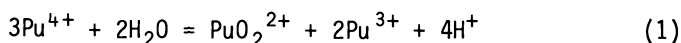
Waste Handling for Unirradiated Plutonium Processing. Higher capacity, better-performing, and more radiation-resistant separation materials such as new ion exchange resins(21) and solvent extractants, similar to dihexyl-N,N-diethylcarbamoylmethylphosphonate,(22) are needed to selectively recover actinides from acidic wastes. The application of membranes and other new techniques should be explored.

The chemistry of waste treatment processes and the development of new processes are fertile areas of research work. The speciation of plutonium in basic and laundry wastes is needed. For example, if soluble plutonium complexes in basic wastes can be destroyed, perhaps ultrafiltration could replace the flocculent-carrier precipitation process. The chemistry of plutonium(VII) and of ferrites--a candidate waste treatment process--needs to be explored.(23)

Applied Plutonium Technology Needs - Irradiated Plutonium Scrap and Waste

Plutonium-238 Processing. The major problems with the reprocessing of neptunium targets to recover ²³⁸Pu is the incomplete partitioning of ²³⁷Np and ²³⁸Pu on the anion exchange columns.(14) This cross-contamination is the result of either incomplete valence adjustments or an unwanted valence readjustment during the partitioning step. A better understanding of oxidation-reduction reaction kinetics and valence states equilibria as a function of the concentrations of valence adjustment chemicals, total plutonium, ²³⁸Pu, neptunium, and temperature is needed.

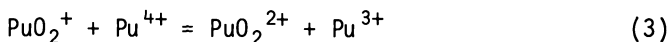
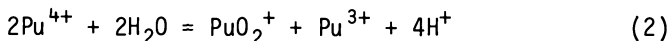
Disproportionation of Pu(IV). There are several needs associated with the occurrence, detection, and mitigation of the disproportionation of Pu(IV) in applied plutonium recovery/purification procedures. First, there is a great need for much more detailed information concerning the effect of typical process conditions [e.g., temperature, concentration of plutonium, hydrogen ion, nitrate ion, nitrite ion, fluoride ion, other metal ions (e.g., Al³⁺, Fe³⁺, etc.), etc.] on the occurrence and extent of the reaction:



Ideally, this information should be made available in the form of easy-to-use nomographs or empirical equations which can be quickly and rapidly solved on a programmable desk calculator. New instrumentation which can be used on an in-line basis to analyze process streams for the concentrations of plutonium in different oxidation states is also needed.

Nitrite ion is often used in plutonium solvent extraction systems to oxidize Pu(III) to Pu(IV) and to reduce Pu(VI) to Pu(IV). But HONO, produced in HNO₃ media, is extractable into TBP-diluent systems and can interfere with subsequent reductive stripping of plutonium. There is thus a need to find a reagent comparable to nitrite ion in its reactions with Pu(III) and Pu(VI), but which does not extract into TBP solutions.

Disproportionation reactions of Pu(IV) (Equations 1 and 2) and Pu(V) (Equation 3) have been known and studied since Manhattan Project days. (24,25)



The importance of Pu(VI) and Pu(III) as products of the disproportionation of both Pu(IV) and Pu(V) is called out by Equations 1 and 3. Equations 1 and 2 also indicate the great dependence of the disproportionation reactions on acidity. For example, at room temperature, measurable disproportionation of Pu(IV) occurs at HNO₃ concentrations below 1.5M, while at 98°C, disproportionation of Pu(IV) occurs at HNO₃ concentrations less than 8M.

Previous studies of the plutonium disproportionation reaction have generally, and understandably, emphasized an academic approach with simple acid solutions to elucidate fundamental plutonium chemistry. These past investigations should provide a firm springboard for the more general and advanced research and

development we are recommending. The approach developed and advocated by Silver(26-29) for calculating the concentrations of plutonium in various oxidation states in aqueous media may prove to be a very valuable tool, particularly when it is supplemented by comprehensive data for disproportionation in solutions typical of those encountered in industrial-scale processes.

Spectrophotometric methods for determining concentration of Pu(III, IV, VI, and "polymer") in nitrate media have been reported.(30) Adaptation of such procedures to routine rapid in-line analysis of feed and raffinate solutions may be possible.

We are not able to suggest a suitable reagent to replace HONO for counteracting disproportionation of Pu(IV) in nitrate media. We can only emphasize the benefits to large-scale plutonium separation (via TBP extraction) of finding such a reagent.

Spent Zirflex Process Decladent. The basic perceived need is to devise and develop a simple process for selective and efficient removal of plutonium (and ^{241}Am) from spent Zirflex process decladent solution. To satisfy this need, it may be necessary--or prove beneficial--to determine, by appropriate physiochemical methods, the nature of the plutonium (and americium) species in the decladding solution. Availability of a satisfactory transuranium removal scheme may be one of the key factors in devising an alternative to storage in expensive double-shell tanks for spent Zirflex process solution at the Hanford site.

Swanson,(31) Smith,(32) Phillips,(33) and others have described many aspects of the Zirflex process but, unfortunately, not the form or charge of plutonium and other actinides in spent decladding solution. Presumably, soluble amounts of these elements are present as fluoride complexes, but this remains to be proven.

We are not aware of any previous studies of the removal of plutonium or americium from $(\text{NH}_4)_2\text{ZrF}_6\text{-NH}_4\text{F-NH}_4\text{NO}_3$ solutions. For ready plant-scale application, precipitation, sorption on inorganic materials, or batch solvent extraction processes may all be satisfactory. An inexpensive inorganic material with great selectivity and capacity for sorbing actinides, and with suitable hydraulic properties, would be especially attractive.

High-Level Waste. Hydrated iron oxide (so-called "sludge") precipitates when NaOH is added to HLW and carries down almost all the plutonium and most of the other actinides in the HLW.

From past production operations at Hanford, approximately 100 old single-shell tanks contain varying amounts of sludge and plutonium.

The exact chemical species of plutonium present in sludge in Hanford single-shell tanks is not known; likely candidates include either hydrated oxide or polymer, or both. Similarly, the size of the precipitated plutonium particles is not known. These data are needed in connection with the desire to use economically favorable in situ passive neutron activation techniques to measure the plutonium content of the Hanford sludge. One preferred technique makes use of the reaction $^{63}\text{Cu} (\alpha, \eta) ^{64}\text{Cu}$ to estimate plutonium content. Sensitivity and calibration of this technique is quite dependent upon the chemical environment of the alpha-emitting plutonium atoms. Specifically, such factors as the number and type of neighboring atoms (e.g., O, Na, Al, etc.) and the diameter (size) of the plutonium species impact the neutron flux, which can activate ^{63}Cu to ^{64}Cu . Experimentation to characterize the nature and properties of the plutonium species produced when Hanford Purex HLW is made alkaline thus needs to be performed. Such experimentation should include effects of aging of sludges at elevated temperatures over long (i.e., years) times.

That freshly precipitated hydrated iron oxide effectively scavenges plutonium (and various other radionuclides) from aqueous waste solution has long been known. Plant-scale use is made of this chemical fact at Rocky Flats and Los Alamos in-site waste management schemes.^(34,35) Sludges produced at the Rocky Flats and Los Alamos sites are believed to be closely akin to those produced and stored in Hanford single-shell tanks. We are not aware of any recent studies to characterize the nature of the plutonium solid forms in any plant-produced sludges. Recent advances in the availability of sensitive microcharacterization equipment (e.g., SEM, STEM, etc.) should enable suitable determination of the nature and properties of plutonium and other actinides in sludge. Techniques applied by Milligan and co-workers in characterizing the nature of the amorphous hydrous gel which precipitates when ammonia or alkali is added to a solution of Am(III), provide a reference point for characterization of sludge.^(36,37)

Acknowledgment

This paper was prepared under U.S. Government contract, and the U.S. Government retains a prior nonexclusive, royalty-free license to publish, translate, reproduce, use, or dispose of the published form of the work, or allow others to do so for U.S. Government purposes.

Literature Cited

1. Mullins, L. J.; Foxx, C. L. Direct Reduction of $^{238}\text{PuO}_2$ to Metal, U.S. DOE Report LA-9073, Los Alamos National Laboratory, Los Alamos, N.M., January 1982.
2. Mullins, L. J.; Christensen, D. C. Babcock, B. R. Fused Salt Processing of Impure Plutonium Dioxide to High-Purity Metal, U.S. DOE Report LA-9154-MS, Los Alamos National Laboratory, Los Alamos, N.M., January 1982.
3. Baker, R. D. Preparation of Plutonium Metal by the Bomb Method, U.S. AEC Report LA-473, Los Alamos National Laboratory, Los Alamos, N.M., 1946.
4. Mullins, L. J.; Leary, J. A.; Morgan, A. N.; Maraman, W. J. I&EC Proc. Des. Dev. 1963, 2.
5. Mullins, L. J.; Morgan, A. N. A Review of Operating Experience at Los Alamos Plutonium Electrorefining Facility, 1963-1977, U.S. DOE Report LA-8943, Los Alamos National Laboratory, Los Alamos, N.M., December 1981.
6. Christensen, E. L.; Maraman, W. J. Plutonium Processing at the Los Alamos Scientific Laboratory, U.S. AEC Report LA-3542, Los Alamos Scientific Laboratory, Los Alamos, N.M., April 1969.
7. Bruns, L. E. in "Preparation of Nuclear Fuels, Nuclear Engineering, Part XVIII," Chemical Engineering Progress Symposium Series No. 80, Vol. 63, pp. 156-182. American Institute of Chemical Engineers, New York, 1967.
8. Bruns, L. E. in "Proceedings of the International Solvent Extraction Conference, The Hague, April 19-23, 1971," Vol. 1, Society of Chemical Industry, London, 1971, p. 186.
9. Environmental Assessment - Waste Form Selection for SRP High-Level Waste. DOE/EA - 0179, Savannah River Operations Office, Aiken, SC, 1982.
10. McKibben, J. M.; Starks, J. B.; Brown, J. K. in "Proceedings of 27th Conference on Remote Systems Technology," American Nuclear Society, La Grange Park, IL., 1979.

11. Hyder, M. L.; Perkins, W. C.; Thompson, M. C.; Burney, G. A.; Russell, E. R.; Holcomb, H. P.; Landon, L. F. Processing of Irradiated, Enriched Uranium Fuels at the Savannah River Plant. U.S. DOE Report DP-1500, E. I. duPont de Nemours & Co., Savannah River Laboratory, Aiken, SC, 1979.
12. Orth, D. A.; McKibben, J. M.; Scotten, W. C. in "Proceedings of the International Solvent Extraction Conference. The Hague, April 19-23, 1971," Vol. 1, Society of Chemical Industry, London, 1971, pp. 514-533.
13. Thompson, M. C.; Burney, G. A.; McKibben, J. M. in "Actinide Separations," J. D. Navratil and W. W. Schulz (eds.), American Chemical Society, Washington, DC, 1980, pp. 515-531.
14. Burney, G. A. Separation of Neptunium and Plutonium by Anion Exchange. U.S. AEC Report DP-689, E. I. duPont de Nemours & Co., Savannah River Laboratory, Aiken, SC, 1962.
15. Gray, L. W.; Burney, G. A.; Reilly, T. A.; Wilson, T. W.; McKibben, J. M. in "Transplutonium Elements - Production and Recovery," J. D. Navratil and W. W. Schulz (eds.), American Chemical Society, Washington, DC, 1981, pp. 93-108.
16. Gray, L. W.; Burney, G. A.; Wilson, T. W.; McKibben, J. M., *ibid*, pp. 223-242.
17. Gray, L. W.; Radke, J. H., in "Actinide Recovery from Waste and Low Grade Sources," J. D. Navratil and W. W. Schulz (eds.), Harwood Academic Publishers, New York, 1982, pp. 3-26.
18. Hagan, P. G.; Navratil, J. D.; Cichorz, R. S. J. Inorg. Nucl. Chem., 1981, 43, 1054.
19. Bray, L. A.; Ryan, J. L. in "Actinide Recovery From Waste and Low-Grade Sources," J. D. Navratil and W. W. Schulz (eds.), Harwood Academic Publishers, New York, 1982, pp. 129-154.
20. Leary, J. A.; Morgan, A. N.; Maraman, W. J. Second Eng. Chem., 1959, 51, 27.
21. Navratil, J. D.; Martella, L. L. Nucl. Technol., 1979, 46, 105.

22. Schulz, W. W.; Navratil, J. D. in "Recent Developments in Separation Science, Vol. VII, N.N.Li (ed.), CRC Press, Boca Raton, Florida, 1982, pp. 31-72.
23. Boyd, T. E.; Kochen, R. L. Ferrite Treatment of Actinide Waste Solutions: A Preliminary Study, U.S. DOE Rept. RFP-3299, Rockwell International, Golden, Colorado, July 30, 1982.
24. Cotton, F. A.; Wilkinson, G. "Advanced Inorganic Chemistry - A Comprehensive Text," 2nd Ed., Interscience, New York, 1968, p. 1180.
25. Katz, J. J.; Seaborg, G. T. "The Chemistry of the Actinide Elements," Methuen, London, 1957, p. 420.
26. Silver, G. L. Effect of Hydrolysis on the Disproportionation of Tetravalent and Pentavalent Plutonium Ions, U.S. AEC Report MLM-1743, Mound Laboratory, Miamisburg, OH, 1970.
27. Silver, G. L. The Three Actinide Equilibrium Problem, U.S. AEC Report MLM-2007, Mound Laboratory, Miamisburg, OH, 1973.
28. Silver, G. L. Minor Problems in Aqueous Plutonium Chemistry, U.S. AEC Report MLM-2075, Mound Laboratory, Miamisburg, OH, 1973.
29. Silver, G. L. Plutonium Disproportionation Reactions: Some Unresolved Problems, U.S. AEC Report MLM-1807, Mound Laboratory, Miamisburg, OH, 1971.
30. Colvin, C. A. Quantitative Determination of Plutonium Oxidation States in Variable Nitric Acid Solutions for Control Laboratories--Spectrophotometric, U.S. AEC Report RL-SA-33, General Electric Co., Richland, WA, 1965.
31. Swanson, J. L. The Selective Dissolution of Zirconium or Zircaloy Cladding by the Zirflex Process, Report A/Conf. 15/2429, June 1958, "Second United Nations International Conference on Peaceful Uses of Atomic Energy," Geneva, 1958.
32. Smith, P. W. The Zirflex Processes Terminal Development Report, U.S. AEC Report HW-65979, General Electric Co., Richland, WA, 1960.

33. Phillips, J. F. Dissolution of Oxide-Coated Zirconium and Zirconium Alloys, U.S. AEC Report BNWL-600, Pacific Northwest Laboratory, Richland, WA, 1968.
34. Emelity, L. A.; Christensen, C. W.; Kline, W. H.; in "Practices in the Treatment of Low- and Intermediate-Level Radioactive Wastes," IAEA, Vienna, 1966, p. 187.
35. Ryan, E. S.; Vance, J. N.; Maas, M. E.; in "Practices in the Treatment of Low- and Intermediate-Level Radioactive Wastes," IAEA, Vienna, 1966, p. 517.
36. Milligan, W. O.; Beasley, M. L.; Lloyd, M. H.; Haire, R. G.; Acta. Crystallog., Sect. B., 1968, 24, 978.
37. Milligan, W. O.; Crystal Structure and Morphology of Hydrrous Oxides and Hydroxides in the Lanthanide and Actinide Series, Final Report June 1, 1969-May 31, 1972. U.S. AEC Report ORO-3955-3, Oak Ridge Operation Office, Oak Ridge, TN, 1972.

RECEIVED December 21, 1982

Plutonium Process Chemistry at Rocky Flats

CHARLES E. BALDWIN and JAMES D. NAVRATIL

Rockwell International, Rocky Flats Plant, Golden, CO 80401

An overview is presented of plutonium process chemistry at Rocky Flats and of research in progress to improve plutonium processing operations or to develop new processes. Both pyrochemical and aqueous methods are used to process plutonium metal scrap, oxide, and other residues. The pyrochemical processes currently in production include electrorefining, fluorination, hydriding, molten salt extraction, calcination, and reduction operations. Aqueous processing and waste treatment methods involve nitric acid dissolution, ion exchange, solvent extraction, and precipitation techniques.

Rocky Flats is a Government-owned and contractor-operated facility which originated in 1952. The plant's primary missions are metal fabrication, assembly, and chemical processing--with emphasis on production-related research and development. Chemical processing activities involve the recovery of plutonium from Rocky Flats Plant scrap, waste materials and residues, and effluent streams. The final product of this recovery and purification effort is high-purity plutonium metal for use in foundry operations.

Both pyrochemical and aqueous methods are used at Rocky Flats to process plutonium metal scrap, oxide, and other residues. The pyrochemical processes currently in production include electrorefining, fluorination, hydriding, molten salt extraction, calcination, and reduction operations. Aqueous processing and waste treatment methods involve nitric acid dissolution, ion exchange, solvent extraction, and precipitation techniques. A brief overview of the chemistry involved in these operations is described. Research to improve these operations, or develop new processes, is also presented.

0097-6156/83/0216-0369\$06.00/0

© 1983 American Chemical Society

Plutonium Processing Overview

Figure 1 shows a simplified flow sheet for plutonium-239 recovery operations at Rocky Flats. Impure plutonium metal is sent through a pyrochemical process, called molten salt extraction (MSE), to remove the elemental impurity americium.* The product plutonium metal, if it meets plant purity requirements, is sent to the foundry. Metal that does not meet foundry requirements is processed further, either through an aqueous process using ion exchange, or through a pyrochemical electro-refining process. The waste chloride salt from MSE is dissolved; then the actinides are precipitated with carbonate and redissolved in 7M HNO₃; finally the plutonium is purified by anion exchange.

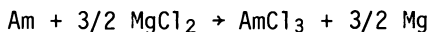
Impure plutonium oxide residues are dissolved in 12M HNO₃-0.1M HF under refluxing conditions and then purified by anion exchange. Plutonium is leached from other residues, such as metal and glass, and is also purified by anion exchange. The purified eluate from the anion exchange process is precipitated with hydrogen peroxide. The plutonium peroxide is calcined to the oxide, and the plutonium oxide is fluorinated. The plutonium tetrafluoride is finally reduced to the metal with calcium.

Acid waste streams are processed through nitric acid recovery and then sent to a secondary plutonium recovery process which uses anion exchange. Acid, basic, and laundry waste streams are sent to waste treatment. A discussion of the process steps shown on Figure 1 follows.

Pyrochemical Processes

Molten Salt Extraction. MSE has been used very successfully at Rocky Flats since 1967 to remove americium from plutonium (1, 2).

Plutonium, in 2-kg batches, is contacted at 750°C with a molten salt of 35 mole % NaCl-35 mole % KCl-30 mole % MgCl₂. The MgCl₂ reacts with the americium according to the reaction:



In addition, some plutonium is also lost to the salt as PuCl₃. A two-step counter-current extraction is used to minimize the amount of salt used in the MSE process, reduce plutonium losses

* Americium grows in the plutonium-239 from the beta decay of plutonium-241.

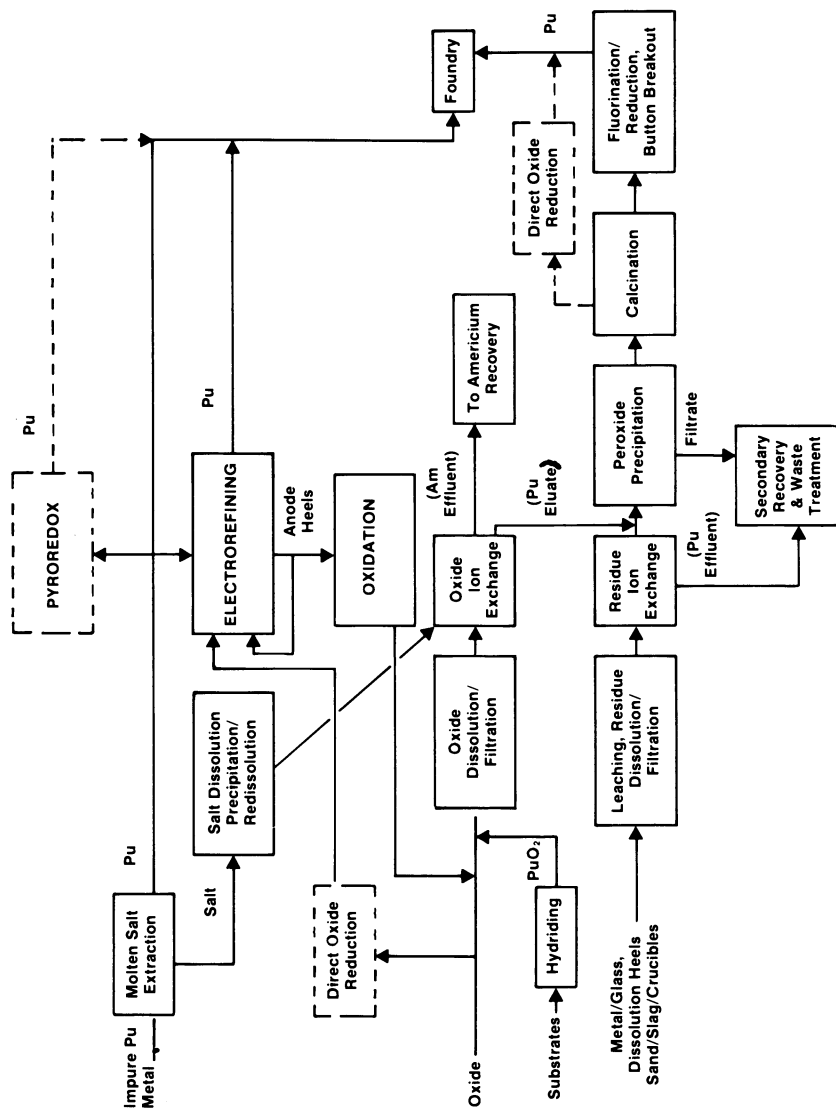


Figure 1. Plutonium recovery process.

to the salt, and achieve the proper level of americium removal (1).

The spent salt from MSE is currently sent to an aqueous dissolution/carbonate precipitation process to recover plutonium and americium. Efforts to recover plutonium and americium from spent NaCl-KCl-MgCl₂ MSE salts using pyrochemistry have been partially successful (3). Metallothermic reductions using Al-Mg and Zn-Mg alloys have been used in the past to recover plutonium and americium, and produce salts which meet plant discard limits. Attempts at direct reductions of MSE salts using calcium metal have been less successful, with a discardable white salt phase, a nondiscardable black salt phase, and little or no metal produced (3). Until recently, pyrochemical alloy products from salt cleanup have not been compatible with other plant operations because of the difficulty in removing impurities, such as aluminum and calcium, from the americium during aqueous processing. Development of the CMP process (*vide infra*), which removes these impurities, has renewed the interest in pyrochemical recovery of spent MSE salt (4). Other salt systems, such as NaCl-CaCl₂-MgCl₂, will again be investigated for MSE. Calcium reductions of CaCl₂-based salts have been shown to be successful in the past and could lead to a more compatible salt system in the future at Rocky Flats for MSE (3).

Electrorefining. Impure plutonium metal from MSE and Direct Oxide Reduction (DOR) is sent to an electrorefining operation (5). In plutonium electrorefining, impure plutonium metal is placed in a molten salt electrolyte of equimolar NaCl-KCl and 3 mole % MgCl₂. Trivalent plutonium ions, required to start electrolysis, are generated *in situ* by the MgCl₂ oxidation of plutonium metal. The impure plutonium metal is made anodic (positive) and a tungsten electrode is made cathodic (negative). When a direct current is applied, plutonium at the anode is anodically dissolved and plutonium metal is deposited at the cathode. The chemical basis for plutonium purification during electrorefining is the difference in the free energy of formation ($-\Delta G_f$) for the chlorides of plutonium and the impurity elements. Elements with values of $-\Delta G_f$ smaller than that for plutonium will remain in the anode. The transfer of impurities is set by the equilibrium distribution coefficient for each element partitioning between the molten anode-salt interface and the molten plutonium-salt interface at the cathode (3).

Spent anode residues from electrorefining (which contain approximately 20-30 percent of the plutonium fed to the process) are either recycled back to electrorefining, or, if high enough in impurities, are oxidized and sent to oxide dissolution. The spent salt is sent to aqueous dissolution (see Figure 1).

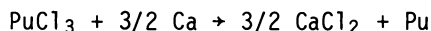
Future work to be done in electrorefining includes evaluation of CaCl_2 -based salts, similar to those considered for use in MSE, which will allow direct reduction of plutonium from the salts. Past research and development using $\text{NaCl-CaCl}_2\text{-MgCl}_2$ for electrorefining looked promising. In situ reduction of plutonium from the salt demonstrated the ability to recover the plutonium with the product metal and produce salt meeting the plant's discard limits (3).

The ability to reuse the salt will be investigated. Pyrochemical techniques to recover plutonium from spent anode heels will also be examined. One technique, called pyroredox (*vide infra*), utilizes ZnCl_2 in a diluent salt of 46 mole % $\text{KCl-54 mole \% CaCl}_2$ to oxidize the plutonium to PuCl_3 (3). The reduced zinc scavenges the impurities and separates from the salt. The salt is reduced in a diluent salt of 26 mole % $\text{KCl-74 mole \% CaCl}_2$ to recover the purified plutonium which can be returned to electrorefining or, if pure enough, to the foundry. Pyroredox is also being investigated as a primary operation to purify plutonium, along with electrorefining.

Pyroredox. This is a three-step plutonium purification process (3). Impure plutonium metal is reacted with ZnCl_2 in a solvent salt of KCl-CaCl_2 , as follows:



Impurities less chemically reactive than plutonium follow the zinc. The salt and zinc are allowed to solidify and are separated. The PuCl_3 , contained in the salt, is reacted with calcium, according to the reaction:



The plutonium reduces and separates from the salt phase. In the third step, distillation is used to separate the more volatile zinc and calcium from the plutonium.

Pyroredox is currently under development. Several problems have been identified and work is underway to overcome these obstacles. As mentioned previously, this process has immediate application as a primary plutonium purification process and as a means to process spent electrorefining anodes for direct recycle back to electrorefining.

Direct Oxide Reduction. Implementation of the DOR process into production is currently underway. Plutonium oxide from foundry operations, hydriding, and other sources is calcined in

air at 800°C to remove any carbon or other volatile impurities. This oxide is then reduced by a 25 percent stoichiometric excess of calcium in a CaCl_2 solvent. The salt-to-oxide ratio, by weight, is 4 to 1. The reaction takes place in a MgO crucible which is heated to approximately 850°C. Upon cooling to room temperature, a well consolidated plutonium product is obtained at better than 98 percent recovery, as well as salt and ceramics which are well below the plant discard limits.

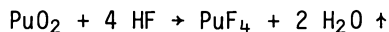
Recent development work has been done defining the above operating parameters and evaluating a CaCl_2 - CaF_2 salt system.

Hydriding. A hydride facility was constructed for recovering plutonium, as plutonium hydride, from various types of metallic substrates (6). Hydriding does not damage certain types of reusable substrates, as does acid leaching. Hydriding also eliminates the use of large volumes of leaching acid solutions and the need for subsequent removal of plutonium from these solutions.

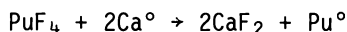
During the hydriding cycle, gaseous hydrogen reacts with plutonium in an oxygen-free reactor to produce plutonium dihydride. It is possible to produce other plutonium-hydrogen compounds having different hydrogen-to-plutonium ratios, depending on operating parameters. For this type of recovery process, however, the formation of nonstoichiometric plutonium hydride compounds is not significant. As plutonium hydride is produced during a hydriding operation, it falls free from the metallic substrate and drops into a tray. Since PuH_2 is a pyrophoric powder, it is oxidized in air to PuO_2 . This change permits safe handling of the material during additional processing. Residual hydrogen that is not used in hydriding operations is pumped from the reactor to an apparatus where the hydrogen is burned in a natural gas flame.

Plutonium has been selectively removed from metallic substrates that do not form hydrides with hydrogen. Plutonium has also been removed from metals that absorb hydrogen (i.e., tantalum), but do not produce a hydride under the hydriding operating conditions used. The hydriding apparatus is used to recover plutonium from reusable equipment, plutonium scrap, plutonium-coated tools, and plutonium melts from tantalum and tungsten crucibles. The hydriding apparatus is also used to oxidize such pyrophoric material as casting residues, plutonium chips and turnings, mixtures of plutonium hydride and plutonium oxide, and plutonium hydride that is generated elsewhere on plantsite.

Fluorination and Reduction. Until recently, plutonium dioxide from the calcination of plutonium peroxide was contacted with HF in a rotary hydrofluorinator. The reaction converted PuO_2 to PuF_4 , according to the following equation:



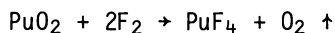
The PuF_4 is then loaded in ceramic (MgO) crucibles, where it is reacted with calcium to form CaF_2 and plutonium metal as follows (7):



The products of the reaction, once cooled to room temperature, are easily separated. The plutonium metal is sent to the foundry, while the CaF_2 salt is stored until it can be dissolved in 9M HNO_3 for recovery of residual amounts of plutonium.

Though both hydrofluorination and reduction were accomplished with relative ease, three significant problems were apparent. First, PuF_4 is a neutron emitter, requiring considerable protective shielding and creating difficulty in handling. Secondly, the use of HF requires costly equipment which must be resistant to corrosion. Finally, the salt from the reduction, CaF_2 , is not discardable, and must be processed to recover residual plutonium.

In the last year, direct fluorination has been used to convert PuO_2 to PuF_4 , as follows (8):



The problems previously discussed are basically the same, with an added problem--disposal of excess fluorine. Studies are underway to find a safe, efficient way to resolve it. Ultimately, the use of DOR, previously discussed, is expected to replace fluorination and reduction. This would result in one process step, rather than two. In addition, the problems previously discussed would be eliminated.

Aqueous Processing

Dissolution. Plutonium is solubilized in nitric acid solutions at Rocky Flats. The feed material consists of oxide, metal and glass, dissolution heels, incinerator ash and sand, slag, and crucible from reduction operations. The residues are contacted with 12M HNO_3 containing CaF_2 or HF to hasten dissolution. Following dissolution, aluminum nitrate is added to these solutions to complex the excess fluoride ion.

Complete dissolution of plutonium residues, especially high temperature calcined plutonium dioxide contained in residues such as incinerator ash, continues to cause problems, despite continued research since the Manhattan Project (9). Methods to improve the Rocky Flats system include the use of additives (e.g., cerium) and electrochemistry, other solvents (HCl-SnCl_2) as well as high-temperature fusion methods (10). High pressure dissolution, HF preleaching, fluorination, and other methods are being investigated.

Solvent Extraction. A modified, one-cycle PUREX process is used at Rocky Flats to recover plutonium from miscellaneous Pu-U residues (11). The process utilizes the extraction of uranium (VI) into tributyl phosphate (TBP), leaving plutonium (III) in the raffinate. The plutonium is then sent to ion exchange for purification. An extraction chromatography method is being studied as a possible substitute for the liquid-liquid extraction process (12); TBP is sorbed on an inert support so ion exchange column equipment can be used. Electrolytic valence adjustment could significantly improve this process.

Acid waste streams are sent through a nitric acid recovery process and then to a secondary plutonium recovery process using anion exchange (Figure 2). Another area of solvent extraction application involves the use of dihexyl-N,N-diethylcarbamoylmethylphosphonate (CMP Process) for removing further amounts of plutonium and americium from the acid waste streams coming from the secondary plutonium recovery columns (4, 13). Alternative solvent extractants, sorbed or bonded on inert support materials so ion exchange column equipment can be used, are being studied to selectively extract only actinides and not impurities.

Precipitation Processes. Plutonium peroxide precipitation is used at Rocky Flats to convert the purified plutonium nitrate solution to a solid (14); the plutonium peroxide is then calcined to PuO_2 and sent to the reduction step. The chemistry of the plutonium peroxide precipitation process is being studied, as well as alternative precipitation processes such as oxalate, carbonate, fluoride, and thermal denitration. The latter method shows the most promise for cost and waste reduction.

Molten salt extraction residues are processed to recover plutonium by an aqueous precipitation process. The residues are dissolved in dilute HCl, the actinides are precipitated with potassium carbonate, and the precipitate redissolved in nitric acid (7M) to convert from a chloride to a nitrate system. The plutonium is then recovered from the 7M HNO_3 by anion exchange and the effluent sent to waste or americium recovery. We are studying actinide (III) carbonate chemistry and looking at new

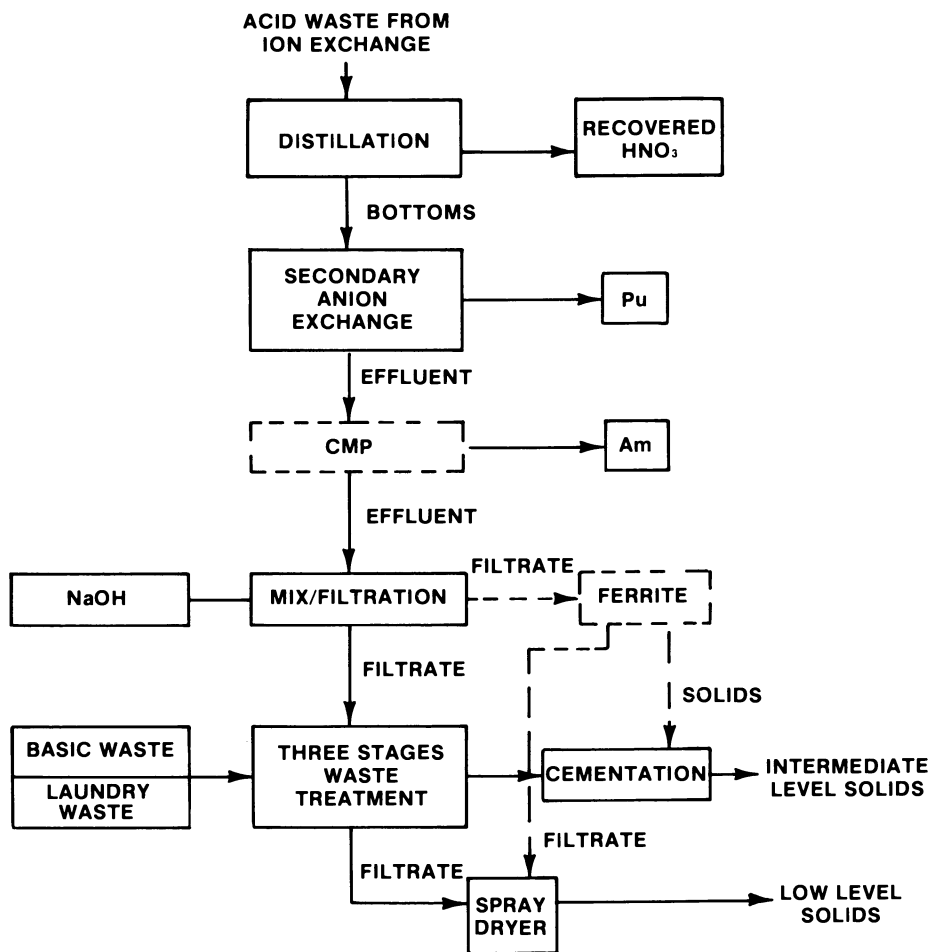


Figure 2. Aqueous waste recovery and treatment processes (broken lines represent processes under development).

cation exchangers as an alternative to carbonate precipitation (15, 16).

Ion Exchange. Very few elements form anions in nitric acid solutions, thus anion exchange is a very effective procedure for purifying plutonium. The plutonium hexanitrate anion is sorbed on the resin from a 7M nitric acid solution. A nitric acid wash is used to remove residual impurities from the resin. Dilute nitric acid is used to elute the purified plutonium from the resin. We have a continuing resin evaluation program to test new gel and macroporous anion exchange resins, as well as inorganic ion exchangers (17).

Waste Treatment. Figure 2 outlines the current waste recovery and treatment processes, and proposed changes. Acid waste streams are sent through nitric acid and secondary plutonium recovery processes before being neutralized with potassium hydroxide and filtered. This stream and basic and laundry waste streams are sent to waste treatment. During waste treatment, the actinides in the aqueous waste are removed by three stages of hydroxide-iron carrier-flocculant precipitation. The filtrate solution is then evaporated to a solid with a spray dryer and the solids are cemented and sent to retrievable storage.

A ferrite waste treatment process is being investigated to determine if it can more effectively remove actinides from waste solution with less solid waste generation than the flocculant precipitation method presently used (18).

Ferrite is introduced into the aqueous media by two techniques. With the in situ method, ferrite is formed within the actinide-containing solution by addition of Fe(II), Fe(III), and sodium hydroxide. With the preformed ferrite method, ferrite solids are prepared separately and added to the actinide solution.

Both preformed and in situ ferrite lowered plutonium concentrations in simulated process waste from 10^{-4} g/l to 10^{-8} g/l in one treatment step. Two or three flocculant precipitations, as currently used for waste processing, were required to achieve the same result. Ferrite waste treatment produced 4.1 g/l solids, while production waste processing during the past year, using the flocculant process, produced 7.9 g/l solids.

The Chemistry Research and Development group has a large variety of plutonium process chemistry projects underway. The work will certainly add to our understanding of plutonium chemistry and will result in plutonium process improvements.

Acknowledgment

The authors wish to thank M. J. Cusick and J. B. Knighton for their assistance in preparing this manuscript. This work was performed under U.S. Government Contract DE-AC04-76DP03533, and the U.S. Government retains a prior nonexclusive, royalty-free license to publish, translate, and reproduce, use, or dispose of the published form of the work, or allow others to do so for U.S. Government purposes.

Literature Cited

1. Knighton, J. B.; Auge, R. C.; Berry, J. W.; Franchini, R. C. "Molten Salt Extraction of Americium from Molten Plutonium Metal," U.S. ERDA Rept. RFP-2365, Dow Chemical Co., Golden, Colorado, March 12, 1976.
2. Knighton, J. B.; Hagan, P. G.; Navratil, J. D.; Thompson, G. H. "Production of Transplutonium Elements," Navratil, J.D.; Schulz, W. W. (Eds.), American Chemical Society, 1981, p. 53.
3. Knighton, J. B. Rockwell International, Rocky Flats Plant, personal communication.
4. Yamada, W. I.; Martella, L. L.; Navratil, J. D. J. *Less Common Metals* 1982, 86, 211.
5. Miner, F. J. "Chemistry Research and Development Progress Report for July 1977 Through April 1978," U.S. DOE Rept. RFP-2803, Rockwell International, Golden, Colorado, November 8, 1978.
6. DeGrazio, R. P. "A Prototype Hydriding Apparatus (Application for Plutonium Recovery)," U.S. ERDA Rept. RFP-2340, Dow Chemical Company, Golden, Colorado, March 17, 1975.
7. Conner, W. V. "Process Studies on the Reduction of Plutonium Tetrafluoride to Metal," U.S. AEC Rept. RFP-728, Dow Chemical Company, Golden, Colorado, May 11, 1966.
8. Standifer, R. L. "Conversion of Plutonium Oxide to Plutonium Tetrafluoride with Fluorine in a Fluid Bed Reactor - Part I, Development Studies," U.S. AEC Rept. RFP-1889, Dow Chemical Company, Golden, Colorado, August 23, 1972.

9. Bray, L. A.; Ryan, J. L. "Actinide Recovery From Waste and Low-Grade Sources," Navratil, J. D.; Schulz, W. W. (Eds.), Harwood Academic Publishers, New York, 1982, p. 129.
10. Navratil, J. D.; Thompson, G. H. *Nucl. Technol.* 1979, 43, 136.
11. Navratil, J. D.; Leeb1, R. G. "Modified Purex Processes for the Separation and Recovery of Plutonium-Uranium Residues," U.S. DOE Rept. RFP-2675, Rockwell International, Golden, Colorado, July 1978.
12. Martella, L. L.; Navratil, J. D. "Recovery of Uranium from Mixed Plutonium-Uranium Residues by an Extraction Chromatography Process," U.S. DOE Rept. RFP-3289, Rockwell International, Golden, Colorado, May 15, 1982.
13. Martella, L. L.; Navratil, J. D.; Saba, M. T. "Actinide Recovery from Waste and Low-Grade Sources," Navratil, J. D.; Schulz, W. W. (Eds.), Harwood Academic Publishers, New York, 1982, p. 27.
14. Hagan, P. G.; Miner, F. J. "Actinide Separations," Navratil, J. D.; Schulz, W. W. (Eds.), American Chemical Society, Washington, D.C., 1980, p. 51.
15. Hagan, P. G.; Navratil, J. D.; Cichorz, R. S. J. *Inorg. Nucl. Chem.* 1981, 43, 1054.
16. Navratil, J. D.; Martella, L. L.; Thompson, G. H. "Actinide Separations," Navratil, J. D.; Schulz, W. W. (eds.), American Chemical Society, Washington, D.C., 1980, p. 455.
17. Navratil, J. D.; Martella, L. L. *Nucl. Technol.* 1979, 46, 105.
18. Boyd, T. E.; Kochen, R. L. "Ferrite Treatment of Actinide Waste Solutions: A Preliminary Study," U.S. DOE Rept. RFP-3299, Rockwell International, Golden, Colorado, July 30, 1982.

RECEIVED January 4, 1983

Pyrochemical Processing of Plutonium

MELVIN S. COOPS—Lawrence Livermore National Laboratory,
Livermore, CA 94550

JAMES B. KNIGHTON—Rockwell International, Rocky Flats Plant,
Golden, CO 80401

LAWRENCE J. MULLINS—Los Alamos National Laboratory,
Los Alamos, NM 87545

Non-aqueous processes are now in routine use for direct conversion of plutonium oxide to metal, molten salt extraction of americium, and purification of impure metals by electrorefining. These processes are carried out at elevated temperatures in either refractory metal crucibles or magnesium-oxide ceramics in batch-mode operation. Direct oxide reduction is performed in units up to 700 gram PuO₂ batch size with molten calcium metal as the reductant and calcium chloride as the reaction flux. Americium metal is removed from plutonium metal by salt extraction with molten magnesium chloride. Electrorefining is used to isolate impurities from molten plutonium by molten salt ion transport in a controlled potential oxidation-reduction cell. Such cells can purify five or more kilograms of impure metal per 5-day electrorefining cycle. The product metal obtained is typically >99.9% pure, starting from impure feeds. Metal scrap and crucible skulls are recovered by hydriding of the metallic residues and recovered either as impure metal or oxide feeds.

The term "Pyrochemical Processing" is commonly applied to a family of chemical processes that utilize oxidation-reduction reactions to effect chemical separations at elevated temperatures.

These reactions are carried out in the total absence of aqueous solvents, and are used to chemically isolate elements, or groups of elements, from impurities in the feed materials.

0097-6156/83/0216-0381\$08.00/0
© 1983 American Chemical Society

Pyrochemical processes have significant advantages over aqueous processes for the purification of actinide metals for several reasons: the size of the equipment used to carry out the chemical processes is very compact, typically an order of magnitude smaller than that needed for aqueous methods; the chemical process can be designed to recycle many of the reagents used, thereby greatly minimizing waste disposal problems; nuclear criticality concerns are alleviated because non-moderating reagents can be used exclusively; pyrochemical processes can readily accept metallic feed stocks and produce high purity metallic products; and because pyrochemical processes require smaller facilities, generate less waste, and use less manpower, they are cheaper to operate. Like aqueous processes, pyrochemical systems utilize several different physical processes including liquid-liquid extraction, precipitation, filtration, evaporation and distillation. These are performed at elevated temperatures in either refractory metal or ceramic equipment. Molten metals and molten salts are used both as solvents and as immiscible extractants in various steps in the chemical purification sequence. Specialized process hardware has been constructed to meet the needs of these highly corrosive processes.

While pyrochemical processes have inherent advantages, they require sophisticated equipment and specialized operating conditions. One of the basic techniques used in pyroprocessing is liquid-liquid extraction between molten salts and molten metals. The process temperatures are typically 1100 K, and because both the process reagents and the refractory materials used to contain them are susceptible to air oxidation, process operations must be carried out in an inert atmosphere. As the actinide elements are inherently radioactive, work on actinide compounds is routinely carried out in tight process enclosures; pyroprocessing operations require that the atmosphere in contact with the process reagents be truly inert and also dry. Recirculating argon or helium atmospheres are used to meet this requirement. Where sealed reaction vessels are used, dry air enclosures are adequate.

In order to obtain maximum efficiency from pyroprocessing, very high purity reagents must be used. Obtaining satisfactory reagents has been a continuing problem but as the demand for high purity metals and salts rises, commercial sources become more available. At present it is necessary to dry all commercially obtained reagent salts prior to use.

The following pages will describe several examples of pyrochemical processing as applied to the recycle of plutonium, and will briefly review the fundamental chemistry of these processes. We shall review the conversion of plutonium oxide to plutonium metal by the direct oxide reduction process (DOR), the removal of americium from metallic plutonium by molten salt extraction (MSE), and the purification of metallic

plutonium from dissolved impurities by the electro-refining technique (ER).

All actinide metals are pyrophoric and it is common practice to burn metallic scrap to oxide as a safety precaution. Plutonium is typically stored as PuO_2 and must be chemically reduced to metal prior to component manufacture. This has traditionally been done by precipitating $\text{Pu}_2(\text{C}_2\text{O}_4)_3$, $\text{Pu}(\text{O}_2)_2$, $\text{Pu}(\text{OH})_3$, or PuF_3 from solution and converting it to PuF_4 for bomb reduction to metal. This method is now being replaced by direct reduction techniques.

Reduction of Plutonium Oxide to Metal

The first successful reduction of PuO_2 to metal with calcium was reported by Wade and Wolf⁽¹⁾ in 1968. Their process was carried out in two stages: an initial thermit reaction between PuO_2 and Ca, followed by a leaching step with CaCl_2 to dissolve the CaO reaction product and any unreacted Ca. The fluid flux permitted finely divided plutonium to coalesce into a pool of metal. Rotation of the inclined reaction vessel was used to promote slag dissolution and metal consolidation. The original process described by Wade has been significantly improved by workers at several DOE sites^(2,3,4).

The DOR process presently used for production work utilizes a CaCl_2 (or $\text{CaCl}_2\text{-CaF}_2$) flux to both dissolve the CaO reaction product at the reaction site and to provide a fresh supply of Ca reductant to keep the reaction going. This process exploits the solubility of Ca and CaO in CaCl_2 while utilizing the insolubility of plutonium metal in the Ca-CaO- CaCl_2 reaction flux to permit metal consolidation. Vigorous stirring is used to keep the reactants in intimate contact so that the reaction is driven to completion. Workers at Los Alamos used the above process for ^{238}Pu metal production in 1975⁽⁴⁾. That work led to a routine 700 gram scale oxide reduction process that has been in use since that time. Recent development work at LANL has increased the batch size to one kilogram of oxide feed. It appears that the ultimate limitation on DOR batch size will be from criticality safety constraints.

The use of this direct oxide reduction process is replacing fluoride reduction as it eliminates neutron exposure to operating personnel (alpha particles from plutonium decay have sufficient energy to eject neutrons from fluorine by the α, n reaction) and eliminates reduction residues which require subsequent recovery.

The reaction is carried out under an inert atmosphere in an open crucible at approximately 830°C. Figure 1 shows typical equipment used for direct oxide reduction. Vitriified magnesium oxide ceramic is commonly used as a container material, but tungsten and tantalum can also be used⁽³⁾. If the latter are used, CaF_2 is added to lower the temperature needed to liquify

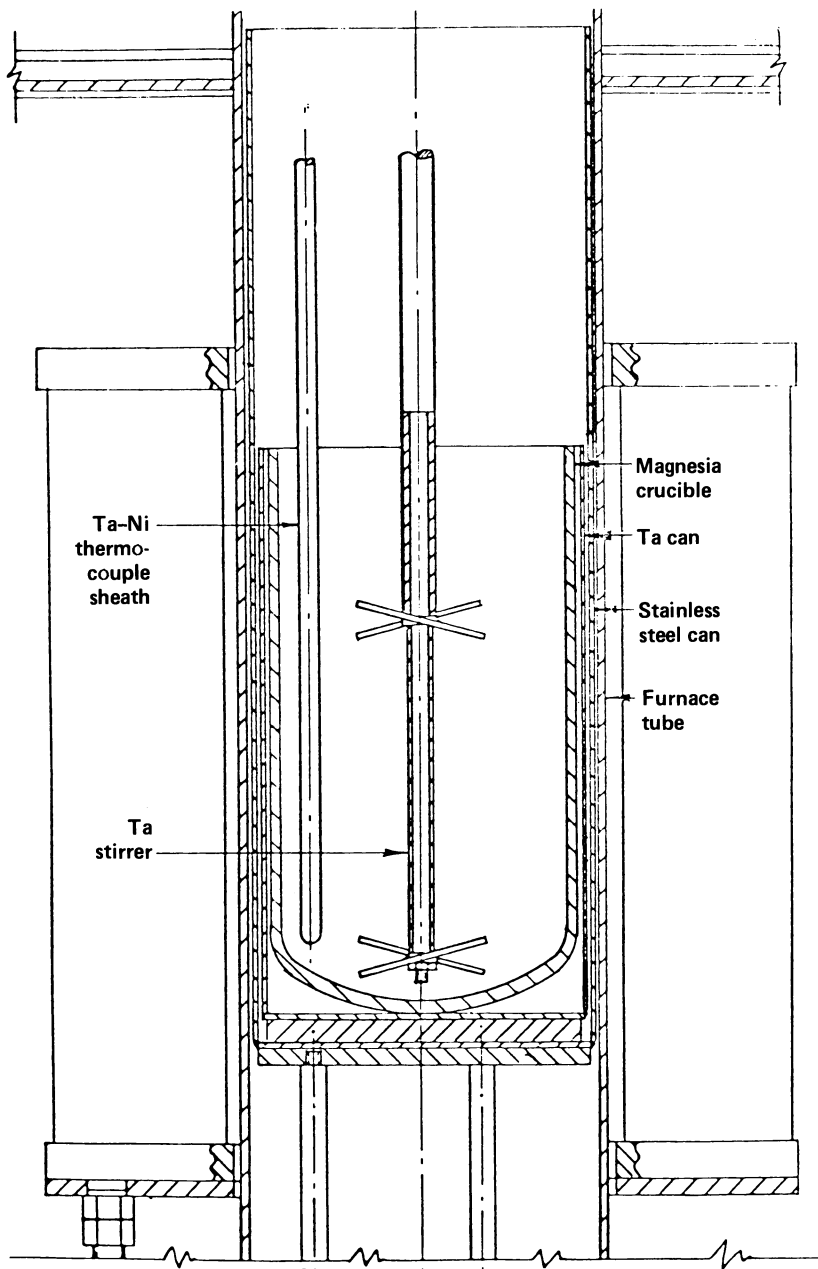
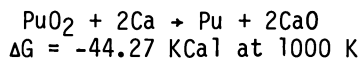


Figure 1. Stationary Extraction Furnace Assembly for Plutonium Reduction and Americium Extraction.

the flux, thereby decreasing the corrosion of the crucible and subsequent contamination of the metal product. Intense stirring is required to keep all the reactants in contact as the very dense PuO_2 sinks and Ca metal floats in the melt. The reaction is exothermic and a temperature rise occurs after initiation. The overall chemical reaction is:

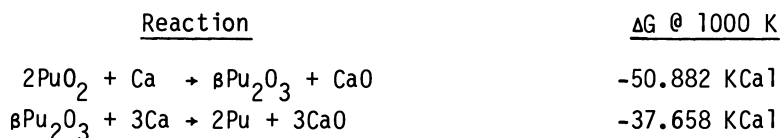


The mechanism for the reaction is not fully understood at present but is believed to take place in several steps. Moseley et-al⁽³⁾ found that $\beta\text{-Pu}_2\text{O}_3$ is formed as a solid residue when insufficient Ca is present to drive the reaction to completion.

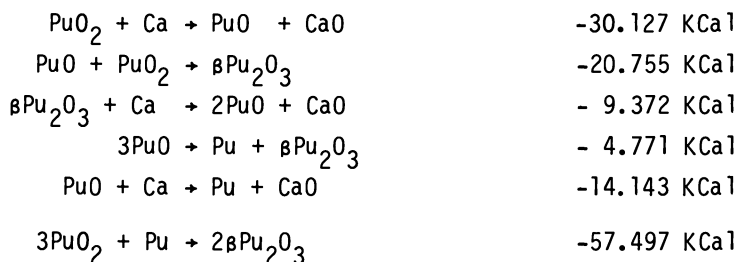
Several of the possible reacting species and their free energy of formation are listed in the table below:

Compound	KCal/mole	<u>ΔG @ 1000 K</u>	
		KCal/gr-at oxygen	Ref
PuO_2	-210.130	-105.065	20
$\alpha\text{-Pu}_2\text{O}_3$	-367.696	-122.565	20
$\beta\text{-Pu}_2\text{O}_3$	-343.942	-114.647	20
PuO	-113.057	-113.057	20
CaO	-127.200	-127.200	21

The reaction mechanism proposed by Moseley is:

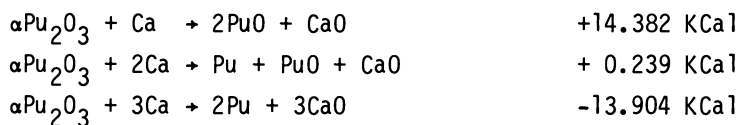


It is also feasible to assume the following mechanism:



An additional back reaction can occur between $\beta\text{Pu}_2\text{O}_3$ and PuO_2 to form $\alpha\text{Pu}_2\text{O}_3$. Conditions leading to the formation of $\alpha\text{Pu}_2\text{O}_3$ are to be avoided as the reaction between a single

atom of Ca and $\alpha\text{Pu}_2\text{O}_3$ is not thermodynamically favorable:



Although the exact chemical mechanism for the direct oxide reduction reaction has not yet been fully characterized, it has been well established that the reaction goes to completion when excess calcium is present, sufficient CaCl_2 is available to dissolve the CaO produced, and adequate stirring is used. As calcium metal is soluble to about 1 wt% in CaCl_2 at 835°C , excess Ca insures that the reaction is driven to completion by mass-action effects.

The CaCl_2 -rich end of the CaO-CaCl_2 and $\text{CaO-CaCl}_2\text{-CaF}_2$ phase diagrams have been worked out by Wenz et-al⁽⁶⁾ and are shown in Figures 2 and 3. The phase diagrams indicate that CaO is soluble to 18.5 mole % in CaCl_2 at 835°C , but if the loading of CaO rises much above 14 mole % the increased viscosity of the melt retards consolidation of the droplets of plutonium into a single pool. The 700-gram PuO_2 reduction process at LANL⁽⁵⁾ uses 50 mole % excess calcium reductant and a CaO loading in CaCl_2 of about 14 mole %, to give product yields in excess of 99.5%. After the melt is allowed to cool, an ingot of plutonium metal can be readily cleaved from the solidified flux. The salt phase contains negligible unreacted PuO_2 . At present, both the $\text{CaCl}_2\text{-CaO}$ salt residue and the excess calcium metal are discarded to waste. These materials are promising candidates for recycle; processes are presently being developed to recover these reagents for reuse.

Extraction of Americium With Molten Salt

All reactor-produced plutonium contains a mixture of several plutonium isotopes. The continuous decay of ^{241}Pu (14.8 year half-life) is the source of ^{241}Am . This isotope decays by alpha emission with the simultaneous emission of 60 kilovolt gamma rays in 80% abundance. In order to minimize personnel exposure, this element is removed from the metal prior to fabrication.

Early experimental work in electrorefining at Los Alamos by Mullins et-al⁽⁷⁾ demonstrated that americium could be partitioned between molten plutonium and a molten NaCl-KCl salt containing Pu^{+3} ions, and Knighton et-al⁽⁸⁾, working at ANL on molten salt separation processes for fuel reprocessing, demonstrated that americium could be extracted from Mg-Zn-Pu-Am alloys with immiscible molten magnesium chloride salts. Work

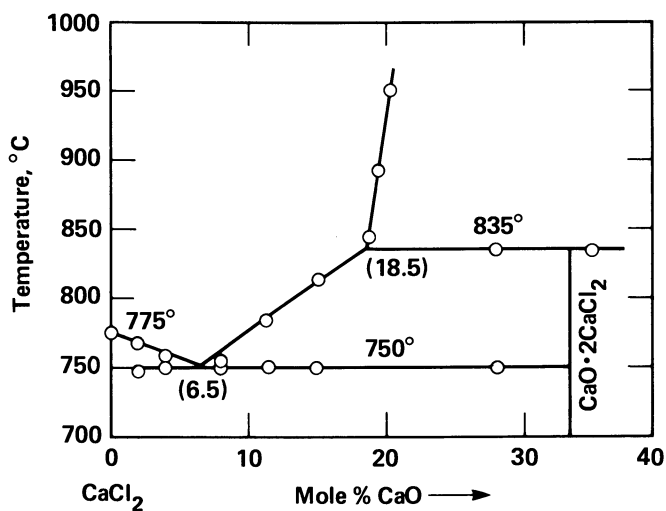


Figure 2. Partial Binary Phase Diagram for the CaO-CaCl₂ System.

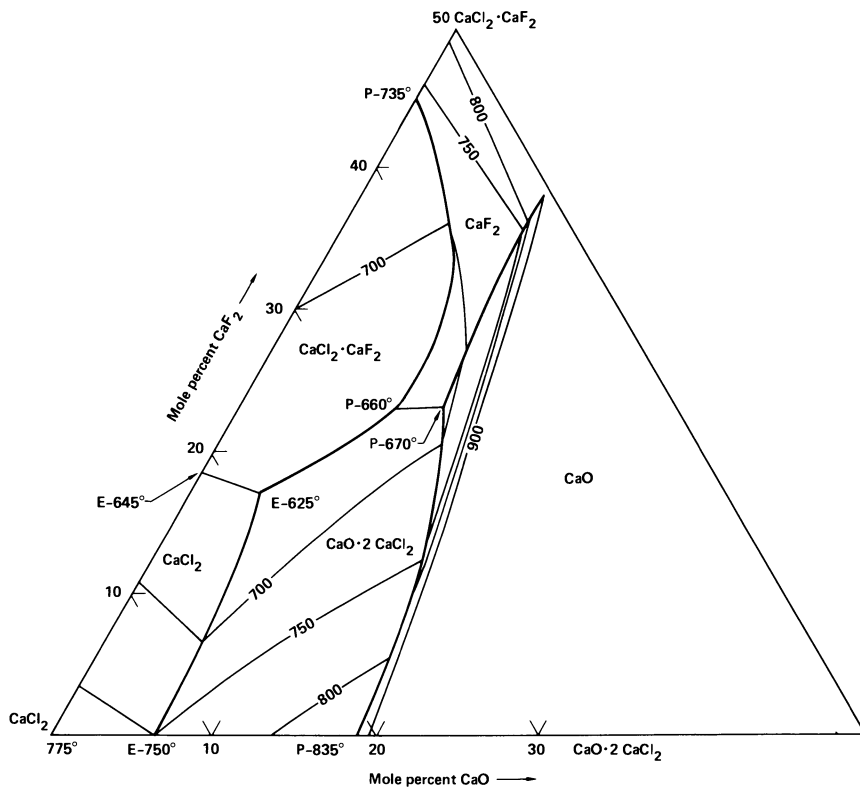
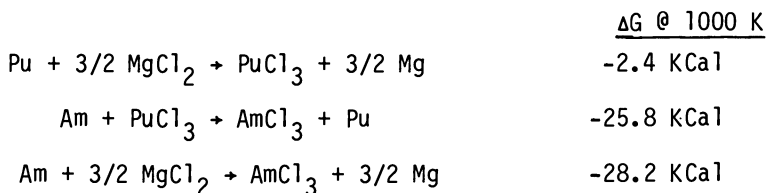


Figure 3. Partial Ternary Phase Diagram for the CaCl_2 -rich Side of the CaCl_2 - CaF_2 - CaO System.

was soon initiated by Long et al.⁽⁹⁾ at Rocky Flats to study the extraction of americium from molten plutonium by contacting with molten NaCl-KCl salt containing a few percent of MgCl₂.

A production process has evolved from this original work, and is presently used for extracting americium from kilogram amounts of plutonium metal. This process is based upon equilibrium partitioning (by oxidation-reduction reactions) of americium and plutonium between the molten chloride salt and the molten plutonium phase. The chemistry of this process is indicated by the following reactions:



The free energies of formation for the actinide compounds above are given by the following table:

Compound	$\Delta G @ 1000 \text{ K}$ (KCal per gram-atom of chlorine)
AmCl ₃	-67.0
PuCl ₃	-58.4
MgCl ₂	-57.6

The thermodynamic activity equilibrium constant (K_a) is expressed in terms of mole fraction (X) and activity coefficient (γ) by the following equation:

$$K_a = \frac{(X_{\text{AmCl}_3})(\gamma_{\text{AmCl}_3})(X_{\text{Mg}})^{3/2}(\gamma_{\text{Mg}})^{3/2}}{(X_{\text{Am}})(\gamma_{\text{Am}})(X_{\text{MgCl}_2})^{3/2}(\gamma_{\text{MgCl}_2})^{3/2}}$$

The term $\frac{X_{\text{AmCl}_3}}{X_{\text{Am}}}$ is defined as the distribution coefficient (D_{Am})

and is simply the ratio of the mole fraction of AmCl₃ in the salt to the atom fraction of Am in the metal.

The activity coefficients in the above equation may be determined by obtaining experimental data for D_{Am} , and relating K_a to the free energy change for the reaction using the equation $\Delta G_f = -RT \ln K$.

In laboratory work the following closely related, but not identical, relationship is used to determine the partition value between phases:

$$K_d = \frac{\text{conc. of AmCl}_3 \text{ in salt phase}}{\text{conc. of Am in metal phase}}$$

by convention, the above ratio is usually expressed in weight percent instead of mole fractions. For extraction work the term α is used for the extraction factor and is related to K_d in the following manner:

$$\alpha = (K_d) \left(\frac{s}{m} \right) (F) (\beta)$$

where

- α = extraction factor = $\frac{\text{Wt of solute in salt phase}}{\text{Wt of solute in metal phase}}$
 K_d = distribution coefficient (as defined above)
 s/m = salt to metal ratio by weight
 F = fraction of equilibrium attained
 β = effects of side reactions

For a multi-stage counter-current extraction operated in true equilibrium without side reactions, the partitioning of a solute into the metal phase (f_m) and the salt phase (f_s) is defined as follows:

$$f_m = \frac{(\alpha - 1)}{(\alpha^{n+1}) - 1} \quad f_s = 1 - f_m$$

where n = number of counter-current stages.

For a cross-current extraction the equation is defined as follows:

$$f_m = \frac{1}{(1+\alpha)^n} \quad f_s = 1 - f_m = \frac{(1+\alpha)^n - 1}{(1+\alpha)^n}$$

Both methods have been used at various times, but the counter-current method is the preferred technique as it minimizes salt use and plutonium losses.

Present production processes use two stage counter-current extraction to remove americium from molten plutonium with magnesium chloride based salts. Both 35 mole % NaCl - 35 mole % KCl - 30 mole % MgCl₂ and 50 mole % NaCl - 26 mole % CaCl₂ - 24 mole % MgCl₂ are used for americium extraction. Figures 4 and 5 show the ternary phase diagrams for these salt systems⁽¹⁰⁾. The above salt fluxes will extract 90% of the americium present when a salt-to-metal mass-ratio of 0.06 is used in a two stage counter-current extraction.

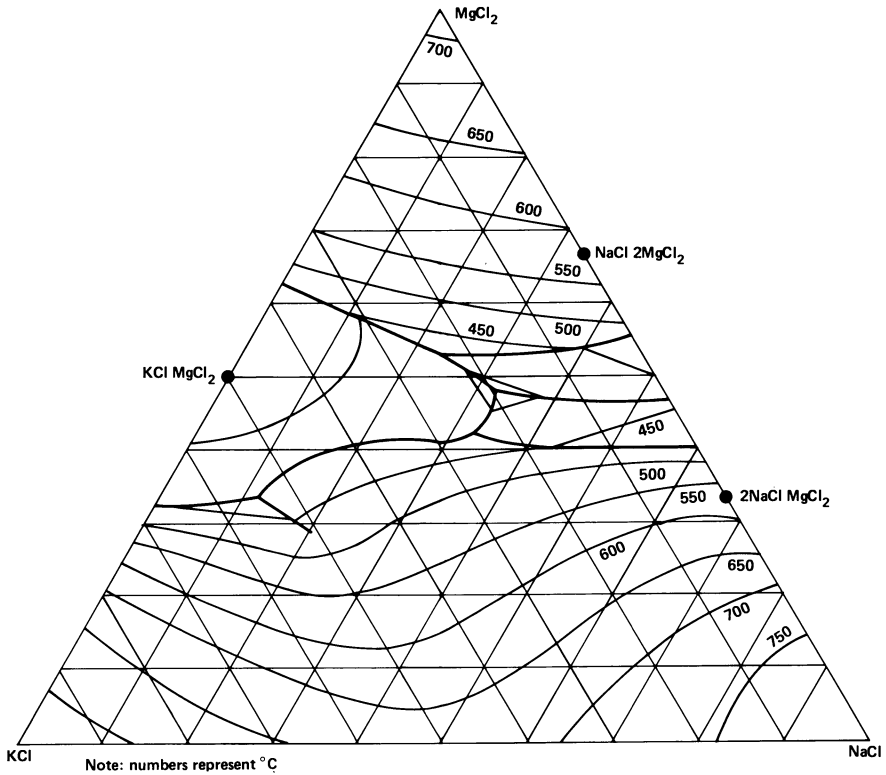


Figure 4. Ternary Phase Diagram for the NaCl-CaCl₂-MgCl₂ System.

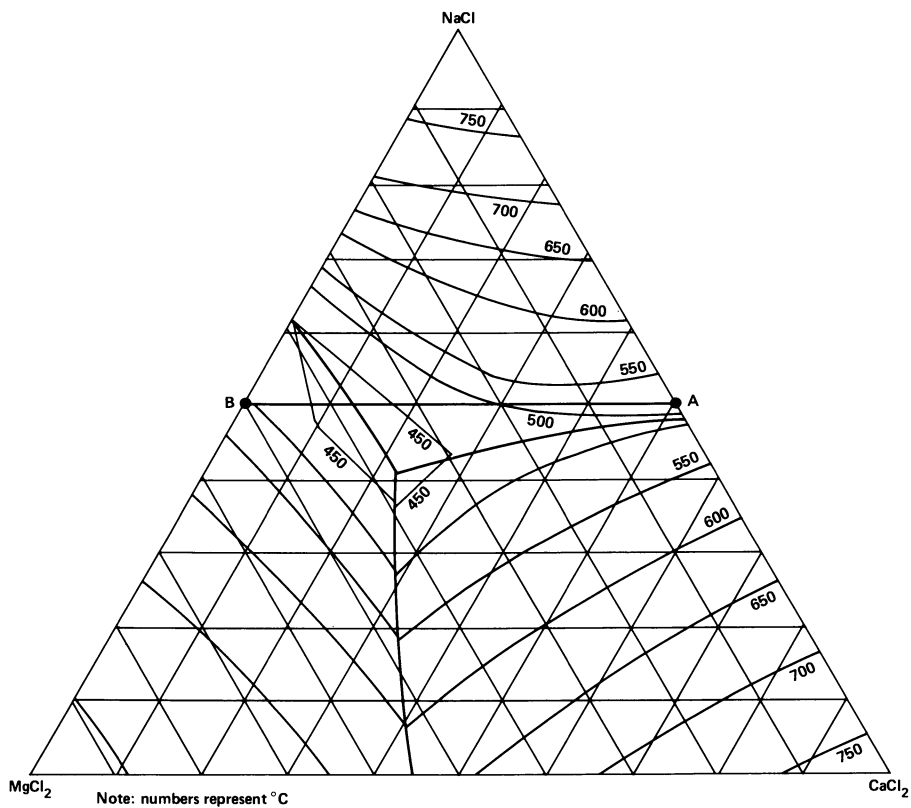


Figure 5. Ternary Phase Diagram for the NaCl-CaCl₂-MgCl₂ System.

The NaCl-KCl eutectic is used when the pregnant extraction salt is to be processed by aqueous recovery (this is the salt currently used at Rocky Flats because calcium follows americium in the present aqueous recovery process). The NaCl-CaCl₂ system is used when the salt is processed by pyrochemical means to recover the americium and residual plutonium. When the pyrochemical recovery technique is used, the NaCl-CaCl₂-MgCl₂ salt is contacted with liquid calcium metal at approximately 850°C in a batch extractor. The calcium reduces AmCl₃, PuCl₃, and MgCl₂ to form a 50/50 mole % NaCl-CaCl₂ salt phase and a molten Am-Pu-Mg-Ca alloy which is immiscible in the above salt⁽¹⁰⁾. After cooling, the metal phase is cleaved away from the salt phase and the salt phase is analyzed. Little, if any, Am or Pu remains in the salt phase and the salt residues can be discarded to waste. Metal recovery begins by evaporating magnesium and calcium from the residual metal button at about 800°C in vacuum. The americium can then be distilled away from the plutonium in a vacuum still operated at 1200°C, using yttria ceramic vessels to contain the molten metal fraction. The bottoms fraction contains the plutonium which is recycled back into the main plutonium stream.

Knighton⁽¹⁰⁾ has calculated the values of K_d for both americium and plutonium in both of the salt diluents mentioned above for varying concentrations of magnesium chloride. These calculations were performed by using the chemical equilibrium values for Pu with 100% MgCl₂ and an empirical equation based on equilibrium values and measured K_d values for salts in the midrange and low end of the curves. The low end Pu data is from the work of Schweikhardt⁽¹¹⁾. Knighton's data is presented in graphic form for both of these salt systems in Figures 6 and 7.

Knighton has also constructed graphs for the relationship between salt-to-metal ratio for the extraction versus the concentration of magnesium chloride in the salt. The graphs for both the NaCl-KCl-MgCl₂ and NaCl-CaCl₂ MgCl₂ salt systems are shown in Figures 8 and 9. These graphs are for two stage counter-current systems with contour lines at 5% intervals from 80 to 99% americium removal efficiencies. Such graphs enable the operators to obtain almost any extraction constant required to lower the americium content to some acceptable personnel exposure value.

Figure 10 shows in graphic form the utility of molten salt extractions for americium removal in one, two, and three stage extractions for various salt-to-metal extraction feeds. This graph demonstrates the impressive power of molten salt extraction systems for purification of plutonium from americium and related rare earth elements.

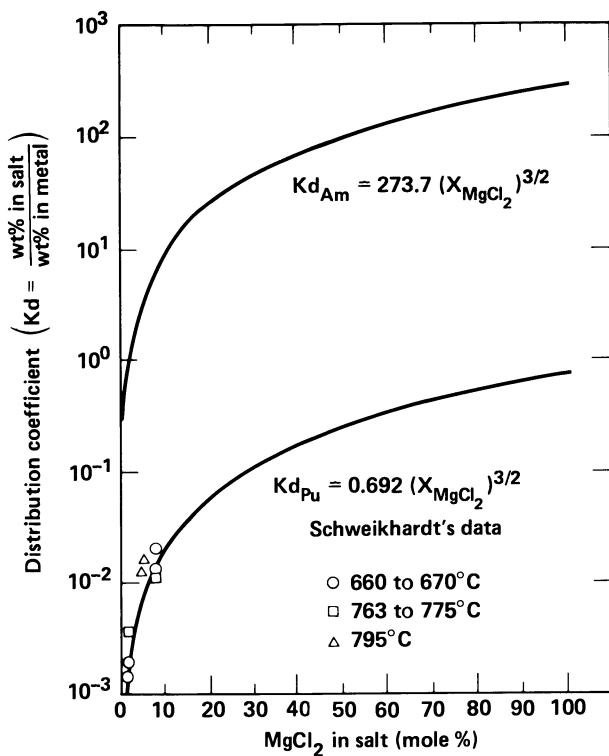


Figure 6. Distribution Coefficients for Americium and Plutonium Extraction vs MgCl₂ Concentration in the NaCl-KCl-MgCl₂ Salt System.

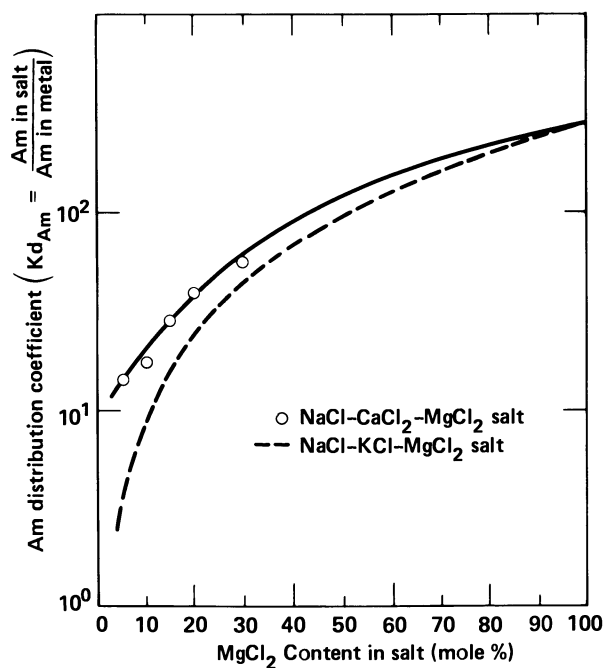


Figure 7. Distribution Coefficient for Americium Extraction vs $MgCl_2$ Concentration in the NaCl-KCl- $MgCl_2$ and NaCl-CaCl₂- $MgCl_2$ Salt Systems.

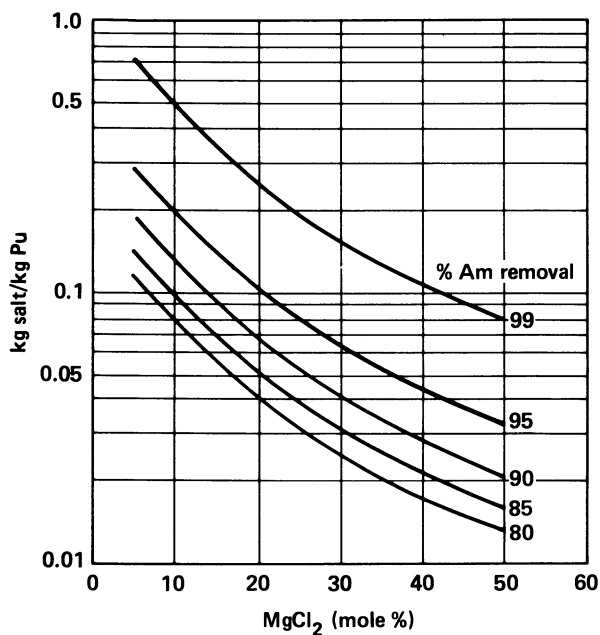


Figure 8. Yield Curves for Salt-To-Pu Ratio vs Concentration of MgCl₂ for Extraction of Americium From NaCl-CaCl₂-MgCl₂ Salt Using 2-Stage Counter-Current Extraction

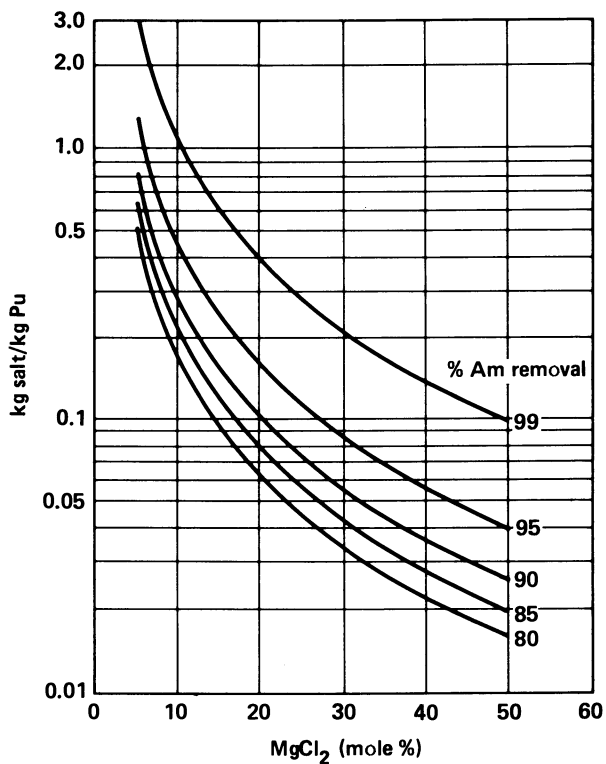


Figure 9. Yield Curves for Salt-To-Pu Ratio vs Concentration of MgCl₂ for Extraction of Americium From NaCl-KCl-MgCl₂ Salt Using 2-Stage Counter-Current Extraction.

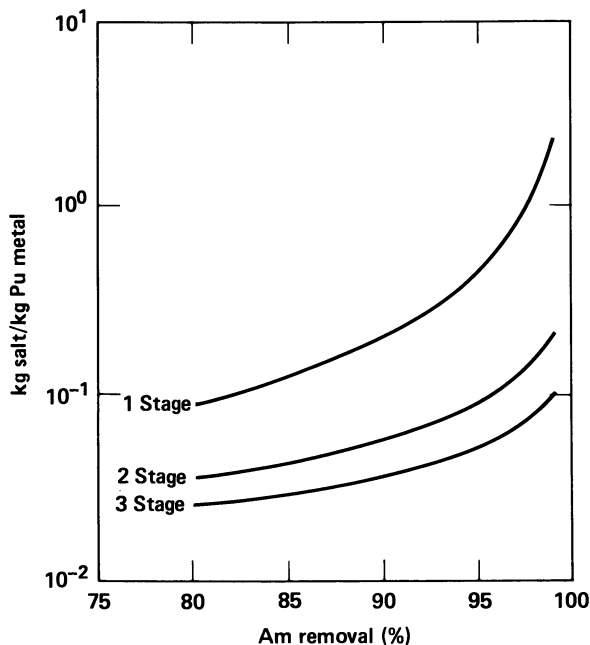


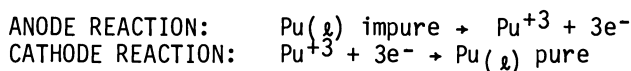
Figure 10. Yield Contours for Americium Extraction vs s/m Ratio for 1, 2, and 3-Stage Counter-Current Extraction. Salt Composition: 30 m/o $MgCl_2$, 35 m/o $NaCl$, 35 m/o KCl .

Plutonium Electrorefining

The first publication related to plutonium electrochemistry dates back to Manhattan Project work at Los Alamos when Kolodney⁽¹²⁾ reported making small amounts of metal by electrolysis. Leary et-al⁽¹³⁾ published an article in the Geneva Proceedings in 1958 on the pyrochemical recovery of plutonium from metallic reactor fuels, and in 1960 Mullins et-al⁽¹⁴⁾ reported a 300 gram scale electrorefining process for making high purity metal. Improvements continued, and in 1962 Mullins et-al⁽¹⁵⁾ reported a production process (three kilogram scale) for routine production of >99.9% pure metal. Recent developments at Los Alamos have expanded the capacity of the electrorefining cells to about six kilograms per batch, with a cycle time of five days⁽¹⁶⁾.

The principle of the electrorefining process is basically simple: plutonium is oxidized at a liquid metal anode containing impure metal feed and the resulting Pu^{+3} ions are transported through molten salt to a cathode where pure metal is produced. The transport salt is usually eutectic NaCl-KCl but NaCl-CaCl₂ can also be used. As liquid plutonium metal builds up on the cathode it drips off into an annular channel surrounding the anode cup where it coalesces into a pool of metal and is recovered after the cell is cooled. The entire chemical process is performed in a molten salt bath.

A schematic representation of an electrorefining cell is shown in Figure 11. The basic chemistry of the electrorefining technique is as follows:



PuCl_3 must be added to the cell prior to operation to maintain a high concentration of Pu^{+3} ions in the salt phase. This PuCl_3 also acts as a salt-phase buffer to prevent dissolution of trace impurities in the metal feed by forcing the anode equilibrium to favor production (retention) of trace impurities as metals, instead of permitting oxidation of the impurities to ions. Metallic impurities in the feed fall into two classes, those more electropositive and those less electropositive than plutonium. Since the cell is operated at temperatures above the melting point of all the feed components, and both the liquid anode and salt are well mixed by a mechanical stirrer, chemical equilibrium is established between all impurities and the plutonium in the salt even before current is applied to the cell. Thus, impurities more electropositive than the liquid plutonium anode will be oxidized by Pu^{+3} and be taken up by the salt phase, while impurities in the electrolyte salt less electropositive than plutonium will be reduced by plutonium metal and be collected in the anode.

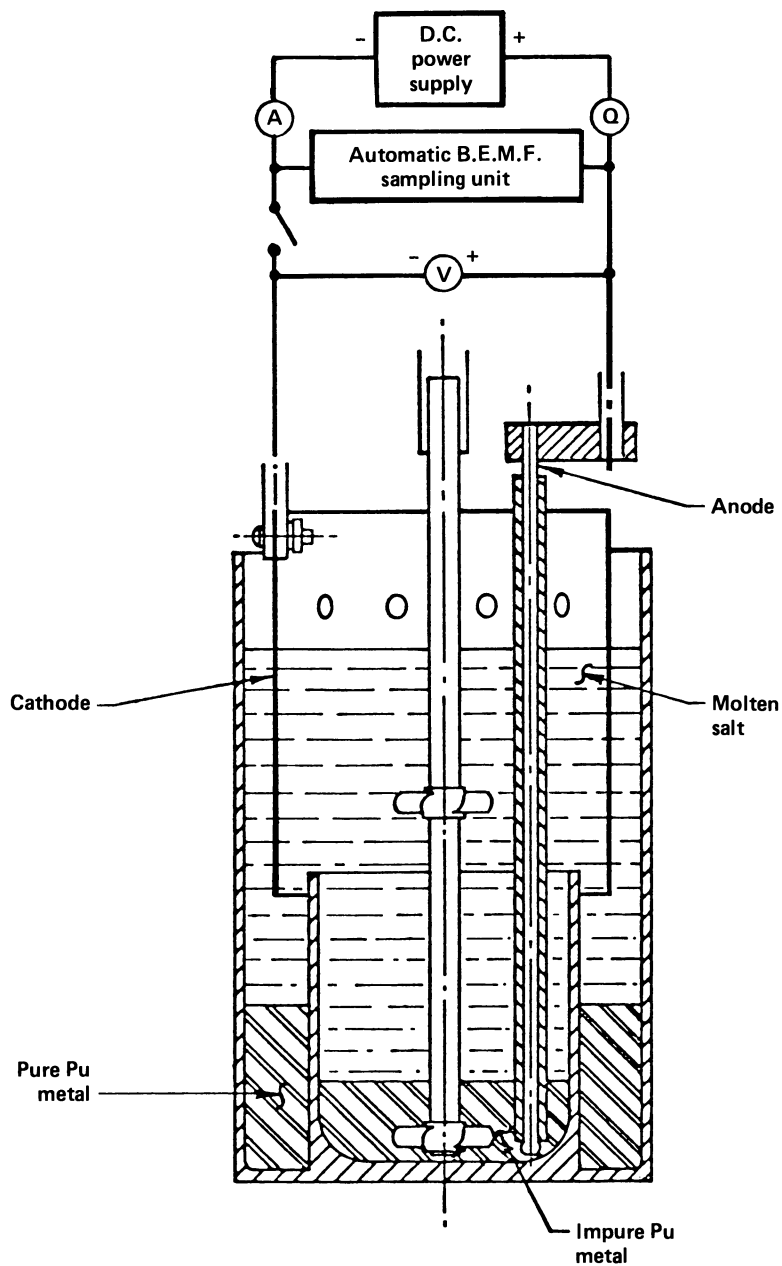
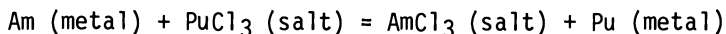


Figure 11. Schematic of Electrorefining Cell Showing Major Features.

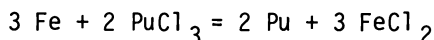
Those impurities less electropositive than plutonium that are already present in the molten anode will remain in the anode. The extent of these reactions will be determined by the reaction free energy and concentration for each of the impurities in the molten anode/electrolyte salt system. Americium can be used as an example of a very electropositive impurity:



When current is passed through the cell, the concentration of impurities in the product obtained at the cathode will depend upon their concentration in the salt. If equilibrium conditions exist in the cell the following equation applies:

$$\frac{(\text{Am})}{(\text{Pu})} \text{ metal product} = \frac{1}{K} \frac{(\text{AmCl}_3)}{(\text{PuCl}_3)}$$

Where the parenthesis refer to the chemical activities of the reactants and K is the equilibrium constant for the previous equation. Similar considerations apply to the oxidation of less electropositive impurities from the anode when a current is passed through the cell. Thus, for the case of iron impurity in the anode, the reaction



favors the production of iron metal instead of ferrous ion since the free energy change for the reaction is +96 kilocalories (+96 KCal is equivalent to an equilibrium constant of 1×10^{-21} at 1000 K).

The composition of the salt electrolyte in the cell does not change during the electrorefining cycle so long as the driving potential of the cell is kept below the decomposition voltage of the electrolyte. The following table gives the decomposition potential of normal components of the electrolyte:

<u>Chloride salt</u>	<u>Decomposition Potential at 800° C</u>
CaCl ₂	3.32
KCl	3.44
NaCl	3.24
MgCl ₂	2.46
PuCl ₃	2.40

Since the energy required to strip the electrons from plutonium metal at the anode is exactly matched by the energy returned at the cathode, the potential required by the process is only that required to overcome time invariant (I^2R) losses in the cell circuit, and time dependent resistance (electrode polarization).

Polarization of the anode occurs after most of the plutonium is transferred across the cell and impurities constitute a large percentage of the anode. The reason for this can be demonstrated by using the case of delta plutonium alloy feed. Delta alloy contains ~ 1 wt % gallium. The normal operating temperature of the electrorefining cell is 750°C and at this temperature the delta alloy melts to form a liquid phase. The phase diagram for Pu-Ga is shown in Figure 12.

As electrorefining proceeds, plutonium is selectively removed from the anode and the composition of the anode becomes enriched in gallium. At approximately 18 mole percent gallium, the lower density eta phase Pu begins to form (at 750°C) and a mixture of solid eta phase and liquid is formed at the anode surface (eta phase floats on the liquid plutonium phase). The back-EMF of the cell will gradually increase as the eta phase is formed. Vigorous stirring will expose liquid plutonium and permit oxidation to proceed at the anode surface, but at 25 mole % gallium the anode will solidify. Continued operation of the cell will now oxidize gallium in the ratio of the composition of the solid anode.

To prevent the passage of impurities, the back-EMF of the cell is monitored at frequent intervals. The current to the electrodes is turned off, and the voltage of the cell is measured. When the back-EMF reaches a predetermined value, operation of the cell is terminated, and the cell is allowed to cool. The cathode product, which consists of very pure plutonium metal, is recovered from the solidified salt mass by breaking the ceramic vessel and brushing the ring free of adhering salt. The product ring typically amounts to about 85% of the original mass of the anode feed metal. The impurity level of the cathode product from electrorefining is usually below normal spectroscopic detectability levels if the cell is run at anode current densities of 0.60 amps per sq. cm. or less.

The level of purification that can be achieved from impurities by the electrorefining process is directly related to the free energy of formation of the chloride salt of each impurity present in the feed metal, as discussed above. Since both the lanthanide and actinide chlorides have very negative free energies of formation, the purification factors achievable for these elements by plutonium electrorefining is considerably lower than for most common impurities. For example, the typical purification factor obtained for americium is approximately 9, and the factor for neptunium is about 3. The decontamination from the lanthanides and americium is easily accomplished by the magnesium chloride based molten salt extraction described in the previous section. Neptunium is a relatively rare contaminant as it grows into plutonium as the daughter of americium-241 (453 year half-life alpha decay). Neptunium is separated with high efficiency in the initial chemistry used to isolate plutonium from irradiated uranium. If additional purification is necessary, neptunium can be extracted from plutonium by the "Salt Transport Method" in a compatible pyrochemical process.

Publication Date: May 19, 1983 | doi: 10.1021/bk-1983-0216.ch025

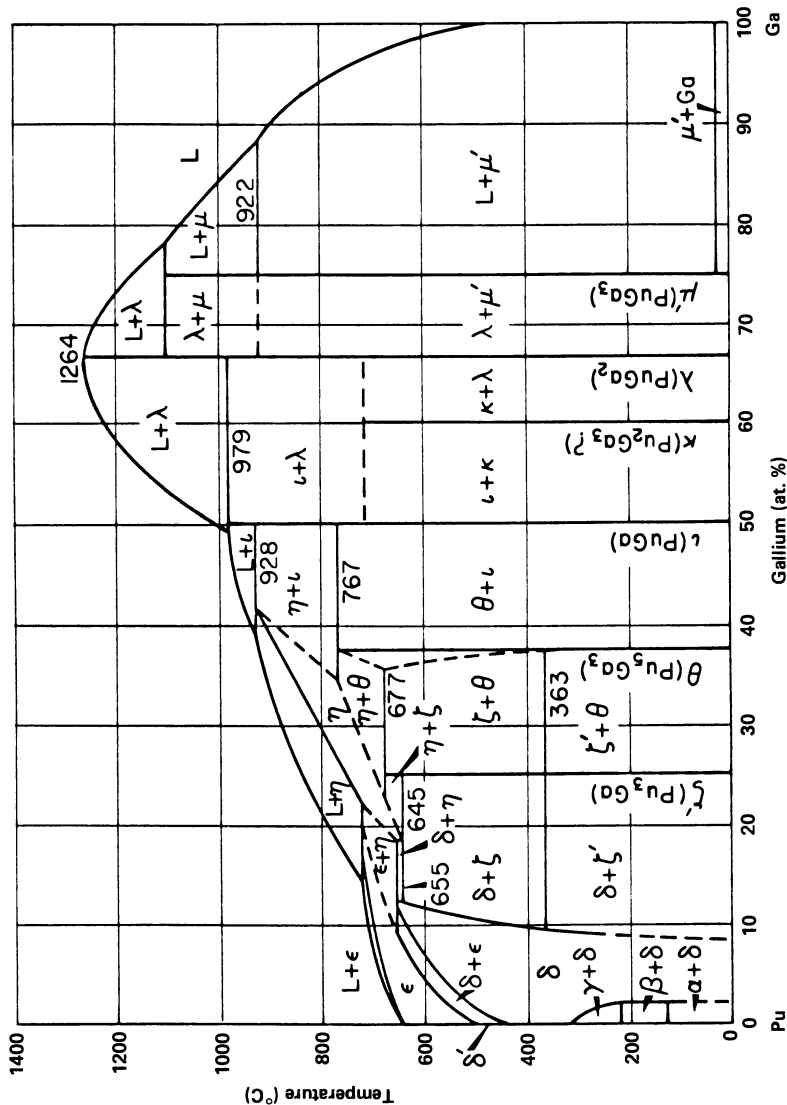


Figure 12. The Gallium-Plutonium Phase Diagram.

The following table, excerpted from a Los Alamos production report, demonstrates typical feed and product purities achievable by the electrorefining method:

Comparison of Purities of Oxide Feed, DOR Metal, and ER Metal Product, Run PMR 162*

Impurity levels reported as micrograms per gram of sample.

<u>Element</u>	<u>Oxide-Feed</u>	<u>DOR Metal Product</u>	<u>ER Product</u>
B	>150	>150	<1
Na	>233	10	6
Mg	>375	300	1
Al	500	500	<5
Si	283	1400	<5
K	>100	50	15
Ca	>750	100	<3
Ti	32	50	<5
Cr	317	360	<5
Mn	20	10	<1
Fe	>1500	>1500	<5
N	880	940	<5
Cu	24	7	<1
Y	>180	25	<25
Zr	>450	500	<100
Nb	85	60	<10
Mo	121	200	<3
Ta	>500	>500	<100
W	>500	>500	100
Pb	38	< 5	<5
Th	421	270	30
U	656	20	7
C	78	790	25
Am	655	795	219
Pu	82.23 (93.29% pure)	98.47%	99.96%

*From LA-9154-MS

The anode residues must be chemically processed to recover the plutonium remaining in the residues. This may amount to about 10% of the feed mass if delta alloy is the feed metal. Either aqueous or pyrochemical processes may be used for anode recovery. One pyrochemical process used for recovery utilizes oxidation of the plutonium with zinc chloride to form plutonium chloride salt, followed by calcium reduction of the PuCl_3 contained in the salt phase to produce pure plutonium metal (the impurities follow the zinc metal obtained from the oxidation reaction and are discarded to waste). Impurities more stable than calcium chloride remain in the salt phase and are also

discarded to waste. This process, known as "Pyroredox" is still under development and is not yet available as a production method.

The electrolyte salt must be processed to recover the ionic plutonium originally added to the cell. This can be done by aqueous chemistry, typically by dissolution in a dilute sodium hydroxide solution with recovery of the contained plutonium as $\text{Pu}(\text{OH})_3$, or by pyrochemical techniques. The usual pyrochemical method is to contact the molten electrolyte salt with molten calcium, thereby reducing any PuCl_3 to plutonium metal which is immiscible in the salt phase. The extraction crucible is maintained above the melting point of the contained salts to permit any fine droplets of plutonium in the salt to coalesce with the pool of metal formed beneath the salt phase. If the original ER electrolyte salt was eutectic NaCl-KCl a third "black salt" phase will be formed between the stripped electrolyte salt and the solidified metal button. This dark-blue phase can contain 10 wt. % of the plutonium originally present in the electrolyte salt; plutonium in this phase can be recovered by an additional calcium extraction step⁽¹⁷⁾.

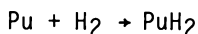
Recent work by Coops et al⁽¹⁸⁾ has suggested that "black salt" is a dispersion of K_3PuCl_6 in a matrix of KCl and NaCl . K_3PuCl_6 is a highly insoluble complex salt that solidifies at 621°C from $\text{PuCl}_3\text{-KCl}$ mixtures, and contains 42% plutonium by weight. This salt apparently can form during the extraction and trap droplets of plutonium metal in a viscous salt phase. K_3PuCl_6 also appears to be more thermodynamically stable than either PuCl_3 or NaCl ; for this reason consideration is now being given to the utilization of either CaCl_2 or NaCl-CaCl_2 as the electrolyte salt for ER instead of NaCl-KCl .

The basic electrorefining process is now being used on a production scale for the purification of non-specification plutonium metal. The technology is sufficiently well developed to permit 24-hour unattended operation of the electrorefining cells, and the quality of the product metal is highly consistent. This technology is rapidly replacing aqueous chemistry for plutonium metal purification.

Metallic Scrap Recycle

The reaction between plutonium metal and hydrogen is exothermic and proceeds quite satisfactorily at room temperature in an atmosphere of pure hydrogen. The reaction is fully reversible and plutonium can be recovered by pumping off the hydrogen in a suitable vacuum system. Plutonium hydride that is formed below 250°C is granular and friable; the particle size is very fine and the hydride does not adhere to the substrate surface. Above 250°C the product is a more adherent flaky scale. The rate of reaction, and hence the temperature of the reaction, is easily controlled by varying the hydrogen pressure in the reaction chamber. Since PuH_2 decomposes readily above

600°C, the rate of reaction tends to be self limiting at hydrogen pressures up to 10 torr. The hydriding technique is used to recover metallic plutonium residues clinging to the walls of ceramic crucibles, and can also be used to recover machining scrap if the feed is free of lubricants or oxides. Mulford and Sturdy⁽¹⁴⁾ have found the heat of formation for the reaction



to be -37.4 ± 1.2 KCal per mole, and observed the decomposition of PuH₂ between 400-800°C to follow the equation:

$$\log P_{\text{mm}} = (10.01 \pm 0.32) - (8165 \pm 263)/T$$

At 650°C the decomposition pressure of PuH₂ is 14.7 Torr.

The very chemically reactive plutonium hydride is usually decomposed in a vacuum-tight furnace capable of attaining a temperature of 700°C. Plutonium hydride that is decomposed under vacuum at temperatures below 400°C forms a very fine (<20 μ) metallic powder; above 500°C the powder begins to sinter into a porous frit which melts at 640°C to form a consolidated metal ingot. This metal typically contains significant oxide slag but is suitable for feed to either molten salt extraction or electrorefining.

The advantage of hydride recovery is its ability to recover a large fraction of the scrap in metallic form. This method therefore has a major economic advantage over chemical recycle and subsequent reduction to metal. It is just beginning to be used as a production aid for metallic scrap recovery.

Acknowledgment

The work presented in this article represents the combined effort of a large number of dedicated scientific workers at many Department of Energy facilities located throughout the United States. Particular credit must be given to the staff at Los Alamos, Argonne, Rocky Flats, Livermore, and Hanford. Without their diligent effort the pyrochemical process technologies described above would not have been developed.

This work was performed under the auspices of the U.S. Department of Energy by Lawrence Livermore National Laboratory under contract No. W-7405-Eng-48.

Literature Cited

1. Wade, Warren Z.; and Wolf T.; "Preparation of Massive Plutonium Metal Directly from its Oxides", J. Nucl. Sci. and Technol. 6 No. 7, 402-407 (1969).

2. Felt, R.E.; "A Pyrochemical Process for the Reduction of Plutonium Dioxide to Metal", Atlantic Richfield Hanford Co. Report ARH-1198, July 1969.
3. Moseley, J.D.; Strickland, W.R.; Domning, W.D.; Auge, R.G.; and Brown, J.C.; unpublished Rocky Flats Plant data; also RFP-1472 (1970) pp. 13-14.
4. Mullins, L.J.; and Foxx, C.L.; "Direct reduction of $^{238}\text{PuO}_2$ to Metal", Los Alamos National Laboratory Report LA-9073 (1982).
5. Mullins, L.J.; Christensen, D.C.; Babcock, B.R.; "Fused Salt Processing of Impure Plutonium Dioxide to High Purity Metal", Los Alamos Nat. Lab. Report LA-9154-MS; also Symposium on Actinide Recovery from Waste and Low Grade Sources, ACS, New York City August 23-28, 1981 (in press).
6. Wenz, D.A.; Johnson, I.; Wolson, R.D.; "CaCl₂-rich Region of the CaCl₂-CaF₂-CaO System", J. Chem. Eng. Data, 14, 2, 250-252 (1969).
7. Mullins, L.J.; Leary, J.A.; Morgan, A.E.; Maraman, W.J.; "Plutonium Electrowinning", Los Alamos Nat. Lab. report LA-2666 (1962).
8. Knighton, J.B.; Steunenberg, R.K.; "Distribution of Transuranium Elements Between Magnesium Chloride and Zinc-Magnesium Alloy", J. of Inorganic and Nuc. Chem. 27 p.p. 1457-1462 (1965).
9. Long, J.L.; Perry, C.C.; "The Molten Salt Extraction of Americium from Plutonium Metal", Nuc. Metal 15 p. 385 (1969).
10. Knighton, J.B.; Auge, R.G.; Berry, J.W.; "Molten Salt Extraction of Americium from Molten Plutonium Metal", Rocky Flats Plant report RFP-2365 (1976).
11. Schweikhardt, R.D.; "Metal-Salt Reactions in Molten Systems of Plutonium Metal and NaCl, NaCl-KCl, and NaCl-KCl-MgCl₂" thesis, Univ. of Denver, August 1966.
12. Kolodney, M.; "Production of Plutonium by Electrolysis", Los Alamos Nat. Lab. report LA-148.

13. Leary, J.A. et-al; "Pyrometallurgical Purification of Plutonium Reactor Fuels", Second Internat. Conf. on Peaceful Uses of Atomic Energy, 17, United Nations, Geneva (1958) p. 376.
14. Mullins, L.J.; Leary, J.A.; Bjorkland, C.W.; "Large Scale Preparation of High Purity Plutonium Metal by Electro-refining", Los Alamos Nat. Lab. report LAMS-2441 (1960).
15. Mullins, L.J.; Leary, J.A.; "Fused Salt Electrorefining of Molten Plutonium by the LAMEX Process", I and EC Process Design and Development, Vol. 4, Pg. 394, October 1965.
16. Mullins, L.J.; Morgan, A.M.; Apgar, S.A. III; and Christensen, D.C.; "Six-Kilogram Scale Electrorefining of Plutonium Metal", Los Alamos National Laboratory Report LA-9469-MS (1982).
17. Christensen, D.C.; Mullins, L.J.; "Salt Stripping, a Pyrochemical Approach to the Recovery of Plutonium Electrorefining Salt Residues", Los Alamos Nat. Lab report LA-9464-MS (1982).
18. Coops, M.S.; Bergin, J.B.; Wallace, P.L.; Work in Progress at Lawrence Livermore National Laboratory; to be published.
19. Mulford, R.N.R.; Sturdy, G.E.; "The Plutonium - Hydrogen System, I, Plutonium Dihydride and Dideuteride", J. Amer. Chem. Soc. 77:3449 (1955).
20. Oetting, F. L.; "The Chemical Thermodynamic Properties of Plutonium Compounds", Chemical Reviews, 67, 261 (1967).
21. Wicks, C. E.; and Block, F. E.; "Thermodynamic Properties of 65 Elements - Their Oxides, Halides, Carbides, and Nitrides", Bureau of Mines, Bulletin 605, 1963.

RECEIVED January 7, 1983

Plutonium Metal Production and Purification at Los Alamos

D. C. CHRISTENSEN and L. J. MULLINS

Los Alamos National Laboratory, Material Science and Technology Division,
Los Alamos, NM 87545

The production of plutonium metal by both fluoride and oxide reduction is well established at Los Alamos. The subsequent purification of this metal by electrorefining is now being performed in production on a 6-kg batch scale. The objective is the production of high-purity plutonium metal.

Recent process development efforts have been devoted to more expeditious and less costly pyrochemical reprocessing of residues created by the metal preparation and purification process. We intend to establish an internal recycle which yields either reusable or discardable residues and recovers all plutonium for feed to the electrorefining purification system. This internal recycle is to be performed in a more timely and less costly operation than in the present reprocessing mode.

The Los Alamos National Laboratory has had a very active program for the production of high purity plutonium metal for both Laboratory and national needs for many years using pyrochemical techniques.

Plutonium pyrochemistry at Los Alamos dates back to 1956. During the period 1956-1962, the Plutonium Chemistry and Metallurgy group was involved in a program on the pyrochemical processing of Plutonium Fast Breeder Reactor Fuels for the Los Alamos Molten Plutonium Reactor Experiment (LAMPRE). Processes such as oxidative slagging, halide slagging, pyroredox, liquation, and electrorefining were spanned in this period. These processes were turned toward national defense programs in 1964. In 1976 the direct oxide reduction (DOR) was developed in support of the artificial heart, plutonium-238 program. In 1978, the DOR process was adopted for use in plutonium-239 programs. This operation gave us two principal processes for making plutonium metal.

0097-6156/83/0216-0409\$06.75/0
© 1983 American Chemical Society

1. The conventional PuF_4 reduction process.
2. Direct oxide reduction process. (DOR).

In addition there are two principle metal purification processes:

1. Electrorefining (ER).
2. Halide Slagging or Molten Salt Extraction (MSE).

Beginning in 1978, the above four processes were put into production in the new TA-55 building at Los Alamos. The source of plutonium for Los Alamos needs was both plutonium dioxide from aqueous recovery processes and metal from fabrication scrap. In 1980, Los Alamos embarked on a program to increase the output of pure metal.¹ Pyrochemical processes were selected as the candidate operations to rapidly and cost effectively achieve the increased throughput. This type of processing offers the potential of large cost reduction over traditional aqueous chemical processes for a number of reasons.

- Plutonium is processed as a liquid, in highly compact equipment, and therefore expensive floor space is conserved.
- Very few steps are needed in order to achieve highly purified products (Figure 1).
- Primary waste generation is small because of the high density nature of the fused salt operations. Nearly all primary waste residues show excellent potential for recycle. (The present main processing sequence for plutonium does not include significant reagent and residue recycle).
- Secondary waste from the processing of waste residue materials is minimal.
- The turnaround of plutonium in residues is very rapid.

The expanded throughput resulted in a commensurate increase in primary residue generation. The increased production of plutonium metal was achieved very easily in existing floor space because of the compact nature of equipment, but the increased needs for aqueous residue handling could not be met with existing floor space. As a result, the residues were stored for future processing. In order to support the process scale-up, R&D efforts have been involved with developing cost-effective, high-throughput pyrochemical processes for handling process materials and residues. In addition, we are evaluating problems in the areas of process and equipment design have been evaluated. Most recent efforts are concerned with the recovery and recycle of plutonium values in the residues.

This document will summarize our present main production sequence and discuss how it was arrived at. It will then discuss the status of our present recycle of plutonium values in residues. Third, it will discuss our proposed recycle of all plutonium in residues. Finally, it will discuss our goal of a fully integrated process sequence where plutonium and salt residues are recycled through the production sequence.

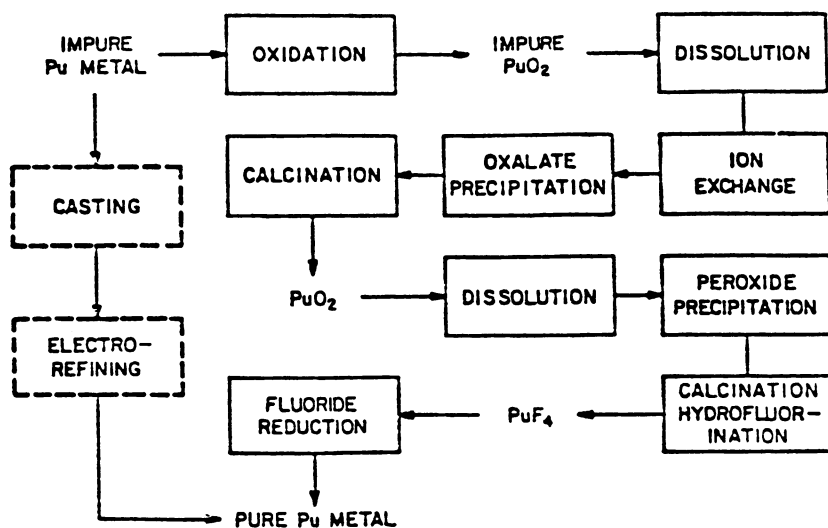
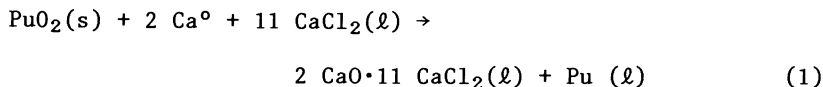


Figure 1. Pyrochemical vs. aqueous flowsheet for metal purification.

Main Process Sequence For Conversion Of Plutonia To High-Purity Metal

A. Process Schematic. A schematic of the main process sequence for the conversion of plutonia scrap to high-purity metal is shown in Figure 2. Plutonia scrap is fed to both the direct oxide reduction (DOR) process and the plutonium tetrafluoride production/reduction process.

Direct Oxide Reduction. In DOR, plutonia is reduced with calcium metal to form plutonium metal and calcium oxide.^{2,3} The reaction takes place in a CaCl₂ solvent which dissolves the calcium oxide and allows the plutonium metal to coalesce in the bottom of the crucible.



The reactants are loaded in a magnesia crucible and heated by a resistance furnace to 800°C (Figure 3). Once the CaCl₂ is molten, a tantalum stirrer and a Ta-Ni thermocouple sheath are lowered into the melt. While stirring, the reaction is monitored with a thermocouple. Once the reaction is complete, the stirrer and thermocouple well are retracted and the melt is allowed to cool. Figure 4 shows a typical DOR product and salt/crucible residue. A typical product button weighs 600 g and the process yield is >99%. Essentially no purification takes place in the reduction step, meaning that the product button is no purer than the feed.

Plutonium Tetrafluoride Production and Reduction. In PuF₄ production/reduction, plutonia is fed first to an HF reaction furnace where the PuO₂ is converted to PuF₄. The PuF₄ is reacted with calcium metal in the presence of iodine to form plutonium metal, CaF₂, and CaI₂.^{2,4,5,6} Calcium and iodine react first to initiate the plutonium reaction. The PuF₄ and calcium react to form plutonium metal and CaF₂. Both the iodine and PuF₄ reactions with calcium are very exothermic, providing enough heat to melt the waste slag and allow the plutonium metal to coalesce in the bottom of the crucible.

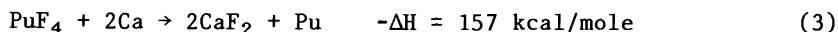
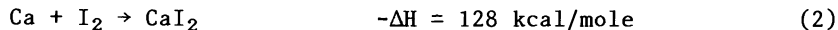


Figure 5 shows a typical PuF₄ product button with the slag and crucible residue. A typical button weighs 1250 g and the yield is 96-98%. Essentially no purification takes place in the reduction step, meaning that the product button is no purer than the feed fluoride.

Molten Salt Extraction. The metal from DOR and PuF₄ reduction is impure and proceeds to the next step in the process sequence

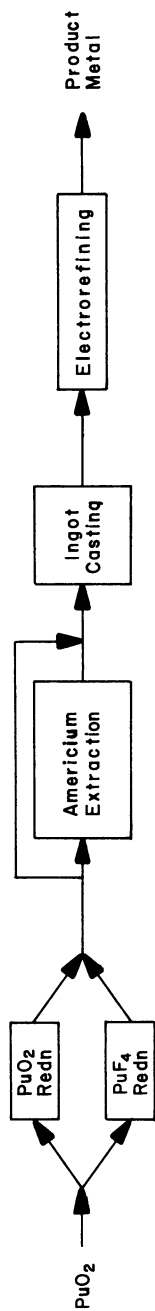


Figure 2. Main production sequence.

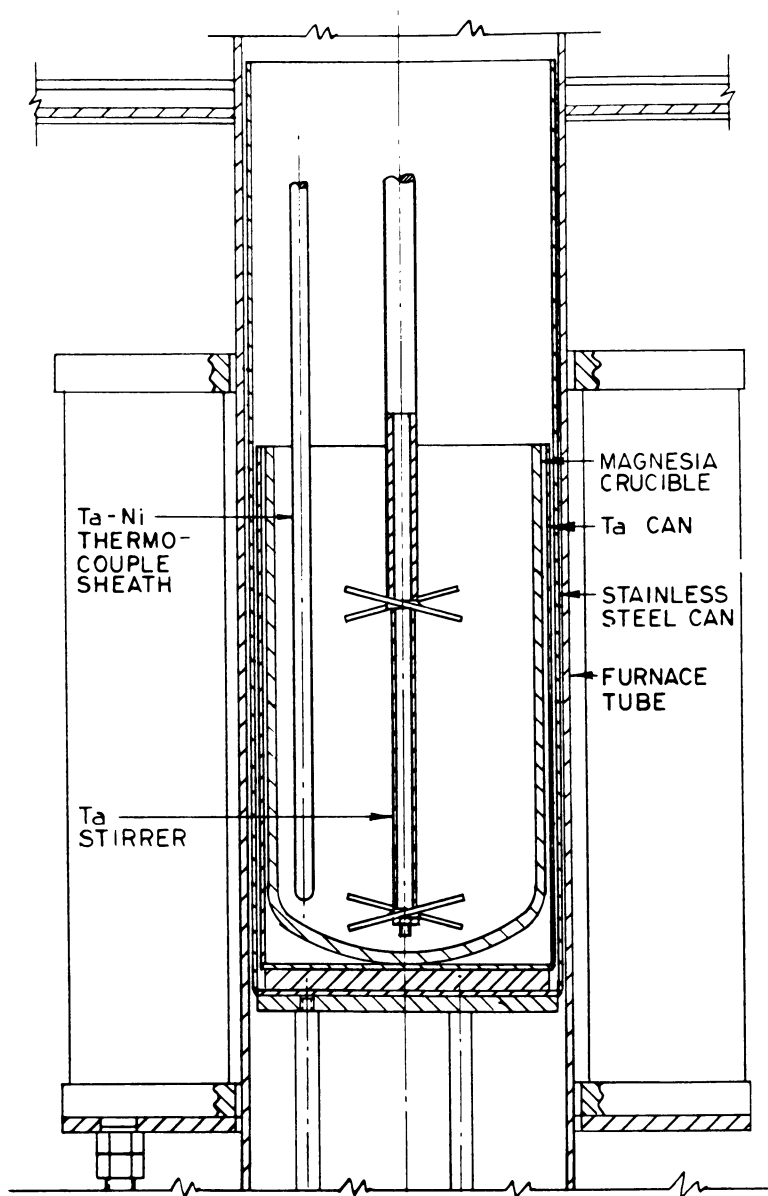


Figure 3. Direct oxide reduction equipment.

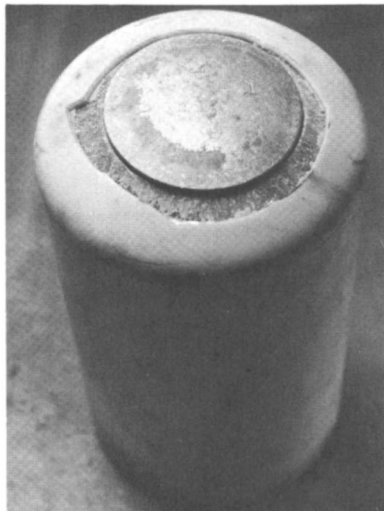


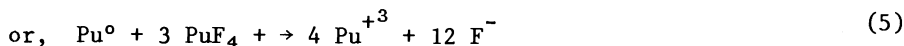
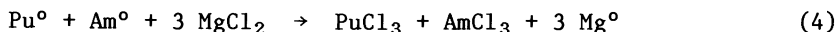
Figure 4. Direct oxide reduction metal product with residues.



Figure 5. Plutonium tetrafluoride reduction slag and product metal.

Americium Extraction (more commonly referred to as Molten Salt Ex- or MSE). This process is specifically designed to reduce the americium content of the plutonium metal. (Am^{241} spontaneously grows into plutonium as a result of Pu^{241} decay.) When the impure metal contains more than 1000 ppm of americium, it is run through the MSE process. Otherwise, it bypasses the MSE step and proceeds directly to electrorefining.

The MSE process was first reported in Reference 7 as the halide or chloride slagging process. It was later optimized and developed into a major production process by workers at the Rocky Flats Plant.⁸ In our process, the feed metal is placed in a magnesia crucible as shown in Figure 3. The extraction procedure is identical to the DOR procedure except that the stirring cycle is 30 minutes instead of only a few minutes. An equal molar $\text{KCl}\cdot\text{NaCl}$ is used as a bulk matrix for the americium reaction. The oxidizing agent typically used is MgCl_2 , although PuF_4 has been used extensively at Los Alamos. The reactions are as follows:



The extent of the first reaction is about 67%, which means that some of the MgCl_2 remains in the bulk salt. In a typical 4.5-kg run containing 3000 ppm americium, 90% of the americium is oxidized at the expense of approximately 100 g plutonium. A typical product weighs 4400 g and contains 98% of the feed plutonium.

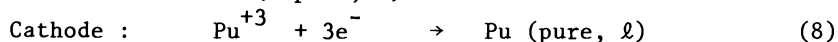
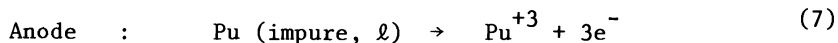
Ingot Casting. After the extraction of americium from the impure metal, the plutonium metal must be put into a shape which is compatible with the electrorefining cell. This requires alloying and casting the metal into a cylindrical ingot shape, hence ingot casting.

The shape of the ingot is a 2 7/8" diam. cylinder which is up to 4" long. The quantity of metal needed for electrorefining is 6 kg. Due to nuclear criticality concerns, 6 kg of α phase (or near full density) metal could not be allowed in the cylindrical configuration. (For an explanation of criticality concerns with respect to the 6-kg electrorefining process, see Ref. 1). As a result, the metal is alloyed during the casting phase with gallium in order to change the bulk density from $>19 \text{ g/cm}^3$ down to $<16.5 \text{ g/cm}^3$. This step involves heating the metal buttons under a vacuum to above the metal melting point. The metal is mixed with the gallium and bottom poured from the furnace tube into the mold. A casting residue, or skull, always occurs. This skull contains any light element impurities, oxide films, or high melting contaminants which exist in the impure metal buttons. The casting yield is typically 95%. A typical ingot can be seen in Figure 6.



Figure 6. Impure metal ingot feed for electrorefining.

Plutonium Electrorefining. Plutonium electrorefining principles are summarized in Refs. 1,3,9. Briefly, the process consists of oxidizing plutonium from an impure metal feed at the anode and reducing it to pure metal at the cathode.



The process is done at 740°C in a molten salt consisting of NaCl-KCl-PuCl₃-MgCl₂, under near-equilibrium conditions. Virtually all of the impurities concentrate in the anode. Of the impurities usually present in plutonium, only americium concentrates in the salt.

The process is performed in a double-cupped vitrified, magnesia crucible (Figure 7). The inner cup contains the impure metal ingot. The crucible is placed inside a tantalum safety can and placed inside the furnace tube. The assembly is heated by a resistance furnace. The schematic in Figure 8 shows the cell in operation. Both the impure metal and the molten salt electrolyte are stirred by a vitrified magnesia stirrer. A tungsten rod is suspended in the impure metal pool to serve as the anode rod. The anode rod is electrically insulated from the salt by a magnesia sleeve. A cylindrically shaped sheet of tungsten is suspended in the annular space between the two cups and serves as the cathode.

The molten salt referred to in Figure 8 is an equal molar NaCl·KCl salt. A small amount of MgCl₂ is added to this salt as an oxidizing agent. The MgCl₂ reacts with the impure metal to both charge the salt with Pu⁺³ and to remove some additional americium from the metal (Equations 4 and 6). The actual electrorefining process is accomplished by stirring at 800 RPM and passing a dc current between anode and cathode. Plutonium oxidizes at the anode and reduces back to metal at the cathode. The metal drips off the cathode and into the annular space. Figure 9 shows a typical product ring after break-out. The product yield from a Pu-1wt% Ga alloy is 83%. Approximately 10% of the residual plutonium remains in the anode as a very impure heel. The remaining plutonium (~7%) ends up in the salt either as uncoalesced metal shot or as Pu⁺³ chloride salt.

Present Plutonium Residue Recycle

Process Schematic. A schematic showing our main production sequence and our present plutonium residue recycle streams is seen in Figure 10. The oval-shaped steps, representing the recycle streams, are as follows:

1. Casting Skull Recycle.
2. Slag Recovery.

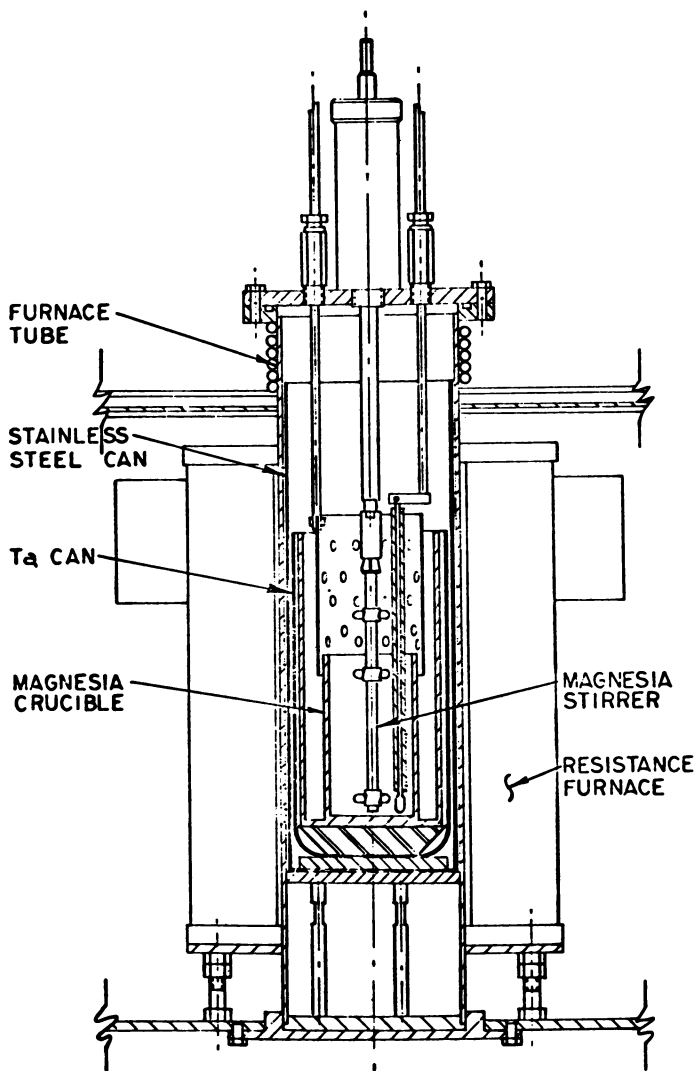


Figure 7. Electrorefining process equipment.

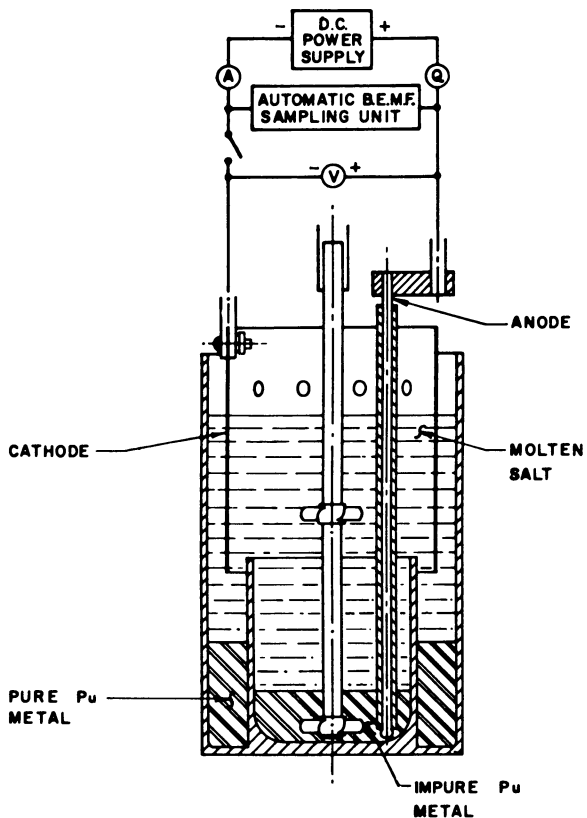


Figure 8. Schematic of electrorefining.



Figure 9. Typical electrorefining product ring.

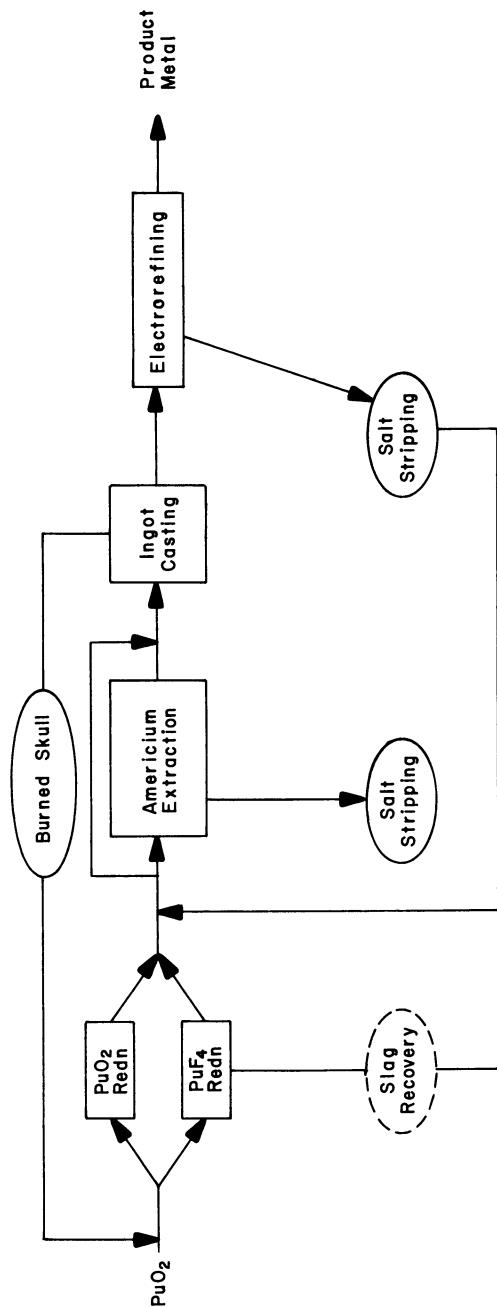


Figure 10. Main production sequence plus present Pu residue recycle.

3. Americium Extraction Salt Recovery.

4. Electrorefining Salt Stripping.

Each of these four streams will be discussed in more depth.

Casting Skull Recycle. After ingot casting, a residue containing up to 5% of the plutonium feed remains behind. Usually the metal buttons fed to the casting operations retain some of the calcium used in the reduction operation, as well as other volatile metals and oxides.

The buttons usually have a film of PuO_2 as a result of exposure to glove-box air. Upon casting, this PuO_2 floats and remains in the skull along with trapped plutonium metal. This portion of the skull is recycled back into the production sequence.

The skull metal and oxide are first completely burned to oxide by heating in air to 400-500°C. The plutonium metal spontaneously burns and is collected as a green PuO_2 powder. This oxide is recycled back as feed for Direct Oxide Reduction. This process is normally 100% efficient with only a small plutonium residue showing up in items such as clean-up rags.

Slag Recovery. An in-depth discussion on the slag recovery process is found in Reference 10.

Periodically, during the PuF_4 reduction process, production misfires occur. The essence of the misfire is that not enough heat is generated during the reduction to melt the CaF_2 by-product. As a result, the plutonium metal remains trapped in the CaF_2 slag and does not flow to the bottom of the crucible and coalesce as a metal button.

In an effort to rapidly recover the plutonium from these residues, a process was developed whereby the CaF_2 slag is dissolved in CaCl_2 at 685°C. The plutonium, which exists either as a finely divided metal fog or as incompletely reduced fluoride salt, is reduced to metal and/or allowed to coalesce as a button in the bottom of the crucible. The process has been demonstrated on slags containing between 250 g and 1000 g of plutonium but it is not restricted to these high-plutonium-bearing residues. The recovery of plutonium in a one-day cycle averages 96% and all of the residues have fallen below our allowable discard limits.

Molten Salt Extraction (MSE) - Salt Recovery. The salt residue from the americium extraction process is made up of NaCl , KCl , MgCl_2 , PuCl_3 , and AmCl_3 . A typical residue weighs approximately 2.0 kg and contains 200 g plutonium, 10-20 g americium, 50 g MgCl_2 with the remaining equimolar NaCl-KCl .

The proposed process will be performed in an MgO crucible at 800°C (Figure 3). A tantalum stirrer will be used to mix the reactants. The salt recovery operation will consist of melting the salt and contacting it with calcium metal. This reduces the PuCl_3 , AmCl_3 , and MgCl_2 to metal. The magnesium metal vaporizes off due to its high vapor pressure at 800°C. The plutonium and americium coalesce together as a button in the bottom of the crucible.

Only a few preliminary tests have been run. We have

successfully removed the plutonium from the salt residue, but the exact disposition of the americium is not clear. Thermodynamically, the americium should be reduced to metal and recovered with the plutonium. Our first indications are that some americium is moved with the plutonium but that some stays behind in the salt.

The stripping approach seems to be practical. Future work will investigate the disposition of the americium. Work will be done to establish proper operating conditions and optimize process yields.

Electrorefining (ER) Salt Recovery. Approximately 8% (500 g) of the plutonium in an electrorefining run is lost to the salt phase. Historically, this waste stream was recovered by aqueous processing.³ The salts are now recovered pyrochemically by salt stripping. This operation consists of contacting the molten salt residue with calcium metal, resulting in the reduction of PuCl_3 to metal and the coalescence of metallic plutonium shot. The process results in the formation of a metallic plutonium button (96% yield), a large white salt phase, and a small black salt phase. The plutonium metal is recycled to MSE and ER. The white salt phase together with the crucible contain less than recoverable amounts of plutonium and are discarded. The black salt phase which contains the unrecovered plutonium is combined with other black salt phases and sent through a second reduction step. Complete details of the process are given in Reference.¹¹

Proposed Plutonium Recycle

Process Schematic. A schematic showing our main production sequence and residue recycle streams is seen in Figure 11. In addition on this figure, (shown in the pentagonal shaped boxes) are two proposed plutonium recycle streams which are under investigation but are not being used in the production sequence.

1. Plutonium and americium recovery from MSE Salt Stripping Product.
2. Electrorefining anode recovery.

The goal of these two processes is to provide a closed loop on the plutonium streams in the metal preparation and purification sequence.

Molten Salt Extraction Salts: Plutonium and Americium Recovery. We have demonstrated the ability to successfully strip the plutonium from the MSE salts. The resulting metal product now contains as much as 10% americium and as a result cannot be fed directly into the metal processing sequence. To use the plutonium we must remove the americium.

Vacuum distillation of the americium away from the plutonium has been demonstrated by Berry and Knighton.¹² In this work the goal was to recover pure americium metal. They demonstrated the ability to recover >50 g batches of americium (>99% pure) in a two-stage distillation.

In the system discussed here, the goal is not necessarily to

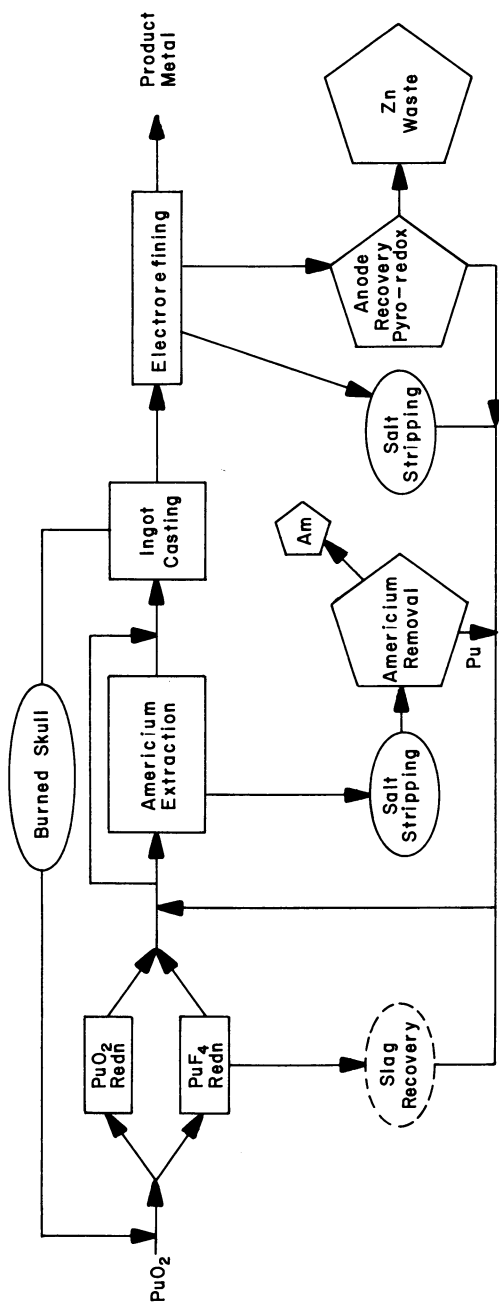


Figure 11. Main production sequence, present Pu residue recycle, plus proposed Pu residue recycle.

recover pure americium but rather to significantly reduce the americium content in the plutonium. In doing so, the plutonium must be conserved such that the americium stream contains an insignificant amount of plutonium.

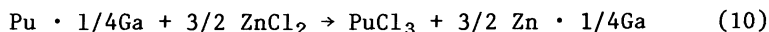
The target for americium concentration in the plutonium is <1000 ppm. This means that a 100-fold reduction of americium concentration is necessary. The vacuum distillation system discussed above seems a likely candidate for this step.

Anode Residue Recovery. Approximately 10% of the plutonium present in a Pu- 1wt% Ga electrorefining feed, ends up in the anode residue. This residue also contains most of the impurities which were present in the metal feed. The following pyrochemical processes have been considered for recovering plutonium from this residue.

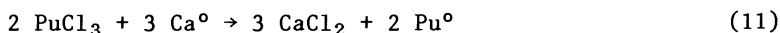
- Electrorefining at temperatures above 1100°C.
- Electrorefining with a solid plutonium anode and a liquid plutonium cathode.
- Pyroredox.

After a study of the three alternatives we concluded that pyroredox offered the most promise for anode residue recovery. Pyroredox is a molten-salt process in which plutonium metal is oxidized chemically into the salt phase and then reduced chemically into the metal phase. Most of the impurities are not oxidized and remain in the metal residue. Thus, for a Pu-Ga anode residual, the reactions would be:

Oxidation



Reduction



The pyroredox process has been studied extensively by workers at Argonne National Laboratory¹³ and Rocky Flats.¹⁴ Reavis of Los Alamos National Laboratory was apparently the first to explore the potential of pyroredox in 1961.^{15,16} Knighton of Rocky Flats recently reported the results of a study in which twelve batches of impure plutonium metal (about 2 kg of plutonium per batch) were fed to the pyroredox process.¹⁴ Processing was done in tungsten crucibles contained in tilt-pour furnaces. The oxidation and reduction yields were excellent, averaging 99.77% and 99.17% respectively. The overall process yield, however, was low, 89.97%, because of plutonium losses caused primarily by salt foaming. The purity of the plutonium metal product was poor because of entrainment of zinc metal in the salt phase. Knighton concluded that the rate of oxidation must be slowed down or the rate of heat removal from the reaction site must be increased in order to control foaming. Although the percent of zinc metal entrainment decreased

from 27.3% for the first experiments to 13% for the last, the entrainment problem was not resolved. Thus, the remaining pyrore-dox problems that Knighton identified were:

1. Foaming of salt.
2. Zinc metal entrainment in salt.

We believe that foaming can be eliminated by:

1. Controlling the rate of oxidation of plutonium by ZnCl_2 , i.e., by controlling the oxidation rate, we can control the temperature.
2. Using pure, anhydrous reagents (note -- In the DOR process, we have noted that wet CaCl_2 results in salt foaming.)

Our experiments to date have been on the 100 g plutonium scale, and have been done in tantalum containers. We have demonstrated:

1. We can control the plutonium oxidation rate by reacting molten ZnCl_2 salt with solid plutonium metal.
2. We can prepare anhydrous $\text{ZnCl}_2\text{-NaCl}$ and $\text{ZnCl}_2\text{-KCl}$.
3. We can eliminate foaming.

We have not demonstrated quantitative phase separation of salt from metal in the oxidation step. Approximately 5% of the gallium was carried over from the feed to the product after the calcium reduction. We are now scaling-up the 100-g experiments to plant-size equipment using magnesia crucibles in the equipment shown in Figure 3.

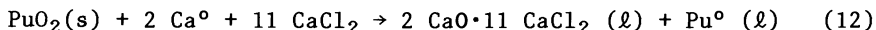
Proposed Reagent Recycle

Process Schematic. The final installation in our main production sequence will be the recycle of reagent salts. There are quite a number of options involved in recycling reagents from nearly every operation. Figure 12 shows the process schematic where the three major salt recycle steps are highlighted by heavy lines.

1. Direct Oxide Reduction.
2. Molten Salt Extraction.
3. Electrowinning.

All three have unique problems in salt reuse.

Direct Oxide Reduction. In DOR, calcium chloride is used as a solvent to dissolve the calcium oxide in the reaction:



As can be seen, there are 11 moles of CaCl_2 needed per mole of PuO_2 . A normal reduction involves 700 g of PuO_2 and requires 3600 g of CaCl_2 . The regeneration/reuse of the salt residue does more than just reduce the cost of CaCl_2 . The biggest area of impact is in waste handling and subsequent disposal.

In order to reuse the $\text{CaO} \cdot \text{CaCl}_2$ salt cake, the CaO must be removed from the matrix, thus liberating fresh CaCl_2 solvent.

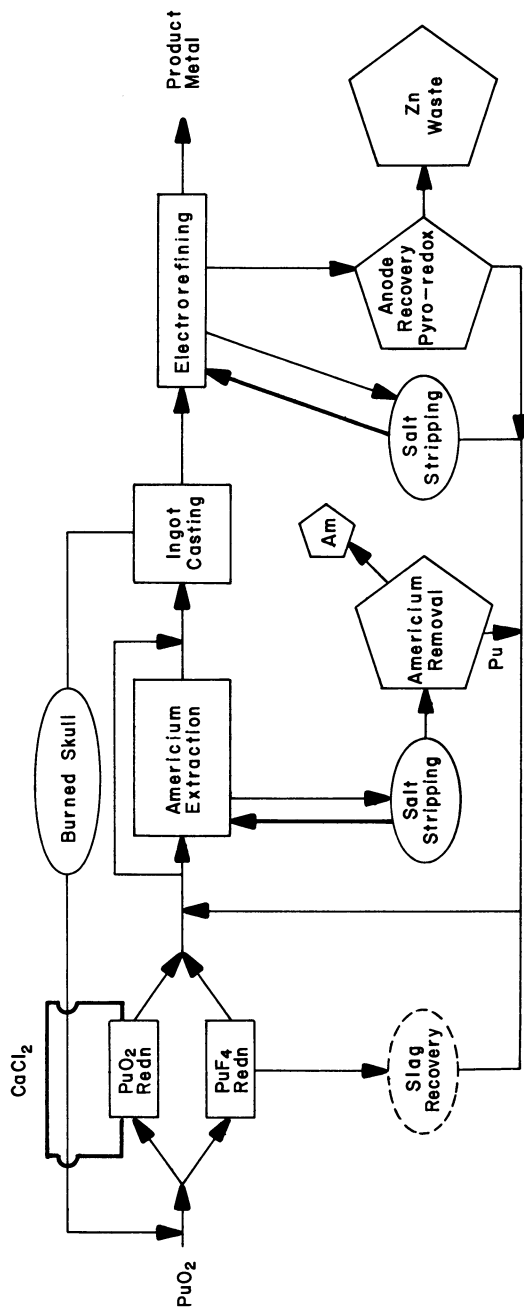


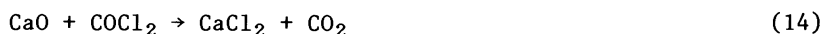
Figure 12. Main production sequence, present Pu residue recycle, proposed Pu residue recycle, and proposed reagent recycle.

There are three mechanisms for achieving this:

1. Physical separation of CaO from the CaCl₂,
2. Chemical conversion of CaO to CaCl₂, and
3. Electrolytic removal of CaO from CaCl₂.

In physical separation, the goal is to find a solvent that can dissolve the CaCl₂ and allow the CaO to settle. The CaCl₂ is soluble in most alcohols and acetone where CaO is essentially insoluble. After the CaO is separated, the alcohol could be evaporated to liberate CaCl₂.

In the chemical conversion of CaO to CaCl₂, the molten salt would be contacted with a strong chlorinating agent such as HCl or COCl₂. The chlorinating agent converts the CaO to CaCl₂ per the following equations:



An electrolytic method for removing CaO from CaCl₂ was suggested by Barletta, et.al.¹⁷ The salt is electrolyzed in a cell with a graphite consumable anode. Oxygen is removed at the anode where it reacts with carbon to form CO and CO₂. Calcium ions are reduced to metal at the cathode. Thus, the electrolytic reduction reaction should be



The competing reaction causes the formation of CO gas:



In all three mechanisms, the reactions are performed at about 800°C and the oxygen-containing by-products (H₂O, and CO₂) are removed in the off-gas stream.

None of the above systems have been demonstrated. There are serious drawbacks to all of them. In the case of Physical Separation, volatile organics are highly undesirable in a glove-box system because of the potential for explosion and fire. In the Chemical Conversion System, HCl and COCl₂ pose serious corrosion problems, particularly so at 800°C. An HCl system can probably be engineered without too much difficulty. A phosgene-handling system would be more difficult because of its greater reactivity. In the Electrolytic System, corrosion should not be a serious problem. Its principal drawback is design of the electrolytic cell.

Molten Salt Extraction and Electrorefining Salt Recycle. The goal in any salt recycle system is to keep the system as simple as possible and to use compatible reagents for each of the steps: processing, recovery, and reprocessing. In evaluating potential recycle schemes, these two considerations will play an important role.

The salt matrix presently used for both Molten Salt Extraction (MSE) and Electrorefining is an equimolar NaCl-KaCl with MgCl₂ added as an oxidizing agent. After the operation, the salt contains these three compounds as well as PuCl₃ and AmCl₃. During the stripping step, plutonium and americium are reduced to metal and removed from the salt as a metal button. The reducing agent presently used is calcium. The resulting salt, after stripping, is made up of KCl, NaCl, MgCl₂ and CaCl₂. Obviously, the salt composition is getting more and more complex. The specific makeup of the salt matrix is not significant as long as it is reasonably pure, absolutely dry, and melts at less than 800°C. But, it is very desirable to know the specific characteristics of the salt being used from a chemical and diagnostics standpoint.

The recycled salt will accumulate MgCl₂ and CaCl₂ with the CaCl₂ being the predominant compound. (The MgCl₂ may or may not be completely reduced to Mg⁰ by Ca⁰ and therefore a residual of MgCl₂ will likely be recycled back in the return salt). As a result of the CaCl₂ build-up, future investigations will involve the use of CaCl₂ instead of KCl·NaCl as the feed salt to MSE and ER.

Calcium metal is the usual reducing agent used in stripping plutonium and americium from these residue salts. Other active metals, such as sodium metal, show good potential for use as a reducing agent. In the case of sodium metal, the reduction by-product would be NaCl per the following reaction.



Since NaCl is already a major constituent of the initial salt matrix, the complexity of the salt does not change. This is highly desirable from a reprocessing standpoint.

These two approaches to salt recycle satisfy the needs to keep the system as simple as possible and to use compatible reagents in each step of the processing. The first approach involves changing matrix salt in order to be more compatible with the calcium metal reducing agent. The second approach involves changing the reducing agent to be compatible with the existing salt matrix. In both instances, the resulting salt matrix after the stripping step remains as simple as possible.

Summary

Plutonium pyrochemical processes are now the principal tools at Los Alamos for producing large amounts of high purity plutonium metal from impure metal and oxide scrap. Pyrochemical processing was selected because of its cost effectiveness. The processes are highly compact and require little floor space and manpower to operate. The processes are also operationally efficient in that one or two steps can be used to supplant multi-step operations found in the classical aqueous chemistry flow streams. The

third major cost impact is in the area of waste generation and reprocessing. In pyrochemical processing, nearly all residues have the potential for recycle. Very little primary or secondary waste is generated. In the classical aqueous process sequence, large volumes of liquids and some solids are usually generated. As a result of following the pyrochemical recycle route rather than the aqueous waste processing route, the plutonium values in the residues can be returned very expeditiously to the main process sequence. The form of the plutonium is metal, which is most desirable from a production standpoint.

In order to achieve this goal of a fully integrated process sequence, a concerted research and process development effort must take place. Present R&D efforts are devoted to the development of cost-effective pyrochemical processes for the recycle of plutonium in residues. Future efforts will be aimed at the recycle of reagents in each individual process. The objectives of the recycle are to produce plutonium metal which can be further purified, and to generate small volumes of residues which can be discarded or recycled.

In the present conceptual design, only two ultimate waste streams would be generated. One waste stream would contain the "noble" impurities and the second would contain the more "active" impurities. All reagents would be regenerated and/or recycled. The simplest systems would be used, meaning that a single solvent salt with a single compatible reducing agent would be used in every process.

Literature Cited

1. Mullins, L. J.; Morgan, A. N.; Apgar, S. A.; Christensen, D. C. "Six-Kilogram Scale Electrorefining of Plutonium Metal," Los Alamos National Laboratory, LA-9469-MS, April, 1982.
2. Mullins, L. J.; Foxx, C. L. "Direct Reduction of $^{238}\text{PuO}_2$ and $^{239}\text{PuO}_2$ to Metal." Los Alamos National Laboratory report LA 9073.
3. Mullins, L. J.; Christensen, D. C.; Babcock, B. R. "Fused Salt Processing of Impure Plutonium Dioxide to High-Purity Metal." Los Alamos National Laboratory report LA-9154-MS.
4. Baker, R. D. "Preparation of Plutonium Metal by the Bomb Method," Los Alamos Scientific Laboratory, LA-473 (1946).
5. Cleveland, J. M. The Chemistry of Plutonium, Gordon and Breach Science Publishers, New York, 1970.
6. Sohn, C. L.; Thorn, C. W.; Christensen, D. C. "Enhanced Production of Plutonium Metal Using PuO_2 in the PuF_4 /Bomb Reduction Process," Los Alamos National Laboratory LA-UR-82-1230, May 1982.
7. Mullins, L. J.; Leary, J. A. and Maraman, W. J. "Removal of Fission Product Elements by Slagging," Ind. Eng. Chem. **52**, 227-230 (1960).

8. Knighton, J. B.; Auge, R. G.; Berry, J. W. "Molten Salt Extraction of Americium from Molten Plutonium Metal," Rockwell International Rocky Flats Plant, RFP-2365, March 12, 1976.
9. Mullins, L. J.; Morgan, A. N. "A Review of Operating Experience at the Los Alamos Plutonium Electrorefining Facility, 1963-1977," Los Alamos National Laboratory, LA 9843, Dec. 1981.
10. Christensen, D. C.; Rayburn, J. A. "Pyrochemical Recovery of Plutonium Fluoride Reduction Slag," Los Alamos National Laboratory, In Press.
11. Christensen, D. C.; Mullins, L. J. "Salt Stripping, A Pyrochemical Approach to the Recovery of Plutonium Electrorefining Salt Residues," Los Alamos National Laboratory, LA-9464-MS October 1982.
12. Berry, J. W.; Knighton, J. B.; Hammel, C. A. "Vacuum Distillation of Americium Metal", Rockwell International, Energy Systems Group, Rocky Flats Plant, RFP 3211, January 22, 1982.
13. Knighton, J. B.; Steunenber, R. K., "Preparation of Metals By Magnesium Zinc Reduction, Part II, Reduction of Plutonium Dioxide," ANL-7059, Argonne National Laboratory, Argonne Illinois, June 1965.
14. Knighton J. B.; Auge, R. G.; Bird, G. D. "Purification of Plutonium Metal by the Pyroredox Process," Rockwell int., Rocky Flats Plant, CRD 80-043, Feb. 1981.
15. Reavis, J. G.; Leary, J. A. "Non-Aqueous Dissolution of Massive Plutonium," U. S. Patent Number 2 886 410, May 12, 1959.
16. Reavis, J. G.; Leary, J. A.; Maraman, W. J. "Method for Obtaining Plutonium Metal from its Trichloride", U. S. Patent Number 3,049,423, August 14, 1962.
17. Barletta, R. E.; Jardine, L. J.; Gerding, T. J.; Kroeck, D. K.; Krumpelt, M. "Molten Salt Recycle, Electrolysis of CaO in Molten Salt", Argonne National Laboratory, ANL 79-99.

RECEIVED December 22, 1982

Carbamoylmethylphosphoryl Derivatives as Actinide Extractants

Their Significance in the Processing and Recovery of Plutonium and Other Actinides

E. PHILIP HORWITZ, HERBERT DIAMOND, and DALE G. KALINA
Argonne National Laboratory, Chemistry Division, Argonne, IL 60439

Three classes of carbamoylmethylphosphoryl extractants were studied for their ability to extract selected tri-, tetra-, and hexavalent actinides from nitric acid. The three extractants are dihexyl-N,N-diethylcarbamoylmethylphosphonate (DHDECMP), hexyl hexyl-N,N-diethylcarbamoylmethylphosphinate (HHDECMP), and octyl(phenyl)-N,N-diisobutylcarbamoylmethylphosphine oxide $O\phi D[IB]CMPO$. The above three extractants were compared on the basis of nitric acid and extractant dependencies for Am(III), solubility of complexes on loading with Nd(III) and U(VI), and selectivity of actinide(III) over fission products. The influence of temperature on D_{Am} from $LiNO_3$ (10^{-2} M HNO_3) and from 3 M HNO_3 using dilute solutions of DHDECMP, HHDECMP, $O\phi D[IB]CMPO$ in o-xylene showed that the increase in D_{Am} in the series phosphonate-phosphinate-phosphine oxide was due primarily to an increase in the enthalpy of extraction.

The above information was used to develop conceptual flowsheets for the extraction of all of the actinides (U, Np, Pu, Am, and Cm) from high-level liquid waste from PUREX processing using 0.4 M $O\phi D[IB]CMPO$ in DEB and for the extraction of all of the actinides from dissolved spent LWR fuel using 0.8 M DHDECMP in DEB. In both flowsheets, no oxidation state of Pu is necessary since the III, IV, and VI state extract into the organic phase.

Recently there has been a renewed interest in the extraction of actinides with various neutral bifunctional organophosphorus extractants (1-9). An excellent review on this subject has been published recently by Schulz and Navratil (9). Interest in neutral bifunctional organophosphorus extractants stems largely from the fact that these compounds have the ability to extract tri-

0097-6156/83/0216-0433\$06.00/0
© 1983 American Chemical Society

valent actinide ions from nitric acid solution. This is important from the standpoint of removing long-lived alpha emitting nuclides from liquid waste streams generated in the reprocessing of spent nuclear fuel.

We have studied the extractant behavior of a series of compounds containing the carbamoylmethylphosphoryl (CMP) moiety in which the basicity of the phosphoryl group and the steric bulk of the substituent group are varied (10,11). These studies have led to the development of extractants which have combinations of substituent groups that impart to the resultant molecule improved ability to extract Am(III) from nitric acid and to withstand hydrolytic degradation. At the same time good selectivity of actinides over most fission products and favorable solubility properties on actinide loading are maintained (11).

This paper describes a comparison of the extraction behavior of selected actinide(III), (IV), and (VI) ions by the dihexyl-N, N-diethyl analogs of carbamoylmethyl-phosphonate and phosphinate and octyl(phenyl)-N,N-diisobutylcarbamoylmethylphosphine oxide. The objective was to evaluate the potential of selected CMP type extractants for the processing and recovery of plutonium from nitric acid.

Experimental

The preparation and purification of DHDECMP, HHDECMP, DHDECMP₀, and O ϕ D[IB]CMPO have been described in earlier publications (7,10,11). All extractants were >97% pure. (See Table I for an explanation of abbreviations.) Extractant solutions were prepared using distilled-in-glass grade o-xylene (Burdick and Jackson Laboratories) and diethylbenzene (DEB) (mixture of isomers, Aldrich Chemical Co.). Hydroxylammonium formate and hydrazium formate were prepared by mixing hydroxylamine (Chem. Service, Inc.) or hydrazine monohydrate (J. T. Baker Chemical Co., Inc.) with an equal molar amount of formic acid. Synthetic high-level liquid waste (HLLW) was prepared using the procedure of Bond and Leuze (12). Other aqueous solutions were prepared using materials described previously (7).

Extraction studies were performed using ²³⁰Th, ²³³U, ²³⁷Np, ²³⁹Np, ²³⁹Pu, ²⁴²Pu, ²⁴¹Am, and ²⁴³Cm. Standard radiometric assay and counting procedures were used throughout. Distribution ratios were determined at 25°C and as a function of temperature using the procedures described previously (7,13). For Np(IV) and Pu(IV) D's, extractions were performed from 3 M HNO₃ containing 0.1 M sulfamic acid-0.05 M ferrous sulfamate, and 0.05 M sodium nitrite, respectively. Multiple scrubs (usually 2 to 3) of the loaded organic phases were performed until two successive equilibrations gave the same distribution ratios. The distribution ratio for Np(V) was measured using a mixture of ²³⁷,²³⁹Np that was separated from Np(IV) and Np(VI) by cation ion exchange from 1 M HNO₃. The distribution ratios of fission products were measured

TABLE I. Abbreviations, Structures and Nomenclature of CMP and CMPO Extractants Employed in this Work

Abbreviations	Extractant	Nomenclature
DHDECMP	$\begin{array}{c} \text{O} \\ \parallel \\ (\text{C}_6\text{H}_{13}\text{O})_2\text{P}-\text{CH}_2-\text{C}-\text{N}(\text{C}_2\text{H}_5)_2 \end{array}$	Dihexyl-N,N-diethylcarbamoylmethylphosphonate
HHDECMP	$\begin{array}{c} \text{O} \\ \parallel \\ \text{C}_6\text{H}_{13} \text{---} \text{P}-\text{CH}_2-\text{C}-\text{N}(\text{C}_2\text{H}_5)_2 \\ \text{C}_6\text{H}_{13}\text{O} \text{---} \end{array}$	Hexyl hexyl-N,N-diethylcarbamoylmethylphosphinate
DHDECMP	$\begin{array}{c} \text{O} \\ \parallel \\ (\text{C}_6\text{H}_{13})_2\text{P}-\text{CH}_2-\text{C}-\text{N}(\text{C}_2\text{H}_5)_2 \end{array}$	Dihexyl-N,N-diethylcarbamoylmethylphosphine oxide
OφD[IB]CMPO	$\begin{array}{c} \text{O} \\ \parallel \\ \text{C}_8\text{H}_{17} \text{---} \text{P}-\text{CH}_2-\text{C}-\text{N}[\text{CH}_2-\text{CH}(\text{CH}_3)_2]_2 \\ \phi \text{---} \end{array}$	n-Octyl(phenyl)-N,N-diisobutylcarbamoylmethylphosphine oxide

from synthetic HLLW using an Instruments SA, Inc. inductively coupled atomic emission spectrometer (argon plasma). Since only aqueous phases could be analyzed, the metal ion constituents of the organic phases were quantitatively back-extracted by first diluting the equilibrated organic phase with 2-ethylhexanol (10% by volume) and then equilibrating the resultant mixture twice with an equal volume of an aqueous solution containing 0.01 M NaCN, 0.05 M diethyltriaminepentaacetate (DTPA), and 0.50 M NH₄OH. Distribution ratios measured by ICP/AES analysis were estimated to have a standard deviation of 20%.

Results and Discussion

General Comparison of the Three Classes of CMP Extractants.

Table II shows a general comparison of three essential properties of a liquid-liquid extraction system; namely, distribution ratio, selectivity, and solubility of loaded organic phase, for hexyl-ethyl analogs of the three classes of CMP extractants and for OφD[IB]CMPO. As described in earlier publications (10,11), there is a progressive increase in D_{Am}, but decrease in selectivity with respect to important fission products and in loading solubility, as the donor strength of the phosphoryl group increases. (The selectivity of Am(III) over Fe(III) is a good indication of selectivity of actinide(III) ions over a number of fission products whose reversible D's are more difficult to measure, *e.g.*, Zr.) Therefore DHDECMPO is not a good candidate as a processing extractant in spite of its high D_{Am} value. On the other hand, the phosphonate and phosphinate analogs have good overall extractant properties except for the low but usable D_{Am} value for DHDECMPO. The D_{Am} for DHDECMPO can be increased by using 0.8 M concentration in a diisopropylbenzenedecalin diluent (3).

As Table II shows, the octyl(phenyl)-N,N-diisobutyl CMPO compensates, to a large degree, for the unfavorable properties

TABLE II. Comparisons of 0.5 M Solution of CMP Extractants in DEB. 3 M HNO₃, 25°C

Extractant	D _{Am}	α _{Am} Fe	% Loading	
			Nd(III)*	U(VI)*
DHDECMPO	1.8	3 × 10 ³	>75	100
HHDECMPO	11	1 × 10 ²	>75	80-85
DHDECMPO	22	4 × 10 ⁻¹	65-70	30-35
OφD[IB]CMPO	41	3 × 10 ¹	>75	40-45

*Percent loadings are based on an extractant-to-metal ratio of 3 for Nd(III) and 2 for U(VI).

of the dihexyl-N,N-diethyl CMPO, although the U(VI) loading of $O\phi D[IB]CMPO$ extractant limits its use to applications involving moderate to low concentrations of U(VI). The absence of alkoxy groups in the CMPO class is noteworthy since this feature imparts improved hydrolytic and probably radiolytic stability to these compounds.

Acid and Extractant Dependencies. Figure 1 shows a comparison between the acid dependencies of D_{Am} using 0.5 M DHDECMP, HHDECMP, and $O\phi D[IB]CMPO$ solution in DEB. Although all show a progressive increase in D_{Am} with increasing acidity, the CMPO extractant shows an impressively high D_{Am} over a range of acidity from 0.1 M to 6 M HNO_3 and probably much higher. Since the CMPO molecule has no alkoxy groups, the stability of this extractant at very high aqueous acidities should be superior to the phosphinate and phosphonate compounds. The peak D_{Am} at 0.8 M HNO_3 for the CMPO extractant is also noteworthy since operation of an extraction process in the moderate to low acid range could be useful if aqueous soluble complexing agents, *e.g.*, oxalic acid, are required.

Figure 2 shows the extractant dependency for D_{Am} from 3 M HNO_3 using the same three extractants. All three extractants show approximately third power dependencies although the CMPO compound shows a tendency toward higher dependencies above 0.5 M. Because of the very strong extraction capability of $O\phi D[IB]CMPO$, a ~ 0.5 M concentration is sufficient whereas ~ 1.0 M is a useful concentration for the phosphinate and phosphonate CMP extractants. At these concentrations the HHDECMP and $O\phi D[IB]CMPO$ compound have comparable D_{Am} values.

Effect of Temperature on D_{Am} . The effect of temperature on D_{Am} from both 2 M $LiNO_3$ (0.01 M HNO_3) and 3 M HNO_3 for the three hexyl-ethyl CMP extractants and for $O\phi D[IB]CMPO$ is shown in Figures 3 and 4. Table III shows a tabulation of the thermodynamic constants for the extraction of Am(III) using third power concentration dependencies for the nitrate ions and the extractant. (Although activities were ignored in the calculation of the thermodynamic constants, the relative ΔH and ΔS values should be valid since the activity of the different extractant molecules should be approximately the same.)

The increase in D_{Am} from DHDECMP to DHDECMP is much greater in low acid $LiNO_3$ than in 3 M HNO_3 because of the increasing competition between Am(III) and hydrogen ion as the basicity of the P=O group increases. This behavior is also reflected in the decrease in ΔH for a given extractant from $LiNO_3$ to HNO_3 and in the increase in $\Delta(\Delta H)$, the difference in the enthalpy of Am extraction between $LiNO_3$ and nitric acid, from the phosphonate to phosphine oxide. This latter quantity is related to the enthalpy of extraction of HNO_3 . In a given medium, the improvement in D_{Am} from DHDECMP to HHDECMP is largely an enthalpy effect, however, entropy

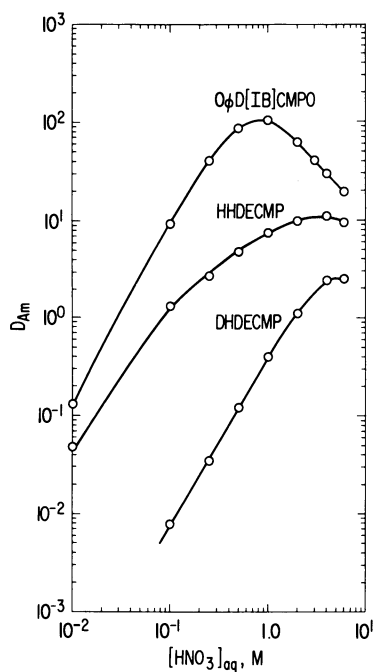


Figure 1.

Distribution ratio of Am(III) versus aqueous nitric acid conc. for carbamoylmethylphosphoryl type extractants, extractant conc. = 0.5 M.

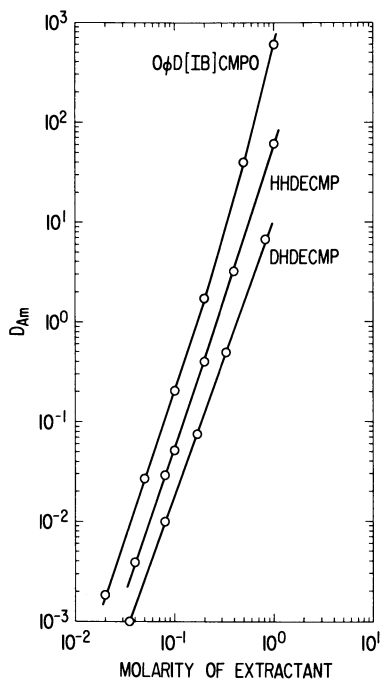


Figure 2.

Extractant dependency of Am(III) for OφD[IB]CMPO in DEB and HHDECMP and DHDECMP in DIPB, 3 M HNO_3 , 25°C.

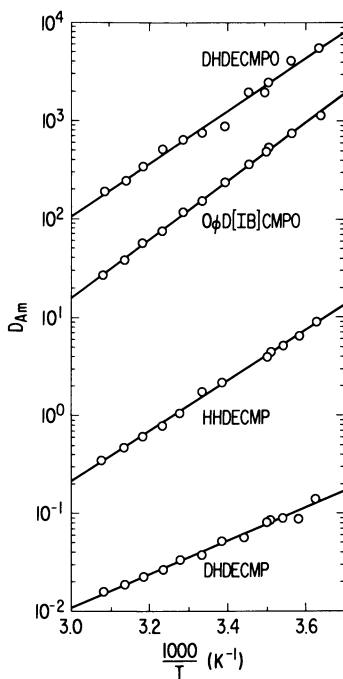


Figure 3.

The effect of temperature on the extraction of Am(III) from 2.00 M LiNO₃/0.01 M HNO₃ by 0.10 M extractant in o-xylene.

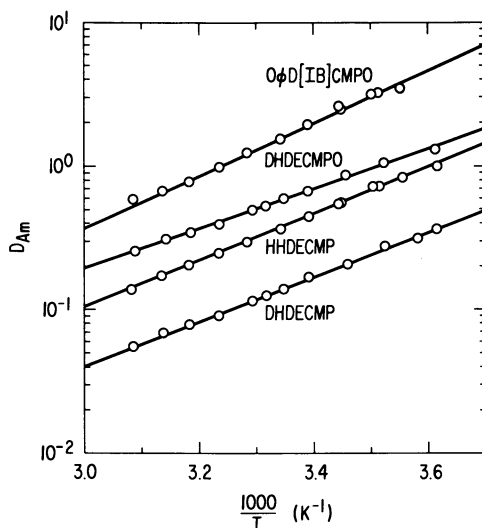


Figure 4.

The effect of temperature on the extraction of Am(III) from 3 M HNO₃ by 0.25 M extractants in o-xylene.

effects are largely responsible for the increasing strength of DHDECMP. The increase in positive ΔS for the DHDECMP extractant may be due to decreased involvement of the carbonyl group because of the large difference in donor strength between the phosphoryl and carbonyl groups.

The superiority of $O\phi D[IB]CMPO$ over DHDECMP in the extraction of Am(III) from nitric acid media is largely an enthalpy effect, which is consistent with the rationale for substituting a phenyl group for a hexyl. In fact the improved extraction of Am(III) from either nitric acid or $LiNO_3$ media in the series DHDECMP, HHDECMP, and $O\phi D[IB]CMPO$ is largely an enthalpy effect. From a practical standpoint, D_{Am} decreases with an increase in temperature for all extractants. However, as a result of the differences in ΔH , the superiority of $O\phi D[IB]CMPO$ over DHDECMP is greater at lower than at higher temperature although the difference is not great.

TABLE III. Equations and Thermodynamic Parameters for the Extraction of Am(III) from Nitrate Media by Carbamoylmethylphosphoryl Derivatives

2 M $LiNO_3$ (0.01 M HNO_3), 0.10 M Extractant in o-xylene				
	DHDECMP	HHDECMP	DHDECMP	$O\phi D[IB]CMPO$
$\ln K_{eq}$	$\frac{3852}{T} - 9.563$	$\frac{5877}{T} - 12.67$	$\frac{6217}{T} - 7.503$	$\frac{6877}{T} - 11.39$
ΔG (kJ/mol)	-8.32	-17.5	-33.1	-28.9
ΔH (kJ/mol)	-32.0	-48.9	-51.7	-57.2
ΔS (J/mol-K)	-79.5	-105	-62.4	-94.7
3 M HNO_3 , 0.25 M Extractant in o-xylene				
	DHDECMP	HHDECMP	DHDECMP	$O\phi D[IB]CMPO$
$\ln K_{eq}$	$\frac{3539}{T} - 10.03$	$\frac{3780}{T} - 9.840$	$\frac{3188}{T} - 7.426$	$\frac{4170}{T} - 9.570$
ΔG (kJ/mol)	-4.559	-7.033	-8.097	-10.95
ΔH (kJ/mol)	-29.42	-31.43	-26.51	-34.67
ΔS (J/mol-K)	-83.38	-81.81	-61.74	-79.56

Fission Product Extraction. Tables IV and V list the distribution ratios for most of the fission products produced in spent fuel. Also included are corrosion products Cr, Fe, and Ni. Extractant concentrations for DHDECMP, HHDECMP, and $O\phi D[IB]CMPO$ were selected on the basis of data in Figure 2. The aqueous acidity

TABLE IV. Distribution Ratios (Measured by ICP/AES)
 from Synthetic HLLW. 50°C

Element	0.8 M DHDECMP in DEB ^a	0.8 M HHDECMP in DEB ^b	0.4 M OφD[IB]CMPO in DEB ^c
*Rb	<0.001	<0.001	<0.001
Sr	0.006	0.003	0.003
Y	0.56	1.7	1.7
Zr	0.017	0.26	0.19
Mo	0.026	0.89	0.66
*Tc	0.50	1.4	1.2
Ru	0.14	0.26	0.083
Rh	<0.04	0.11	0.10
Pd	0.077	0.62	0.19
Ag	<0.5	-	<0.6
Cd	<0.03	0.057	0.056
*Cs	<0.001	<0.001	<0.001
Ba	<0.007	<0.007	<0.007
Cr	<0.09	<0.09	<0.09
Fe	<0.03	0.08	0.08
Ni	<0.2	<0.2	<0.2

*Radiochemical Measurements

^aHLLW - 2.9 M HNO₃, 0.05 M H₂C₂O₄, O/A = 1.0^bHLLW - 2.4 M HNO₃, 0.05 M H₂C₂O₄, O/A = 1.0^cHLLW - 2.4 M HNO₃, 0.075 M H₂C₂O₄, O/A = 1.0.
 TABLE V. Distribution Ratios (Measured by ICP/AES)
 from Synthetic HLLW. 50°C

Element	0.8 M DHDECMP in DEB ^a	0.8 M HHDECMP in DEB ^b	0.4 M OφD[IB]CMPO in DEB ^c
La	2.1	6.7	2.4
Ce	1.8	4.9	3.4
Pr	1.8	6.1	4.5
Nd	1.9	6.8	5.6
Pm	-	-	-
Sm	1.5	11.0	9.1
Eu	1.3	8.8	8.0
Gd	0.73	2.1	1.9
*Am	2.2	9.1	9.4
*Cm	1.7	6.8	7.2

*Radiochemical Measurements

^aHLLW - 2.9 M HNO₃, 0.05 M H₂C₂O₄, O/A = 1.0^bHLLW - 2.4 M HNO₃, 0.05 M H₂C₂O₄, O/A = 1.0^cHLLW - 2.4 M HNO₃, 0.075 M H₂C₂O₄, O/A = 1.0.

and temperature were adjusted to correspond to conditions which would occur in the feed plus scrub processes (see section below on conceptual flowsheets). The D's for Am(III) and Cm(III) were included to evaluate selectivity. As can be seen from the data, Am(III) and Cm(III), which are the least extractable actinides [Pu(III) follows Am(III) closely], are selectively extracted from all of the fission products except lanthanides for each of the three extractants. The presence of oxalic acid is required to complex Zr(IV) and Mo(VI) as shown previously by McIsaac (3). The data for Tc indicates that poor decontamination from this fission product would be achieved. Also the D's for Pd and Ru are mixed distribution ratios. The fraction of Pd and Ru which extracts does not readily scrub out of a loaded organic phase.

Of the three extractants, DHDECMP shows the best selectivity for actinides(III) over fission products. However, because of the low D_{Am} obtained using DHDECMP an organic to aqueous phase ratio of one or higher and a number of stages are required to ensure a good decontamination of the feed solution. HHDECMP and $O\phi D[IB]CMPO$ have slightly less selectivity than the phosphonate but would require less organic phase because of higher extractability of actinides(III).

Extraction of Actinides(IV) and (VI). Table VI shows the D's for representative hexa- and tetravalent actinides from 3 M HNO_3 at 50°C for DHDECMP, HHDECMP, and $O\phi D[IB]CMPO$. The same concentration of extractants in DEB were chosen as used to measure the fission product D's. The D for Np(V) was found to be 0.64 from 3 M HNO_3 at 50°C using 0.5 M $O\phi D[IB]CMPO$ in DEB. The data for U(VI), Np(IV), and Pu(IV) for DHDECMP are in general agreement but somewhat higher than the values reported by Schulz and McIsaac (1). This disparity is probably due primarily to the lower purity of the CMP extractant used in the earlier work. The trends in distribution ratios for tetravalent actinides and uranium follow the same trends as D_{Am} for the three classes of CMP extractants. In addition, the increase in D's from Th(IV) to Pu(IV) and D's for tetravalent $> D_U$ are expected (14).

Although the D's for U(VI) and tetravalent actinides are very high, the data in Table VII show that formic acid (HCOOH) will readily back-extract these elements as well as Am(III) from all the extractants except in the case of U(VI) with $O\phi D[IB]CMPO$. This latter situation affords a good method for separating uranium from plutonium. Hydroxylammonium formate (HAF) and hydrazium formate (NHF) were added to the formic acid to reduce Pu(IV) to Pu(III) to aid in plutonium recovery, although formic acid alone will strip tetravalent actinides, *e.g.*, Th(IV) from $O\phi D[IB]CMPO$, once excess HNO_3 present in the organic phase is removed. Thus, formic acid with HAF and NHF affords an excellent method for stripping all the actinides from these very powerful CMP extractants. Under the above conditions Am(III) and Cm(III) present in

TABLE VI. Distribution Ratios for Selected Actinides from 3 M HNO₃ 50°C

	U(VI)	Th(IV)	Np(IV)	Pu(IV)
0.8 M DHDECMP in DEB	5.3×10^1	2.0×10^2	2.6×10^2	3.0×10^2
0.8 M HHDECMP in DEB	4.8×10^2	-	5.7×10^3	7.0×10^3
0.4 M OφD[IB]CMPO in DEB	1.1×10^3	1.0×10^4	1.6×10^4	2.0×10^4

TABLE VII. Distribution Ratios for Selected Actinides from 1 M HCOOH - 0.05 M HAF* - 0.05 M HNF**. 50°C

	U(VI)	Np(IV)	Pu(IV)	Am(III)
0.8 M DHDECMP in DEB	0.06	0.008	0.061	<0.01
0.8 M HHDECMP in DEB	1.4	0.082	0.062	<0.01
0.4 M OφD[IB]CMPO in DEB	5.0	0.17	0.15	<0.01

*HAF - hydroxylammonium formate

**HNF - hydrazinium formate

processing feed solutions will follow plutonium through the separation procedure and can serve as denaturing nuclides.

Conceptual Flowsheet for the Extraction of Actinides from HLLW. Figure 5 shows a conceptual flowsheet for the extraction of all the actinides (U, Np, Pu, Am, and Cm) from HLLW using 0.4 M OφD[IB]CMPO in DEB. The CMPO compound was selected for this process because of the high D_{Am} values attainable with a small concentration of extractant and because of the absence of macro-concentrations of uranyl ion. Distribution ratios relevant to the flowsheet are shown in previous tables, IV, V, VI, and VII and figures 1 and 2. One of the key features of the flowsheet is that plutonium is extracted from the feed solution and stripped from the organic phase without the addition of any nitric acid or use of ferrous sulfamate. However, oxalic acid is added to complex Zr and Mo (see Table IV). The presence of oxalic acid reduces any Np(VI) to Np(IV) (15). The presence of ferrous ion, which is

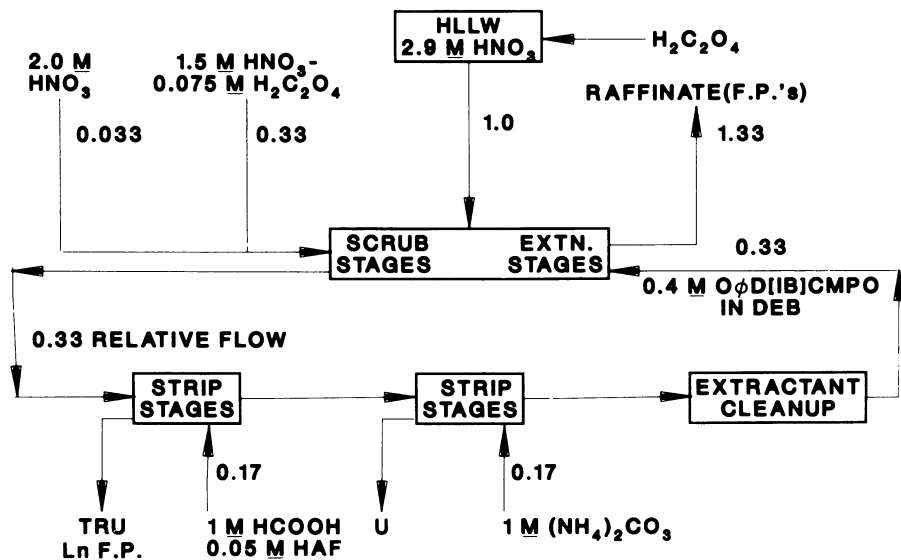


Figure 5.

Conceptual flowsheet for the extraction of actinides from high-level liquid waste using 0.4 M OφD[IB]CMPO in DEB.

always present in stainless steel equipment containing nitric acid, catalyzes the reduction. A test with synthetic HLLW in which $^{237,239}\text{Np}$ was added as Np(V) confirmed that most of the neptunium (>99.9%) was converted to an extractable form, which was probably Np(IV) .

The loaded $0\phi\text{D[IB]CMPO}$ is scrubbed successively with $1.5 \text{ M HNO}_3 - 0.075 \text{ M H}_2\text{C}_2\text{O}_4$ and 2 M HNO_3 . The oxalate scrub gives additional decontamination from fission products other than lanthanides. High concentrations of lanthanides (at least 0.1 M) in the extractant can be tolerated during scrubbing without the precipitation of lanthanide oxalates because of the high distribution ratio for La-Eu from 1.5 M HNO_3 . The 2 M HNO_3 scrub is used to remove the small quantity of oxalic acid which extracts during the previous scrubbing operation.

The stripping operation occurs in two steps. The first step involves the back-extraction of the transuranium elements (TRU) together with the lanthanide fission products using formic acid containing hydroxylammonium formate. This operation requires several equilibrations of the organic phase to remove excess nitric acid before the TRU's are readily removed. After the first strip, uranium is removed from the extractant with ammonium carbonate. Since the phase ratio is two, both stripping operations concentrate the product. Overall the TRU's and uranium are concentrated by a factor of six relative to their concentrations in the feed solution. The extractant cleanup stages involve a simple Na_2CO_3 scrub as in the PUREX process. However, since $0\phi\text{D[IB]CMPO}$ is much more stable to hydrolysis and probably to radiation than TBP, the cleanup step should be required less often than with TBP.

The major fission products which will limit overall decontamination (other than from the lanthanides) are Tc, Ru, and Pd. formed to evaluate the actual decontaminations which can be achieved.

Conceptual Flowsheet for the Extraction of Actinides from Spent LWR Fuel. Figure 6 shows a conceptual flowsheet for the extraction of all the actinides from dissolved spent LWR fuel using 0.8 M DHDECMP in DEB. The phosphonate compound was selected for this process because of its more favorable uranium loading properties (see Table II). The relative flows are based on a feed solution containing 1 M uranyl nitrate. Although the D_{Am} values for DHDECMP are much smaller than those obtained with the phosphinate and phosphine oxide compounds, the large phase ratios used in the spent fuel reprocessing flowsheet partially compensate for the low D_{Am} . Distribution ratios relevant to the flowsheet are shown in tables IV, V, VI, and VII and in figures 1 and 2. The flowsheet in Figure 6 is somewhat analogous to that proposed and tested by McIsaac, Baker, Krupa, LaPointe, Meikrantz, and Schroeder (3) for processing HLLW from LWR using DHDECMP. The major differences are the larger phase ratios in the extraction

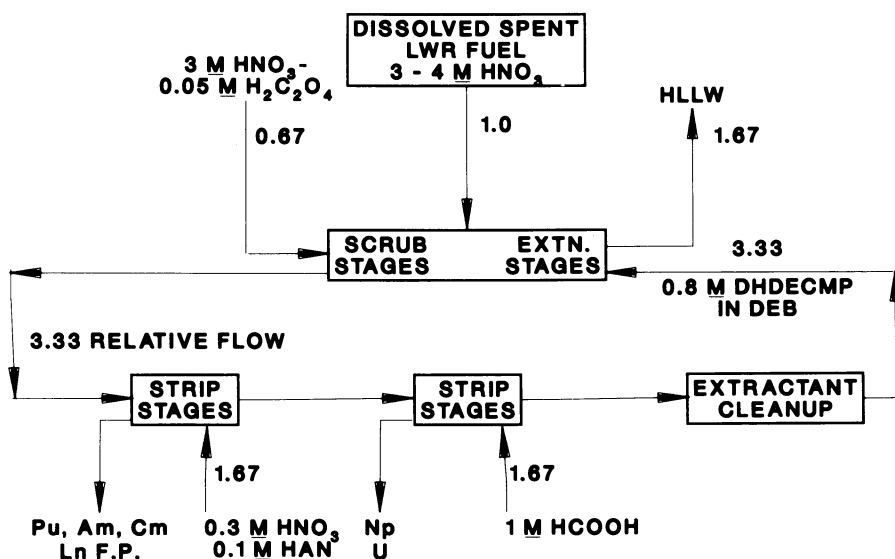


Figure 6.

Conceptual flowsheet for the extraction of actinides from dissolved spent LWR fuel using 0.8 M DHDECMP in DEB.

American Chemical
Society Library
1155 16th St., N.W.
Washington, D. C. 20036

stages in our flowsheet, which are necessary because of the large quantity of uranyl nitrate present, and in the stripping stages.

As was the case in the previous flowsheet (Figure 5), no oxidation state adjustment is necessary for plutonium or neptunium. Oxalic acid in nitric acid is again used for scrubbing to ensure a high decontamination from Zr and Mo (3). However, a 3 M nitric acid concentration is required because D_{Am} decreases with decreasing acid concentration unlike the CMPO extractants. The first stripping agent for the LWR flowsheet is a dilute nitric acid-hydroxylammonium nitrate mixture. These conditions enable one to separate Pu, Am, and Cm from U and Np. The Pu-Am-Cm fraction would require further processing to separate the lanthanides. However, the Am and Cm would remain with the Pu thus serving as denaturing nuclides. Following the first stripping operation the resultant organic phase is then stripped with 1 M formic acid, which removes U and Np (see Table VII). The extractant cleanup involves a Na_2CO_3 scrub as was the case for O ϕ D[IB]CMPO. However, the presence of two alkoxy groups in DHDECMP does result in increased hydrolytic degradations compared to the CMPO extractants and thus more extensive extractant cleanup would be required as described in (1).

Major limitations in fission product decontamination will require tests with mixer-settlers. However, we anticipate from the distribution ratio measurements that Tc, Ru, and Pd will limit the overall decontamination from beta activity (other than from lanthanides).

Summary and Conclusions

Extractants derived from the carbamoylmethylphosphoryl moiety (CMP) were studied in the phosphonate, phosphinate, and phosphine oxide classes. Our studies focused on dihexyl-N,N-diethylcarbamoylmethylphosphonate, DHDECMP, hexyl hexyl-N,N-diethylcarbamoylmethylphosphinate, HHDECMP, and octyl(phenyl)-N,N-diisobutylcarbamoylmethylphosphine oxide, O ϕ D[IB]CMPO. The three types of CMP extractants were compared on the basis of nitric acid and extractant dependencies for Am(III), solubility of complexes on loading with Nd(III) and U(VI), and selectivity over fission products. On the basis of the above data two conceptual flowsheets were developed. The first flowsheet involves the extraction of all of the actinides from HLLW using 0.4 M O ϕ D[IB]CMPO in DEB. The second flowsheet involves the extraction of all of the actinides from dissolved spent LWR fuel using 0.8 M DHDECMP in DEB.

An important feature of both flowsheets is that the oxidation state of plutonium does not have to be adjusted because all three states, III, IV, and VI, extract. Another feature of the flowsheets is that Am(III) and Cm(III) follow Pu through the separation scheme and thus behave as denaturing nuclides.

Although the O ϕ D[IB]CMPO is a particularly strong extractant for actinides in the III, IV, and VI oxidation states and has good

selectivity over fission products and very good hydrolytic stability, its major disadvantages are that it forms two organic phases on heavy loading with uranyl nitrate and is expensive to prepare. DHDECMP on the other hand requires higher ratios to extract actinide(III) ions, but has excellent solubility properties on loading with uranyl nitrate, has good selectivity over fission products, and is much less costly to prepare. The HHDECMP properties lie between those of the phosphonate and phosphine oxide with regard to its solubility on loading and extractant strength. Thus, the phosphinate would represent a good compromise extractant if it were not for the fact that it is even more difficult to synthesize and purify than the other two extractants. Therefore, final choice of which CMP extractant to employ depends on many factors. However, all three compounds described above are effective actinide extractants and give the separation chemist many new options.

Acknowledgment

The authors wish to thank Mr. Edmund Huff of the Chemical Technology Division for performing the inductively couple plasma atomic emission spectrographic analyses. Work performed under the auspices of the Office of Basic Energy Sciences, Division of Chemical Sciences, U. S. Department of Energy under contract number W-31-109-ENG-38.

Literature Cited

1. Schulz, W. W.; McIsaac, L. D. in "Proceedings of the International Solvent Extraction Conference," Toronto, Canada, September 9-16, 1977, Vol. 2, p. 619, Canadian Institute of Mining and Metallurgy, Montreal, Quebec, 1979.
2. Shown, R. R.; McDowell, W. J.; Weaver, B. in "Proceedings of the International Solvent Extraction Conference," Toronto, Canada, September 9-16, 1977, Vol. 1, p. 101, Canadian Institute of Mining and Metallurgy, Montreal, Quebec, 1979.
3. McIsaac, L. D.; Baker, J. D.; Krupa, J. F.; LaPointe, R. E.; Meikrantz, D. H.; Schroeder, N. C. "Study of Bidentate Compounds for the Separation of Actinides from Commercial LWR Reprocessing Waste," Allied Chemical Idaho Chemical Programs Report ICP-1180, Idaho Falls, Idaho, February 1979.
4. Petrzilova, H.; Binka, J.; Kuca, L. *Radioanal. Chem.* 1979, 51, 107.
5. Filippov, E. A.; Yakshin, V. V.; Belov, V. A.; Arkhipova, G. G.; Tymonyuk, M. I.; Laskorin, B. N. *Radiochem.* 1980, 22, 162.
6. Chmutova, M. K.; Kochetkova, N. E.; Myasoedov, B. F. *J. Inorg. Nucl. Chem.* 1980, 42, 897.
7. Horwitz, E. P.; Kalina, D. G.; Muscatello, A. C. *Sep. Sci. Technol.* 1981, 16, 403.

8. Horwitz, E. P.; Muscatello, A. C.; Kalina, D. G.; Kaplan, L. *Sep. Sci. Technol.* 1981, 16, 417.
9. Schulz, W. W.; Navratil, J. D. in "Recent Developments in Separation," Vol. VII, N. N. Li (ed.), CRC Press, Inc., Boca Raton, Florida, 1981, p. 31.
10. Kalina, D. G.; Horwitz, E. P.; Kaplan, L.; Muscatello, A. C. *Sep. Sci. Technol.* 1981, 16, 1127.
11. Horwitz, E. P.; Kalina, D. G.; Kaplan, L.; Mason, G. W.; Diamond, H. *Sep. Sci. Technol.* 1982, 17, 1261.
12. Bond, W.; Leuze, R. "Feasibility Studies of the Partitioning of Commercial High-Level Wastes Generated in Spent Nuclear Fuel Reprocessing: Annual Progress Report for FY-1974," ORNL-5012, Oak Ridge, Tennessee, January 1975.
13. Kalina, D. G.; Mason, G. W.; Horwitz, E. P. *J. Inorg. Nucl. Chem.* 1981, 43, 159.
14. Keller, C. "The Chemistry of the Transuranium Elements," Verlag Chemie GmbH, Weinheim/Bergstr., Germany, 1971, p. 229.
15. Shilin, V.; Romyantseva, T. A. *Radiokhimiya*, 1973, 15, 513.

RECEIVED January 5, 1983

APPENDIX A

Status of Plutonium Chemistry—Round Table Discussion

R. A. PENNEMAN

Los Alamos National Laboratory, University of California, Los Alamos, NM 87545

Remarks by R. A. Penneman, Round Table Discussion Leader:

"This program on the 40th year of plutonium chemistry reminds us anew that plutonium has an exceedingly complicated chemistry. The near identity of its oxidation/reduction couples makes all oxidation states accessible and provides a wealth of chemistry not exceeded in any other element.

"Indeed, plutonium marks an important turning point along the actinide series of elements, both in its chemistry and in the metallic state. The metallic state of plutonium is the most complicated known. Metals beyond plutonium are abruptly simpler. Also, the chemistry changes dramatically for elements beyond plutonium. For plutonium, valences 3 - 7 are known, with oxidation states of 3 through 6 being common. For the elements americium and curium, just beyond plutonium, their tetravalent states are such powerful oxidants [~ 1.5 to 2 volts higher than that for Pu(IV)] that their tetravalent ions are essentially missing from aqueous chemistry. Without powerful oxidative intervention accompanied by complexation, this barrier of the tetravalent states beyond plutonium is not surpassed. This denies access to the pentavalent and hexavalent states of americium in ground waters, for example. In contrast, the higher valent states of plutonium can be prominent in aqueous solution, especially at ground water pH's frequently encountered.

"In this symposium we have heard papers describing process chemistry, new complexing extractants, pyrochemical processing methods, spectroscopy, and photochemistry. The groundwork for these approaches is of earlier origin just now being pursued, however elegantly. Further, we saw several papers on plutonium hydrolytic behavior, leaching and speciation at midrange pH's. A pattern seems obvious and indicates to me the consequences of diminished funding for investigations of basic plutonium chemistry and funding focused on certain problem areas.

"Where do we stand? Many needed complexity constants are unknown or poorly known. Questions of solubility under a variety of circumstances remain largely unanswered. Prof. Fuger summed

0097-6156/83/0216-0453\$06.00/0
© 1983 American Chemical Society

up his presentation with the conclusion that plutonium thermochemistry is not in good overall shape. The field of organometallic chemistry is largely untouched. It is obvious that much remains to be done."

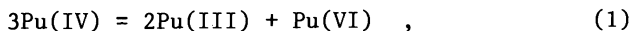
Speakers and audience members were encouraged to submit written versions of their participation. Edited versions follow.

There was considerable corridor discussion after a presentation by Dr. G. L. Silver, who "got the attention of the audience" by taking plutonium chemists to task concerning (according to him) their erroneous use of a (too) simplified summary equation involving the disproportionation of Pu(IV) and their lack of appreciation of alpha coefficients. Dr. Silver stressed the use of alpha coefficients and equations which explicitly involve acidity, hydrolysis of Pu(IV), and especially the presence of Pu(V), which is too frequently ignored.

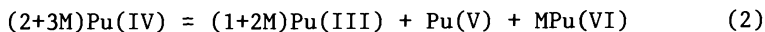
To illustrate the points of contention, accounts of Dr. Silver's arguments and a reply by Dr. Bell (edited and softened) are given.

Dr. G. L. Silver, Monsanto Research Corp., Mound, Miamisburg, OH 45342:

"In plutonium chemistry I find certain deficiencies which impede the orderly development of this science. One of these deficiencies is continued use of the equation:



which is supposed to represent the disproportionation of initially pure tetravalent plutonium. This equation is wrong for the purpose because it violates mass and charge conservation. I suggest the following equation as a replacement for Eq. (1):



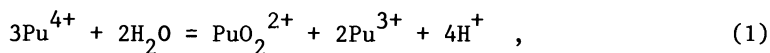
in which M is the equilibrium ratio $[\text{Pu(VI)}]/[\text{Pu(V)}]$, and is found as the sole positive root of a cubic equation. This cubic equation contains coefficients which are functions of the acidity. The consequence is that Eq. (2) shows that both the extent of disproportionation and the stoichiometry of disproportionation are dependent upon the acidity, something lacking in Eq. (1). But having said this, I disavow Eq. (2) as inadequate for the general description of plutonium in solution. Both Eqs. (1) and (2) place too much emphasis on oxidation number $N = 4.00$. We need a method which explicitly defines the oxidation state distribution for any value of N, for any acidity, and for any degree of sequestration of the four oxidation states. These advantages are accomplished with the aforementioned cubic equation. It is found as Eq. (3) in *Radiochimica Acta* **21**, 54 (1974) and is used with Eqs. (7)-(10) therein for determining fractional distributions of oxidation states for selected values of N ($3 < N < 6$) and acidity.

Plutonium in solution is a function of six variables. The first two of these variables may be selected almost at pleasure. If plutonium oxidation number N and acidity are selected, the

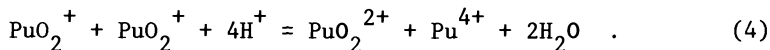
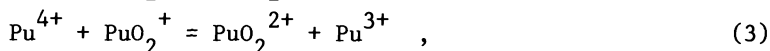
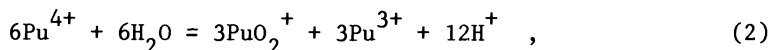
aforementioned cubic equation results. A calculator program and a commentary for this approach are given in MLM-2809 (1981). Specifying N restricts permissible oxidation state distributions in a way not generally appreciated. If measured system redox potential and acidity are selected, the system is even easier to solve. This approach is discussed in MLM-2727 (1980) and references cited therein, and will be illustrated again in the journal Marine Chemistry in 1983. Many other selections for the first two variables are possible. The latter four variables I take as the four alpha coefficients, one for each oxidation state of the plutonium. I choose alpha coefficients because they are easy to handle in the algebra of oxidation state distributions, and because their introduction suggests a new and potentially useful method of studying environmental plutonium. The alpha coefficient is the ratio of the total concentration of soluble oxidation state, including all complexes, to the concentration of the uncomplexed oxidation state."

Dr. J. T. Bell, Chem Tech Division, ORNL, Oak Ridge, TN 37830:

"A major thrust of Silver's comments was directed toward the reaction which is commonly and accurately called the disproportionation of Pu(IV). The reaction is frequently written as



and is generally understood to be the sum or "net reaction" of three reactions as follows:



Plutonium chemists use reaction (1) as the net reaction for reactions (2), (3), and (4). This is clearly documented in the Plutonium Handbook edited by Wick, and in Cleveland's book, The Chemistry of Plutonium. Reaction (1) is an accurate representation of an equilibrium and the equilibrium concentration quotient is the product of the quotients for reactions (2), (3), and (4). Therefore, it is correct to discuss equilibrium concentrations of Pu(IV), Pu(VI), and Pu(III), without Pu(V). Circumstances where the net reaction has not been properly considered are those where concentrations of oxidation states in solutions with low acidity are calculated without consideration of Pu(IV) hydrolysis and polymerization. The distributions of Pu oxidation states (including Pu(V) and Pu(IV) polymer in nitric acid systems) were reported in JINC 35, 609 (1973), and Silver has not included those experimental results in any comparison of experimental information with his computed results. The Pu(IV) hydrolysis and polymerization reactions have more effects on the oxidation states

in reaction (1) at low acidities than any other reaction, and failure to consider the hydrolysis is negligence by choice.

Silver was critical of the lack of use by plutonium chemists of α -coefficients. Assuming that Silver was referring to α -coefficients defined as the fraction of the total concentration of a substance that exists as a particular species, he was wrong to say that plutonium chemists have not used them. Phil Horwitz at ANL has used them. Publications from ORNL have reported them to easily show relative concentrations of plutonium species, and L. M. Toth used such α -coefficients as percent of Pu(IV) polymer in his symposium talk Tuesday. Alpha coefficients are a commonly used, simple concept - certainly since Ringbom's article in the Journal of Chemical Education in 1958."

Dr. Silver:

"Any one of Bell's Eqs. (2), (3), or (4) is a linear combination of the other two, and therefore it contributes no new information. The disproportionation can be represented by combining two such equations, but every value of the solution acidity has its own particular combination, usually not expressible with small integers, and no single combination is suitable for all acidities - see Radiochem. Radioanal. Letters 27 (4), 243 (1976)."

REFERENCES TO REMARKS BY G. L. SILVER

1. Silver, G. L., "Method for Estimating Acidity Changes in Plutonium Solutions," Radiochimica Acta 1974, 21, 54.
2. Silver, G. L., "Comment on the Evaluation of the Chemical Forms of Plutonium in Seawater and Other Aqueous Solutions," to be published in Marine Chemistry (1983).
3. Silver, G. L., "Simplex Characterization of Equilibrium: Application to Plutonium," Radiochem. Radioanal. Lett. 1976, 27 (4), 243.
4. Silver, G. L., in "Mound Facility Activities in Chemical and Physical Research: July-December 1980" (April 10, 1981), MLM-2809, 50 pp.
5. Silver, G. L., in "Mound Facility Activities in Chemical and Physical Research: July-December 1979" (June 18, 1980), MLM-2727, 54 pp.

W. W. Schulz, Rockwell Hanford Operations, Energy Systems Group, P.O. Box 800, Richland, WA 99352:

"I am not going to comment on plutonium process chemistry or process R&E needs since I had done all that in my paper on Tuesday.

"I emphasized and seconded what Rai called out - namely the great need for experimental work to determine solubility data for plutonium in its various oxidation states under typical expected geologic repository conditions (e.g., pH, Eh, temperature, etc.).

"I mentioned that new computer codes - RAFSCATT 1 and RAFSCATT 2 have been very recently formulated by Dr. Gary Jacobs and Mr. William Anderson of Rockwell Hanford's Basalt Waste Isolation Project. These codes relate required engineered barrier (i.e., waste packages and seals performance to draft NRC and EPA criteria). A key part of these codes is that they partition

radionuclides in those whose release are solubility-controlled (e.g. plutonium) and those whose release are not solubility-controlled (i.e., radiocesium). Reliable plutonium solubility data are thus a prerequisite to successful application of RAFSCATT 2.

"Regarding plutonium solubilities, judgment needs to be made upon how much time and money to spend determining exact Pu solubilities when all that may be required is to demonstrate that Pu solubilities are acceptably low for repository licensability purposes.

Phil Horwitz asked me to comment on what I saw as potential disadvantages of the various plutonium pyrochemical processes extolled by speakers in the Tuesday sessions. I, too, am a fan of pyrochemical techniques. I recognize that pyrochemical processes for Pu processing are just in their infancy - on batch plant-scale. To be truly useful, such processes need to be operated on a continuous basis. Scientists and engineers concerned with such technology need to develop equipment and procedures required to operate pyrochemical processes in a cost-effective, continuous manner."

Dana C. Christensen, Group MST-13, MS E511, Los Alamos National Laboratory, Los Alamos, NM 87545.

"A. The 'Twenty Year Retrieval Storage' has allowed us to continue operating while alternate methods of disposal could be established. The twenty year retrieval concept will become one of three things in the not too distant future.

1. Twenty Year Retrievable Interim sites will become permanent disposal sites. Or
2. The waste material will be exhumed and placed in permanent disposal sites. Or
3. The waste material will be exhumed and reprocessed. New waste criteria will be applied to the subsequent residues which will be compatible with the permanent disposal sites.

"The ultimate disposition of existing wastes is of major concern, particularly if they must go through additional processing in order to be handled in permanent disposal sites. The real concern is that we continue to generate wastes which must go through interim storage before they reach their grave. Most liquid wastes are reduced in volume by evaporation and blended with the solid material and cement to make a solid concrete matrix. This concrete is then sent to the twenty year retrievable storage site.

"At Los Alamos, we are making a concerted effort to reduce this waste volume to a minimum. In effect, we are trying to look beyond the need for permanent waste repositories by evaluating new processing and recycle concepts.

"B. A major effort is going into the pyrochemical processing area. Pyrochemical processing affords the luxury of working with high-density feeds and reagents thus requiring reduced floor space. The reagents are typically metal/salt couples which are essentially radiation resistant. Since we are working with plutonium in

the high-density form (preferably molten metal), self attenuations reduce personnel exposures. The reagent salts have a high potential for recycle with little waste generation. We have demonstrated essentially every unit operation in a plutonium-recovery sequence with the exception of total-reagent recycle. Therefore, the near term requirement for the plutonium processing industry is to develop and demonstrate an integrated process sequence where the only wastes are those undesirable elements which entered with the plutonium feed. The emphasis should be to recycle all reagents.

"The longer term goal for pyrochemical processing is to convert the present batch systems to remotely operated hot cell environments. Pyrochemical processes typically involve reactions of chloride-based salts with plutonium at around 800°C. To date, designing systems with compatible materials of construction has been a great challenge. Two options exist in applying these systems to remote operations: 1) The hot cells must adapt to batch-type operations; or, 2) The batch systems must adapt to the conventional continuous/semicontinuous flow schemes of the present hot cells. The biggest engineering challenge will be to apply the fully integrated process sequence to remote facilities, with the emphasis on generating the smallest quantity of ultimate waste.

"The success of the entire nuclear industry in the United States rests almost exclusively on our ability to properly handle reprocessing wastes. Pyrochemical processes, as demonstrated in the plutonium industry, show great promise toward generating only a small volume of ultimate waste through high-yield processes and high (potential) reagent reuse. A concerted engineering effort, primarily in the process applications area, is needed to apply these new processing and recycle concepts to our processing facilities of the future."

RECEIVED December 22, 1982

APPENDIX B

Summary of the Nuclear Properties, Availability, and Applications of Selected Plutonium Isotopes

JOHN L. BURNETT

U.S. Department of Energy, Processes and Techniques Branch, Division of
Chemical Sciences, Office of Basic Energy Sciences, Washington, DC 20545

According to the 7th Ed. of the Table of Isotopes, (1), the known isotopes of Pu range in mass number from 232 to 246 and in half-life from 21 minutes for Pu-233 to 8×10^7 years for Pu-244. Certain of these isotopes have found a variety of applications in research and technology and are produced in varying amounts ranging from tracer levels to metric tons. Research quantities are available to properly authorized recipients from the Oak Ridge Isotope Sales Office. Some information on such isotopes is indicated below.

<u>Isotope</u>	<u>Half-life</u>	<u>Decay</u>	<u>Preparation</u>
Pu-236	2.85y	α (5.77 MeV)	U-235 (99.9%)[22 MeV(d,n)]
Pu-237	45.6d	α (5.65 MeV)	U-235(99.9%)[36 MeV(α ,2n)]
Pu-238	87.7y	α (5.50 MeV)	Np-237(n, γ)Np-238(β^-)
Pu-239	2.41×10^4 y	α (5.16 MeV)	U-238(n, γ)U-239(β^-)
Pu-240	6.57×10^3 y	α (5.17 MeV)	Cm-244(α)
Pu-241	14.36y	β^-	U-238(xn)isotope separation
Pu-242	3.76×10^5 y	α (4.90 MeV)	U-238(xn)isotope separation
Pu-244	8.05×10^7 y	α (4.59 MeV)	U-238(xn)isotope separation

Pu-236 and Pu-237 are popular environmental and biological chemical tracers. Both are available by the microcurie.

Pu-238 is available in various isotopic enrichments ranging from 99+% to 78%. Uses are for small thermal and electric power generators.

Pu-239 is used as a fast reactor fuel, in nuclear weapons, and frequently in chemical research where production grade material of mixed isotopic content is suitable. Available enrichments range from 99.99+% to 97%.

This chapter not subject to U.S. copyright.
Published 1983, American Chemical Society.

Pu-240 is principally used in flux monitors for fast reactors. Available enrichments range from 99+% to 93%.

Pu-241 is the parent from which high assay Am-241 can be isolated for industrial purposes. 93% samples are available.

Pu-242 samples are available in enrichments ranging from 99.9+% to 95%; production-grade material ranges from 85% to 95%. Uses are for the study of plutonium physical properties and as a mass spectroscopy tracer and standard.

Only one isotope, Pu-244, is presently available as a NBS Standard Reference Material and can be obtained from the DOE New Brunswick Laboratory. A second NBS/SRM as a 1:1 mixture of Pu-239 and Pu-242 is in preparation and a third, Pu-239, is planned for the future. All the isotopes are available from the ORNL Isotopes Sales Office, Oak Ridge National Laboratory, P. O. Box X, Oak Ridge, Tennessee, 37830.

Literature Cited

1. Lederer, C. M.; Shirley, V. S.; Eds.; "Table of Isotopes", 7th Ed.; Wiley, New York, 1978.

RECEIVED January 5, 1983

INDEX

A

- Absorption
 IR
 of $\text{PuI}_3\text{C}_2\text{H}_4 \cdot 4\text{THF}$ and
 $\text{PuI}_2\text{C}_2\text{H}_3$ 43–48
 of $\text{Pu}_2(\text{OH})_2(\text{SO}_4)_3(\text{H}_2\text{O})_4$ 58–62
 UV, of plutonyl ion 265–67
 Absorption band structure, PuF_6 156–59
 Absorption spectra of various alkali
 metal PuF_6 compounds 203–6
 Absorption spectrophotometry,
 oxidation state analysis of
 dissolved Pu ions 319, 326–27
 Acid constant, hydration 223
 of disproportionation,
 stoichiometry 454–56
 Acid dependence
 of polymerization of hydrolysis
 products in uranyl
 nitrate 231, 237–39
 of stability constants, Pu(III) and
 Pu(IV) sulfate complexes 251–61
 Acid, nitric
 and extractant dependencies,
 Am(III) 433–49
 and Pu purification 360
 Acid systems, perchloric and nitric,
 photochemical Pu reduction 265–72
 Acid waste streams and nitric acid
 recovery process 353
 Acidity—*See also* pH
 Acidity and complexation 213–29
 Actinides—*See also the specific
 elements*
 and dissolved organic carbon in
 filtered lake water,
 concentration 300*t*
 electronic configurations 180–93
 energy level diagram of gas
 phase hexafluorides 157–59
 and magnetic properties 25–26
 entropies and enthalpies of
 sulfate complexes 261*t*
 extraction from high-level
 liquid waste 444–49
 hydration sphere of cation 90
 hydrothermal hydrolysis
 spectroscopic studies 58–62
 structural studies 53–57
 synthetic studies 50–53
 Actinides (*continued*)
 lattice parameter for rock-salt
 structure 69–71
 photochemistry 263–72
 radii plot 69–71
 spectra, parametric model 184–89
 stability constants of sulfate
 complexes 261*t*
 temperature dependence of free
 energy of formation 105–6
 Actinyl(VI) ion electrode 227–29
 Activation energy for $\text{PuF}_6(\text{g}) +$
 $\text{PuF}_6(\text{g})$ reaction 168
 Activity
 alpha, early work 11, 13, 15
 specific
 nuclear reactors 276
 Pu(IV) , early work 15
 238-PuO_2 319
 thermodynamic, equilibrium
 constant, actinide chlorides 389
 Addition, ligand, and stability
 constants, Pu sulfate complexes 251–61
 Adsorber, solid, competitive
 equilibrium with Pu(IV) 308–13
 Adsorption
 carbon dioxide, on dried Pu(IV)
 polymer 235–37
 Pu on geologic media 286–92
 Aggregation of hydrolysis products
 of Pu(IV) 231–32
 Algae, impact of Pu waste 275–92
 ALI—*See* Annual limit of intake
 Alkali fluorouranates(V), stabilization
 enthalpies 200*t*
 Alkali PuF_6 compounds, absorption
 spectra 203–6
 Alkaline earth metal Pu complexes
 and their reactions 80
 Alkalinity, ground-water
 compositions 337, 343–44
 Allotropic crystal structures, metallic
 radii plot 72, 72*f*
 Alloy phase diagrams, binary 66, 68–69
 Alloys—*See also the specific alloys*
 Alloys, aluminum–magnesium and
 zinc–magnesium, metallothermic
 reductions 372
 Alpha activity, early work 11, 13, 15
 Alpha coefficient, disproportionation
 equation of Pu(VI) 454–56

- Alpha phase of Pu, reaction with diiodoethane 41-48
- Aluminum-magnesium alloys, metallothermic reductions 372
- Americium
extraction—*See also* Molten salt extraction
magnesium chloride based salts 390-98
molten salt extraction at Rocky Flats, reaction 370-72
stationary extraction furnace assembly 384f
solution absorption spectra 186-93
sorption 288f
and uptake of Pu on geologic material and in living organisms 278
- Americium-Pu alloys, atomic volume and superconductivity 71-73
- Americium(III)
distribution coefficients between aluminum, silicon, and chloride oxides 287, 289f
nitric acid and extractant dependencies 433-49
- Americium-241 460
- Ammonia, concentration in natural waters 281t
- Ammonium-Pu reactions 80
- Anaerobic system of solution-phase Np(V) and Pu(V) via glucose ... 305-6
- Analyses
environmental, reducing agent 302
mathematical—*See* Data analysis
- Angles, bond, between SiO₄ tetrahedra 150-52
- Animals, impact of Pu waste 275-92
- Anion
carbonate, and complexation of Pu(IV) ion 317-32
halide, hydration sphere 90
- ANL—*See* Argonne National Laboratory
- Annual limits of intake, Pu concentration in drinking water 290-91
- Anode reaction, electrorefining technique 399-405, 418
- Anode residue recovery from electrorefining 372, 425-26
- Antiferromagnetic transition of PuCl₃ and β -Pu₂O₃ 33, 35
- Antimonide-actinide compounds, lattice parameter for rock-salt structure 69-71
- Apatite, sorption of Pu and Am 288f
- Apparatus—*See also* Techniques
- Apparatus, experimental, fluorescence 159-62
- Applications, isotopes 459-60
- Applied technology needs, overview of Pu processing chemistry 349-64
- Aquatic chemistry, Pu reactions 275-86, 297-313
- Aqueous media
photochemistry 263-72
thermodynamics of halides and halogeno complexes 86-93
- Aqueous processing
overview 359
at Rocky Flats
ion exchange 378
nitric acid dissolution 375-76
precipitation 376-78
solvent extraction 376
waste treatment 378
- Aqueous vs. pyrochemical processes, large-scale purification 409-11
- Argonne National Laboratory, oxidation state studies 302-8
- Atmospheric carbon dioxide, equilibrium with Pu 285f
- Atmospheric fallout from nuclear weapon tests and aquatic ecosystems 298-99
- Atomic volume and bonding, actinides 67-71
- Attapulgit, sorption of Pu and Am .. 288f
- Availability, isotopes 459-60

B

- Bands, vibrational, hydrolytic polymers 235-37
- Basalt, Pu transport processes 335-44
- Battelle static leach test 337-38
- Bedrock granite, Pu repository 290-92
- Bedrock water, composition 281t
- Bicarbonate-carbonate solutions and Pu(IV) ion, complexation studies 317-22
- Bifunctional organophosphorus complexes as actinide extractants 433-49
- Binary alloy phase diagrams 66, 68-69
- Binary phase diagram for CaO-CaC₁₂ system 387-88
- Binary silicate-based glasses, x-ray photoemission spectroscopic studies of U, Np, and Pu 145-54
- Binding of organic ligands in natural waters, stability constants 308-13
- Biotite, sorption of Pu and Am 288f
- Bis(cyclooctatetraenyl)plutonium(IV), magnetic and electronic properties 33, 34f
- Bis(μ -hydroxo)tetraaquadiplutonium(IV) sulfate, hydrothermal hydrolysis spectroscopic studies 58-62

- Bis(μ -hydroxo)tetraaquadiplutonium (IV) sulfate, hydrothermal hydrolysis (*continued*)
 structural studies 53-57
 synthetic studies 50-53
- Bismuth phosphate oxidation-reduction process 17-19
- Bombardment experiments, neutron, early work 6, 13, 15
- Bombay harbor, Pu distribution coefficients 299-302
- Bond angles between SiO₄ tetrahedra 150-52
- Bond lengths, α -phase of Pu 66, 67f
- Bond structure, double, of Pu₃C₂H₄•4THF and Pu₂C₂H₃ 46-48
- Bond, uranyl-to-Pu(IV) polymer, Raman spectroscopy 235
- Bonding electrons and photochemical reduction 265-67
- Bonding, *f*-character, and actinides 66-74
- Bonding model, Wigner-Seitz approximation 105
- Boron, oxide additives in silicate-based glasses, x-ray photoemission spectroscopic spectra 151f
- Bridges
 double hydroxide, structure of hydroxysulfate compounds 56
 hydroxyl, Pu(IV) polymeric network 235-39
 oxygen, silicate glasses 152-53
- Bromide complexes
 thermodynamic data 84-86, 92-93
- Bromide, concentration in natural waters 281t
- C**
- Calcium
 concentration in natural waters 281t
 ground-water compositions . 337, 343-44
- Calcium carbonate, reduction of Pu concentrations 305
- Calcium chloride, direct oxide reduction 412-15
- Calcium oxide
 additives in silicate-based glasses .. 151f
 direct oxide reduction—*See* Direct oxide reduction
 pyroreox at Rocky Flats 373-74
- Calcium oxide-calcium chloride flux system and phase diagrams 383-88
- Calculations—*See* Data analysis
- Carbamoylmethylphosphoryl derivatives as actinide extractants 433-49
- Carbon dioxide
 adsorption on dried Pu(IV) polymer 235-37
- Carbon dioxide (*continued*)
 equilibrium with Pu 285f
- Carbon, dissolved organic, influence on Pu solubility 297-313
- Carbonate
 concentration in natural waters 281t
 formation in Pu reduction 305
- Carbonate-bicarbonate solutions and Pu(IV) ion, complexation studies 317-22
- Casting, ingot 416-17
- Casting skull recycle 422
- Cathode reaction, electrorefining technique 399-405, 418
- Cation, actinide, hydration sphere 90
- Cation-anion, internuclear distance in free energy calculations 223-29
- Cation-exchange techniques, stability constant determination of Pu sulfate complexes 251-61
- Cell
 electrorefining 399-400
 galvanic, standard free energy of formation measurements, PuO₂(s) 112
 iridium effusion, mass spectrometric measurements, heats of sublimation of PuO₂(s) 100-101, 105
 tungsten effusion, vapor pressure measurements of PuO₂ 112
 tungsten, preparation 100
 unit, of α -Pu 67f
- Cell constants, cesium and hafnium . 53, 55t
- Cell coupled with absorption spectrophotometry, electrochemical reactions 319
- Cesium, cell constants 53, 55t
- Cesium plutonium hexafluoride, stability and electronic spectrum 199-209
- Characterization of Pu, summary of early work 2-21
- Characterization of sludge 363-64
- Charge—*See* Ions and Oxidation states
- Charge conservation and disproportionation of Pu(IV) 454-56
- Chelate rings 226
- Chemical processes for scrap recovery at Los Alamos 352f
- Chemical properties, summary of early work 1-21
- Chemisorption on geologic media 286-92
- Chloride
 calcium, direct oxide reduction 412-15
 concentration in natural waters 281t
 ground-water compositions . 337, 343-44
 zinc, pyroreox at Rocky Flats 373-74

- Chloride compounds
 PuCl₃, antiferromagnetic transition 35
 R₂PuCl₆ 30–31, 80–84
 thermodynamic data 90–92
- Chloride salt, decomposition potential, electrorefining 401
- Chloride slagging process—*See* Molten salt extraction
- Citrate, Pu, impact on ecosystem 278–92
- CMP—*See* Dihexyl-*N,N*-diethylcarbamoylmethylphosphonate process
- Coastal plants and animals, impact of Pu waste 275–92
- Coefficient, distribution, in equation for thermodynamic activity equilibrium constant 389–90
- Coefficients, alpha, disproportionation reaction of Pu(VI) 454–56
- Coefficients, distribution—*See* Distribution coefficients
- Coefficients of free energy of formation equation, Pu oxide vapor 127*t*
- Colloid formation 287–89
- Complex formation constants 282–84
- Complex formation, Pu with Ir, Os, Pt, Rh, Ru, and U 100
- Complexation of Pu
 in carbonate-bicarbonate solutions 317–32
 by HSO₄ 251–52
 oxidation states and hydrolysis 222–29
 and solubility in natural waters 301–2, 308–13
- Composition
 borosilicate glass 338*t*
 condensed phase, Pu-oxide systems 119–21
 salt electrolyte, electrorefining 401
 water, and Pu leaching studies 335–44
 water, swamps, ponds, lakes, and oceans 281*t*
- Compounds, coordination and organometallic, electronic and magnetic properties 25–38
- Computer codes, RAFSCATT 1 and RAFSCATT 2, waste packages and seals performance 456–58
- Concentration
 carbonate formation, Pu reduction 305
 fluoride ion, ground-water leaching ability 335–44
 Pu
 hydrated cationic species, and pH effect 220*f*
- Concentration dependence, polymerization of hydrolysis products with uranyl nitrate 231, 237–39
- Condensed phase composition, oxygen and Pu oxide systems 119–21, 124–41
- Condensed phases and thermodynamic functions 130–33
- Configuration, electronic
 actinide 180–93
 and magnetic properties 26–29, 33
 PuI₃C₂H₄ • 4THF and PuI₂C₂H₃ 46–48
 Pu(I) isotope shift 176, 178–80
 Pu(I) and Pu(II), spectral analysis 174–86
- Constants
 acid, hydration 223
 cell, cesium and hafnium 53, 55*t*
 Debye-Hückel 89
 dielectric and complexation 223–29
 equilibrium, between O(s) and Pu ions 128–29
 formation 282–84
 formation, Pu(IV) hydroxides, hydroxycarbonates, and carbonates 320–32
 stability 222–23
 halide complexes 88*t*, 91*t*, 93*t*
 organic ligands 308–13
 sulfate complexes, acid dependence 251–61
- Constants, thermodynamic activity equilibrium, actinide chlorides 389
- Coordination
 cubic, PuO₂, Lee, Leask, Wolf diagram 29
 planar six-fold, α-phase of Pu 66, 67*f*
- Coordination compounds, electronic and magnetic properties 25–38
- Coordination numbers 214–17
- Coordination sphere, geometry, Pu₂(OH)₂⁶⁺ 53–57
- Copper, stability constants for organic complexes 312–13
- Cost analysis, Pu processing 409–14
- Coupling, *jj*, organometallic and coordination compounds 25–38
- Covalency and orbital reduction data, organometallic and coordination compounds 25–38
- Cretaceous shale, ground-water leaching 335–44
- Crucibles for pyrochemical processes 412–30
- Crystal-field effects 186
- Crystal-field parameters for hexahalide 5f1-actinide ions 190–96
- Crystal field state
 organometallic and coordination compounds 25–38
 PuI₃C₂H₄ • 4THF and PuI₂C₂H₃ 46–48

- Crystal structures
 allotropic, and metallic radii 71, 72f
 spectra 186-93
 tetravalent metals 53-57
 Crystallographic distortion, actinides 66-69
 Cubic coordination, PuO₂, Lee,
 Leask, Wolf diagram 29
 Curie behavior, halides 35
 Curie-Weiss behavior, PuF₄ 29-30
 Curie-Weiss paramagnetism 46-48
 Curium isotopes
 Cu-243, extraction by carbamoyl-
 methylphosphoryl
 derivatives 433-49
 and preparation of Pu isotopes 459
 Cycle, oxidation-reduction—*See*
 Oxidation
 Cyclotron experiments, early
 work 6, 13, 15
- D**
- Data analysis
 distribution ratios of Pu and
 dissolved organic carbon in
 natural waters 308-13
 mathematical treatment, solubility
 products and formation con-
 stants of Pu(IV) hydroxides,
 hydroxycarbonates, and
 carbonates 319
 Pu migration in granite bedrock 291-92
 radial integrals, Hartree-Fock
 method 184-88
 stability constants for Pu sulfate
 complexes 253-62
 vapor pressure measurement 100-102
 vapor pressure from spectroscopic
 data 125f
 Debye-Hückel relation, modification,
 and ionic strengths 89
 Decay channels and rate, nonradia-
 tive, PuF₆(g) fluorescence
 studies 163-70
 Decay, isotopes 459
 Decladent
 spent Zirflex process 363
 storage tanks 355
 Decomposition potential, chloride
 salt, in electrorefining 401
 Decomposition of Pu oxyfluorides 79
 Dehydration enthalpy of halides and
 halogeno solid compounds 76-86
 Density, electron, and isotope shift
 for Pu(I) configurations 176, 178-80
 Depolymerization reaction by
 UV-irradiation 270-72
 Deprotonation in Pu sulfate systems 260-61
 Detector, IR fluorescence measure-
 ments of PuF₆(g) 162
 Diamagnetism of Pu(C₈H₈)₂, tempera-
 ture dependence 33
 Dielectric constant and
 complexation 223-29
 Differential pulse polarography,
 oxidation state analysis of dis-
 solved Pu ions 319, 326-27
 N,N'-Diheptyl-N,N',6,6-tetramethyl-
 4,8-dioxaundecane, ion
 electrode 227-29
 Dihexyl-N,N-diethylcarbamoylmethyl-
 phosphine oxide and dihexyl-
 N,N-diethylcarbamoylmethyl-
 phosphonate, actinide
 extractant 371, 433-49
 Dihydride, Pu 374
 Dihydroxide ion, diplutonium, spec-
 troscopy and coordination
 sphere 53-57
 Diiodoethane, reactions with Pu 41-48
 Dioxide ions, Pu, standard potentials .. 283t
 Dioxide, Pu
 complexation in carbonate-bicar-
 bonate solutions 317-32
 cubic coordination and Lee, Leask,
 Wolf diagram 29
 direct oxide reduction—*See* Direct
 oxide reduction
 purification from reactor fuel 353-55
 and x-ray diffraction technique,
 early work 20
 α-Diplutonium trioxide, back
 reaction 385-86
 β-Diplutonium trioxide, specific heat
 and magnetic measurements 33
 Direct oxide reduction (DOR) 350, 382-88
 at Los Alamos 412-15, 426-28
 at Rocky Flats 373-74
 Disilicate glasses 153-54
 Disposal, waste 456-58
 Disproportionation of Pu(IV)
 in applied Pu recovery/purification
 procedures 362
 photo shift 268-70
 Disproportionation of Pu(VI) 454-56
 Dissociation limit of gas-phase
 actinide hexafluoride 156-69
 Dissolution media, aqueous—*See also*
 Aqueous media and Aqueous
 processing
 Dissolution media, aqueous, proces-
 sing overview 359
 Dissolved organic carbon (DOC),
 influence on Pu solubility 297-313
 Distortion, crystallographic, and
 symmetry of actinides 66-69
 Distribution coefficients
 Pu in natural waters 276-78, 287,
 289-302

- Distribution coefficients (*continued*)
 Pu sulfate complexes 253-62
 in thermodynamic activity equilibrium constant equation ... 389-90
- Distribution ratio
 actinides, and aqueous nitric acid concentration for carbamoylmethylphosphoryl extractants 437-43
 in aquatic systems, definition ... 300-302
- DOC—*See* Dissolved organic carbon
- Dodecahedral geometry, Pu₂(OH)₂⁶⁺ ... 53-57
- DOR—*See* Direct oxide reduction
- Double bond structure of
 Pu₃C₂H₄ • 4THF and PuI₂C₂H₃ 46-48
- Double hydroxide bridges, structure of hydroxysulfate compounds ... 56
- E**
- Ecological impact, Pu waste 275-92
- Ecosystems, freshwater and marine, impact of Pu waste 297-313
- Efficiency of ionization of Pu 102
- Effusion rates, vapor pressure determination 100-101
- Eigenvectors 184
- Electrochemical reaction cell coupled with absorption spectrophotometry 319
- Electrode, ion, uranyl-specific 227-29
- Electron density and isotope shift for configurations in Pu(I) 176, 178-80
- Electron-exchange reaction, Pu(IV) disproportionation 268
- Electronic configuration—*See also* Energy levels
 actinides 66-74
 actinides, spectral analyses 180-93
 PuF₆(s) 156-59, 164, 168-69, 203-9
 Pu₃C₂H₄ • 4THF and PuI₂C₂H₃ ... 46-48
- Electronic properties, organometallic and coordination compounds 25-38
- Electrons, bonding, and photochemical reduction 265-67
- Electropositive impurities and electrorefining 401
- Electrorefining (ER) 399-405
 impure metal ingot feed 416-17
 at Los Alamos 351*f*, 418-20, 423
 at Rocky Flats 372-73
 salt recycle 423, 428-30
- Electrostatic adsorption by geologic media 286-92
- Electrostatic parameters for Pu(IV) .. 190
- Elements
 Group IVB, actinide, and lanthanide, hydrothermal hydrolysis spectroscopic studies 58-62
- Elements (*continued*)
 Group IVB, actinide and lanthanide hydrothermal hydrolysis (*continued*)
 structural studies 53-57
 synthetic studies 50-53
 rare earth, Pu purification 393-98
- Energy
 Fermi, actinides 66-69
 free—*See* Free energy
- Energy of activation for PuF₆(g) + PuF₄(g) reaction 168
- Energy band, f-electron 66, 68-69
- Energy of extraction of Am(III) by carbamoylmethylphosphoryl derivatives 437-41
- Energy of formation
 actinide chlorides 385, 389
 atomic oxygen for Pu oxides 112-16, 113*f*
 Pu oxides 126-33
- Energy gap for Pu(C₈H₈)₂ as function of orbital reduction factor 34*f*
- Energy levels
 free-ion spectral analysis 174-86
 plutonyl ion 263-68
 PuF₄ 30
 PuF₆ 156-59, 164, 168-69, 206-9
 Pu₃C₂H₄ • 4THF and PuI₂C₂H₃ ... 46-48
- Energy levels, transitions
 actinides 66-74
 core level excitation of actinide oxides in silicate-based glasses 145-54
- Enewetak Lagoon, Pu distribution coefficients 299-302
- Enhancement, photo, and degradation of Pu(IV) polymer 270-72
- Enrichment
 oxygen, in PuO₂ relative to condensed phase 134, 136*f*
 Pu isotopes 459-60
- Enthalpy of extraction of Am(III) by carbamoylmethylphosphoryl derivatives 437-41
- Enthalpy of formation, actinide intermetallics 105-7
- Enthalpy of formation, solution, and dehydration, halides and halogeno solid compounds 76-86
- Enthalpy of fusion, Pu-oxygen systems 129
- Enthalpy of stabilization, alkali fluorouranates(V) 199-200
- Enthalpy of vaporization, partial, calculations 115
- Entropy of extraction of Am(III) by carbamoylmethylphosphoryl derivatives 437-41

- Entropy of formation, actinide intermetallics 104-7
- Entropy of formation, solution, and dehydration, halides and halogeno solid compounds 77-86
- Entropy of fusion, Pu-oxygen systems 129
- Entropy of ionization, HSO_4^- 257
- Entropy of sublimation, Pu-intermetallics 104*f*
- Environmental impact
Pu waste 275-92
Pu waste and ground-water leaching 335-36
- Environmental research, sources of Pu and its aquatic chemistry 297-313
- Equation, thermodynamic activity equilibrium constant 389-90
- Equations
competitive equilibrium between Pu(IV) and soluble complexing ligands and solid adsorber 308-13
enthalpy of stabilization, alkali fluorouranates(V) 199
extraction of Am(III) from nitrate media 437, 441
extraction factor, partitioning between metal and salt phase 390-97
free energy of formation, hypostoichiometric condensed phase 132
free energy of formation, PuO(g), PuO₂(g) 114-16
free energy of protonation, and hydration 223-29
- Knudsen, total vapor pressure calculation 101
- reaction—*See* Reactions
- retention factor of Pu in granite bedrock 291-92
- stability constants for Pu sulfate complexes 253-62
- vapor pressure calculation of Pu oxides 114-15
- vapor pressure calculations at high temperatures 124-41
- Vasil'ev's modification of Debye-Huckel relation 89
- Equilibrium
CsPuF₆ 203
Pu dioxide system 124-29
Pu and HSO₄⁻ 251-61
Pu oxides and fluorides 77
Pu(IV) polymer growth with uranyl nitrate 231-35
Pu(IV) and soluble complexing ligands and solid adsorber 308-13
solubility, and sorption of carbonate ion 327*f*
- Equilibrium constant
equilibrium between O(g) and Pu ions 128-29
thermodynamic activity, actinide chlorides 389
- Equilibrium partitioning in molten salt extraction 389
- Equilibrium vapor pressure determination, Pu-noble metal compounds 100-107
- Equipment, electrorefining process 419*f*
- ER—*See* Electrorefining
- Ethylenic stretching frequencies of PuI₂C₂H₄ • THF and PuI₂C₂H₃ 43-48
- Exchange, ion, use at Rocky Flats 378
- Excitation, fluorescence, of PuF₆(g) 162
- Excited states and magnetic measurements of PuF₄ 29-30
- Excited states, plutonyl ion 263-68
- Experimental data vs. calculated solubilities for hydrolysis reactions 325-30
- Experimental data vs. Hartree-Fock methods, energy level parameters 184-90
- Experimental heats of formation, Pu intermetallics vs. corresponding heats calculated from Miedema model 105-7
- Experimental preparation—*See* Preparation 201-3
- Experimental procedure
actinide extraction by carbamoylmethylphosphoryl derivatives 433-49
leaching speciation studies 336-39
- Pu distribution ratios and dissolved organic carbon determination in natural waters 308-13
- 238-PuO₂ and complexation of ion in carbonate solutions 318-19
- stability constant determination of Pu sulfate complexes 252-61
- Experimental techniques—*See* Techniques
- Extractants, actinide, and carbamoylmethylphosphoryl derivatives 433-49
- Extraction, Am—*See also* Molten salt extraction
at Los Alamos 412, 416, 422-25, 428-30
molten salt 353, 358-59, 386-98
at Rocky Flats 370-72
solvent 360-61, 376
solvent, stability constant, Pu sulfate complexes 252-61
- Extraction factor, partitioning between metal and salt phase 390-97

F

- Fallout, atmospheric, from nuclear weapon tests, and aquatic ecosystems 298-99
- Fast reactor fuel, Pu isotopes 459-60
- f*-character, actinides and bonding 66-74
- crystal field parameter 190-96
- Fermi energy, actinides 66-69
- Ferrite waste treatment process 378
- Film formation, photodecomposition of PuF₆(g) 162
- First-order kinetics, Pu(IV) polymerization 237-39
- Fish, impact of Pu waste 275-92
- Fission products
isolation of Pu, Plutonium Project .. 2-7
selectivity of actinide(III) 441-43
- Fluence, photodecomposition of PuF₆ 155-70
- Fluorescence, laser-induced 155
- Fluorescence photon and quantum yield, definition 163-65
- Fluoride compounds of Pu
gas photophysics and photochemistry 155-70
initial isolation and tracer studies .. 2-7
magnetic measurements of PuF₄ .. 29-30
production and reduction of PuF₄ 350-53, 412
solubility in various media .. 10-11, 14-15
spectra and energy level analysis 190-96, 199-209
thermodynamic data 76-80, 87-90
- Fluoride compounds of U(V), alkali, stabilization enthalpies 200t
- Fluoride ion concentrations, ground-water leaching ability 281t, 335-44
- Fluoride precipitation technique of rare earth metals 302
- Fluorination at Rocky Flats 375
- Food, impact of Pu waste 275-92
- Formation constants, Pu complexes .. 282-84
- Formation constants, Pu(IV) hydroxides, hydroxycarbonates, and carbonates 320-32
- Formation of Pu colloids 287-89
- Formation of Pu-noble metal complexes 99-107
- Formation of Pu(IV) peroxy complex 267
- Formation of Pu(IV) polymer and low-acid reprocessing streams .. 231-39
- Formation, thermodynamic functions
enthalpy
halides and halogeno solid compounds 76-86
hydriding reaction 406
- Formation, thermodynamic functions (continued)
enthalpy (continued)
experimental heats, Pu intermetallics vs. corresponding heats calculated from Miedema model 104-7
- film, photodecomposition of PuF₆(g) 162
- free energies, actinide chlorides 389
- free energy of 385
- free energy, Pu oxygen system 112-16, 126-33
- Formulae—See Equations
- Fourier-transform spectroscopic studies, spectra of Pu-240, -242, -244 isotopes 176f, 177f
- FPY and FQY—See Fluorescence photon and quantum yield
- Free energy of extraction of Am(III) by carbamoylmethylphosphoryl derivatives 437-41
- Free energy of formation 385
actinide chlorides 389
actinide intermetallics, temperature dependence 105-6
atomic oxygen for Pu oxides 112-16
Pu oxygen system 126-33
- Free energy of protonation, and hydration, equations 223-29
- Free-ion interactions, PuO₂ 29
- Free-ion spectra, energy level analysis 174-86
- Frequencies, ethylenic stretching, of Pu₁₃C₂H₄ • 4THF and Pu₁₂C₂H₃ 43-48
- Freshwater systems, Pu distribution coefficients 298-302
- Fuel
dissolved spent LWR, extraction of actinides 446-49
fast reactor, Pu isotopes 459-60
irradiated reactor, Hanford Plant 353-55
- Fuel reprocessing plants and marine and freshwater systems 298-99
- Fuel safety 290
- Functional groups and Pu waste impact on ecosystem 278-92
- Functions
solid and liquid Pu-oxygen system
heat capacity 132
thermodynamic—See Thermodynamic functions
wave, bonding in actinides 69
- Furnace, stationary extraction, assembly for Pu reduction and Am extraction 384f
- Fusion, enthalpy and entropy, Pu oxygen systems 129

G

- Gallium-Pu phase diagram402-3
 Galvanic cell measurements, standard
 free energy of formation
 of $\text{PuO}_2(\text{s})$ 112
 Gas phase
 CsPuF_6 203*t*
 Pu-oxygen system
 oxygen-to-Pu molar ratio 124
 uncertainties of thermo-
 dynamic functions139-40
 vapor pressure calculations 116
 Gas photophysics and photochemistry
 of PuF_6 155-70
 Geological impact, Pu waste286-92
 Geological impact, Pu waste and
 ground-water leaching335-36
 Geometry of coordination sphere,
 $\text{Pu}_2(\text{OH})_2^{6+}$ 53-57
 Gibbs free energy function, enthalpy
 of sublimation 102
 Glass
 borosilicate, composition 338*t*
 silicate, structure150-54
 waste, Pu leaching by ground
 waters335-44
 Glucose, anaerobic system of solu-
 tion-phase Np(V) and Pu(V)305-6
 Grand Ronde basalt, ground-water
 leaching335-44
 Granite bedrock, Pu repository290-92
 Granite, Pu transport processes335-44
 Ground-water composition and Pu
 transport processes, leaching
 studies335-44
 Group IVB elements
 spectroscopic studies58-62
 structural studies53-57
 synthetic studies50-53

H

- Hafnium, cell constants53, 55*t*
 Half-lives of isotopes 459
 Halide anion, hydration sphere 90
 Halide compounds of Pu—*See also*
 Chloride compounds *and*
 Fluoride compounds
 crystal field parameters190-96
 gas photophysics and photo-
 chemistry155-70
 high temperature magnetic
 measurements 35
 stability and electronic spectrum157-59,
 199-209
 thermodynamics
 in aqueous solutions 86-93
 in the solid state75-86, 93

- Halide slagging process—*See* Molten
 salt extraction
 Halogeno compounds, thermodynamics
 in aqueous solutions 86-93
 in the solid state75-86, 93
 Hamiltonian operators, correction for
 parametric model for actinide
 and lanthanide spectra184-86
 Hanford Plant, Pu processing353-55
 Hartree-Fock calculations of radial
 integrals184-88
 Health standards, radiological 275
 Heat capacity function for solid and
 liquid Pu-oxygen system 132
 Heat of formation
 Pu intermetallics, experimental vs.
 corresponding heats calculated
 from Miedema model105-7
 for hydriding reaction 406
 Heat of ionization, HSO_4^- 257
 Heat of reaction, PuF_4 reduction
 process 412, 415*f*
 Heat of sublimation, partial,
 $\text{PuO}_2(\text{g})$ and $\text{PuO}(\text{g})$ 114-15
 Heat of sublimation, Pu-intermetallics 104*t*
 Hexachloro complexes30-31
 Hexafluoride Pu complexes
 gas-phase actinide, electronic
 energy level diagram157-59
 gas photophysics and photo-
 chemistry155-70
 stability and electronic spectrum 199-209
 Hexahalide $5f^1$ -actinide ions, crystal-
 field parameters190-96
 Hexaaxial complexes, reciprocal
 molar susceptibility vs.
 temperature 28*f*
 Hexavalent Pu—*See* Valence states
 Hexyl hexyl-*N,N*-diethylcarbamoyl-
 methylphosphinate, actinide
 extractant433-49
 High-temperature studies
 oxygen potential measurements
 above Pu oxide systems119-21
 reduction of $242\text{-Pu}_2\text{O}_3$ 116
 vapor pressures and vapor compo-
 sitions above Pu oxide
 systems123-41
 History, Plutonium Project and
 summary of early work 1-21
 Homogeneity of Pu_2O_3 phase 116
 Hudson River, Pu distribution
 coefficients299-302
 Humans, impact of Pu waste275-92
 Hybridization, *f*-electron wavefunc-
 tion overlap in actinides69, 71-74
 Hydrated iron oxide363-64
 Hydration—*See also* Solution
 chemistry

- Hydration and Pu oxidation states 216-29
 Hydration sphere, actinide cation and halide anion 90
 Hydrating at Rocky Flats 374
 Hydrocarbonates, Pu(IV) complexation 320-32
 Hydrochloric acid processing plant, future possibilities 359-60
 Hydrofluorination, metal preparation line 350-53, 375
 Hydrogen reduction 405-6
 Hydrogen reduction, preparation of the Pu sesquioxide sample 118f
 Hydrolysis—*See also* Solution chemistry
 products with uranyl nitrate and polymerization of Pu(IV) 231-39
 reactions 213-29, 320-21
 Hydroxide bridges, double, structure of hydroxysulfate compounds 56
 Hydroxides, Pu 320-32
 formation constants 282-84
 impact on ecosystem 278-92
 solubility, early work 14-15
 Hydroxyl bridges in Pu(IV) polymeric network 235-39
 Hydroxysulfate compounds, structure 56-57
 Hypostoichiometric Pu dioxide condensed phase, vapor pressures and vapor compositions 124-41
- I**
- ICRP—*See* International Commission on Radiological Protection
 Impurity levels after electrorefining process 401-4, 404f
 Industry, nuclear power—*See also* Plants
 Industry, nuclear power, production of Pu 276, 457-58
 Ingot casting for electrorefining 416-17
 Inorganic matter, Pu waste impact on ecosystem 278-92
 Instruments—*See* Apparatus
 Intake, annual limits 290-91
 Integrals, radial, Hartree-Fock calculations 184-88
 International Atomic Energy Agency, solidus and liquidus for PuO₂ system 130
 International Commission on Radiological Protection, recommendations 290-91
 Inverse magnetic susceptibilities of Pu₁₃C₂H₄•4THF and Pu₁₂C₂H₃ 47f
 Iodate complexes, solubility in various media, early work 14-15
 Iodide complexes, thermodynamic data 84-86, 92-93
 Iodine, PuF₄ reduction 412, 415f
 Iodometric titration technique 42
 Ion complexes
 diplutonium dihydroxide, spectroscopy and coordination sphere 53-57
 halides, thermodynamic data 87-93
 hexahalide actinides, crystal field parameters 190-96
 Ion electrode, uranyl-specific 227-29
 Ion exchange capacity, sorption on geologic media 286-92
 Ion exchange technique at Rocky Flats 378
 Ion intensity measurements, vapor pressure calculations 101-2
 Ionic model reaction of PuO₂(s) 129
 Ionic radii 56, 214-17
 Ionic strength
 Debye-Hückel relation, modification 87, 89
 dependence of stability constants of Pu sulfate complexes 251-61
 Ionization efficiency curve measurements 102
 Ionization potentials
 of molecules and atoms in equilibrium with Pu dioxide condensed phase 133
 of Pu and PuO₂ 283f
 Ionization, heat, and entropy, HSO₄⁻ 257
 Ions
 carbonate, and complexation of Pu(IV) 317-32
 concentration in natural waters 281f, 335-44
 diplutonium dihydroxide, spectroscopy and coordination sphere 53-57
 plutonyl
 spectra, energy level analysis 174-86
 nitrite, and Pu solvent extraction 362
 stability 263-68
 Pu(IV) reduction, x-ray photoemission spectroscopic study in silicate-based glasses 147, 150
 PuO₂, free ion and crystal field interactions 29
 uranyl, and Pu polymer 231-39
 IR
 detector for fluorescence measurements of PuF₆(g) 162
 Raman, spectroscopic studies, polymerization of Pu(IV) hydrolysis products 233, 235-39
 spectra
 PuI₃C₂H₄•4THF and PuI₂C₂H₃ 43-46
 Pu₂(OH)₂(SO₄)₃(H₂O)₄ 58-62
 Iridium effusion cells, mass spectrometric measurements of heats of sublimation of PuO₂(g) 114-15
 Iridium-Pu compound formation 100

- Irish Sea, Pu distribution
coefficients299-302
- Iron
impurity in electrorefining reaction 401
solubility and ground-water
compositions285*f*, 337, 343-44
- Iron oxide, hydrated363-64
- Irradiated reactor fuel,
Hanford Plant353-55
- Irradiation, photochemistry of
aqueous Pu solutions263-72
- Isolation of Pu from U and fission
products, Plutonium Project 2-7
- Isotope shift for Pu(I) configurations
as a function of central electron
density176, 178-80
- Isotopes
nuclear properities, availability
and applications459-60
of U and slow neutron fission 3-4
- Isotopes of Pu
Fourier-transform spectroscopic
studies, Pu-240, -242, -244 ..176-77
- K**
- KBS—*See* Nuclear Fuel Safety Project
- Kinetics, first-order Pu(IV)
polymerization237-39
- Knudsen effusion technique and
equation, vapor pressure
determination100-101
- L**
- Laboratory, Argonne National,
studies on oxidation states302-8
- Laboratory, Los Alamos National
Pu process chemistry, overview 349-64
Pu production and purification409-30
- Laboratory, Oak Ridge National,
liquid wastes299, 304-7
- Lakes, impact of Pu waste275-92
- Lakes, Pu distribution coefficients299-302
- LAMPRE—*See* Los Alamos Molten
Pu Reactor Experiment
- Landé g_J (k) values
Pu(C_8H_8)₂33
Pu(I) and Pu(II)176, 178-80
- Lanthanides
hydrothermal hydrolysis
spectroscopic studies58-62
structural studies53-57
synthetic studies50-53
spectra, parametric model184-89
trivalency69
- Lanthanum fission product, radio-
active, tracer experiments,
early work7, 10
- Large-scale production, cost analysis
of Pu processing techniques409-14
- Latimer's method, entropy81
- Laws of Thermodynamics, Second
and Third
consistency for Pu-oxygen
system139-40
heats and entropies of sublimation
and formation of Pu-inter-
metallics102-4
- Leaching studies, ground-water com-
position and Pu transport
processes335-44
- Least squares analyses, linear, vapor
pressure vs. reciprocal
temperature102
- Lee, Leask, Wolf diagram, and cubic
coordination of Pu dioxide29
- Lengths, bond, α -phase of Pu66, 67*f*
- Levels, energy—*See* Energy levels
- Lichen, impact of Pu waste275-92
- Lifetimes, fluorescence, PuF₆(g)162-63
- Ligands and Pu complex formation282-84
competitive equilibrium308-13
Pu sulfates, stability constants251-61
Pu(IV) hydroxides, hydroxocar-
bonates, and carbonates317-19
and Pu valency222-29
- Linear least squares analyses, vapor
pressure vs. reciprocal
temperature102
- Liquid PuO₂, oxygen potential126-38
- Liquid wastes
and actinides extraction444-49
at Oak Ridge National
Laboratory299, 304-7
- Lithium oxides of Pu, magnetic
measurements and reciprocal
molar susceptibility vs.
temperature26, 28*f*
- Localization of electrons and energy
levels in actinides66-74
- Los Alamos Molten Pu Reactor
Experiment (LAMPRE)409
- Los Alamos National Laboratory, Pu
process chemistry,
overview349-64, 409-30
- M**
- Magnesium chloride-based salts,
Am removal390-98
- Magnesium concentration in natural
waters and ground-water
leaching281*t*, 337-44
- Magnetic properties
metallic Pu systems71-74
organometallic and coordination
compounds25-38

- Magnetic susceptibilities of
 $\text{Pu}_3\text{C}_2\text{H}_4 \cdot 4\text{THF}$ and
 $\text{Pu}_2\text{C}_2\text{H}_3$ 46-48
- Manganese, ground-water
 compositions 337, 343-44
- Marine systems, Pu distribution
 coefficients 298-302
- Mass, disproportionation of Pu(IV) 454-56
- Mass number, Pu-236 to -244, nuclear
 properties, availability, and
 applications 459-60
- Mass spectrometer-target collection
 technique, measurement of
 effusion rates 100-101, 105
- Mass spectrometric measurements
 with iridium effusion cells, heat of
 sublimation of $\text{PuO}_2(\text{g})$ 114-15
- Mathematical analysis—*See* Data
 analysis
- Maximum permissible concentration
 of Pu in water 290
- Mechanisms
 direct oxide reduction reaction 385-88
 oxidation of Pu(IV) in aquatic
 environments 304-5
 sorption on geologic media 286-92
- Mediterranean Sea, Pu distribution
 coefficients 299-302
- Metal phase partitioning, molten
 salt extraction 390-98
- Metal preparation line (MPL) 350
- Metallic radii, light actinide
 elements 69-71
- Metallic scrap recycle 405-6
- Metallothermic reductions, aluminum-
 magnesium and zinc-magnesium
 alloys 372
- Metallurgical Project 3-6
- Metals
 alkaline earth, and Pu compounds .. 80
 noble, and Pu compounds,
 thermodynamics 99-107
 tetravalent, hydrothermal
 hydrolysis 50-53
- Methods—*See* Data analysis, Preparation,
 Procedures, Processes, and
 Techniques
- Microscopic tracer studies,
 summary of early work 2-3
- Miedema model calculated heats vs.
 experimental heats of formation,
 Pu intermetallics 105-7
- Migration of Pu through granite
 bedrock 291-92
- Minerals and Pu waste impact on
 ecosystem 278-92
- Models
 actinide ion incorporation in
 silicate glass 152
 bonding, Wigner-Seitz
- Models (*continued*)
 approximation 105
 hydration 216-19
 ionic reaction, $\text{PuO}_2(\text{s})$ 129
 Miedema, calculated heats vs.
 experimental heats of formation,
 Pu intermetallics 105-7
 octahedral site, trigonally distorted,
 CsPuF_6 206-9
 oxygen potential 126-38
 parametric, actinide and
 lanthanide spectra 184-89
 point charge and Mulak, PuF_4 29-30
- Moisture content, homogeneity of
 Pu_2O_3 phase 116-19
- Molar ratio, oxygen to Pu,
 in gas phase 124
- Molar susceptibility, reciprocal, vs.
 temperature of Li_3PuO_6 28f
- Molecular symmetry and magnetic
 measurements of organometallic
 and coordination compounds 25-38
- Molecular weight of pure Pu com-
 pound, initial work 7, 10-13
- Molten chloride salts, future
 possibilities 359-60
- Molten salt extraction 353, 358-59,
 386-98
 at Los Alamos 412, 416, 422-25,
 428-30
 at Rocky Flats 370-72
- Monoclinic crystal structure,
 α -phase of Pu 66, 67f
- Montmorillonite, sorption of Pu
 and Am 288f
- MPL—*See* Metal preparation line
- Mulak model, PuF_4 29-30
- N
- Near-IR spectra,
 $\text{Pu}(\text{OH})_2(\text{SO}_4)_3(\text{H}_2\text{O})_4$ 61f
- Neodymium(III) loading and solubility
 of Pu complexes 436-49
- Neptunium
 complexes
 CsNpF_6 , structural comparison
 to CsPuF_6 199
 distribution coefficients between
 aluminum, silicon, and
 chloride oxides 287, 289f
 hexafluorides, gas phase, elec-
 tronic energy level
 diagram 157-59
 redox potential diagram 215f
 solution absorption spectra 186-93
 solution-phase, anaerobic
 system 305-6

- Neptunium, complexes (*continued*)
 stability constants, enthalpies,
 and entropies 261*t*
 x-ray photoemission spectroscopy
 of oxides in silicate-based
 glasses 145–54
 isotopes
 Np-239, extraction by carba-
 moylmethylphosphoryl
 derivatives 433–49
 as target for Pu production 356–58,
 459
 and uptake of Pu on geologic
 material and living organisms .. 278
 Neptunium-239, extraction by
 carbamoylmethylphosphoryl
 derivatives 433–49
 Network propagation of Pu(IV)
 polymer and uranyl nitrate 236*f*
 Neutron bombardment experiments,
 early work 6, 13, 15
 Neutron diffraction measurements
 of β -Pu₂O₃ 33
 Neutron fission, slow, and
 uranium isotopes 3–4
 Nevada Test Site, ground-water
 leaching 335–44
 Nitrate, concentration in natural
 waters 281*t*
 Nitrate, uranyl, polymerization of
 Pu(IV) hydrolysis products 231–39
 Nitric acid media
 dissolution at Rocky Flats 375–76
 and extractant dependencies,
 Am(III) 433–49
 Pu photochemical studies 265–72
 Nitric acid recovery process and acid
 waste streams 353
 Noble metal–Pu compounds,
 thermodynamics 99–107
 Nomenclature of carbamoylmethyl-
 phosphoryl extractants 435*f*
 Nonbridging oxygen bonds in
 silicate-based glasses 152–54
 Nonradiative decay channels, PuF₆(g)
 fluorescence studies 165–70
 Nuclear chain reaction and the
 Plutonium Project 2–3
 Nuclear fuel reprocessing, aqueous
 Pu photochemistry 264
 Nuclear fuel safety project 290
 Nuclear properties, isotopes 459–60
 Nuclear reactors, prevalence and
 capacity 276
 Nuclear waste 299, 304–7
 environmental impact 275–92
 repository site-selection criterion
 and ground-water leaching 335–36
 treatment, overview 349–64
 Nuclear weapon tests, atmospheric
 fallout, and aquatic ecosystems 298–99
- O**
- Oak Ridge National Laboratory,
 liquid wastes 299, 304–7
 Ocean, impact of Pu waste 275–92, 297
 Octahedral CsPuF₆ site, model of
 trigonal distortion 206–9
 Octahedral symmetry of Pu(VII) 26
n-Octyl(phenyl)-*N,N*-diisobutylcarba-
 moylmethylphosphine oxide,
 actinide extractant 433–49
 Operators, Hamiltonian, correction
 for parametric model for actinide
 and lanthanide spectra 184–86
 Optical absorption
 gas-phase actinide hexafluoride 156–69
 Pu(VII) 26
 Orbital reduction, covalency, and
 magnetic properties of organo-
 metallic and coordination
 compounds 25–38
 Orbitals, bonding, and photochemical
 reduction 265–67
 Organic carbon, dissolved, influence
 on Pu solubility 297–313
 Organic ligand complexes
 and Pu valency 222–29
 stability constants 308–13
 Organic matter, Pu waste impact
 on ecosystem 275–92
 Organometallic compounds, electronic
 and magnetic properties 25–38
 Organophosphorus bifunctional com-
 plexes as actinide extractants 433–49
 ORNL—*See* Oak Ridge National
 Laboratory
 Osmium–Pu compound formation 100
 Oxidation reactions
 in electrorefining process 418
 mechanisms in aquatic environ-
 ments, Pu(IV) 304–5
 Oxidation–reduction reactions in
 molten salt extraction 389
 Oxidation state determination, CsPuF₆
 product, thermogravimetric
 technique 201
 Oxidation states
 actinides
 (III), extraction studies 433–49
 (IV), spectra and energy level
 analysis 188–96
 Am(III), nitric acid and extractant
 dependencies 433–49
 Nd(III) complexes, extraction
 studies 433–49
 Np(IV), x-ray photoemission spec-
 troscopy of oxide complexes 146–48

Oxidation states (*continued*)

Pu	
coordination number and ionic radii	214-17
hydrothermal hydrolysis spectroscopic studies	58-62
structural studies	53-57
isolation studies, early work	2-7
and magnetic properties, review	25-38
photochemistry and reduction in aqueous solutions	263-72
Pu(I) and Pu(II), spectra and configurational analysis	174-86
Pu(I), Pu(II), and Pu(III), Hartree-Fock calculations for electronic configurations	184-86
Pu(III)	
early work	19
stability constants	87-89
Pu(III) and Pu(IV)	
thermodynamic parameters	251-61
x-ray photoemission spectroscopy of oxide complexes	145-54
Pu(IV)	
complexes	
in carbonate-bicarbonate solutions	317-32
halide and halogeno, thermodynamic data	75-93
polymerization of hydrolysis products with uranyl nitrate	231-39
Pu(C ₈ H ₈) ₂ , magnetic and electronic properties	33, 34f
PuO ₂ — <i>See also</i> Plutonium dioxide	
PuO ₂ , vapor pressures and compositions	304-5
disproportionation	
in applied Pu recovery/purification processes ..	362
and lack of alpha coefficients	454
equilibrium between soluble complexing ligands and a solid adsorber	308-13
hydrothermal hydrolysis, synthetic studies	50-53
laser-induced fluorescence studies	155-70
specific activity, early work	15
spectra and energy level analyses	188-96
Pu(IV) and Pu(V), absorption spectra and calculated energy levels	
	203-6
solubility and influence of dissolved organic carbon	
	302-8

Oxidation states (*continued*)

Pu (<i>continued</i>)	
and transport processes	335-44
U	
U(IV) and U(VI), x-ray photoemission spectroscopy of oxide complexes	146-48, 150
U(V), stabilization enthalpies for alkali fluorouranates	200f
U(VI)	
complexes, extraction studies	433-49
vapor pressure, comparison to Pu-oxygen system 134, 137-41	
Oxide	
dihexyl- <i>N,N</i> -diethylcarbamoyl-methylphosphine, actinide extractant	433-49
hydrated iron	363-64
<i>n</i> -octyl(phenyl)- <i>N,N</i> -diisobutylcarbamoylmethylphosphine, actinide extractant	433-49
Pu	
dissolution	359
processing and purification at Rocky Flats	369-78
Oxide phases in Pu-oxygen system	109
Oxide reduction process, direct	
with calcium	350
at Los Alamos	412, 426-28
at Rocky Flats	373-74
Oxides	
mixed, U-Pu, oxygen potentials and pressures	138-39
Pu	
free energies of formation and direct oxide reduction reaction	385-88
high-temperature oxygen potential measurements	119-21
impact on ecosystem	278-92
initial weighing, Plutonium Project	11-13
magnetic measurements	26
oxidation states, coordination number, and hydrolysis	214-29
partial pressure as function of temperature and condensed phase composition	123-41
standard free energy of formation	112-16, 113f
Oxidizing agents for initial isolation ..	2
Oxo-bridges in Pu(IV) polymer network	237-39
Oxychlorides and oxyfluorides, thermodynamic data	76-80
Oxygen— <i>See also</i> Oxides	
bonds, bridging and nonbridging, in silicate-based glasses	152-54

- Oxygen (*continued*)
 concentration in natural waters 281*t*, 302
 partial pressure as function of temperature and condensed phase composition 123-41
 standard free energy of formation and partial molar free energies 112-16, 113*t*
- Oxygen potential for Pu-oxide systems 119-21, 126-38
- Oxygen-to-Pu molar ratio in gas phase 124
- P**
- Paramagnetism
 Curie-Weiss, of $\text{PuI}_2\text{C}_2\text{H}_4 \cdot 4\text{THF}$ and $\text{PuI}_2\text{C}_2\text{H}_3$ 46-48
 temperature-independent, for various oxidation states 26-29
- Parameters
 crystal-field
 for hexahalide $5f^1$ -actinide ions 190-96
 for Pu oxides 29
 CsPuF_6 model, electronic structure 206-9
 thermodynamic—*See* Thermodynamic functions
- Parametric model, actinide and lanthanide spectra 184-89
- Parametric studies, polymer growth 237-39
- Partial enthalpy of vaporization, calculations 115
- Partial heats of sublimation of complexes 256-60
 $\text{PuO}_2(\text{g})$ and $\text{PuO}(\text{g})$ 114-15
- Partial molar free energies of atomic oxygen for Pu oxides 112-16, 113*t*
- Partial pressure of oxygen and Pu oxides as function of temperature and condensed phase composition 123-41
- Partial pressure of $\text{PuO}(\text{g})$, free energy of formation and temperature dependency 112-18
- Particles, alpha, disintegrations per minute, early work 11, 13, 15
- Perchlorate acid media
 $\text{Pu}(\text{III})$ and $\text{Pu}(\text{IV})$ sulfate complexes, thermodynamic parameters 251-61
 Pu photochemical studies 265-72
- Periodicity
 early work 2
 Pu vs. actinides, volume, magnetism, and superconductivities 65-74
- Perlman, Isadore 3-4
- Peroxy precipitation at Rocky Flats 376
- Peroxy complex, $\text{Pu}(\text{IV})$, formation .. 267
- pH and composition natural waters 280-82, 337, 343-44
- pH dependent chemistry
 formation constants of $\text{Pu}(\text{IV})$ hydroxides, hydroxycarbonates, and carbonates 320-32
 hydrolysis 213-29
 polymerization of hydrolysis products with uranyl nitrate 231, 237-39
 and Pu solubility in natural waters 282-86
 stability constants, Pu sulfate
- Phase diagrams
 binary alloys 66, 67-68
 binary alloys, gallium-Pu 402-3
 $\text{CaO}-\text{Cl}_2$ system 387-88
 Pu-oxygen system 125*f*
- α -Phase of Pu, monoclinic crystal structure 66, 67*f*
- Phase relationships, Pu-oxygen system 109-11, 116-19
- Phase transitions and temperatures for Pu and PuO_2 132
- Phase transitions and vapor pressure calculation for Pu-noble metal compounds 99-107
- Phases
 condensed, thermodynamic functions 130-33
 gaseous, CsPuF_6 203*t*
 homogeneity, Pu_2O_3 116
- Photo effects on degradation of $\text{Pu}(\text{IV})$ polymer 270-72
- Photo shift in $\text{Pu}(\text{IV})$ disproportionation reaction 268-70
- Phosphate
 bismuth, and oxidation-reduction process 17-19
 concentration in natural waters 281*t*, 337, 343-44
 tributyl, solvent extraction 371
- Photochemistry, aqueous Pu solutions 263-72
- Photochemistry, Pu hexafluoride gas 155-70
- Photodecomposition, $\text{PuF}_6(\text{g})$ 162
- Photoelectron escape depth, x-ray photoemission spectroscopic study of actinide oxides 147
- Photon yields, fluorescence, $\text{PuF}_6(\text{g})$ 163-65
- Photophysics, Pu hexafluoride gas 155-60
- Physical adsorption, geologic media 286-92
- Physical constants, $\text{Pu}(\text{III})$ and $\text{IV})$ sulfate complexes 251-61
- Physical properties, silicate glasses 152-54
- Phytoplankton, impact of Pu waste 275-92
- pKa, hydration 223
- Planar six-fold coordination, α -phase of Pu 66, 67*f*
- Plankton, impact of Pu waste 275-92

- Plants
 fuel reprocessing, and marine and
 freshwater systems 298-99
 impact of Pu waste 275-92
 Pu processing
 Hanford 353-55
 Rocky Flats 350-53
 Savannah River 355-58
 Plutonium-Pu compound formation 100
 Plutonium-Am alloys, atomic volume
 and superconductivity 71-73
 Plutonium carbonates, formation
 constants 320-32
 Plutonium citrate, impact on
 ecosystem 278-92
 Plutonium colloids, formation 287-89
 Plutonium dihydride 374
 Plutonium dioxide
 complexation in carbonate-bicar-
 bonate solutions 317-32
 condensed phase, ionization
 potentials of molecules and
 atoms in equilibrium 133
 cubic coordination and Lee,
 Leask, Wolf diagram 29
 direct oxide reduction—*See* Direct
 oxide reduction
 ions standard potentials 283*t*
 phase-transition temperatures 132
 purification from reactor fuel 353-55
 single phase preparation 116
 solid and liquid, oxygen
 potential 126-38
 specific heat and magnetic
 measurements 33
 x-ray diffraction technique, early
 work 20
 Plutonium hexafluoride
 laser-induced fluorescence spec-
 troscopic studies 155
 photophysics and photochemistry 155-70
 stability and electronic spectrum 203-9
 Plutonium hexaoxide, reciprocal
 molar susceptibility 28*f*
 Plutonium hydroxides, impact on
 ecosystem 278-92
 Plutonium hydroxocarbonate
 reactions 321-32
 Plutonium-noble metal compounds,
 thermodynamics 99-107
 Plutonium oxides
 dissolution 359
 free energies of formation and
 direct oxide reduction
 reaction 385-88
 impact on ecosystem 278-92
 initial weighing 11-13
 partial pressure as function of
 temperature and condensed
 phase composition 123-41
 Plutonium oxides (*continued*)
 phase relationships 109-11, 116-19
 processing and purification at
 Rocky Flats 369-78
 and silicate-based glasses, x-ray
 photoemission spectroscopy 145-54
 standard free energy of
 formation 112-16, 113*t*
 thermodynamics 109-21
 vaporization behavior 110, 112-21
 Plutonium peroxide precipitation
 at Rocky Flats 376
 Plutonium polymer—*See* Polymer,
 Pu(IV)
 Plutonium process chemistry—*See*
 Processes and Processing
 Plutonium Project 2-21
 Plutonium residue recycle processes
 at Los Alamos 418, 421-30
 Plutonium reclamation facility,
 Hanford site 355
 Plutonium tetrafluoride
 Mulak model 29-30
 production and reduction at
 Los Alamos 412
 Plutonium trichloride, antiferro-
 magnetic transition 35
 Plutonium-238 processing 361
 Plutonium-239 recovery operations
 at Rocky Flats 370-71
 Plutonyl ion
 stability 263-68
 UV photoreduction, spectra 258*f*
 Point charge model, calculations
 for PuF₄ 30
 Point groups of organometallic and
 coordination compounds 25-38
 Polarography, differential pulse,
 oxidation state analysis of dis-
 solved Pu ions 319, 326-27
 Polydentate ligand systems 226
 Polymer, Pu(IV)
 hydrolysis products with uranyl
 nitrate 231-39
 photo effects on degradation 270-72
 spectroscopic studies 56-62
 Polymeric hydroxide, formation 287-89
 Polymerization and hydration 213-29
 Ponds, Pu distribution coefficients 299-302
 Potassium, concentration in natural
 waters 281*t*, 337, 343-44
 Potential
 decomposition, chloride salt in
 electrorefining 401
 ionization, of molecules and atoms
 in equilibrium with Pu dioxide
 condensed phase 133
 oxygen
 measurements above Pu-oxide
 systems, high temperature 119-21

- Potential (*continued*)
 oxygen (*continued*)
 solid and liquid PuO₂ 126-38
 standard, Pu and PuO₂ ions 283*t*
- Precipitation processes
 Pu
 early work 2-3, 6-21
 at Rocky Flats 376-78
 Pu(IV) hydroxide for 238-PuO₂
- Preparation
 CsPuF₆ 201-3
 isotopes 459
 Pu, Los Alamos National
 Laboratory 350
 Pu(IV) polymer 233-39
 238-PuO₂ 318-19
 β-Pu₂O₃, single phase 116
 Pu sulfate complexes for stability
 constant determination
 reaction of Pu with diiodoethane .42-43
 tungsten cell 100
 XPS study of actinide oxides in
 silicate-based glass 146
- Pressure, partial
 of oxygen and Pu oxides, function
 of temperature and condensed
 phase composition 124
 of PuO(g), temperature
 dependency 112-18
- Pressure, vapor
 hypostoichiometric Pu dioxide
 condensed phase 123-41
 over intermetallics, temperature
 dependence 103*f*
 Pu-noble metal compounds 100-107
 PuO₂ 112-16
- PRF—*See* Plutonium reclamation
 facility, Hanford site
- Procedure
 for actinide extraction by carba-
 moylmethylphosphoryl
 derivatives 433-49
 for dissolved organic carbon deter-
 mination in natural waters .308-13
 for large-scale production and
 purification at Los Alamos .409-30
 for reduction of Pu oxide
 to metal 382-88
 for stability constant determination
 of Pu sulfate complexes 252-61
- Process chemistry at Los Alamos
 National Laboratory, overview 349-64
- Process chemistry, at Rocky Flats,
 overview 369-78
- Processes
 bismuth phosphate oxidation-
 reduction 17-19
 disproportionation, Pu(IV) 454-56
 halide or chloride slagging—*See*
 Molten salt extraction
- Processes (*continued*)
 isolation via
 oxidation-reduction
 cycle, Plutonium Project 2-3
 Pu transport, and ground-water
 composition, leaching
 studies 335-44
 pyrochemical—*See* Pyrochemical
 processes
 separation
 at Savannah River plant 357*f*
 summary of early work 2-7
- Processing
 aqueous, at Rocky Flats
 ion exchange 378
 nitric acid dissolution 375-76
 precipitation 376-78
 solvent extraction 376
 waste treatment 378
 pyrochemical 359, 370-75,
 381-406, 412-30, 457
- Processing techniques, Pu, large-scale
 production, cost analysis 409-14
- Production, large-scale, cost analysis,
 Pu processing techniques 409-14
- Project, Metallurgical 3-6
- Project, Nuclear Fuel Safety 290
- Project, Plutonium 2-21
- Propagation of Pu(IV) polymer
 network, and uranyl nitrate 236*f*
- Properties
 chemical, summary of early work .. 1-21
 magnetic and electronic, organo-
 metallic and coordination
 compounds 25-38
 nuclear, isotopes 459-60
 physical, silicate glasses 152-54
 thermodynamic—*See* Thermo-
 dynamic functions
 thermophysical—*See* Vapor
 pressure
- Protonation, free energies 223-29
- Pseudoaxial D_{8h} symmetry,
 Pu(C₈H₈)₂ 33
- Pseudoaxial symmetry, PuF₄ 29-30
- Pseudo-spiral magnetic structure
 of β-Pu₂O₃ 33
- Pulse polarography, differential,
 oxidation state analysis of dis-
 solved Pu ions 319, 326-27
- Pump laser photon absorption, fluo-
 rescence photon yield 163-64
- Purification processes
 large-scale
 at Los Alamos 350, 409-30
 at Rocky Flats 369-78
 nuclear waste treatment 349-64, 457
 PuO₂ from reactor fuel 353-55
 pyrochemical—*See* Pyrochemical
 processes

- Pyrochemical processes
 calcination at Rocky Flats 373-75
 direct oxide reduction at
 Los Alamos 412-15, 426-28
 electrorefining 399-405
 at Rocky Flats 372-73
 at Los Alamos 418-20, 423
 fluorination at Rocky Flats 374
 hydriding 375, 405-6
 molten salt extraction 386-98
 at Los Alamos 412, 416, 422-25,
 428-30
 at Rocky Flats 370-72
 reduction
 chloride, at Rocky Flats 373-75
 fluoride at Los Alamos 412, 415f, 422
 separations 359
- Pyrochemical vs. aqueous processes,
 large-scale Pu purification 409-11
- Pyroreodox purification reaction at
 Rocky Flats 373
- Q**
- Quantum number J, lowest level
 of each configuration of Pu(I)
 and Pu(II) 176, 178-80
- Quantum yield
 fluorescence, definition 163-65
 photochemical studies 263-71
- Quartz, sorption of Pu and Am 288f
- R**
- Radial integrals, Hartree-Fock
 calculations 184-88
- Radiative lifetime, fluorescence
 quantum yield 165
- Radii, ionic
 light actinide elements 69-71
 tetravalent metals 56
- Radioactive nuclear waste—*See*
 Recovery and Waste
- Radiological health standards 275
- Radiometrical determination
 technique 42
- RAFSCATT 1 and RAFSCATT 2,
 computer codes, waste packages
 and seals performance 456-58
- Rainwater, composition 281f
- Raman spectroscopic studies, poly-
 merization of Pu(IV) hydrolysis
 products 233, 235-39
- Rare earth elements, Pu purification
 by molten salt extraction 393-98
- Rare earth fluoride precipitation
 technique 302
- Rates
 decay, in PuF₆(g) fluorescence 163
- Rates (*continued*)
 effusion, in vapor pressure
 determination 100-101
 leaching, borosilicate-glass waste
 forms 335-44
 of movement in soil 276
 of reduction, disproportionation, and
 depolymerization reactions 264-72
- Ratios
 distribution
 for actinides for carbamoyl-
 methylphosphoryl
 extractants 437-43
 in aquatic systems, definition 300-302
 molar, oxygen to Pu, in gas phase .. 124
 Pu oxidation state, in filtered
 lake water 300f
 salt to metal, in molten salt
 extraction 393-98
- Reaction cell, electrochemical,
 coupled with absorption spectro-
 photometry 319
- Reactions
 Americium removal, molten salt
 extraction at Rocky Flats 370-71
 of ammonium and alkaline earth
 metal-Pu complex 80
 at anode and cathode in electro-
 refining technique 399-405, 418
 depolymerization, UV-irradiation 270-71
 diiodoethane and Pu 41-48
 direct oxide reduction 382-88, 412-15
 disproportionation of
 Pu(IV) 268-70, 362
 equilibrium sublimation, Pu-noble
 metal compounds 101
 fluorination 375
 free energy of formation of
 PuO₂(g) 112-14
 hydrogen and Pu 405-6
 hydrolysis 320-21
 and aggregation, Pu(IV) 231-39
 and pH 219
 hydrothermal hydrolysis 49-62
 ionic model, PuO₂(s) 129
 iron impurity, in electrorefining 401
 oxidation-reduction, molten salt
 extraction 389
 photochemical reduction of aqueous
 Pu(VI) and Pu(IV) 263-68
 Pu and HSO₄⁻ 251-52
 Pu hydroxycarbonates 321-32
 PuF₄ reduction process 412, 415f
 PuF₆(g) and PuF₄(g) 168
 pyroreodox, at Rocky Flats 373
 single phase, ground water 335-44
 Reactor fuel, fast, Pu isotopes 459-60
 Reactor fuel, irradiated, Hanford
 Plant 353-55

- Reactor safety analysis, thermo-
dynamics of Pu–oxygen system 109–21
- Reagent recycle, salt 426–30
- Reciprocal molar susceptibility vs.
temperature, Li_5PuO_6 28*f*
- Recovery
anode residue 425
from PuF_4 reduction process 422
Pu-239, operations at Rocky
Flats 370–71
salt, in electrorefining 423
salt, in molten salt extraction 422–25
waste treatment and solution
chemistry, overview 349–64
- Recycle
metallic scrap 405–6
reagent, salt 426–30
residue, processes at
Los Alamos 418, 421–30
- Redox potential diagram for U,
Np, and Pu 215*f*
- Reducing agent for environmental
analyses 302
- Reduction
alloys, aluminum–magnesium and
zinc–magnesium 372
in anaerobic system 305–6
direct oxide 282–86, 350, 373–74,
382–88, 412, 426–28
in electrorefining process at anode 418
furnace assembly 384*f*
in natural waters 282–86
photochemical, aqueous Pu(VI)
and Pu(IV) 263–68
 PuF_4 412
 PuF_4 , metal preparation line 350–53
Pu(IV) ions, x-ray photoemission
spectroscopy in silicate-based
glasses 147, 150
242-PuO₂ at high temperature 116
- Reflux experiments, polymer growth 237–39
- Regression analysis, stability constants
for Pu sulfate complexes 253–62
- Repository, radioactive waste
deep granite bedrock 290–92
site-selection criterion and ground-
water leaching 335–36
- Reprocessing plants, fuel, and
aquatic ecosystems 298–99
- Reprocessing streams, low acid
polymer formation 231–39
- Reprocessing wastes 456–58
aqueous Pu photochemistry 264
prevalence and capacity 276
- Research and development, Pu produc-
tion and purification 369–78, 409–30
- Residue processing and purification
at Los Alamos 418, 421–30
at Rocky Flats 369–78
- Residue recovery at anode 425
- Retention factor, Pu in granite
bedrock 291
- Retrieval storage, 20 year 457
- Rhodium–Pu compound formation 100
- Rings, chelate 226
- Rivers, impact of Pu
waste 275–92, 299–302
- Rock, Pu transport processes 335–44
- Rock–salt structure of actinide–anti-
monide compounds, lattice
parameter 69–71
- Rocky Flats Plant, processing,
overview 350–53, 369–78
- Rotation axes of organometallic and
coordination compounds 25–38
- Russell–Saunders coupling for
different configurations 27*t*
- Ruthenium–Pu compound formation .. 100
- S**
- Safety
nuclear fuel 290
reactor, thermodynamics of
Pu–oxygen system 109–21
- Salt, concentration in natural waters .. 281*t*
- Salt electrolyte composition,
electrorefining 401
- Salt extraction process, molten 353, 358,
370–72, 386–98, 412,
422–25, 428–30
- Salt-to-metal ratio, molten salt
extraction 393–98
- Salt phase partitioning, molten salt
extraction 390–98
- Salt reagent recycle 426–30
- Salt recovery
in electrorefining 423
in molten salt extraction (MSE) ... 422–25
- Salts
chloride, decomposition potential,
electrorefining 390–98
magnesium chloride-based,
americium removal 390–98
molten chloride, future
possibilities 359–60
- Samarium metals in tetrahydrofuran
solutions of diiodoethane 41
- Savannah River Plant
impact on ecosystem 278–92
Pu processing 355–58
- Savannah River, Pu distribution
coefficients 299–302
- Scrap processing and purification at
Rocky Flats 369–78
- Scrap processing and
recovery 350, 352*f*, 355, 405–6
- Sea, impact of Pu waste 275–92, 297

- Seaborg, Glenn T., summary of work with Pu 1-21
- Seals performance and waste packages, computer codes, RAFSCATT 1 and RAFSCATT 2 456-58
- Second Law of Thermodynamics consistency for Pu-oxygen system 139-40
- and heats and entropies of sublimation and formation of Pu-intermetallics 102-4
- Sediment, ocean, impact of Pu waste 275-92
- Selection criterion for radioactive nuclear waste repository site and ground-water leaching 335-36
- Selectivity of actinide(III) over fission products 441-43
- Separation processes isotopes 459
- at Savannah River Plant 356-58
- summary of early work 2-7
- Sesquioxide, Pu, phase diagram of Pu-oxygen system 116, 121
- Shale, Pu transport processes 335-44
- Shannon's radii 216-17
- Silica, ground-water compositions 337, 343-44
- Silicate glasses, physical properties 150-54
- Single-phase reactions, ground-water 335-44
- Site, ground-water leaching, Nevada test 335-44
- Site-selection criterion, radioactive nuclear waste repository and ground-water leaching 335-36
- Skull recycle, casting 422
- Slag recovery from PuF_4 reduction process 422
- Slagging process, halide or chloride—*See* Molten salt extraction
- Slow neutron fission and isotopes of uranium 3-4
- Sludge, characterization 363-64
- Sodium carbonate solutions and complexation of Pu(IV) ion 317-32
- Sodium concentrations in natural waters and ground-water leaching 281*t*, 337-41, 343-44
- Sodium oxide of Pu, magnetic measurements 26
- Sodium silicate glass, medium for actinide oxides 145-54
- Soil, impact of Pu waste 275-92
- Solid adsorber, competitive equilibrium with Pu(IV) 308-13
- Solid state CsPuF₆ 203*t*
- halides and halogeno complexes, thermodynamic data 76-83, 93
- Solid state (*continued*) PuO₂ oxygen potential 126-38
- standard free energy of formation 112-13
- Solidus, Pu-oxygen system 130-31
- Solid waste form, ground-water leaching 335-44
- Solubilities actinide oxides in sodium silicate glass 146-47, 150, 153
- calculated, vs. experimental, hydrolysis reactions 325-30
- ground-water leaching 339-44
- on loading with uranium(VI) and neodymium(III) 436-49
- Pu compounds in various media 10-11, 14-15
- Pu in natural waters 282-86
- and U(VI) and Nd(III) loading 436-49
- Solubility product of PuO₂ 319-24
- Solution chemistry of halides and halogeno solid compounds, enthalpy 76-86
- polymerization of hydrolysis products with uranyl nitrate 231-39
- Pu oxidation states and influence of dissolved organic carbon 302-13
- Pu(IV) complexation in carbonate-bicarbonate solutions 317-32
- review 213-29, 349-64
- roundtable discussion 454-57
- Solutions, aqueous photochemistry 263-74
- thermodynamic data of halide and halogeno complexes 86-93
- Solvent extraction, Pu purification 360-61
- Solvent extraction at Rocky Flats 376
- Solvent extraction techniques, stability constant determination of Pu sulfate complexes 252-61
- Solvents early work 14-15
- perchloric and nitric acid, photochemical studies of aqueous Pu 265-72
- Sorption of Pu on geologic media 286-92
- Sources of Pu for environmental research 276, 298-99
- Speciation studies 282-86, 336-39
- Specific activity nuclear reactors 276
- Pu(IV) oxidation state, early work 15
- Spectra absorption, of Pu ions 327*f*
- absorption, of various alkali metal PuF₆ compounds 203-6
- actinide and lanthanide, parametric model 184-89
- crystal 186-93

- Spectra (*continued*)
 fluorescence emission,
 PuF₆(g) 160-62, 164-67
 Fourier transform, of Pu-240,
 -242, -244 isotopes 177f
 free-ion, energy level analysis 174-86
 IR, near-IR,
 and visible, of
 Pu₂(OH)₂(SO₄)₃(H₂O)₄ 58-62
 IR of potassium bromide pellets
 containing Pu(IV) polymer
 precipitates 236f
 optical, of Pu(VII) 26
 of PuI₃C₂H₄ • 4THF and
 PuI₂C₂H₃ 43-46
 UV photoreduction of plutonyl
 ion 258f
 visible, of Pu₂(OH)₂(SO₄)₃(H₂O)₄ 58-62
 x-ray photoemission, of actinide
 oxides 148f, 149f, 151f
 Spectrometric measurements, mass,
 with iridium effusion cells, heats
 of sublimation of PuO₂(g) 114-15
 Spectrophotometric measurements,
 oxychloro complexes 92
 Spectroscopic studies
 absorption, oxidation state analysis
 of dissolved Pu ions 319, 326-27
 Fourier-transform, Pu-240,
 -242, -244 isotopes 176-77
 hydrothermal, hydrolysis and
 hydroxy sulfate Pu complexes 58-62
 IR, of PuI₃C₂H₄ • 4THF and
 PuI₂C₂H₃ 43-48
 IR-Raman, polymerization of
 Pu(IV) hydrolysis
 products 233, 235-39
 laser-induced fluorescence, PuF₆(g) 155
 mass spectrometer-target collec-
 tion for effusion rate
 measurement 100-102, 105
 procedure for calculation of vapor
 pressures 125f
 UV-visible
 polymerization of Pu(IV) hydroly-
 sis products 233, 235-39
 reduction, disproportionation,
 and depolymerization
 reactions 264-74
 x-ray photoemission, U, Np, and
 Pu oxides in silicate-based
 glasses 145-54
 Zeeman pattern for Pu(I) 175f
 Sphere complexation, inner vs.
 outer 213
 Spin-orbit coupling, actinides 25
 Spin-orbit parameters for Pu(IV) 190
 Splitting, crystal field, of octa-
 hedral(VI) oxidation state 26
 Stability constants 222-23
 halide, bromide complexes 88t, 91t, 93t
 organic ligands 308-13
 plutonyl ion 263-68
 sulfate complexes, acid
 dependence 251-61
 Stability of oxidation states, effect of
 pH and complexation 2-3, 223-29
 Stability spectrum of cesium pluto-
 nium hexafluoride 199-203
 Stabilization enthalpies of alkali
 fluorouranates(V) 199-200
 Standard free energy of formation of
 atomic oxygen for Pu oxides 112-16
 Standard potentials, Pu and PuO₂
 ions 283t
 Stationary extraction furnace assembly
 for Pu reduction and ameri-
 cium extraction 348f
 Stoichiometry of reaction
 disproportionation, dependence on
 acidity 454-56
 Pu metal with a THF solution
 of C₂H₄I₂ 43
 Stoichiometry of TTA extraction
 process, Pu sulfate complexes 251-61
 Storage, nuclear waste 275-92
 Storage, nuclear waste, x-ray photo-
 emission spectroscopic study of
 actinides in silicate-based
 glasses 150
 Storage, retrieval, 20 year 457
 Storage tanks, spent decladding
 solution 355
 Streams, Pu distribution
 coefficients 299-302
 Strengths, ionic, Debye-Hückel
 relation, modification 89
 Stretching frequencies, ethylenic, of
 PuI₃C₂H₄ • 4THF and PuI₂C₂H₃ 43-48
 Strontium, ground-water
 compositions 337, 343-44
 Structural studies
 CsNpF₆, comparison to CsPuF₆ 199
 IR-Raman spectroscopy of poly-
 merization of Pu(IV) hydrolysis
 products 233, 235-39
 tetravalent metals 53-57
 Structure
 of carbamoylmethylphosphoryl
 extractants 435f
 crystal, allotropic, of metallic
 radii 71, 72f
 double bond, of PuI₃C₂H₄ • 4THF
 and PuI₂C₂H₃ 46-48
 electronic, of CsPuF₆ 206-9
 hydroxysulfate compounds 56-57
 monoclinic crystal, α-phase
 of Pu 66, 67f
 plutonyl ion 263-68

- Structure (*continued*)
 pseudo-spiral magnetic,
 of β -Pu₂O₃ 33
 silicate glasses 150-54
 Sublimation
 heats and entropies, of
 Pu-intermetallics 104*t*
 partial heats, of PuO₂(g)
 and PuO(g) 114-15
 Sulfate
 complexes
 bis(μ -hydroxo)tetraaquadipluto-
 nium(IV)
 spectroscopic studies 58-62
 structural studies 53-57
 synthetic studies 50-53
 concentration, ground-water leach-
 ing and composition 337, 343-44
 stability constants, enthalpies,
 and entropies 251-61
 Superconductivity in metallic
 Pu systems 71-74
 Symmetry
 crystallographic distortion of
 actinides 66-69
 of organometallic and coordina-
 tion compounds 25-38
 of Pu₃C₂H₄ · 4THF and Pu₂C₂H₃ 46-48
 of Pu₂(OH)₂(SO₄)₃(H₂O)₄ 58-62
 Synthesis of PuF₆ 159
 Synthetic studies, hydrothermal
 hydrolysis of Pu(IV) and
 sulfate 50-53
- T**
- Tanks, spent decladding solution
 storage 355
 Target collection technique, mass
 spectrometer, and measurement
 of effusion rates 100-101, 105
 TBP—*See* Tributyl phosphate
 Techniques
 absorption spectrophotometry and
 differential pulse polarography
 to determine oxidation state
 stability 319
 aqueous processing at Rocky
 Flats 375-78
 cost analysis for large-scale
 production 409-11
 high-temperature transpiration 116
 Pu processing and scrap recovery,
 overview 349-64
 pyrochemical
 direct oxide reduction, at
 Los Alamos 412-15, 428-30
 electrorefining 399-405
 electrorefining at Los
 Alamos 418-20, 423
 hydriding 405-6
 molten salt extraction 386-98
 molten salt extraction at Los
 Alamos 412, 416, 422-25,
 428-30
 PuF₄ reduction at Los
 Alamos 412, 415*f*, 422
 at Rocky Flats 370-75
 radiometrical determination 42
 recovery for waste recycle 418-30
 reflux, polymer growth 237-39
 separation processes, early work 6-21
 thermogravimetric, oxidation state
 determination of CsPuF₆
 product 201
 ultramicrochemistry, early work 6-21
 vapor pressure determination,
 Knudsen effusion 100-101
 x-ray diffraction, early work
 with Pu dioxide 20
 Technology, applied, overview of Pu
 processing chemistry 349-64
 Temperature dependence
 in Am(III) extraction 437-45
 diamagnetism of Pu(C₂H₅)₂ 33
 of free energy of formation of
 actinide intermetallics 105-6
 of magnetic moment, of organo-
 metallic and coordination
 compounds 31*f*, 32*f*, 36*f*
 of partial pressure of PuO(g), free
 energy of formation 112-18
 of polymer degradation 368-72
 of polymerization of hydrolysis
 products with nitrate 231, 237-39
 of Pu disproportionation 268-70
 of Pu vapor pressure over
 intermetallics 103*f*
 of reciprocal molar susceptibility
 of Li₃PuO₆ 28*f*
 of stability constants, Pu sulfate
 complexes 256-60
 of total pressures in equilibrium
 with condensed-phase com-
 position, PuO 134, 136*f*
 Temperature, phase-transition,
 Pu and PuO₂ 132
 Ternary phase diagram for
 NaCl-CaCl₂-MgCl₂ system 391-92
 Test site, Nevada, and ground-water
 leaching 335-44
 Testing
 Battelle static leach 337-38
 environmental, reducing agent 302
 nuclear weapons
 and aquatic ecosystems 298-99
 and production of Pu 276
 Tetracatechoylamide complex 220*f*
 Tetrafluoride Pu complex
 metal preparation line 350-53

- Tetrafluoride Pu complex (*continued*)
 Mulak model 29-30
 production and reduction at
 Los Alamos 412
- Tetragonal distortion in VII
 oxidation state 26
- Tetrahedra, SiO₄, bond angles 150-52
- Tetrapositive Pu, carrier 17-19
- Tetravalent metals, hydrothermal
 hydrolysis 50-62
- Thenyltrifluoroacetone (TTA),
 solvent extraction
 equilibrium 252-53, 258-61
- Thermodynamic functions 126-33
 activity equilibrium constant of
 actinide chlorides 389
 condensed phases 130-33
 halides and halogeno complexes
 in aqueous media 86-93
 in the solid state 75-86, 93
 PuF₆ 156-59, 164, 168-69
 Pu-noble metal compounds 99-107
 Pu oxides 109-21
- Thermogravimetric technique for
 oxidation state determination
 of CsPuF₆ product 201
- Third Law of Thermodynamics
 consistency for Pu-oxygen
 system 139-40
 heats and entropies of sublimation
 and formation of Pu-inter-
 metallics 102-4
- Thorium hydroxysulfate structure 57f
- Thorium(IV), distribution coefficients
 between aluminum, silicon, and
 chloride oxides 287, 289f
- Thorium-230, extraction by
 carbamoylmethylphosphoryl
 derivatives 433-49
- Titanium, x-ray photoemission spec-
 troscopic spectra 148f, 149f, 151f
- Titration, iodometric 42
- Tracer studies
 environmental, aquatic
 chemistry 297-313
 oxidation states, early work 2-3
 radioactive lanthanum fission
 product, early work 7, 10
- Tributyl phosphate (TBP), solvent
 extraction 371
- Trichloride compound, antiferro-
 magnetic transition 35
- Trigonally distorted octahedral
 CsPuF₆ site, model 206-9
- Trioxide, α -diplutonium, back
 reaction 385-86
- Trioxide, β -diplutonium, specific heat
 and magnetic measurements 33
- Triplet state, plutonyl ion 263-68
- Tripositive bismuth, carrier 17-19
- Trisilicate glass, sodium, and
 solubility of actinide
 oxides 146-47, 150, 153
- Trivalency
 actinides and lanthanides 69
 Pu₃C₂H₄ · 4THF and Pu₂C₂H₃ 46-48
- Tungsten cells
 preparation 100
 for vapor pressure measurements
 of PuO₂ 112
- U**
- Ultramicroscopic studies, early work .. 6-15
- Unit cell of α -Pu 67f
- Uranium
 compounds
 alkali fluorouranates, stabiliza-
 tion enthalpies 200t
 cesium hexafluoride, structural
 comparison to CsPuF₆ 199
 hexafluorides, gas-phase, elec-
 tronic energy level 157-59
 hydrothermal hydrolysis 50-53
 nitrate
 neutron-irradiated, and initial
 isolation of Pu 6-7
 and polymerization of Pu(IV)
 hydrolysis products 231-39
 oxides
 of aluminum, silicon, and chlo-
 ride, distribution
 coefficients 287-89
 oxygen potentials and
 pressures 138-39
 in silicate-based glasses, x-ray
 photoemission spec-
 troscopy 145-54
 vapor pressure and com-
 position 134, 137-41
 Pu compound formation 100
 separations at Savannah River
 Plant 356-58
 solubility of complexes on
 loading 436-49
 solution absorption spectra 186-93
 stability constants 261t, 312-13
 isotopes
 and neutron fission 3-4
 and preparation of Pu
 isotopes 2-7, 459
 redox potential diagram 215f
 and uptake of Pu on geologic mate-
 rial and living organisms 278
- Uranyl-specific ion electrode 227-29
- UV spectrophotometric studies of
 reduction, disproportionation,
 and depolymerization
 reactions 264-72

UV-visible spectroscopic studies of polymerization of Pu(IV) hydrolysis products233, 235-39

V

Valence electrons—*See* Electron configurations

Valence state transitions, x-ray photoemission spectroscopic study of actinide oxides145-54

Vaporization behavior of Pu-oxygen system110, 112-21

Vaporization, partial enthalpy of, calculations 115

Vapor pressure hypostoichiometric Pu dioxide condensed phase123-41

intermetallics, temperature dependence 103f

procedure for calculation from spectroscopic data 125f

Pu-noble metal compounds100-107

PuO₂112-16

Vasil'ev's equation, modification of Debye-Hückel relation 89

Vegetation, impact of Pu waste275-92

Velocities, migration, of Pu in granite bedrock 291

Vibrational bands of hydrolytic polymers235-37

Vibrations, IR, of PuI₃C₂H₄ • 4THF and PuI₃C₂H₃43-48

Visible spectra of Pu₂(OH)₂(SO₄)₃(H₂O)₄58-62

Visible spectroscopic studies of polymerization of Pu(IV) hydrolysis products233, 237-39

of reduction, disproportionation, and depolymerization reactions264-72

Volume, atomic, and bonding of actinides69-71

W

Waste disposal456-58

Waste glass, Pu leaching by ground waters335-44

Waste handling for unirradiated Pu processing 361

Waste, liquid, and actinides extraction444-49

Waste packages and seals performance, computer codes, RAFSCATT 1 and RAFSCATT 2456-58

Waste, repository site-selection criterion, ground-water leaching335-36

Waste storage, nuclear x-ray photoemission spectroscopic study of actinides in silicate-based glasses 150

Waste streams and environmental impact272-92

at Oak Ridge National Laboratory299, 304-7

Waste treatment, overview349-64

Waste treatment process, ferrite 378

Waste treatment at Rocky Flats 378

Water drinking, and Pu concentration290-91

and Pu transport processes, leaching studies225-44

vapor, homogeneity of Pu₂O₃ phase116-19

Wavefunction bonding 5f¹66-69

Weapon testing and aquatic ecosystems298-99

and production of Pu 276

Weight, molecular, of pure Pu compound, initial work7, 10-13

Wigner-Seitz approximation 105

X

x-Ray diffraction technique, early work with Pu dioxide 20

x-Ray photoemission spectroscopic (XPS) study, U, Np, and Pu oxides in silicate-based glasses 145-54

x-Ray powder diffraction pattern CsPuF₆201-2

Pu(IV) sulfate53-57

Y

Yields, fluorescence photon, PuF₆(g)163-64

Ytterbium metals in tetrahydrofuran solutions of diiodoethane 41

Z

Zeeman pattern for Pu(I) 197f

Zinc chloride, pyroreodox at Rocky Flats373-74

Zinc, oxide additives in silicate-based glasses, x-ray photoemission spectroscopic spectra 151f

Zinc-magnesium alloys, metal-thermic reductions 372

Zirconium compound, hydrothermal hydrolysis and crystal structure52-57

Zirflex, decladent 363

Zooplankton, impact of Pu waste275-92